universidad de salamanca

FACULTAD DE FARMACIA

DEPARTAMENTO DE CIENCIAS FARMACÉUTICAS

Área de Química Farmacéutica

NUEVOS ANTIMITÓTICOS BASADOS EN SULFONAMIDAS: DISEÑO, SÍNTESIS Y EVALUACIÓN COMO AGENTES ANTITUMORALES Y LEISHMANICIDAS

Memoria para optar al Grado de Doctor

Myriam González Díaz

Bajo la dirección de

Dr. Rafael Peláez, Dra. Raquel Álvarez, Dr. Manuel Medarde

Salamanca, 2021

NOVEL ANTIMITOTICS BASED ON SULFONAMIDES: DESIGN, SYNTHESIS AND EVALUATION AS ANTITUMOR AND ANTILEISHMANIAL AGENTS

Memoria presentada por Myriam González Díaz para optar al grado de Doctor en Farmacia con Mención Internacional por la Universidad de Salamanca.

Fdo. Dña. Myriam González Díaz

El **Dr. Rafael Peláez Lamamié de Clairac Arroyo**, Profesor Titular del Departamento de Ciencias Farmacéuticas de la Facultad de Farmacia de la Universidad de Salamanca, la **Dra. Raquel Álvarez Lozano**, Profesora Contratada Doctor del Departamento de Ciencias Farmacéuticas de la Facultad de Farmacia de la Universidad de Salamanca y el **Dr. Manuel Medarde Agustín**, Catedrático del Departamento de Ciencias Farmacéuticas de la Facultad de Farmacia de la Universidad de Salamanca,

CERTIFICAN

Que la memoria en formato compendio de artículos titulada "**Nuevos antimitóticos basados en sulfonamidas: diseño, síntesis y evaluación como agentes antitumorales y leishmanicidas**", presentada por la Graduada en Farmacia por la Universidad de Salamanca **Dña. Myriam González Díaz** para optar al Grado de Doctor en Farmacia con Mención Internacional por la Universidad de Salamanca, ha sido realizada bajo su dirección en el Laboratorio de Química Farmacéutica del Departamento de Ciencias Farmacéuticas, área de Química Farmacéutica, de la Facultad de Farmacia de la Universidad de Salamanca. Considerando que cumple con las condiciones necesarias, autorizan su presentación a fin de que pueda ser defendido ante el tribunal correspondiente.

Y para que así conste a efectos oportunos, expiden y firman el presente certificado en Salamanca, a 10 de junio de 2021.

Fdo. Dr. Rafael Peláez Fdo. Dra. Raquel Álvarez Fdo. Dr. Manuel Medarde

La doctoranda ha disfrutado, durante la realización de esta Tesis Doctoral, de un contrato predoctoral de personal investigador de la Junta de Castilla y León, cofinanciado por el Fondo Social Europeo, según Orden EDU/529/2017 de 26 de junio.

El desarrollo del trabajo experimental ha sido financiado en parte con cargo a los siguientes proyectos:

- Nuevos inductores de la degradación selectiva de proteínas esenciales como alternativa a la quimioterapia convencional en la búsqueda de nuevos agentes antitumorales y antiparasitarios. **SA116P20**. Consejería de Educación de la Junta de Castilla y León y fondos FEDER, 2021-2023. Rafael Peláez.
- Alternativas terapéuticas a los benzimidazoles para las zoonosis parasitarias mediante diseño basado en la diana. **RTI2018-099474-B-I00**. Ministerio de Ciencia, Innovación y Universidades, 2019-2021. Rafael Peláez.
- Diseño, síntesis y evaluación de análogos de combretastatina funcionalizados para su inclusión en sistemas de liberación dirigida. Fundación Memoria de D. Samuel Solórzano Barruso, 2019. Raquel Álvarez.
- Combinación de nuevos agentes antitubulina y análogos alquilfosfolípidos como una nueva estrategia frente a cáncer y Leishmaniosis. **SA262P18**. Consejería de Educación de la Junta de Castilla y León y fondos FEDER, 2018-2021. Rafael Peláez.
- Nuevos agentes antimitóticos activos frente a células resistentes: diseño, síntesis y evaluación. **SA030U16**. Consejería de Educación de la Junta de Castilla y León y fondos FEDER, 2016-2018. Rafael Peláez.
- Diseño, síntesis y evaluación de nuevos análogos antitumorales polares de combretastatinas. Fundación Memoria de D. Samuel Solórzano Barruso, 2015. Pilar Puebla.
- Optimización de antitumorales inhibidores de tubulina por mejora de las propiedades farmacocinéticas. **SA147U13**. Consejería de Educación de la Junta de Castilla y León y fondos FEDER, 2013-2015. Rafael Peláez.

La escritura principal de esta Tesis Doctoral corresponde a un compendio de tres artículos de investigación publicados, como a continuación se describen:

ARTÍCULO 1

Myriam González, María Ovejero-Sánchez, Alba Vicente-Blázquez, Raquel Álvarez, Ana B. Herrero, Manuel Medarde, Rogelio González-Sarmiento and Rafael Peláez. Microtubule Destabilizing Sulfonamides as an alternative to taxane-based chemotherapy. International Journal of Molecular Sciences. 2021, 22, 1907. DOI: 10.3390/ijms22041907.

ARTÍCULO 2

Myriam González, María Ovejero-Sánchez, Alba Vicente-Blázquez, Manuel Medarde, Rogelio González-Sarmiento and Rafael Peláez. Methoxy and bromo scans on *N*-(5-methoxyphenyl) methoxybenzenesulphonamides reveal potent cytotoxic compounds, especially against the human breast adenocarcinoma MCF7 cell line. Journal of Enzyme Inhibition and Medicinal Chemistry. 2021, 36:1, 1029-1047. DOI: 10.1080/14756366.2021.1925265.

ARTÍCULO 3

Myriam González, Pedro José Alcolea, Raquel Álvarez, Manuel Medarde, Vicente Larraga and Rafael Peláez. New diarylsulfonamide inhibitors of *Leishmania infantum* amastigotes. International Journal for Parasitology: Drugs and Drug Resistance. 2021, 16, 45-64. DOI: 10.1016/j.ijpddr.2021.02.006.

Trabajo adicional realizado durante este periodo ha contribuido a la publicación de los siguientes artículos de investigación:

- **González, M.**; Ellahioui, Y.; Álvarez, R.; Gallego-Yerga, L.; Caballero, E.; Vicente-Blázquez, A.; Ramudo, L.; Marín, M.; Sanz, C.; Medarde, M. and Pelaéz, R. The Masked Polar Group Incorporation (MPGI) strategy in drug design: Effects of nitrogen substitutions on combretastatin and isocombretastatin tubulin inhibitors. Molecules **2019**, 24 (23), 4319.
- Vicente-Blázquez, A.; **González, M.**; Álvarez, R.; Del Mazo, S.; Medarde, M. and Peláez, R. Antitubulin sulfonamides: The successful combination of an established drug class and a multifaceted target. Med. Res. Rev. **2019**, 39 (3), 775–830.
- Majumder, I.; Álvarez, R.; Chakraborty, P.; **González-Díaz, M.**; Peláez, R.; Bauza, A.; Ellahioui, Y.; Frontera, A.; Zangrando, E.; Gómez-Ruiz, S. and Das, D. Bioactive Heterometallic Cu^{II}-Zn^{II} Complexes with Potential Biomedical Applications. ACS Omega **2018**, 3, 13343 - 12353.
- Álvarez, R.; Aramburu, L.; Puebla, P.; Caballero, E.; **González, M.**; Vicente, A.; Medarde, M. and Peláez, R. Pyridine based antitumour compounds acting at the colchicine site. Curr. Med. Chem. **2016**, 23 (11), 1100–1130.
- Jiménez, C.; Ellahioui, Y.; Álvarez, R.; Aramburu, L.; Riesco, A.; **González, M.**; Vicente, A.; Dahdouh, A.; Ibn Mansour, A.; Jiménez, C.; Martín, D.; Sarmiento, R. G.; Medarde, M.; Caballero, E. and Peláez, R. Exploring the size adaptability of the B ring binding zone of the colchicine site of tubulin with para-nitrogen substituted isocombretastatins. Eur. J. Med. Chem. **2015**, 100, 210–222.

A mis padres, Herminia y Gabriel, por su apoyo incondicional.

A mi compañero de vida, Raúl, por caminar siempre a mi lado.

Quiero expresar mi agradecimiento a mis directores de tesis Rafa, Raquel y Manolo por haber confiado en mí desde el primer momento y abrirme las puertas tanto de su investigación como de su amistad; por haberme dado todo su apoyo y dedicación durante estos años; por las enseñanzas transmitidas; por orientarme en todo momento (aunque no siempre siguiera sus sabios consejos); por su infinita paciencia con mi peculiar memoria. En definitiva, gracias por ayudarme a cumplir este sueño.

Gracias al Dr. Nathaniel I. Martin del *Institute of Biology Leiden* (*The Netherlands*), al Dr. Vicente Larraga del Centro de Investigaciones Biológicas Margarita Salas (Madrid) y al Dr. Rogelio González del Departamento de Medicina de la Facultad de Medicina (Salamanca) por blindarme la oportunidad de realizar estancias de investigación. Gracias a ellas he podido completar mi formación adquiriendo un aprendizaje multidisciplinar y la capacidad de adaptación a nuevas formas de trabajar. Además, me han permitido conocer gente maravillosa a los que no podría estar más agradecida por su ayuda, Ned, Pedro y María, gracias por todo.

Por último, quiero agradecer a todas las personas que, de una manera u otra, han hecho posible que haya llegado hasta aquí:

A todos mis compañeros de laboratorio, en especial a Alba, por trabajar mano a mano conmigo todos estos años, complementarme y ayudarme siempre.

A mis padres, por su amor y dedicación; por apoyarme y motivarme a elegir el camino de la investigación y recorrerlo a mi lado; por hacer de mí la persona que soy.

A mis hermanos, por ser un pilar fundamental en mi vida y el mejor ejemplo a seguir.

A mi segunda familia, por acogerme y quererme como una hija y hermana más.

A mis amigos, por estar siempre a mi lado por muchos años que pasen y por muchas vueltas que de la vida, haciéndome disfrutar de cada segundo en su compañía.

A Raúl, por hacer de este mundo un verdadero juego de niños; por amarme, respetarme, apoyarme y ayudarme en todo lo posible y lo imposible; por ser una parte más de mí, mi favorita. En definitiva, por ser mi mejor amigo.

Muchas gracias a todos por formar parte de mi vida.

resumen

Los agentes antimitóticos, que se utilizan como antineoplásicos, antiparasitarios, antifúngicos y herbicidas, bloquean la división celular al interferir con la maquinaria mitótica. El cáncer y la leishmaniasis son enfermedades que tienen un enorme impacto y cuyos tratamientos presentan múltiples limitaciones. Este trabajo de Tesis Doctoral tiene como objetivo principal diseñar y sintetizar nuevas *N*-fenilbencenosulfonamidas que se unan al dominio de colchicina en tubulina, y evaluar su actividad antitumoral y leishmanicida.

Los microtúbulos son polímeros dinámicos, formados por la asociación de dímeros de α,β-tubulina, que se encuentran implicados en procesos esenciales para la supervivencia celular tales como la formación del huso mitótico, la motilidad y el mantenimiento de la morfología celular, entre otros.

Los ligandos de unión al dominio de colchicina en tubulina son moléculas estructuralmente sencillas y de pequeño tamaño, lo que las hace sintéticamente accesibles. Además, su estructura sencilla les permite evadir resistencias mediadas por proteínas transportadoras de membrana (MDR). Basándose en las estructuras de rayos X descritas de complejos proteína-ligando, el dominio de la colchicina se ha dividido en 3 zonas consecutivas: zonas 1, 2 y 3. Los ligandos diseñados en este trabajo actúan uniéndose simultáneamente a las zonas 1-2. Para ello, deben estar formados por dos anillos aromáticos conectados entre sí por un puente de longitud variable que permita su disposición *cisoide* y no coplanar, premisa que se cumple con la elección del esqueleto común de *N*-fenilbencenosulfonamida.

Este trabajo ha dado lugar al diseño y la síntesis de una biblioteca de 350 nuevas *N*-fenilbencenosulfonamidas en las que se han explorado numerosas modificaciones estructurales, variando tanto los sustituyentes como el patrón de sustitución de ambos anillos aromáticos e introduciendo una gran variedad de sustituyentes de diferente longitud y naturaleza sobre el nitrógeno de la sulfonamida. A pesar de que la tubulina es una proteína altamente conservada, existen diferencias suficientes entre el dominio de la colchicina de mamíferos y el de *Leishmania* spp. Estas diferencias en las secuencias se han aprovechado para el diseño selectivo de ligandos con actividad antitumoral y/o leishmanicida.

La biblioteca de sulfonamidas sintetizada ha sido evaluada *in vitro* frente a líneas celulares tumorales humanas y formas extra- e intra- celulares de parásitos de *Leishmania infantum*. Los resultados sugieren que ejercen su acción antimitótica por unión al dominio de colchicina en la β-tubulina. Los ligandos evaluados no fueron sustrato de las MDR, lo que sugiere que no son susceptibles de sufrir resistencias mediadas por MDR. Además, la solubilidad acuosa fue apreciablemente mayor que la de los ligandos de referencia. Los compuestos citotóxicos presentaron actividad antitumoral con potencias en el rango submicromolar y nanomolar. En el estudio del mecanismo de acción antitumoral los compuestos se comportaron como agentes de unión a tubulina, causando una clara desestabilización de la red microtubular, la inhibición de la polimerización de tubulina *in vitro* y la parada del ciclo celular en la región G_2/M seguida por la muerte celular mediada por apoptosis. La evaluación de la actividad antiparasitaria alcanzó tasas de éxito de más del 10% y potencias similares o incluso mejores que los fármacos de referencia actualmente en clínica. Por lo tanto, podemos concluir que este trabajo contribuye al desarrollo de ligandos antimitóticos de unión a tubulina, con potencial aplicación en terapias antitumorales o antiparasitarias.

abstract

Antimitotic agents, which are used as antineoplastics, antiparasitics, antifungals, and herbicides, block cell division by interfering with the mitotic machinery. Cancer and leishmaniasis are diseases that have a huge impact and whose treatments have multiple limitations. The main objective of this Ph.D. thesis is to design and synthesize new *N*-phenylbenzenesulfonamides aimed to bind to the colchicine domain in tubulin, and to evaluate their antitumor and antileishmanial activity.

Microtubules are dynamic polymers built up by polymerization of α,β-tubulin dimers, they are highly involved in pivotal functions for cell survival such as the formation of the mitotic spindle, motility, and maintenance of cell shape, among others.

Colchicine-site binding ligands are structurally simple small molecules, making them synthetically accessible. Furthermore, their small structure allows them to avoid resistance mechanisms mediated by membrane transporter proteins (MDR). Based on the described X-ray structures of protein-ligand complexes, the colchicine domain has been divided into 3 consecutive zones: zones 1, 2, and 3. The ligands designed in this work act by binding simultaneously to zones 1-2. For this purpose, they must be constituted by two aromatic rings connected to each other by a bridge of variable length that allows their arrangement in a *cisoid* and non-coplanar disposition, a premise that is fulfilled with the choice of the common *N*-phenylbenzenesulfonamide scaffold.

This work has completed the design and synthesis of a focused library of 350 novel *N*-phenylbenzenesulfonamides in which numerous structural modifications have been explored, varying both the substituents and the substitution pattern of both aromatic rings, and introducing a wide variety of substituents of different length and nature on the sulfonamide nitrogen. Despite tubulin is a highly conserved protein, there are some differences in the colchicine domain between mammals and *Leishmania* spp. These sequence differences have been exploited for the selective design of ligands with antitumor and/or antileishmanial activity.

The synthesized sulfonamide library was evaluated *in vitro* against human tumor cell lines and against extra- and intra- cellular stages of *Leishmania infantum*. Our results suggest that they exert their antimitotic activity by binding to the colchicine domain in β-tubulin. The assayed ligands were not substrates of MDR proteins, suggesting that they are not susceptible to MDR-mediated resistance. Furthermore, the aqueous solubility was appreciably higher than that of the reference ligands. The antitumor activity evaluation revealed many compounds with submicromolar and nanomolar cytotoxic potencies. During the study of the antitumor mechanism of action, compounds behaved as tubulin binding agents, causing a clear disruption of the microtubular network, the *in vitro* inhibition of tubulin polymerization and the arrest of the cell cycle in the G_2/M region followed by apoptosis-mediated cell death. The antiparasitic activity evaluation achieved success rates of more than 10% and potencies similar or even greater than the reference drugs currently in clinical use. Therefore, we can conclude that this work contributes to the development of tubulin-binding antimitotic ligands, with potential application in antitumor or antiparasitic therapies.

índice

abreviaturas y acrónimos

A

A	Activo
Ac	Acetilo
Acetone-D_6	Acetona deuterada
AcOH	Ácido acético
ADM	Agentes Desestabilizadores de Microtúbulos
ADN	Ácido desoxirribonucleico
AEM	Agentes Estabilizadores de Microtúbulos
AnV	Anexina V
APC/C^{Cdc20}	Complejo promotor de la anafase o Ciclosoma, del inglés *Anaphase Promoting 21omplexo r Cyclosome*
Ar_A	Anillo aromático A
Ar_B	Anillo aromático B
Ar_C	Anillo aromático C
ATP	Adenosín trifosfato, del inglés, *Adenosine triphosphate*
AURKA	Aurora Kinasa A
AURKB	Aurora Kinasa B
AVL	Leishmaniasis visceral antroponótica, del inglés, *Anthroponotic Visceral Leishmaniasis*

B

bd	Doblete ancho, del inglés, *broad doublet*
β-ME	Beta-mercaptoetanol
Bn	Bencilo
bs	Singlete ancho, del inglés, *broad singlet*
BSA	Albúmina de suero bobino, del inglés, *Bovine Serum Albumin*

C

C	Citotóxico
C1	Concentración 1
C2	Concentración 2
CA-4	Combretastatina A-4
CDK1	Kinasa dependiente de ciclina 1, del inglés, *Cyclin-Dependent Kinase 1*
CENP-E	Proteína centromérica E, del inglés, *Centromere-associated Protein E*
CI_{50}	Concentración inhibitoria 50%
CL	Leishmaniasis cutánea, del inglés, *Cutaneous Leishmaniasis*

D

d	Doblete, del inglés, *doublet*
DAPI	4',6-diamidino-2-fenilindol
dd	Doble doblete, del inglés, *double doublet*
DMEM	Del inglés, *Dulbecco's Modified Eagle Medium*
DMF	Dimetilformamida
DMSO	Dimetil sulfóxido
DMSO-D_6	Dimetil sulfóxido deuterado
DNA	Ácido desoxirribonucleico, del inglés, *Deoxyribonucleic acid*

E

EA	Apoptosis temprana, del inglés, *Early Apoptosis*
EDTA	Ácido etilendiaminotetraacético, del inglés, *Ethylene Diamine Tetraacetic Acid*
EGTA	Ácido etilenglicoltetraacético, del inglés, *Ethylene Glycol Tetraacetic Acid*
EMA	Agencia europea del medicamento, del inglés, *European Medicines Agency*
Et	Etilo
et al.	Y otros
EtOAc	Acetato de etilo

F

FDA	Del inglés, *Food and Drug Administration*
Fig.	Figura
FITC	Isotiocianato de fluoresceína

G

GC-MS	Cromatografía de gases-espectrometría de masas, del inglés, *Gas Chromatography-Mass Spectrometry*
GDP	Guanosín difosfato, del inglés, *Guanosine diphosphate*
GLOBOCAN	Del inglés, *Global Cancer Observatory*
GTP	Guanosín trifosfato, del inglés, *Guanosine triphosphate*

H

h	Hora
HDAC	Histona desacetilasa
HIFBS	Suero fetal bovino inactivado por calor, del inglés, *Heat-Inactivated Fetal Bovine Serum*
HRMS	Espectrometría de masas de alta resolución, del inglés, *High-Resolution Mass Spectrometry*

I

IC_{50}	Concentración inhibitoria 50%, del inglés, *half-maximal inhibitory concentration*
IR	Infrarrojo

J

JADOPPT	Del inglés, *Java based AutoDock Preparing and Processing Tool*
J	Constante de acoplamiento

K

KNIME	Del inglés, *Konstanz Information Miner*
KSP/EG5	Kinesina del huso acromático EG5, del inglés, *Kinesin-Spindle Protein EG5*

L

LA	Apoptosis tardía, del inglés, *Late Apoptosis*
LGA	Algoritmo genético lamarckiano, del inglés, *Lamarckian Genetic Algorithm*
LUT	Ligandos de Unión a Tubulina
LLM/PEL	Laulimalida Pelorusida

M

m	Multiplete, del inglés, *multiplet*
M^+	Ion molecular
MAPs	Proteínas asociadas a microtúbulos, del inglés, *Microtubule-Associated Proteins*
MCL	Leishmaniasis mucocutánea, del inglés, *Mucocutaneous Leishmaniasis*
MDA	Agentes desestabilizadores de microtúbulos, del inglés, *Microtubule Destabilizing Agents*
MDR	Resistencia a múltiples fármacos, del inglés, *Multiple Drug Resistance*
MDS	Sulfonamidas desestabilizadoras de microtúbulos, del inglés, *Microtubule Destabilizing Sulfonamides*
Me	Metilo
MeOH	Metanol
MES	Ácido 2-(*N*-morfolino)etanosulfónico
min	Minutos
M.p.	Punto de fusión, del inglés, *Melting Point*
MPF	Factor promotor de la maduración, del inglés, *Maturation Promoting Factor*
MSA	Agentes estabilizadores de microtúbulos, del inglés, *Microtubule Stabilizing Agents*

N

NA	No Activo
NBS	*N*-bromosuccinimida
$nBu_4N^+HSO_4^-$	Hidrógeno sulfato de tetrabutilamonio
NC	No Citotóxico
n.d. o ND	No Determinado
NMR	Resonancia magnética nuclear, del inglés, *Nuclear Magnetic Resonance*

O

OMS	Organización Mundial de la Salud

P

PBS	Tampón fosfato salino, del inglés, *Phosphate-Buffered Saline*
PDB	Del inglés, *Protein Data Bank*
Pd(C)	Paladio sobre carbón activo
P-gp	Glicoproteína-P
Ph	Fenilo, del inglés, *phenyl*
PI	Yoduro de propidio, del inglés, *Propidium Iodide*
PLK1	Del inglés, *Polo-Like* Kinasa 1
PMA	Del inglés, *Phorbol 12-Myristate 13-Acetate*
ppm	Partes por millón
PVDF	Fluoruro de polivinilideno
Py	Piridina, del inglés, *pyridine*

Q

q	Cuartete, del inglés, *quartet*

R

REA	Relación Estructura-Actividad
REP	Relación Estructura-Propiedades
RES	Relación Estructura-Selectividad
Rho/ROCK	Del inglés, *Rho-associated coiled coil-containing protein kinase 1*
RMN	Resonancia Magnética Nuclear
RNase A	Ribonucleasa A
rpm	Revoluciones por minuto
rt	Temperatura ambiente, del inglés, r*oom temperature*

S

s	Singlete, del inglés, *singlet*
SAC	Punto de control del huso mitótico, del inglés, *Spindle Assembly Checkpoint*
SAR	Relación estructura-actividad, del inglés, *Structure-Activity Relationship*
SDS-PAGE	Del inglés, *Sodium Dodecyl Sulfate Polyacrylamide Gel Electrophoresis*
SQSTM1	Del inglés, *Sequestosome 1*

T

t	Triplete, del inglés, *triplet*
TBS-T	Tampón tris salino con Tween20, del inglés, *Tris Buffered Saline with Tween 20*
THF	Tetrahidrofurano
TLC	Cromatografía en capa fina, del inglés, *Thin Layer Chromatography*
TMP	3,4,5-trimetoxifenilo
TPI	Inhibición de la polimerización de tubulina, del inglés, *Tubulin Polymerization Inhibition*

U-Z

UV	Ultravioleta
VDA	Agentes disruptores de la vasculatura, del inglés, *Vascular Disrupting Agents*
Verap.	Verapamilo
VL	Leishmaniasis visceral, del inglés, *Visceral Leishmaniasis*
vs.	*Versus*
WHO	Del inglés, *World Health Organization*
ZVL	Leishmaniasis visceral zoonótica, del inglés, *Zoonotic Visceral Leishmaniasis*

Símbolos

δ	Desplazamiento químico

introducción

"Nothing in life is to be feared, only understood. Now is the time to understand more, so we can fear less."

Marie Curie

1. AGENTES ANTIMITÓTICOS

Los agentes antimitóticos son sustancias que bloquean la división celular al interferir con la maquinaria mitótica, produciendo la parada de la célula en mitosis e impidiendo su correcta progresión.

1.1. Mitosis

El ciclo celular es el conjunto de estadios mediante los cuales una célula aumenta su tamaño y duplica su material genético para finalmente dividirse en dos células hijas idénticas. Se desarrolla en cuatro fases o etapas denominadas G_1, S, G_2 y M (Fig. 1). Las fases G_1, S y G_2 se suelen agrupar en la denominada interfase. La fase G_1 es la más larga de todas y es en la que se produce el crecimiento celular hasta alcanzar el tamaño óptimo. La fase S, o síntesis, es la encargada de la duplicación del ADN. La fase G_2 es una segunda etapa de crecimiento, más breve que la primera (G_1), durante la cual la célula se prepara para entrar en mitosis. Por último, la fase M o mitosis es el proceso mediante el cual se divide el material genético en dos células idénticas.[1]

La progresión de la mitosis transcurre en cuatro fases: profase, metafase, anafase y telofase (Fig. 1). Durante la profase, los cromosomas (previamente duplicados en la interfase) condensan, desaparece el nucleolo y se rompe la envuelta nuclear. El huso mitótico comienza a formarse mediante la migración de los centrosomas a los polos opuestos de la célula. Los microtúbulos que emanan de los centrosomas se unen a los cromosomas a través de los cinetocoros. Durante la metafase, los cromosomas se alinean en el plano ecuatorial, uniéndose cada una de las cromátidas hermanas a través de los cinetocoros a microtúbulos de centrosomas opuestos. En la anafase, las cromátidas se separan y migran hacia los polos opuestos de la célula. Finalmente, el huso mitótico se descompone, las cromátidas descondensan y se rodean de nuevas envolturas nucleares durante la telofase. La mitosis va seguida inmediatamente del proceso de citoquinesis, mediante el cual se produce la división del citoplasma para originar las dos células hijas idénticas.[1] Proteínas como la tubulina, las kinasas mitóticas AURKA, AURKB y PLK1 o las kinesinas mitóticas KSP/EG5 o CENP-E son las responsables directas de la correcta formación y funcionamiento del huso mitótico, así como de una adecuada condensación y segregación cromosómica durante el proceso de mitosis.[2]

Existen múltiples puntos de control que aseguran la progresión del ciclo celular de forma correcta. Cabe destacar, el punto de control del huso mitótico, del inglés, *Spindle Assembly Checkpoint* (SAC), encargado de garantizar la distribución equitativa de los cromosomas en las células hijas durante el proceso de la mitosis. Con el fin de prevenir la segregación errónea de los cromosomas, la ausencia o defectos en la unión de los microtúbulos del huso mitótico a los cromosomas activan el SAC, bloqueando la transición de la metafase a la anafase.[3,4]

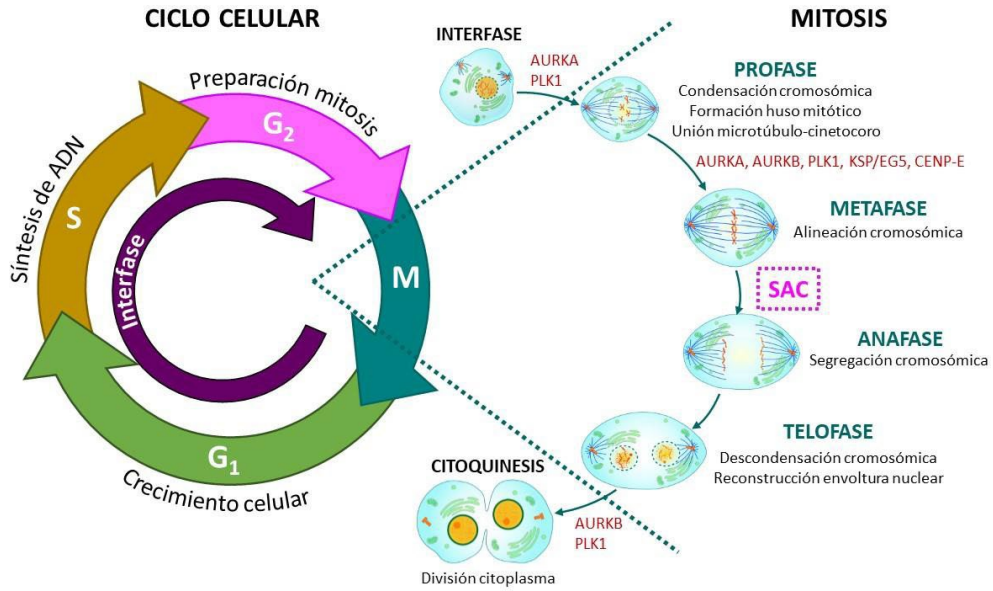

Figura 1. Representación esquemática de las diferentes fases de las que se componen el ciclo celular y la mitosis.

1.2. Mecanismo de acción de los agentes antimitóticos

La progresión del ciclo mitótico está regulada por cascadas de señalización que implican múltiples proteínas (Fig. 2). La profase comienza cuando la CiclinaB y la kinasa CDK1 forman el complejo denominado Factor Promotor de la Maduración (MPF), fosforilado principalmente por las kinasas Wee1 y CAK. La activación por PLK1 de las fosfatasas Cdc25 elimina los grupos fosfato del MPF dando lugar a la entrada en metafase. La forma activa de CDK1 desencadena una cascada de fosforilación de sustratos mitóticos. El inicio de la anafase ocurre cuando el complejo promotor de la anafase (APC/C^{Cdc20}) ubiquitina a la CiclinaB para ser posteriormente degradada por la vía del proteasoma 26S. De esta manera, la CiclinaB ya no estaría disponible para formar el complejo MPF con CDK1.[5]

Los agentes antimitóticos actúan a través de la unión a sus respectivas dianas (ver apartado 1.3), alterando la maduración y segregación del centrosoma, la formación y funcionamiento del huso mitótico, la unión microtúbulo-cinetocoro, el alineamiento y la segregación cromosómica o la activación del MPF o del APC/C^{Cdc20}, entre otros; conduciendo a la activación del SAC (Fig. 2). La activación del SAC bloquea la actividad ubiquitina ligasa mediada por el complejo promotor de la anafase APC/C^{Cdc20}, permaneciendo activado el complejo CDK1/CiclinaB (MPF). Esta activación sostenida no permite a las células completar el ciclo mitótico y es la responsable de la parada en G_2/M del ciclo celular observada en los experimentos de cultivo celular por citometría de flujo.[6–8] Finalmente, niveles sostenidos de la kinasa CDK1 hacen que múltiples proteínas de la familia de Bcl-2 sean fosforiladas, induciendo así la permeabilización de la membrana mitocondrial.[9,10] La alteración de la integridad de la membrana mitocondrial permite la liberación del citocromo c al citoplasma y la posterior activación de la cascada de fosforilación de las caspasas, desencadenando la muerte celular por apoptosis.[11]

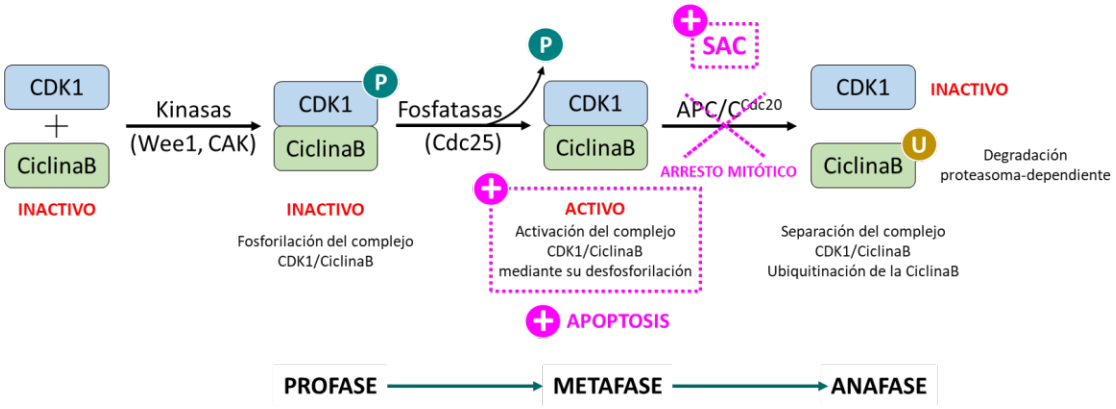

Figura 2. Principales cascadas de señalización que regulan la mitosis. Sobre ellas, el mecanismo de acción de los agentes antimitóticos señalado en color **rosa**.

1.3. Clasificación y aplicaciones terapéuticas

Tradicionalmente, los agentes antimitóticos han sido considerados como sinónimo de fármacos que actúan sobre la dinámica de los microtúbulos. Sin embargo, son múltiples las dianas celulares sobre las que los antimitóticos ejercen su acción, todas ellas con un rol decisivo en la división celular.[2,12–15] En función de su diana se clasifican en:

- Ligandos de unión a tubulina. La tubulina es la proteína encargada de la formación de los microtúbulos. Los microtúbulos se encuentran altamente implicados en el proceso de división celular, ya que son los responsables directos de la formación del huso mitótico. Se describen en profundidad a lo largo de este trabajo.
- Inhibidores de kinasas mitóticas. Las kinasas son proteínas muy importantes en la regulación del ciclo celular. Su función consiste en la fosforilación de múltiples sustratos, (Ej.: MPF, Cdc25, etc.) conduciendo a su activación o inactivación. Algunas de las más importantes que intervienen en el proceso de la mitosis son las Aurora Kinasas A (AURKA) y B (AURKB) y la *Polo-Like* Kinasa 1 (PLK1). La AURKA juega un papel fundamental en el mantenimiento de la bipolaridad del huso mitótico al comienzo de la profase al estar altamente implicada en la maduración y la separación de los centrosomas. La AURKB está implicada en procesos como la unión microtúbulo-cinetocoro y la condensación y el alineamiento de los cromosomas, asegurando la alineación cromosómica bipolar. Además, la AURKB contribuye al correcto funcionamiento del SAC y del proceso de citoquinesis. La PLK1 interviene en los procesos mitóticos de maduración del centrosoma, formación del huso mitótico, segregación cromosómica y citoquinesis; así como en la activación del Cdc25, del APC/C^{Cdc20} o del SAC, entre otros.
- Inhibidores de fosfatasas mitóticas. Las proteínas fosfatasas aseguran que la fosforilación sea un proceso reversible, mediante la desfosforilación de múltiples sustratos. Las fosfatasas Cdc25 son esenciales en el proceso de la mitosis ya que son las encargadas de la activación del MPF mediante su desfosforilación.
- Inhibidores de kinesinas. Las kinesinas son una familia de proteínas motoras que utilizan la energía del ATP para trasladarse a lo largo de los microtúbulos. Intervienen en diversas funciones del ciclo celular como la formación del huso mitótico, la regulación de la dinámica de los microtúbulos o la segregación y alineamiento de los cromosomas, entre otras. Las más destacables en el proceso mitótico son la *Kinesin-Spindle Protein* EG5 (KSP/EG5) y la proteína centromérica E (CENP-E). La KSP/EG5 es necesaria para la establecer la bipolaridad del huso mitótico a través de la separación del centrosoma y para la segregación adecuada de las cromátidas hermanas. La kinesina CENP-E interviene en la unión microtúbulo-cinetocoro y por lo tanto es esencial para la progresión normal de la mitosis al contribuir a la correcta congresión cromosómica.
- Inhibidores de proteínas asociadas a microtúbulos (MAPs). Las MAPs son una serie de proteínas unidas a los microtúbulos, encargadas de regular su estabilidad y su comportamiento dinámico (polimerización/despolimerización). Las más destacadas son Map1, Map2, Map4 y Tau.

En la siguiente imagen (Fig. 3) se detalla la estructura química de inhibidores representativos y característicos de cada uno de los grupos de agentes antimitóticos descritos.

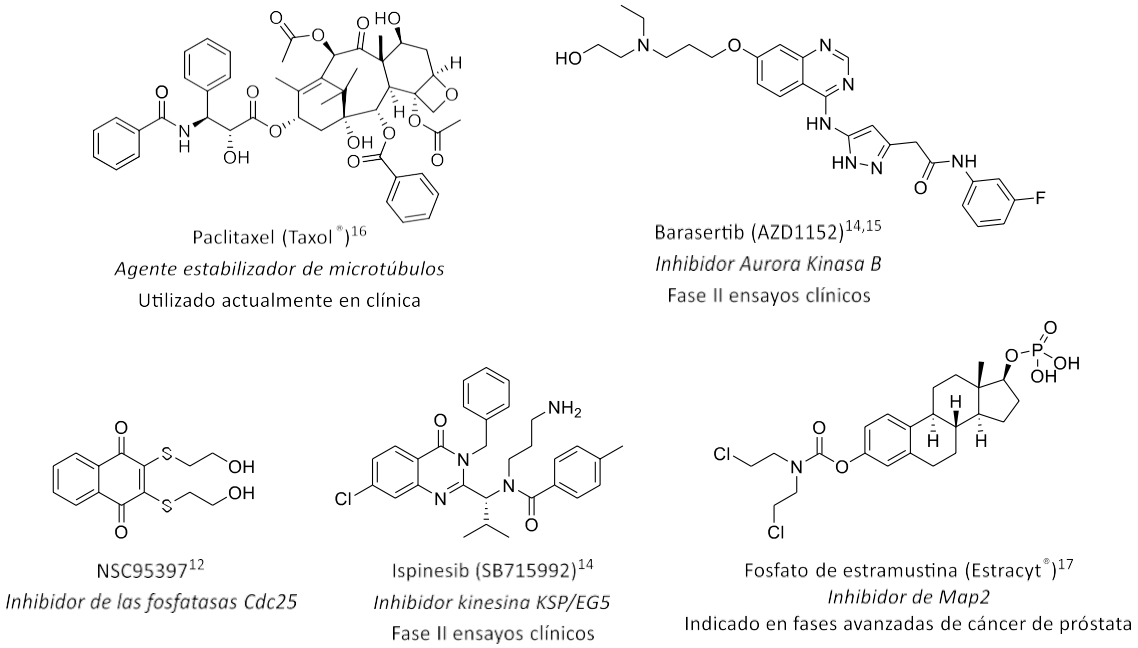

Figura 3. Ligandos representativos de los diferentes grupos de agentes antimitóticos según su diana celular.

Además de los agentes antimitóticos citados anteriormente, los cuales interfieren de forma directa con la maquinaria mitótica, existen multitud de ligandos que pueden provocar la parada del ciclo celular en G_2/M al interferir indirectamente con el proceso de la mitosis, y que en algunas ocasiones pueden llegar a ser considerados fármacos antimitóticos.[12] Algunos de ellos pueden ser, por ejemplo:

- Inhibidores del proteasoma. El proteasoma es un importante complejo multiproteico responsable de la degradación de la mayoría de las proteínas de las células eucariotas. Durante la mitosis, es el encargado de degradar las proteínas ubiquitinadas por el complejo APC/C^{Cdc20}, conduciendo a la célula a la salida de la mitosis.
- Inhibidores de las topoisomerasas. Las ADN topoisomerasas (ej.: Topoisomerasa II) son enzimas nucleares esenciales que modifican el superenrollamiento del ADN.
- Inhibidores de las histonas desacetilasas (HDACs). Las HDACs son las enzimas que catalizan la hidrólisis de los residuos acetil-lisina de las proteínas. Se encuentran altamente implicadas en el control de la expresión génica.
- Inhibidores de actina. La actina constituye uno de los componentes fundamentales del citoesqueleto celular, encargada de funciones como la motilidad, el tráfico intracelular y la citoquinesis, entre otras.

La aplicación de los agentes que interfieren con la progresión de la mitosis está indicada en procesos fisiopatológicos en los que la división celular se encuentra alterada o en aquellos en los que se pretende acabar con agentes exógenos no deseados. El cáncer, al ser una enfermedad caracterizada por una hiperproliferación incontrolada de células malignas, constituye la principal aplicación terapéutica de los agentes antimitóticos. Fármacos antimitóticos como el Taxol®, se incluyen en tratamientos antitumorales utilizados actualmente en clínica.[18] Además, las terapias antimitóticas se emplean en el tratamiento de enfermedades provocadas por agentes exógenos como parásitos u hongos.[19–22] Por lo tanto, podemos concluir que los agentes antimitóticos presentan aplicaciones antitumorales, antiparasitarias, antifúngicas y herbicidas.

Este trabajo de Tesis Doctoral se centra, de entre todos los agentes antimitóticos, en aquellos que tienen como objetivo la alteración de la dinámica de los microtúbulos. Los Ligandos de Unión a Tubulina (LUT) han sido y son fármacos ampliamente utilizados en la clínica de diversas enfermedades (ej.: tumores sólidos y hematológicos, gota, parasitosis, etc.), mientras que, hasta ahora, ninguno de los inhibidores de kinasas mitóticas y kinesinas ha conseguido ser aprobado para su uso clínico.[23] LUT como el Taxol®, y los alcaloides de la vinca (Vincristina y Vinblastina) continúan siendo tratamientos de primera línea para varios tipos de cáncer[18,24] y fármacos como el albendazol, el mebendazol o el triclabendazol,[22] son antiparasitarios de uso extendido que ejercen su acción al inhibir la polimerización de los microtúbulos.

2. LA TUBULINA COMO DIANA

La tubulina es una diana ampliamente validada en el tratamiento del cáncer y de las enfermedades parasitarias, entre otras.[25–27] Es la responsable de la formación de los microtúbulos, los cuales forman parte del citoesqueleto, intervienen en procesos esenciales como la motilidad celular, el transporte de orgánulos y vesículas, el mantenimiento de la morfología celular y la transducción de señales y son los componentes principales del huso mitótico.[28] Los microtúbulos además, constituyen el esqueleto principal de estructuras móviles como cilios y flagelos. En *Leishmania* son un componente esencial de flagelos y microtúbulos subpeliculares, dos estructuras relacionadas con la patogenicidad del parásito.[29,30]

La tubulina es una proteína heterodimérica globular formada por dos subunidades: α y β (Fig. 4). Las subunidades α y β se encuentran codificadas por familias de genes muy relacionadas entre sí, presentando una identidad de secuencia de aproximadamente el 40%.[31,32] Ambos monómeros tienen una masa molecular aproximada de 50 kDa cada uno y sus estructuras tridimensionales son muy similares. Actualmente, se conocen ocho isotipos de α-tubulina y nueve de β-tubulina en humanos.[33] Los genes que codifican estos isotipos se encuentran ubicados en diferentes cromosomas y su expresión está relacionada con el tipo de tejido.[34] Asociaciones longitudinales de dímeros de α y β tubulina, mediante enlaces entre subunidades diferentes (α-β), dan lugar a la formación de protofilamentos. La asociación lateral de 13 protofilamentos, mediante enlaces entre subunidades iguales (α-α, β-β), origina estructuras poliméricas organizadas llamadas microtúbulos (Fig. 4).[35] Los microtúbulos son cilindros huecos, de longitud variable, 25 nm de diámetro y distancia interior de 15 nm.[36] Su estructura no se compone de un solo isotipo de tubulina, sino que están formados por varios de ellos que coexisten según el tipo de célula. Los microtúbulos son polímeros dinámicos en equilibrio que alternan procesos, dependientes de GTP/GDP, de crecimiento (polimerización) y acortamiento (despolimerización) por la asociación y disociación reversible de unidades de α/β tubulina en sus dos extremos. El extremo + (subunidad β) o de crecimiento rápido es mucho más dinámico y puede mostrar un crecimiento neto, mientras que el extremo – (subunidad α) o de crecimiento lento es menos dinámico y puede mostrar un acortamiento neto.[37–39]

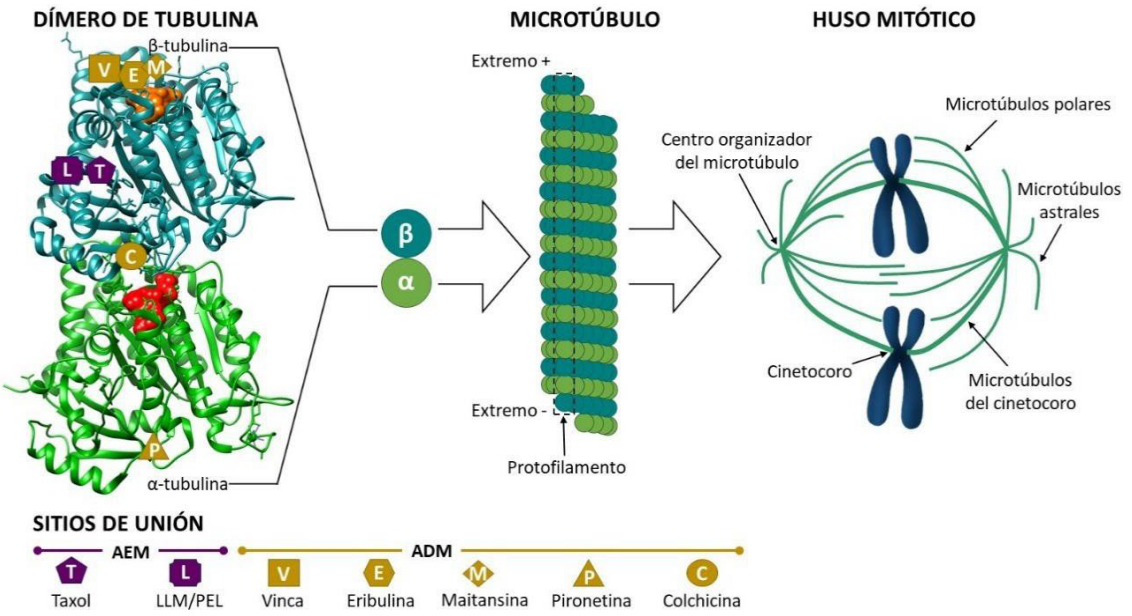

Figura 4. Estructuras del dímero de tubulina, del microtúbulo y del huso mitótico. Sitios de unión a tubulina indicados sobre el dímero de tubulina mediante formas de colores. En color **rojo**, sitio de unión para GTP; en **naranja** sitio de unión para GDP; en **morado**, sitios de unión de Agentes Estabilizadores de Microtúbulos (AEM); en **mostaza**, sitios de unión de Agentes Desestabilizadores de Microtúbulos (ADM).

En el heterodímero de tubulina, además de los dos sitios de unión para GTP, uno intercambiable (sitio E), y otro no intercambiable (sitio N), actualmente se encuentran descritos siete sitios de unión sobre los que actúan los agentes antimitóticos (Fig. 4). Estos sitios llevan el nombre del primer compuesto por el que se descubrieron y corresponden a los siguientes: el sitio del Taxol®, el de la laulimalida/pelorusida, el de los alcaloides de la *Vinca minor,* el de la eribulina, el de la maitansina, el de la pironetina y el de la colchicina (Fig. 5).[21,40] Según el sitio de unión y su efecto sobre la dinámica de los microtúbulos, los LUT se dividen en dos grandes grupos:

- Agentes Estabilizadores de Microtúbulos (AEM): Se unen al microtúbulo estabilizándolo y por lo tanto inhibiendo su despolimerización, lo que impide a las células completar el ciclo mitótico de manera adecuada. La acción estabilizadora ocurre al reforzar los contactos laterales entre los protofilamentos adyacentes.[41,42] Los AEM ejercen su acción por unión a dos de los sitios presentes en el dímero de tubulina: el sitio del taxol®, situado en una hendidura hidrofóbica profunda en la β-tubulina frente a la superficie luminal de los microtúbulos; y el sitio de la laulimalida/pelorusida (LLM/PEL), situado en la superficie exterior de la β-tubulina.
- Agentes Desestabilizadores de Microtúbulos (ADM): Se unen al dímero de tubulina, preferentemente a los dímeros solubles, y actúan inhibiendo la polimerización de los microtúbulos y favoreciendo su despolimerización. La acción desestabilizadora ocurre al bloquear los contactos longitudinales de los protofilamentos. Los ADM ejercen su acción por unión a cinco de los sitios presentes en el dímero de tubulina: el sitio de los alcaloides de la *Vinca minor*, situado en la interfaz interdímero, compartiendo residuos de ambas subunidades; el de la eribulina, se encuentra en la interfaz interdímero, en una región cercana al sitio de la vinca; el de la maitansina, localizado también cerca del sitio de la vinca en la β-tubulina; el de la pironetina, en un bolsillo de la subunidad α, cerca de la interfaz interdímero; y el dominio de la colchicina, situado en una región hidrofóbica en la interfaz intradímero entre las subunidades α y β.[43]

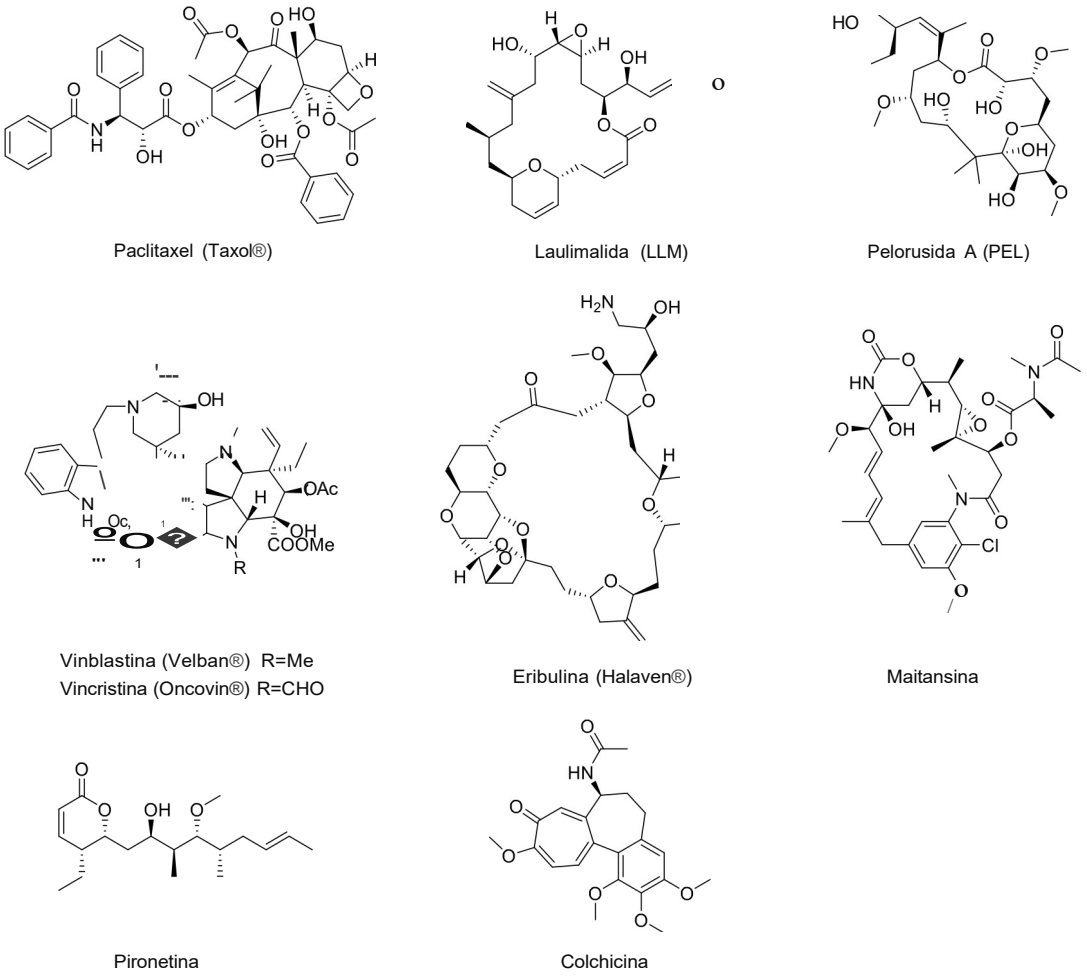

Figura 5. Estructura de los ligandos que dan nombre a los sitios de unión a tubulina descritos.

2.1. El dominio de la colchicina

Los agentes antimitóticos que se presentan en este trabajo de Tesis Doctoral están diseñados para ejercer su acción como LUT a través de su unión al dominio de la colchicina. A pesar de que los únicos LUT aprobados actualmente por la FDA en el tratamiento de tumores sólidos y enfermedades hematológicas corresponden a ligandos de unión al sitio del Taxol® y al de los alcaloides de la *Vinca minor*,[44] en los últimos años, los agentes antimitóticos que actúan por unión al dominio de la colchicina han despertado un gran interés, llegando a alcanzar en algunos casos los ensayos clínicos o incluso su aprobación como medicamentos huérfanos por la Agencia Europea del Medicamento (EMA).[45–48] Algunos de los beneficios del dominio de la colchicina frente al resto de sitios de unión del dímero de tubulina, y que justifican su elección como diana terapéutica en este trabajo de Tesis Doctoral, se describen a continuación.

Los ligandos del dominio de colchicina son moléculas estructuralmente sencillas y de pequeño tamaño, lo que las hace sintéticamente accesibles. Además, su pequeña estructura les permite evadir resistencias mediadas por proteínas transportadoras de membrana (MDR), ya que dichas bombas exportan preferentemente moléculas grandes e hidrófobas.[49] Por otra parte, la principal ventaja que presenta el dominio de la colchicina es su doble mecanismo de acción terapéutica al producir además un efecto sobre la neovasculatura tumoral.[50] Los ligandos que interactúan con este dominio son generalmente denominados agentes disruptores de la vasculatura, del inglés *Vascular Disrupting Agents* (VDAs), puesto que *in vivo*, provocan un colapso rápido de la vasculatura asociada al tumor, lo que lleva al bloqueo del flujo sanguíneo al núcleo del tumor y culmina con su muerte por necrosis.[45,51] Este segundo mecanismo de acción está asociado a interferencias con la vía Rho/ROCK. La alteración en la dinámica de los microtúbulos lleva a la activación de la GTPasa Rho, la cual desencadena una cascada de fosforilación que culmina con el colapso de la vasculatura, perturbando la correcta adhesión, quimiotaxis y migración de las células endoteliales requeridas para la construcción de nuevos vasos sanguíneos.[52–54] Cabe destacar que la dosis a la que los ligandos de unión a colchicina ejercen la acción como VDAs es mucho menor que la requerida para el efecto antimitótico.[55] En muchas ocasiones, se propone su uso en combinación con otros agentes quimioterapéuticos, lo que permite la disminución de la dosis de ambos fármacos y por lo tanto minimiza la toxicidad y los efectos adversos de la quimioterapia convencional.[46,51,56]

2.1.1. Estructura del dominio de la colchicina

El dominio de colchicina es una región hidrofóbica situada en la interfaz intradímero entre las subunidades α y β, con la mayor parte del hueco ocupando la subunidad β y quedando ocupada solamente una pequeña región poco profunda de la subunidad α. La unión de los ligandos a este hueco intradímero obstaculiza la transición del dímero de la conformación curva a recta, necesaria para su incorporación estable al microtúbulo y por lo tanto para su polimerización.[57] Este dominio generalmente se divide en 3 zonas consecutivas: zonas 1, 2 y 3 (Fig. 6).

- La zona 1 se encuentra localizada en la interfaz intradímero, en contacto con la subunidad α, pero ocupando mayoritariamente la región de la subunidad β. Es una zona hidrofóbica, pero con posibilidad de formar enlaces de hidrógeno con los ligandos. En esta zona se acomoda el anillo de tropolona de la colchicina, generalmente conocido como anillo B, estableciendo enlaces de Van der Waals con los aminoácidos S178α y V181α. Además, el grupo carbonilo actúa como aceptor de enlaces de hidrógeno con el residuo V181α.

- La zona 2 tiene su localización en la subunidad β. Corresponde a una región muy hidrofóbica con una pequeña zona polar dada por el aminoácido C241β. En esta región se ubica el anillo de trimetoxifenilo de la colchicina, conocido como anillo A, capaz de establecer enlaces de Van der Waals con los aminoácidos L242β, A250β, L255β, A316β, N350β, K352β y L378β. Cabe destacar además la interacción establecida entre el metoxilo central y el grupo tiol del residuo C241β. Las zonas 1 y 2 se encuentran interconectadas por una región del dímero generalmente ocupada por un espaciador: el puente, responsable de mantener una disposición *cisoide* y no coplanar entre los anillos A y B.
- La zona 3 es una región menos hidrofóbica profundamente enterrada en la subunidad β que incluye los residuos N167β, E200β y Y202β, entre otros. Anillos A voluminosos, como el trimetoxifenilo de la colchicina, disponen la cadena lateral del aminoácido de la zona 2 L255β (situado en la frontera entre las zonas 2-3) de tal forma que se bloquea el acceso a la zona 3, quedando esta sin ocupar.[57]

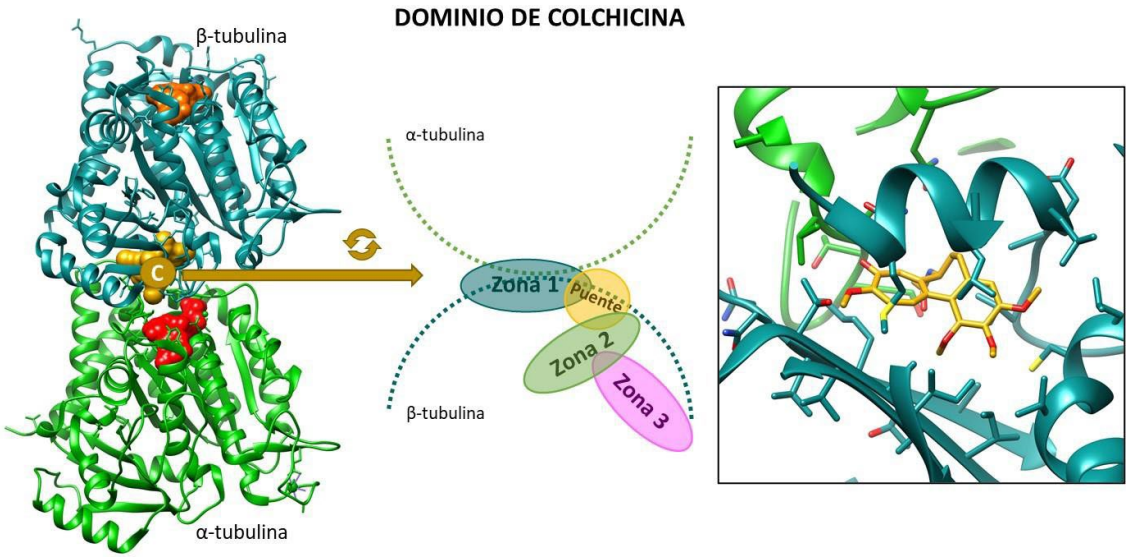

Figura 6. Izqda.: Estructura esquemática del sitio de colchicina en tubulina con las diferentes zonas de unión indicadas. Dcha.: Imagen de rayos X del complejo tubulina-colchicina (PDB ID: 4O2B). La α-tubulina se encuentra representada en color **verde**, la β -tubulina en color **azul** y el ligando en color **amarillo**.

2.1.2. Ligandos del dominio de la colchicina

A pesar de su elevada potencia citotóxica, la colchicina no se utiliza como fármaco antitumoral en clínica debido a su estrecho margen terapéutico y a su alta toxicidad, caracterizada por efectos adversos tales como neutropenia, anemia, malestar gastrointestinal y daño en la médula ósea.[58,59] Por lo tanto, a lo largo de los años se han invertido y se siguen invirtiendo grandes esfuerzos en el descubrimiento de nuevos ligandos del sitio de la colchicina con perfiles terapéuticos mejorados. Según las zonas con las que interactúan basándonos en las estructuras de rayos X de complejos tubulina-ligando disponibles en la base de datos *Protein Data Bank* (PDB), los ligandos del dominio de la colchicina se han dividido en (Fig. 7):

- Ligandos de zonas 1-2. Corresponden a la mayoría de los ligandos descritos y están representados por la colchicina y la combretastatina A-4 (CA-4), un producto natural originariamente aislado de la corteza del *Combretum caffrum* con elevada potencia citotóxica pero baja solubilidad acuosa.[60] Los ligandos clásicos que se unen a estas dos zonas están formados por dos anillos aromáticos (A y B) no coplanares, conectados entre sí por un puente y cumplen unos requerimientos estructurales que se revisan en profundidad en el apartado de diseño de este trabajo. Estructuralmente, pueden ser clasificados según la naturaleza del puente que conecta ambos anillos, habiéndose descrito multitud de puentes con diferentes longitudes y geometrías. Si nos basamos en el número de átomos que separan ambos anillos aromáticos podemos encontrarnos con: ligandos con puentes de 0 átomos como la colchicina; ligandos con puentes de 1 átomo como isocombretastatinas (1,1-diariletenos),[61,62] fenstatinas (diarilcetonas)[63,64] o diarilaminas[65,66]; ligandos con puentes de 2 átomos como combretastatinas (1,2-diariletenos)[67], sulfonamidas[68] o β-lactamas[69,70]; con puentes de 3 átomos como chalconas[71] u oxadiazolinas[72]; de 4 átomos como derivados de azol-carbonilo[73]; y ligandos con puentes formando parte de sistemas heterocíclicos que generalmente oscilan entre 2 y 4 átomos.[65,74] De todos ellos, el puente de sulfonamida – seleccionado en este trabajo – representa una alternativa ampliamente validada y exitosa,[68] con múltiples ventajas que estudiaremos en profundidad en el apartado 3 de la presente introducción. Dentro de los ligandos de unión a zonas 1-2 con estructura de sulfonamida cabe destacar el compuesto T138067, una sulfonamida sintética con un anillo de benceno pentafluorado (anillo A) cuya unión con la proteína ocurre de manera covalente.[75,76] Los ligandos covalentes han resurgido recientemente como una alternativa en la quimioterapia contra el cáncer, ya que evitarían las resistencias mediadas por las proteínas transportadoras de membrana, responsables de la mayoría de los fracasos terapéuticos de los tratamientos antitumorales.[77]
- Ligandos de zonas 2-3. Estructuralmente muy diferentes a los anteriores, ya que a pesar de compartir la unión a la región de la zona 2, éstos interactúan con la proteína de una manera sustancialmente diferente, acomodando en el hueco el fragmento correspondiente al anillo A de una manera distinta, permitiendo así el acceso a la zona 3. El primer ligando descrito por ocupar estas zonas fue TN16,[76] seguido de muchos otros con disposiciones similares y estructuras variadas, tales como MI-181[78] o el antiparasitario nocodazol,[79] entre otros.
- Ligandos de zonas 1-2-3. Actualmente, existen solo tres estructuras de rayos X de complejos tubulina-ligando que se unan simultáneamente a las tres zonas: ABT-751,[76] Lexibulina[79] y MT189.[80] Todos ellos están formados por tres anillos aromáticos conectados por diferentes espaciadores, destacando la sulfonamida sintética ABT-751[81], cuyo anillo de piridilendiamina (anillo A) permite realojar la cadena lateral del aminoácido fronterizo de la zona 2 (L255β) y por lo tanto abrir paso hacia la zona 3 (anillo C).

Figura 7. Izqda.: Ligandos de unión a zonas 1-2, 2-3 y 1-2-3 del dominio de la colchicina con las fracciones de la molécula que se unen a cada zona indicadas mediante formas coloreadas. En color **azul** fracción correspondiente a la zona 1, en **amarillo** zona del puente, en **verde** zona 2 y en **rosa** zona 3. Dcha.: Imágenes de rayos X de los complejos tubulina-combretastatina A-4 (PDB ID: 5LYJ), tubulina-nocodazol (PDB ID: 5CA1) y tubulina-ABT-751 (PDB ID: 3HKC). La α-tubulina se encuentra representada en color **verde**, la β -tubulina en **azul** y los ligandos en **amarillo**.

Son muchos los ligandos del dominio de la colchicina que han alcanzado los ensayos clínicos como agentes antitumorales o antiparasitarios. La CA-4,[67] debido a su escasa solubilidad acuosa, ha sido formulada como profármacos, dando lugar al derivado de serina de la aminocombretastatina AVE-8062 (Ombrabulina),[82] con buenos resultados en combinación con docetaxel en tumores sólidos avanzados[83] y actualmente en fase III; y al fosfato de combretastatina Fosbretabulina,[84] en fase II/III en combinación con otros antitumorales[85] o con radioterapia. Cabe destacar que la Fosbretabulina trometamol fue aprobada por la EMA como medicamento huérfano, por su acción como agente disruptor de la vasculatura tumoral, en el tratamiento del cáncer de ovario (EU/3/13/1154) en el año 2013[48] y en el tratamiento de los tumores neuroendocrinos gastroenteropancreáticos (EU/3/16/1633) en el año 2016.[86] Los benzimidazoles derivados del nocodazol, como el albendazol o el triclabendazol han superado con éxito los ensayos clínicos, estando aprobado su uso como agentes antihelmínticos.[87] También las sulfonamidas ABT-751 y T138067 han alcanzado en múltiples ocasiones los ensayos clínicos para su uso como antitumorales, ya sean solos o en combinación.[68] No obstante, las propiedades farmacocinéticas desfavorables de los ligandos del dominio de la colchicina causadas por una baja solubilidad acuosa, la supervivencia de las células del borde del tumor y el desarrollo de resistencias,[88] así como la inestabilidad de las combretastatinas[60] o la insuficiente potencia de ABT-751,[68] están impidiendo su desarrollo completo.[89] Por lo tanto, existe una gran demanda de nuevos ligandos del sitio de la colchicina con una mayor potencia citotóxica y unas propiedades farmacocinéticas más favorables.

2.1.3. El dominio de la colchicina en mamíferos vs. Leishmania spp.

En los tratamientos antiparasitarios la selectividad es de gran importancia, ya que éstos deben ser inocuos para el mamífero hospedador del parásito. LUT con aplicación antitumoral en humanos como el Taxol® o los alcaloides de la vinca han demostrado ser potentes inhibidores de la tubulina de parásitos,[90–92] sugiriendo una gran similitud entre ambas proteínas en sus sitios de unión, lo que los inhabilita para el desarrollo de agentes antiparasitarios. Sin embargo, la colchicina, ligando arquetípico del domino en mamíferos, no presenta ningún efecto sobre la viabilidad de parásitos como *Leishmania* spp.,[93] lo que hace pensar que puedan existir diferencias suficientes entre ambas proteínas para el diseño selectivo de ligandos con aplicaciones antitumorales o antiparasitarias. Esta toxicidad selectiva ha permitido el tratamiento de parasitosis por helmintos y hongos con benzimidazoles antimitóticos por unión al dominio de la colchicina tales como el triclabendazol o el albendazol.[87]

A pesar de que la tubulina es una proteína altamente conservada, los microtúbulos de tripanosomátidos presentan hasta once aminoácidos diferentes en el sitio de unión de la colchicina, con respecto a los mamíferos.[94] Estas diferencias se identificaron mediante el alineamiento de las secuencias de mamíferos y *Leishmania* y su posterior comparación, lo que permitió identificar los residuos mutados (Fig. 8). En la zona 1 del dominio existe una gran conservación en la secuencia entre los parásitos de *Leishmania* y los humanos, con la única excepción del reemplazo A316βS. Esta modificación hace que el hueco sea más pequeño y polar debido a la presencia del grupo hidroxilo de la cadena lateral de serina. En la zona del puente, la presencia de un grupo hidroxilo en la tubulina de *Leishmania* respecto a la secuencia de mamífero por la sustitución A250βS, favorece la introducción de puentes polares como las sulfonamidas. En la Zona 2 las secuencias de tubulina de *Leishmania* muestran dos sustituciones de alaninas por serinas (A316βS y A354βS), una cisteína por treonina (C241βT) y una valina por leucina (V318βL). Estos cambios hacen el hueco menor y más polar debido a la presencia de tres grupos hidroxilo adicionales. Finalmente, en la zona 3 se producen varias sustituciones que

modifican la geometría y el tamaño del hueco, haciéndolo más pequeño y menos polar (N167βI y Y202βM); las cuales podrían permitir el acceso de un tercer anillo aromático. Las diferencias aquí descritas permiten diseñar nuevos agentes antimitóticos con modificaciones en puntos estratégicos que dirijan su efecto hacia la proteína de mamíferos (ligandos más grandes y menos polares) o de parásitos (ligandos más pequeños y polares).

DOMINIO DE COLCHICINA *LEISHMANIA* SPP.

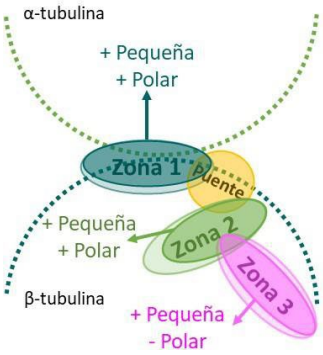

SUBUNIDAD	POSICIÓN	AMINOÁCIDO	
		Mamíferos	Parásitos
β	316	Alanina	Serina
β	250	Alanina	Serina
β	241	Cisteína	Treonina
β	316	Alanina	Serina
β	318	Valina	Leucina
β	354	Alanina	Serina
β	167	Asparagina	Isoleucina
β	202	Tirosina	Metionina

Figura 8. Principales modificaciones en la secuencia de aminoácidos del dominio de la colchicina de *Leishmania* spp. con respecto al de mamíferos y su efecto sobre las diferentes zonas de unión de los ligandos.

3. LAS SULFONAMIDAS COMO FÁRMACOS DE ÉXITO

Las sulfonamidas son las amidas de los ácidos sulfónicos, con una fórmula general $RSO_2NR_1R_2$. Dependiendo del grado de sustitución en el nitrógeno, se las conoce como sulfonamidas primarias (R_1 y R_2 iguales a H), secundarias (R_1 o R_2 iguales a H) o terciarias (R_1 y R_2 diferentes de H).

Las sulfonamidas son compuestos estables y accesibles sintéticamente, con una amplia y exitosa trayectoria en la clínica.[95] Son uno de los grupos funcionales más frecuentes entre los fármacos,[96] habiéndose descrito una gran diversidad de aplicaciones terapéuticas, como: antibacterianas, hipoglucémicas, diuréticas, antiinflamatorias, anticonvulsivas, antitiroideas, herbicidas, antivirales, antitumorales y antiparasitarias.[95] En algunos casos, los efectos antitumorales y antiparasitarios se deben a la inhibición de la dinámica de los microtúbulos por unión al dominio de la colchicina en tubulina.[25,68]

Las sulfonamidas presentan una serie de propiedades que justifican su frecuente elección en el diseño de nuevos fármacos, como son la accesibilidad sintética, alta estabilidad, la capacidad de establecer enlaces de hidrógeno, la polaridad y un adecuado equilibrio entre hidrofobicidad e hidrofilia.[97,98] Las sulfonamidas primarias y secundarias son dadoras de enlaces de hidrógeno y ácidos débiles cuyos valores de pK_a pueden modificarse variando los sustituyentes. Esta acidez determina el grado de ionización que presentan en disolución, que a su vez condiciona la unión a la diana (en algunos casos, la especie activa es la base conjugada, mientras que en otros es la forma neutra), la solubilidad, la permeabilidad y la distribución.[98] Además, los átomos de oxígeno de la sulfonamida son aceptores débiles de enlace de hidrógeno.[97] Su gran versatilidad y la posibilidad de modular sus propiedades las convierten en esqueletos privilegiados en la búsqueda de nuevos fármacos.

Tras el descubrimiento de la actividad inhibidora de la polimerización de tubulina de las bencenosulfonamidas antitumorales ABT-751, T138067 y su profármaco T900607 se han descrito un gran número de compuestos relacionados.[99] Otras sulfonamidas como el herbicida orizalina actúan sobre los microtúbulos de protozoos parásitos y de vida libre sin afectar a la tubulina de hongos o vertebrados.[90] A continuación, se describe la Relación Estructura-Actividad encontrada para las sulfonamidas antimitóticas.[68]

3.1. Relación Estructura-Actividad de las sulfonamidas antimitóticas

Teniendo en cuenta la división del dominio de la colchicina en tres zonas y los ligandos de referencia que a ellas se unen, en el grupo de trabajo hemos realizado una revisión de las sulfonamidas antimitóticas (Anexo 1) en la que han sido clasificadas según su similitud estructural a CA-4 (zonas 1-2) o a ABT-751 (zonas 1-2-3).[68] A continuación, se resumen las modificaciones estructurales más significativas para ambos grupos de sulfonamidas, con especial énfasis en las primeras por su analogía con los ligandos que se describen en este trabajo.

3.1.1. Sulfonamidas antimitóticas tipo CA-4

Las combretastatinas A son *cis* estilbenos, por lo que las sulfonamidas antimitóticas análogas de CA-4 incluidas en este grupo son *N*-fenilbencenosulfonamidas, en las que la sulfonamida sustituye al puente olefínico de las combretastatinas. En líneas generales, esta sustitución reduce la potencia antiproliferativa, aunque se mantienen en muchos casos potencias submicromolares, pero se mejoran las solubilidades acuosas. Las modificaciones llevadas a cabo en este tipo de compuestos se han realizado en los sustituyentes de los dos anillos aromáticos (A y B) y el puente de sulfonamida, incluyendo la dirección del mismo, la sustitución en el átomo de nitrógeno y la formación de ciclos adicionales (Fig. 9).

- Modificaciones en el puente: En la mayoría de los casos, la dirección de la sulfonamida no tiene efectos relevantes sobre la actividad biológica. De entre las posibles sustituciones en el nitrógeno (R_N) la metilación conduce a un aumento significativo de la potencia cuando se compara con sus análogos sin sustituir, pero a costa de una disminución en la solubilidad. Una estrategia llevada a cabo de forma exitosa ha sido la fijación de la conformación *cisoide* mediante la ciclación intramolecular del puente con la posición *orto* del anillo aromático A, como es el caso del compuesto CID20959075.

Los anillos aromáticos A (Ar_A) y B (Ar_B) han sido tanto modificados en sus patrones de sustitución y sus sustituyentes como reemplazados por policiclos aromáticos, en la mayoría de los casos heterociclos nitrogenados benzofusionados tales como indoles, benzimidazoles, indazoles, carbazoles o carbolinas. La sustitución por policiclos se da de forma individual, afectando solo a uno de los dos anillos, o de forma simultánea en ambos anillos, en este último caso, únicamente combinaciones indol-naftaleno mantienen la actividad antiproliferativa. A continuación, se revisan las modificaciones estructurales más exitosas sobre cada uno de los anillos aromáticos.

- Modificaciones en Ar_B: La mayoría de las modificaciones llevadas a cabo sobre este anillo se centran en las posiciones 3 y 4. El reemplazo del grupo hidroxilo de la posición 3 de la CA-4 por un grupo amino o su eliminación mantiene la potencia citotóxica. La sustitución del metoxilo de la posición 4 por grupos metilo, amino o acetamido disminuye la potencia antiproliferativa, sin embargo, su sustitución por grupos extendidos como 2-oxoimidazolidin-1-ilo da lugar a compuestos altamente citotóxicos (PIB-SAs). Sistemas bicíclicos de *N*-metil-5-indolilo reemplazando el Ar_B combinados con Ar_A de trimetoxifenilo (A-293620) originan derivados muy potentes. Las sulfonamidas con restos de *N*-alquil-carbazol-3-ilo presentan valores de citotoxicidad en el rango nanomolar que se mantienen incluso cuando el Ar_A convencional de trimetoxifenilo se sustituye por un anillo de 4-cloro-2,5-dimetoxifenilo o 2,6-dimetoxipirid-3-ilo (IG-105). Grupos hidroxilo o amino sobre las posiciones 6 o 7 del anillo de carbazol mejoran tanto

la solubilidad acuosa como la citotoxicidad. Carbolinas, benzotiazoles, 2,3-dihidroindenos y antracenos disminuyen la potencia.

- Modificaciones en Ar_A: Tradicionalmente, el anillo de trimetoxifenilo ha sido considerado esencial para el mantenimiento de la actividad citotóxica tanto en derivados de combretastatinas como en sulfonamidas.[100,101] Sin embargo, en los últimos años se han descrito numerosas sulfonamidas en las que se ha reemplazado con éxito. La eliminación de los grupos metoxilo y su sustitución por grupos 2-acetamido o 2-etilureido conduce a compuestos con potencias similares, así como el derivado pentafluorado T138067. Anillos de 7-indolilo sustituidos en la posición 2 con un átomo de cloro (ER68378) o con un grupo hidroxilo llevan a compuestos activos. Los indazoles unidos a través de las posiciones 4 o 7 conducen a compuestos citotóxicos submicromolares, preferentemente sin sustituir en el nitrógeno del indazol y con un átomo de cloro en la posición 3.

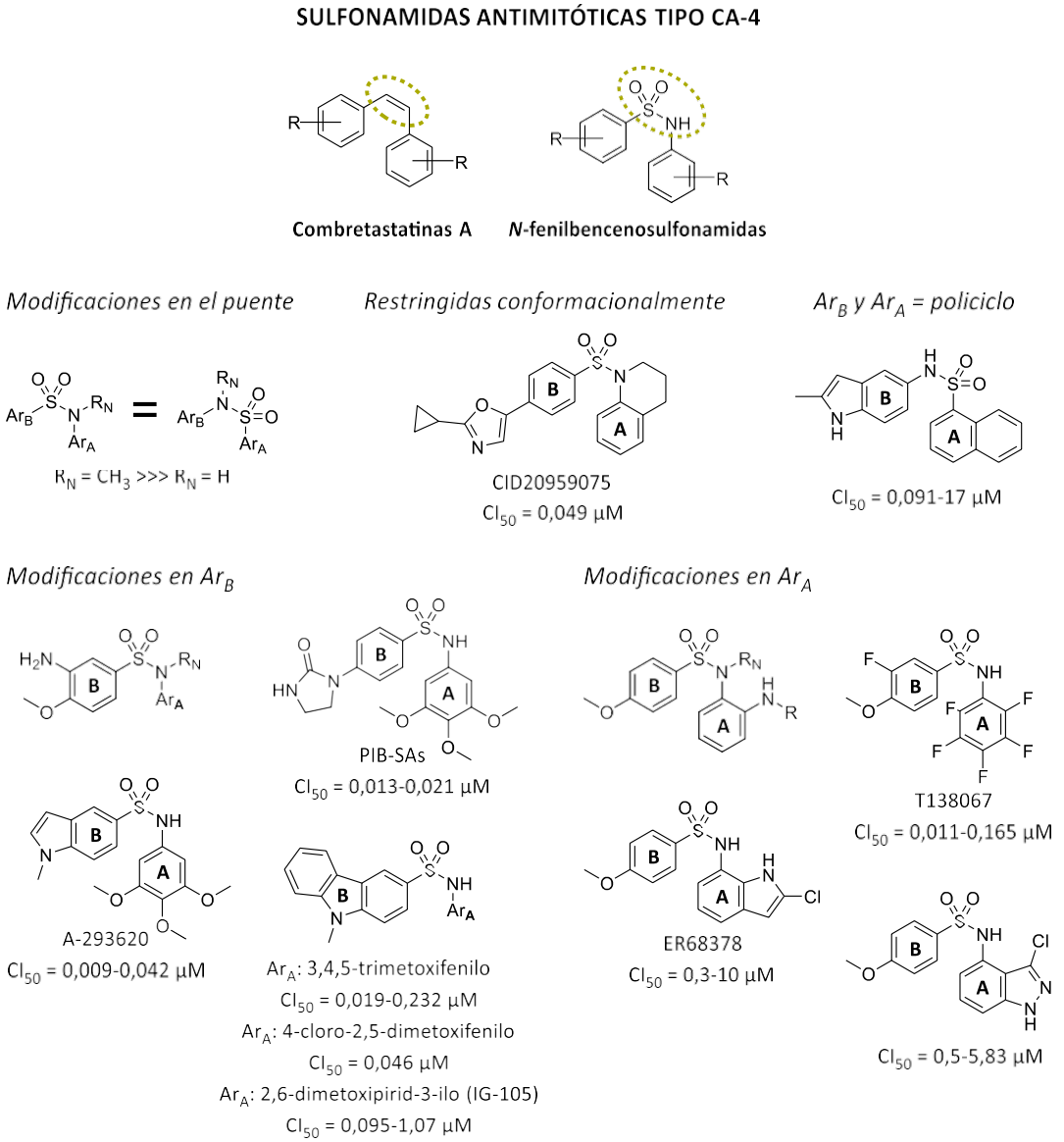

Figura 9. Sulfonamidas antimitóticas tipo CA-4 representativas de las modificaciones estructurales que mantienen o mejoran la potencia citotóxica. Ar_A: Anillo aromático A; Ar_B: Anillo aromático B.

3.1.2. Sulfonamidas antimitóticas tipo ABT-751

Las sulfonamidas análogas de ABT-751 se subdividen en dos grupos diferenciados (Fig. 10):

a) Sulfonamidas que mantienen la estructura clásica de ABT-751, caracterizada por la presencia de tres anillos aromáticos: B (Ar_B), A (Ar_A) y C (Ar_C); y dos puentes que los interconectan: Puente BA (SO_2N-R_N) y puente AC (Y). Las modificaciones llevadas a cabo sobre el esqueleto principal tienen lugar en cinco partes diferentes de la molécula: sustituyentes de los anillos aromáticos B (R_B), A (R_A) y C (R_C), sustituyentes sobre el nitrógeno de la sulfonamida (R_N) y variaciones estructurales del puente AC (Y). La mayoría de estas modificaciones se realizan generalmente de manera simultánea.

- R_B: La mejor actividad antiproliferativa se observa para el grupo metoxilo original, ya que su sustitución por grupos alquilo, alcoxi o amino de pequeño tamaño no la mejoran.
- R_A: Modificaciones en el Ar_A incluyen cambios en la molécula de piridina, en el patrón de sustitución 2,3 o en la introducción de sustituyentes adicionales. Todos estos cambios dan lugar a disminuciones en la potencia.
- R_C: Las variaciones del Ar_C incluyen tanto la introducción de sustituyentes adicionales, como su reemplazo por heterociclos aromáticos. Sustituyentes etoxilo en la posición *para* o átomos de flúor en cualquier posición mantienen la potencia de los compuestos. La sustitución de la posición *para* por un grupo nitrilo en derivados que carecen de puente AC conduce a un aumento de hasta 10 veces en la potencia. El reemplazo del Ar_C por heterociclos tales como 2-piridina o 2-pirimidina resulta en un aumento de unas 8 veces de media en la potencia.
- R_N: La orientación de la sulfonamida no conlleva cambios significativos en la actividad antiproliferativa, sin embargo, la sustitución del nitrógeno de la sulfonamida resulta en un incremento en la potencia de hasta 4 veces.
- Y: El puente de amina originariamente presente en ABT-751 conectando los anillos A-C se reemplaza con éxito por otros puentes tales como amidas u olefinas o incluso se elimina, obteniéndose los mejores resultados con los puentes tipo amida.

b) Sulfonamidas restringidas conformacionalmente mediante la ciclación de alguno de los puentes (BA o AC) sobre alguno de los anillos aromáticos (Ar_B, Ar_A o Ar_C), fijando así una geometría preferente. Se dividen en tres grupos estructurales:

- Sulfonamidas tricíclicas fusionadas: Se producen mediante la ciclación del puente AC sobre la posición 2 del Ar_B. Estos derivados solo son activos cuando el Ar_C se mueve al nitrógeno de la piridina del Ar_A tras tautomerización.
- *N*-bencenosulfonil(aza)indol(ina): Se dan por la formación de un ciclo entre el puente BA y el Ar_A. Sus potencias antiproliferativas son similares a las de ABT-751.
- *N*-indol-7-ilsulfonamidas: Derivados formados por el cierre del anillo entre el puente AC y el Ar_A, con potencias en el mejor de los casos similares a ABT-751.

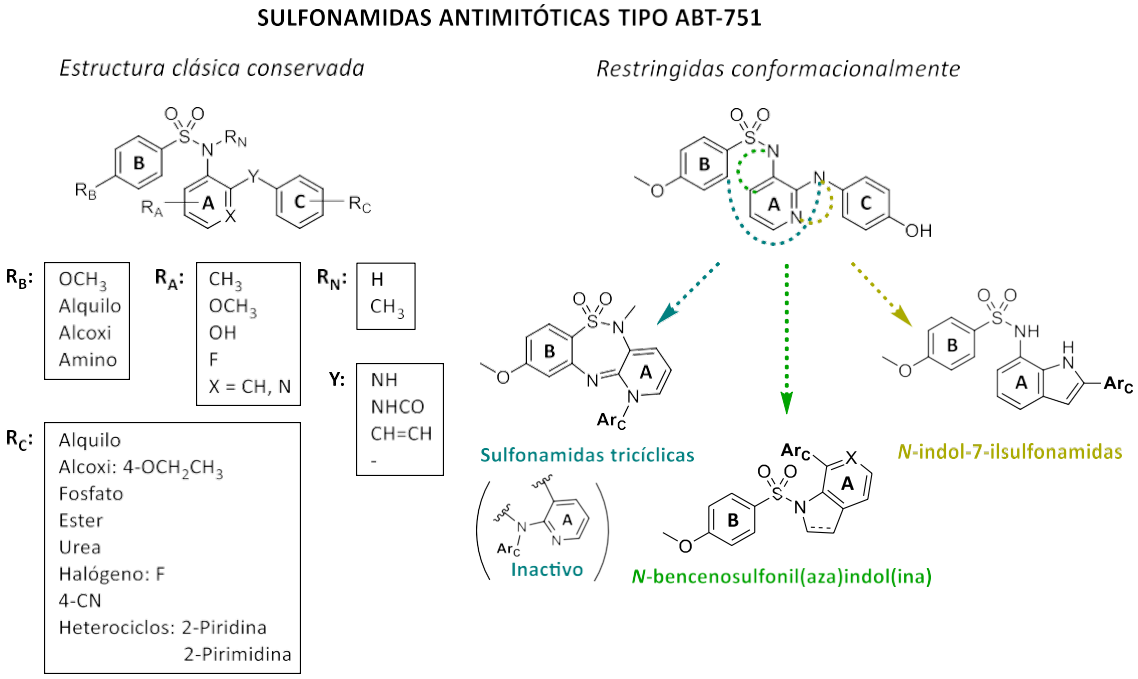

Figura 10. Estructura general de las sulfonamidas antimitóticas tipo ABT-751 descritas. Ar_C: Anillo aromático C.

4. APLICACIONES TERAPÉUTICAS: CÁNCER Y LEISHMANIASIS

El cáncer y la leishmaniasis son enfermedades responsables de un gran número de muertes tanto en países desarrollados como en desarrollo y tienen un enorme impacto en las sociedades que las sufren.[102] En un intento de reducir el impacto de estas enfermedades, la OMS ha propuesto estrategias basadas en el desarrollo de los métodos de prevención, el avance en la detección precoz y en el desarrollo de nuevos tratamientos y la combinación exhaustiva de los existentes que puedan mejorar la supervivencia y la calidad de vida. No obstante, nuevas terapias efectivas y selectivas son ampliamente demandadas por la sociedad actual.

Los nuevos agentes antimitóticos basados en sulfonamidas que se describen en este trabajo de Tesis Doctoral tienen por objetivo su posible aplicación selectiva en el tratamiento de tumores o de infecciones causadas por el parásito *Leishmania* spp., mediante la alteración de una diana común y esencial para las células eucariotas, la tubulina.

A continuación, se presenta una breve introducción sobre la epidemiología de ambas enfermedades, así como de los tratamientos actualmente utilizados en clínica y sus principales limitaciones, prestando mayor atención a aquellos que ejercen su mecanismo de acción por alterar la dinámica de los microtúbulos.

4.1. Cáncer

El cáncer es un conjunto heterogéneo de enfermedades en las que fallan los sistemas de regulación de la proliferación celular y la homeostasis, produciéndose una división incontrolada de células.[103,104] Estas células pueden invadir los tejidos circundantes y/o diseminarse a través del torrente sanguíneo o linfático, provocando lo que se conoce como metástasis, siendo ésta la principal causa de muerte por cáncer.[105]

La enfermedad del cáncer es la segunda causa de muerte en el mundo, representando alrededor de 10 millones de decesos en 2020. Se estima que casi una de cada seis defunciones a nivel mundial se debe a esta enfermedad. Además, el número total de casos está aumentando, de forma que la OMS prevé que la mortalidad por cáncer aumentará en un 45% entre 2007 y 2030.[106–108] Alrededor de un tercio de las muertes por cáncer se debe a los cinco principales factores de riesgo conductuales y dietéticos: índice de masa corporal elevado, ingesta reducida de frutas y verduras, falta de actividad física, consumo de tabaco y consumo de alcohol. Pese a los enormes esfuerzos de la sociedad y de la comunidad biomédica y a las inversiones económicas realizadas para el estudio y tratamiento del cáncer, los avances alcanzados son limitados debido a la complejidad y a la gran capacidad adaptativa de las poblaciones de células tumorales. Con las terapias actuales - cirugía, trasplante de médula, radioterapia y/o quimioterapia[109] - entre el 30 y el 40% de los pacientes que sufren cáncer acaban falleciendo por causa de la enfermedad, lo que pone de manifiesto la necesidad de tratamientos nuevos.[110]

4.1.1. Cánceres de mama, ovario y cérvix: tratamientos actuales y principales limitaciones

El cáncer de mama femenino y los tumores ginecológicos, englobados bajo el término de cánceres *Pan-Gyn*, son los cánceres con mayor incidencia y mortalidad en la población femenina.[111] Las líneas celulares utilizadas en este trabajo para el estudio de los agentes antimitóticos como posibles fármacos antitumorales corresponden principalmente a líneas tumorales humanas de cáncer de mama (MCF7), ovario (SKOV3) y cérvix (HeLa). Según

GLOBOCAN (*Global Cancer Observatory*), el cáncer de mama es el tipo de cáncer más frecuentemente diagnosticado a nivel mundial entre las mujeres (24%), y el segundo a nivel global (12%), representando el 15% de las muertes por cáncer entre las mujeres.[102] El cáncer de ovario, alcanza los índices de mortalidad más altos (63%), ya que debido a la ausencia de síntomas durante los estadios tempranos de la enfermedad, la mayoría de las pacientes (80% de los casos aproximadamente) son diagnosticadas en un estadio avanzado y generalmente con metástasis abdominal.[112] La alta mortalidad se atribuye no solo al estadio avanzado en el momento del diagnóstico, sino también a las limitadas opciones de tratamiento disponibles para las pacientes que desarrollan resistencia adquirida a la quimioterapia convencional. El cáncer de útero, tanto de cuello (cérvix) como de cuerpo de útero, es responsable de más del 11% de los nuevos casos de cáncer diagnosticados anualmente entre las mujeres y del 10% de las muertes.

Los tratamientos de primera línea para estos tres tipos de tumores incluyen agentes estabilizadores de los microtúbulos: taxanos secuenciados o en combinación con antraciclinas para cáncer de mama en estadio avanzado y metastático,[113–116] regímenes de combinación platinos-taxanos (preferentemente carboplatino-paclitaxel)[117] en el tratamiento del cáncer de ovario[112,118,119] y combinaciones cisplatino-paclitaxel en cánceres de útero metastásicos, recurrentes o persistentes.[120–123] Sin embargo, pese a ser ampliamente utilizados en clínica, los taxanos presentan tres limitaciones principales que en muchas ocasiones conducen al fracaso terapéutico: una baja solubilidad acuosa, un estrecho margen terapéutico debido a una alta toxicidad y el desarrollo de resistencias adquiridas a los tratamientos. Su baja solubilidad acuosa requiere su formulación en complejos sistemas solubilizantes asociados con la aparición en el paciente de reacciones de hipersensibilidad aguda caracterizadas por dificultad respiratoria, hipotensión, angioedema, urticaria generalizada y erupción.[124–126] Los efectos adversos intrínsecos asociados a la toxicidad de los taxanos y que limitan sus dosis incluyen neuropatías periféricas y mialgias/artralgias para paclitaxel y mielosupresión y neutropenia primaria para docetaxel.[127] No obstante, la mayor causa de fracaso terapéutico[128] descrita en los cánceres de mama, [129,130] ovario[131,132] y útero[121,133] ha sido la aparición de resistencias adquiridas a los tratamientos de primera línea. Los mecanismos de resistencia a taxanos son generalmente debidos a la sobreexpresión de proteínas transportadoras de membrana (glicoproteína-P, P-gp).[134] La alteración en la expresión de los isotipos de tubulina (especialmente sobreexpresión del isotipo βIII) o niveles aberrantes de tubulina, se han asociado también a mecanismos de resistencia.[33,88,135,136] Resistencias específicas a la quimioterapia basada en taxanos han sido descritas en el tratamiento del cáncer de mama, con aproximadamente un 30% de recurrencia,[137,138] en el de ovario, en el cual un 50% de las pacientes recaen con enfermedad quimiorresistente en los dos primeros años posteriores al diagnóstico[139,140] y en el cáncer de útero.[141] El reducido éxito en el tratamiento de estas enfermedades y las limitaciones de su principal quimioterapia, los taxanos, hacen necesaria la búsqueda de tratamientos alternativos.

4.2. Leishmaniasis

La leishmaniasis es una enfermedad tropical desatendida causada por un protozoo parásito del género *Leishmania* (Kinetoplastida: Trypanosomatidae), clasificada por la OMS como un problema de salud internacional, emergente y descontrolado.[142] Afecta a las poblaciones más pobres del planeta[142] y su incidencia es de 700.000-2.000.000 casos, causando entre 20.000 y 30.000 muertes anuales, siendo la novena enfermedad más lesiva a nivel mundial.[143] Es producida por más de 20 especies diferentes y se transmite a los mamíferos por la picadura de flebótomos infectados, siendo el *Phlebotomus perniciosus* (Diptera: Psychodidae) el vector más común en el centro y el este de la cuenca mediterránea.[106] Se presenta en tres formas principales: i) Leishmaniasis Visceral (VL) o Kala-azar, cursa con episodios irregulares de fiebre, pérdida de peso, hepatoesplenomegalia y anemia. Se estima que cada año se producen en el mundo entre 50.000 y 90.000 nuevos casos, la mayoría en el subcontinente indio, África oriental y Brasil.[107] *L. donovani* es la responsable de los casos de VL en el este de África e India, mientras que en Europa, el norte de África y América latina la especie causante es *L. infantum*, también conocida como *L. chagasi*.[144] ii) Leishmaniasis cutánea, es la manifestación más común, se caracteriza por la presencia de lesiones cutáneas ulcerosas. Se calcula que cada año se producen en el mundo entre 600.000 y 1 millón de casos nuevos. La mayor parte de ellos tienen lugar en las Américas, la cuenca del Mediterráneo, Oriente Medio y Asia Central. Las especies de *L. major* y *L. tropica* suelen producir lesiones cutáneas benignas y autolimitadas y son endémicas de Asia, mientras que en las Américas la infección está causada por más de 15 especies diferentes, siendo las más importantes: *L. mexicana*, *L. amazonensis*, *L. venezuelensis*, *L. braziliensis*, *L. panamensis*, *L. peruviana* y *L. guyanensis*.[145] iii) Leishmaniasis mucocutánea, cursa con la destrucción parcial o completa de las membranas mucosas de la nariz, la boca y la garganta. Más del 90% de los casos de leishmaniasis mucocutánea se producen en Brasil, el Estado Plurinacional de Bolivia, Etiopía y Perú. Las especies responsables de la leishmaniasis mucocutánea son *L. braziliensis* y *L. panamensis* y son endémicas de Latinoamérica.[107] Cabe destacar que hace aproximadamente una década se registró en España un importante brote en humanos provocado por la especie *L. infantum*, agente causante de la leishmaniasis visceral.[146–148]

4.2.1. Ciclo vital del parásito

El ciclo vital de *Leishmania* spp. es digenético y por lo tanto se desarrolla en dos etapas: promastigotes y amastigotes (Fig. 11). El promastigote es el estadio fusiforme extracelular con un flagelo surgiendo del cuerpo celular y el amastigote es la etapa inmóvil esférica con un flagelo no emergente. Cuando la mosca infectada se alimenta de un huésped mamífero (1), inyecta en la dermis promastigotes altamente infectivos (promastigotes metacíclicos). Éstos son internalizados por fagocitos (2) y se diferencian en amastigotes (3). Los amastigotes se multiplican en las células infectadas que los distribuyen a los distintos tejidos (4), originando las diferentes manifestaciones clínicas de la leishmaniasis. Con una nueva picadura, el insecto se infecta al ingerir sangre con macrófagos infectados (5 y 6). Los amastigotes se transforman en promastigotes procíclicos dentro de la membrana peritrófica y comienzan a diferenciarse a las formas metacíclicas. El proceso de desarrollo de los promastigotes se conoce como metaciclogénesis y tiene lugar dentro del intestino del vector, el flebótomo (7). Finalmente, los promastigotes migran hacia el intestino anterior medio para acabar en la probóscide (8), comenzando así de nuevo el ciclo biológico.[27,149]

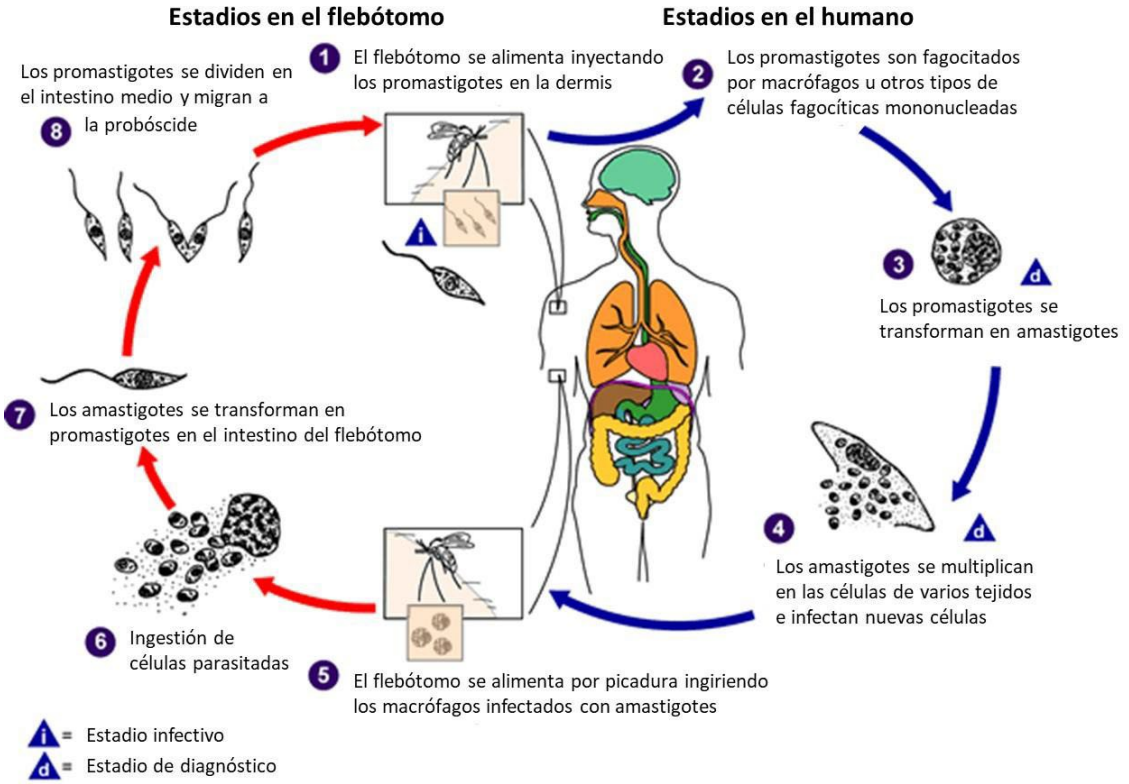

Figura 11. Ciclo vital de *Leishmania* spp.
Imagen adaptada de: https://www.cdc.gov/parasites/leishmaniasis/biology.html

4.2.2. Tratamientos actuales y principales limitaciones

Las estrategias terapéuticas de prevención de la leishmaniasis, entre ellas las vacunas potenciales, se encuentran en etapas preclínicas o clínicas de desarrollo temprano, por lo que el tratamiento de esta enfermedad se basa en la quimioterapia. El número de fármacos disponibles es limitado y presentan toxicidad, efectos adversos, resistencias, largas duraciones y altos costes económicos.[150–153] Además, su eficacia varía en función de la especie, los síntomas o la región geográfica de la parasitosis.[154] La farmacopea actual contra esta enfermedad incluye los tratamientos descritos a continuación con sus correspondientes limitaciones.

- Derivados de primera línea de antimonio (SbV). Los antimoniales pentavalentes pueden presentarse en dos formulaciones, el estibogluconato sódico (100 mg/100 mL) y el antimoniato de meglumina (85 mg/100 mL). Ambas formulaciones presentan mala absorción oral y se administran por vía intramuscular o intravenosa. El fármaco se acumula en los tejidos debido a la larga duración del tratamiento, causando efectos secundarios graves como arritmia cardíaca y pancreatitis aguda.[152,155] Además, durante la década de los noventa, se detectó una disminución de la eficacia en las zonas más endémicas de la India.[156] La aparición de resistencias a estos tratamientos ha sido atribuida a la sobreexpresión de proteínas transportadoras de membrana, especialmente a ABCI4, ABCG2, MRPA y MDR1,[157] y a mutaciones en la acuaporina de macrófagos AQP1.[158]
- Anfotericina B. La anfotericina B es una macrolida poliénica antibiótica con una potente actividad antifúngica y leishmanicida. Sin embargo, presenta múltiples limitaciones: efectos adversos como nefrotoxicidad, hipopotasemia, anafilaxia y fiebre, alto coste económico, baja solubilidad en agua a pH fisiológico, inestabilidad gástrica y mala

permeabilidad a través de las membranas.[159,160] Su formulación convencional se realiza a través de una suspensión micelar de desoxicolato sódico (Fungizone®) administrada por vía intravenosa, por lo que el paciente debe ser hospitalizado y monitorizado durante 4-5 semanas.[152,155,161] Posteriormente se han desarrollado formulaciones lipídicas de anfotericina B (AmBisome®) las cuales permiten dosis más bajas, reduciendo así los efectos secundarios, pero quedando su uso restringido debido al alto coste.[151] Además, aunque la administración de anfotericina-B liposomal está teniendo buenos resultados en el control de leishmaniasis visceral en el subcontinente indio, esta sigue siendo ineficaz o inadecuada en otras áreas geográficas.[162] Dado que la anfotericina se une a los esteroles de las membranas de células eucariotas e induce estrés oxidativo, los mecanismos de resistencia a este fármaco se han asociado a cambios en las enzimas esterol metiltransferasas que alteran la biosíntesis del ergosterol.[163]

- Miltefosina. La alquilfosfocolina oral miltefosina, fue aprobada como tratamiento de primera línea en el año 2002, reemplazando a los antimoniales pentavalentes en la mayoría de las regiones debido a las resistencias adquiridas.[152,164] Este fármaco mostró inicialmente una potente actividad leishmanicida, pero poco después, se observó un aumento gradual de las recaídas.[165,166] La pérdida de eficacia, probablemente debida a la aparición de resistencias ligadas a las proteínas transportadoras,[167–169] junto con los efectos secundarios del fármaco redujeron considerablemente su uso.
- Pentamidina. La pentamidina se utilizó como terapia de segunda línea en los casos de leishmaniasis visceral refractaria en la India, pero fue reemplazada por Fungizone® en la década de los noventa debido a su toxicidad y a la aparición de resistencias, probablemente debidas al transportador de membrana PRP1.[152,170]
- Paromomicina. Fármaco de uso muy reducido debido a sus efectos secundarios como la ototoxicidad.[155,171]

Diferentes tipos de fármacos, como los aminopirazoles, los nitroimidazoles, los oxaboroles, los inhibidores del proteasoma y los inhibidores de kinasas, se encuentran actualmente en desarrollo contra la leishmaniasis visceral, pero aun así, problemas como la baja biodisponibilidad oral, la falta de seguridad y eficacia y el alto coste siguen estando muy presentes.[172] Esto, junto con las limitaciones descritas a los tratamientos actuales, resaltan la necesidad de desarrollar nuevas terapias leishmanicidas que actúen sobre dianas terapéuticas alternativas, como la tubulina.

hipótesis y objetivos

"Lo que importa verdaderamente en la vida no son los objetivos que nos marcamos, sino los caminos que seguimos para lograrlo."

Peter Bamm

Tal y como queda reflejado en la introducción de este trabajo de Tesis Doctoral, la búsqueda de nuevas alternativas terapéuticas a los fármacos convencionales que se utilizan en el tratamiento del cáncer y la leishmaniasis es una necesidad urgente, siendo la tubulina una diana prometedora para su desarrollo. Por lo tanto, el **objetivo general** de este trabajo se centra en diseñar y sintetizar nuevos ligandos antimitóticos por unión al dominio de colchicina en tubulina con una estructura común de sulfonamida para finalmente evaluarlos como agentes antitumorales o leishmanicidas.

1. DISEÑAR

El diseño de los ligandos que se defienden en este trabajo de Tesis Doctoral está dirigido a las zonas 1-2 del dominio de la colchicina en tubulina.

1.1. Requerimientos estructurales ligandos de zonas 1-2

Las estructuras de rayos X de DAMA-colchicina (PDB ID: 1SA0) y podofilotoxina (PDB ID: 1SA1) en complejo con tubulina permitieron describir estructuralmente el dominio de la colchicina.[43] Partiendo de estas estructuras, se propuso un modelo de farmacóforo con los requerimientos estructurales mínimos para los ligandos que ocupan las zonas 1-2 del dominio de la colchicina de mamíferos (Fig. 12).[173] Estos requerimientos estructurales se resumen en 7 puntos: 3 aceptores de enlace de hidrógeno (**A1**, **A2** y **A3**), 1 dador de enlace de hidrógeno (**D1**), 2 centros hidrofóbicos (**H1** y **H2**) y 1 grupo plano (**P1**); dispuestos en 2 planos, correspondientes a los dos anillos aromáticos, conectados por puentes de longitud variable que permitan una disposición *cisoide* y no coplanar.

La colchicina, alcaloide tricíclico originariamente aislado del *Colchicum autumnale*[174] y la combretastatina A-4, olefina aislada del *Combretum caffrum*,[60] son ligandos representativos de las zonas 1-2. Las combretastatinas, por su pequeño tamaño, accesibilidad sintética y elevada potencia se han tomado como modelo para el diseño de los nuevos ligandos, ya que su estructura resume muchos de los requerimientos estructurales del sitio de la colchicina.

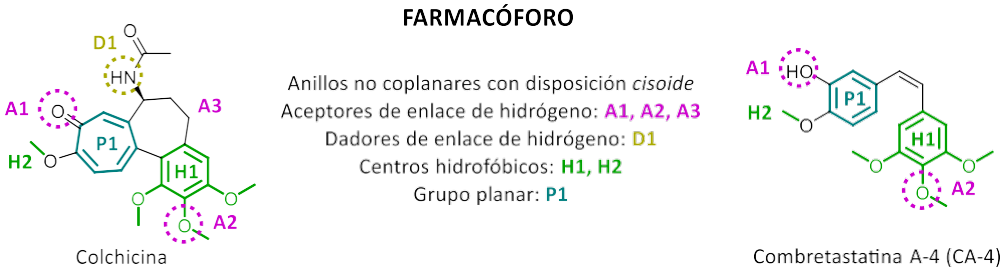

Figura 12. Modelo del farmacóforo propuesto por Nguyen *et al.* donde se definen los requerimientos estructurales para los ligandos que ocupan las zonas 1-2 del dominio de la colchicina de mamíferos.

1.2. Limitaciones de la Combretastatina A-4

Pese a su alta potencia citotóxica, la CA-4 presenta múltiples limitaciones (Fig. 13), destacando: i) su baja solubilidad acuosa, ii) la inestabilidad configuracional del doble enlace *cis* y iii) la aparición de resistencias. La baja solubilidad acuosa de la CA-4 reduce considerablemente su biodisponibilidad, por lo que se ha recurrido a su formulación como profármacos (fosbretabulina y ombrabulina[175176]). La disposición *cis* (*Z*) del doble enlace – considerada esencial para la actividad biológica[60] – puede isomerizarse al isómero *trans* (*E*) (más estable pero mucho menos activo[177]) tanto por el efecto del calor, la luz o el pH ácido, como por reacciones metabólicas *in vivo* durante su almacenamiento, administración y metabolismo. El anillo de trimetoxifenilo, crucial en la interacción con la proteína,[101,178–180] confiere una gran hidrofobicidad a la molécula y sufre reacciones metabólicas de *O*-desmetilación a fenoles inactivos, que facilitan la isomerización a la olefina *trans*.[177,181,182] La aparición de diversos mecanismos de resistencia implica el restablecimiento de la vasculatura tumoral, la adaptación de las células tumorales a las condiciones hipóxicas y la resistencia directa al fármaco.[88,183] El grupo hidroxilo del anillo aromático B posibilita la inactivación por reacciones de glucuronidación metabólica.[184] Además, se han descrito resistencias asociadas a procesos autofágicos.[183]

1.3. Diseño de los ligandos como híbridos de CA-4 y ABT-751

Los nuevos LUT se diseñan como híbridos del ligando clásico CA-4 y la sulfonamida ABT-751 (Fig. 13). La sustitución del puente olefínico de la CA-4 por un grupo funcional de sulfonamida pretende incrementar la solubilidad acuosa, mejorar las propiedades farmacocinéticas y evitar la isomerización adoptando una conformación *cisoide* preferente.[68] Por otra parte, se mantiene la estructura clásica para la unión a las zonas 1-2 de *N*-fenilbencenosulfonamida, que ha conducido a los compuestos más activos de la familia.[14]

Basándonos en los antecedentes descritos, en los requerimientos estructurales para la unión al dominio de la colchicina y en las diferencias entre las tubulinas de parásitos y mamíferos, se plantea el diseño de los ligandos mediante las siguientes modificaciones estructurales sobre el esqueleto principal de biarilsulfonamida: a) Modificación de los sustituyentes del anillo B (Ar_B) de CA-4 y eliminación del grupo hidroxilo metabólicamente inestable. b) Introducción de una amplia variedad de sustituyentes de diferente longitud y naturaleza sobre el nitrógeno de la sulfonamida (R_N) que permitan reforzar la interacción con la proteína y la disposición *cisoide* de ambos anillos aromáticos. c) Sustitución del anillo considerado esencial de trimetoxofenilo (Ar_A) por otros novedosos que contribuyan tanto al aumento en la potencia, como al aumento en la polaridad de las moléculas.

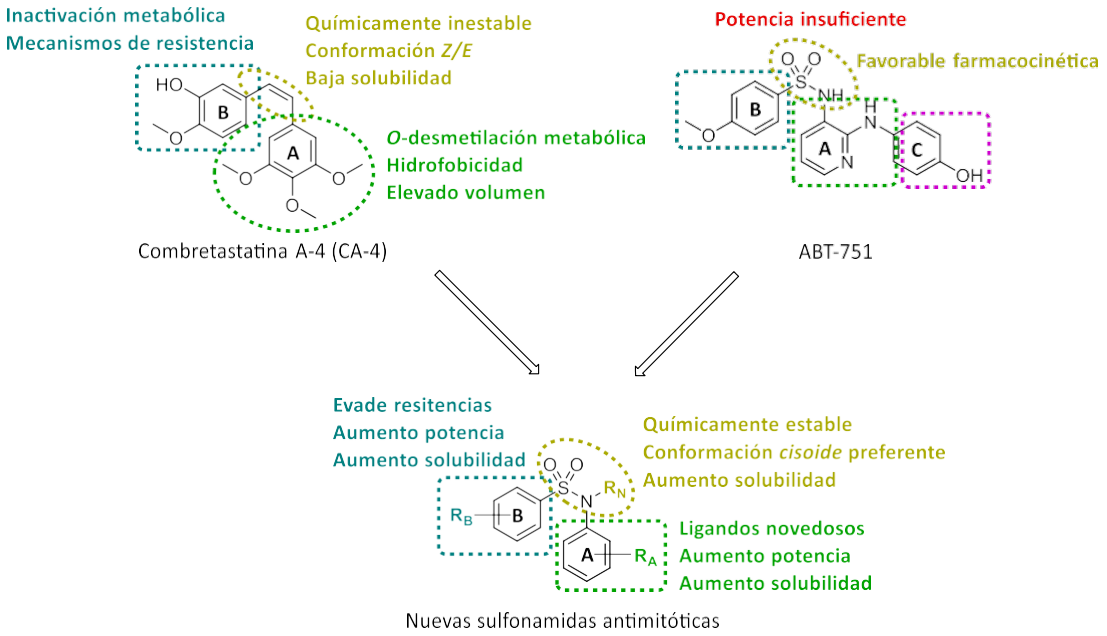

Figura 13. Diseño de las nuevas sulfonamidas antimitóticas como híbridos de CA-4 y ABT-751 y principales limitaciones estructurales de la CA-4.

1.3.1. Modificaciones en Ar_B

El Ar_B es uno de los fragmentos sobre el que han sido descritas un mayor número de modificaciones exitosas. En primer lugar, se plantea la eliminación del grupo hidroxilo de la CA-4, asociado con la aparición de resistencias y el metabolismo rápido de los fármacos, diseñando ligandos con un Ar_B de 4-metoxifenilo, idéntico al presente en ABT-751 (Fig. 14). Posteriormente, se plantea su sustitución por anillos de 4-dimetilamino- y 3-amino-4-metoxifenilo, descritos en la bibliografía como alternativas potentes al anillo convencional de 4-metoxifenilo.[74,185–187] Además, se propone la introducción de grupos amino primarios o secundarios que contribuyan tanto al aumento de la solubilidad acuosa así como a la interacción con la proteína, pudiendo suplir los enlaces de hidrógeno presentes entre el grupo hidroxilo de la CA-4 y los aminoácidos V181α y T179α de la zona 1 del dominio.[188] Con el fin de estudiar la Relación Estructura-Actividad (REA) en mayor profundidad, se plantea la derivatización de los grupos amino en las posiciones 3 y 4 con sustituyentes de diferente longitud y naturaleza, de forma que, teniendo en cuenta las diferencias entre la tubulina de mamíferos y la de *Leishmania* spp., puedan tener mayor afinidad por una u otra proteína.

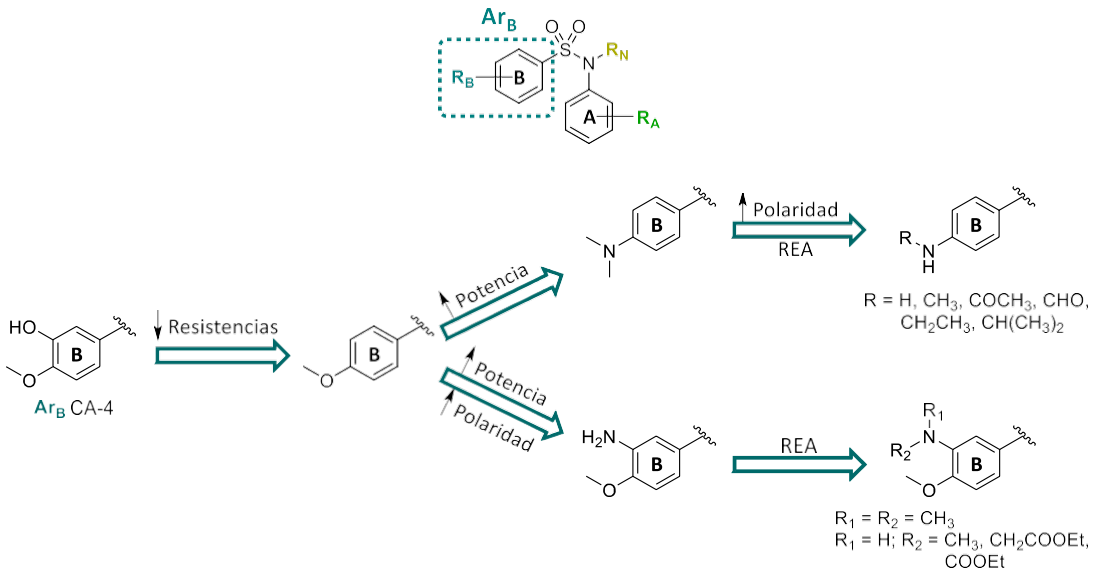

Figura 14. Modificaciones estructurales planteadas para el anillo aromático B (Ar_B) y su contribución a la estructura-actividad de la molécula.

1.3.2. Modificaciones sobre el nitrógeno de la sulfonamida (R_N)

El puente de sulfonamida elegido para el diseño de los nuevos ligandos puede ser extensamente modificado mediante la introducción de diversos sustituyentes que reemplacen el hidrógeno de la sulfonamida secundaria, produciéndose un elevado aumento en la potencia cuando se comparan con sus análogos sin sustituir.[68] Además de explorar la interfaz entre las zonas 1-2 y establecer nuevas interacciones con la proteína, esta modificación nos va a permitir introducir grupos solubilizadores que mejoren las propiedades farmacocinéticas y/o farmacodinámicas de las moléculas (Fig. 15). Si tenemos en cuenta la sustitución A250βS en la tubulina de *Leishmania* spp. respecto a la secuencia de mamíferos en la zona del puente, la cual reduce el espacio disponible, podremos plantear el diseño selectivo según su aplicación, al ser incompatible la introducción de sustituyentes voluminosos en el diseño de ligandos antiparasitarios. Por último, aunque las sulfonamidas adoptan preferentemente la disposición *cisoide* indispensable para el mantenimiento de la actividad, se propone su fijación mediante la ciclación intramolecular del nitrógeno de la sulfonamida con la posición *orto* del Ar_A.

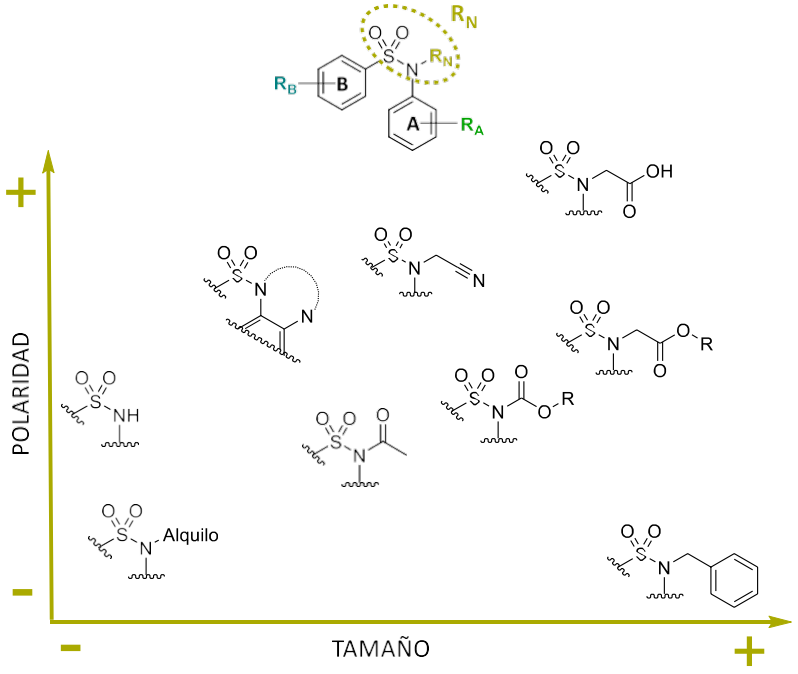

Figura 15. Modificaciones estructurales planteadas para el nitrógeno de la sulfonamida (R_N) organizadas según su aportación al tamaño y a la polaridad de las moléculas. Para la distribución aproximada de la polaridad se ha utilizado la predicción del área de superficie polar de ChemDraw®.

1.3.3. Modificaciones en Ar_A

El Ar_A de trimetoxifenilo ha sido considerado esencial para el mantenimiento de la actividad citotóxica debido a la importancia de su interacción con la cadena lateral de la C241β de la zona 2 del dominio de la colchicina.[57,100,101] Las modificaciones sobre el anillo de trimetoxifenilo son escasas, estando presente en la mayoría de los LUT activos.[58,100,189–195] Sin embargo, los problemas asociados a la alta lipofilia y labilidad metabólica del anillo de trimetoxifenilo hacen muy deseables estructuras alternativas que proporcionen altas potencias y propiedades farmacocinéticas más adecuadas. En los últimos años, se ha descrito su posible reemplazo manteniendo potencias razonables por heterociclos nitrogenados con o sin sustituir[61,65,196–201] o por diferentes anillos aromáticos en los que se ha modificado el patrón de sustitución de los metoxilos[187,202,203] o se han introducido derivados halogenados[75]. En la figura 16 se proponen una amplia variedad de Ar_A donde se pretende explorar la importancia de los grupos metoxilos en la interacción con la diana (modificando su número y posición), así como su posible sustitución por grupos más polares que permitan mejorar la solubilidad de las moléculas. Además, se proponen derivados de menor tamaño y/o mayor polaridad (ej.: 2,5- o 3,5-dimetoxifenilo y 3-carboxi-5-aminofenilo) que se ajusten mejor a los requerimientos estructurales del dominio de la colchicina de *Leishmania* spp., tratando de conferir a los ligandos más afinidad por la tubulina del parásito que por la del mamífero hospedador.

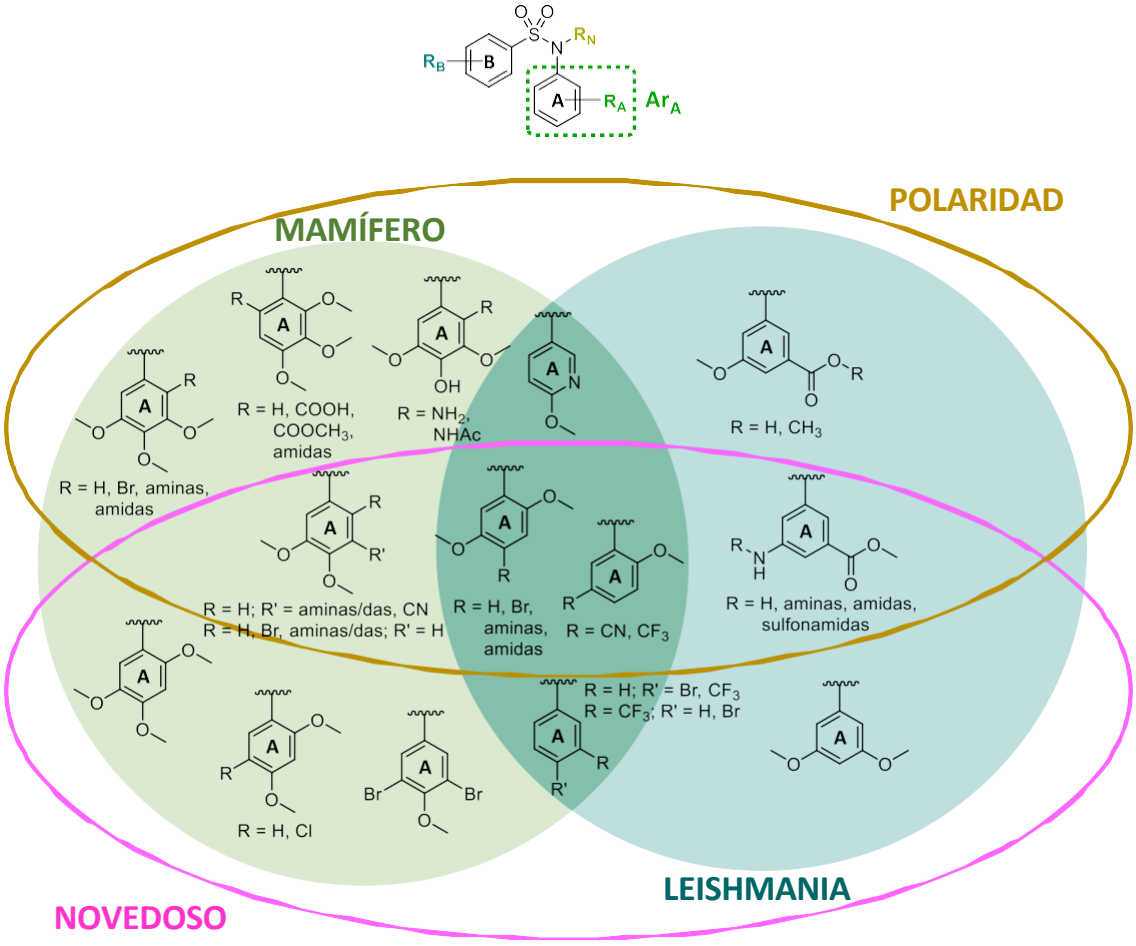

Figura 16. Modificaciones estructurales planteadas para el anillo aromático A (Ar_A). Los círculos **verde** y **azul** diferencian las modificaciones en función de su afinidad teórica a la tubulina de **mamíferos** y/o de ***Leishmania***, respectivamente, basado en las diferencias descritas en la estructura de ambas proteínas. El óvalo **amarillo** engloba las modificaciones que contribuyen al aumento de la **polaridad** de las moléculas. Dentro del óvalo **rosa** se incluyen las modificaciones propuestas más **novedosas** según los LUT descritos.

Por lo tanto, los **objetivos específicos** correspondientes al diseño de los ligandos serán los siguientes:

- Diseñar nuevos ligandos dirigidos al dominio de la colchicina en tubulina con una estructura común de sulfonamida.
- Seleccionar modificaciones estructurales que permitan mejorar el perfil farmacocinético de los ligandos y evadir los mecanismos de resistencia.
- Modificar los ligandos según las variaciones estructurales del dominio de la colchicina en mamíferos y *Leishmania* spp. para su aplicación selectiva como fármacos antitumorales o antiparasitarios.

2. SINTETIZAR

Una de las razones de la amplia aplicación de las sulfonamidas para diferentes fines terapéuticos es su accesibilidad sintética. Aunque existen múltiples rutas sintéticas para su formación, la más extendida y la más eficaz es la que hace reaccionar derivados de ácido sulfónico y aminas.[68] Es por ello que, en este trabajo de Tesis Doctoral, la formación del puente de sulfonamida para la síntesis de los compuestos se plantea mediante la reacción entre un cloruro de sulfonilo y la amina aromática correspondiente (Fig. 17). Las anilinas de partida no comerciales se pueden obtener mediante nitración del correspondiente anillo aromático y su posterior reducción catalítica. Tras la construcción del esqueleto de sulfonamida se modifican los sustituyentes de ambos anillos aromáticos. La síntesis de los sustituyentes derivados de amina se plantea partiendo de sus precursores nitro, los cuales son reducidos a sus aminas primarias, para ser posteriormente derivatizadas. La sustitución del nitrógeno de la sulfonamida se puede realizar en último lugar con el fin de obtener compuestos finales homólogos sustituidos y sin sustituir que permitan su comparación directa. Su síntesis se plantea mediante reacción de la sulfonamida secundaria con el derivado halogenado correspondiente en presencia de una base. Todos los compuestos sintetizados se purifican mediante técnicas generales de cristalización y/o cromatografía y se caracterizan mediante las metodologías habituales de Resonancia Magnética Nuclear (RMN) de ^{1}H y ^{13}C, infrarrojo (IR), punto de fusión y espectrometría de masas.

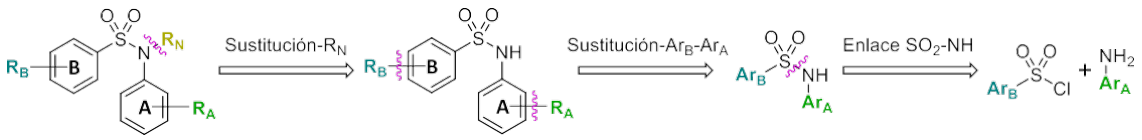

Figura 17. Esquema general retrosintético de los LUT diseñados con estructura de sulfonamida.

Por lo tanto, los **objetivos específicos** correspondientes a la síntesis de los ligandos serán los siguientes:

- Sintetizar materiales de partida y esqueletos principales de sulfonamida en cantidades suficientes y rendimientos adecuados para su posterior derivatización.
- Sintetizar series de compuestos en cantidad y pureza suficiente para su posterior evaluación.
- Sintetizar familias completas de compuestos análogos entre sí, que permitan la comparación intra- e inter- familia.

3. EVALUAR

El objetivo final de este trabajo consiste en evaluar los ligandos diseñados y sintetizados, como posibles agentes de unión al dominio de colchicina en tubulina como antitumorales o leishmanicidas con propiedades farmacocinéticas mejoradas. La estrategia de evaluación se plantea en el siguiente orden (Fig. 18):

1º. Evaluación de la actividad antitumoral. Se propone estudiar la capacidad de los ligandos de impedir la proliferación celular *in vitro*. Para ello se puede trabajar con cultivos celulares de células humanas procedentes de diferentes tipos de tumores (ej.: cérvix, mama, colon). La evaluación comienza con la determinación preliminar de la actividad antiproliferativa de todos los ligandos sintetizados, a una concentración lo suficientemente elevada que nos permita discernir entre ligandos citotóxicos (+) o no citotóxicos (-). Posteriormente, se procede a la determinación de la CI_{50} (concentración de compuesto que inhibe la proliferación celular en un 50%) para todos aquellos compuestos que hayan superado el cribado inicial. Una vez dispongamos de esta información, los resultados obtenidos se comparan para llevar a cabo estudios de REA con el fin de establecer cómo afectan las modificaciones estructurales a la actividad antiproliferativa.

2º. Evaluación de la actividad antiparasitaria. El parásito *Leishmania infantum* presenta dos estadios diferentes según su hospedador: i) el promastigote, presente en el vector flebótomo y ii) el amastigote, presente en el huésped mamífero.[204] Por lo tanto, se propone la evaluación leishmanicida de los ligandos frente a ambas formas parasitarias. Para ello, se puede trabajar con cultivos extracelulares de ambos estadios y con formas intracelulares del estadio causante de la enfermedad en el humano, el amastigote. La evaluación comienza con un cribado inicial de todos los ligandos sintetizados sobre las formas parasitarias extracelulares y continúa con la determinación de la CI_{50} para todos aquellos que muestren inicialmente un resultado positivo (+). Todos los ligandos que no hayan resultado ser citotóxicos para la célula hospedadora en la evaluación antitumoral se evalúan posteriormente sobre formas parasitarias intracelulares. Finalmente, los resultados obtenidos se comparan entre sí para establecer estudios de REA sobre la actividad antiparasitaria.

3º. Evaluación de la selectividad mamíferos/parásitos. La capacidad de las modificaciones estructurales de conferir selectividad frente a una u otra especie permite establecer Relaciones Estructura-Selectividad (RES) mamíferos *vs.* parásitos, a través de la comparación de los resultados obtenidos en ambas evaluaciones anteriores.

4º. Evaluación del mecanismo de acción antimitótico. Los LUT ejercen su acción al alterar la dinámica de los microtúbulos, lo que desencadena la interrupción de la división celular en la transición de la metafase a la anafase y la posterior muerte celular por apoptosis.[6,11] Por lo tanto, la hipótesis propuesta de que los ligandos ejerzan su actividad biológica por unión al dominio de colchicina en tubulina se puede contrastar mediante los siguientes experimentos de evaluación: Inhibición de la Polimerización de Tubulina (IPT) *in vitro*, interacciones ligando-proteína *in silico* (*docking*), parada del ciclo celular en G_2/M, muerte celular mediada por apoptosis y desestabilización de la red de microtúbulos. Para ello se utilizan técnicas espectrofotométricas, modelado molecular, citometría de flujo e inmunofluorescencia. Para los estudios por citometría de flujo e inmunofluorescencia se propone seleccionar únicamente los ligandos más prometedores.

5º. Evaluación de la solubilidad acuosa. La mala farmacocinética, debida en gran parte a la escasa solubilidad acuosa, de los LUT en ensayos clínicos ha impedido en muchas ocasiones su desarrollo completo.[47] Por lo tanto, en este trabajo se propone la introducción de grupos solubilizadores en las moléculas que permitan mejorar la

solubilidad de los compuestos de referencia, estableciendo Relaciones Estructura-Propiedades (REP). Esta hipótesis puede ser contrastada mediante la evaluación de la solubilidad acuosa de los ligandos sintetizados utilizando técnicas espectrofotométricas.

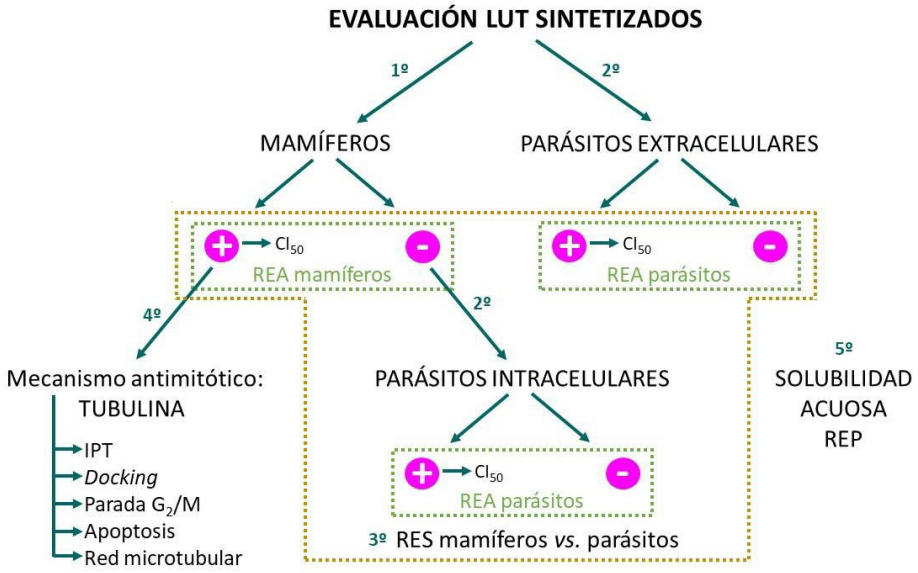

Figura 18. Esquema de evaluación planteado para los LUT diseñados y sintetizados.

Por lo tanto, los **objetivos específicos** correspondientes a la evaluación de los ligandos serán los siguientes:

- Evaluar la actividad antiproliferativa *in vitro* de los ligandos sintetizados frente a líneas celulares tumorales humanas y establecer relaciones estructura-actividad (REA).
- Evaluar la actividad antiparasitaria *in vitro* frente a cultivos extra- e intra- celulares del parásito *Leishmania infantum* y establecer REA.
- Comparar las evaluaciones de la actividad antitumoral y antiparasitaria y establecer relaciones estructura-selectividad (RES) mamíferos *vs.* parásitos.
- Examinar el efecto de los ligandos sobre los microtúbulos, estudiar su mecanismo de acción y muerte celular y confirmar la tubulina como la diana molecular de la actividad biológica.
- Evaluar y optimizar la solubilidad acuosa de los ligandos y establecer relaciones estructura-propiedades (REP).

artículos de investigación

"Lo que sabemos es una gota de agua,
lo que ignoramos es el océano."

Isaac Newton

artículo 1

Microtubule Destabilizing Sulfonamides as an Alternative to Taxane-Based Chemotherapy

Myriam González, María Ovejero-Sánchez, Alba Vicente-Blázquez, Raquel Álvarez, Ana B. Herrero, Manuel Medarde, Rogelio González-Sarmiento, Rafael Peláez.

Int. J. Mol. Sci. **2021**, 22, 1907.
DOI: 10.3390/ijms22041907

RESUMEN

El objetivo de este trabajo es la búsqueda de una alternativa terapéutica a los fármacos de primera línea – taxanos – en el tratamiento del cáncer de mama femenino y de los tumores ginecológicos, englobados bajo el término de cánceres *Pan-Gyn*. La baja solubilidad acuosa de los taxanos requiere su compleja formulación en sistemas lipídicos, implicados en una amplia variedad de efectos secundarios al tratamiento. Además, estos fármacos están frecuentemente asociados con un estrecho margen terapéutico debido a su alta toxicidad, y con la aparición de resistencias múltiples mediadas por MDR. Por lo tanto, se propone como alternativa el diseño y la síntesis de 52 nuevos ligandos de unión al dominio de colchicina en tubulina con estructura común de *N*-fenilbencenosulfonamida. El pequeño tamaño de los nuevos compuestos no solo ofrece ventajas farmacocinéticas, sino que los hace menos propensos a los mecanismos de resistencia mediados por MDR. La determinación de la solubilidad acuosa pone de manifiesto la mejora en la solubilidad con respecto a los ligandos de referencia. Para la mayoría de los compuestos, la actividad citotóxica no varía en presencia de inhibidores de MDR, lo que sugiere que no son sustrato de dichas proteínas. Las sulfonamidas más prometedoras muestran potencias antiproliferativas nanomolares contra células tumorales humanas de cánceres de ovario, mama y cérvix, superando en algunos casos a paclitaxel. Finalmente, los compuestos se comportaron como agentes de unión a tubulina, causando una clara desestabilización de la red de microtúbulos, la inhibición de la polimerización de tubulina *in vitro* y la parada del ciclo celular en la región G_2/M seguida por la muerte celular mediada por apoptosis. Por lo tanto, los resultados sugieren que las nuevas sulfonamidas desestabilizadoras de microtúbulos pueden ser alternativas prometedoras a la quimioterapia basada en taxanos en cánceres *Pan-Gyn* quimiorresistentes.

International Journal of
Molecular Sciences

MDPI

Article

Microtubule Destabilizing Sulfonamides as an Alternative to Taxane-Based Chemotherapy

Myriam González [1,2,3,†], María Ovejero-Sánchez [2,4,5,†], Alba Vicente-Blázquez [1,2,3], Raquel Álvarez [1,2,3], Ana B. Herrero [2,4,5], Manuel Medarde [1,2,3], Rogelio González-Sarmiento [2,4,5,*] and Rafael Peláez [1,2,3,*]

1 Laboratorio de Química Orgánica y Farmacéutica, Departamento de Ciencias Farmacéuticas, Facultad de Farmacia, Universidad de Salamanca, 37007 Salamanca, Spain; mygondi@usal.es (M.G.); avicenteblazquez@usal.es (A.V.-B.); raquelalvarez@usal.es (R.Á.); medarde@usal.es (M.M.)
2 Instituto de Investigación Biomédica de Salamanca (IBSAL), Hospital Universitario de Salamanca, 37007 Salamanca, Spain; maría.os@usal.es (M.O.-S.); anah@usal.es (A.B.H.)
3 Centro de Investigación de Enfermedades Tropicales de la Universidad de Salamanca (CIETUS), Facultad de Farmacia, Universidad de Salamanca, 37007 Salamanca, Spain
4 Unidad de Medicina Molecular, Departamento de Medicina, Facultad de Medicina, Universidad de Salamanca, 37007 Salamanca, Spain
5 Laboratorio de Diagnóstico en Cáncer Hereditario, Laboratorio 14, Centro de Investigación del Cáncer, Universidad de Salamanca-CSIC, 37007 Salamanca, Spain
* Correspondence: gonzalez@usal.es (R.G.-S.); pelaez@usal.es (R.P.); Tel.: +34-923-294500 (R.G.-S.); +34-677-554-890 (ext. 1837) (R.P.)
† These authors contributed equally to this work.

Abstract: Pan-Gyn cancers entail 1 in 5 cancer cases worldwide, breast cancer being the most commonly diagnosed and responsible for most cancer deaths in women. The high incidence and mortality of these malignancies, together with the handicaps of taxanes—first-line treatments—turn the development of alternative therapeutics into an urgency. Taxanes exhibit low water solubility that require formulations that involve side effects. These drugs are often associated with dose-limiting toxicities and with the appearance of multi-drug resistance (MDR). Here, we propose targeting tubulin with compounds directed to the colchicine site, as their smaller size offer pharmacokinetic advantages and make them less prone to MDR efflux. We have prepared 52 new Microtubule Destabilizing Sulfonamides (MDS) that mostly avoid MDR-mediated resistance and with improved aqueous solubility. The most potent compounds, *N*-methyl-*N*-(3,4,5-trimethoxyphenyl-4-methylaminobenzenesulfonamide **38**, *N*-methyl-*N*-(3,4,5-trimethoxyphenyl-4-methoxy-3-aminobenzenesulfonamide **42**, and *N*-benzyl-*N*-(3,4,5-trimethoxyphenyl-4-methoxy-3-aminobenzenesulfonamide **45** show nanomolar antiproliferative potencies against ovarian, breast, and cervix carcinoma cells, similar or even better than paclitaxel. Compounds behave as tubulin-binding agents, causing an evident disruption of the microtubule network, in vitro Tubulin Polymerization Inhibition (TPI), and mitotic catastrophe followed by apoptosis. Our results suggest that these novel MDS may be promising alternatives to taxane-based chemotherapy in chemoresistant Pan-Gyn cancers.

Keywords: tubulin; sulfonamide; antitumor; taxane; combretastatin A-4; breast cancer; gynecologic cancer

Citation: González, M.; Ovejero-Sánchez, M.; Vicente-Blázquez, A.; Álvarez, R.; Herrero, A.B.; Medarde, M.; González-Sarmiento, R.; Peláez, R. Microtubule Destabilizing Sulfonamides as an Alternative to Taxane-Based Chemotherapy. *Int. J. Mol. Sci.* **2021**, *22*, 1907. https://doi.org/10.3390/ijms22041907

Academic Editor: Peter Van Dam

Received: 12 January 2021
Accepted: 11 February 2021
Published: 14 February 2021

1. Introduction

Gynecologic (i.e., ovarian, uterine, vulva, and vagina) and women breast cancer share relevant similarities at the molecular level that cluster them together (Pan-Gyn) and distinguish them from other tumor types [1,2]. According to GLOBOCAN estimates, Pan-Gyn cancers accounted for 19% of new diagnoses worldwide in 2018 and entailed 40% of new cancer cases among females [3]. 39% of women with Pan-Gyn cancers died from them, representing 30% of all female cancer deaths and 13% of total cancer deaths globally.

The high incidence and mortality of female breast [4,5], ovarian [6,7], and uterine [8,9] cancers and the acquired resistance to first-line treatments highlight the need for new therapeutic alternatives.

Since the FDA approved the use of Taxol® for advanced ovarian carcinoma in 1992 and metastatic breast cancer in 1994 [10], taxane-based chemotherapy has become the basis for treating breast and ovarian cancers [11]. First-line chemotherapy involves a platinum-taxane combination for ovarian cancer [12–14], preferably carboplatin/paclitaxel [15], and taxanes sequenced or combined with anthracyclines for advanced and metastatic breast cancer [16–19]. Furthermore, the combination of cisplatin and paclitaxel is considered a standard regimen in the palliative setting for patients with metastatic, recurrent, or persistent uterine cancer [9,20–22].

However, the clinical efficacy of taxanes is limited by an intrinsic low aqueous solubility (<2 μg/mL [23–25]), dose-limiting toxicities, and the development of drug resistance [26]. The low solubility (remaining challenging) requires complex solvent-system formulations that can alter the pharmacokinetic profiles [27,28] and have been associated with toxicity [29,30]. The development of resistance to these drugs is usually ascribed to Pgp-mediated efflux and alterations in tubulin (mutations in the tubulin genes, altered tubulin isotype expression, or aberrant levels of tubulin) [31–33]. Specific resistance to taxane-based chemotherapy has been described for female breast cancer, with an approximately 30% of recurrence [34,35], ovarian cancer, in which 50% of patients relapse with the chemoresistant disease within the first two years post-diagnosis [36,37], and uterine cancer [38].

Taxanes bind to microtubules, stabilizing lateral contacts between protofilaments, thus promoting assembly and inhibiting depolymerization at high concentrations. At lower concentrations, they alter microtubule dynamics and preclude cells from properly completing mitosis [39,40], which leads to cell cycle arrest at G_2/M and, subsequently, to cell death mainly triggered by apoptosis [41,42]. There are other drug binding sites in tubulin that affect microtubule dynamics similarly to taxanes, but whose engagement results in microtubule depolymerization at high concentrations, such as the colchicine, the vinca alkaloids, the maytansine, the pironetin, and the hemiasterlin sites [43]. The only approved drugs belong to the vinca alkaloids site binding ligands, which are used against hematological malignancies and solid tumors, including breast cancer. However, they share with taxanes the problems of toxic side effects, difficult pharmacokinetics, and complex hydrophobic structures that make them substrates of drug efflux pumps [44].

The colchicine site offers advantages for drug design since its ligands exhibit simple chemical structures and are synthetically accessible. Colchicine-site ligands display antiproliferative effects (characterized by cell cycle arrest at G_2/M phase followed by the induction of apoptosis [45]) and act as vascular disrupting agents, affording additional odds against solid tumors [46]. Representatives such as the stilbene combretastatin A-4 (CA-4) and the sulfonamide ABT-751 have reached clinical trials [47]. However, the *Z* olefin of combretastatins is chemically unstable and readily isomerizes to the more stable but inactive *E* isomer. The low solubility of CA-4 requires the use of phosphate prodrugs on the phenolic hydroxyl group, which is, in turn, the target for metabolic inactivation by glucuronidation in resistant cells, such as the colon adenocarcinoma HT-29 cell line [48]. ABT-751 is an orally administered sulfonamide with modest potency against human cancer cell lines and xenograft models. Despite its favorable pharmacokinetics, ABT-751 has not found clinical application due to insufficient potency [49].

In this work, we have designed and synthesized a new family of Microtubule Destabilizing Sulfonamides (MDS) hybrids of CA-4 and ABT-751. The effects of replacing the chemically unstable CA-4 olefin with a sulfonamide bridge, the removal or substitution of the phenolic hydroxyl group, and the introduction of several modifications on the aromatic rings and the sulfonamide bridge have been explored while maintaining the 3,4,5-trimethoxyphenyl ring that has been long considered essential for high potency [50,51] (Figure 1). The resulting compounds have been evaluated for tubulin inhibition in vitro

and antiproliferative activity against several human tumor cell lines. We have also studied whether MDR1 pumps could compromise their effectiveness by the pharmacological inhibition of Pgp using verapamil. After a comprehensive preliminary evaluation, three promising MDS have been further screened against several representative cancer cell lines representative of the tumor types that are associated with the highest mortalities: breast, ovarian, and uterine, accounting for 51%, 15%, and 32% of cancer deaths in women, respectively. The effect of the compounds on cancer cell proliferation has been studied and compared with paclitaxel, CA-4, and ABT-751. The mechanism of action of these novel MDS has been studied by ascertaining their effect on the microtubule network in vitro. These MDS induce mitotic arrest, followed by apoptotic cell death with differences arising from different genetic backgrounds of the studied cell lines. The favorable pharmacodynamic and pharmacokinetic profiles compared to reference drugs, including solubility, absence of Pgp-mediated resistance, and improved potency indicate that MDS are promising candidates for the treatment of this kind of malignancies.

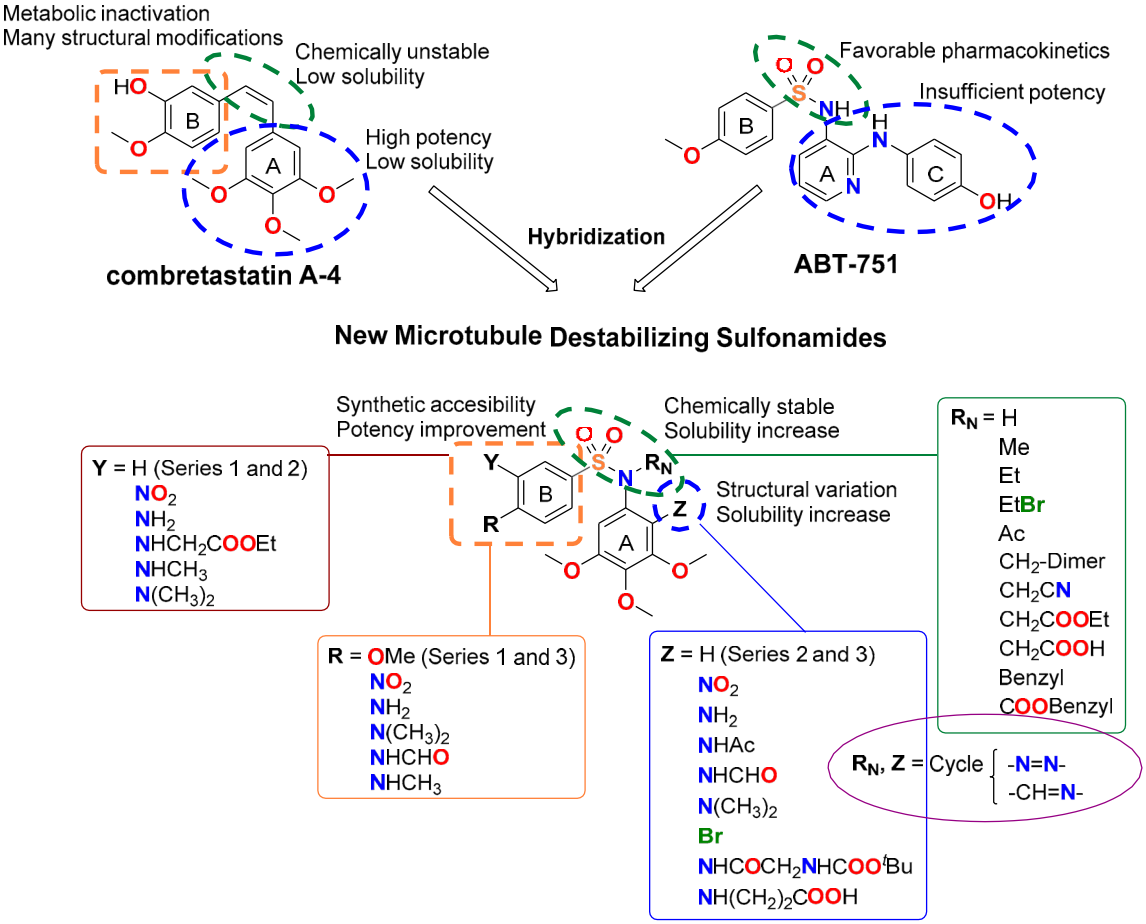

Figure 1. Representative ligands binding at the colchicine site used as a starting point for the rational design of new Microtubule Destabilizing Sulfonamides (MDS). General structure and structure variations of new MDS.

2. Results

2.1. Synthesis of MDS

52 new MDS (Figure 1) were prepared following the synthetic approach shown in Figure 2 (detailed synthetic procedures and NMR spectra can be found in Supplemental Figure S1 and Methods SP1,2). The synthesized compounds were divided into three series according to the substituents on the aromatic B ring (Ar_B): series 1 (compounds **1a**-**24**), series 2 (**25**–**38**), and series 3 (**39**–**48b**) (Table 1). Sulfonamides were built up by the reaction between 4-methoxy- (series 1), 4-nitro- (series 2), or 4-methoxy-3-nitro- (series 3)

benzenesulfonyl chlorides and 3,4,5-trimethoxyaniline, providing crystalline products in excellent yields (90–96%). Nitro groups were reduced to amines by palladium-catalyzed hydrogenation (82–98% yields). The subsequent amino derivatization by alkylation, acylation, and/or formylation-reduction sequences allowed the introduction of varied *Z*, *R*, and *Y* substituents (Figure 1). Substitutions at the sulfonamide nitrogen were conducted by alkylation reactions with alkyl halides in KOH/CH_3CN (methylations with methyl iodide in 63–98% yields) or K_2CO_3/DMF (ethyl, acetyl, acetonitrile, benzyl, or ethyl acetate substituents in 40–99% yields).

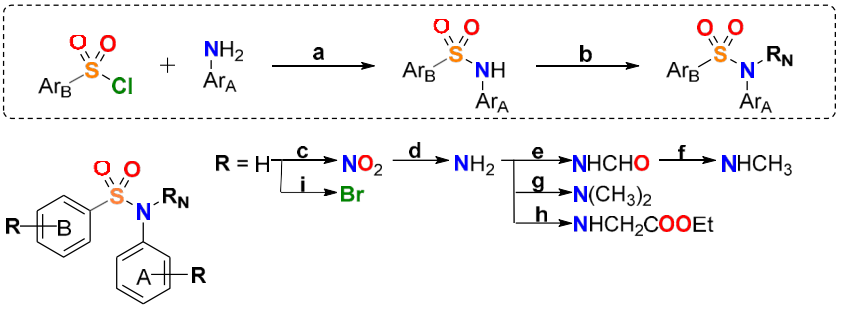

Figure 2. General synthetic approach. Reagents, conditions, and yields: (**a**) Pyridine, CH_2Cl_2, rt, 4–8 h, 90–96% (**b**) R_N = CH_3, CH_3I, KOH, CH_3CN, rt, 24 h, 63–98%; R_N = Ac, acetic anhydride, pyridine, CH_2Cl_2, reflux, 8–12 h, 61–83%; R_N = CH_3 and Ac, R_N-halogen, K_2CO_3, dry DMF, rt, 24–48 h, 40–99% (**c**) *tert*-Butyl nitrite, CH_3CN, 45 °C, 24 h, 60% (**d**) H_2, Pd/C, EtOAc, rt, 48–72 h, 82–98% (**e**) Formic acid, CH_2Cl_2, rt, 24–48 h, 62–82% (**f**) Trichloroacetic acid, $NaBH_4$, dry THF, 0 °C, 24 h, 97% (**g**) Paraformaldehyde, $NaBH_3CN$, AcOH, MeOH, rt, 72–96 h, 95% (**h**) Ethyl 2-bromoacetate, NaI, acetone/THF 1:1, reflux, 48 h, 19% (**i**) NBS, CH_2Cl_2, rt, 6 h, 43%.

Table 1. Chemical structure, antiproliferative activity against human tumor cell lines, and Tubulin Polymerization Inhibition (TPI) of novel Microtubule Destabilizing Sulfonamides (MDS). Compounds have been divided into three different series according to the substituents on the aromatic B ring (Ar_B). TM: 3,4,5-trimethoxyphenyl.

Series 1: 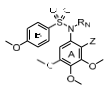			**Antiproliferative Activity IC_{50} (nM)**		**TPI**	
					TPI %	
Z	**R_N**	**Compound**	**HeLa**	**MCF7**	**10 μM**	**IC_{50} (μM)**
H	H	**1a**	240	375	0	>20
H	SO_2-4-OMePh	**1b**	>1000	>1000	0	>20
H	Me	**2a**	71	127	35	>20
H	CH_2-Dim	**2b**	>1000	>1000	0	>20
H	Et	**3**	99	87	25	>20
H	EtBr	**4**	94	340	30	>20
H	Ac	**5**	287	270	0	>20
H	CH_2CN	**6**	143	275	0	>20
H	CH_2COOEt	**7**	217	335	21	>20
H	CH_2COOH	**8**	>1000	>1000	0	>20
H	Benzyl	**9**	750	830	21	>20
H	COOBenzyl	**10**	>1000	>1000	11	>20
NO_2	H	**11**	>1000	>1000	10	>20
NH_2	H	**12**	>1000	>1000	0	>20
NH_2	Me	**13**	>1000	>1000	0	>20
NH_2	CH_2-Dim	**14**	>1000	>1000	0	>20
NHAc	H	**15**	>1000	>1000	0	>20
NHAc	Me	**16**	>1000	>1000	0	>20
NHCHO	H	**17**	>1000	>1000	4	>20
$N(CH_3)_2$	H	**18**	>1000	>1000	0	>20
$N(CH_3)_2$	Me	**19**	>1000	>1000	0	>20
Br	H	**20**	>1000	>1000	0	>20
Gly-*t*BOC	H	**21**	>1000	>1000	0	>20

Table 1. *Cont.*

Succinic	H	**22**	>1000	>1000	0	>20
-N=N-		**23**	>1000	>1000	0	>20
-N=CH-		**24**	>1000	>1000	0	>20

Series 2: 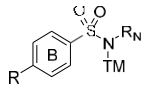			**Antiproliferative Activity IC_{50} (nM)**		**TPI**	
					TPI %	
R	**R_N**	**Compound**	**HeLa**	**MCF7**	**10 μM**	**IC_{50} (μM)**
NO_2	H	**25**	>1000	>1000	0	>20
NH_2	H	**26**	>1000	>1000	0	>20
NH_2	Me	**27**	>1000	>1000	0	>20
$N(CH_3)_2$	H	**28**	230	173	0	>20
$N(CH_3)_2$	Me	**29a**	63	30	40	>20
$N(CH_3)_2$	CH_2-Dim	**29b**	>1000	>1000	0	>20
$N(CH_3)_2$	Et	**30**	66	81	45	>20
$N(CH_3)_2$	Ac	**31**	183	135	38	14
$N(CH_3)_2$	CH_2CN	**32**	55	120	17	>20
$N(CH_3)_2$	CH_2COOEt	**33**	99	91	14	>20
$N(CH_3)_2$	CH_2COOH	**34**	>1000	>1000	6	>20
$N(CH_3)_2$	Benzyl	**35a**	330	100	72	5.3
$N(CH_3)_2$	COOBenzyl	**35b**	>1000	>1000	0	>20
NHCHO	H	**36**	>1000	>1000	0	>20
$NHCH_3$	H	**37**	607	>1000	7	>20
$NHCH_3$	Me	**38**	44	61	47	10

Series 3: 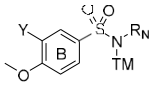			**Antiproliferative Activity IC_{50} (nM)**		**TPI**	
					TPI %	
Y	**R_N**	**Compound**	**HeLa**	**MCF7**	**10 μM**	**IC_{50} (μM)**
NO_2	H	**40**	>1000	>1000	0	>20
NH_2	H	**41**	260	96	15	>20
NH_2	Me	**42**	23	26	41	12
NH_2	Et	**43**	38	14	37	>20
NH_2	CH_2CN	**44**	60	8	5	>20
NH_2	Benzyl	**45**	25	48	75	3.7
$NHCH_2COOEt$	Me	**46**	210	48	13	>20
$NHCH_2COOEt$	CH_2COOEt	**47**	>1000	>1000	0	>20
$NHCH_3$	Me	**48a**	440	1190	2	>20
$N(CH_3)_2$	Me	**48b**	>1000	>1000	0	>20
Paclitaxel [52]			2.6	2.5	n.d. [1]	n.d.
Combretastatin A-4			2	1	100	3
ABT-751			388	180	69	4.4

[1] n.d.: not determined.

2.2. Replacement of CA-4 Olefin by a Sulfonamide Highly Increased Aqueous Solubility

Aqueous solubility of representative compounds was spectrophotometrically measured in pH 7.0 phosphate buffer (Table 2). UV absorbance at three maximum absorbance wavelengths of selected compounds was measured after 48 h shaking and subsequent microfiltration. Replacement of the CA-4 olefinic bridge by a sulfonamide group highly increased aqueous solubility when compared to paclitaxel and to CA-4 (4- up to 1700-fold increase). Similar or even better results were obtained when compared with the orally administered sulfonamide ABT-751 (up to 42-fold increase). The best results were achieved by the introduction of amino acid derivatives at the *Z* position (compounds **21** and **22**).

Table 2. Aqueous solubility in μg/mL of representative compounds.

Compound	Solub (μg/mL)	Compound	Solub (μg/mL)	Compound	Solub (μg/mL)
1a	83	**22**	1690	**37**	43
1b	108	**23**	41	**38**	16
2a	27	**26**	28	**41**	89
3	30	**27**	25	**42**	108
5	38	**28**	15	**43**	58
6	33	**29a**	7	**44**	46
11	88	**29b**	4	**45**	14
12	158	**30**	6	**CA-4**	1
15	230	**31**	18	**ABT-751**	40
20	87	**32**	8	**Paclitaxel** [23–25]	<2
21	357	**36**	27	–	–

2.3. MDS Inhibit Cell Proliferation in Breast, Cervix, and Ovarian Tumor Cells

The in vitro antiproliferative activity of MDS at 1 μM after 72 h treatments was evaluated by a colorimetric method against the human tumor cell lines HeLa (cervix epithelioid carcinoma) and MCF7 (breast adenocarcinoma). Compounds showing more than 40% inhibition at 1 μM in at least three independent assays were evaluated in a range of concentrations between 0.1 nM and 10 μM for the determination of half-maximal inhibitory concentrations (IC_{50}) (Table 1). Paclitaxel [52], CA-4, and ABT-751 were used as references.

HeLa and MCF7 cells showed similar sensitivities to MDS, both cell lines displayed less than two-fold changes in IC_{50} values between them in most cases. The most potent compounds (e.g., **29a**, **30**, **38**, **42**, **43**, **44**, and **45**) showed IC_{50} values in the double-digit nanomolar range, less potent than paclitaxel and CA-4 but more than ABT-751. Substitutions on the trimethoxyphenyl ring resulted in inactive compounds (**11–24**). Alkylations of the sulfonamide improved the potency, with methyl groups yielding the lowest IC_{50} values in most cases (e.g., **29a**, **30**, and **42**). Larger substituents gave worse results except for some benzyl (e.g., **45**) and cyanomethyl (e.g., **44**) derivatives. Replacement of the 4-methoxy group on the B ring in series 1 by an amino substituent (series 2) and introduction of an amino group on position 3 as a primary amine (series 3) gave favorable results. Substituents with a hydrogen bond donor, such as methylamines (**38**) in series 2, or primary amines in series 3 (**42–45**), resulted in the most potent MDS. Based on antiproliferative results, we selected 3 out of the 7 most potent compounds (**38**, **42**, and **45**) as representative leaders for further investigation.

The in vitro antiproliferative activity of compounds **38**, **42**, and **45** against a panel of five human ovarian carcinoma cell lines (SKOV3, IGROV-1, A2780, OVCAR-8, and OVCAR-3) was evaluated by a colorimetric method (Table 3) and compared with paclitaxel [14]. Paclitaxel and MDS showed a similar comparative behavior against the highly paclitaxel-sensitive A2780 and OVCAR-8 and the less sensitive IGROV-1 cell line, with paclitaxel being one order of magnitude more potent than MDS. Concerning OVCAR-3, paclitaxel is less potent, but MDS maintain their potency range, thus resulting in similar effects of both types of drugs. For SKOV3, the potency reduction observed for paclitaxel together with a sustained or improved (**42** with a 7 nM IC_{50} value) potency for MDS results in a more favorable profile of the MDS compared to paclitaxel.

2.4. Lead Compounds Overcome MDR-Mediated Resistance

The antiproliferative activity of MDS against the CA-4-resistant cell line HT-29 (colon adenocarcinoma) in the absence or the presence of 10 μM verapamil, a non-selective Pgp/MDR1 inhibitor, was measured 72 h post-treatment by a colorimetric method (Supplementary Table S1). Verapamil itself did not affect cell proliferation at that concentration. Detecting changes in drug potency when inhibiting MDR-mediated efflux reflect that these transporters reduce the intracellular drug concentration. HT-29 has been

reported to express moderate levels of MDR1, accounting for a resistant phenotype [53]. A comparison of the antiproliferative IC_{50} values of each MDS in the presence or absence of verapamil provides an estimate of the susceptibility of each compound to efflux pumps. Most of the compounds, including leading derivatives **38**, **42**, and **45** (Table 4 and Supplementary Table S1), showed no significant differences (up to two-fold change) between pairs of IC_{50} values, thus suggesting that they are not substrates of MDR pumps. Compounds **3**, **29a**, and **30** showed higher potencies against HT-29 cells when combined with verapamil (comparables to that of obtained against sensitive HeLa an MCF7 cells), thus validating the assay as positive controls.

Table 3. Antiproliferative activity of the lead compounds and paclitaxel against several human ovarian tumor cell lines.

	Antiproliferative Activity IC_{50} (nM)				
Compound	**SKOV3**	**IGROV-1**	**A2780**	**OVCAR-8**	**OVCAR-3**
38	46	248	68	74	31
42	7	400	42	37	72
45	48	492	104	48	58
Paclitaxel [1]	81	39	3	6	17

[1] IC_{50} values against A2780, OVCAR-8, and OVCAR-3 cell lines from Bicaku, E. et al. evaluation [14].

Table 4. Antiproliferative activity against the CA-4 resistant cancer cell line HT-29 and sensitivity of the lead MDS to MDR pumps.

	Antiproliferative Activity IC_{50} (nM)	
Compound	**HT-29**	**HT-29 Verapamil 10 μM**
38	59	50
42	81	79
45	300	276
CA-4	305	327

2.5. Lead Compounds Induce G_2/M Arrest in Breast, Ovarian and Cervix Tumor Cells

The effect of the lead MDS on the cell cycle of MCF7, SKOV3, and HeLa cells was analyzed in time-course experiments at 24, 48, and 72 h post-treatment by DNA staining and flow cytometry quantification. The working concentration for each compound (600 nM for **38**, 50 nM for **42**, and 400 nM for **45**) was established at the complete inhibition of cell proliferation in view of individually assays run in parallel for each cell line.

For breast adenocarcinoma MCF7 cells (Figure 3a) a pronounced and sustained G_2/M arrest was observed for all the treatments from 24 h (70–80%) to 72 h (60–76%), compared to untreated MCF7 cells, which maintained a 32–40% population at G_2/M throughout the time course. A moderate increase of the percentage of cells at the $SubG_0/G_1$ region was observed, which slightly increased over time (from 4–6% at 24 h to 6–12% at 72 h) accompanied by the decrease in the G_2/M population.

Compounds **38**, **42**, and **45** (Figure 3b) arrested ovarian carcinoma SKOV3 cells at the G_2/M phase 24 h post-treatment (44%) compared to untreated cells (30%). The percentage of $SubG_0/G_1$ treated SKOV3 cells was already elevated at 24 h (20% to 22%) compared to untreated controls (always <14%). Treatments with compounds **38** and **42** increased the percentage of $SubG_0/G_1$ modestly at 48 h (35% and 34%, respectively), and notably at 72 h (43% and 53%, respectively). This increase presumably occurred at the expense of cells arrested at the G_2/M phase. The effect of compound **45** was notably higher, with 46% of cells at $SubG_0/G_1$ region 48 h post-treatment and 63% at 72 h.

Treatment of HeLa cells with **38** and **45** (Figure 3c) caused a significant arrest at the G_2/M phase after 24 h (80%) and a more modest one for compound **42** (44%) accompanied by a limited increase in the percentage of cells of the $SubG_0/G_1$ population (9–16% vs. <4% in untreated controls). At subsequent time points, around 50% of the cells for all three

treatments were allocated to the SubG$_0$/G$_1$ region of the cell cycle histogram at the expense of the G$_2$/M phase.

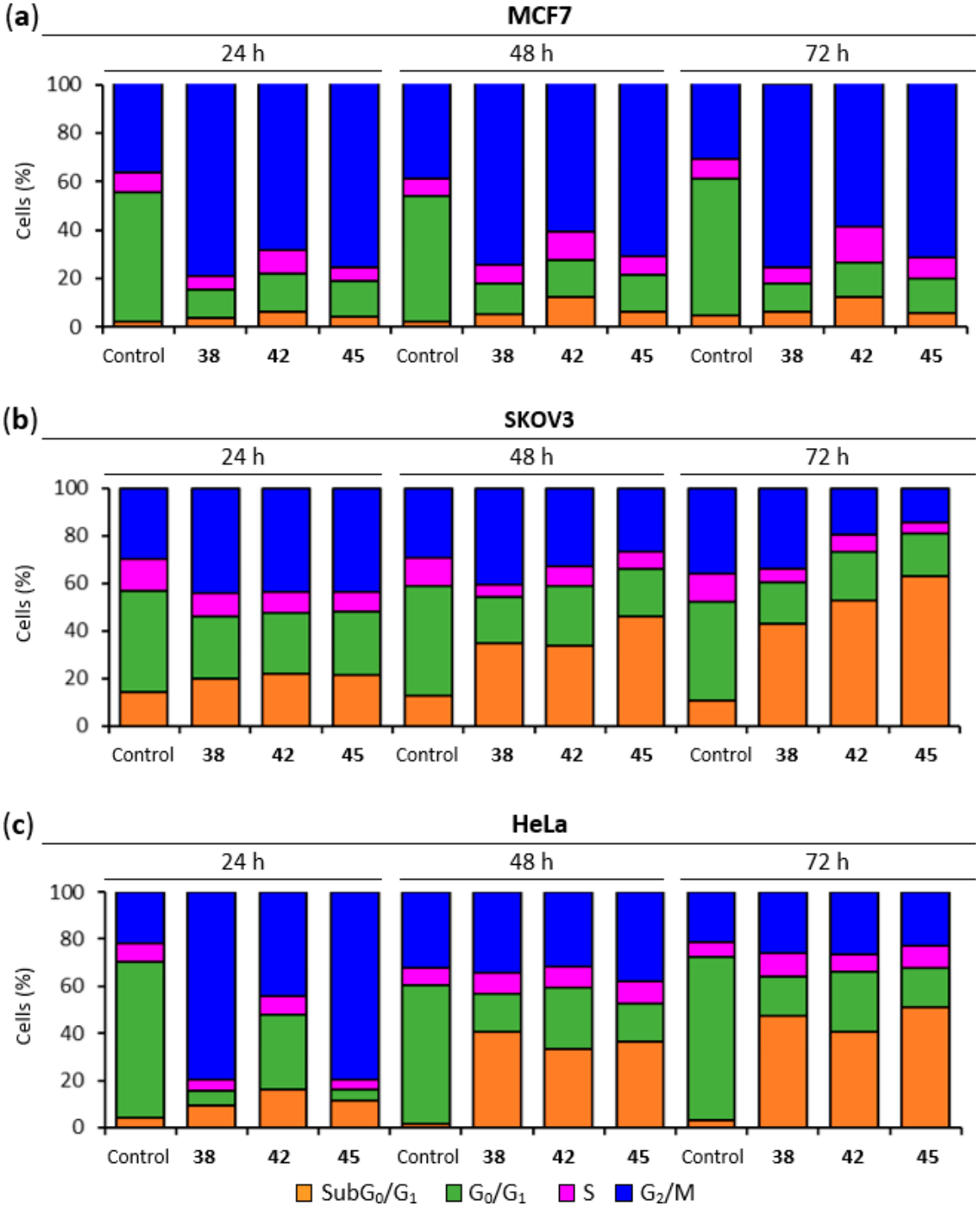

Figure 3. Cell cycle analysis. (**a**) MCF7 cell cycle distribution. Cells were arrested in G$_2$/M phase. (**b**) SKOV3 cell cycle distribution. Cells arrested in G$_2$/M phase experienced time-dependent cell death (SubG$_0$/G$_1$ region). (**c**) HeLa cell cycle distribution. Cells were arrested in the G$_2$/M phase followed by cell death (SubG$_0$/G$_1$ region). Cells were incubated with the lead compounds at 600 nM (**38**), 50 nM (**42**), or 400 nM (**45**) for 24, 48, and 72 h, stained with propidium iodide (PI) and their DNA content was analyzed by flow cytometry. Untreated samples were analyzed in parallel. The different cell cycle populations were quantified, expressed in percentages, and represented in bar charts. Data shown are representative of three independent experiments.

2.6. Lead Compounds Trigger Apoptotic Cell Death

To determine whether the cytotoxic/antiproliferative effect of the MDS was due to apoptosis induction, cells were treated with variable concentrations of the drug for 72 h or 6 days, stained with Annexin V-FITC (AnV) and propidium iodide (PI), and analyzed by flow cytometry. Double negative cells (AnV^-/PI^-) were classified as live cells (L), cells positive for AnV and negative for PI (AnV^+/PI^-) were considered in Early Apoptosis (EA), cells negative for AnV and positive for PI (AnV^-/PI^+) were considered necrotic (N), and double-positive cells (AnV^+/PI^+) as Late Apoptosis (LA). In all cases, the compounds were used at the same concentrations previously used in cell cycle studies (Table 5).

Table 5. Cell death quantification in Annexin V-FITC/PI double staining experiments. MCF7, SKOV3, and HeLa cells were incubated with the lead compounds for 72 h and/or 6 days, stained with Annexin V-FITC (AnV) and PI, and analyzed by flow cytometry. The results are expressed in percentage as the average of three independent experiments. Untreated samples were analyzed in parallel. Cells were classified into double-negatives (live cells), AnV-positive cells (early apoptosis), double-positives (late apoptosis), and PI-positive cells (necrosis).

	Compound	Annexin V-FITC/PI 72 h (%)				Annexin V-FITC/PI 6 Days (%)			
		Live	EA [1]	LA [2]	Necrosis	Live	EA	LA	Necrosis
MCF7	**38** (600 nM)	60.5	29.0	5.4	5.1	52.0	45.0	2.7	0.3
	42 (50 nM)	87.7	8.5	2.3	1.4	79.1	18.9	1.7	0.3
	45 (400 nM)	70.5	20.1	7.5	1.9	56.7	39.3	3.8	0.3
	CA-4 (50 nM)	58.3	31.7	3.3	6.7	44.5	52.4	2.7	0.4
	Control	93.6	1.8	2.9	1.7	97.4	0.2	0.8	1.6
SKOV3	**38** (600 nM)	62.3	30.5	5.4	1.8				
	42 (50 nM)	85.1	12.2	2.0	0.7				
	45 (400 nM)	72.7	23.4	2.6	1.3				
	Paclitaxel (10 nM)	90.7	3.8	3.1	2.4				
	Control	99.2	0.5	0.3	0.1				
HeLa	**38** (600 nM)	0.6	1.1	87.6	10.6				
	42 (50 nM)	7.3	1.4	82.0	9.4				
	45 (400 nM)	0.8	1.5	84.9	12.7				
	Control	90.5	1.7	5.5	2.4				

[1] Early Apoptosis (EA). [2] Late Apoptosis (LA).

Breast cancer MCF7 cells treated with compound **42** for 72 h were mostly classified as live cells (88%), whereas lower percentages of live cells were found when treated with compounds **38** (60%), **45** (71%) and the reference compound CA-4 (58%). This lower percentage of live cells was accompanied by a higher proportion of EA cells for **38** (29%), **45** (20%), and CA-4 (32%) compared to the treatment with **42** (9%). Longer treatment exposures of 6 days confirmed this trend, with **38**, **45**, and CA-4 showing significantly lower percentages of live cells (45–57%) and higher EA populations (39–52%) than **42**, which showed live-cell percentages of 79% and EA of 19%.

Similar results were found 72 h post-treatment for SKOV3 ovarian tumor cells for MCF7 cells. SKOV3 cells treated with compounds **38** and **45** showed modest percentages of EA cells (31% and 23%, respectively) whereas a lower apoptotic population was found for compound **55** (12%). These percentages of apoptotic cells for compounds **38** and **55** were accompanied by low percentages of live cells (62% and 73%, respectively), with 10 nM paclitaxel showing high percentages of live cells (91%).

Treatment of the cervical cancer HeLa cells with compounds **38**, **42**, and **45** resulted in a severe reduction of live cells down to less than 7% and an accumulation of LA (82–88%) and necrotic (9–13%) cells after 72 h.

2.7. Lead Compounds Disrupt the Microtubule Network and Inhibit Tubulin Polymerization

The effect of MDS **38** and **45** on the tubulin cytoskeleton was analyzed in MCF7, SKOV3, and HeLa cells after 72-h treatments. The microtubule network was visualized by confocal microscopy staining α-tubulin in green, and cell nuclei were stained in blue with DAPI (4′,6-diamidino-2-phenylindole) (Figure 4). Compounds **38** and **45** disrupted the microtubule system of MCF7, SKOV3, and HeLa cells (Figure 4a), which loses the hairy appearance of untreated cells and shows up as a diffuse gauze. Treated cells showed multilobulated nuclei resembling bunches of grapes (Figure 4b).

The effect of all the synthesized compounds on the in vitro tubulin polymerization was evaluated at 10 μM. All the compounds that inhibited polymerization more than 30% were also assayed at 20 μM. IC_{50} values were calculated for those compounds inhibiting tubulin polymerization by at least 50% at 20 μM (Table 1 and Supplemental Figure S2). Most antiproliferative *N*-alkylated sulfonamides interfere to a greater or lesser extent with tubulin polymerization, with the highest effect shown by compound **45** (IC_{50} = 3.7 μM), with a benzyl group on the sulfonamide nitrogen, close to CA-4 (IC_{50} = 3 μM) and better than ABT-751 (IC_{50} = 4.4 μM). Compounds **38** and **42** showed moderate to good IC_{50} values of 10 and 12 μM, respectively.

The binding mode of the active compounds at the colchicine site of tubulin was studied by flexible docking studies. The protein conformational variability was represented by using 55 protein structures with different binding sites, as previously described [54,55]. Two frequently used docking programs with different scoring functions were used for the flexible docking of the ligands in the binding sites. Several thousand poses were generated for each ligand which were automatically classified according to their occupation of the subsites of the colchicine domain, and the poses with the best consensus scores were selected (Figure 5). The selected ligands bind in similar dispositions to combretastatin A-4, with a good overlap of the trimethoxyphenyl ring, which is inserted edgewise towards the surface of sheets S8 and S9 between the sidechains of Ala316β, Val318β, Ala354β, and covered by helices H7 and H8 and the H7-H8 loop and interacting with Cys241β, Leu242β, Leu248β, Ala250β, and Leu255β. The sulfonamide bridges are placed close to the olefin binding zone of CA-4, with the other aromatic ring behind helix H8 and above the sidechains of Ala316β and the methylenes of Lys352β, with the substituents on the sulfonamide nitrogen projecting towards a hydrophobic region of the interdimer interface, thus explaining the preference for small hydrophobic substituents such as methyl or cyanomethyl groups.

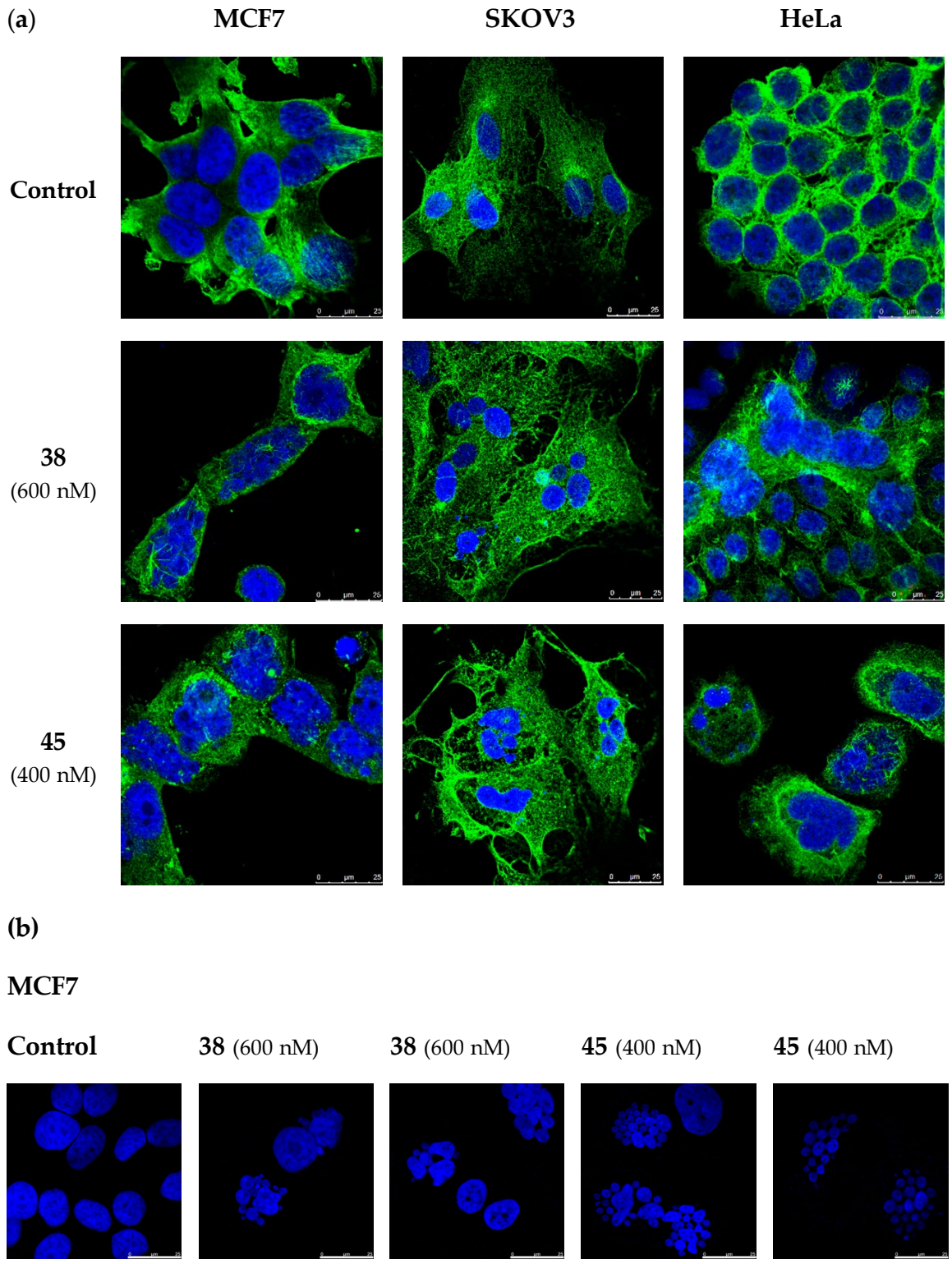

Figure 4. Confocal microscopy experiments in MCF7, SKOV3, and HeLa cells. Cells were incubated in the absence (Control) or the presence of **38** (600 nM) and **45** (400 nM) for 72 h. (**a**) Visualization of the microtubule network. α-Tubulin was stained in green, and nuclei were stained with DAPI (blue fluorescence). (**b**) Multilobulated nuclei (blue) resembling bunches of grapes in MCF7 cells. Photomicrographs are representative of three independent experiments. Scale bar: 25 μm.

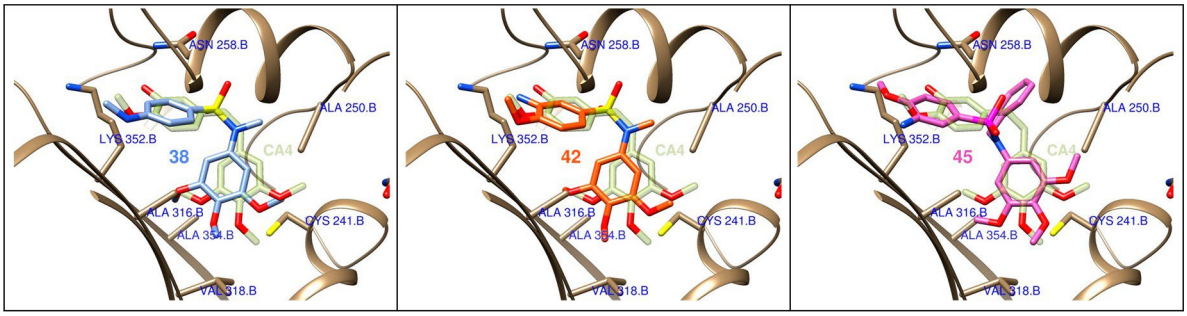

Figure 5. Docking poses for compounds **38**, **42**, and **45** at the colchicine site of tubulin. Combretastatin A-4 (**CA-4**) is shown in diffuse green as a reference.

3. Discussion

Taxanes—usually paclitaxel alone or in combination regimens—entail the first-line chemotherapy for breast and gynecological cancers [9,13,18,20]. However, limitations related to toxicity, pharmacokinetic problems, and the appearance of resistance [31] prompt the search for new treatments. This work has yielded a new family of tubulin inhibitors with a sulfonamide scaffold as hybrids of combretastatin A-4 and ABT-751, two colchicine site ligands in clinical trials that present shortcomings of opposite nature whose hybridization might alleviate (Figure 1).

Therefore, a focused library of sulfonamides was designed, and 52 representatives were synthesized following a synthetic methodology that involves first the assembly of the sulfonamide followed by functional group manipulations at different points of the main scaffold. A breadth of substituents was thus introduced to explore the chemical space for optimal pharmacokinetic and pharmacodynamic properties (Figure 1). One of the main drawbacks of taxanes and CA-4 is their low water solubility, making necessary drug administration as formulations with several associated adverse effects [27,28,47]. New sulfonamide derivatives show moderate to good solubilities (Table 2). Improvements up to 1700 times in solubility were found when compared with reference drugs paclitaxel and CA-4 and even surpass the solubility of the orally administered ABT-751 up to 42 times.

The antiproliferative activity of the synthesized compounds was evaluated against two Pan-Gyn representative human tumor cell lines (HeLa and MCF7) (Table 1). Many compounds showed growth inhibitory activities at submicromolar concentrations, thus validating the adequacy of the selected diarylsulfonamide scaffold. Most potent derivatives inhibited cell proliferation at very low drug concentrations, with IC_{50} values in the low to medium nanomolar range. Compounds **2a**, **29a**, **30**, **32**, **38**, and **42–45** display antiproliferative IC_{50} values comparable to those of paclitaxel and CA-4 and better than ABT-751, a tubulin colchicine-site inhibiting sulfonamide in clinical trials used as a reference [49]. Alkylation of the sulfonamide nitrogen significantly increases potency compared to the unsubstituted sulfonamides, probably due to a combination of a favoring of the *cisoid* disposition of both aromatic rings, an essential requirement for colchicine-site-binding drugs, with a more favorable interaction with the target [56]. Small alkyl groups, such as methyl or ethyl (e.g., **2a**, **29a**, **38**, or **42**), are usually preferred over longer chains such as carboxylic acid derivatives. All the modifications attempted on the trimethoxyphenyl ring abolished the activity, whereas the introduction of hydrogen bond donor amines on the B ring translated into more potent analogs, such as the secondary amines in the *para* position of the sulfonamide group (**38**) and the primary amines *ortho* to the methoxy group of B ring (**42–45**). Both modifications improve the polarity and aqueous solubility. The potency improvement suggests favorable hydrogen bonding with the target. Thus, B-ring amines improve both the pharmacokinetics and the pharmacodynamics.

The antiproliferative IC_{50} values of each compound against HeLa and MFC7 cell lines were quite similar, whereas the CA-4-resistant HT-29 cell line was less or at best equally sensitive to MDS (Supplementary Table S1). When differences in antiproliferative potencies

occur, they are not due to multidrug-resistance by the described moderate expression of MDR1 or MDR3 proteins in HT-29 colon carcinoma cell line [48,53,57], as only a handful of compounds experienced a potency increase in the presence of the Ppg/MDR1 inhibitor, verapamil [58]. Therefore, none of our lead compounds (**38**, **42**, and **45**) seemed to be MDR substrates and even compounds **38** and **42** overcame the resistance shown by CA-4 in the HT-29 cell line (IC_{50} = 59, 81, and 305 nM, respectively) (Table 4).

The microtubule disruption caused by the lead compounds in MCF7 cells winded up in the accumulation of cells in the G_2/M region (Figure 3a), as previously reported for CA-4 and ABT-751, used as references [59,60]. This sustained mitotic arrest lasted at least 72 h with percentages of cells showing DNA fragmentation below 12%. The mild response regarding this apoptotic marker is in line with the results observed in AnV/PI staining experiments (Table 5). Compounds **38** and **45** triggered phosphatidylserine exposure in 28–34% of MCF7 cells; 11% in the case of **42**. The lack of PI staining within the apoptotic population reveals the integrity of the plasma membrane in most Annexin V-positive cells. This slight apoptotic response might be related to the expression levels of caspase 3, the hub effector of the apoptotic machinery. MCF7 cells have been reported to be deficient in caspase 3 [61,62]. Despite MCF7 cells suffer a weak apoptotic response upon treatment with the lead compounds for 72 h, the percentage of early apoptotic cells increases after 6-day treatments, still preserving the integrity of the plasma membrane. This slow build-up of the apoptotic response in MCF7 cells may putatively rely on the other two effector caspases 6 and 7, as described for DNA damaging agents [11,63,64].

Lead compounds **38**, **42**, and **45** were then assayed against a panel of human ovarian tumor cell lines. Ovarian serous adenocarcinoma cell lines (SKOV3, OVCAR-8, and OVCAR-3), the most common type of ovarian cancer, were more sensitive than endometrioid cell lines (IGROV-1 and A2780). The metastatic cell line SKOV3 was found quite resistant to paclitaxel and CA-4 (IC_{50} of 81 and 380 nM [65], respectively) but was sensitive to MDS (Table 3). Time-course analysis of the cell cycle distribution (Figure 3b) showed a strong mitotic arrest for **42**, **38, and 45** 24 h after treatment. The mitotic arrest readily triggered apoptosis 48 h after treatment. Compound **45** elicits a higher $SubG_0/G_1$ population than **38** and **42** at 72 h. Dual staining experiments confirm the apoptotic response with Annexin V-positive cells at 72 h ranging from 14–36%, notably higher when compared with paclitaxel (7%).

Studies on the mechanism of action of MDS on the cervical cancer cell line HeLa were also performed (Figure 3c). After the common mitotic arrest at G_2/M phase 24 h after treatment (more pronounced for **38** and **45** than for **42**) HeLa cells exhibited strikingly high percentages of $SubG_0/G_1$ cells (around 50%) from 48 h after drug exposure. AnV/PI staining experiments revealed a strong and advanced apoptotic response with rates of double-positives cells above 82%, indicating the permeabilization of the plasma membrane. At this point, we wished to verify if the observed effect was due to the disruption of microtubule assembly. Tubulin immunofluorescence analysis of cells treated with compounds **38** and **45** revealed a clear disruption in the microtubule network (Figure 4a). Furthermore, as interference with microtubule dynamics is expected to affect chromatin organization, cell nuclei were stained with DAPI. Accumulation of multiple micronuclei characteristic of mitotic catastrophe was observed, widely linked to tubulin-binding drugs [66,67]. In vitro tubulin polymerization inhibition experiments confirmed the effect of the compounds on tubulin, and molecular docking experiments suggest a similar binding mode to that of CA-4 to the colchicine site of tubulin (Figure 5). However, no correlation was observed between TPI and antiproliferative IC_{50} values, as has previously been found for many tubulin polymerization inhibitors [68]. This discrepancy can be explained by an antiproliferative effect dependent on the alteration of microtubule dynamics and not on polymer mass, as measured in TPI assays.

In conclusion, a new family of MDS has been designed and synthesized. MDS antiproliferative effects against several representative cell lines of Pan-Gyn cancers have been studied. The effects of the compounds vary depending on the structural modifi-

cations, the most potent derivatives being those with a small alkyl substituent on the sulfonamide nitrogen. The molecular mechanism of action studies revealed a pronounced G_2/M arrest mainly followed by a $SubG_0/G_1$ increase over time. The different behavior between MCF7, SKOV3 and HeLa cells seems to be related to the rate at which each cell line builds up its apoptotic response to the initial unsolved mitotic arrest. Inhibition of tubulin polymerization in vitro was observed for most potent MDS, as well as disruption of microtubule network by immunofluorescence, probably by binding similarly to CA-4 to the colchicine site of tubulin. The improved aqueous solubility, lack of Pgp-mediated resistance, and antiproliferative potencies comparable to paclitaxel—first-line treatment of Pan-Gyn cancers—make MDS interesting for future application as antitumor agents.

4. Materials and Methods

4.1. Chemistry

4.1.1. Chemical Synthesis

Detailed synthetic procedures and characterization of compounds can be found in Supplemental methods SP1 and SP2.

4.1.2. Chemical Characterization of Lead MDS **38**, **42**, and **45**

MDS 38. M.p.: 147–150 °C (CH_2Cl_2/Hexane). IR (KBr): 3390, 1599, 1502, 835 cm^{-1}. ^1H NMR (400 MHz, $CDCl_3$): δ 2.83 (3H, *s*), 3.07 (3H, *s*), 3.71 (6H, *s*), 3.80 (3H, *s*), 6.28 (2H, *s*), 6.51 (2H, *d, J* = 8.8), 7.35 (2H, *d, J* = 8.8). ^{13}C NMR (100 MHz, $CDCl_3$): δ 30.0 (CH_3), 38.4 (CH_3), 56.1 ($2CH_3$), 60.8 (CH_3), 104.6 (2CH), 110.8 (2CH), 122.6 (C), 130.0 (2CH), 137.2 (C), 137.8 (C), 152.7 (C), 152.8 (2C). HRMS ($C_{17}H_{22}N_2O_5S + H^+$): calcd 367.1322 ($M + H^+$), found 367.1325.

MDS 42. M.p.: 124–126 °C (MeOH). ^1H NMR (400 MHz, $CDCl_3$): δ 3.11 (3H, *s*), 3.73 (6H, *s*), 3.83 (3H, *s*), 3.90 (3H, *s*), 3.94 (2H, *s*), 6.30 (2H, *s*), 6.78 (1H, *d, J* = 8.8), 6.90 (1H, *d, J* = 2.4), 6.99 (1H, *dd, J* = 8.8 and 2.4). ^{13}C NMR (50 MHz, $CDCl_3$): δ 38.5 (CH_3), 55.7 (CH_3), 56.0 ($2CH_3$), 60.8 (CH_3), 104.6 (2CH), 109.1 (CH), 113.2 (CH), 118.8 (CH), 128.0 (C), 136.5 (C), 137.3 (C), 137.7 (C), 150.2 (C), 152.8 (2C). HRMS ($C_{17}H_{22}N_2O_6S + H^+$): calcd 383.1271 ($M + H^+$), found 383.1263.

MDS 45. ^1H NMR (200 MHz, $CDCl_3$): δ 3.63 (6H, *s*), 3.78 (3H, *s*), 3.93 (3H, *s*), 4.63 (2H, *s*), 6.14 (2H, *s*), 6.83 (1H, *d, J* = 8.4), 7.02 (1H, *d, J* = 2), 7.11 (1H, *dd, J* = 8.4 and 2), 7.23 (5H, *bs*). ^{13}C NMR (100 MHz, $CDCl_3$): δ 55.3 (CH_2), 55.8 (CH_3), 55.9 ($2CH_3$), 60.8 (CH_3), 106.7 (2CH), 109.3 (CH), 113.1 (CH), 118.8 (CH), 127.6 (CH), 128.3 (2CH), 128.7 (2CH), 130.5 (C), 134.9 (C), 136.2 (C), 136.6 (C), 137.6 (C), 150.3 (C), 152.7 (2C). HRMS ($C_{23}H_{26}N_2O_6S + H^+$): calcd 459.1584 ($M + H^+$), found 459.1589.

4.1.3. Aqueous Solubility

The aqueous solubility of the sulfonamides was determined using an approach based on the saturation shake-flask method. Tested compounds (1–2 mg) were stirred in pH 7.0 phosphate buffer (300 µL) for 48 h at room temperature. The resulting suspension was filtered over a 45 µm filter to discard insoluble residues, and the concentration in the supernatant was measured by UV absorbance. To determine the concentration, a scan between 270 and 400 nm was performed in a Helios-α UV-320 Spectrophotometer (Thermo-Spectronic, Thermo Fischer Scientific, Waltham, MA, USA) for each tested compound. Then, three maximum wavelengths of absorbance per compound were selected from the previous scan and calibration curves were performed at these three wavelengths. Solubility results are given as the average of the three measurements.

4.2. Biological Evaluation

4.2.1. Cell Lines and Cell Culture Conditions

MCF7 (human breast carcinoma), SKOV-3 (human ovarian carcinoma), OVCAR-3 (human ovarian carcinoma), OVCAR-8 (human ovarian carcinoma), and HeLa (human cervical carcinoma) cell lines were cultured in Dulbecco's Modified Eagle's Medium (DMEM)

(Gibco, Thermo Fischer Scientific) containing 10% (*v*/*v*) heat-inactivated fetal bovine serum (HIFBS) (Lonza-Cambrex, Karlskoga, Sweden), 2 mM L-glutamine (Lonza-Cambrex, Karlskoga, Sweden), 100 µg/mL streptomycin, and 100 IU/mL penicillin (Lonza-Cambrex) at 37 °C in humidified 95% air and 5% CO_2. HT-29 (human colon carcinoma), IGROV-1 (human ovarian carcinoma), and A2780 (human ovarian carcinoma) cell lines were cultured in RPMI 1640 medium (Gibco, Thermo Fischer Scientific) supplemented with 10% HIFBS, 100 µg/mL streptomycin, and 100 IU/mL penicillin at 37 °C in humidified 95% air and 5% CO_2 atmosphere. The presence of mycoplasma was routinely checked with MycoAlert kit (Lonza-Cambrex) and only mycoplasma-free cells were used in the experiments. Ovarian tumor cell lines were originally acquired from Dr Atanasio Pandiella from Centro de Investigación del Cáncer (CIC), Salamanca, Spain. HeLa, HT-29 and MCF7 tumor cell lines were provided by Dr Faustino Mollinedo from Centro de Investigaciones Biológicas Margarita Salas, Madrid, Spain.

4.2.2. Cell Proliferation Assay

MCF7, HeLa, and HT-29 cell proliferation, when treated with the corresponding compounds, were determined using the XTT (sodium 3′-[1(phenylaminocarbonyl)-3,4-tetrazolium]-bis(4-methoxy-6-nitro)-benzenesulfonic acid hydrate) cell proliferation kit (Roche Molecular Biochemicals, Mannheim, Germany). A freshly prepared mixture of XTT labeling reagent with 0.02% (*v*/*v*) PMS (*N*-methyl-dibenzopyrazine methyl sulfate) electron coupling reagent was added to cells (50 µL/well in 96-well plates, total volume of 160 µL/well). Cells were incubated under standard culture conditions for 4 h (MCF7 and HeLa) or 6 h (HT-29). The absorbance of the formazan product generated was measured at 450 nm using a multi-well plate reader. SKOV-3, OVCAR-3, OVCAR-8, IGROV-1, A-2780 cell proliferation, when treated with the corresponding compound, were determined using MTT (3-(4,5-dimethylthiazol-2-yl)-2,5-diphenyl-2*H*-tetrazolium bromide) (Sigma-Aldrich, St. Louis, MO, USA). MTT in Phosphate Buffer Saline (PBS) (5 mg/ml) was added to cells (110 µL/well in 24-well plates, total volume of 1110 µL/well). After 1 hour of incubation, the medium was aspirated, and formazan violet crystals were dissolved in dimethyl sulfoxide (DMSO) (500 µL/well). Absorbance was measured at 570 nm in a plate reader (Ultra Evolution, Tecan, Männedorf, Suiza). To determine cell viability, cells in exponential growth phase were seeded (100 µL/well in 96-well plates and 1000 µL/well in 24-well plates) with appropriate cell line concentration ($1.5 \cdot 10^4$ cells/mL for MCF7 and HeLa, $3 \cdot 10^4$ cells/mL for HT-29, and 1 10^4 cells/mL for SKOV-3, OVCAR-3, OVCAR-8, IGROV-1, and A-2780) in complete RPMI 1640 or DMEM medium at 37°C and 5% CO_2 atmosphere. After 24 h incubation, to allow cells to attach to the plates, all compounds were added at 1 µM concentration and the effect on the proliferation was evaluated 72 h post-treatment. Compounds showing antiproliferative effects at tested concentration were selected for IC_{50} calculation (50% inhibitory concentration with respect to the untreated controls) from 10^{-5} to 10^{-10} M concentration. Non-linear curves fitting the experimental data were carried out for each compound. Compounds were dissolved in DMSO and the final solvent concentrations never exceeded 0.5% (*v*/*v*). The control wells included treated cells with 0.5% (*v*/*v*) DMSO and the positive control. 10 µM verapamil was included as a control for the HT-29 cell line. Measurements were performed in triplicate, and each experiment was repeated three times.

4.2.3. Cell Cycle Analysis

Cell cycle analysis was performed in MCF7, SKOV-3, and HeLa cells by quantifying the DNA content by flow cytometry. Cells in the exponential growth phase at $2 \cdot 10^4$ cells/mL were seeded in 24-well plates (1 mL/well). After 24 h incubation, cells were treated with different concentrations of the selected compounds and the effect of treated and untreated cells was measured 24, 48, and 72 h post-treatment. Live and dead cells were collected and fixed in ice-cold ethanol/PBS (7:3) and stored at 4 °C for later use. Cells were rehydrated with PBS, treated with 100 µg/mL RNase A (Sigma-Aldrich Co., St. Louis, MO, USA) and

stained overnight in darkness at room temperature with 50 µg/mL PI (Sigma-Aldrich Co.). Cell cycle profiles were then analyzed by flow cytometry using BD Accuri™ C6 Plus Flow Cytometer (BD Biosciences, San José, CA, USA). Data were analyzed with BD Accuri™ C6 Software (version 1.0.264.21, BD Biosciences, San José, CA, USA) and compared to control cells. Compounds were dissolved in DMSO and the final solvent concentration never exceeded 0.5% (*v*/*v*). Control wells included cells with 0.5% (*v*/*v*) DMSO.

4.2.4. Apoptotic Cell Death Quantification

MCF7, SKOV-3, and HeLa apoptotic cells were quantified using an Annexin V-FITC/PI apoptosis detection kit (Immunostep, Salamanca, Spain) according to the manufacturer's guidelines. 1.5 mL/well of cells in the exponential growth phase at $2 \cdot 10^4$ cells/mL were seeded onto 12-well plates and left to attach overnight. After 24 h incubation, cells were treated with selected compounds. After 72 h (MCF7, SKOV-3, and HeLa) and 6 days (MCF7) post-treatment, attached and floating cells of treated and untreated wells were collected, centrifuged, resuspended in Annexin V binding buffer, and stained with Annexin V-FITC/PI. Cells were then incubated in darkness at room temperature for 15 min and a total of 30,000 cells were acquired and analyzed using the BD Accuri™ C6 Plus Flow Cytometer and Software (version 1.0.264.21, BD Biosciences, San José, CA, USA), respectively. Compounds were dissolved in DMSO and the final solvent concentration never exceeded 0.5% (*v*/*v*). Control wells included cells with 0.5% (*v*/*v*) DMSO.

4.2.5. Immunofluorescence

MCF7, SKOV-3, and HeLa cells were grown on glass coverslips coated with poly-L-lysine (12 mm diameter). To reach appropriate cell confluence, coverslips were manipulated in 6-well plates (3 coverslips/well) seeding 3 mL/well of cells in the exponential growth phase at 2×10^4 cells/mL. After 24 h incubation, cells were treated with selected compounds and incubated for 72 h. Cells were washed with PBS, fixed with 4% formaldehyde in PBS for 10 min, permeabilized with 0.5% Triton X-100 (Boehringer Mannheim, Ingelheim am Rhein, Germany) in PBS for 10 min and blocked with 10% BSA in PBS for 30 min. Microtubule detection was performed by incubation with anti-α-tubulin mouse monoclonal antibody (1:200 in 3% BSA/PBS) (Sigma-Aldrich) for 1.5 h. After PBS washing, coverslips were incubated with fluorescent secondary antibody Alexa Fluor 488 goat anti-mouse IgG (1:400 in 1% BSA/PBS) (Molecular Probes, Invitrogen, Thermo Fischer Scientific) for 1 h in darkness. After being washed with PBS, cell nuclei were stained with DAPI (dihydrochloride of 4′,6-diamidino-2-phenylindole) (diluted 1:10,000 in mq H_2O) (Roche, Basel, Switzerland) for 5 min in darkness. DAPI excess was removed by washing with PBS. Mowiol reagent (Calbiochem, Sigma-Aldrich) was used to mount preparations on slides. Cells were analyzed by confocal microscopy using a LEICA SP5 microscope DMI-6000V model coupled to a LEICA LAS AF software computer.

4.2.6. Tubulin Isolation

Microtubular protein was isolated from calf brain according to the modified Shelanski method [69,70] by two cycles of temperature-dependent assembly/disassembly and stored at −80 °C. Before each use, protein concentration was determined by the Bradford method [71] taking BSA as standard.

4.2.7. Tubulin Polymerization Inhibition (TPI) Assay

Tubulin polymerization was monitored using a Helios α spectrophotometer by measuring the increase in turbidity at 450 nm, caused by a shift from 4 °C to 37 °C, which allows the in vitro microtubular protein to depolymerize and polymerize, respectively. The assay was carried out in quartz cuvettes containing 1.5 mg/mL microtubular protein and the ligand (except for control cuvette with only DMSO at the same concentration) in a mixture of 0.1 M MES buffer, 1 mM EGTA, 1 mM $MgCl_2$, 1 mM β-ME, and 1.5 mM GTP at pH 6.7 (final volume 500 µL). Cuvettes were preincubated at 20 °C for 30 min, to allow

ligand binding to tubulin, and subsequently cooled on ice for 10 min. Then, the experiment starts at 4 °C to establish the initial baseline. The assembly process was initiated by a temperature shift to 37 °C and the turbidity produced by tubulin polymerization can be measured by an absorbance increase. After reaching a stable plateau, the temperature was switched back to 4 °C to return to the initial absorption values (to confirm the reversible nature of the monitored process and to determine whether or not the microtubular tubular protein has stabilized). The difference in amplitude between the stable plateau and the initial baseline of the curves was taken as the degree of tubulin polymerization for each experiment. Comparison with control curves under identical conditions but without ligands yielded TPI as a percentage value. All compounds were tested at 10 μM concentration. Compounds that inhibited tubulin polymerization by at least 30% at 10 μM were tested at 20 μM. IC_{50} values were calculated for compounds that inhibit tubulin polymerization by more than 50% at 20 μM. Compounds were dissolved in DMSO, and the final solvent concentration never exceeded 4% (*v*/*v*), which has been reported not to interfere with the assembly process. All the measurements were carried out in at least two independent experiments using microtubular protein from different preparations.

4.3. Computational Studies

Docking studies were carried out as previously described [45]. Briefly, dockings were performed in parallel with PLANTS [72] with default settings and 10 runs per ligand and with AutoDock 4.2 [73] runs applying the Lamarckian genetic algorithm (LGA) 100−300 times for a maximum of 2.5 10^6 energy evaluations, 150 individuals, and 27,000 generations maximum. The retrieved poses were automatically assigned to the colchicine subzones using in-house KNIME pipelines [74]. The programs' docking scores were converted into Z-scores and the poses with best consensus scores were selected as the docking results. Docked poses were analyzed with Chimera [75], Marvin [76], OpenEye [77], and JADOPPT [78].

Supplementary Materials: The following are available online at https://www.mdpi.com/1422-0067/22/4/1907/s1, Figure S1: Synthetic procedures of new Microtubule Destabilizing Sulfonamides, Table S1: Antiproliferative activity against HT-29 and sensitivity to MDR pumps, Figure S2: Tubulin Polymerization Assay data. IC_{50} calculation, Methods SP1: Chemistry. General chemical techniques and chemical synthesis, Methods SP2: ^{1}H NMR and ^{13}C NMR spectra

Author Contributions: Conceptualization, M.G. and R.P.; Data curation, M.G. and R.P.; Formal analysis, M.G., M.O.-S., A.V.-B. and A.B.H.; Funding acquisition, R.G.-S. and R.P. Investigation, R.Á., M.M., R.G.-S. and R.P.; Methodology, M.G. and M.O.-S.; Project administration, R.G.-S. and R.P.; Resources, R.G.-S. and R.P.; Software, R.P.; Supervision, R.G.-S. and R.P.; Validation, M.M., R.G.-S. and R.P.; Visualization, M.G. and M.O.-S.; Writing—original draft, M.G.; Writing—review and editing, A.V.-B., A.B.H., M.M., R.G.-S. and R.P.; All authors have read and agreed to the published version of the manuscript.

Funding: This research was funded by the Consejería de Educación de la Junta de Castilla y León (SA030U16, SA262P18 and SA116P20), co-funded by the EU's European Regional Development Fund-FEDER, the Spanish Ministry of Science, Innovation and Universities (RTI2018-099474-BI00) and the health research program of the Instituto de Salud Carlos III (Spanish Ministry of Economy and Competitiveness, PI16/01920 and PI20/01569) co-funded with FEDER founds.

Institutional Review Board Statement: Not applicable.

Informed Consent Statement: Not applicable.

Data Availability Statement: The data that support the findings of this study are available from the corresponding author upon reasonable request.

Acknowledgments: We thank the people at Frigoríficos Salamanca S.A slaughterhouse for providing us with the calf brains, "Servicio General de NMR" and "Servicio General de Espectrofotometría de Masas" of the University of Salamanca for equipment. M.G. acknowledges a predoctoral fellowship from the Junta de Castilla y León (ORDEN EDU/529/2017 de 26 de junio). M.O.-S. acknowledges

a predoctoral fellowship from the IBSAL (IBpredoc17/00010). A.V.-B. acknowledges a predoctoral fellowship from the Spanish Ministerio de Educación, Cultura y Deporte (FPU15/02457).

Conflicts of Interest: The authors declare no conflict of interest.

References

1. Berger, A.C.; Korkut, A.; Kanchi, R.S.; Hegde, A.M.; Lenoir, W.; Liu, W.; Liu, Y.; Fan, H.; Shen, H.; Ravikumar, V.; et al. A Comprehensive Pan-Cancer Molecular Study of Gynecologic and Breast Cancers. *Cancer Cell* **2018**, *33*, 690–705.e9. [CrossRef] [PubMed]
2. Hoadley, K.A.; Yau, C.; Hinoue, T.; Wolf, D.M.; Lazar, A.J.; Drill, E.; Shen, R.; Taylor, A.M.; Cherniack, A.D.; Thorsson, V.; et al. Cell-of-Origin Patterns Dominate the Molecular Classification of 10,000 Tumors from 33 Types of Cancer. *Cell* **2018**, *173*, 291–304.e6. [CrossRef] [PubMed]
3. Bray, F.; Ferlay, J.; Soerjomataram, I.; Siegel, R.L.; Torre, L.A.; Jemal, A. Global cancer statistics 2018: GLOBOCAN estimates of incidence and mortality worldwide for 36 cancers in 185 countries. *CA. Cancer J. Clin.* **2018**, *68*, 394–424. [CrossRef]
4. Rivera, E.; Gomez, H. Chemotherapy resistance in metastatic breast cancer: The evolving role of ixabepilone. *Breast Cancer Res.* **2010**, *12*, S2. [CrossRef] [PubMed]
5. Gonzalez-Angulo, A.M.; Morales-Vasquez, F.; Hortobagyi, G.N. Overview of Resistance to Systemic Therapy in Patients with Breast Cancer. In *Breast Cancer Chemosensitivity*; Madame Curie Biosci. Database; Springer: Berlin/Heidelberg, Germany, 2013.
6. Agarwal, R.; Kaye, S.B. Ovarian cancer: Strategies for overcoming resistance to chemotherapy. *Nat. Rev. Cancer* **2003**, *3*, 502–516. [CrossRef] [PubMed]
7. Pokhriyal, R.; Hariprasad, R.; Kumar, L.; Hariprasad, G. Chemotherapy Resistance in Advanced Ovarian Cancer Patients. *Biomark. Cancer* **2019**, *11*, 1179299X1986081. [CrossRef] [PubMed]
8. Chaudhry, P.; Asselin, E. Resistance to chemotherapy and hormone therapy in endometrial cancer. *Endocr. Relat. Cancer* **2009**, *16*, 363–380. [CrossRef] [PubMed]
9. Moxley, K.M.; McMeekin, D.S. Endometrial Carcinoma: A Review of Chemotherapy, Drug Resistance, and the Search for New Agents. *Oncologist* **2010**, *15*, 1026–1033. [CrossRef]
10. U.S. Food and Drug Administration. Available online: https://www.fda.gov/ (accessed on 27 May 2020).
11. Ofir, R.; Seidman, R.; Rabinski, T.; Krup, M.; Yavelsky, V.; Weinstein, Y.; Wolfson, M. Taxol-induced apoptosis in human SKOV3 ovarian and MCF7 breast carcinoma cells is caspase-3 and caspase-9 independent. *Cell Death Differ.* **2002**, *9*, 636–642. [CrossRef]
12. Jayson, G.C.; Kohn, E.C.; Kitchener, H.C.; Ledermann, J.A. Ovarian cancer. *Lancet* **2014**, *384*, 1376–1388. [CrossRef]
13. McGuire, W.P.; Markman, M. Primary ovarian cancer chemotherapy: Current standards of care. *Br. J. Cancer* **2003**, *89*, S3–S8. [CrossRef]
14. Bicaku, E.; Xiong, Y.; Marchion, D.C.; Chon, H.S.; Stickles, X.B.; Chen, N.; Judson, P.L.; Hakam, A.; Gonzalez-Bosquet, J.; Wenham, R.M.; et al. In vitro analysis of ovarian cancer response to cisplatin, carboplatin, and paclitaxel identifies common pathways that are also associated with overall patient survival. *Br. J. Cancer* **2012**, *106*, 1967–1975. [CrossRef] [PubMed]
15. Ozols, R.F.; Bundy, B.N.; Greer, B.E.; Fowler, J.M.; Clarke-Pearson, D.; Burger, R.A.; Mannel, R.S.; DeGeest, K.; Hartenbach, E.M.; Baergen, R.; et al. Phase III trial of carboplatin and paclitaxel compared with cisplatin and paclitaxel in patients with optimally resected stage III ovarian cancer: A Gynecologic Oncology Group study. *J. Clin. Oncol.* **2003**, *21*, 3194–3200. [CrossRef] [PubMed]
16. Ghersi, D.; Wilcken, N.; Simes, R.J. A systematic review of taxane-containing regimens for metastatic breast cancer. *Br. J. Cancer* **2005**, *93*, 293–301. [CrossRef] [PubMed]
17. Friedrichs, K.; Hölzel, F.; Jänicke, F. Combination of taxanes and anthracyclines in first-line chemotherapy of metastatic breast cancer: An interim report. *Eur. J. Cancer* **2002**, *38*, 1730–1738. [CrossRef]
18. Telli, M.L.; Carlson, R.W. First-line chemotherapy for metastatic breast cancer. *Clin. Breast Cancer* **2009**, *9*, S66–S72. [CrossRef] [PubMed]
19. Piccart-Gebhart, M.J.; Burzykowski, T.; Buyse, M.; Sledge, G.; Carmichael, J.; Lück, H.J.; Mackey, J.R.; Nabholtz, J.M.; Paridaens, R.; Biganzoli, L.; et al. Taxanes alone or in combination with anthracyclines as first-line therapy of patients with metastatic breast cancer. *J. Clin. Oncol.* **2008**, *26*, 1980–1986. [CrossRef] [PubMed]
20. Pectasides, D.; Pectasides, E.; Economopoulos, T. Systemic therapy in metastatic or recurrent endometrial cancer. *Cancer Treat. Rev.* **2007**, *33*, 177–190. [CrossRef] [PubMed]
21. Serkies, K.; Jassem, J. Systemic therapy for cervical carcinoma—Current status. *Chin. J. Cancer Res.* **2018**, *30*, 209–221. [CrossRef]
22. Boussios, S.; Seraj, E.; Zarkavelis, G.; Petrakis, D.; Kollas, A.; Kafantari, A.; Assi, A.; Tatsi, K.; Pavlidis, N.; Pentheroudakis, G. Management of patients with recurrent/advanced cervical cancer beyond first line platinum regimens: Where do we stand? A literature review. *Crit. Rev. Oncol. Hematol.* **2016**, *108*, 164–174. [CrossRef] [PubMed]
23. Konno, T.; Watanabe, J.; Ishihara, K. Enhanced solubility of paclitaxel using water-soluble and biocompatible 2-methacryloyloxyethyl phosphorylcholine polymers. *J. Biomed. Mater. Res. Part A* **2003**, *65*, 209–214. [CrossRef]
24. Hamada, H.; Ishihara, K.; Masuoka, N.; Mikuni, K.; Nakajima, N. Enhancement of water-solubility and bioactivity of paclitaxel using modified cyclodextrins. *J. Biosci. Bioeng.* **2006**, *102*, 369–371. [CrossRef] [PubMed]
25. Yang, T.; Cui, F.-D.; Choi, M.-K.; Lin, H.; Chung, S.-J.; Shim, C.-K.; Kim, D.-D. Liposome Formulation of Paclitaxel with Enhanced Solubility and Stability. *Drug Deliv.* **2007**, *14*, 301–308. [CrossRef] [PubMed]
26. Eric, K.; Rowinsky, M.D.; Ross, C.; Donehower, M.D. Paclitaxel (Taxol®). *N. Engl. J. Med.* **1995**, *332*, 1004–1014. [CrossRef]

27. Hennenfent, K.L.; Govindan, R. Review Novel formulations of taxanes: A review. Old wine in a new bottle? *Ann. Oncol.* **2006**, *17*, 735–749. [CrossRef] [PubMed]
28. Ten Tije, A.J.; Verweij, J.; Loos, W.J.; Sparreboom, A. Pharmacological effects of formulation vehicles: Implications for cancer chemotherapy. *Clin. Pharmacokinet.* **2003**, *42*, 665–685. [CrossRef] [PubMed]
29. Weiss, R.B. Hypersensitivity reactions from taxol. *J. Clin. Oncol.* **1990**, *8*, 1263–1268. [CrossRef] [PubMed]
30. Gligorov, J.; Lotz, J.P. Preclinical Pharmacology of the Taxanes: Implications of the Differences. *Oncologist* **2004**, *9*, 3–8. [CrossRef] [PubMed]
31. Orr, G.A.; Verdier-Pinard, P.; McDaid, H.; Horwitz, S.B. Mechanisms of Taxol resistance related to microtubules. *Oncogene* **2003**, *22*, 7280–7295. [CrossRef]
32. Kavallaris, M. Microtubules and resistance to tubulin-binding agents. *Nat. Rev. Cancer* **2010**, *10*, 194–204. [CrossRef] [PubMed]
33. Yusuf, R.; Duan, Z.; Lamendola, D.; Penson, R.; Seiden, M. Paclitaxel Resistance: Molecular Mechanisms and Pharmacologic Manipulation. *Curr. Cancer Drug Targets* **2003**, *3*, 1–19. [CrossRef] [PubMed]
34. Murray, S.; Briasoulis, E.; Linardou, H.; Bafaloukos, D.; Papadimitriou, C. Taxane resistance in breast cancer: Mechanisms, predictive biomarkers and circumvention strategies. *Cancer Treat. Rev.* **2012**, *38*, 890–903. [CrossRef] [PubMed]
35. Tommasi, S.; Mangia, A.; Lacalamita, R.; Bellizzi, A.; Fedele, V.; Chiriatti, A.; Thomssen, C.; Kendzierski, N.; Latorre, A.; Lorusso, V.; et al. Cytoskeleton and paclitaxel sensitivity in breast cancer: The role of β-tubulins. *Int. J. Cancer* **2007**, *120*, 2078–2085. [CrossRef] [PubMed]
36. Chong, T.; Sarac, A.; Yao, C.Q.; Liao, L.; Lyttle, N.; Boutros, P.C.; Bartlett, J.M.S.; Spears, M. Deregulation of the spindle assembly checkpoint is associated with paclitaxel resistance in ovarian cancer. *J. Ovarian Res.* **2018**, *11*, 27. [CrossRef] [PubMed]
37. Kavallaris, M.; Kuo, D.Y.S.; Burkhart, C.A.; Regl, D.L.; Norris, M.D.; Haber, M.; Horwitz, S.B. Taxol-resistant epithelial ovarian tumors are associated with altered expression of specific β-tubulin isotypes. *J. Clin. Investig.* **1997**, *100*, 1282–1293. [CrossRef] [PubMed]
38. Peng, X.; Gong, F.; Chen, Y.; Jiang, Y.; Liu, J.; Yu, M.; Zhang, S.; Wang, M.; Xiao, G.; Liao, H. Autophagy promotes paclitaxel resistance of cervical cancer cells: Involvement of Warburg effect activated hypoxia-induced factor 1-α-mediated signaling. *Cell Death Dis.* **2014**, *5*, 1–11. [CrossRef]
39. Horwitz, S.B.; Lothstein, L.; Manfredi, J.J.; Mellado, W.; Parness, J.; Roy, S.N.; Schiff, P.B.; Sorbara, L.; Zeheb, R. Taxol: Mechanisms of Action and Resistance. *Ann. New York Acad. Sci.* **1986**, *466*, 733–744. [CrossRef]
40. Schiff, P.B.; Fant, J.; Horwitz, S.B. Promotion of microtubule assembly in vitro by taxol. *Nature* **1979**, *277*, 665–667. [CrossRef] [PubMed]
41. Dumontet, C.; Jordan, M.A. Microtubule-binding agents: A dynamic field of cancer therapeutics. *Nat. Rev. Drug Discov.* **2010**, *9*, 790–803. [CrossRef]
42. Mollinedo, F.; Gajate, C. Microtubules, microtubule-interfering agents and apoptosis. *Apoptosis* **2003**, *8*, 413–450. [CrossRef]
43. Vicente-Blázquez, A.; González, M.; Álvarez, R.; del Mazo, S.; Medarde, M.; Peláez, R. Antitubulin sulfonamides: The successful combination of an established drug class and a multifaceted target. *Med. Res. Rev.* **2019**, *39*, 775–830. [CrossRef] [PubMed]
44. Lee, C.-T.; Huang, Y.-W.; Yang, C.-H.; Huang, K.-S. Drug Delivery Systems and Combination Therapy by Using Vinca Alkaloids. *Curr. Top. Med. Chem.* **2015**, *15*, 1491–1500. [CrossRef]
45. Álvarez, R.; Aramburu, L.; Gajate, C.; Vicente-Blázquez, A.; Mollinedo, F.; Medarde, M.; Peláez, R. Potent colchicine-site ligands with improved intrinsic solubility by replacement of the 3,4,5-trimethoxyphenyl ring with a 2-methylsulfanyl-6-methoxypyridine ring. *Bioorg. Chem.* **2020**, *98*, 103755. [CrossRef]
46. Lee, R.M.; Gewirtz, D.A. Colchicine site inhibitors of microtubule integrity as vascular disrupting agents. *Drug Dev. Res.* **2008**, *69*, 352–358. [CrossRef]
47. Tron, G.C.; Pirali, T.; Sorba, G.; Pagliai, F.; Busacca, S.; Genazzani, A.A. Medicinal chemistry of combretastatin A4: Present and future directions. *J. Med. Chem.* **2006**, *49*, 3033–3044. [CrossRef] [PubMed]
48. Cummings, J.; Zelcer, N.; Allen, J.D.; Yao, D.; Boyd, G.; Maliepaard, M.; Friedberg, T.H.; Smyth, J.F.; Jodrell, D.I. Glucuronidation as a mechanism of intrinsic drug resistance in colon cancer cells: Contribution of drug transport proteins. *Biochem. Pharmacol.* **2004**, *67*, 31–39. [CrossRef] [PubMed]
49. ABT-751 ClinicalTrials.gov. Available online: https://clinicaltrials.gov/ (accessed on 21 May 2020).
50. Seddigi, Z.S.; Malik, M.S.; Saraswati, A.P.; Ahmed, S.A.; Babalghith, A.O.; Lamfon, H.A.; Kamal, A. Recent advances in combretastatin based derivatives and prodrugs as antimitotic agents. *Medchemcomm* **2017**, *8*, 1592–1603. [CrossRef] [PubMed]
51. Chaudhary, A.; Pandeya, S.; Kumar, P.; Sharma, P.; Gupta, S.; Soni, N.; Verma, K.; Bhardwaj, G. Combretastatin A-4 Analogs as Anticancer Agents. *Mini Rev. Med. Chem.* **2007**, *7*, 1186–1205. [CrossRef] [PubMed]
52. Liebmann, J.E.; Cook, J.A.; Lipschultz, C.; Teague, D.; Fisher, J.; Mitchell, J.B. Cytotoxic studies of paclitaxel (Taxol®) in human tumour cell lines. *Br. J. Cancer* **1993**, *68*, 1104–1109. [CrossRef] [PubMed]
53. Naret, T.; Khelifi, I.; Provot, O.; Bignon, J.; Levaique, H.; Dubois, J.; Souce, M.; Kasselouri, A.; Deroussent, A.; Paci, A.; et al. 1,1-Diheterocyclic Ethylenes Derived from Quinaldine and Carbazole as New Tubulin-Polymerization Inhibitors: Synthesis, Metabolism, and Biological Evaluation. *J. Med. Chem.* **2019**, *62*, 1902–1916. [CrossRef]
54. Alvarez, R.; Medarde, M.; Pelaez, R. New Ligands of the Tubulin Colchicine Site Based on X-Ray Structures. *Curr. Top. Med. Chem.* **2014**, *14*, 2231–2252. [CrossRef] [PubMed]

55. Goodsell, D.S.; Zardecki, C.; Di Costanzo, L.; Duarte, J.M.; Hudson, B.P.; Persikova, I.; Segura, J.; Shao, C.; Voigt, M.; Westbrook, J.D.; et al. RCSB Protein Data Bank: Enabling biomedical research and drug discovery. *Protein Sci.* **2020**, *29*, 52–65. [CrossRef] [PubMed]
56. Nguyen, T.L.; McGrath, C.; Hermone, A.R.; Burnett, J.C.; Zaharevitz, D.W.; Day, B.W.; Wipf, P.; Hamel, E.; Gussio, R. A common pharmacophore for a diverse set of colchicine site inhibitors using a structure-based approach. *J. Med. Chem.* **2005**, *48*, 6107–6116. [CrossRef] [PubMed]
57. Schobert, R.; Effenberger-Neidnicht, K.; Biersack, B. Stable combretastatin A-4 analogues with sub-nanomolar efficacy against chemoresistant HT-29 cells. *Int. J. Clin. Pharmacol. Ther.* **2011**, *49*, 71–72. [CrossRef] [PubMed]
58. Sharom, F.J. The P-glycoprotein multidrug transporter. *Essays Biochem.* **2011**, *50*, 161–178. [CrossRef]
59. Wei, R.J.; Lin, S.S.; Wu, W.R.; Chen, L.R.; Li, C.F.; De Chen, H.; Chou, C.T.; Chen, Y.C.; Liang, S.S.; Chien, S.T.; et al. A microtubule inhibitor, ABT-751, induces autophagy and delays apoptosis in Huh-7 cells. *Toxicol. Appl. Pharmacol.* **2016**, *311*, 88–98. [CrossRef] [PubMed]
60. Kanthou, C.; Greco, O.; Stratford, A.; Cook, I.; Knight, R.; Benzakour, O.; Tozer, G. The tubulin-binding agent combretastatin A-4-phosphate arrests endothelial cells in mitosis and induces mitotic cell death. *Am. J. Pathol.* **2004**, *165*, 1401–1411. [CrossRef]
61. Jänicke, R.U.; Sprengart, M.L.; Wati, M.R.; Porter, A.G. Caspase-3 is required for DNA fragmentation and morphological changes associated with apoptosis. *J. Biol. Chem.* **1998**, *273*, 9357–9360. [CrossRef]
62. Yang, X.H.; Sladek, T.L.; Liu, X.; Butler, B.R.; Froelich, C.J.; Thor, A.D. Reconstitution of caspase 3 sensitizes MCF-7 breast cancer cells to doxorubicin- and etoposide-induced apoptosis. *Cancer Res.* **2001**, *61*, 348–354. [PubMed]
63. Walker, P.R.; Leblanc, J.; Carson, C.; Ribecco, M.; Sikorska, M. Neither Caspase-3 nor DNA Fragmentation Factor Is Required for High Molecular Weight DNA Degradation in Apoptosis. *Ann. N. Y. Acad. Sci.* **1999**, *887*, 48–59. [CrossRef]
64. Kagawa, S.; Gu, J.; Honda, T.; McDonnell, T.J.; Swisher, S.G.; Roth, J.A.; Fang, B. Deficiency of caspase-3 in MCF7 cells blocks Bax-mediated nuclear fragmentation but not cell death. *Clin. Cancer Res.* **2001**, *7*, 1474–1480. [PubMed]
65. Stefański, T.; Mikstacka, R.; Kurczab, R.; Dutkiewicz, Z.; Kucińska, M.; Murias, M.; Zielińska-Przyjemska, M.; Cichocki, M.; Teubert, A.; Kaczmarek, M.; et al. Design, synthesis, and biological evaluation of novel combretastatin A-4 thio derivatives as microtubule targeting agents. *Eur. J. Med. Chem.* **2018**, *144*, 797–816. [CrossRef]
66. Vakifahmetoglu, H.; Olsson, M.; Zhivotovsky, B. Death through a tragedy: Mitotic catastrophe. *Cell Death Differ.* **2008**, *15*, 1153–1162. [CrossRef] [PubMed]
67. Castedo, M.; Perfettini, J.L.; Roumier, T.; Andreau, K.; Medema, R.; Kroemer, G. Cell death by mitotic catastrophe: A molecular definition. *Oncogene* **2004**, *23*, 2825–2837. [CrossRef] [PubMed]
68. González, M.; Ellahioui, Y.; Álvarez, R.; Gallego-Yerga, L.; Caballero, E.; Vicente-Blázquez, A.; Ramudo, L.; Marín, M.; Sanz, C.; Medarde, M.; et al. The Masked Polar Group Incorporation (MPGI) Strategy in Drug Design: Effects of Nitrogen Substitutions on Combretastatin and Isocombretastatin Tubulin Inhibitors. *Molecules* **2019**, *24*, 4319. [CrossRef]
69. Shelanski, M.L.; Gaskin, F.; Cantor, C.R. Microtubule assembly in the absence of added nucleotides. *Proc. Natl. Acad. Sci. USA* **1973**, *70*, 765–768. [CrossRef]
70. Dumortier, C.; Gorbunoff, M.J.; Andreu, J.M.; Engelborghs, Y. Different Kinetic Pathways of the Binding of Two Biphenyl Analogues of Colchicine to Tubulin. *Biochemistry* **1996**, *35*, 4387–4395. [CrossRef] [PubMed]
71. Bradford, M. A Rapid and Sensitive Method for the Quantitation of Microgram Quantities of Protein Utilizing the Principle of Protein-Dye Binding. *Anal. Biochem.* **1976**, *72*, 248–254. [CrossRef]
72. Korb, O.; Stützle, T.; Exner, T.E. Empirical scoring functions for advanced Protein-Ligand docking with PLANTS. *J. Chem. Inf. Model.* **2009**, *49*, 84–96. [CrossRef]
73. Forli, S.; Huey, R.; Pique, M.E.; Sanner, M.F.; Goodsell, D.S.; Olson, A.J. Computational protein-ligand docking and virtual drug screening with the AutoDock suite. *Nat. Protoc.* **2016**, *11*, 905–919. [CrossRef] [PubMed]
74. Berthold, M.R.; Cebron, N.; Dill, F.; Gabriel, T.R.; Kötter, T.; Meinl, T.; Ohl, P.; Sieb, C.; Thiel, K.; Wiswedel, B. KNIME: The Konstanz Information Miner. In *Studies in Classification, Data Analysis, and Knowledge Organization*; Springer: Berlin/Heidelberg, Germany, 2007; pp. 319–326.
75. Pettersen, E.F.; Goddard, T.D.; Huang, C.C.; Couch, G.S.; Greenblatt, D.M.; Meng, E.C.; Ferrin, T.E. UCSF Chimera-A visualization system for exploratory research and analysis. *J. Comput. Chem.* **2004**, *25*, 1605–1612. [CrossRef] [PubMed]
76. Marvin 17.8 ChemAxon. Available online: https://www.chemaxon.com (accessed on 2 May 2020).
77. OpenEye Scientific Software, Inc. Santa Fe. Available online: https://www.eyesopen.com/ (accessed on 2 May 2020).
78. Garcia-Perez, C.; Pelaez, R.; Theron, R.; Luis Lopez-Perez, J. JADOPPT: Java based AutoDock preparing and processing tool. *Bioinformatics* **2017**, *33*, 583–585. [CrossRef] [PubMed]

MATERIAL SUPLEMENTARIO

El material suplementario del artículo 1 se encuentra disponible *online* en la siguiente dirección:

https://www.mdpi.com/1422-0067/22/4/1907/s1

Se compone de los siguientes apartados, lo cuales se desarrollan a continuación de esta página:

Figure S1. Synthetic procedures of new Microtubule Destabilizing Sulfonamides.

Table S1. Antiproliferative activity against HT-29 and sensitivity to MDR pumps.

Figure S2. Tubulin Polymerization Assay data. IC_{50} calculation.

Methods SP1. Chemistry. General chemical techniques and chemical synthesis.

Methods SP2. ^{1}H NMR and ^{13}C NMR spectra (online and Anexo digital 2.d).

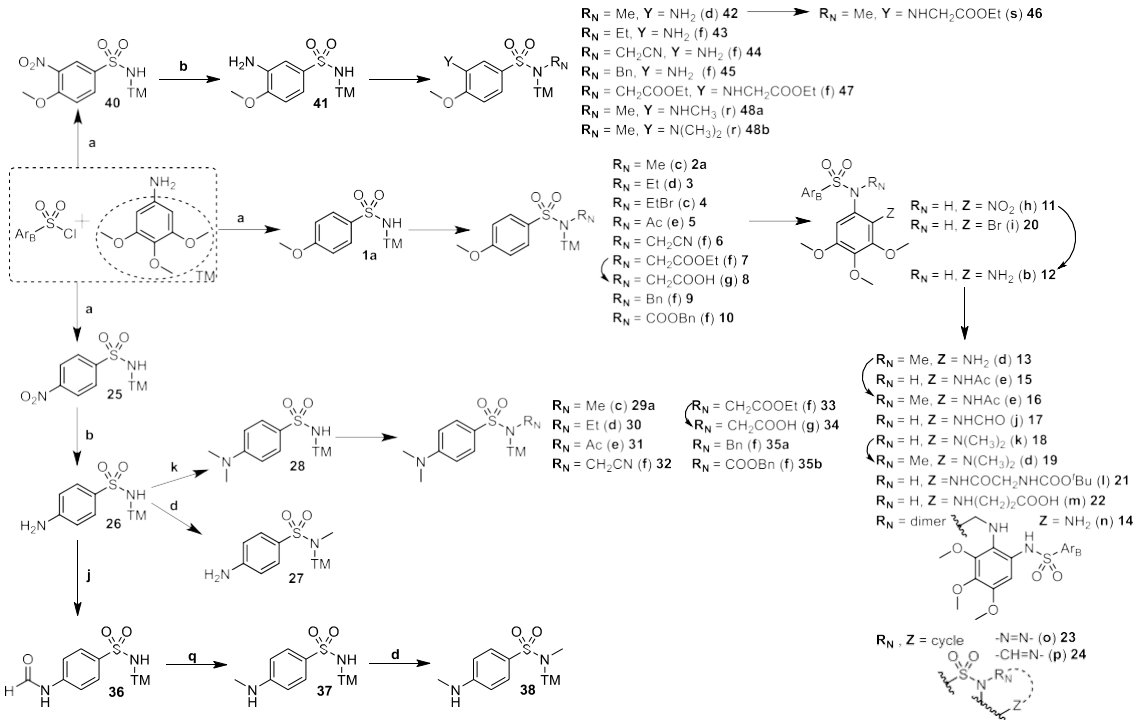

Figure S1. Synthetic procedures of new Microtubule Destabilizing Sulfonamides. Reagents, conditions, and yields: (**a**) Pyridine, CH_2Cl_2, rt, 4-8 h, 90-96% (**b**) H_2, Pd/C, EtOAc, rt, 48-72 h, 82-98% (**c**) R_N-halogen, NaOH or KOH, nBu$_4$N$^+$HSO$_4^-$, CH_2Cl_2, rt, 48-72 h, 26-78% (**d**) R_N-halogen, KOH, CH_3CN, rt, 24 h, 63-98% (**e**) Acetic anhydride, pyridine, CH_2Cl_2, rt or reflux, 8-12 h, 61-84% (**f**) R_N-halogen, K_2CO_3, dry DMF, rt, 24-48 h, 40-99% (**g**) KOH, MeOH, rt, 30 min, 63-89% (**h**) *tert*-Butyl nitrite, CH_3CN, 45 °C, 24 h, 60% (**i**) NBS, CH_2Cl_2, rt, 6 h, 43% (**j**) Formic acid, CH_2Cl_2, rt, 24-48 h, 62-82% (**k**) Paraformaldehyde, $NaBH_3CN$, AcOH, MeOH, rt, 72-96 h, 95% (**l**) (*tert*-butoxycarbonyl)glycine, EDCI, 4-DMAP, CH_2Cl_2, rt, 24 h, 53% (**m**) Succinic anhydride, pyridine, CH_2Cl_2, rt or reflux, 24-72 h, 23-35% (**n**) KOH, nBu$_4$N$^+$HSO$_4^-$, CH_2Cl_2, rt, 72 h, 35% (**o**) *tert*-Butyl nitrite, CH_3CN, H_2O, AcOH, 0 °C, 24 h, 30% (**p**) Triethyl orthoformate, CH_3CN, reflux, 2 h, 87% (**q**) Trichloroacetic acid, $NaBH_4$, dry THF, 0°C, 24 h, 97% (**r**) $(CH_3)_2SO_4$, K_2CO_3, acetone, reflux, 12 h, 11-32% (**s**) Ethyl 2-bromoacetate, NaI, acetone/THF 1:1, reflux, 48 h, 19%.

Table S1. Chemical structure, antiproliferative activity against the CA-4 resistant cancer cell line HT-29, and sensitivity to MDR pumps of novel Microtubule Destabilizing Sulfonamides (MDS). Compounds have been divided into three different series according to the substituents on the aromatic B ring (Ar_B). TM: 3,4,5-trimethoxyphenyl.

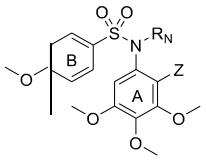

Series 1:			Antiproliferative activity IC_{50} (nM)	Sensivity to MDR pumps IC_{50} (nM)
Z	**R_N**	**Compound**	**HT-29**	**HT-29 Verapamil 10 µM**
H	H	**1a**	897	975
H	SO_2-4-OMePh	**1b**	>1000	n.d. [1]
H	Me	**2a**	143	117
H	CH_2-Dim	**2b**	>1000	n.d.
H	Et	**3**	913	328
H	EtBr	**4**	503	460
H	Ac	**5**	747	683
H	CH_2CN	**6**	230	458
H	CH_2COOEt	**7**	237	398
H	CH_2COOH	**8**	>1000	n.d.
H	Benzyl	**9**	>1000	n.d.
H	COOBenzyl	**10**	>1000	n.d.
NO_2	H	**11**	>1000	n.d.
NH_2	H	**12**	>1000	n.d.
NH_2	Me	**13**	>1000	n.d.
NH_2	CH_2-Dim	**14**	>1000	n.d.
NHAc	H	**15**	>1000	n.d.
NHAc	Me	**16**	>1000	n.d.
NHCHO	H	**17**	>1000	n.d.
$N(CH_3)_2$	H	**18**	>1000	n.d.
$N(CH_3)_2$	Me	**19**	>1000	n.d.
Br	H	**20**	>1000	n.d.
Gly-*t*BOC	H	**21**	>1000	n.d.
Succinic	H	**22**	>1000	n.d.
-N=N-		**23**	>1000	n.d.
-N=CH-		**24**	>1000	n.d.

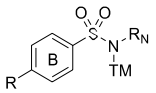

Series 2:			Antiproliferative activity IC_{50} (nM)	Sensivity to MDR pumps IC_{50} (nM)
R	**R_N**	**Comp**	**HT-29**	**HT-29 Verapamil 10 µM**
NO_2	H	**25**	>1000	n.d.
NH_2	H	**26**	>1000	n.d.
NH_2	Me	**27**	>1000	n.d.
$N(CH_3)_2$	H	**28**	887	1170
$N(CH_3)_2$	Me	**29a**	103	43
$N(CH_3)_2$	CH_2-Dim	**29b**	>1000	n.d.
$N(CH_3)_2$	Et	**30**	460	84
$N(CH_3)_2$	Ac	**31**	140	240

$N(CH_3)_2$	CH_2CN	**32**	123	237
$N(CH_3)_2$	CH_2COOEt	**33**	863	850
$N(CH_3)_2$	CH_2COOH	**34**	>1000	n.d.
$N(CH_3)_2$	Benzyl	**35a**	165	287
$N(CH_3)_2$	COOBenzyl	**35b**	690	n.d.
NHCHO	H	**36**	>1000	n.d.
$NHCH_3$	H	**37**	807	n.d.
$NHCH_3$	Me	**38**	59	50

Series 3: 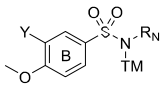			**Antiproliferative activity IC_{50} (nM)**	**Sensivity to MDR pumps IC_{50} (nM)**
Y	**R_N**	**Comp**	**HT-29**	**HT-29 Verapamil 10 µM**
NO_2	H	**40**	>1000	n.d.
NH_2	H	**41**	277	260
NH_2	Me	**42**	81	79
NH_2	Et	**43**	63	58
NH_2	CH_2CN	**44**	61	62
NH_2	Benzyl	**45**	300	276
$NHCH_2COOEt$	Me	**46**	113	317
$NHCH_2COOEt$	CH_2COOEt	**47**	>1000	n.d.
$NHCH_3$	Me	**48a**	>1000	n.d.
$N(CH_3)_2$	Me	**48b**	>1000	n.d.
Paclitaxel [52]			2.8	n.d.
Combretastatin A-4			305	327
ABT-751			213	250

[1] n.d.: not determined.

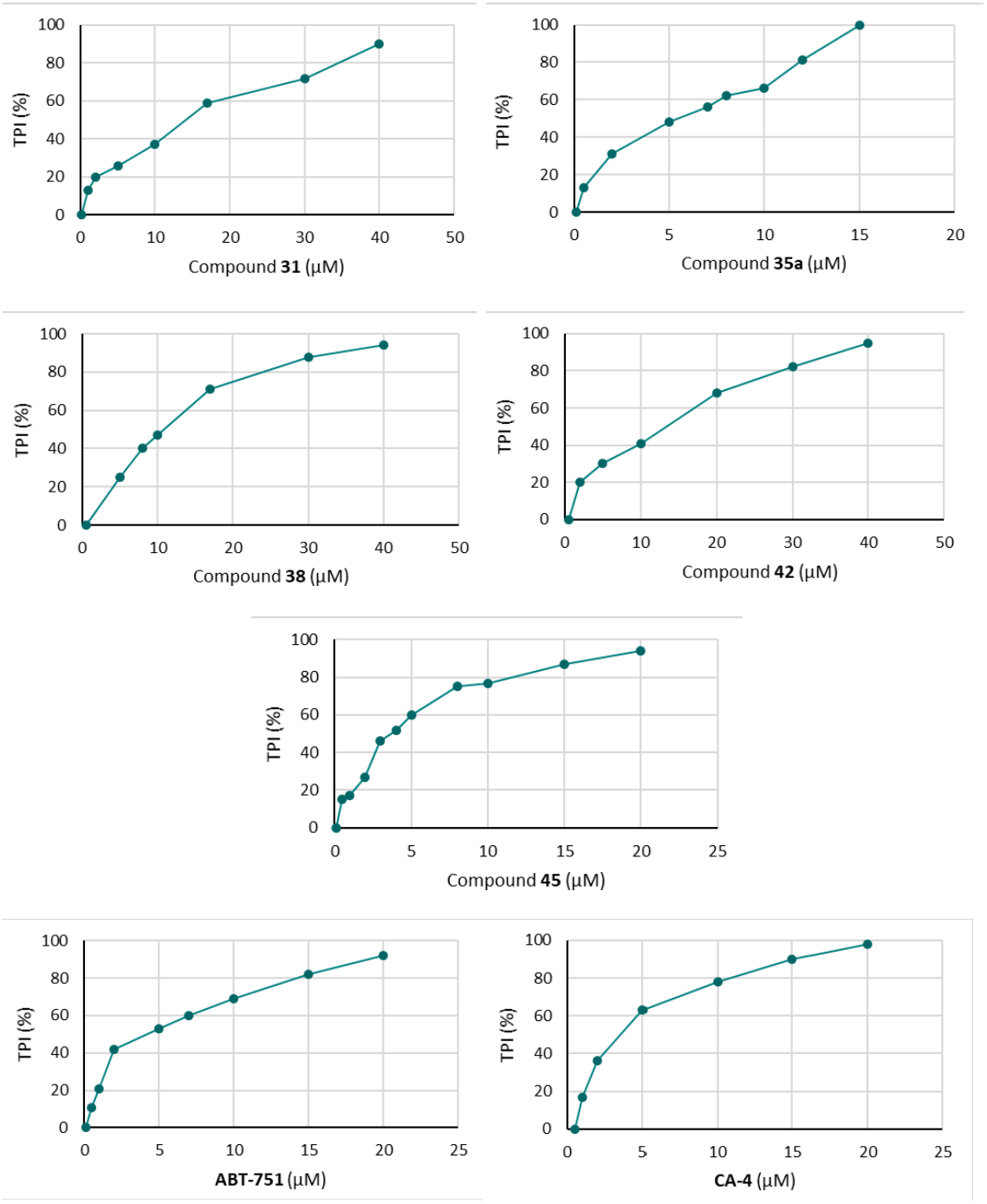

Figure S2. Tubulin Polymerization Assay data. IC_{50} calculation. Tubulin Polymerization Inhibition (TPI) percentages are the average of three independent experiments.

Methods SP1

Chemistry

General chemical techniques

Reagents were used as purchased without further purification. Solvents (EtOAc, DMF, CH_2Cl_2, MeOH, CH_3CN, toluene) were stored over molecular sieves. THF was refluxed with sodium/benzophenone, and hexane was dried by distillation and stored over $CaCl_2$. TLC was performed on precoated silica gel polyester plates (0.25 mm thickness) with a UV fluorescence indicator 254 (Polychrom SI F254). Chromatographic separations were performed on silica gel columns by flash (Kieselgel 40, 0.040-0.063; Merck) chromatography. Melting points were determined on a Buchi 510 apparatus and are uncorrected. ^{1}H NMR and ^{13}C NMR spectra were recorded in $CDCl_3$, CD_3OD, DMSO-D6, or acetone-D6 on a Bruker WP 200-SY spectrometer operating at 200/50 MHz, or a Bruker SY spectrometer at 400/100 MHz. Chemical shifts (δ) are given in ppm downfield from tetramethylsilane and coupling constants (*J* values) are given in Hz. IR spectra in KBr disk were run on a Nicolet Impact 410 Spectrophotometer. A hybrid QSTAR XL quadrupole/time of flight spectrometer was used for HRMS analyses. GC-MS spectra were performed using a Hewlett-Packard 5890 series II mass detector. A Helios-α UV-320 from Thermo-Spectronic was used for UV spectra.

Chemical synthesis

4-Methoxy-*N*-(3,4,5-trimethoxyphenyl)benzenesulfonamide (**1a**) and 4-methoxy-*N*-((4-methoxyphenyl)sulfonyl)-*N*-(3,4,5-trimethoxyphenyl)benzenesulfonamide (**1b**). 3,4,5-Trimethoxyaniline (2.64 g, 14.45 mmol) was added to a solution of 4-methoxybenzenesulfonyl chloride (2.97 g, 14.45 mmol) in CH_2Cl_2 (100 mL) and triethylamine (6 mL), and stirred at room temperature. After 4 h, the reaction was treated with 2N HCl and 5% $NaHCO_3$, washed with brine to neutrality, dried over anhydrous Na_2SO_4, and concentrated under vacuum. Successive crystallizations in EtOH and EtOAc provided compounds **1a** (3.58 g, 10.14 mmol, 70%) and **1b** (0.95 g, 1.82 mmol, 25%), respectively. Another synthetic methodology was performed to obtain **1a** in better yield as a single product. 4-Methoxybenzenesulfonyl chloride (2.22 g, 10.76 mmol) dissolved in CH_2Cl_2 (50 mL) was dropwise added to a solution of 3,4,5-trimethoxyaniline (1.97 g, 10.76 mmol) in CH_2Cl_2 (100 mL) and pyridine (3 mL). The mixture was stirred at room temperature for 4 h. The reaction was then treated with 2N HCl and 5% $NaHCO_3$, washed with brine, dried over anhydrous Na_2SO_4, and concentrated under vacuum yielding 3.65 g (10.34 mmol, 96%) of **1a**. **1a:** M.p.: 115-116 °C (EtOH). IR (KBr): 3283, 1601, 1578, 1497, 1335 cm^{-1}. ^{1}H NMR (400 MHz, $CDCl_3$): δ 3.75 (6H, *s*), 3.78 (3H, *s*), 3.84 (3H, *s*), 6.23 (1H, *s*), 6.27 (2H, *s*), 6.91 (2H, *d, J* = 9.2), 7.69 (2H, *d, J* = 9.2). ^{13}C NMR (100 MHz, $CDCl_3$): δ 56.1 (CH_3), 56.4 ($2CH_3$), 61.3 (CH_3), 99.7 (2CH), 114.5 (2CH), 130.3 (2CH), 131.4 (C), 133.2 (C), 135.7 (C), 153.8 (2C), 163.5 (C). HRMS ($C_{16}H_{19}NO_6S + H^+$): calcd 354.1006 ($M + H^+$), found 354.1009. **1b:** M.p.: 192-193 °C (EtOAc). IR (KBr): 1592, 1576, 1495, 1376, 1356 cm^{-1}. ^{1}H NMR (400 MHz, $CDCl_3$): δ 3.68 (6H, *s*), 3.87 (3H, *s*), 3.91 (6H, *s*), 6.18 (2H, *s*), 7.00 (4H, *d, J* = 8.8), 7.90 (4H, *d, J* = 8.8). ^{13}C NMR (100 MHz, $CDCl_3$): δ 55.7 ($2CH_3$), 56.0 ($2CH_3$), 60.9 (CH_3), 108.9 (2CH), 114.0 (4CH), 129.5 (C), 129.6 (2C), 130.9 (4CH), 139.5 (C), 153.0 (2C), 163.9 (2C). HRMS ($C_{23}H_{25}NO_9S_2 + H^+$): calcd 524.1043 ($M + H^+$), found 542.1060.

4-Methoxy-*N*-methyl-*N*-(3,4,5-trimethoxyphenyl)benzenesulfonamide (**2a**) and *N*,*N*'-methylenebis(4-methoxy-*N*-(3,4,5-trimethoxyphenyl)benzenesulfonamide) (**2b**). CH_3I (81 µL, 1.30 mmol) was added to a mixture of **1a** (229 mg, 0.65 mmol), NaOH (30 mg, 1.30 mmol), and $n Bu_4N^+HSO_4^-$ (260 mg, 1.30 mmol) in CH_2Cl_2 (100 mL). The reaction was stirred at room temperature under nitrogen atmosphere for 3 days. The solution was poured onto brine, extracted with CH_2Cl_2, and then dried over Na_2SO_4. After concentration, the residue was purified by silica gel column chromatography (hexane/EtOAc, 6:4) to give **2a** (187 mg, 0.51 mmol, 78%) and **2b** (39 mg, 0.05 mmol, 17%). **2a:** M.p.: 123-124 °C (CH_2Cl_2/Hexane). IR (KBr): 1595, 1468,

1336 cm^{-1}. ^{1}H NMR (400 MHz, $CDCl_3$): δ 3.05 (3H, *s*), 3.66 (6H, *s*), 3.76 (3H, *s*), 3.79 (3H, *s*), 6.21 (2H, *s*), 6.87 (2H, *d, J* = 8.8), 7.48 (2H, *d, J* = 8.8). ^{13}C NMR (100 MHz, $CDCl_3$): δ 38.5 (CH_3), 55.6 (CH_3), 56.1 ($2CH_3$), 60.9 (CH_3), 104.5 (2CH), 113.8 (2CH), 128.0 (C), 130.1 (2CH), 137.3 (C), 137.4 (C), 152.9 (2C), 163.0 (C). HRMS ($C_{17}H_{21}NO_6S + H^+$): calcd 368.1162 ($M + H^+$), found 368.1154. **2b:** M.p.: 178-179 °C (EtOAc). IR (KBr): 1594, 1464, 1349 cm^{-1}. ^{1}H NMR (400 MHz, $CDCl_3$): δ 3.63 (12H, *s*), 3.83 (6H, *s*), 3.84 (3H, *s*), 5.52 (2H, *s*), 6.11 (4H, *s*), 6.83 (4H, *d, J* = 8.8), 7.34 (4H, *d, J* = 8.8). ^{13}C NMR (100 MHz, $CDCl_3$): δ 55.6 ($2CH_3$), 55.9 ($4CH_3$), 60.9 ($2CH_3$), 65.7 (CH_2), 106.9 (4CH), 113.8 (4CH), 129.7 (4CH), 130.4 (2C), 132.9 (2C), 138.0 (2C), 152.9 (4C), 163.0 (2C). HRMS ($C_{33}H_{38}N_2O_{12}S_2 + H^+$): calcd 719.1939 ($M + H^+$), found 719.1959.

N-ethyl-4-methoxy-*N*-(3,4,5-trimethoxyphenyl)benzenesulfonamide (**3**). 101 mg (0.28 mmol) of compound **1a** were dissolved in CH_3CN (50 mL) and 39 mg (0.56 mmol) of crushed KOH were added. After 30 min stirring at room temperature, 42.7 µL (0.56 mmol) of bromoethane were added to the solution. The reaction mixture was stirred at room temperature for 24 h. The mixture was evaporated to dryness. The residue was diluted with water, and the solution was extracted with EtOAc. The extract was dried over Na_2SO_4 and evaporated to dryness yielding 103 mg (0.27 mmol, 94%) of **3**. The residue was crystallized from CH_2Cl_2/hexane to give 78 mg (0.20 mmol, 71%) of compound **3**. M.p.: 140-143 °C (CH_2Cl_2/Hexane). ^{1}H NMR (400 MHz, $CDCl_3$): δ 1.09 (3H, *t, J* = 7.2), 3.54 (2H, *q, J* = 7.2), 3.72 (6H, *s*), 3.84 (3H, *s*), 3.86 (3H, *s*), 6.23 (2H, *s*), 6.94 (2H, *s, J* = 8.8), 7.60 (2H, *d, J* = 8.8). ^{13}C NMR (100 MHz, $CDCl_3$): δ 14.1 (CH_3), 45.7 (CH_2), 55.5 (CH_3), 56.1 ($2CH_3$), 60.9 (CH_3), 106.5 (2CH), 113.8 (2CH), 129.9 (2CH), 130.0 (C), 134.5 (C), 137.7 (C), 153.0 (2C), 162.9 (C). HRMS ($C_{18}H_{23}NO_6S + H^+$): calcd 382.1319 ($M + H^+$), found 382.1322.

N-(2-bromoethyl)-4-methoxy-*N*-(3,4,5-trimethoxyphenyl)benzenesulfonamide (**4**). A mixture of **1a** (161 mg, 0.45 mmol), KOH (51 mg, 0.91 mmol), $nBu_4N^+HSO_4^-$ (309 mg, 0.91 mmol), and 1,2-dibromoethane (79 µL, 0.91 mmol) in CH_2Cl_2 (100 mL) was stirred at room temperature for 3 days. The reaction was washed with brine, extracted with CH_2Cl_2, and dried over Na_2SO_4. After concentration, the crude material was purified by column chromatography using hexane/EtOAc 6:4 as eluants to give **4** (55 mg, 0.12 mmol, 26%) and **2b** (121 mg, 0.17 mmol, 74%). M.p.: 101-102 °C (CH_2Cl_2/Hexane). IR (KBr): 1593, 1498, 1352 cm^{-1}. ^{1}H NMR (400 MHz, $CDCl_3$): δ 3.41 (2H, *t, J* = 7.2), 3.57 (2H, *t, J* = 7.2), 3.72 (6H, *s*), 3.84 (3H, *s*), 3.87 (3H, *s*), 6.25 (2H, *s*), 6.95 (2H, *d, J* = 8.8), 7.61 (2H, *d, J* = 8.8). ^{13}C NMR (100 MHz, $CDCl_3$): δ 41.3 (CH_2), 52.7 (CH_2), 55.6 (CH_3), 56.1 ($2CH_3$), 60.8 (CH_3), 106.5 (2CH), 113.9 (2CH), 129.7 (C), 129.9 (2CH), 134.4 (C), 138.1 (C), 153.2 (2C), 163.1 (C). HRMS ($C_{18}H_{22}BrNO_6S + H^+$): calcd 460.0424 and 462.0404 ($M + H^+$), found 460.0394 and 462.0382.

N-((4-methoxyphenyl)sulfonyl)-*N*-(3,4,5-trimethoxyphenyl)acetamide (**5**). Acetic anhydride (304 µL, 323 mmol) was added to a solution of **1a** (114 mg, 0.32 mmol) in CH_2Cl_2 (50 mL) and pyridine (1 mL). The reaction mixture was heated under reflux for 12 h. After cooling, the mixture was poured onto ice. The organic layer was separated, washed with 2N HCl, 5% $NaHCO_3$, and brine, dried (Na_2SO_4), filtered, and concentrated under vacuum to yield 107 mg (0.27 mmol, 83%) of compound **5**. The product was purified by crystallization in CH_2Cl_2/Hexane (50 mg, 0.13 mmol, 39%). M.p.: 190-195 °C (CH_2Cl_2/Hexane). ^{1}H NMR (400 MHz, $CDCl_3$): δ 1.86 (3H, *s*), 3.76 (6H, *s*), 3.81 (3H, *s*), 3.82 (3H, *s*), 6.37 (2H, *s*), 6.93 (2H, *d, J* = 8.8), 7.92 (2H, *d, J* = 8.8). ^{13}C NMR (100 MHz, $CDCl_3$): δ 24.7 (CH_3), 55.7 (CH_3), 56.3 ($2CH_3$), 61.0 (CH_3), 107.2 (2CH), 113.8 (2CH), 130.2 (C), 131.5 (2CH), 132.2 (C), 139.2 (C), 153.7 (2C), 163.9 (C), 170.2 (C). HRMS ($C_{18}H_{21}NO_7S + H^+$): calcd 396.1111 ($M + H^+$), found 396.1126.

N-(cyanomethyl)-4-methoxy-*N*-(3,4,5-trimethoxyphenyl)benzenesulfonamide (**6**). 2-Chloroacetonitrile (37 µL, 0.59 mmol) was added after 30 min to a stirred solution of **1a** (104 mg, 0.29 mmol) and K_2CO_3 (81 mg, 0.59 mmol) in DMF (5 mL). After 24 h, the reaction mixture was dried under vacuum, re-dissolved in EtOAc, and washed with brine. After drying over Na_2SO_4 and removal of the solvent, the residue was purified by preparative TLC (hexane/EtOAc 1:1) to

give **6** (57 mg, 0.15 mmol, 49%). ^{1}H NMR (400 MHz, $CDCl_3$): δ 3.67 (6H, *s*), 3.79 (3H, *s*), 3.82 (3H, *s*), 4.49 (2H, *s*), 6.34 (2H, *s*), 6.92 (2H, *d, J* = 8.8), 7.62 (2H, *d, J* = 8.8). ^{13}C NMR (100 MHz, $CDCl_3$): δ 40.1 (CH_2), 56.1 ($2CH_3$), 56.5 (CH_3), 61.3 (CH_3), 106.3 (2CH), 114.5 (2CH), 115.5 (C), 129.1 (C), 130.8 (2CH), 134.3 (C), 139.0 (C), 153.8 (2C), 164.1 (C). HRMS ($C_{18}H_{20}N_2O_6S + H^+$): calcd 393.1115 ($M + H^+$), found 393.1097.

Ethyl *N*-((4-methoxyphenyl)sulfonyl)-*N*-(3,4,5-trimethoxyphenyl)glycinate (**7**). K_2CO_3 (78 mg, 0.56 mmol) was added to a solution of **1a** (100 mg, 0.28 mmol) in DMF (5 mL), and the resulting mixture was stirred for 30 min. Then, ethyl 2-bromoacetate (63 µL, 0.56 mmol) was added. After 24 h, the solvent was evaporated to dryness and the residue was dissolved in brine and extracted with EtOAc. The organics were dried over Na_2SO_4 before concentration under reduced pressure to yield compound **7** (121 mg, 0.28 mmol, 97%). The crude product obtained was recrystallized from CH_2Cl_2/Hexane (51 mg, 0.12 mmol, 41%). M.p.: 123-127 °C (CH_2Cl_2/Hexane). ^{1}H NMR (400 MHz, $CDCl_3$): δ 1.25 (3H, *t, J* = 7.2), 3.71 (6H, *s*), 3.83 (3H, *s*), 3.86 (3H, *s*), 4.17 (2H, *q, J* = 7.2), 4.37 (2H, *s*), 6.42 (2H, *s*), 6.93 (2H, *d, J* = 8.8), 7.67 (2H, *d, J* = 8.8). ^{13}C NMR (100 MHz, $CDCl_3$): δ 14.1 (CH_3), 52.9 (CH_2), 55.6 (CH_3), 56.0 ($2CH_3$), 60.8 (CH_2), 61.4 (CH_3), 106.4 (2CH), 113.7 (2CH), 130.1 (2CH), 130.4 (C), 135.3 (C), 137.8 (C), 153.0 (2C), 163.1 (C), 168.9 (C). HRMS ($C_{20}H_{25}NO_8S$ + H^+): calcd 440.1374 ($M + H^+$), found 440.1363.

N-((4-methoxyphenyl)sulfonyl)-*N*-(3,4,5-trimethoxyphenyl)glycine (**8**). Compound **7** (91 mg 0.21 mmol) was diluted with methanolic KOH for saponification. After 30 min stirring at room temperature, the solution was acidified with 2N HCl and extracted with EtOAc. The extract was washed with brine, dried over Na_2SO_4, and evaporated to dryness to afford 77 mg (0.19 mmol, 89%) of the desired compound (**8**). The residue was purified by crystallization in CH_2Cl_2/Hexane (54 mg, 0.13 mmol, 63%). M.p.: 151-158 °C (CH_2Cl_2/Hexane). ^{1}H NMR (400 MHz, $CDCl_3$): δ 3.71 (6H, *s*), 3.82 (3H, *s*), 3.86 (3H, *s*), 4.41 (2H, *s*), 6.39 (2H, *s*), 6.94 (2H, *d, J* = 8.8), 7.65 (2H, *d, J* = 8.8). ^{13}C NMR (100 MHz, $CDCl_3$): δ 52.7 (CH_2), 55.7 (CH_3), 56.1 ($2CH_3$), 60.8 (CH_3), 106.3 (2CH), 113.8 (2CH), 130.0 (C), 130.1 (C), 135.2 (2CH), 137.9 (C), 153.1 (2C), 163.2 (C), 174.0 (C). HRMS ($C_{18}H_{21}NO_8S + H^+$): calcd 412.1061 ($M + H^+$), found 412.1053.

N-benzyl-4-methoxy-*N*-(3,4,5-trimethoxyphenyl)benzenesulfonamide (**9**). A solution of **1a** (80 mg, 0.22 mmol) and K_2CO_3 (60 mg, 0.44 mmol) in DMF (5 mL) was stirred for 30 min at room temperature. Then, benzyl chloride (31.5 µL, 0.27 mmol) was added and the reaction mixture was stirred for 24 h. When completed, solvent was removed under vacuum and the residue was washed with brine, extracted with EtOAc, dried (Na_2SO_4), filtered, and evaporated to dryness to afford 93 mg (0.21 mmol, 93%) of **9.** The crude reaction product was purified by crystallization in methanol (85 mg, 0.19 mmol, 85%). M.p.: 170-171 °C (MeOH). ^{1}H NMR (400 MHz, $CDCl_3$): δ 3.60 (6H, *s*), 3.77 (3H, *s*), 3.86 (3H, *s*), 4.64 (2H, *s*), 6.10 (2H, *s*), 6.96 (2H, *d, J* = 8.8), 7.22 (5H, *bs*), 7.65 (2H, *d, J* = 8.8). ^{13}C NMR (100 MHz, $CDCl_3$): δ 55.2 (CH_2), 55.6 (CH_3), 56.0 ($2CH_3$), 60.8 (CH_3), 106.7 (2CH), 113.9 (2CH), 127.6 (CH), 128.3 (2CH), 128.7 (2CH), 129.9 (2CH), 130.4 (C), 134.6 (C), 136.1 (C), 137.7 (C), 152.8 (2C), 163.0 (C). HRMS ($C_{23}H_{25}NO_6S + Na^+$): calcd 466.1295 ($M + Na^+$), found 466.1284.

Benzyl ((4-methoxyphenyl)sulfonyl)(3,4,5-trimethoxyphenyl)carbamate (**10**). K_2CO_3 (70 mg, 0.51 mmol) and benzyl chloroformate (43.6 µL, 0.30 mmol) were added to a solution of **1a** (90 mg, 0.25 mmol) in DMF (5 mL), and the solution was stirred at room temperature for 24 h. The reaction mixture was evaporated and re-dissolved in EtOAc, washed with brine, and dried over Na_2SO_4. After concentration, the residue was purified by crystallization in MeOH to give product **10** (30 mg, 0.06 mmol, 24%). M.p.: 179-184 °C (MeOH). ^{1}H NMR (400 MHz, $CDCl_3$): δ 3.80 (6H, *s*), 3.88 (6H, *s*), 5.11 (2H, *s*), 6.43 (2H, *s*), 6.93 (2H, *d, J* = 8.8), 7.17 (2H, *m*), 7.30 (3H, *m*), 7.89 (2H, *d, J* = 8.8). ^{13}C NMR (100 MHz, $CDCl_3$): δ 55.7 (CH_3), 56.2 ($2CH_3$), 60.9 (CH_3), 68.7 (CH_2), 107.1 (2CH), 113.9 (2CH), 127.9 (2CH), 128.4 (2CH), 128.5 (CH), 130.2 (C), 131.2 (2CH), 131.3 (C), 134.7

(C), 138.8 (C), 152.2 (C), 153.3 (2C), 163.8 (C). HRMS ($C_{24}H_{25}NO_8S + Na^+$): calcd 510.1193 ($M + Na^+$), found 510.1193.

4-Methoxy-*N*-(3,4,5-trimethoxy-2-nitrophenyl)benzenesulfonamide (**11**). *tert*-Butyl nitrite (257 µL, 1.94 mmol) was added to a solution of **1a** (1.37 g, 3.89 mmol) in CH_3CN (50 mL), and stirred at 45 °C. After 1 h, additional 1.94 mmol *tert*-butyl nitrite was added to the reaction mixture and it was stirred at 45 °C for 24 h. The mixture was poured onto ice and basified with 5% $NaHCO_3$, and extracted with EtOAc. The organic layers were washed with brine, dried over Na_2SO_4, and concentrated under vacuum. The residue was purified by silica gel column chromatography (hexane/EtOAc 6:4) to give pure product **11** (924 mg, 2.32 mmol, 60%). M.p.: 122-123 °C (CH_2Cl_2/Hexane). IR (KBr): 3268, 1597, 1495, 876 cm^{-1}. ^1H NMR (400 MHz, $CDCl_3$): δ 3.82 (3H, *s*), 3.84 (3H, *s*), 3.89 (3H, *s*), 3.94 (3H, *s*), 6.89 (2H, *d, J* = 9.2), 7.05 (1H, *s*), 7.60 (2H, *d, J* = 9.2), 8.08 (1H, *s*). ^{13}C NMR (100 MHz, $CDCl_3$): δ 55.6 (CH_3), 56.4 (CH_3), 61.1 (CH_3), 62.3 (CH_3), 102.4 (CH), 114.5 (2CH), 127.5 (C), 129.1 (2CH), 129.5 (C), 131.9 (C), 140.2 (C), 148.1 (C), 156.7 (C), 163.6 (C). HRMS ($C_{16}H_{18}N_2O_8S + H^+$): calcd 399.0857 ($M^+ + H^+$), found 399.0855.

N-(2-amino-3,4,5-trimethoxyphenyl)-4-methoxybenzenesulfonamide (**12**). A mixture of **11** (907 mg, 2.28 mmol), 10 mg of Pd/C, and 125 mL of EtOAc was maintained under low hydrogen pressure and stirred at room temperature. After 48 h, uptake of H_2 was completed and the solution was filtered through Celite. The filtrate was concentrated under vacuum to give product **12** (823 mg, 2.24 mmol, 98%). The residue was purified by crystallization in CH_2Cl_2/Hexane (670 mg, 1.82 mmol, 80%). M.p.: 119-120 °C (CH_2Cl_2/Hexane). IR (KBr): 3469, 3377, 1595, 839 cm^{-1}. ^1H NMR (400 MHz, $CDCl_3$): δ 3.47 (3H, *s*), 3.77 (6H, *s*), 3.79 (3H, *s*), 5.82 (1H, *s*), 5.92 (1H, *s*), 6.87 (2H, *d, J* = 9.2), 7.62 (2H, *d, J* = 9.2). ^{13}C NMR (100 MHz, $CDCl_3$): δ 55.6 (CH_3), 56.1 (CH_3), 60.5 (CH_3), 60.8 (CH_3), 107.7 (CH), 114.0 (2CH), 116.5 (C), 129.6 (2CH), 130.6 (C), 132.5 (C), 141.9 (C), 142.3 (C), 144.9 (C), 163.1 (C). HRMS ($C_{16}H_{21}N_2O_6S + H^+$): calcd 369.1115 ($M + H^+$), found 369.1114.

N-(2-amino-3,4,5-trimethoxyphenyl)-4-methoxy-*N*-methylbenzenesulfonamide (**13**). CH_3I (69 µL, 1.10 mmol) was added to 202 mg (0.55 mmol) of **12** and 61 mg (1.10 mmol) of KOH in CH_3CN, and stirred for 24 h. The CH_3CN solution was concentrated under reduced pressure, the residue dissolved in EtOAc and washed with brine. The organics were dried over Na_2SO_4, filtered, and evaporated. The crude material was purified by column chromatography using hexane/EtOAc 7:3 as eluant to give 169 mg (0.44 mmol, 80%) of **13.** ^1H NMR (400 MHz, $CDCl_3$): δ 3.10 (3H, *s*), 3.47 (3H, *s*), 3.86 (3H, *s*), 3.87 (3H, *s*), 3.88 (3H, *s*), 5.69 (1H, *s*), 6.97 (2H, *d, J* = 8.4), 7.66 (2H, *d, J* = 8.4). ^{13}C NMR (100 MHz, $CDCl_3$): δ 38.7 (CH_3), 55.6 (CH_3), 56.3 (CH_3), 60.4 (CH_3), 60.8 (CH_3), 106.6 (CH), 113.9 (2CH), 121.5 (C), 128.7 (C), 130.3 (2CH), 134.8 (C), 141.7 (C), 142.9 (C), 144.4 (C), 163.1 (C). HRMS ($C_{17}H_{22}N_2O_6S + H^+$): calcd 383.1271 ($M + H^+$), found 383.1271.

N-(2-amino-3,4,5-trimethoxyphenyl)-4-methoxy-*N*-(((2,3,4-trimethoxy-6-((4-methoxyphenyl)sulfonamido)phenyl)amino)methyl)benzenesulfonamide (**14**). A mixture of **12** (110 mg, 0.30 mmol), KOH (33 mg, 0.60 mmol), and $n Bu_4N^+HSO_4^-$ (203 mg, 0.60 mmol) in CH_2Cl_2 (100 mL) was stirred at room temperature for 3 days. The reaction was washed with brine, extracted with CH_2Cl_2, and dried over Na_2SO_4. After concentration, the crude material was purified by column chromatography using hexane/EtOAc 6:4 as eluant to give **14** (35 mg, 0.05 mmol, 31%). ^1H NMR (400 MHz, $CDCl_3$): δ 3.35 (3H, *s*), 3.47 (3H, *s*), 3.74 (3H, *s*), 3.82 (3H, *s*), 3.84 (3H, *s*), 3.85 (3H, *s*), 3.89 (3H, *s*), 3.93 (3H, *s*), 5.25 (1H, *d, J* = 13.6), 5.56 (1H, *d, J* = 13.6), 5.73 (1H, *s*), 5.88 (1H, *s*), 6.85 (2H, *d, J* = 8.8), 6.87 (2H, *d, J* = 9.2), 7.43 (2H, *d, J* = 9.2), 7.54 (2H, *d, J* = 8.8). ^{13}C NMR (100 MHz, $CDCl_3$): δ 55.6 (CH_3), 55.8 ($2CH_3$), 56.2 ($2CH_3$), 60.4 ($2CH_3$), 60.8 (CH_3), 60.9 (CH_2), 108.7 (CH), 109.8 (CH), 113.8 (2CH), 113.9 (2CH), 118.0 (2C), 129.7 (2C), 130.1 (2CH), 130.3 (2CH), 135.5 (2C), 141.7 (2C), 143.3 (2C), 144.4 (2C), 163.1 (2C). HRMS ($C_{33}H_{40}N_4O_{12}S_2 + H^+$): calcd 749.2157 ($M + H^+$), found 749.2155.

N-(2,3,4-trimethoxy-6-((4-methoxyphenyl)sulfonamido)phenyl)acetamide (**15**). Acetic anhydride (44 µL, 0.47 mmol) was added to **12** (143 mg, 0.39 mmol) in CH_2Cl_2 (40 mL) and pyridine (2 mL), and allowed to react at room temperature overnight. Then, the reaction mixture was washed with 2N HCl, 5% $NaHCO_3$, and brine, dried over anhydrous Na_2SO_4, and concentrated under vacuum. The residue was purified by preparative TLC (hexane/EtOAc 3:7) to afford **15** (109 mg, 0.27 mmol, 68%). ^{1}H NMR (400 MHz, $CDCl_3$): δ 2.05 (3H, *s*), 3.49 (3H, *s*), 3.82 (3H, *s*), 3.84 (6H, *s*), 6.79 (1H, *s*), 6.88 (2H, *d, J* = 8.4), 7.60 (2H, *d, J* = 8.4), 8.19 (1H, *s*). ^{13}C NMR (100 MHz, $CDCl_3$): δ 23.6 (CH_3), 55.6 (CH_3), 56.0 (CH_3), 61.1 (CH_3), 61.3 (CH_3), 106.4 (CH), 113.9 (2CH), 118.7 (C), 126.1 (C), 128.9 (2CH), 132.1 (C), 140.2 (C), 145.7 (C), 151.7 (C), 162.8 (C), 169.8 (C). HRMS ($C_{18}H_{22}N_2O_7S$ + H^+): calcd 411.1220 (M + H^+), found 411.1219.

N-(2,3,4-trimethoxy-6-((4-methoxy-*N*-methylphenyl)sulfonamido)phenyl)acetamide (**16**). Acetic anhydride (18 µL, 0.19 mmol) was added to a solution of **13** (60 mg, 0.15 mmol) in CH_2Cl_2 (40 mL) and pyridine (2 mL). After stirring for 12 h, the solution was washed with 2N HCl, 5% $NaHCO_3$, and brine, dried over anhydrous Na_2SO_4, and concentrated under vacuum to give compound **16** (56 mg, 0.13 mmol, 84%). The crude product obtained was crystallized from CH_2Cl_2/Hexane (31 mg, 0.07 mmol, 46%). M.p.: 205-210 °C (CH_2Cl_2/Hexane). ^{1}H NMR (400 MHz, $CDCl_3$): δ 2.20 (3H, *s*), 3.09 (3H, *s*), 3.54 (3H, *s*), 3.87 (3H, *s*), 3.88 (3H, *s*), 3.91 (3H, *s*), 5.83 (1H, *s*), 6.97 (2H, *d, J* = 8.8), 7.22 (1H, *s*), 7.58 (2H, *d, J* = 8.8). ^{13}C NMR (100 MHz, $CDCl_3$): δ 23.3 (CH_3), 38.5 (CH_3), 55.6 (CH_3), 55.9 (CH_3), 60.9 (CH_3), 61.0 (CH_3), 105.5 (CH), 113.9 (2CH), 123.9 (C), 128.3 (C), 130.5 (2CH), 132.9 (C), 142.8 (C), 150.9 (C), 152.1 (C), 163.2 (C), 169.7 (C). HRMS ($C_{19}H_{24}N_2O_7S$ + H^+): calcd 425.1377 (M + H^+), found 425.1382.

N-(2,3,4-trimethoxy-6-((4-methoxyphenyl)sulfonamido)phenyl)formamide (**17**). A solution of **12** (100 mg, 0.27 mmol) and formic acid (15 µL, 0.32 mmol) in CH_2Cl_2 (50 mL) was stirred at room temperature for 48 h. The reaction mixture was washed with brine, dried, and concentrated under vacuum to produce 67 mg (0.17 mmol, 62%) of crude reaction product **17**, which was purified by preparative TLC (CH_2Cl_2/MeOH 98:2) (45 mg, 0.11 mmol, 41%). ^{1}H NMR (400 MHz, $CDCl_3$): δ 3.78 (6H, *s*), 3.82 (6H, *s*), 6.77 (1H, *s*), 6.86 (2H, *d, J* = 9.2), 7.33 (1H, *bs*), 7.58 (2H, *d, J* = 9.2), 8.02 (1H, *s*), 8.21 (1H, *s*). ^{13}C NMR (100 MHz, $CDCl_3$): δ 55.6 (CH_3), 56.0 (CH_3), 61.1 (CH_3), 61.3 (CH_3), 106.2 (CH), 113.9 (2CH), 117.7 (C), 125.7 (C), 129.0 (2CH), 131.8 (C), 140.2 (C), 145.5 (C), 152.0 (C), 159.7 (C), 162.9 (CH). HRMS ($C_{17}H_{20}N_2O_7S$ + H^+): calcd 397.1064 (M + H^+), found 397.1064.

N-(2-(dimethylamino)-3,4,5-trimethoxyphenyl)-4-methoxybenzenesulfonamide (**18**). Compound **12** (250 mg, 0.68 mmol) was dissolved in MeOH (100 mL) with paraformaldehyde (41 mg, 1.36 mmol) and acetic acid (one drop). After 1 h stirring at room temperature, sodium cyanoborohydride (85 mg, 1.36 mmol) was added to the solution. The reaction mixture was allowed to react for 4 days. The methanol solution was concentrated under reduced pressure, the residue dissolved in EtOAc, and washed with 5% $NaHCO_3$ and brine. The organics were dried over sodium sulfate and evaporated to afford **18** (258 mg, 0.65 mmol, 96%). The residue was purified by crystallization in CH_2Cl_2/Hexane (174 mg, 0.44 mmol, 64%). M.p.: 125-130 °C (CH_2Cl_2/Hexane). IR (KBr): 3117, 1596, 1496, 841 cm^{-1}. ^{1}H NMR (400 MHz, $CDCl_3$): δ 2.40 (6H, *s*), 3.72 (3H, *s*), 3.75 (3H, *s*), 3.79 (3H, *s*), 3.83 (3H, *s*), 6.83 (2H, *d, J* = 8.8), 6.94 (1H, *s*), 7.67 (2H, *d, J* = 8.8), 8.31 (1H, *bs*). ^{13}C NMR (100 MHz, $CDCl_3$): δ 43.9 ($2CH_3$), 55.5 (CH_3), 56.0 (CH_3), 60.6 (CH_3), 60.7 (CH_3), 97.3 (CH), 113.8 (C), 114.0 (2CH), 127.8 (C), 129.2 (2CH), 131.0 (C), 138.5 (C), 151.9 (C), 153.0 (C), 163.0 (C). HRMS ($C_{18}H_{24}N_2O_6S$ + H^+): calcd 397.1428 (M + H^+), found 397.1414.

N-(2-(dimethylamino)-3,4,5-trimethoxyphenyl)-4-methoxy-*N*-methylbenzenesulfonamide (**19**). KOH (46 mg, 0.82 mmol) and 52 µL of methyl iodide (0.82 mmol) were added to a solution of **18** (165 mg, 0.41 mmol) in CH_3CN (50 mL) and stirred at room temperature for 24 h. Then, the reaction mixture was concentrated, re-dissolved in EtOAc, washed with brine, dried over anhydrous Na_2SO_4, filtered, and concentrated under vacuum to produce 159 mg (0.39 mmol,

93%) of **19**. The crude reaction product was purified by flash chromatography in hexane/EtOAc 6:4 (107 mg, 0.26 mmol, 62%). ^{1}H NMR (400 MHz, $CDCl_3$): δ 2.76 (6H, *s*), 3.16 (3H, *s*), 3.62 (3H, *s*), 3.85 (3H, *s*), 3.87 (3H, *s*), 3.89 (3H, *s*), 6.11 (1H, *s*), 6.98 (2H, *d, J* = 8.8), 7.76 (2H, *d, J* = 8.8). ^{13}C NMR (100 MHz, $CDCl_3$): δ 38.9 (CH_3), 43.6 ($2CH_3$), 55.6 (CH_3), 55.8 (CH_3), 60.6 (CH_3), 60.7 (CH_3), 106.8 (CH), 106.9 (C), 113.8 (2CH), 129.9 (2CH), 131.0 (C), 133.0 (C), 139.1 (C), 149.3 (C), 152.4 (C), 162.8 (C). HRMS ($C_{19}H_{26}N_2O_6S$ + H^+): calcd 411.1584 (M + H^+), found 411.1585.

N-(2-bromo-3,4,5-trimethoxyphenyl)-4-methoxybenzenesulfonamide (**20**). *N*-bromosuccinimide (127 mg, 0.70 mmol) was added to a solution of **1a** (247 mg, 0.70 mmol) in CH_2Cl_2 (20 mL). The reaction was stirred at room temperature for 6 h and evaporated to dryness. After concentration, the residue was purified by silica gel column chromatography (hexane/EtOAc 6:4) to give pure product **20** (131 mg, 0.30 mmol, 43%). IR (KBr): 3264, 1597, 1485, 595 cm^{-1}. ^{1}H NMR (400 MHz, $CDCl_3$): δ 3.73 (3H, *s*), 3.76 (3H, *s*), 3.77 (3H, *s*), 3.81 (3H, *s*), 6.83 (2H, *d, J* = 8.8), 6.89 (1H, *s*), 7.06 (1H, *s*), 7.63 (2H, *d, J* = 8.8). ^{13}C NMR (100 MHz, $CDCl_3$): δ 55.1 (CH_3), 55.8 (CH_3), 60.5 (CH_3), 60.7 (CH_3), 102.3 (CH), 102.6 (C), 113.6 (2CH), 129.0 (2CH), 129.6 (C), 130.2 (C), 140.0 (C), 150.2 (C), 152.6 (C), 162.9 (C). HRMS ($C_{16}H_{18}BrNO_6S$ + H^+): calcd 432.0111 and 434.0091 (M + H^+), found 432.0117 and 434.0094.

Tert-butyl (2-oxo-2-((2,3,4-trimethoxy-6-((4-methoxyphenyl)sulfonamido)phenyl)amino) ethyl)carbamate (**21**). A solution of (*tert*-butoxycarbonyl)glycine (121 mg, 0.65 mmol), EDCI (164 mg, 0.75 mmol), and 4-DMAP (33 mg, 0.25 mmol) in CH_2Cl_2 (20 mL) was stirred for 10 min. Then, compound **12** (177 mg, 0.50 mmol) was added to this solution and the reaction mixture was stirred at room temperature for 24 h. The solution was washed with 2N HCl, 5% $NaHCO_3$, and brine. After drying (Na_2SO_4) and removal of the solvent, compound (**21**) was isolated by flash column chromatography using as eluent hexane/EtOAc 7:3 (138 mg, 0.26 mmol, 53%). IR (KBr): 3349, 1695, 1596, 1498, 836 cm^{-1}. ^{1}H NMR (400 MHz, $CDCl_3$): δ 1.45 (9H, *s*), 3.78 (3H, *s*), 3.80 (2H, *s*), 3.81 (6H, *s*), 3.82 (3H, *s*), 5.21 (1H, *bs*), 6.75 (1H, *s*), 6.86 (2H, *d, J* = 9.2), 7.57 (2H, *d, J* = 9.2), 7.83 (1H, *s*), 8.29 (1H, *s*). ^{13}C NMR (100 MHz, $CDCl_3$): δ 28.2 ($3CH_3$), 44.8 (CH_2), 55.6 (CH_3), 56.0 (CH_3), 61.0 (CH_3), 61.4 (CH_3), 80.7 (C), 106.0 (CH), 113.9 (2CH), 118.2 (C), 126.1 (C), 129.0 (2CH), 131.8 (C), 140.2 (C), 146.1 (C), 151.8 (C), 156.1 (C), 162.9 (C), 169.4 (C). HRMS ($C_{23}H_{31}N_3O_9S$ + H^+): calcd 526.1854 (M + H^+), found 526.1877.

4-Oxo-4-((2,3,4-trimethoxy-6-((4-methoxyphenyl)sulfonamido)phenyl)amino)butanoic acid (**22**). A mixture of **12** (83 mg, 0.22 mmol), succinic anhydride (27 mg, 0.27 mmol), and pyridine drops in CH_2Cl_2 (50 mL) was stirred at room temperature for 24 h. The reaction mixture was washed with 2N HCl and brine, dried over anhydrous Na_2SO_4, and filtered. The solution was evaporated to dryness and the residue was purified by preparative TLC (CH_2Cl_2/MeOH 9:1) to give **22** (24 mg, 0.05 mmol, 23%). M.p.: 159-160 °C (CH_2Cl_2/Hexane). ^{1}H NMR (400 MHz, $CDCl_3$): δ 2.53 (2H, *bs*), 2.77 (2H, *bs*), 3.80 (3H, *s*), 3.82 (9H, s), 6.80 (1H, *s*), 6.87 (2H, *d, J* = 8.8), 7.06 (1H, *s*), 7.60 (2H, *d, J* = 8.8), 7.92 (1H, *s*). ^{13}C NMR (100 MHz, $CDCl_3$): δ 28.9 (CH_2), 30.8 (CH_2), 55.6 (CH_3), 56.0 (CH_3), 61.1 (CH_3), 61.3 (CH_3), 105.7 (CH), 113.8 (2CH), 117.9 (C), 126.6 (C), 129.1 (2CH), 131.7 (C), 140.1 (C), 146.3 (C), 151.9 (C), 162.9 (C), 171.2 (C), 176.6 (C). HRMS ($C_{20}H_{24}N_2O_9S$ + H^+): calcd 469.1275 (M + H^+), found 469.1269.

4,5,6-Trimethoxy-1-((4-methoxyphenyl)sulfonyl)-1*H*-benzo[d][1,2,3]triazole (**23**). *tert*-Butyl nitrite (34.4 µL, 0.26 mmol) was added to a solution of **12** (96 mg, 0.26 mmol) in CH_3CN (20 mL) and H_2O (200 µL) at 0 °C. After 1 h, acetic acid (20 µL) was added to the reaction mixture and stirred for 24 h to room temperature. Then, the mixture was concentrated, re-dissolved in EtOAc, and treated with 5% $NaHCO_3$. The organic layers were washed with brine to neutrality, dried over Na_2SO_4, and concentrated under vacuum. The residue was chromatographed on silica TLC preparative (hexane/EtOAc 1:1) to afford the purified compound **23** (30 mg, 0.08 mmol, 30%). IR (KBr): 1593, 1497, 802 cm^{-1}. ^{1}H NMR (400 MHz, $CDCl_3$): δ 3.84 (3H, *s*), 3.85 (3H, *s*), 4.01 (3H, *s*), 4.48 (3H, *s*), 6.97 (2H, *d, J* = 8.8), 7.15 (1H, *s*), 8.03 (2H, *d, J* = 8.8). ^{13}C NMR (100 MHz,

$CDCl_3$): δ 55.8 (CH_3), 56.6 (CH_3), 61.3 (CH_3), 61.6 (CH_3), 86.0 (CH), 114.8 (2CH), 128.1 (C), 129.8 (C), 130.3 (2CH), 133.2 (C), 136.9 (C), 144.1 (C), 157.1 (C), 164.8 (C). HRMS ($C_{16}H_{17}N_3O_6S$ + H^+): calcd 380.0911 (M + H^+), found 380.0907.

4,5,6-Trimethoxy-1-((4-methoxyphenyl)sulfonyl)-1*H*-benzo[d]imidazole (**24**). A mixture of **12** (93 mg, 0.25 mmol) and triethyl orthoformate (52 µL, 0.30 mmol) in CH_3CN (25 mL) was heated under reflux for 2 h. CH_3CN was removed under reduced pressure and the residue was washed with brine, extracted with EtOAc, and dried over Na_2SO_4. After concentration, the residue was purified by preparative TLC (CH_2Cl_2/MeOH 98:2) and compound **24** was isolated (84 mg, 0.22 mmol, 87%). IR (KBr): 1594, 1487, 805 cm^{-1}. ^1H NMR (400 MHz, $CDCl_3$): δ 3.74 (3H, *s*), 3.75 (3H, *s*), 3.85 (3H, *s*), 4.21 (3H, *s*), 6.88 (2H, *d, J* = 8.8), 6.96 (1H, *s*), 7.82 (2H, *d, J* = 8.8), 8.08 (1H, *s*). ^{13}C NMR (100 MHz, $CDCl_3$): δ 55.8 (CH_3), 56.5 (CH_3), 61.2 (CH_3), 61.3 (CH_3), 89.4 (CH), 114.9 (2CH), 127.9 (C), 128.6 (C), 129.4 (2CH), 130.1 (C), 137.9 (C), 138.5 (CH), 144.9 (C), 152.9 (C), 164.5 (C). HRMS ($C_{17}H_{18}N_2O_6S$ + H^+): calcd 379.0958 (M + H^+), found 379.0944.

4-Nitro-*N*-(3,4,5-trimethoxyphenyl)benzenesulfonamide (**25**). 4-Nitrobenzenesulfonyl chloride (3.02 g, 13.65 mmol) was slowly added to a solution of 3,4,5-trimethoxyaniline (2.50 g, 13.65 mmol) in CH_2Cl_2 (100 mL) and pyridine (3 mL). The reaction mixture was stirred at room temperature for 4 h. Then, it was treated with 2N HCl and 5% $NaHCO_3$. The organics were washed with brine, dried over Na_2SO_4, filtered, and concentrated under vacuum to yield compound **25** (4.56 g, 12.39 mmol, 90%), which was purified by crystallization in CH_2Cl_2/Hexane (3.92 g, 10.65 mmol, 78%). M.p.: 138-140 °C (CH_2Cl_2/Hexane). IR (KBr): 3167, 1604, 1531, 1348 cm^{-1}. ^1H NMR (400 MHz, $CDCl_3$): δ 3.75 (6H, *s*), 3.78 (3H, *s*), 6.29 (2H, *s*), 6.43 (1H, *s*), 7.93 (2H, *d, J* = 8.8), 8.30 (2H, *d, J* = 8.8). ^{13}C NMR (100 MHz, $CDCl_3$): δ 56.2 ($2CH_3$), 61.0 (CH_3), 100.1 (2CH), 124.4 (2CH), 128.6 (2CH), 131.4 (C), 136.2 (C), 144.5 (C), 150.3 (C), 153.1 (2C). HRMS ($C_{15}H_{16}N_2O_7S$ + Na^+): calcd 391.0570 (M + Na^+), found 391.0562.

4-Amino-*N*-(3,4,5-trimethoxyphenyl)benzenesulfonamide (**26**). The sulfonamide **25** (4.56 g, 12.39 mmol) in ethyl acetate (100 mL) and Pd/C (10 mg) was stirred at room temperature under H_2 atmosphere for 72 h. The reaction mixture was filtered over Celite, and the filtrate was evaporated to dryness to give compound **26** (4.01 g, 11.87 mmol, 96%). The crude reaction product was purified by crystallization (MeOH/EtOAc) to give pure product **26** (2.97 g, 8.79 mmol, 71%). M.p.: 177-179 °C (MeOH/EtOAc). IR (KBr): 3469, 1643, 1600 cm^{-1}. ^1H NMR (400 MHz, $CDCl_3$): δ 3.75 (6H, *s*), 3.78 (3H, *s*), 4.11 (2H, *s*), 6.19 (1H, *s*), 6.27 (2H, *s*), 6.61 (2H, *d, J* = 8.8), 7.53 (2H, *d, J* = 8.8). ^{13}C NMR (100 MHz, $CDCl_3$): δ 56.1 ($2CH_3$), 61.0 (CH_3), 99.3 (2CH), 113.9 (2CH), 126.5 (C), 129.5 (2CH), 135.1 (C), 135.2 (C), 151.1 (C), 153.4 (2C). HRMS ($C_{15}H_{18}N_2O_5S$ + H^+): calcd 339.1009 (M + H^+), found 339.1016.

4-Amino-*N*-methyl-*N*-(3,4,5-trimethoxyphenyl)benzenesulfonamide (**27**). A mixture of **26** (205 mg, 0.61 mmol) and KOH (68 mg, 1.21 mmol) in CH_3CN (25 mL) was stirred at room temperature for 30 min. Then, CH_3I (77 µL, 1.21 mmol) was added to the solution and stirred for 24 h. The solvent was evaporated under reduced pressure and the residue was re-dissolved in EtOAc, washed with brine, dried over Na_2SO_4, and concentrated. The residue was crystallized in CH_2Cl_2/Hexane to isolate compound **27** (135 mg, 0.38 mmol, 63%). M.p.: 147-148 °C (CH_2Cl_2/Hexane). IR (KBr): 3428, 1594, 1457 cm^{-1}. ^1H NMR (400 MHz, $CDCl_3$): δ 3.10 (3H, *s*), 3.73 (6H, *s*), 3.82 (3H, *s*), 6.29 (2H, *s*), 6.63 (2H, *d, J* = 7.2), 7.37 (2H, *d, J* = 7.2). ^{13}C NMR (50 MHz, $CDCl_3$): δ 38.4 (CH_3), 56.0 ($2CH_3$), 60.8 (CH_3), 104.5 (2CH), 113.5 (2CH), 124.4 (C), 130.1 (2CH), 137.0 (C), 137.6 (C), 150.8 (C), 152.8 (2C). HRMS ($C_{16}H_{20}N_2O_5S$ + H^+): calcd 353.1166 (M + H^+), found 353.1176.

4-(Dimethylamino)-*N*-(3,4,5-trimethoxyphenyl)benzenesulfonamide (**28**). A mixture of **26** (2.54 g, 7.50 mmol), paraformaldehyde (2.25 g, 75 mmol), acetic acid (drops), and sodium cyanoborohydride (980 mg, 15 mmol) in 100 mL of MeOH was stirred at room temperature for 72 h. The reaction mixture was concentrated under reduced pressure, diluted with EtOAc,

washed with 5% $NaHCO_3$ and brine, dried (Na_2SO_4), filtered, and concentrated under vacuum to give 2.62 g (7.16 mmol, 95%) of **28**, which was purified by crystallization in EtOAc (1.87 g 68%). M.p.: 169-170 °C (EtOAc). IR (KBr): 1593, 1449, 818 cm^{-1}. ^1H NMR (400 MHz, $CDCl_3$): δ 3.01 (6H, *s*), 3.75 (6H, *s*), 3.76 (3H, *s*) 6.28 (2H, *s*), 6.35 (1H, *s*), 6.59 (2H, *d, J* = 8.8), 7.59 (2H, *d, J* = 8.8). ^{13}C NMR (100 MHz, $CDCl_3$): δ 40.0 ($2CH_3$), 56.0 ($2CH_3$), 60.9 (CH_3), 99.0 (2CH), 110.7 (2CH), 123.8 (C), 129.2 (2CH), 133.1 (C), 135.1 (C), 152.9 (C), 153.3 (2C). HRMS ($C_{17}H_{22}N_2O_5S + H^+$): calcd 367.1322 ($M + H^+$), found 367.1306.

4-(Dimethylamino)-*N*-methyl-*N*-(3,4,5-trimethoxyphenyl)benzenesulfonamide (**29a**) and *N*,*N*'-methylenebis(4-(dimethylamino)-*N*-(3,4,5-trimethoxyphenyl)benzenesulfonamide) (**29b**). CH_3I (73 µL, 1.16 mmol) was added to a mixture of **28** (212 mg, 0.58 mmol), NaOH (27 mg, 1.16 mmol), and $nBu_4N^+HSO_4^-$ (232 mg, 1.16 mmol) in CH_2Cl_2 (100 mL). The reaction was stirred at room temperature under nitrogen atmosphere for 2 days. The solution was poured onto brine, extracted with CH_2Cl_2, and dried over Na_2SO_4. After concentration, the residue was purified by silica gel column chromatography (hexane/EtOAc, 6:4) to give **29a** (129 mg, 0.34 mmol, 58%) and **29b** (79 mg, 0.11 mmol, 36%). **29a:** M.p.: 134-140 °C (EtOAc). IR (KBr): 2938, 1598, 1455, 822 cm^{-1}. ^1H NMR (400 MHz, $CDCl_3$): δ 3.00 (6H, *s*), 3.07 (3H, *s*), 3.71 (6H, *s*), 3.80 (3H, *s*), 6.28 (2H, *s*), 6.58 (2H, *d, J* = 8.8), 7.39 (2H, *d, J* = 8.8). ^{13}C NMR (100 MHz, $CDCl_3$): δ 38.4 (CH_3), 44.0 ($2CH_3$), 56.1 ($2CH_3$), 60.9 (CH_3), 104.5 (2CH), 110.4 (2CH), 121.5 (C), 129.8 (2CH), 137.0 (C), 137.9 (C), 152.8 (2C), 152.9 (C). HRMS ($C_{18}H_{24}N_2O_5S + H^+$): calcd 381.1479 ($M + H^+$), found 381.1472. **29b:** M.p.: 191-193 °C (EtOAc). IR (KBr): 2938, 1597, 1460, 835 cm^{-1}. ^1H NMR (400 MHz, $CDCl_3$): δ 3.03 (12H, *s*), 3.64 (12H, *s*), 3.86 (6H, *s*), 5.46 (2H, *s*), 6.15 (4H, *s*), 6.53 (4H, *d, J* = 8.8), 7.25 (4H, *d, J* = 8.8). HRMS ($C_{35}H_{44}N_4O_{10}S_2 + Na^+$): calcd 767.2391 ($M + Na^+$), found 767.2385.

4-(Dimethylamino)-*N*-ethyl-*N*-(3,4,5-trimethoxyphenyl)benzenesulfonamide (**30**). A solution of **28** (106 mg, 0.29 mmol) and KOH (32 mg, 0.58 mmol) in CH_3CN (25 mL) was stirred for 30 min. Then, bromoethane (43 µL, 0.58 mmol) was added. After 24 h, the solvent was evaporated to dryness and the crude residue was re-dissolved in EtOAc, washed with brine, dried over Na_2SO_4, filtered, and concentrated under vacuum to give 98 mg (0.25 mmol, 86%) of **30**. The crude product was purified by crystallization in CH_2Cl_2/Hexane (90 mg, 0.23 mmol, 79%). M.p.: 134-135 °C (CH_2Cl_2/Hexane). IR (KBr): 2941, 1505, 1470, 793 cm^{-1}. ^1H NMR (400 MHz, $CDCl_3$): δ 1.06 (3H, *t, J* = 7.2), 3.03 (6H, *s*), 3.51 (2H, *q, J* = 7.2), 3.72 (6H, *s*), 3.84 (3H, *s*), 6.26 (2H, *s*), 6.63 (2H, *d, J* = 8.8), 7.48 (2H, *d, J* = 8.8). ^{13}C NMR (100 MHz, $CDCl_3$): δ 14.5 (CH_3), 40.5 ($2CH_3$), 46.0 (CH_2), 56.5 ($2CH_3$), 61.3 (CH_3), 106.9 (2CH), 110.9 (2CH), 124.1 (C), 130.1 (2CH), 135.5 (C), 137.9 (C), 153.2 (C), 153.3 (2C). HRMS ($C_{19}H_{26}N_2O_5S + H^+$): calcd 395.1635 ($M + H^+$), found 395.1634.

N-((4-(dimethylamino)phenyl)sulfonyl)-*N*-(3,4,5-trimethoxyphenyl)acetamide (**31**). 105 mg (0.29 mmol) of **28** were dissolved in CH_2Cl_2 (50 mL). Acetic anhydride (32.4 µL, 0.34 mmol) and pyridine (1 mL) were added to the solution and the mixture was heated under reflux for 8 h. The reaction mixture was poured into ice and extracted with CH_2Cl_2. The organic layers were washed with 2N HCl, 5% $NaHCO_3$, and brine, dried over Na_2SO_4, filtered, and concentrated. The residue was purified by preparative TLC (CH_2Cl_2/MeOH 98:2) to give **31** (71 mg, 0.17 mmol, 61%). M.p.: 198-200 °C (CH_2Cl_2/Hexane). IR (KBr): 2938, 1698, 1597, 1448, 814 cm^{-1}. ^1H NMR (400 MHz, $CDCl_3$): δ 1.94 (3H, *s*), 3.08 (6H, *s*), 3.84 (6H, *s*), 3.89 (3H, *s*), 6.45 (2H, *s*), 6.72 (2H, *d, J* = 8.8), 7.87 (2H, *d, J* = 8.8). ^{13}C NMR (100 MHz, $CDCl_3$): δ 24.8 (CH_3), 40.0 ($2CH_3$), 56.3 ($2CH_3$), 60.9 (CH_3), 107.3 (2CH), 110.3 (2CH), 123.5 (C), 131.1 (2CH), 132.7 (C), 139.0 (C), 153.6 (C), 153.6 (2C), 170.2 (C). HRMS ($C_{19}H_{24}N_2O_6S + H^+$): calcd 409.1428 ($M + H^+$), found 409.1429.

N-(cyanomethyl)-4-(dimethylamino)-*N*-(3,4,5-trimethoxyphenyl)benzenesulfonamide (**32**). A solution of **28** (110 mg, 0.30 mmol) and K_2CO_3 (83 mg, 0.60 mmol) in dry DMF (5 mL) was stirred at room temperature for 1 h. To this solution, 2-chloroacetonitrile (38 µL, 0.60 mmol) was added and the reaction mixture was stirred for 24 h. The solvent was removed under reduced pressure. The residue was dissolved in EtOAc and washed with brine, dried (Na_2SO_4), and concentrated

under vacuum to afford 110 mg (0.27 mmol, 90%) of **32**. The crude product was purified by crystallization in methanol (73 mg, 0.18 mmol, 60%). M.p.: 155-157 °C (MeOH). IR (KBr): 2360, 1594, 1503, 804 cm^{-1}. ^{1}H NMR (400 MHz, $CDCl_3$): δ 3.05 (6H, *s*), 3.73 (6H, *s*), 3.84 (3H, *s*), 4.51 (2H, *s*), 6.41 (2H, *s*), 6.64 (2H, *d, J* = 8.8), 7.53 (2H, *d, J* = 8.8). ^{13}C NMR (100 MHz, $CDCl_3$): δ 39.6 ($2CH_3$), 40.0 (CH_2), 56.1 ($2CH_3$), 60.8 (CH_3), 105.9 (2CH), 110.6 (2CH), 115.4 (C), 122.0 (C), 130.0 (2CH), 134.3 (C), 138.5 (C), 153.6 (C), 153.4 (2C). HRMS ($C_{19}H_{23}N_3O_5S + H^+$): calcd 406.1431 (M + H^+), found 406.1422.

Ethyl *N*-((4-(dimethylamino)phenyl)sulfonyl)-*N*-(3,4,5-trimethoxyphenyl)glycinate (**33**). K_2CO_3 (116 mg, 0.84 mmol) was added to a solution of **28** (153 mg, 0.42 mmol) in dry DMF (3 mL). After 1 h at room temperature, 93 µL (0.84 mmol) of ethyl 2-bromoacetate were added and stirred for 24 h. The reaction mixture was concentrated, re-dissolved in EtOAc, washed with brine, dried over anhydrous Na_2SO_4, filtered, and concentrated under vacuum to produce 187 mg (0.41 mmol, 99%) of crude reaction product from which 89 mg (0.20 mmol, 47%) of **33** were purified by crystallization. M.p.: 146-148 °C (CH_2Cl_2/Hexane). ^{1}H NMR (400 MHz, $CDCl_3$): δ 1.24 (3H, *t, J* = 7.2), 3.03 (6H, *s*), 3.71 (6H, *s*), 3.81 (3H, *s*), 4.16 (2H, *q, J* = 7.2), 4.34 (2H, *s*), 6.42 (2H, s), 6.61 (2H, *d, J* = 9.2), 7.54 (2H, *d, J* = 9.2). ^{13}C NMR (50 MHz, $CDCl_3$): δ 14.0 (CH_3), 39.9 ($2CH_3$), 52.7 (CH_2), 55.9 ($2CH_3$), 60.7 (CH_3), 61.2 (CH_2), 106.3 (2CH), 110.3 (2CH), 123.7 (C), 129.7 (2CH), 135.8 (C), 137.6 (C), 152.9 (3C), 169.0 (C). HRMS ($C_{21}H_{28}N_2O_7S + H^+$): calcd 453.1690 (M + H^+), found 453.1681.

N-((4-(dimethylamino)phenyl)sulfonyl)-*N*-(3,4,5-trimethoxyphenyl)glycine (**34**). Compound **33** (150 mg 0.33 mmol) was diluted with methanolic KOH for saponification. After 30 min stirring at room temperature, the solution was acidified with 2N HCl and extracted with EtOAc. The extract was washed with brine, dried over Na_2SO_4, and evaporated to dryness to afford 88 mg (0.21 mmol, 63%) of compound **34**. The residue was purified by crystallization in methanol (58 mg, 0.14 mmol, 41%). M.p.: 168-170 °C (MeOH). ^{1}H NMR (400 MHz, $CDCl_3$): δ 3.04 (6H, *s*), 3.75 (6H, *s*), 3.82 (3H, *s*), 4.35 (2H, *s*), 6.38 (2H, *s*), 6.62 (2H, *d, J* = 8.4), 7.52 (2H, *d, J* = 8.4). ^{13}C NMR (100 MHz, $CDCl_3$): δ 40.0 ($2CH_3$), 52.6 (CH_2), 56.1 ($2CH_3$), 60.8 (CH_3), 106.3 (2CH), 110.5 (2CH), 123.2 (C), 129.8 (2CH), 135.8 (C), 137.8 (C), 153.0 (3C), 173.3 (C). HRMS ($C_{19}H_{24}N_2O_7S + H^+$): calcd 425.1377 (M + H^+), found 425.1381.

N-benzyl-4-(dimethylamino)-*N*-(3,4,5-trimethoxyphenyl)benzenesulfonamide (**35a**) and benzyl ((4-(dimethylamino)phenyl)sulfonyl)(3,4,5-trimethoxyphenyl)carbamate (**35b**). K_2CO_3 (33 mg, 0.24 mmol) and benzyl chloroformate (20.1 µL, 0.14 mmol) were added to a solution of **28** (43 mg, 0.12 mmol) in dry DMF (5 mL), and the solution was stirred at room temperature for 24 h. The reaction mixture was evaporated and re-dissolved in EtOAc, washed with brine, and dried over Na_2SO_4. After concentration, the residue was purified by preparative TLC (hexane/EtOAc 1:1) to give products **35a** (10 mg, 0.02 mmol, 19%) and **35b** (30 mg, 0.06 mmol, 51%). **35a:** ^{1}H NMR (400 MHz, $CDCl_3$): δ 3.04 (6H, *s*), 3.61 (6H, *s*), 3.76 (3H, *s*), 4.61 (2H, *s*), 6.14 (2H, *s*), 6.65 (2H, *d, J* = 8.8), 7.24 (5H, *m*), 7.54 (2H, *d, J* = 8.8). ^{13}C NMR (100 MHz, $CDCl_3$): δ 40.0 ($2CH_3$), 55.0 (CH_2), 56.0 ($2CH_3$), 60.8 (CH_3), 106.7 (2CH), 110.6 (2CH), 124.0 (C), 127.4 (CH), 128.2 (2CH), 128.6 (2CH), 129.7 (2CH), 135.2 (C), 136.4 (C), 137.5 (C), 152.7 (C), 152.9 (2C). HRMS ($C_{24}H_{28}N_2O_5S$ + H^+): calcd 457.1792 (M + H^+), found 457.1788. **35b:** IR (KBr): 3446, 1721, 1599, 1505 cm^{-1}. ^{1}H NMR (400 MHz, $CDCl_3$): δ 3.07 (6H, *s*), 3.80 (6H, *s*), 3.88 (3H, *s*), 5.12 (2H, *s*), 6.45 (2H, *s*), 6.61 (2H, *d, J* = 9.2), 7.17 (2H, *bs*), 7.29 (3H, *m*), 7.77 (2H, *d, J* = 9.2). ^{13}C NMR (100 MHz, $CDCl_3$): δ 40.0 ($2CH_3$), 56.2 ($2CH_3$), 60.8 (CH_3), 68.3 (CH_2), 107.2 (2CH), 110.3 (2CH), 123.6 (C), 127.8 (2CH), 128.2 (CH), 128.4 (2CH), 130.9 (2CH), 131.8 (C), 135.0 (C), 138.7 (C), 152.4 (C), 153.2 (2C), 153.5 (C). HRMS ($C_{25}H_{28}N_2O_7S + Na^+$): calcd 523.1509 (M + Na^+), found 523.1511.

N-(4-(*N*-(3,4,5-trimethoxyphenyl)sulfamoyl)phenyl)formamide (**36**). A solution of **26** (620 mg, 1.83 mmol) and formic acid (7 mL, 18.32 mmol) in pyridine (5 mL) and CH_2Cl_2 (50 mL) was stirred for 24 h. Then, the reaction mixture was washed with 2N HCl, 5% $NaHCO_3$, and brine, dried over

Na_2SO_4, filtered, and evaporated to dryness to afford 550 mg (1.50 mmol, 82%) of **36**. The crude reaction product was purified by crystallization in methanol (429 mg, 1.17 mmol, 62%). M.p.: 203-204 °C (MeOH). IR (KBr): 3329, 3251, 1697, 1592, 816 cm^{-1}. ^1H NMR (400 MHz, CD_3OD): δ 3.66 (3H, *s*), 3.71 (6H, *s*), 6.37 (2H, *s*), 7.70 (4H, *bs*), 8.30 (1H, *s*). ^{13}C NMR (100 MHz, acetone-D6): δ 55.4 ($2CH_3$), 59.6 (CH_3), 98.9 (2CH), 118.8 (2CH), 128.5 (2CH), 133.6 (C), 134.3 (C), 142.2 (C), 153.6 (C), 159.5 (C), 159.6 (C), 159.6 (CH). HRMS ($C_{16}H_{18}N_2O_6S$ + Na^+): calcd 389.0778 (M + Na^+), found 389.0776.

4-(Methylamino)-*N*-(3,4,5-trimethoxyphenyl)benzenesulfonamide (**37**). Trichloroacetic acid (536 mg, 3.27 mmol) diluted in dry THF (10 mL) was added dropwise to a solution of **36** (400 mg, 1.09 mmol) and $NaBH_4$ (124 mg, 3.27 mmol) in dry THF (15 mL) at 0 °C, then warmed to room temperature. The reaction mixture was stirred for 24 h, concentrated, and re-dissolved in EtOAc, washed with brine, dried over anhydrous Na_2SO_4, filtered, and solvent evaporated under vacuum to afford compound **37** (376 mg, 1.07 mmol, 97%). The residue was purified by crystallization. M.p.: 200-206 °C (CH_2Cl_2). IR (KBr): 3374, 3248, 1604, 1468, 814 cm^{-1}. ^1H NMR (400 MHz, $CDCl_3$): δ 2.86 (3H, *s*), 3.75 (6H, *s*), 3.77 (3H, *s*), 6.15 (1H, *s*), 6.27 (2H, *s*), 6.51 (2H, *d, J* = 8.8), 7.55 (2H, *d, J* = 8.8). ^{13}C NMR (100 MHz, acetone-D6): δ 39.1 (CH_3), 55.4 ($2CH_3$), 59.6 (CH_3), 98.3 (2CH), 110.6 (2CH), 125.3 (C), 129.1 (2CH), 134.5 (C), 134.9 (C), 153.3 (C), 153.5 (2C). HRMS ($C_{16}H_{20}N_2O_5S$ + H^+): calcd 353.1166 (M + H^+), found 353.1172.

N-methyl-4-(methylamino)-*N*-(3,4,5-trimethoxyphenyl)benzenesulfonamide (**38**). 80 mg (0.23 mmol) of **37** were dissolved in CH_3CN (25 mL) with 26 mg (0.46 mmol) of KOH. After 30 min stirring at room temperature, CH_3I (29 µL, 0.46 mmol) was added to the solution and the reaction mixture was stirred for 24 h. The solvent was removed under reduced pressure. The residue was dissolved in EtOAc and washed with brine, dried (Na_2SO_4), and concentrated under vacuum to afford 64 mg (0.17 mmol, 76%) of **38**. The crude product was purified by crystallization in CH_2Cl_2/Hexane (40 mg, 0.11 mmol, 47%). M.p.: 147-150 °C (CH_2Cl_2/Hexane). IR (KBr): 3390, 1599, 1502, 835 cm^{-1}. ^1H NMR (400 MHz, $CDCl_3$): δ 2.83 (3H, *s*), 3.07 (3H, *s*), 3.71 (6H, *s*), 3.80 (3H, *s*), 6.28 (2H, *s*), 6.51 (2H, *d, J* = 8.8), 7.35 (2H, *d, J* = 8.8). ^{13}C NMR (100 MHz, $CDCl_3$): δ 30.0 (CH_3), 38.4 (CH_3), 56.1 ($2CH_3$), 60.8 (CH_3), 104.6 (2CH), 110.8 (2CH), 122.6 (C), 130.0 (2CH), 137.2 (C), 137.8 (C), 152.7 (C), 152.8 (2C). HRMS ($C_{17}H_{22}N_2O_5S$ + H^+): calcd 367.1322 (M + H^+), found 367.1325.

4-Methoxy-3-nitrobenzenesulfonyl chloride (**39**). Nitric acid (0.95 mL, 21.36 mmol) was dropwise added to a solution of 4-methoxybenzenesulfonyl chloride (4.41 g, 21.36 mmol) in CH_2Cl_2 (20 mL) and H_2SO_4 (5 mL) at 0 °C. After 4 h under N_2 atmosphere, the reaction was poured onto ice and the mixture was kept at 4 °C for 30 min. Then, the precipitate was filtered under vacuum to dryness to obtain 4.97 g (19.80 mmol, 92%) of **39**. The product was used without further purification. ^1H NMR (400 MHz, $CDCl_3$): δ 4.11 (3H, *s*), 7.33 (1H, *d, J* = 8.8), 8.20 (1H, *dd, J* = 8.8 and 2.4), 8.48 (1H, *d, J* = 2.4). ^{13}C NMR (100 MHz, $CDCl_3$): δ 57.0 (CH_3), 114.0 (CH), 124.8 (CH), 127.1 (C), 132.2 (CH), 135.0 (C), 157.1 (C). GC-MS ($C_7H_6ClNO_5S$): 251 (M^+).

4-Methoxy-3-nitro-*N*-(3,4,5-trimethoxyphenyl)benzenesulfonamide (**40**). Sulfonyl chloride **39** (1.39 g, 5.54 mmol) in CH_2Cl_2 (20 mL) was slowly added to a solution of 3,4,5-trimethoxyaniline (1.01 g, 5.54 mmol) in CH_2Cl_2 (80 mL) and pyridine (2 mL). The reaction mixture was stirred at room temperature for 8 h and then treated with 2N HCl and 5% $NaHCO_3$. The organic layer was washed with brine, dried over Na_2SO_4, filtered, and evaporated to dryness to give 1.99 g (5.00 mmol, 90%) of **40**. The product was purified by crystallization. M.p.: 157-158 °C (CH_2Cl_2/Hexane). IR (KBr): 3258, 1538, 1493, 898 cm^{-1}. ^1H NMR (400 MHz, $CDCl_3$): δ 3.75 (6H, *s*), 3.78 (3H, *s*), 4.01 (3H, *s*), 6.34 (2H, *s*), 6.85 (1H, *s*), 7.12 (1H, *d, J* = 8.8), 7.87 (1H, *dd, J* = 8.8 and 2.4), 8.29 (1H, *d, J* = 2.4). ^{13}C NMR (100 MHz, $CDCl_3$): δ 56.1 ($2CH_3$), 57.1 (CH_3), 60.9 (CH_3), 99.8 (2CH), 113.8 (CH), 125.3 (CH), 130.7 (CH), 131.9 (C), 133.1 (C), 135.8 (C), 138.9 (C), 153.5 (C), 155.9 (2C). HRMS ($C_{16}H_{18}N_2O_8S$ + H^+): calcd 399.0857 (M + H^+), found 399.0855.

3-Amino-4-methoxy-*N*-(3,4,5-trimethoxyphenyl)benzenesulfonamide (**41**). Sulfonamide **40** (1.81 g, 4.56 mmol) in ethyl acetate (125 mL) and Pd/C (10 mg) was stirred at room temperature under H_2 atmosphere for 48 h. The reaction mixture was filtered through Celite, and the filtrate was evaporated to dryness to yield 1.38 g (3.75 mmol, 82%) of sulfonamide **41**, which was purified by crystallization in CH_2Cl_2/Hexane. M.p.: 134-140 °C (CH_2Cl_2/Hexane). IR (KBr): 3469, 3273, 1603, 822 cm^{-1}. ^1H NMR (400 MHz, $CDCl_3$): δ 3.63 (6H, *s*), 3.70 (3H, *s*), 3.77 (3H, *s*), 4.04 (2H, *bs*), 6.33 (2H, *s*), 6.64 (1H, *d, J* = 8.4), 7.11 (1H, *dd, J* = 8.4 and 2.4), 7.18 (1H, *d, J* = 2.4), 7.68 (1H, *bs*). ^{13}C NMR (100 MHz, $CDCl_3$): δ 55.6 (CH_3), 55.9 ($2CH_3$), 60.8 (CH_3), 99.2 (2CH), 109.2 (CH), 112.4 (CH), 118.6 (CH), 130.4 (C), 132.9 (C), 135.1 (C), 136.9 (C), 150.5 (C), 153.2 (2C). HRMS ($C_{16}H_{20}N_2O_6S + H^+$): calcd 369.1115 ($M + H^+$), found 369.1116.

3-Amino-4-methoxy-*N*-methyl-*N*-(3,4,5-trimethoxyphenyl)benzenesulfonamide (**42**). KOH (162 mg, 2.90 mmol) was added to a solution of **41** (535 mg, 1.45 mmol) in CH_3CN (30 mL). After 1 h at room temperature, 182 µL (2.90 mmol) of CH_3I were added and stirred for 24 h. The solution was concentrated under vacuum, re-dissolved in EtOAc, washed with brine, dried over Na_2SO_4, and evaporated to dryness to give 547 mg (1.43 mmol, 98%) of **42**. The crude reaction product was purified by crystallization in methanol (392 mg, 1.03 mmol, 71%). M.p.: 124-126 °C (MeOH). ^1H NMR (400 MHz, $CDCl_3$): δ 3.11 (3H, *s*), 3.73 (6H, *s*), 3.83 (3H, *s*), 3.90 (3H, *s*), 3.94 (2H, *s*), 6.30 (2H, *s*), 6.78 (1H, *d, J* = 8.8), 6.90 (1H, *d, J* = 2.4), 6.99 (1H, *dd, J* = 8.8 and 2.4). ^{13}C NMR (50 MHz, $CDCl_3$): δ 38.5 (CH_3), 55.7 (CH_3), 56.0 ($2CH_3$), 60.8 (CH_3), 104.6 (2CH), 109.1 (CH), 113.2 (CH), 118.8 (CH), 128.0 (C), 136.5 (C), 137.3 (C), 137.7 (C), 150.2 (C), 152.8 (2C). HRMS ($C_{17}H_{22}N_2O_6S + H^+$): calcd 383.1271 ($M + H^+$), found 383.1263.

3-Amino-*N*-ethyl-4-methoxy-*N*-(3,4,5-trimethoxyphenyl)benzenesulfonamide (**43**). 88 mg (0.24 mmol) of **41** and 66 mg (0.48 mmol) of K_2CO_3 were dissolved in dry DMF (3 mL). After 30 min stirring at room temperature, 2-bromoethane (35.7 µL, 0.48 mmol) was added to the solution and stirred for 24 h. The reaction mixture was concentrated under reduced pressure, dissolved in EtOAc, washed with brine, dried (Na_2SO_4), filtered, and concentrated under vacuum to give 69 mg (0.17 mmol, 73%) of crude reaction product **43**, from which 40 mg (0.10 mmol, 42%) were purified by crystallization in methanol. M.p.: 132-133 °C (MeOH). IR (KBr): 3465, 3364, 1594, 838 cm^{-1}. ^1H NMR (200 MHz, $CDCl_3$): δ 1.07 (3H, *t, J* = 7.2), 3.49 (2H, *q, J* = 7.2), 3.73 (6H, *s*), 3.84 (3H, *s*), 3.90 (3H, *s*), 6.26 (2H, *s*), 6.79 (1H, *d, J* = 8.2), 6.95 (1H, *d, J* = 2), 7.04 (1H, *dd, J* = 8.2 and 2). ^{13}C NMR (100 MHz, $CDCl_3$): δ 14.0 (CH_3), 45.8 (CH_2), 55.7 (CH_3), 56.1 ($2CH_3$), 60.8 (CH_3), 106.5 (2CH), 109.2 (CH), 113.2 (CH), 118.8 (CH), 130.1 (C), 134.7 (C), 136.4 (C), 137.6 (C), 150.2 (C), 152.9 (2C). HRMS ($C_{18}H_{24}N_2O_6S + H^+$): calcd 397.1428 ($M + H^+$), found 397.1425.

3-Amino-*N*-(cyanomethyl)-4-methoxy-*N*-(3,4,5-trimethoxyphenyl)benzenesulfonamide (**44**). A mixture of **41** (80 mg, 0.21 mmol) and K_2CO_3 (59 mg, 0.43 mmol) in dry DMF (3 mL) was stirred at room temperature for 30 min. Then, 2-chloroacetonitrile (27.6 µL, 0.43 mmol) was added. After 24 h, the solvent was evaporated under reduced pressure. The residue was dissolved in EtOAc and washed with brine, dried (Na_2SO_4), and concentrated under vacuum. The product was isolated by crystallization in methanol (**44**, 35 mg, 0.08 mmol, 40%). M.p.: 139-145 °C (MeOH). ^1H NMR (200 MHz, $CDCl_3$): δ 3.74 (6H, *s*), 3.85 (3H, *s*), 3.92 (3H, *s*), 4.01 (2H, *s*), 4.52 (2H, *s*), 6.40 (2H, *s*), 6.82 (1H, *d, J* = 8.4), 6.99 (1H, *d, J* = 2.4), 7.09 (1H, *dd, J* = 8.4 and 2.4). ^{13}C NMR (100 MHz, $CDCl_3$): δ 39.8 (CH_2), 56.0 (CH_3), 56.1 ($2CH_3$), 60.8 (CH_3), 106.1 (2CH), 109.4 (CH), 112.9 (CH), 115.1 (C), 119.1 (CH), 128.9 (C), 134.0 (C), 136.9 (C), 138.6 (C), 150.9 (C), 153.4 (2C). HRMS ($C_{18}H_{21}N_3O_6S + H^+$): calcd 408.1224 ($M + H^+$), found 408.1228.

3-Amino-*N*-benzyl-4-methoxy-*N*-(3,4,5-trimethoxyphenyl)benzenesulfonamide (**45**). 63 mg (0.46 mmol) of K_2CO_3 were added to a solution of **41** (86 mg, 0.23 mmol) in 3 mL of dry DMF. After 1 h at room temperature, 54.2 µL (0.46 mmol) of benzyl chloride were added and stirred for 24 h. The reaction mixture was concentrated, re-dissolved in EtOAc, washed with brine, dried over anhydrous Na_2SO_4, filtered, and concentrated under vacuum to obtain 101 mg (0.22

mmol, 94%) of **45**. Crude reaction product was then crystallized in methanol (58 mg, 0.13 mmol, 54%). M.p.: 160-163 °C (MeOH). ^{1}H NMR (200 MHz, $CDCl_3$): δ 3.63 (6H, *s*), 3.78 (3H, *s*), 3.93 (3H, *s*), 4.63 (2H, *s*), 6.14 (2H, *s*), 6.83 (1H, *d, J* = 8.4), 7.02 (1H, *d, J* = 2), 7.11 (1H, *dd, J* = 8.4 and 2), 7.23 (5H, *bs*). ^{13}C NMR (100 MHz, $CDCl_3$): δ 55.3 (CH_2), 55.8 (CH_3), 55.9 ($2CH_3$), 60.8 (CH_3), 106.7 (2CH), 109.3 (CH), 113.1 (CH), 118.8 (CH), 127.6 (CH), 128.3 (2CH), 128.7 (2CH), 130.5 (C), 134.9 (C), 136.2 (C), 136.6 (C), 137.6 (C), 150.3 (C), 152.7 (2C). HRMS ($C_{23}H_{26}N_2O_6S + H^+$): calcd 459.1584 ($M + H^+$), found 459.1589.

Ethyl (2-methoxy-5-(*N*-methyl-*N*-(3,4,5-trimethoxyphenyl)sulfamoyl)phenyl)glycinate (**46**). Ethyl 2-bromoacetate (242 µL, 2.17 mmol) and NaI (65 mg, 0.43 mmol) were added to a solution of **42** (83 mg, 0.22 mmol) and K_2CO_3 (59 mg, 0.43 mmol) in acetone/THF 1:1 (40 mL). The reaction mixture was heated at 70 °C for 48 h. After cooling, the reaction mixture was concentrated and re-dissolved in EtOAc, washed with brine, dried over Na_2SO_4, filtered, and evaporated to dryness. The residue was purified by preparative TLC (hexane/EtOAc 4:6) to afford compound **46** (20 mg, 0.04 mmol, 19%). ^{1}H NMR (400 MHz, $CDCl_3$): δ 1.28 (3H, *t, J* = 7.2), 3.10 (3H, *s*), 3.72 (6H, *s*), 3.80 (2H, *s*), 3.82 (3H, *s*), 3.91 (3H, *s*), 4.22 (2H, *q, J* = 7.2), 6.28 (2H, *s*), 6.57 (1H, *d, J* = 2), 6.77 (1H, *d, J* = 8.4), 6.99 (1H, *dd, J* = 8.4 and 2). ^{13}C NMR (50 MHz, $CDCl_3$): δ 14.1 (CH_3), 38.4 (CH_3), 44.9 (CH_2), 55.8 (CH_3), 56.1 ($2CH_3$), 60.8 (CH_3), 61.4 (CH_2), 104.6 (2CH), 108.2 (CH), 108.3 (CH), 118.2 (CH), 128.2 (C), 136.9 (C), 137.2 (C), 137.5 (C), 150.1 (C), 152.8 (2C), 170.3 (C). HRMS ($C_{21}H_{28}N_2O_8S + H^+$): calcd 469.1639 ($M + H^+$), found 469.1632.

Ethyl (5-(*N*-(2-ethoxy-2-oxoethyl)-*N*-(3,4,5-trimethoxyphenyl)sulfamoyl)-2-methoxyphenyl) glycinate (**47**). Ethyl 2-bromoacetate (72.6 µL, 0.65 mmol) was added after 30 min to a solution of **41** (80 mg, 0.22 mmol) and K_2CO_3 (59 mg, 0.43 mmol) in dry DMF (3 mL). The reaction mixture was then stirred for 48 h, concentrated under vacuum, re-dissolved in EtOAc, washed with brine, dried (Na_2SO_4), and evaporated to dryness. The residue was purified by preparative TLC (CH_2Cl_2/EtOAc 7:3) to give **47** (34 mg, 0.06 mmol, 29%). ^{1}H NMR (400 MHz, $CDCl_3$): δ 1.22 (3H, *t, J* = 7.2), 1.28 (3H, *t, J* = 7.2), 3.69 (6H, *s*), 3.79 (3H, *s*), 3.84 (2H, *s*), 3.89 (3H, *s*), 4.15 (2H, *q, J* = 7.2), 4.22 (2H, *q, J* = 7.2), 4.31 (2H, *s*), 6.38 (2H, *s*), 6.71 (1H, *d, J* = 2), 6.75 (1H, *d, J* = 8.4), 7.06 (1H, *dd, J* = 8.4 and 2). ^{13}C NMR (100 MHz, $CDCl_3$): δ 14.1 (CH_3), 14.1 (CH_3), 45.0 (CH_2), 52.9 (CH_2), 55.8 (CH_3), 56.0 ($2CH_3$), 60.8 (CH_3), 61.3 (CH_2), 61.5 (CH_2), 106.4 (2CH), 108.2 (CH), 108.3 (CH), 118.2 (CH), 130.5 (C), 135.5 (C), 137.1 (C), 137.8 (C), 150.2 (C), 152.9 (2C), 168.8 (C), 170.3 (C). HRMS ($C_{24}H_{32}N_2O_{10}S + H^+$): calcd 541.1850 ($M + H^+$), found 541.1830.

4-Methoxy-*N*-methyl-3-(methylamino)-*N*-(3,4,5-trimethoxyphenyl)benzenesulfonamide (**48a**) and 3-(dimethylamino)-4-methoxy-*N*-methyl-*N*-(3,4,5-trimethoxyphenyl) benzenesulfonamide (**48b**). $(CH_3)_2SO_4$ (272 µL, 2.85 mmol) was dropwise added to a solution of **41** (140 mg, 0.38 mmol) and K_2CO_3 (525 mg, 3.80 mmol) in acetone (20 mL) and heated under reflux overnight. Then, the reaction mixture was filtered, poured onto ice, and extracted with CH_2Cl_2. The organic layers were dried over anhydrous Na_2SO_4, filtered, and evaporated to dryness. Compounds **48a** (48 mg, 0.12 mmol, 32%) and **48b** (17 mg, 0.04 mmol, 11%) were isolated by preparative TLC (toluene/EtOAc 4:6). **48a:** IR (KBr): 3426, 1594, 1500, 803 cm^{-1}. ^{1}H NMR (400 MHz, $CDCl_3$): δ 2.76 (3H, *s*), 3.12 (3H, *s*), 3.74 (6H, *s*), 3.82 (3H, *s*), 3.89 (3H, *s*), 6.32 (2H, *s*), 6.63 (1H, *d, J* = 2), 6.75 (1H, *d, J* = 8), 6.99 (1H, *dd, J* = 8 and 2). ^{13}C NMR (100 MHz, $CDCl_3$): δ 30.0 (CH_3), 38.4 (CH_3), 55.7 (CH_3), 56.0 ($2CH_3$), 60.8 (CH_3), 104.7 (2CH), 107.7 (CH), 107.8 (CH), 117.1 (CH), 128.4 (C), 137.3 (C), 137.7 (C), 139.1 (C), 149.9 (C), 152.8 (2C). HRMS ($C_{18}H_{24}N_2O_6S + H^+$): calcd 397.1428 ($M + H^+$), found 397.1432. **48b:** ^{1}H NMR (400 MHz, $CDCl_3$): δ 2.64 (6H, *s*), 3.05 (3H, *s*), 3.66 (6H, *s*), 3.75 (3H, *s*), 3.88 (3H, *s*), 6.23 (2H, *s*), 6.82 (1H, *d, J* = 8.4), 6.89 (1H, *d, J* = 2), 7.24 (1H, *dd, J* = 8.4 and 2). ^{13}C NMR (100 MHz, $CDCl_3$): δ 37.9 (CH_3), 42.5 ($2CH_3$), 55.4 (CH_3), 55.7 ($2CH_3$), 60.5 (CH_3), 104.1 (2CH), 109.7 (CH), 117.3 (CH), 122.5 (CH), 127.4 (C), 136.8 (C), 137.1 (C), 141.9 (C), 152.5 (2C), 155.2 (C). HRMS ($C_{19}H_{26}N_2O_6S + H^+$): calcd 411.1584 ($M + H^+$), found 411.1570.

artículo 2

Methoxy and bromo scans on N-(5-methoxyphenyl) methoxybenzenesulphonamides reveal potent cytotoxic compounds, especially against the human breast adenocarcinoma MCF7 cell line

Myriam González, María Ovejero-Sánchez, Alba Vicente-Blázquez, Manuel Medarde, Rogelio González-Sarmiento, Rafael Peláez.

J. Enzyme Inhib. Med. Chem. **2021**, 36:1, 1029-1047
DOI: 10.1080/14756366.2021.1925265

RESUMEN

El objetivo de este artículo es estudiar el efecto en la actividad biológica de las sustituciones de los átomos de hidrógeno del Ar_A de *N*-(5-metoxifenil)-4-metoxibenceno sulfonamidas por grupos metoxilo y/o bromo – definido como *scan* estructural – en un intento de reemplazar el anillo de trimetoxifenilo de los clásicos inhibidores de microtúbulos. De esta forma, se diseñan y sintetizan 37 nuevas sulfonamidas con diferentes patrones de sustitución sobre el anillo de *N*-fenilo, combinados con diversos sustituyentes en el nitrógeno de la sulfonamida. 21 de los 37 nuevos ligandos presentan potencias citotóxicas submicromolares contra líneas celulares humanas de cáncer de cérvix (HeLa) y colon (HT-29), siendo especialmente potentes contra la línea celular de cáncer de mama MCF7. El co-tratamiento de la línea celular resistente a CA-4, HT-29, con el inhibidor de las MDR verapamilo, sugiere que los nuevos ligandos no son sustratos de las MDR y por lo tanto no son susceptibles de sufrir resistencias mediadas por MDR, una de las principales desventajas de las quimioterapias actuales. Además, la solubilidad acuosa de los ligandos sintetizados es apreciablemente mayor que la de los compuestos de referencia. Las moléculas más potentes presentan un patrón de sustitución de *N*-2,5-dimetoxifenilo, y son aún mejores cuando tienen un átomo de bromo en la posición 4, seleccionándose entre ellas el compuesto **25** (*N*-(4-bromo-2,5-dimetoxifenil)-*N*-(cianometil)-4-metoxibencenosulfonamida) para el estudio del mecanismo de acción. La hipótesis de que actúan como agentes desestabilizadores de los microtúbulos por unión al dominio de colchicina en tubulina, fue corroborada mediante experimentos de inmunofluorescencia, citometría de flujo, inhibición enzimática, *western blot* y estudios computacionales, dando lugar respectivamente a los siguientes resultados: i) Disrupción de la red microtubular, ii) Arresto mitótico de las células en la región G_2/M y muerte celular por apoptosis, iii) Inhibición de la polimerización de tubulina *in vitro* a concentraciones micromolares, iv) Inducción de la autofagia y v) Unión al sitio de la colchicina en tubulina. Por lo tanto, podemos concluir que estos compuestos novedosos abren las puertas al diseño de ligandos antimitóticos de unión a tubulina desprovistos del anillo de trimetoxifenilo considerado esencial, como tratamientos prometedores en la terapia antitumoral.

JOURNAL OF ENZYME INHIBITION AND MEDICINAL CHEMISTRY
2021, VOL. 36, NO. 1, 1029–1047
https://doi.org/10.1080/14756366.2021.1925265

Taylor & Francis
Taylor & Francis Group

RESEARCH PAPER

Methoxy and bromo scans on *N*-(5-methoxyphenyl) methoxybenzenesulphonamides reveal potent cytotoxic compounds, especially against the human breast adenocarcinoma MCF7 cell line

Myriam Gonzalez[a,b,c], Mar ıa Ovejero-Sanchez[b,d,e], Alba Vicente-Blazquez[a,b,c], Manuel Medarde[a,b,c], Rogelio Gonzalez-Sarmiento[b,d,e] and Rafael Pelaez[a,b,c]

[a]Laboratorio de Qu ımica Organica y Farmaceutica, Departamento de Ciencias Farmaceuticas, Facultad de Farmacia, Universidad de Salamanca, Salamanca, Spain; [b]Instituto de Investigacion Biomedica de Salamanca (IBSAL), Hospital Universitario de Salamanca, Salamanca, Spain; [c]Centro de Investigacion de Enfermedades Tropicales de la Universidad de Salamanca (CIETUS), Facultad de Farmacia, Universidad de Salamanca, Salamanca, Spain; [d]Unidad de Medicina Molecular, Departamento de Medicina, Facultad de Medicina, Universidad de Salamanca, Salamanca, Spain; [e]Laboratorio de Diagnostico en Cancer Hereditario, Centro de Investigacion del Cancer, Universidad de Salamanca-CSIC, Salamanca, Spain

ABSTRACT

Thirty seven *N*-(5-methoxyphenyl)-4-methoxybenzenesulphonamide with methoxy or/and bromo substitutions (series 1-4) and with different substituents on the sulphonamide nitrogen have been synthesised. 21 showed sub-micromolar cytotoxicity against HeLa and HT-29 human tumour cell lines, and were particularly effective against MCF7. The most potent series has 2,5-dimethoxyanilines, especially the 4-brominated compounds 23–25. The active compounds inhibit microtubular protein polymerisation at micromolar concentrations, thus pointing at tubulin as the target. Co-treatment with the MDR inhibitor verapamil suggests that they are not MDR substrates. Compound 25 showed nanomolar antiproliferative potency. It severely disrupts the microtubule network in cells and arrests cells at the G_2/M cell-cycle phase, thus confirming tubulin targeting. 25 triggered apoptotic cell death, and induced autophagy. Docking studies suggest binding in a distinct way to the colchicine site. These compounds are promising new antitumor agents acting on tubulin.

GRAPHICAL ABSTRACT

ARTICLE HISTORY
Received 18 February 2021
Revised 7 April 2021
Accepted 28 April 2021

KEYWORDS
Sulphonamides; tubulin; antimitotic; structure–activity relationships; colchicine

Introduction

Microtubule dynamics is a very well-established target in antitumor, antiparasitic, herbicidal, and antifungal chemotherapy[1,2]. Many microtubule-targeting drugs act by binding to tubulin, with some of them causing microtubule destabilisation (MDA, such as colchicine or vincristine), and others stabilisation (MSA, such as the taxanes) through binding to several binding sites[3]. The colchicine domain of tubulin is a highly hydrophobic region located at the intradimer interface between the *a*- and *b*-tubulins[4], and ligand binding prevents the dimer transition from curved to straight, which is necessary for polymerization[5]. Several colchicine-site ligands have reached clinical use as antiparasitic and antitumor drugs, such as the benzimidazoles nocodazole and albendazole[6], the stilbene combretastatin A-4 (CA-4)[7], or the sulphonamides ABT-751 or T138067[3]. However, each class of colchicine site drugs has liabilities, such as the low aqueous solubility and the instability of combretastatins[7], the insufficient potency of ABT-751[3], or the development of resistance by cancer cells[8], which urge for new medicinal chemistry efforts.

Diarylsulphonamides are privileged scaffolds in medicinal chemistry and well-known anticancer agents[3], with benzenesulphonamides carrying 3,4,5-trimethoxyphenyl (TMP) rings acting as tubulin inhibitors, such as *N*-(3,4,5-trimethoxyphenyl)-4-methoxybenzenesulphonamides[3]. The TMP ring has long been considered important for strong tubulin-binding through interactions with the sidechain of Cys241*b* amongst others and potent cytotoxic effects[4,9,10], but it is also a bulky hydrophobic moiety that lowers the aqueous solubility and suffers from metabolic inactivation by *O*-demethylation reactions of the aromatic methoxy groups[11–13]. Recently, successful substitutions of the TMP ring have appeared in several tubulin inhibitory structural families, such as the combretastatins, the isocombretastatins, and the phenstatins, some of them even featuring polar azines replacing the phenyl ring[14–17].

Here, we have explored new replacements for the *N*-TMP ring (Figure 1): keeping the 5-methoxy group to preserve the polar interaction with the sidechain of Cys241*b* and exploring the effect of the addition of methoxy groups (methoxy scan) and/or of bromine atoms (bromo scan) at different positions of the phenyl ring, as similar in size groups but with different bonding characteristics (weak hydrogen bonding acceptors for the methoxy groups and halogen bonding for the bromines[18,19]). We have combined these changes with different substituents on the sulphonamide nitrogen, exploring from hydrogen (unsubstituted) to small alkyls (methyl or ethyl) and more polar and larger acetates or acetonitriles or even to the much larger benzyl groups. We have assayed the new benzenesulphonamides against several

CONTACT RAFAEL Pelaez pelaez@usal.es Ciencias Farmaceuticas, Facultad de Farmacia, Universidad de Salamanca, Campus Miguel de Unamuno, Facultad de Farmacia, Salamanca, 37008 Spain

Supplemental data for this article can be accessed here.

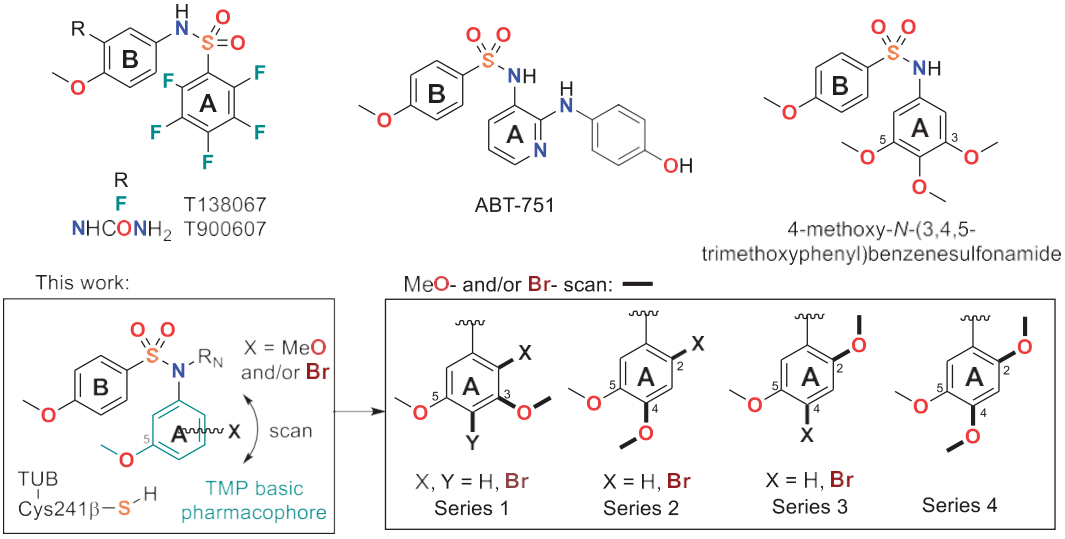

Figure 1. Chemical structure of tubulin inhibitor sulphonamides and summary of diarylsulphonamide scaffolds proposed in this work.

human tumour cell lines with different sensitivity towards CA-4, against the non-tumorigenic cell line HEK293, and for tubulin inhibitory activity *in vitro*. We have also ascertained the sensitivity to MDR pumps by comparing the cytotoxicity of the compounds alone or combined with the MDR inhibitor verapamil[20]. The new family of compounds encompasses potent inhibitors of cell proliferation and tubulin polymerisation, in particular the 4-bromo-2,5-dimethoxyphenyl series. We have shown that the designed compounds are antitumor agents interfering with the mitotic machinery by studying their effect on the microtubules of cancer cells by immunofluorescence, and assessed the effects on the cell cycle by flow cytometry, showing initial G_2/M arrest followed by apoptotic cell death. As for the reference ligands CA-4[21] and ABT-751[22], an increased autophagy response has been observed upon treatment. We have also studied the binding mode of the new benzenesulphonamides to the colchicine site of tubulin. These results show that the methoxy and bromo scans provide new antimitotic benzenesulphonamides devoid of the trimethoxyphenyl ring which are promising new antiproliferative agents.

Materials and methods

General chemical techniques

Reagents were used as purchased without further purification. Solvents (EtOAc, DMF, CH_2Cl_2, MeOH, CH_3CN, toluene) were stored over molecular sieves. TLC was performed on precoated silica gel polyester plates (0.25 mm thickness) with a UV fluorescence indicator 254 (Polychrom SI F254). Chromatographic separations were performed on silica gel columns by flash (Kieselgel 40, 0.040–0.063; Merck) chromatography. Melting points were deter- mined on a Bu€chi 510 apparatus and are uncorrected. ^{1}H NMR and ^{13}C NMR spectra were recorded in $CDCl_3$ or CD_3OD on a Bruker WP 200-SY spectrometer operating at 200/50 MHz, or Varian Mercury or Bruker SY spectrometers operating at 400/ 100 MHz. Chemical shifts (d) are given in ppm downfield from tetramethylsilane and coupling constants (J values) are given in Hz. IR spectra were run on KBr discs on a Nicolet Impact 410 Spectrophotometer. A hybrid QSTAR XL quadrupole/time of flight spectrometer was used for HRMS analyses. GC-MS spectra were performed using a Hewlett-Packard 5890 series II mass detector. A Helios-*a* UV-320 from Thermo-Spectronic was used for UV spectra.

General synthetic procedures

General procedure A for the formation of the sulphonamide bridge

To a stirred solution of the corresponding aniline (1 mmol) in CH_2Cl_2 (50 ml) and pyridine (2 ml), 4-methoxybenzenesulphonyl chloride (1 mmol) was slowly added. The mixture was stirred for 6 h at room temperature. Then the reaction was treated with 2 N HCl and 5% $NaHCO_3$, washed with brine, dried over anhydrous Na_2SO_4 and the solvent evaporated to dryness. Crude reaction products were purified by crystallisation to afford the corresponding sulphonamides (1, 11, 21, and 32).

General procedure B for alkylation of the sulphonamide nitrogen

B1: R_N ¼ CH_3. A mixture of the corresponding sulphonamide (1 mmol) and crushed KOH (2 mmol) in CH_3CN (50 ml) was stirred for 30 min. Then, CH_3I (2 mmol) was added and stirred at room temperature for 24 h. The solvent was removed under reduced pressure. The residue was re-dissolved in EtOAc and washed with brine, dried (Na_2SO_4), and concentrated in vacuum. Crude reaction products were further purified to afford the corresponding methylated sulphonamides (2, 12, 14, 22, 24, and 33).

B2: R_N 6¼ CH_3. To a solution of the sulphonamide derivative (1 mmol) in dry DMF (3 ml), K_2CO_3 (2 mmol) was added and the mixture was stirred for 1 h at room temperature. Then, the appropriate alkyl halide (2 mmol) was added, and the mixture was stirred at room temperature for 24 h. The solution was concentrated in a vacuum and redissolved in EtOAc. Then, it was washed with brine, dried over Na_2SO_4, and evaporated to dryness to give a crude reaction product which was further purified (3–7, 15–18, 25–28, and 34–37).

General procedure C for bromination

A mixture of the corresponding sulphonamide (1 mmol) and *N*-bromosuccinimide (1–2 mmol) in CH_2Cl_2 (50 ml) was stirred at room temperature overnight. The reaction mixture was washed with brine, dried, and concentrated under a vacuum. Crude reaction products were further purified to afford the brominated sulphonamides (8a–10c, 13, and 23).

General procedure D for the nitration of Ar_A precursors

To a stirred solution at 0 °C of the corresponding Ar_A precursor (1 mmol) in acetic acid (5 ml), nitric acid (1 mmol) in acetic acid (5 ml) was dropwise added under nitrogen atmosphere. After 4 h, the reaction was poured onto ice and the mixture was kept at 4 °C for 30 min. Then, the precipitate was washed with cold water and filtered under vacuum to dryness. Crude reaction products were then used without further purification (19 and 30).

General procedure E for the reduction of nitro precursors

The nitro derivatives were dissolved in EtOAc. Pd(C) (10 mg) was added to the solution and stirred at room temperature under H_2 atmosphere for 48 h. The reaction mixture was filtered through Celite® and the solvent vacuum evaporated. Crude reaction products were then used without further purification (20 and 31).

Chemical synthesis and characterisation

N-(3,5-dimethoxyphenyl)-4-methoxybenzenesulphonamide (1)

Following general procedure A, 3,5-dimethoxyaniline (290 mg, 1.89 mmol) and 4-methoxybenzenesulphonyl chloride (390 mg, 1.89 mmol) gave sulphonamide 1. Yield, crude: 97% (596 mg); crystals: 71% (438 mg). M.p.: 115–122 °C (CH_2Cl_2/hexane). IR (KBr): 3234, 1595, 824 cm $^{-1}$. ^{1}H NMR (400 MHz, $CDCl_3$): *d* 3.66 (6H, s), 3.77 (3H, s), 6.13 (1H, t, *J* ¼ 2), 6.17 (2H, d, *J* ¼ 2), 6.85 (2H, d, *J* ¼ 8.8), 7.68 (2H, d, *J* ¼ 8.8). ^{13}C NMR (100 MHz, $CDCl_3$): *d* 55.3 ($2CH_3$), 55.5 (CH_3), 97.0 (CH), 98.9 (2CH), 114.2 (2CH), 129.5 (2CH), 130.4 (C), 138.6 (C), 161.1 (2C), 163.1 (C). HRMS ($C_{15}H_{17}NO_5S$ þ Hþ): calcd 324.0909 (M þ Hþ), found 324.0900.

N-(3,5-dimethoxyphenyl)-4-methoxy-N-methylbenzenesulphonamide (2)

Following general procedure B1, compound 1 (205 mg, 0.63 mmol) was methylated with CH_3I (79 mL, 1.27 mmol). Yield, crude: 89% (190 mg); crystals 50% (108 mg). M.p.: 120–128 °C (MeOH). ^{1}H NMR (400 MHz, $CDCl_3$): *d* 3.10 (3H, s), 3.72 (6H, s), 3.85 (3H, s), 6.26 (2H, d, *J* ¼ 2), 6.35 (1H, t, *J* ¼ 2), 6.91 (2H, d, *J* ¼ 9.2), 7.53 (2H, d, *J* ¼ 9.2). ^{13}C NMR (100 MHz, $CDCl_3$): *d* 38.1 (CH_3), 55.4 ($2CH_3$), 55.5 (CH_3), 99.4 (CH), 104.9 (2CH), 113.8 (2CH), 128.2 (C), 129.9 (2CH), 143.5 (C), 160.5 (2C), 163.0 (C). HRMS ($C_{16}H_{19}NO_5S$ þ Hþ): calcd 338.1057 (M þ Hþ), found 338.1050.

N-(3,5-dimethoxyphenyl)-N-ethyl-4-methoxybenzenesulphonamide (3)

Following general procedure B2, compound 1 (274 mg, 0.85 mmol) was alkylated using bromoethane (252 mL, 3.40 mmol) as alkylating agent. Yield, crude: 87% (260 mg); crystals: 67% (201 mg). M.p.: 109–118 °C (MeOH). IR (KBr): 1605, 1497, 1162, 838 cm $^{-1}$. ^{1}H NMR (400 MHz, $CDCl_3$): *d* 1.07 (3H, t, *J* ¼ 7.2), 3.52 (2H, q, *J* ¼ 7.2), 3.71 (6H, s), 3.85 (3H, s), 6.20 (2H, d, *J* ¼ 2), 6.39 (1H, t, *J* ¼ 2), 6.93 (2H, d, *J* ¼ 8.8), 7.58 (2H, d, *J* ¼ 8.8). ^{1} C NMR (100 MHz, $CDCl_3$): *d* 13.9 (CH_3), 45.5 (CH_2), 55.4 ($2CH_3$), 55.5 (CH_3), 100.1 (CH), 107.1 (2CH), 113.8 (2CH), 129.8 (2CH), 130.0 (C), 140.7 (C), 160.6 (2C), 162.8 (C). HRMS ($C_{17}H_{21}NO_5S$ þ Hþ): calcd 352.1213 (M þ Hþ), found 352.1219.

N-(cyanomethyl)-N-(3,5-dimethoxyphenyl)-4-methoxybenzenesulphonamide (4)

Following general procedure B2, compound 1 (113 mg, 0.35 mmol) was alkylated using 2-chloroacetonitrile (44 mL, 0.70 mmol) as alkylating agent. Yield, crude: 89% (113 mg); crystals: 53% (67 mg). M.p.: 92–96 °C (MeOH). ^{1}H NMR (400 MHz, $CDCl_3$): *d* 3.70 (6H, s), 3.85 (3H, s), 4.51 (2H, s), 6.34 (2H, d, *J* ¼ 2), 6.43 (1H, t, *J* ¼ 2), 6.95 (2H, d, *J* ¼ 8.8), 7.65 (2H, d, *J* ¼ 8.8). ^{13}C NMR (100 MHz, $CDCl_3$): *d* 39.4 (CH_2), 55.5 ($2CH_3$), 55.6 (CH_3), 101.2 (CH), 106.1 (2CH), 114.2 (2CH), 115.0 (C), 128.8 (C), 130.2 (2CH), 140.2 (C), 161.1 (2C), 163.7 (C). HRMS ($C_{17}H_{18}N_2O_5S$ þ Hþ): calcd 363.1009 (M þ Hþ), found 363.1003.

Ethyl N-(3,5-dimethoxyphenyl)-N-((4-methoxyphenyl)sulphonyl)glycinate (5)

Following general procedure B2, compound 1 (110 mg, 0.34 mmol) was alkylated using ethyl 2-bromoacetate (76 mL, 0.68 mmol) as alkylating agent and purified by preparative TLC (hexane:EtOAc 1:1). Yield, crude: 97% (135 mg); preparative: 80% (112 mg). ^{1}H NMR (400 MHz, $CDCl_3$): *d* 1.22 (3H, t, *J* ¼ 7.6), 3.68 (6H, s), 3.83 (3H, s), 4.14 (2H, q, *J* ¼ 7.6), 4.35 (2H, s), 6.35 (3H, bs), 6.90 (2H, d, *J* ¼ 8.8), 7.66 (2H, d, *J* ¼ 8.8). ^{13}C NMR (100 MHz, $CDCl_3$): *d* 14.0 (CH_3), 52.6 (CH_2), 55.3 ($2CH_3$), 55.5 (CH_3), 61.4 (CH_2), 100.3 (CH), 106.4 (2CH), 113.8 (2CH), 130.0 (2CH), 130.4 (C), 141.7 (C), 160.7 (2C), 163.0 (C), 168.8 (C). HRMS ($C_{19}H_{23}NO_7S$ þ Hþ): calcd 410.1268 (M þ Hþ), found 410.1262.

N-benzyl-N-(3,5-dimethoxyphenyl)-4-methoxybenzenesulphonamide (6)

Following general procedure B2, compound 1 (90 mg, 0.28 mmol) was alkylated using benzyl chloride (48.5 mL, 0.42 mmol) as alkylating agent. Yield, crude: 90% (104 mg); crystals: 70% (81 mg). M.p.: 146–150 °C (MeOH). IR (KBr): 3467, 1458, 806 cm $^{-1}$. ^{1}H NMR (400 MHz, $CDCl_3$): *d* 3.62 (6H, s), 3.87 (3H, s), 4.65 (2H, s), 6.12 (2H, d, *J* ¼ 2), 6.28 (1H, t, *J* ¼ 2), 6.94 (2H, d, *J* ¼ 8.8), 7.22 (5H, m), 7.63 (2H, d, *J* ¼ 8.8). ^{13}C NMR (100 MHz, $CDCl_3$): *d* 54.7 (CH_2), 55.3 ($2CH_3$), 55.6 (CH_3), 100.0 (CH), 107.2 (2CH), 113.9 (2CH), 127.5 (CH), 128.3 (2CH), 128.5 (2CH), 129.8 (2CH), 130.3 (C), 136.1 (C), 140.9 (C), 160.4 (2C), 162.9 (C). HRMS ($C_{22}H_{23}NO_5S$ þ Hþ): calcd 414.1370 (M þ Hþ), found 414.1369.

Benzyl (3,5-dimethoxyphenyl)((4-methoxyphenyl)sulphonyl)carbamate (7)

Following general procedure B2, compound 1 (77 mg, 0.24 mmol) was alkylated using benzyl chloroformate (70 mL, 0.48 mmol) as alkylating agent and purified by preparative TLC (hexane:EtOAc 6:4). Yield 23% (25 mg). M.p.: 129–131 °C (MeOH). ^{1}H NMR (400 MHz, $CDCl_3$): *d* 3.78 (6H, s), 3.88 (3H, s), 5.11 (2H, s), 6.40 (2H, d, *J* ¼ 2.4), 6.53 (1H, t, *J* ¼ 2.4), 6.92 (2H, d, *J* ¼ 8.8), 7.16 (2H, bs), 7.29 (3H, bs), 7.90 (2H, d, *J* ¼ 8.8). ^{1} C NMR (100 MHz, $CDCl_3$): *d* 56.3 ($2CH_3$), 56.5 (CH_3), 69.5 (CH_2), 102.5 (CH), 108.9 (2CH), 114.7 (2CH), 128.7 (2CH), 129.2 (CH), 129.3 (2CH), 131.2 (C), 132.1 (2CH), 135.6 (C), 138.2 (C), 152.8 (C), 161.6 (2C), 164.6 (C). HRMS ($C_{23}H_{23}NO_7S$ þ Na^+): calcd 480.1087 (M þ Na^+), found 480.1074.

N-(4-bromo-3,5-dimethoxyphenyl)-4-methoxy-N-methylbenzenesulphonamide (8a) and N-(2-bromo-3,5-dimethoxyphenyl)-4-methoxy-N-methylbenzenesulphonamide (8b)

Following general procedure C, compound 2 (190 mg, 0.56 mmol) was brominated. *N*-bromosuccinimide (150 mg, 0.84 mmol). 8a and 8b were isolated by flash column chromatography (hexane:EtOAc 8:2). Yield, 8a: 54% (127 mg); 8b: 14% (34 mg). 8a: M.p.: 156–160 °C (MeOH). ^{1}H NMR (200 MHz, $CDCl_3$): *d* 3.15 (3H, s), 3.77 (6H, s), 3.86 (3H, s), 6.30 (2H, s), 6.93 (2H, d, *J* ¼ 8.8), 7.53 (2H, d, *J* ¼ 8.8). ^{13}C NMR (100 MHz, $CDCl_3$): *d* 38.2 (CH_3), 55.6 (CH_3), 56.5 ($2CH_3$), 99.9 (C), 103.6 (2CH), 113.9 (2CH), 127.9 (C), 130.1 (2CH), 142.1 (C), 156.8 (2 C), 163.1 (C). HRMS ($C_{16}H_{18}BrNO_5S$ þ Hþ): calcd 416.0162 and 418.0141 (M þ Hþ), found 416.0158 and 418.0134. 8b: M.p.: 158–164 °C (MeOH). IR (KBr): 1592, 1498, 1151, 666 cm^{-1}. ^{1}H NMR (200 MHz, $CDCl_3$): *d* 3.14 (3H, s), 3.73 (3H, s), 3.85 (3H, s), 3.87 (3H, s), 6.39 (1H, d, *J* ½ 2.6), 6.46 (1H, d, *J* 2.6), 6.97 (2H, d, *J* ¼ 9), 7.79 (2H, d, *J* ¼ 9). ^{13}C NMR (100 MHz, $CDCl_3$): *d* 38.1 (CH_3), 55.6 (CH_3), 56.4 (CH_3), 56.7 (CH_3), 99.8 (CH), 105.4 (C), 106.7 (CH), 114.1 (2CH), 130.1 (2CH), 130.7 (C), 141.7 (C), 157.5 (C), 159.6 (C), 163.0 (C). HRMS ($C_{16}H_{18}BrNO_5S$ þ Naþ): 437.9981 and 439.9961 calcd (M þ Naþ), found 437.9976 and 439.9961.

N-(4-bromo-3,5-dimethoxyphenyl)-N-ethyl-4-methoxybenzenesulphonamide (9a) and N-(2-bromo-3,5-dimethoxyphenyl)-N-ethyl-4-methoxybenzenesulphonamide (9b)

Following general procedure C, compound 3 (190 mg, 0.54 mmol) was brominated. *N*-bromosuccinimide (192 mg, 1.08 mmol). 9a and 9b were isolated by flash column chromatography (hexane:EtOAc 8:2). Yield, 9a: 38% (90 mg); 9b: 16% (37 mg). 9a: M.p.: 141–144 °C (MeOH). ^{1}H NMR (200 MHz, $CDCl_3$): *d* 1.09 (3H, t, *J* ¼ 7), 3.57 (2H, q, *J* ¼ 7), 3.75 (6H, s), 3.86 (3H, s), 6.23 (2H, s), 6.93 (2H, d, *J* 9), 7.58 (2H, d, *J* ¼ 9). ^{13}C NMR (100 MHz, $CDCl_3$): *d* 14.0 (CH_3), 45.6 (CH_2), 55.6 (CH_3), 56.5 ($2CH_3$), 100.6 (C), 105.7 (2CH), 113.8 (2CH), 129.7 (C), 129.9 (2CH), 139.4 (C), 156.9 (2 C), 163.0 (C). HRMS ($C_{17}H_{20}BrNO_5S$ þ Hþ): calcd 430.0318 and 432.0298 (M Hþ), found 430.0313 and 432.0289. 9b: M.p.: 146–150 °C (MeOH). ^{1}H NMR (200 MHz, $CDCl_3$): *d* 1.09 (3H, t, *J* ¼ 7), 3.59 (2H, m), 3.73 (3H, s), 3.86 (3H, s), 3.87 (3H, s), 6.33 (1H, d, *J* ½ 2.6), 6.47 (1H, d, *J* ½ 2.6), 6.95 (2H, d, *J* ¼ 9), 7.76 (2H, d, *J* 9). ^{13}C NMR (100 MHz, $CDCl_3$): *d* 13.7 (CH_3), 45.9 (CH_2), 55.5 (CH_3), 55.6 (CH_3), 56.4 (CH_3), 99.9 (CH), 106.9 (C), 108.2 (CH), 113.9 (2CH), 130.1 (2CH), 131.5 (C), 139.2 (C), 157.5 (C), 159.4 (C), 162.9 (C). HRMS ($C_{17}H_{20}BrNO_5S$ þ Hþ): calcd 430.0318 and 432.0298 (M Hþ), found 430.0312 and 432.0281.

N-benzyl-N-(4-bromo-3,5-dimethoxyphenyl)-4-methoxybenzenesulphonamide (10a), N-benzyl-N-(2-bromo-3,5-dimethoxyphenyl)-4-methoxybenzenesulphonamide (10b) and N-benzyl-N-(2,4-dibromo-3,5-dimethoxyphenyl)-4-methoxybenzenesulphonamide (10c)

Following general procedure C, compound 6 (195 mg, 0.47 mmol) was brominated. *N*-bromosuccinimide (168 mg, 0.94 mmol). 10a, 10b and 10c were isolated by flash column chromatography (hexane:EtOAc 8:2). Yield, 10a: 50% (116 mg); 10b: 10% (24 mg); 10c: 2% (6 mg). 10a: M.p.: 199–203 °C (MeOH). IR (KBr): 3435, 1589, 836 cm^{-1}. ^{1}H NMR (200 MHz, $CDCl_3$): *d* 3.65 (6H, s), 3.88 (3H, s), 4.68 (2H, s), 6.12 (2H, s), 6.97 (2H, d, *J* ¼ 9), 7.22 (5H, bs), 7.65 (2H, d, *J* ¼ 9). ^{13}C NMR (100 MHz, $CDCl_3$): *d* 54.9 (CH_2), 55.7 (CH_3), 56.4 ($2CH_3$), 100.5 (C), 105.8 (2CH), 114.0 (2CH), 127.8 (CH), 128.4 (2CH), 128.6 (2CH), 129.9 (C), 130.0 (2CH), 135.7 (C), 139.4 (C), 156.7 (2 C), 163.1 (C). HRMS ($C_{22}H_{22}BrNO_5S$ þ Hþ): calcd 492.0475 and 494.0454 (M þ Hþ), found 492.0473 and 494.0440. 10b: IR (KBr): 2938, 1593, 831 cm^{-1}. ^{1}H NMR (200 MHz, $CDCl_3$): *d* 3.57 (3H, s), 3.80 (3H, s), 3.87 (3H, s), 4.60 (1H, d, *J* ¼ 14.4), 4.89 (1H, d, *J* ¼ 14.4), 6.14 (1H, d, *J* ¼ 2.8), 6.38 (1H, d, *J* ¼ 2.8), 6.94 (2H, d, *J* ¼ 9), 7.20 (5H, bs), 7.74 (2H, d, *J* ¼ 9). ^{13}C NMR (100 MHz, $CDCl_3$): *d* 54.4 (CH_2), 55.5 (CH_3), 55.6 (CH_3), 56.3 (CH_3), 100.0 (CH), 105.9 (C), 109.4 (CH), 113.9 (2CH), 127.7 (CH), 128.2 (2CH), 129.4 (2CH), 130.1 (2CH), 131.8 (C), 135.7 (C), 138.8 (C), 157.2 (C), 158.9 (C), 163.0 (C). HRMS ($C_{22}H_{22}BrNO_5S$ þ Hþ): calcd 492.0475 and 494.0454 (M þ Hþ), found 492.0467 and 494.0447. 10c: IR (KBr): 2935, 1595, 835 cm^{-1}. ^{1}H NMR (200 MHz, $CDCl_3$): *d* 3.60 (3H, s), 3.77 (3H, s), 3.87 (3H, s), 4.55 (1H, d, *J* ¼ 14.4), 4.97 (1H, d, *J* ¼ 14.4), 6.30 (1H, s), 6.95 (2H, d, *J* ¼ 9), 7.22 (5H, m), 7.73 (2H, d, *J* ¼ 9). ^{13}C NMR (100 MHz, $CDCl_3$): *d* 54.2 (CH_2), 55.6 (CH_3), 56.5 (CH_3), 60.5 (CH_3), 108.8 (C), 112.4 (C), 112.8 (CH), 114.0 (2CH), 128.0 (CH), 128.3 (2CH), 129.4 (2CH), 130.0 (2CH), 131.5 (C), 135.4 (C), 137.4 (C), 155.6 (C), 155.7 (C), 163.2 (C). HRMS ($C_{22}H_{21}Br_2NO_5S$ þ Hþ): calcd 569.9580 and 571.9559 (M þ Hþ), found 569.9577 and 571.9558.

N-(3,4-dimethoxyphenyl)-4-methoxybenzenesulphonamide (11)

Following general procedure A, 3,4-dimethoxyaniline (2.49 g, 16.26 mmol) and 4-methoxybenzenesulphonyl chloride (3.61 g, 16.26 mmol) gave sulphonamide 11. Yield, crude: 99% (5.29 g); crystals: 75% (4.04 g). M.p.: 101–102 °C (CH_2Cl_2/hexane). IR (KBr): 3224, 1498, 801 cm^{-1}. ^{1}H NMR (400 MHz, $CDCl_3$): *d* 3.75 (3H, s), 3.79 (3H, s), 3.80 (3H, s), 6.53 (1H, dd, *J* ¼ 8.8 and 2.8), 6.66 (1H, d, *J* ¼ 8.8), 6.70 (1H, d, *J* ¼ 2.8), 6.86 (2H, d, *J* ¼ 8.8), 7.66 (2H, d, *J* ¼ 8.8). ^{13}C NMR (100 MHz, $CDCl_3$): *d* 55.5 (CH_3), 55.9 (CH_3), 55.9 (CH_3), 107.7 (CH), 111.1 (CH), 114.0 (2CH), 115.4 (CH), 129.4 (2CH), 129.5 (C), 130.3 (C), 147.2 (C), 149.1 (C), 163.0 (C). HRMS ($C_{15}H_{17}NO_5S$ þ Hþ): calcd 324.0900 (M þ Hþ), found 324.0906.

N-(3,4-dimethoxyphenyl)-4-methoxy-N-methylbenzenesulphonamide (12)

Following procedure B1, compound 11 (205 mg, 0.63 mmol) was methylated and purified by silica gel column chromatography (hexane:EtOAc, 6:4). CH_3I (79 mL, 1.27 mmol). Yield 84% (180 mg). IR (KBr): 3435, 1595, 1508, 823 cm^{-1}. ^{1}H NMR (400 MHz, $CDCl_3$): *d* 3.06 (3H, s), 3.72 (3H, s), 3.80 (3H, s), 6.46 (1H, dd, *J* ¼ 8.8 and 2.0), 6.62 (1H, d, *J* ¼ 2.0), 6.69 (1H, d, *J* ¼ 8.8), 6.87 (2H, d, *J* ¼ 9.2), 7.44 (2H, d, *J* ¼ 9.2). ^{13}C NMR (100 MHz, $CDCl_3$): *d* 38.5 (CH_3), 55.6 (CH_3), 55.8 (CH_3), 55.9 (CH_3), 110.5 (CH), 111.1 (CH), 113.8 (2CH), 118.5 (CH), 127.8 (C), 130.0 (2CH), 134.5 (C), 148.2 (C), 148.6 (C), 162.9 (C). HRMS ($C_{16}H_{19}NO_5S$ þ Hþ): calcd 338.1057 (M Hþ), found 338.1058.

N-(2-bromo-4,5-dimethoxyphenyl)-4-methoxybenzenesulphonamide (13)

Following general procedure C, compound 11 (195 mg, 0.60 mmol) was brominated. *N*-bromosuccinimide (129 mg, 0.72 mmol). Yield, crude: 95% (232 mg); crystals: 32% (77 mg). M.p.: 162–167 °C (CH_2Cl_2/hexane). IR (KBr): 3265, 1594, 1510, 895 cm^{-1}. ^{1}H NMR (400 MHz, $CDCl_3$): *d* 3.80 (3H, s), 3.82 (3H, s), 3.89 (3H, s), 6.59 (1H, s), 6.81 (1H, s), 6.86 (2H, d, *J* ¼ 9.2), 7.62 (2H, d, *J* ¼ 9.2). ^{13}C NMR (100 MHz, $CDCl_3$): *d* 55.5 (CH_3), 56.1 ($2CH_3$), 107.1 (C), 108.1 (CH), 114.0 (2CH), 114.3 (CH), 127.6 (C), 129.5 (2CH), 130.1 (C), 147.4 (C), 148.8 (C), 163.2 (C). HRMS ($C_{15}H_{16}BrNO_5S$ þ Hþ): calcd 402.0005 and 403.9985 (M þ Hþ), found 402.0008 and 403.9972.

N-(2-bromo-4,5-dimethoxyphenyl)-4-methoxy-N-methylbenzenesulphonamide (14)

Following procedure B1, compound 13 (54 mg, 0.13 mmol) was methylated. CH_3I (16 mL, 0.26 mmol). Yield, crude: 88% (49 mg); crystals: 52% (29 mg). M.p.: 136–141 °C (MeOH). IR (KBr): 1596, 1507, 833 cm $^{-1}$. ^{1}H NMR (400 MHz, $CDCl_3$): *d* 3.15 (3H, s), 3.72 (3H, s), 3.84 (3H, s), 3.85 (3H, s), 6.62 (1H, s), 6.95 (2H, d, *J* ¼ 9.2), 6.99 (1H, s), 7.73 (2H, d, *J* ¼ 9.2). ^{13}C NMR (100 MHz, $CDCl_3$): *d* 38.3 (CH_3), 55.6 (CH_3), 56.0 (CH_3), 56.2 (CH_3), 113.0 (CH), 113.9 (2CH), 114.7 (C), 115.4 (CH), 130.1 (2CH), 130.6 (C), 132.4 (C), 148.4 (C), 149.4 (C), 163.0 (C). HRMS ($C_{16}H_{18}BrNO_5S$ þ HÞ): calcd 416.0162 and 418.0141 (M þ HÞ), found 416.0168 and 418.0155.

N-(2-bromo-4,5-dimethoxyphenyl)-N-ethyl-4-methoxybenzenesulphonamide (15)

Following general procedure B2, compound 13 (91 mg, 0.22 mmol) was alkylated using bromoethane (34 mL, 0.45 mmol) as alkylating agent. Yield, crude: 72% (71 mg); crystals: 39% (38 mg). M.p.: 111–117 °C (MeOH). ^{1}H NMR (200 MHz, $CDCl_3$): *d* 1.10 (3H, t, *J* ¼ 7.2), 3.49 (2H, m), 3.74 (3H, s), 3.87 (6H, s), 6.57 (1H, s), 6.95 (2H, d, *J* ¼ 9.0), 7.03 (1H, s), 7.72 (2H, d, *J* ¼ 9.0). ^{1}C NMR (100 MHz, $CDCl_3$): *d* 13.8 (CH_3), 45.9 (CH_2), 55.6 (CH_3), 56.0 (CH_3), 56.2 (CH_3), 113.9 (2CH), 114.1 (CH), 115.5 (CH), 116.4 (C), 129.8 (C), 130.0 (2CH), 131.3 (C), 148.2 (C), 149.4 (C), 162.9 (C). HRMS ($C_{17}H_{20}BrNO_5S$ þ HÞ): calcd 430.0318 and 432.0298 (M þ HÞ), found 430.0313 and 432.0285.

N-(2-bromo-4,5-dimethoxyphenyl)-N-(cyanomethyl)-4-methoxybenzenesulphonamide (16)

Following general procedure B2, compound 13 (103 mg, 0.25 mmol) was alkylated using 2-chloroacetonitrile (32.5 mL, 0.51 mmol) as alkylating agent. Yield, crude: 83% (94 mg); crystals: 51% (58 mg). M.p.: 76–84 °C (MeOH). ^{1}H NMR (400 MHz, $CDCl_3$): *d* 3.72 (3H, s), 3.85 (6H, s), 4.21 (1H, bd), 4.88 (1H, bd), 6.74 (1H, s), 6.97 (2H, d, *J* ¼ 9.2), 7.02 (1H, s), 7.72 (2H, d, *J* ¼ 9.2). ^{1}C NMR (100 MHz, $CDCl_3$): *d* 38.8 (CH_2), 55.7 (CH_3), 56.1 (CH_3), 56.3 (CH_3), 114.0 (CH), 114.3 (2CH), 115.0 (C), 115.2 (C), 115.5 (CH), 128.5 (C), 129.9 (C), 130.3 (2CH), 148.6 (C), 150.4 (C), 163.7 (C). HRMS ($C_{17}H_{17}BrN_2O_5S$ þ HÞ): calcd 441.0114 and 443.0094 (M þ HÞ), found 441.0101 and 443.0091.

Ethyl N-(2-bromo-4,5-dimethoxyphenyl)-N-((4-methoxyphenyl)sulphonyl)glycinate (17)

Following general procedure B2, compound 13 (98 mg, 0.24 mmol) was alkylated using ethyl 2-bromoacetate (54 mL, 0.48 mmol) as alkylating agent. Yield, crude: 87% (104 mg); crystals: 44% (52 mg). M.p.: 116–126 °C (MeOH). IR (KBr): 1751, 1739, 1596, 1507, 831 cm $^{-1}$. ^{1}H NMR (200 MHz, $CDCl_3$): *d* 1.25 (3H, t, *J* ¼ 7), 3.76 (3H, s), 3.84 (3H, s), 3.85 (3H, s), 4.16 (4H, m), 6.91 (2H, d, *J* ¼ 9.2), 6.93 (1H, s), 7.12 (1H, s), 7.66 (2H, d, *J* ¼ 9.2). ^{1}C NMR (100 MHz, $CDCl_3$): *d* 14.1 (CH_3), 51.9 (CH_2), 55.5 (CH_3), 56.0 (CH_3), 56.2 (CH_3), 61.3 (CH_2), 113.8 (2CH), 114.6 (C), 115.0 (CH), 116.7 (CH), 130.0 (2CH), 130.1 (C), 131.7 (C), 148.0 (C), 149.7 (C), 163.1 (C), 169.3 (C). HRMS ($C_{19}H_{22}BrNO_7S$ þ HÞ): calcd 488.0373 and 490.0353 (M þ HÞ), found 488.0364 and 490.0346.

N-benzyl-N-(2-bromo-4,5-dimethoxyphenyl)-4-methoxybenzenesulphonamide (18)

Following general procedure B2, compound 13 (107 mg, 0.26 mmol) was alkylated using benzyl chloride (62 mL, 0.53 mmol) as alkylating agent. Yield, crude: 82% (107 mg); crystals: 26% (34 mg). M.p.: 114–120 °C (MeOH). ^{1}H NMR (400 MHz, $CDCl_3$): *d* 3.54 (3H, s), 3.79 (3H, s), 3.83 (3H, s), 4.57 (1H, d, *J* ¼ 14), 4.86 (1H, d, *J* ¼ 14), 6.33 (1H, s), 6.89 (1H, s), 6.93 (2H, d, *J* 8.4), 7.19 (5H, bs), 7.71 (2H, d, *J* 8.4). ^{13}C NMR (100 MHz, $CDCl_3$): *d* 54.8 (CH_2), 55.9 (CH_3), 56.2 (CH_3), 56.4 (CH_3), 114.3 (2CH), 115.6 (CH), 115.8 (C), 116.1 (CH), 128.2 (CH), 128.6 (2CH), 129.8 (C), 129.9 (2CH), 130.4 (2CH), 132.0 (C), 136.0 (C), 148.2 (C), 149.6 (C), 163.4 (C). HRMS ($C_{22}H_{22}BrNO_5S$ þ HÞ): calcd 492.0475 and 494.0454 (M þ HÞ), found 492.0469 and 494.0451.

1,4-Dimethoxy-2-nitrobenzene (19)

Following general procedure D, 1,4-dimethoxybenzene (2.35 g, 17 mmol) was nitrated. HNO_3 (1.13 ml, 17 mmol). Yield 94% (2.92 g). M.p.: 71.8–72.5 °C (CH_2Cl_2/hexane). IR (KBr): 1528, 874, 763 cm $^{-1}$. ^{1}H NMR (400 MHz, $CDCl_3$): *d* 3.82 (3H, s), 3.92 (3H, s), 7.03 (1H, d, *J* ¼ 9.6), 7.12 (1H, dd, *J* 9.6 and 3.2), 7.4 (1H, d, *J* 3.2). ^{1}C NMR (100 MHz, $CDCl_3$): *d* 55.9 (CH_3), 56.9 (CH_3), 109.9 (CH), 115.0 (CH), 120.8 (CH), 139.3 (C), 147.3 (C), 152.7 (C). GC-MS ($C_8H_9NO_4$): 183 (MÞ).

2,5-Dimethoxyaniline (20)

Following general procedure E, compound 19 (2.92 g, 15.95 mmol) was reduced. Yield 99% (2.42 g). IR (KBr): 3459, 1519, 839 cm $^{-1}$. ^{1}H NMR (400 MHz, $CDCl_3$): *d* 3.72 (3H, s), 3.79 (3H, s), 6.24 (1H, dd, *J* 9.2 and 3.2), 6.33 (1H, d, *J* 3.2), 6.69 (1H, d, *J* 9.2). ^{13}C NMR (100 MHz, $CDCl_3$): *d* 54.5 (CH_3), 55.1 (CH_3), 100.9 (CH), 101.1 (CH), 110.3 (CH), 136.2 (C), 140.9 (C), 153.3 (C). GC-MS ($C_8H_{11}NO_2$): 153 (MÞ).

N-(2,5-dimethoxyphenyl)-4-methoxybenzenesulphonamide (21)

Following general procedure A, aniline 20 (2.42 g, 15.84 mmol) and 4-methoxybenzenesulphonyl chloride (3.27 g, 15.84 mmol) gave sulphonamide 21. Yield, crude: 95% (4.9 g); crystals: 84% (4.29 g). M.p.: 114–115 °C (CH_2Cl_2/hexane). IR (KBr): 3313, 1578, 830 cm $^{-1}$. ^{1}H NMR (400 MHz, $CDCl_3$): *d* 3.62 (3H, s), 3.74 (3H, s), 3.81 (3H, s), 6.53 (1H, dd, *J* ¼ 9.2 and 3.2), 6.65 (1H, d, *J* 9.2), 6.86 (2H, d, *J* 9.2), 7.01 (1H, bs), 7.14 (1H, d, *J* 3.2), 7.72 (2H, d, *J* 9.2). ^{13}C NMR (100 MHz, $CDCl_3$): *d* 55.5 (CH_3), 55.7 (CH_3), 56.2 (CH_3), 106.8 (CH), 109.5 (CH), 111.4 (CH), 113.9 (2CH), 126.8 (C), 129.4 (2CH), 130.7 (C), 143.4 (C), 153.8 (C), 163.0 (C). HRMS ($C_{15}H_{17}NO_5S$ þ HÞ): calcd 324.0900 (M þ HÞ), found 324.0900.

N-(2,5-dimethoxyphenyl)-4-methoxy-N-methylbenzenesulphonamide (22)

Following general procedure B1, compound 21 (615 mg, 1.90 mmol) was methylated. CH_3I (242 mL, 3.80 mmol). Yield, crude: 95% (611 mg); crystals: 57% (366 mg). M.p.: 105–110 °C (CH_2Cl_2/hexane). IR (KBr): 3467, 2948, 1595, 818 cm $^{-1}$. ^{1}H NMR (400 MHz, $CDCl_3$): *d* 3.09 (3H, s), 3.32 (3H, s), 3.65 (3H, s), 3.76 (3H, s), 6.65 (1H, d, *J* 8.8), 6.73 (1H, dd, *J* 8.8 and 3.2), 6.78 (1H, d, *J* 3.2), 6.84 (2H, d, *J* 8.8), 7.54 (2H, d, *J* 8.8). ^{13}C NMR (100 MHz, $CDCl_3$): *d* 38.2 (CH_3), 55.9 (CH_3), 56.0 (CH_3), 56.1 (CH_3), 112.9 (CH), 114.1 (2CH), 114.9 (CH), 117.6 (CH), 130.0 (2CH), 131.5 (C), 151.0 (C), 153.6 (C), 163.1 (C). HRMS ($C_{16}H_{19}NO_5S$ þ HÞ): calcd 338.1057 (M þ HÞ), found 338.1059.

N-(4-bromo-2,5-dimethoxyphenyl)-4-methoxybenzenesulphonamide (23)

Following general procedure C, compound 21 (1.00 g, 3.09 mmol) was brominated. *N*-bromosuccinimide (550 mg, 3.09 mmol). Yield, crude: 94% (1.17 g), crystals: 68% (852 mg). M.p.: 118–119 °C (CH_2Cl_2/hexane). IR (KBr): 3238, 1597, 1503, 828 cm $^{-1}$. ^{1}H NMR (400 MHz, $CDCl_3$): *d* 3.59 (3H, s), 3.81 (3H, s), 3.84 (3H, s), 6.86 (2H, d, *J* ¼ 8.8), 6.91 (1H, s), 6.97 (1H, s), 7.20 (1H, s), 7.67 (2H, d, *J* ¼ 8.8). ^{13}C NMR (100 MHz, $CDCl_3$): *d* 55.6 (CH_3), 56.4 (CH_3), 56.8 (CH_3), 105.9 (CH), 106.3 (C), 114.0 (2CH), 115.9 (CH), 125.9 (C), 129.3 (2CH), 130.4 (C), 143.8 (C), 150.2 (C), 163.1 (C). HRMS ($C_{15}H_{16}BrNO_5S$ þ H^+): calcd 402.0005 and 403.9985 (M þ H^+), found 402.0006 and 403.9992.

N-(4-bromo-2,5-dimethoxyphenyl)-4-methoxy-N-methylbenzenesulphonamide (24)

Following general procedure B1, compound 23 (90 mg, 0.22 mmol) was methylated and purified by preparative TLC (hexane:EtOAc 7:3). CH_3I (28 mL, 0.44 mmol). Yield, crude: 89% (83 mg); preparative: 82% (76 mg); crystals: 62% (60 mg). M.p.: 132–133 °C (CH_2Cl_2/hexane). IR (KBr): 1596, 1503, 833 cm $^{-1}$. ^{1}H NMR (400 MHz, $CDCl_3$): *d* 3.17 (3H, s), 3.37 (3H, s), 3.83 (3H, s), 3.86 (3H, s), 6.92 (2H, d, *J* ¼ 8.8), 6.92 (1H, s), 7.61 (2H, d, *J* ¼ 8.8). ^{13}C NMR (100 MHz, $CDCl_3$): *d* 37.7 (CH_3), 55.6 (2CH_3), 56.8 (CH_3), 111.4 (C), 113.6 (2CH), 115.9 (CH), 116.6 (CH), 128.6 (C), 129.6 (2CH), 130.8 (C), 149.6 (C), 150.5 (C), 162.7 (C). HRMS ($C_{16}H_{18}BrNO_5S$ þ Na^+): calcd 437.9981 and 439.9961 (M þ Na^+), found 437.9969 and 439.9944.

N-(4-bromo-2,5-dimethoxyphenyl)-N-(cyanomethyl)-4-methoxybenzenesulphonamide (25)

Following general procedure B2, compound 23 (308 mg, 0.76 mmol) was alkylated using 2-chloroacetonitrile (97 mL, 1.53 mmol) as alkylating agent. Yield, crude: 79% (306 mg); crystals: 65% (254 mg). M.p.: 296–297 °C (MeOH). ^{1}H NMR (400 MHz, $CDCl_3$): *d* 3.40 (3H, s), 3.81 (3H, s), 3.84 (3H, s), 4.52 (2H, s), 6.91 (2H, d, *J* ¼ 8.8), 6.93 (1H, s), 7.00 (1H, s), 7.58 (2H, d, *J* ¼ 8.8). ^{13}C NMR (100 MHz, $CDCl_3$): *d* 38.3 (CH_2), 55.7 (2CH_3), 56.8 (CH_3), 113.2 (C), 113.9 (2CH), 115.3 (C), 116.1 (CH), 116.8 (CH), 124.8 (C), 129.9 (2CH), 130.0 (C), 150.0 (C), 150.0 (C), 163.4 (C). HRMS ($C_{17}H_{17}BrN_2O_5S$ þ Na^+): calcd 462.9934 and 464.9913 (M þ Na^+), found 462.9942 and 464.9916.

Ethyl N-(4-bromo-2,5-dimethoxyphenyl)-N-((4-methoxyphenyl)sulphonyl)glycinate (26)

Following general procedure B2, compound 23 (248 mg, 0.61 mmol) was alkylated using ethyl 2-bromoacetate (137 mL, 1.23 mmol) as alkylating agent and purified by flash column chromatography (hexane:EtOAc 3:7). Yield, crude: 95% (286 mg); column: 89% (268 mg). ^{1}H NMR (400 MHz, $CDCl_3$): *d* 1.16 (3H, t, *J* ¼ 7.2), 3.31 (3H, s), 3.75 (3H, s), 3.76 (3H, s), 4.07 (2H, q, *J* ¼ 7.2), 4.29 (2H, s), 6.83 (2H, d, *J* ¼ 9.2), 6.90 (1H, s), 7.08 (1H, s), 7.52 (2H, d, *J* ¼ 9.2). ^{13}C NMR (100 MHz, $CDCl_3$): *d* 15.7 (CH_3), 52.4 (CH_2), 57.2 (CH_3), 57.3 (CH_3), 58.3 (CH_3), 62.8 (CH_2), 113.6 (C), 115.2 (2CH), 117.9 (CH), 119.2 (CH), 127.8 (C), 131.2 (2CH), 133.1 (C), 151.1 (C), 151.6 (C), 164.4 (C), 170.8 (C). HRMS ($C_{19}H_{22}BrNO_7S$ þ H^+): calcd 488.0373 and 490.0353 (M þ H^+), found 488.0367 and 490.0348.

Ethyl (4-bromo-2,5-dimethoxyphenyl)((4-methoxyphenyl)sulphonyl)carbamate (27)

Following general procedure B2, compound 23 (230 mg, 0.57 mmol) was alkylated using ethyl chloroformate (220 mL, 2.28 mmol) as alkylating agent and purified by flash column chromatography (CH_2Cl_2:hexane 98:2). Yield 31% (84 mg). ^{1}H NMR (400 MHz, $CDCl_3$): *d* 1.10 (3H, t, *J* ¼ 6.8), 3.64 (3H, s), 3.86 (3H, s), 3.87 (3H, s), 4.09 (2H, q, *J* ¼ 6.8), 6.91 (1H, s), 6.96 (2H, d, *J* ¼ 8.8), 7.14 (1H, s), 7.94 (2H, d, *J* ¼ 8.8). ^{13}C NMR (100 MHz, $CDCl_3$): *d* 14.0 (CH_3), 55.6 (CH_3), 55.9 (CH_3), 56.9 (CH_3), 63.3 (CH_2), 113.0 (C), 113.4 (2CH), 115.7 (CH), 116.7 (CH), 124.1 (C), 130.4 (C), 131.5 (2CH), 149.9 (2 C), 151.9 (C), 163.7 (C). HRMS ($C_{18}H_{20}BrNO_7S$ þ Na^+): calcd 496.0036 and 498.0016 (M þ Na^+), found 496.0018 and 497.9997.

N-(4-bromo-2,5-dimethoxyphenyl)-4-methoxy-N-(oxiran-2-ylmethyl) benzenesulphonamide (28)

Following general procedure B2, compound 23 (139 mg, 0.35 mmol) was alkylated using epichlorohydrin (108 mL, 1.38 mmol) as alkylating agent and purified by preparative TLC (toluene:EtOAc 3:7). Yield 45% (71 mg). ^{1}H NMR (400 MHz, $CDCl_3$): *d* 2.45 (1H, dd, *J* ¼ 2.4), 2.71 (1H, bt), 3.17 (1H, m), 3.33 (3H, s), 3.73 (2H, bs), 3.84 (3H, s), 3.85 (3H, s), 6.91 (2H, d, *J* ¼ 8.8), 6.96 (1H, s), 6.97 (1H, s), 7.59 (2H, d, *J* ¼ 8.8). ^{13}C NMR (100 MHz, $CDCl_3$): *d* 45.5 (CH_2), 50.7 (CH_2), 52.5 (CH), 55.5 (CH_3), 55.6 (CH_3), 56.8 (CH_3), 112.1 (C), 113.6 (2CH), 116.5 (CH), 116.9 (CH), 126.7 (C), 129.6 (2CH), 131.4 (C), 149.8 (C), 150.2 (C), 162.8 (C). HRMS ($C_{18}H_{20}BrNO_6S$ þ Na^+): calcd 480.0087 and 482.0066 (M þ Na^+), found 480.0077 and 482.0048.

N-(4-bromo-2,5-dimethoxyphenyl)-N-((4-methoxyphenyl)sulphonyl)-glycine (29)

Compound 26 (220 mg 0.45 mmol) was diluted with methanolic KOH for saponification. After 30 min stirring at room temperature, the solution was acidified with 2N HCl and extracted with EtOAc. The extract was washed with brine, dried over anhydrous Na_2SO_4 and evaporated to dryness. Yield, crude: 87% (181 mg); crystals: 68% (141 mg). M.p.: 180–184 °C (CH_2Cl_2/hexane). ^{1}H NMR (400 MHz, $CDCl_3$): *d* 3.46 (3H, s), 3.79 (3H, s), 3.85 (3H, s), 4.35 (2H, s), 6.91 (2H, d, *J* ¼ 9.2), 6.97 (1H, s), 7.00 (1H, s), 7.60 (2H, d, *J* ¼ 9.2). ^{13}C NMR (100 MHz, $CDCl_3$): *d* 51.0 (CH_2), 55.6 (CH_3), 55.7 (CH_3), 56.8 (CH_3), 112.4 (C), 113.7 (2CH), 116.5 (CH), 117.2 (CH), 126.1 (C), 129.7 (2CH), 131.0 (C), 149.8 (2C), 163.0 (C), 174.2 (C). HRMS ($C_{17}H_{18}BrNO_7S$ þ Na^+): calcd 481.9880 and 483.9859 (M þ Na^+), found 481.9876 and 483.9848.

1,2,4-Trimethoxy-5-nitrobenzene (30)

Following general procedure D, 1,2,4-trimethoxybenzene (3.66 ml, 23.8 mmol) was nitrated. HNO_3 (1.54 ml, 23.8 mmol). Yield 85% (4.30 g). ^{1}H NMR (200 MHz, $CDCl_3$): *d* 3.89 (3H, s), 3.97 (3H, s), 6.56 (1H, s), 7.59 (1H, s). GC-MS ($C_9H_{11}NO_5$): 213 (M^+).

2,4,5-Trimethoxyaniline (31)

Following general procedure E, compound 30 (3.20 g, 15.0 mmol) was reduced. Yield 99% (2.72 g). ^{1}H NMR (200 MHz, $CDCl_3$): *d* 3.80 (3H, s), 3.81 (3H, s), 3.82 (3H, s), 6.39 (1H, s), 6.53 (1H, s). GC-MS ($C_9H_{13}NO_3$): 183 (M^+).

4-Methoxy-N-(2,4,5-trimethoxyphenyl)benzenesulphonamide (32)

Following general procedure A, aniline 31 (465 mg, 2.54 mmol) and 4-methoxybenzenesulphonyl chloride (629 mg, 3.05 mmol) gave sulphonamide 32. Yield, crude: 99% (893 mg); crystals: 65% (587 mg). M.p.: 112–114 °C (MeOH). ^{1}H NMR (200 MHz, $CDCl_3$): *d* 3.49 (3H, s), 3.81 (6H, s), 3.85 (3H, s), 6.33 (1H, s), 6.52 (1H, bs), 6.84 (2H, d, *J* ¼ 9), 7.16 (1H, s), 7.61 (2H, d, *J* ¼ 9). ^{13}C NMR (100 MHz, $CDCl_3$): *d* 55.5 (CH_3), 56.2 (CH_3), 56.3 (CH_3), 56.5 (CH_3), 97.2 (CH), 108.1 (CH), 113.7 (2CH), 117.9 (C), 129.4 (2CH), 130.6 (C), 143.1 (C), 144.8 (C), 147.0 (C), 162.8 (C). HRMS ($C_{16}H_{19}NO_6S$ þ Na^+): calcd 376.0825 (M þ Na^+), found 376.0825.

4-Methoxy-N-methyl-N-(2,4,5-trimethoxyphenyl)benzenesulphonamide (33)

Following procedure B1, compound 32 (103 mg, 0.29 mmol) was methylated. CH_3I (36 mL, 0.58 mmol). Yield, crude: 90% (97 mg); crystals: 70% (75 mg). M.p.: 137–143 °C (MeOH). IR (KBr): 1595, 1523, 1152, 893 cm^{-1}. ^{1}H NMR (200 MHz, $CDCl_3$): *d* 3.18 (3H, s), 3.43 (3H, s), 3.79 (3H, s), 3.86 (3H, s), 3.87 (3H, s), 6.38 (1H, s), 6.79 (1H, s), 6.93 (2H, d, *J* ¼ 9), 7.64 (2H, d, *J* ¼ 9). ^{13}C NMR (100 MHz, $CDCl_3$): *d* 38.0 (CH_3), 55.5 (CH_3), 55.6 (CH_3), 56.1 (CH_3), 56.5 (CH_3), 97.2 (CH), 113.5 (2CH), 114.9 (CH), 120.7 (C), 129.7 (2CH), 131.2 (C), 142.4 (C), 149.5 (C), 150.8 (C), 162.6 (C). HRMS ($C_{17}H_{21}NO_6S$ þ Na^+): calcd 390.0982 (M þ Na^+), found 390.0986.

N-ethyl-4-methoxy-N-(2,4,5-trimethoxyphenyl)benzenesulphonamide (34)

Following general procedure B2, compound 32 (102 mg, 0.29 mmol) was alkylated using bromoethane (43 mL, 0.58 mmol) as alkylating agent and purified by preparative TLC (hexane:EtOAc 1:1). Yield, crude: 95% (105 mg); preparative: 87% (96 mg). IR (KBr): 1594, 1504, 1110, 804 cm^{-1}. ^{1}H NMR (400 MHz, $CDCl_3$): *d* 1.01 (3H, t, *J* ¼ 7.2), 3.39 (3H, s), 3.55 (2H, bs), 3.75 (3H, s), 3.80 (3H, s), 3.83 (3H, s), 6.36 (1H, s), 6.70 (1H, s), 6.87 (2H, d, *J* ¼ 9.2), 7.59 (2H, d, *J* ¼ 9.2). ^{13}C NMR (100 MHz, $CDCl_3$): *d* 14.3 (CH_3), 44.7 (CH_2), 55.5 (CH_3), 55.6 (CH_3), 56.0 (CH_3), 56.4 (CH_3), 97.0 (CH), 113.4 (2CH), 116.3 (CH), 117.8 (C), 129.5 (2CH), 132.2 (C), 142.2 (C), 149.6 (C), 151.3 (C), 162.4 (C). HRMS ($C_{18}H_{23}NO_6S$ þ Na^+): calcd 404.1138 (M þ Na^+), found 404.1138.

N-(cyanomethyl)-4-methoxy-N-(2,4,5-trimethoxyphenyl)benzenesulphonamide (35)

Following general procedure B2, compound 32 (87 mg, 0.24 mmol) was alkylated using 2-chloroacetonitrile (31 mL, 0.49 mmol) as alkylating agent. Yield, crude: 72% (70 mg); crystals: 56% (55 mg). M.p.: 173–180 °C (MeOH). ^{1}H NMR (200 MHz, $CDCl_3$): *d* 3.45 (3H, s), 3.79 (3H, s), 3.86 (3H, s), 3.88 (3H, s), 4.54 (2H, s), 6.38 (1H, s), 6.84 (1H, s), 6.93 (2H, d, *J* ¼ 9.2), 7.63 (2H, d, *J* ¼ 9.2). ^{13}C NMR (100 MHz, $CDCl_3$): *d* 38.7 (CH_2), 55.5 (CH_3), 55.6 (CH_3), 56.1 (CH_3), 56.4 (CH_3), 96.9 (CH), 113.8 (2CH), 115.3 (CH), 115.4 (C), 116.8 (C), 129.9 (2CH), 130.5 (C), 142.7 (C), 150.6 (C), 150.6 (C), 163.2 (C). HRMS ($C_{18}H_{20}N_2O_6S$ þ Na^+): calcd 415.0934 (M þ Na^+), found 415.0934.

Ethyl N-((4-methoxyphenyl)sulphonyl)-N-(2,4,5-trimethoxyphenyl)-glycinate (36)

Following general procedure B2, compound 32 (95 mg, 0.27 mmol) was alkylated using ethyl 2-bromoacetate (60 mL, 0.54 mmol) as alkylating agent. Yield, crude: 99% (117 mg); crystals: 69% (82 mg). M.p.: 127–132 °C (MeOH). ^{1}H NMR (200 MHz, $CDCl_3$): *d* 1.24 (3H, t, *J* ¼ 7.2), 3.43 (3H, s), 3.78 (3H, s), 3.84 (3H, s), 3.85 (3H, s), 4.15 (2H, q, *J* ¼ 7.2), 4.38 (2H, s), 6.34 (1H, s), 6.90 (2H, d, *J* ¼ 9), 7.02 (1H, s), 7.63 (2H, d, *J* ¼ 9). ^{13}C NMR (100 MHz, $CDCl_3$): *d* 14.1 (CH_3), 51.4 (CH_2), 55.5 ($2CH_3$), 56.0 (CH_3), 56.3 (CH_3), 61.1 (CH_2), 96.6 (CH), 113.4 (2CH), 116.7 (CH), 118.3 (C), 129.8 (2CH), 132.0 (C), 142.2 (C), 149.8 (C), 150.3 (C), 162.7 (C), 169.6 (C). HRMS ($C_{20}H_{25}NO_8S$ þ Na^+): calcd 462.1193 (M þ Na^+), found 462.1193.

N-benzyl-4-methoxy-N-(2,4,5-trimethoxyphenyl)benzenesulphonamide (37)

Following general procedure B2, compound 32 (95 mg, 0.27 mmol) was alkylated using benzyl chloride (62.4 mL, 0.54 mmol) as alkylating agent. Yield, crude: 99% (118 mg); crystals: 82% (98 mg). M.p.: 130–139 °C (MeOH). IR (KBr): 1596, 1492, 1184, 809 cm^{-1}. ^{1}H NMR (200 MHz, $CDCl_3$): *d* 3.37 (3H, s), 3.62 (3H, s), 3.82 (3H, s), 3.87 (3H, s), 4.70 (2H, bs), 6.30 (1H, s), 6.49 (1H, s), 6.93 (2H, d, *J* ¼ 9), 7.20 (5H, bs), 7.68 (2H, d, *J* ¼ 9). ^{13}C NMR (100 MHz, $CDCl_3$): *d* 53.7 (CH_2), 55.5 (CH_3), 55.6 (CH_3), 55.9 (CH_3), 56.3 (CH_3), 96.7 (CH), 113.5 (2CH), 116.8 (CH), 117.9 (C), 127.4 (CH), 128.1 (2CH), 128.8 (2CH), 129.7 (2CH), 132.5 (C), 136.8 (C), 142.1 (C), 149.6 (C), 151.0 (C), 162.5 (C). HRMS ($C_{23}H_{25}NO_6S$ þ Na^+): calcd 466.1295 (M Na^+), found 466.1287.

Aqueous solubility

The aqueous solubility was determined in a Helios-*a* UV-320 Spectrophotometer Thermo-Spectronic, Thermo Fischer Scientific, Waltham, MA, USA) using an approach based on the saturation shake-flask method. 1–2 mg of each selected compound was suspended in 300 mL pH 7.0 buffer and stirred for 48 h at room temperature. The resulting mixture was filtered through a 45 mm filter to discard the insoluble residues. A scan between 270 and 400 nm for the tested compound was performed and three wavelengths of maximum absorbance were selected. Calibration curves were performed at these wavelengths and the concentration in the supernatant was measured by UV absorbance. The final value was given as the average of the three measurements.

Cell lines and cell culture conditions

MCF7 (human breast carcinoma), HeLa (human cervical carcinoma), and HEK-293 (human embryonic kidney) cells were cultured in Dulbecco's Modified Eagle's Medium (DMEM) (Gibco, Thermo Fischer Scientific) containing 10% (v/v) heat-inactivated foetal bovine serum (HIFBS) (Lonza-Cambrex, Karlskoga, Sweden), 2 mM L-glutamine (Lonza-Cambrex) and 100 *l*g/mL streptomycin-100 IU/mL penicillin (Lonza-Cambrex) at 37 °C in 95% humidified and 5% CO_2 air. HT-29 (human colon carcinoma) cells were cultured in RPMI 1640 medium (Gibco) supplemented with 10% HIFBS and 100 *l*g/mL streptomycin-100 IU/mL penicillin at 37 °C in humidified 95% air and 5% CO_2 atmosphere. The presence of mycoplasma was routinely checked with MycoAlert kit (Lonza-Cambrex) and only mycoplasma-free cells were used in the experiments. Tumour cell lines were kindly provided by Dr Faustino Mollinedo from Centro de Investigaciones Biolo gicas Margarita Salas, Madrid, Spain.

Cell growth assay

To determine cell growth, cells in exponential growth phase were seeded (100 mL/well in 96-well plates) with appropriate cell

concentration (1.5×10^4 cells/mL for MCF7, HeLa and HEK-293 and 3×10^4 cells/mL for HT-29) in complete DMEM or RPMI 1640 medium (see above) at 37 °C and 5% CO_2 atmosphere. After 24 h incubation, to allow cells to attach to the plates, all compounds were added at 1 mM concentration (10 mL/well in 96-well plates) and the effect on the proliferation was evaluated 72 h post-treatment. Compounds showing antiproliferative effects at tested concentration were selected for IC_{50} calculation (50% inhibitory concentration compared to the untreated controls) from 10^{-5} to 10^{-10} M concentration. Nonlinear curves fitting the experimental data were carried out for each compound. MCF7, HeLa, HT-29, and HEK-293 cell growth, when treated with the corresponding compound, were determined using the XTT (sodium 3'-[1(phenylaminocarbonyl)-3,4-tetrazolium]-bis(4-methoxy-6-nitro)-benzenesulphonic acid hydrate) cell proliferation kit (Roche Molecular Biochemicals, Mannheim, Germany). A freshly prepared mixture solution of XTT labelling reagent with 0.02% (v/v) PMS (N-methyldibenzopyrazine methyl sulfate) electron coupling reagent was added to cells (50 mL/well in 96-well plates, the total volume of 160 mL/well) and were incubated during the corresponding time according to each cell line (4 h for MCF7 and HeLa and 6 h for HT-29 and HEK-293) in a humidified atmosphere (37 °C, 5% CO_2). The absorbance of the formazan product generated was measured at a test wavelength of 450 nm using a multi-well plate reader (Ultra Evolution, Tecan, M€annedorf, Suiza). Compounds were dissolved in DMSO and the final solvent concentrations never exceeded 0.5% (v/v). The control wells included treated cells with 0.5% (v/v) DMSO and the positive control. 10 mM verapamil was included as a control for the HT-29 cell line. Measurements were performed in triplicate, and each experiment was repeated three times.

Cell cycle analysis

MCF7, HeLa, and HT-29 cell cycle analyses were performed by quantifying the DNA content by flow cytometry. Cells in the exponential growth phase at 2×10^4 cells/mL were seeded in 24-well plates (1 ml/well). After 24 h incubation, cells were treated with compound 25 at 87.5 or 175 nM. After 24, 48, and 72 h treatments, live and dead cells were collected and fixed in ice-cold ethanol:PBS (7:3) and stored at 4 °C for later use. Cells were rehydrated with phosphate-buffered saline (PBS), treated with 100 mg/mL RNase A (Sigma-Aldrich Co., St. Louis, MO, USA), and stained overnight in darkness at room temperature with 50 mg/mL propidium iodide (PI) (Sigma-Aldrich Co.). Cell cycle profiles were then analysed by flow cytometry using BD Accuri™ C6 Plus Flow Cytometer (BD Biosciences, San Jos e, CA, USA). Data were analysed with BD Accuri™ C6 Software (version 1.0.264.21, BD Biosciences, San Jos e, CA, USA) and compared to control cells treated with 0.5% (v/v) DMSO. Compounds were dissolved in DMSO and the final solvent concentrations never exceeded 0.5% (v/v).

Apoptotic cell death quantification

MCF7, HeLa, and HT-29 apoptotic cells were quantified using an Annexin V-FITC/PI apoptosis detection kit (Immunostep, Salamanca, Spain) according to the manufacturer's guidelines. 1.5 ml/well of cells in the exponential growth phase at 2×10^4 cells/mL were seeded onto 12-well plates and left to attach overnight. After 24 h incubation, cells were treated with compound 25 at 87.5 or 175 nM. 72 h post-treatment, attached and floating cells of treated and untreated wells were collected, centrifuged, resuspended in the Annexin V binding buffer, and stained with Annexin V-FITC/PI. Cells were then incubated in darkness at room temperature for 15 min and a total of 30,000 cells were acquired and analysed using the BD Accuri™ C6 Plus Flow Cytometer and Software (version 1.0.264.21, BD Biosciences, San Jos e, CA, USA), respectively. Compounds were dissolved in DMSO and the final solvent concentrations never exceeded 0.5% (v/v). Control wells included cells with 0.5% (v/v) DMSO.

Western blotting

MCF7, HeLa and HT-29 cells in an exponential growth phase at 2×10^4 cells/mL were seeded in Petri dishes (20 100 mm) (10 ml/dish). After 24 h incubation, cells were treated with compound 25 at 175 nM, and the levels of p-62 in treated and untreated cells were measured at 24 h post-treatment. The culture medium was removed, cells were washed with PBS and resuspended in 1 ml lysis buffer (50 mM Tris, 130 mM NaCl, 1 mM EDTA, 1% Triton X-100) containing protease inhibitors (Complete, Roche Applied Science, Indianapolis). Cells were harvested and incubated with lysis buffer for 30 min at 4 °C in constant agitation. Cell extracts were centrifuged at 12,000 rpm for 15 min at 4 °C and the supernatants were stored at 80 °C. Protein concentrations were determined using Bradford (BioRad, Hercules, CA) method taking BSA (Bovine Serum Albumin) as standard. Protein extracts were used for electrophoresis mixing with loading buffer (4% SDS, 0.05% bromophenol blue, 20% glycerine, 2% *b*-mercaptoethanol, and Tris 100 mM at pH 6.8). Proteins were then denatured at 95 °C for 7 min. Protein samples (50 *l*g/lane) were subjected to electrophoresis on 8% acrylamide gel and SDS-PAGE running buffer at constant voltage (140 V). Then, acrylamide gels were transferred to a PVDF membrane (Merck Millipore, Burlington, Massachusetts, USA) using a semi-dry transfer system for 30 min at constant voltage (15 V). After blocking with TBS-T (NaCl 140 mM, Tween20 0.05%, Tris 10 mM at pH 7.5) with 5% of skimmed milk powder, membranes were incubated overnight at 4 °C with p-62 (1:1000, ab109012, Abcam, Cambridge, UK) or *b*-actin (1:10000, Sigma-Aldrich Co.) antibodies, in 3% BSA/TBS-T. *b*-actin was used as the loading control. Immunoblots were incubated for 50 min at room temperature with secondary antibodies (Horseradish peroxidase linked-sheep (anti-mouse) (NXA931, GE Healthcare, Chicago, Illinois, USA) or goat (anti-rabbit) (AP307P, Merck Millipore)) at a 1:10,000 dilution in 7% of skimmed milk powder/TBS-T. Bands were visualised using an enhanced chemiluminescence western blotting detection kit (Thermo Fisher Scientific) based on the oxidation of luminol in the presence of hydrogen peroxide.

Immunofluorescence

MCF7, HeLa, and HT-29 cells were grown on round glass coverslips coated with poly-L-lysine (12 mm diameter). To reach appropriate cell confluence, coverslips were manipulated in 6-well plates (3 coverslips/well) seeding 3 ml/well of cells in the exponential growth phase at 2×10^4 cells/mL. After 24 h incubation, cells were treated with compound 25 at 175 nM and incubated for 72 h. Cells were washed with PBS, fixed with 4% formaldehyde in PBS for 10 min, permeabilized with 0.5% Triton X-100 (Boehringer Mannheim, Ingelheimam Rhein, Germany) in PBS for 10 min, and blocked with 10% BSA in PBS for 30 min. Then, coverslips were incubated with anti-*a*-tubulin mouse monoclonal antibody (diluted 1:200 in 3% BSA/PBS) (Sigma-Aldrich Co.) and anti-SQSTM1/p62 rabbit monoclonal antibody (diluted 1:100 in 3% BSA/PBS) (Abcam) for 1 h 30 min. After PBS washing, coverslips were incubated with fluorescent secondary antibodies Alexa Fluor 488 goat

anti-mouse IgG and Alexa Fluor 594 anti-rabbit (both diluted 1:400 in 1% BSA/PBS) (Molecular Probes, Invitrogen, Thermo Fischer Scientific) for 1 h in darkness. After being washed with PBS, cell nuclei were stained with DAPI (dihydrochloride of 4⁰,6-diamidino-2-phenylindole) (diluted 1:10,000 in milli-Q H_2O) (Roche, Basel, Switzerland) for 5 min in darkness, DAPI excess was removed by washing with PBS. Finally, Mowiol reagent (Calbiochem, Sigma-Aldrich Co.) was used to mount preparations on slides. Cells were analysed by confocal microscopy using a LEICA SP5 microscope DMI-6000V model coupled to a LEICA LAS AF software computer.

Tubulin isolation and inhibition of tubulin polymerisation

Microtubular protein was isolated from calf brain according to the modified Shelanski method[23,24] by two cycles of temperature-dependent assembly/disassembly and stored at 80 °C. Before each use, protein concentration is determined by Bradford method[25] taking BSA as standard. Tubulin polymerisation was monitored using a Helios *α* spectrophotometer by measuring the increase in turbidity at 450 nm, caused by a shift from 4 °C to 37 °C, which allows the *in vitro* microtubular protein to depolymerise and to polymerise, respectively. The assay was carried out in quartz cuvettes containing 1.5 mg/mL microtubular protein and the ligand (except for control cuvette with only DMSO at the same concentration) in a mixture of 0.1 M MES buffer, 1 mM EGTA, 1 mM $MgCl_2$, 1 mM *b*-ME, and 1.5 mM GTP at pH 6.7 (final volume 500 μL). Cuvettes were preincubated at 20 °C for 30 min, to allow ligand binding to tubulin, and subsequently cooled on ice for 10 min. Then, the experiment starts at 4 °C to establish the initial baseline. The assembly process was initiated by a temperature shift to 37 °C and the turbidity produced by tubulin polymerisation can be measured by an absorbance increase. After reaching a stable plateau, the temperature was switched back to 4 °C to return to the initial absorption values (to confirm the reversible nature of the monitored process and to determine whether or not the microtubular protein has stabilized). The difference in amplitude between the stable plateau and the initial baseline of the curves was taken as the degree of tubulin polymerisation for each experiment. Comparison with control curves under identical conditions but without ligands yielded TPI as a percentage value. All compounds were tested at 10 μM concentration. IC_{50} values were calculated for compounds that inhibit tubulin polymerisation more than 50% at 10 μM. Compounds were dissolved in DMSO and the final solvent concentrations never exceeded 4% (v/v), which has been reported not to interfere with the assembly process. All the measurements were carried out in at least two independent experiments using microtubular protein from different preparations.

Computational studies

Docking studies were carried out as previously described[26]. The protein flexibility was taken into account by using 50 tubulin complexes with different ligands bound at the colchicine site retrieved from the pdb. The proteins were superimposed using the amino acids within 8 Å of any of the ligands and used in the docking experiments. Five additional structures came from a molecular dynamics run of a complex with an indolecombretastatin bound at the colchicine site[26]. Dockings were performed in parallel with PLANTS with default settings[27] and 10 runs per ligand and with AutoDock 4.2[28] runs applying the Lamarckian genetic algorithm (LGA) 100 300 times for a maximum of 2.5×10^6 energy evaluations, 150 individuals, and 27,000 generations maximum. For each virtual ligand 550 poses were generated with PLANTS and AutoDock generated from 550 to more than 1500 poses. The colchicine subzones occupied by every pose were automatically assigned using in-house KNIME pipelines[29]. The programs' docking scores were converted into Z-scores and the poses with best scores were visually compared until a consensus pose obtaining the best consensus scores for both programs could be selected and taken as the docking result. Docked poses were analysed with Chimera[30], Marvin[31], OpenEye[32], and JADOPPT[33].

Results and discussion

Chemistry

The TMP ring is common to many colchicine site ligands and is considered important for high antiproliferative activity and tubulin binding. In an attempt to find new antimitotic sulphonamides with TMP replacements we have explored the effect of additional methoxy (methoxy scan) and/or bromo (bromo scan) substituents at different positions on the basic pharmacophore of the TMP moiety: a phenyl ring with a 5-methoxy aimed at recognising the thiol group of Cys241*b* of tubulin. Therefore, a new family of 4-methoxybenzenesulphonamides with methoxy and bromo substituents at different positions of the *N*-(5-methoxyphenyl) ring and with different substitutions on the sulphonamide nitrogen has been synthesised (Scheme 1 and Table 1). As a result of the methoxy scan, four main structural families have been sampled (Figure 1): 1) 3,5-dimethoxyphenyl (series 1); 2) 3,4-dimethoxyphenyl (series 2); 3) 2,5-dimethoxyphenyl (series 3); and 4) 2,4,5-trimethoxyphenyl (series 4). For the first three, substitutions of aromatic hydrogens by bromo atoms have been additionally carried out, with the fourth one being the methoxylated equivalent of the 4-bromo-2,5-dimethoxyphenyls of series 3. The 3,5- and 3,4-dimethoxyphenyl are the mono demethoxylated analogs of the TMP, and have been previously shown to result in severe potency reductions, with occasional exceptions such as in the 3,5-dimethoxyphenyl triazole analogs of combretastatin A-4[34]. The 2,5-dimethoxyphenyl substitution pattern has as well yielded modest results at best[15,35–38], and only combined with bulky and hydrophobic B ring derivatives such as the carbazolesulphonamides[38,39] or quinazolinone sulfamates[40] achieved good antiproliferative results.

Thirty seven new benzenesulphonamides (series 1–4) were synthesised following the synthetic approach outlined in Scheme 1. The basic diphenylsulphonamide skeletons of the four series (1, 11, 21, and 32) were built up in good yields (95–99%) by the reaction between the corresponding anilines and 4-methoxybenzenesulphonyl chloride. For series 3 and 4, anilines 20 and 31 were previously prepared by nitration-reduction reaction sequences. Substituents of different length, polarity, and size (e.g. small alkyl chains such as methyl or ethyl, more polar acetonitrile or acyl derivatives, or larger benzyl groups) were appended on the sulphonamide bridge through alkylation reactions carried out under basic conditions that favour the formation of the nucleophilic sulphonamide anion. Methylations with methyl iodide and KOH in dry acetonitrile were achieved in good yields (84–95%) to give 2, 12, 14, 22, 24, and 33. Other substitutions were performed with the corresponding alkyl halides and K_2CO_3 as a base in dry DMF (3–7, 15–18, 25–28, and 34–37). Brominations (8a–10c, 13, and 23) were carried out using NBS as a source of electrophilic bromine. The positions of the bromine atom(s) were established by the proton couplings in the ^1H NMR spectra. The synthesised

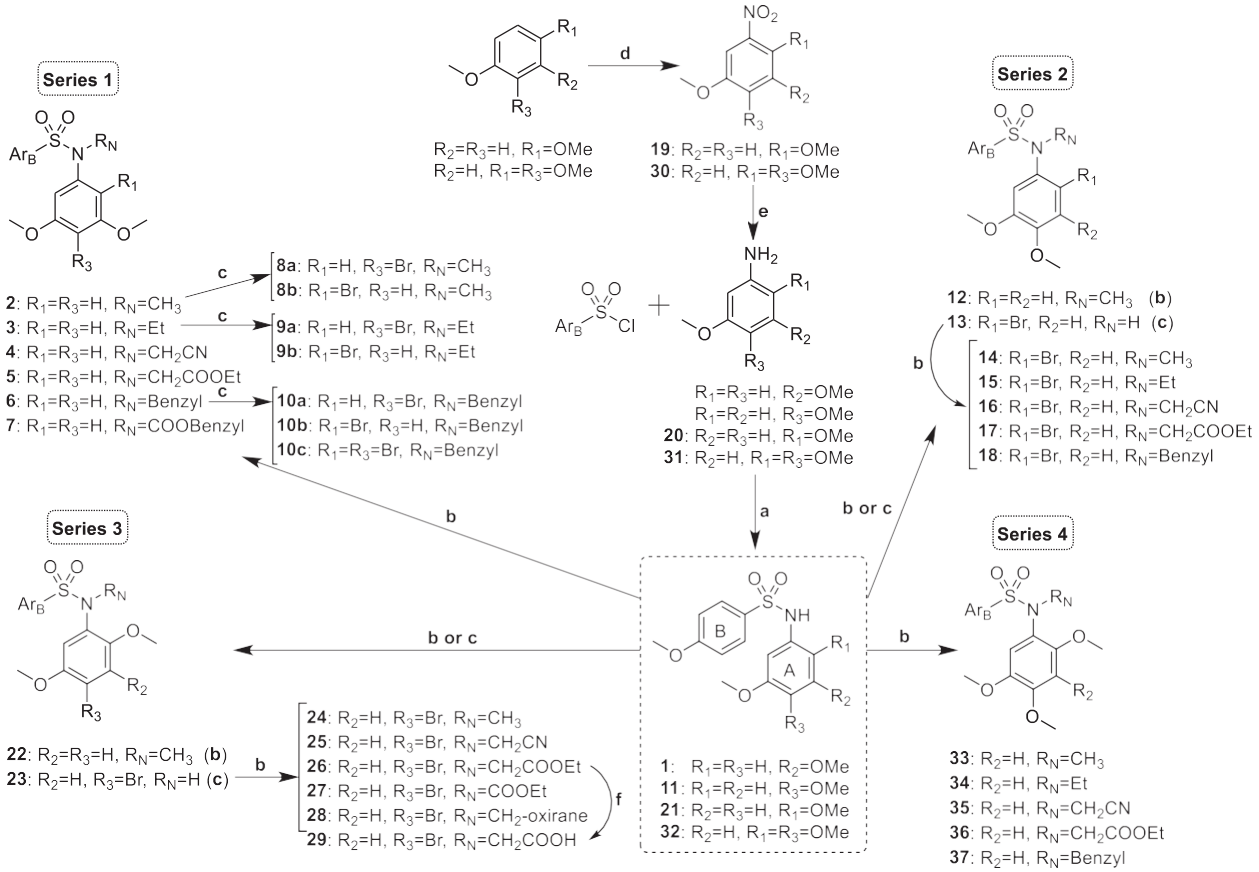

Scheme 1. Synthesis of new tubulin inhibiting sulphonamides. Ar_B: *p*-methoxyphenyl. Reagents, conditions, and yields: (a) Pyridine, CH_2Cl_2, rt, 6 h, 95–99%. (b) R_N ¼ CH_3: CH_3I, KOH, CH_3CN, rt, 24 h, 84–95%; R_N CH_3: R_N-halogen, K_2CO_3, dry DMF, rt, 24 h, 72–99%. (c) NBS, CH_2Cl_2, rt, 12 h, 62–95%. (d) HNO_3, AcOH, 0 °C, 4 h, 85–94%. (e) H_2, Pd(C), EtOAc, rt, 48 h, 99%. (f) KOH/MeOH, rt, 30 min, 87%.

compounds were characterised by ^1H and ^{13}C NMR, IR, HRMS, and melting points (if crystals), and agree with the proposed molecular structures.

The highly hydrophobic nature of the colchicine domain drives the physicochemical properties of the colchicine-site ligands towards non-drug-like physicochemical properties and makes the aqueous insolubility one of the recurrent problems of colchicine site ligands. The aqueous solubilities (Table 2) of representative compounds in pH 7 phosphate buffer were spectrophotometrically measured, showing improvements with respect to the marginal solubility of CA-4 (1 μg/mL). The best results were obtained for series 4, with values 100–200 times higher than that obtained for CA-4. Moreover, 6 out of 16 tested compounds were up to five times more soluble than the orally administered tubulin-inhibiting sulphonamide ABT-751 (40 μg/mL). The introduction of substituents at the sulphonamide and/or of bromo atoms led to a solubility decrease compared to the unsubstituted pairs.

Diphenylsulphonamides are potent in vitro antiproliferative agents: analysis of the structural-modification scans and structure-activity relationships

We screened by the XTT method all the synthesised sulphonamides in three independent assays at 1 μM for antiproliferative effect 72 h after treatment against the human tumour cell lines HeLa (cervix epithelioid carcinoma), MCF7 (breast adenocarcinoma), and HT-29 (colon adenocarcinoma). We classified benzenesulphonamides inhibiting cell proliferation by more than 40% in the screening phase as actives and the rest as inactives. More than half (21 out of 37) of the benzenesulphonamides were actives, with more actives in series 3 (8 out of 9) and 4 (5 out of 6) than in series 1 (4 out of 14) and 2 (4 out of 8). Methoxybenzenesulphonamides of trisubstituted anilines represented most of the actives (18 out of 21), thus indicating that a larger size is important to achieve sub-micromolar potency. We further assayed the actives at concentrations between 10 μM and 0.1 nM and IC_{50} (half-maximal inhibitory concentration) values were calculated (Table 1) along with those of CA-4, ABT-751, and *N*-(3,4,5-trimethoxyphenyl)-4-methoxyphenylsulphonamide[41], used as references. The distributions of the number of actives and relative potencies within the series were similar, thus indicating that the substitution pattern is an important factor for the antiproliferative potency. Interestingly, the series with the most similar substitution patterns to the 3,4,5-trimethoxyphenyl ring (series 1, 2, and 4) are not the ones with more potent representatives (IC_{50} values lower than 100 nM), which correspond to the 4-bromo-2,5-dimethoxyphenyl derivatives (23–25) clustered in series 3. The most sensitive cell line was the human breast cancer cell line MCF7 (6 compounds with IC_{50} values lower than 100 nM), followed by HeLa (3 compounds with IC_{50} values lower than 100 nM), and HT-29 (2 compounds with IC_{50} values lower than 100 nM) was the least sensitive. The lower sensitivity of HT-29 is not unexpected, as it is often observed for tubulin inhibitors and has been associated with efflux by MDR proteins[42], autophagy induction[21], and/or

Table 1. Structures and biological evaluation of new synthetised sulphonamides.

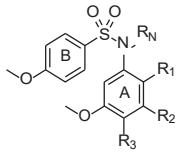

					Antiproliferative activity IC_{50} (nM)[a]				TPI[b]	
R_1	R_2	R_3	R_N	Comp	HeLa	MCF7	HT-29	HT-29 Verap[c]	TPI % 10 μM	IC_{50} (μM)
Series 1										
H	OCH_3	H	H	1	>1000	>1000	>1000	n.d.	0	>10
H	OCH_3	H	CH_3	2	877	765	>1000	n.d.	10	>10
H	OCH_3	H	Et	3	>1000	>1000	>1000	n.d.	0	>10
H	OCH_3	H	CH_2CN	4	>1000	>1000	>1000	n.d.	0	>10
H	OCH_3	H	CH_2COOEt	5	>1000	>1000	>1000	n.d.	0	>10
H	OCH_3	H	Benzyl	6	>1000	>1000	>1000	n.d.	0	>10
H	OCH_3	H	COOBenzyl	7	>1000	>1000	>1000	n.d.	0	>10
H	OCH_3	Br	CH_3	8a	497	99	495	293	10	>10
H	OCH_3	Br	Et	9a	417	n.d.	610	n.d.	0	>10
H	OCH_3	Br	Benzyl	10a	310	335	450	533	0	>10
Br	OCH_3	H	CH_3	8b	>1000	>1000	>1000	n.d.	0	>10
Br	OCH_3	H	Et	9b	>1000	>1000	>1000	n.d.	0	>10
Br	OCH_3	H	Benzyl	10b	>1000	>1000	>1000	n.d.	0	>10
Br	OCH_3	Br	Benzyl	10c	>1000	>1000	>1000	n.d.	0	>10
Series 2										
H	H	OCH_3	H	11	>1000	>1000	>1000	n.d.	4	>10
H	H	OCH_3	CH_3	12	>1000	>1000	>1000	n.d.	0	>10
Br	H	OCH_3	H	13	510	n.d.	543	n.d.	0	>10
Br	H	OCH_3	CH_3	14	557	n.d.	907	n.d.	0	>10
Br	H	OCH_3	Et	15	313	660	365	500	24	>10
Br	H	OCH_3	CH_2CN	16	407	575	360	750	16	>10
Br	H	OCH_3	CH_2COOEt	17	>1000	>1000	>1000	n.d.	0	>10
Br	H	OCH_3	Benzyl	18	>1000	>1000	>1000	n.d.	38	>10
Series 3										
OCH_3	H	H	H	21	227	350	187	187	0	>10
OCH_3	H	H	CH_3	22	177	153	250	305	4	>10
OCH_3	H	Br	H	23	45	25	72	30	65	6.9
OCH_3	H	Br	CH_3	24	33	19	123	160	59	7.6
OCH_3	H	Br	CH_2CN	25	36	86	97	85	51	7.6
OCH_3	H	Br	CH_2COOEt	26	577	700	2100	867	28	>10
OCH_3	H	Br	COOEt	27	377	220	525	170	44	>10
OCH_3	H	Br	CH_2-oxirane	28	495	n.d.	860	n.d.	32	>10
OCH_3	H	Br	CH_2COOH	29	>1000	>1000	>1000	n.d.	8	>10
Series 4										
OCH_3	H	OCH_3	H	32	410	580	360	553	3	>10
OCH_3	H	OCH_3	CH_3	33	413	99	500	577	0	>10
OCH_3	H	OCH_3	Et	34	313	715	500	1070	19	>10
OCH_3	H	OCH_3	CH_2CN	35	500	67	365	415	5	>10
OCH_3	H	OCH_3	CH_2COOEt	36	>1000	>1000	>1000	n.d.	0	>10
OCH_3	H	OCH_3	Benzyl	37	833	n.d.	1250	n.d.	7	>10
H	OCH_3	OCH_3	H	TMP[41]	240	375	897	975	0	>20
H	OCH_3	OCH_3	CH_3	TMP[41]	71	127	143	117	35	>20
Combretastatin A-4					2	1	305	327	100	3
ABT-751					388	180	213	250	69	4.4

Compounds have been grouped in four different series regarding the position of the methoxy groups on the aromatic A ring.
[a]Drug concentration required to inhibit the growth of selected human tumour cell lines by 50%, relative to untreated controls after 72 h of drug exposure.
[b]*In vitro* tubulin polymerisation inhibition.
[c]IC_{50} in human colon adenocarcinoma HT-29 cell line in the presence of the Pgp/MDR1 inhibitor verapamil (10 μM).
[d]n.d.: not determined.

metabolic glucuronidation reactions[43]. However, MCF7 is not usually more sensitive than HeLa as observed here, in particular for compounds 8a, 33, and 35 which are 4–7 fold more potent against MCF7 than against HeLa.

For simplicity, in the following, we will use the IC_{50} values of the *N*-methylated sulphonamides as representative for the pairwise comparison of the different substitution patterns on the aniline rings (series 1–4). Similar effects, usually with lower potencies, are obtained for other substituents on the sulphonamide nitrogen. Regarding the methoxy scan, the more favourable substitution pattern for the dimethoxylated anilines is the 2,5- (series 3: 22) with potencies just slightly lower than those of the TMP analogues[41], while the structurally more similar to the TMP (just differing in the removal of one of the methoxy groups) 3,5- (series 1: 2), and 3,4- (series 2: 12) are inactive or active in the micromolar range. This result is different from similar modifications with other bridges between the aromatic rings, for instance with triazoles where the 3,5-dimethoxyphenyl ring yielded equally potent analogs as the TMP[34].

The methoxy or bromo scans of additional substituents on the disubstituted anilines resulted mostly in potency improvements, thus confirming that larger sizes are preferred. This favourable

Table 2. Aqueous solubility in pH 7.0 phosphate buffer of some representative compounds. Solubility values are expressed in μg/mL.

Comp	Solub (μg/mL)	Comp	Solub (μg/mL)	Comp	Solub (μg/mL)
2	35	16	13	32	213
11	82	21	13	33	157
12	70	22	25	34	122
13	22	23	9	35	15
14	61	24	1	CA-4	1
15	26	25	1	ABT-751	40

effect on the antiproliferative potency varies with the initial dimethoxy substitution pattern and the position and nature of the substituents. For series 1, the introduction of an additional bromo substituent on the 3,5-dimethoxy is slightly favourable at position 4 (e.g. compare 2 with 8a) where it gives a much TMP-like 3,4,5-substitution pattern, whereas it is detrimental at position 2 (e.g. compare 2 with 8 b) where it results in a 2,3,5- substitution pattern. Similarly, for series 2 an additional bromo or methoxy group (series 4) at position 2 of the 4,5-dimethoxy (2,4,5-substitution pattern) results in modest potency improvements (compare 12 vs. 14 for bromo, or 12 vs. 33 for methoxy). Remarkably, an additional bromo at position 4 is highly favourable for the 2,5-dimethoxy series 3 (compare 22 vs. 24) whereas a methoxy group, usually considered an important pharmacophoric element of the TMP ring for the interaction with tubulin[44,45], is detrimental at this position except for MCF7 (compare 22 vs. 33), both again for the 2,4,5-substitution pattern. The structure-activity relationships (SAR) results show an interesting pattern of especially high antiproliferative potency against the human breast cancer cell line MCF7 for the series with 2,4,5-trisubstituted anilines, even compared to the usually highly sensitive HeLa cells[41]. A comparison of the compounds with 2,4,5-trisubstituted anilines shows that a 2,4,5-trimethoxyphenyl ring (33) is worse than the 3,4,5-trimethoxyphenyl ring, except for MCF7, against which they are of similar potency. Replacement of one of the methoxy groups with a bromine atom is slightly detrimental at position 2 (e.g. 14) but highly favourable at position 4 (e.g. 24), where it results in the most potent compounds, even compared to their TMP pairs.

Finally, for the bromo scan, the introduction of the additional bromo substituent at position 4 results in high potency improvements (e.g. compare 2 vs. 8a for series 1, or 22 vs. 24 for series 3), whereas at position 2 it is neutral or even detrimental (e.g. compare 2 vs. 8b for series 1, 12 vs. 14 for series 2, or 33 vs. 14 for series 4). The introduction on the basic pharmacophore of a substituent at position 2 (either a methoxy or a bromo) is favourable, whereas at position 3 (a methoxy) it is detrimental or neutral at best. Finally, a substituent at position 4 is also favourable, more for bromo than for methoxy groups. The structural combination of these favourable modifications is also positive, thus resulting in the highest antiproliferative potencies, even better than those of the well-established TMP.

Concerning the substituent on the sulphonamide nitrogen, hydrogen or small groups (methyl, ethyl, or acetonitrile) resulted in optimal potency for every series (2, 8a, 9a, 13–16, 21–25, and 32–35), whereas larger substituents such as acetates (5, 17, 26, 29, and 36), carboxylates (7 and 27), or benzyls (10b–c, 18, and 37) showed reduced potencies or rendered the compounds inactive, except for the benzyl group of the 3,4,5- trisubstituted compound 10a of the series 1. These results are different from previously described sulphonamides, including those with TMP phenyl rings, where methyl groups are usually strongly preferred[3,46,47]. Acetonitrile substitutions on the sulphonamide nitrogen (16, 25, and 35) showed similar potencies (IC_{50} HeLa ¼ 407, 36, and 500 nM, respectively) with respect to the less polar methylated analogs (14, 24, and 33) (IC_{50} HeLa ¼ 557, 33, and 413 nM, respectively).

In summary, best outcomes were achieved by the 2,4,5-trisubstitution pattern instead of the 3,4,5- of the TMP ring, with optimal results for a 2,5-dimethoxy phenyl ring together with a 4-bromo atom (23–25). Compound 25, which combines these structural characteristics with the novel acetonitrile moiety on the sulphonamide bridge was therefore selected for further characterisation of the mechanism of action in HeLa, MCF7, and HT-29 human tumour cell lines.

Benzenesulphonamides are in vitro *antiproliferative agents against the CA-4 resistant cell line HT-29 and do not suffer from MDR efflux or UDPGluc-transferase conjugation reactions*

The human colon adenocarcinoma cell line HT-29 shows low sensitivity towards CA-4 and other colchicine site ligands. This low sensitivity has been attributed to drug efflux by MDR expression[42], autophagy induction[21], and drug metabolism by UDP glucuronyltransferase enzymes[12]. All the synthesised sulphonamides were evaluated against this cell line (Table 1), both in the absence and the presence of the non-selective Pgp/MDR1 inhibitor verapamil at a concentration of 10 μM, which was shown to not affect HT-29 cell proliferation[20,48]. A comparison of the pairs of IC_{50} values provides a measure of the sensitivity of the drugs to efflux by MDR pumps, as previously described[49,50]. Potency differences higher than 3-fold were considered indicative of sensitivity to MDR efflux. Compound 27 was the only active benzenesulphonamide with a difference in IC_{50} values larger than 3-fold arising from the co-treatment with the MDR inhibitor. These results suggest that the benzenesulphonamides are not substrates of the MDR efflux, which is one of the main ways tumour cells use to develop resistance against tubulin inhibitors[8].

Most of the active compounds showed similar potencies against HeLa and HT-29, with IC_{50} values encompassed within a 3 to 4-fold range. These differences are much lower than that observed for CA-4 (>100 fold) and result in a potency improvement of the new sulphonamides of series 3 (i.e. 21–25) against HT-29 compared with CA-4. The different sensitivity to CA-4 compared to the benzenesulphonamides seems not to be due to drug efflux, as co-treatment with verapamil did not result in a potency increase for CA-4. Alternatively, the lack of the 3 hydroxy group that is the point of metabolism by UDP-glucuronyltransferases in CA-4 might explain the observed difference. Sulphonamides are potential substrates of UDP-glucuronyltransferases, but we have found no differences between unsubstituted and substituted sulphonamides against HT-29 (e.g. compare 23 with 24 and 25), thus suggesting that they do not experience the inactivating conjugation reaction and providing an explanation for the higher effect against this cell line.

In vitro *cell growth inhibition against the human non-tumorigenic cell line HEK293*

The antiproliferative IC_{50} values of sulphonamides 22–25 against the embryonic kidney human cell line HEK293 were used as a surrogate for toxicity against non-tumorigenic cells (Table 3). HeLa and MCF7 tumour cells were more sensitive than the non-tumorigenic HEK293 cells towards sulphonamides 22 (IC_{50} values of 177 and 153 nM compared with 517 nM) and 24 (IC_{50} values of 33 and 19 nM, compared with 91 nM), thus showing promising selectivity indexes up to 3- to 5-fold. The tumour cell lines were similarly sensitive to sulphonamides 23 (IC_{50} values of 45 and 25 nM,

compared with 43 nM for the non-tumorigenic cells) and 25 (IC_{50} values of 36 and 86 nM, compared with 45 nM), with selectivity indexes from 0.5 to 2-fold. These results suggest that the new diarylsulphonamides have a modest safety profile for potential application in the treatment of tumour cells.

Diarylsulphonamides of series 3 are tubulin polymerization inhibitors (TPI) in vitro

To confirm that the antiproliferative effect of the compounds is due to inhibition of tubulin, all the synthesised sulphonamides were screened at a concentration of 10 μM for inhibition of the thermally induced assembly of microtubular protein isolated from calf brain. Only compounds from series 3 (23–28) showed consistently inhibition of tubulin polymerisation, with the rest of the series showing low inhibition percentages or no inhibition at all, even for compounds with sub-micromolar antiproliferative potencies (e.g. 8a–10a, 13–16, or 33–37). For those compounds of series 3 that reduced polymerisation by more than 50% at the tested concentration, we determined the IC_{50} values of tubulin polymerisation inhibition (Table 1 and Supplemental Figure 1). Only the most potent antiproliferative compounds of series 3 (23–25) showed IC_{50} values below 10 μM (IC_{50} ¼6.9, 7.6, and 7.6 μM, respectively). These compounds are also the most potent ones in proliferation assays, thus suggesting TPI as the potential mechanism of action. As previously reported for many anti-tubulin agents[15], no correlation is often observed between the IC_{50} values of TPI and the cell growth inhibition values, and compounds with different scaffolds show very different TPI to antiproliferative ratios. This discrepancy is probably due to the accepted proposal that the antiproliferative effects observed at low treatment doses are caused by the interference with microtubule dynamics but not by the alteration of polymer mass, which only occurs at high drug concentrations[1].

Table 3. Cell growth inhibition of the most potent compounds against the non-tumorigenic human embryonic kidney cell line HEK293.

Antiproliferative activity IC_{50} (nM)	
Comp	HEK293
22	517
23	43
24	91
25	45

Diarylsulphonamide 25 interferes with the microtubule network in cells and causes mitotic arrest followed by apoptotic cell death

The time-course effects of compound 25 (87.5 and 175 nM) on the cell cycle populations of MCF7, HeLa, and HT-29 cells were studied to further interrogate its mechanism of action. Cells were stained with Propidium Iodide (PI) and the DNA content measured by fluorescence flow cytometry was used to evaluate the distribution of cells along the cell cycle at 24 h time steps from 24 to 72 h post-treatment (Figures 2 and 3).

Compound 25 at both concentrations measured (87.5 nM and 175 nM) arrested almost completely cervix cancer HeLa cells (82% and 86%, respectively) and colon adenocarcinoma HT-29 cells (90% and 83%) at the G_2/M phase 24 h after treatment. The mitotic arrest was sustained at the 48 h time point for HT-29 (84%) cells along with a small increase of the subG$_0$/G$_1$ population (9%), and later followed at 72 h by a further increase of the subG$_0$/G$_1$ population (23% and 31%) at the expense of the G_2/M phase (58% and 54%). For the HeLa cells, this trend was reproduced but in a shorter timescale, with the subG$_0$/G$_1$ population (34% and 29%) increasing significantly at 48 h at the expense of the G_2/M phase (54% and 48%), showing a small additional advance in this direction at the 72 h timepoint (subG$_0$/G$_1$ population: 38%; G_2/M phase 41% and 49%). Breast cancer MCF7 cells showed a more modest G_2/M arrest at 24 h for both drug concentrations (66% and 60%), accompanied by an early increase in the subG$_0$/G$_1$ (apoptotic) populations (12% and 16%). After the initial 24 h timepoint, differences for the two drug concentrations were apparent. At the lower dose, the distribution of cells remained mostly unchanged for 72 h, whereas for the higher dose an increment in the subG$_0$/G$_1$ population (24%) at the expense of the G_2/M phase (55%) was observed at 48 h and maintained at 72 h

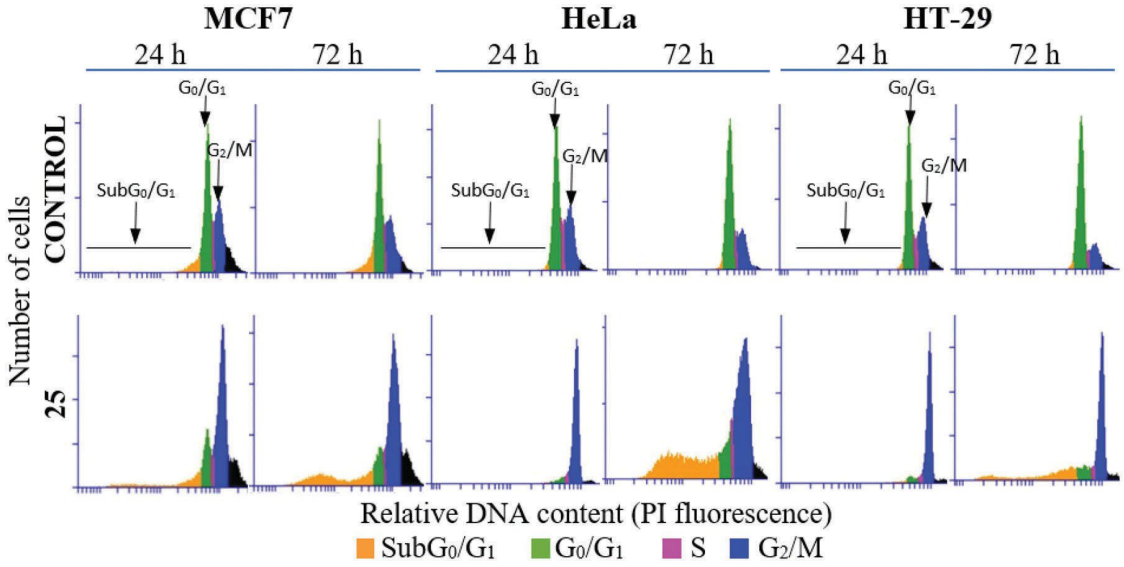

Figure 2. DNA content frequency histograms representing the progression on the cell cycle profile from 24 to 72 h in MCF7, HeLa, and HT-29 cell lines untreated (control) or treated with compound 25 at 175 nM. The position of subG$_0$/G$_1$, G$_0$/G$_1$, and G_2/M peaks are indicated by arrows. Most of the cells are arrested at G_2/M peak after 24 h treatment. Cell death is observed 72 h post-treatment by the increase in the percentage of cells at subG$_0$/G$_1$ region. The histograms shown are representative of three independent experiments. Control cells were run in parallel.

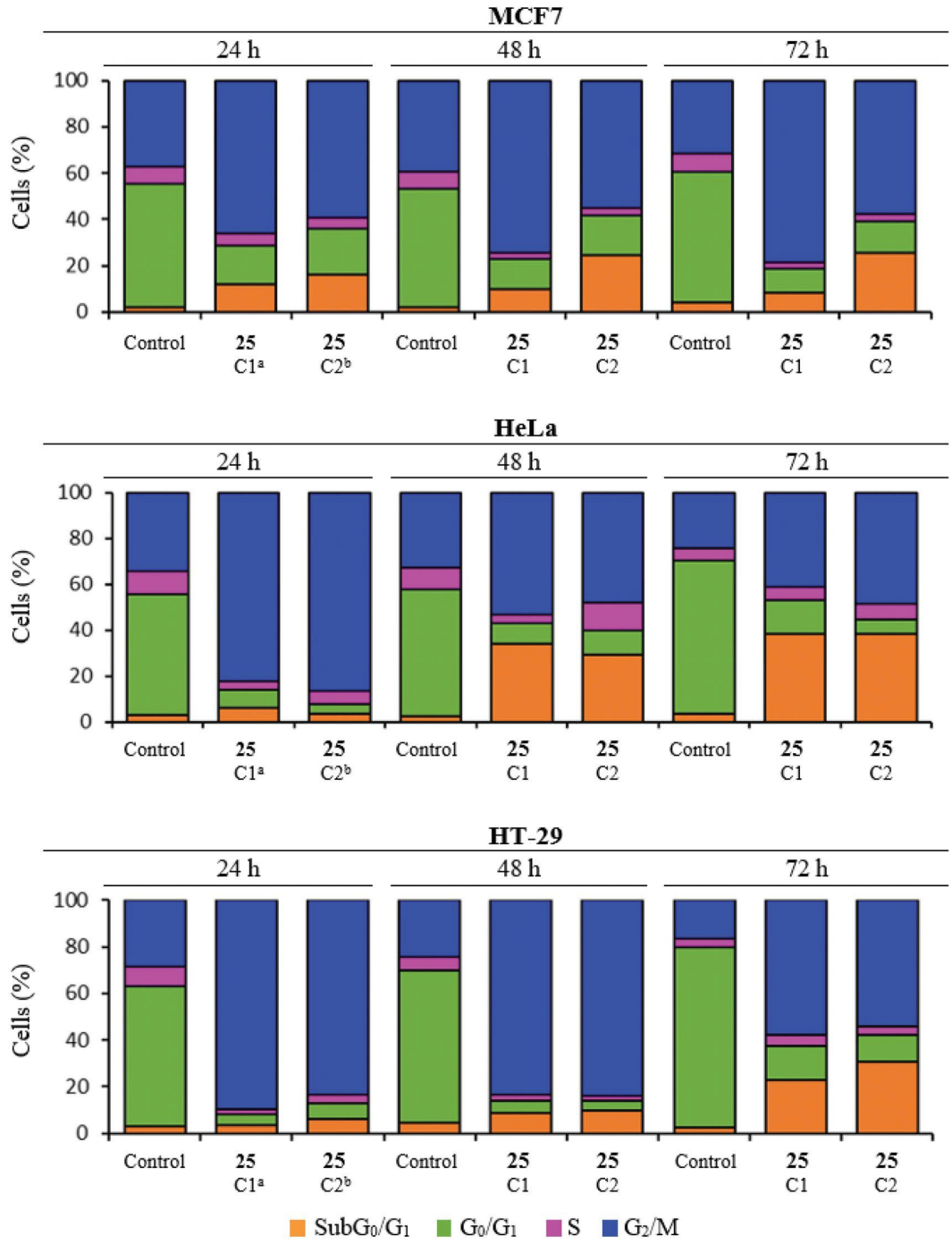

Figure 3. Time-course effect of compound 25 on cell cycle distribution in MCF7, HeLa, and HT-29 cell lines. [a]C1: 87.5 nM. [b]C2: 175 nM. Cells were incubated in the absence (control) or the presence of compound 25 at 87.5 or 175 nM for 24, 48, and 72 h, stained with PI, and their DNA content was analysed by fluorescence flow cytometry. The proportion of cells in each phase of the cell cycle was quantified and expressed in percentages. The data shown are the average of three independent experiments. Control cells were run in parallel.

(subG$_0$/G$_1$ population: 26%; G$_2$/M phase 58%), in a similar way as that observed for HeLa cells but with a lower advance of the subG$_0$/G$_1$ population.

Therefore, the lead compound 25 caused a mitotic arrest of the cell cycle at the G$_2$/M phase and an increase in the subG$_0$/G$_1$ population that varied depending on the cell line in the time of onset and advance, and in the concentration dependency. These results agree with the proposed mechanism of action affecting the mitotic machinery by interfering with tubulin polymerization[1].

To further ascertain the apoptotic cell death suggested by the cell cycle studies, MCF7, HeLa, and HT-29 cells were double-stained with Annexin V-FITC (AnV) and propidium iodide (PI) and then analysed by flow cytometry 72 h after treatment with compound 25 at 87.5 and 175 nM. Cells were considered alive as being double negative (AnV−/PI−), in Early Apoptosis (EA) as being AnV+/PI−, in Late Apoptosis (LA) as being double-positive (AnV + /PI+) and in necrosis as being AnV−/PI + (Table 4). Live control cells were always >90%. Consistently with the cell cycle results, an

apoptotic response was observed for the HT-29 cell line (23% to 36%), and for HeLa cells, which had an almost complete apoptotic profile (>90%). A concentration-dependent apoptotic response similar to that observed in the cell cycle experiments was observed for treated MCF7 cells, with 18% apoptotic cells at the lowest concentration, which increased to 33% with the concentration shift. The weak build-up of the apoptotic response in MCF7 cells may putatively depend on its deficiency of caspase 3[51,52], the hub effector of the apoptotic machinery. These results are in line with the cell cycle experiments and suggest that the lead compound 25 exhibits its antitumor effect by causing a mitotic arrest that triggers an apoptotic response, as has been previously described for other antimitotic agents[53].

Table 4. Cell death quantification.

	MCF7	HeLa	HT-29
CONTROL			
Live[a]	91.1	96.8	92.3
Early apoptosis[b]	0.9	0.6	3.3
Late apoptosis[c]	5.9	1.9	4.1
Necrosis[d]	2.1	0.6	0.2
25			
87.5 nM			
Live	82.1	6.5	76.2
Early apoptosis	11.7	52.3	16.4
Late apoptosis	5.8	39.7	6.8
Necrosis	0.5	1.5	0.7
175 nM			
Live	65.7	4.1	61.7
Early apoptosis	23.8	47.5	20.4
Late apoptosis	9.5	45.3	15.3
Necrosis	1.0	3.1	2.5

MCF7, HeLa, and HT-29 cell lines were incubated in the absence (control) or the presence of compound 25 at 87.5 or 175 nM for 72 h, double-stained with Annexin V-FITC (AnV) and propidium iodide (PI) and analysed by flow cytometry. Data shown represent the average of three independent experiments and are expressed in percentages. Control cells were run in parallel.

[a]Cells were considered live as being double-negative (AnV−/PI−).

[b]In early apoptosis as being AnV-positive.

[c]In late apoptosis as being double-positive (AnV+/PI+).

[d]In necrosis as being PI-positive.

To confirm the effect on the microtubular system of treated cells, the microtubule network of MCF7, HeLa, and HT-29 cell lines was studied by immunofluorescent microscopy. Microtubules (green fluorescence) were stained with anti-*α*-tubulin antibody after 72-h exposure to compound 25 at 175 nM, the p-62 autophagosome marker (red fluorescence) was stained with anti-SQSTM1/p62 antibody and cell nuclei (blue fluorescence) were stained with DAPI (Figure 4). Compound 25 disrupted the microtubule network of MCF7, HeLa, and HT-29 cell lines. Besides, as expected for tubulin-binding drugs[54,55], alterations in chromatin organisation could be observed. Condensation and fragmentation of chromatin in multilobulated nuclei resembling bunches of grapes are clear in treated MCF7 and HT-29 cells; whereas giant nuclei are present in HeLa cells. These results further support that the lead compound 25 exhibits its antitumor effect by interfering with the microtubule network.

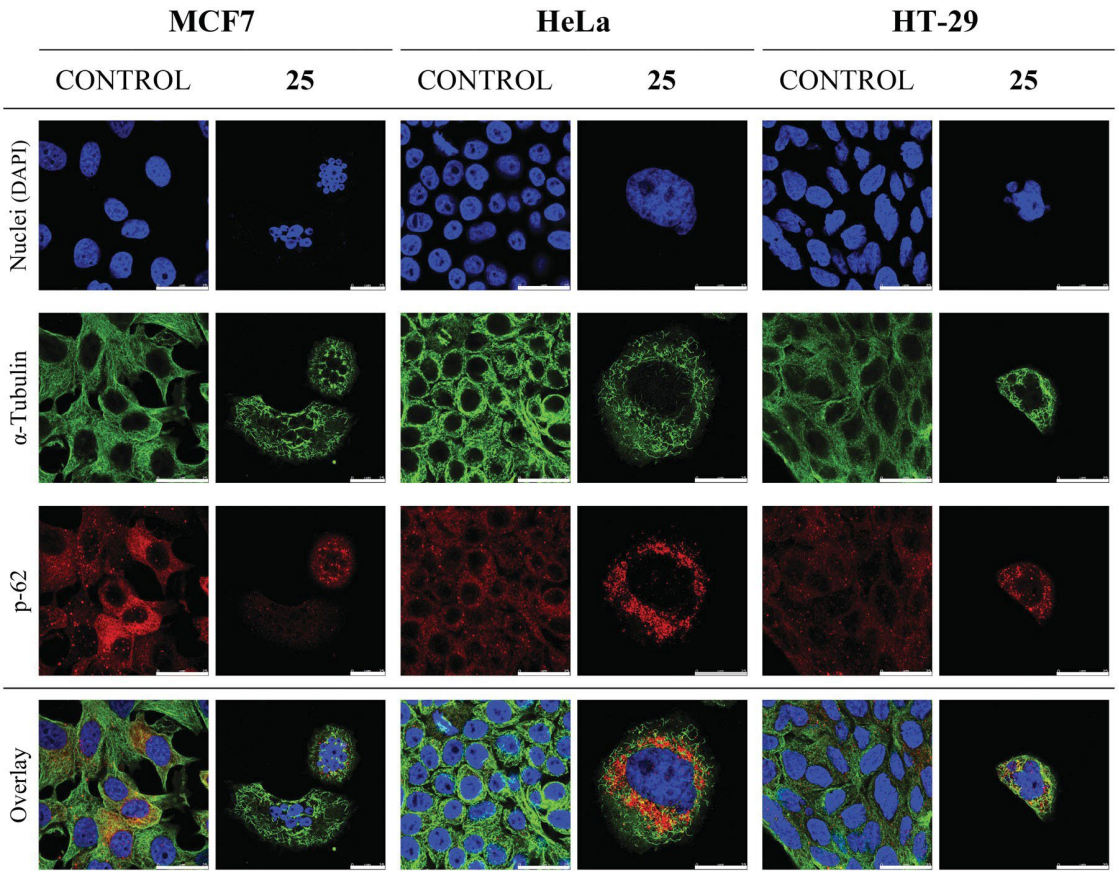

Figure 4. Effect of compound 25 (175 nM) on the microtubule system and autophagy of MCF7, HeLa, and HT-29 cells after 72 h of treatment. Microtubules were stained with anti-a-tubulin antibody (green fluorescence), p-62 protein with anti-SQSTM1/p62 antibody (red fluorescence), and cell nuclei with DAPI (blue fluorescence). Preparations were analysed by confocal microscopy. Control cells were run in parallel. Scale bar: 25 μm. The photomicrographs shown are representative of three independent experiments.

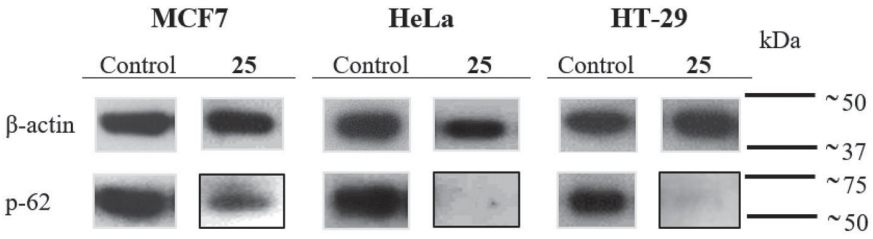

Figure 5. Western blot analysis of autophagosome marker p-62, on MCF7, HeLa and HT-29 cell extracts after 24 h of treatment with compound 25 at 175 nM. b-actin constitutive protein was used as an internal control. Control cells were run in parallel.

Diarylsulphonamide 25 causes a downregulation of the autophagosome marker p-62

The confocal microscopy studies showed downregulation and perinuclear clumps of autophagosome marker p-62 upon drug treatment, in accordance with activated autophagy[56] (Figure 4). Additional evidence of this mechanism was pursued by western blot analysis of the autophagosome marker p-62 after treatment with compound 25 at 175 nM (Figure 5). Treatment with compound 25 caused decay in p-62 levels in the MCF7 cell line and an almost complete reduction in the expression of p-62 in HeLa and the HT-29 cell lines after 24 h treatment. These results reveal activation of the autophagic process, which is associated with decreased p-62 levels[57], and sustain that compound 25 exerts its action by interfering with microtubule dynamics and by activation of autophagy.

Molecular docking studies

The binding mode of the sulphonamides at the colchicine site has been studied using flexible docking studies. The protein conformational space has been sampled employing ensemble docking[58] into 55 tubulin structures with different colchicine domain configurations induced by different ligands. Two docking programs with different scoring functions have been combined for the docking and scoring processes. For each ligand, the common pose shared by the two docking programs and with the highest (corresponding to lowest scoring energies) combined normalised scores for the two scoring functions was selected as the ligand-binding mode (Supplemental Table 1). All the ligands bound to the colchicine domain with the two phenyl rings (*p*-methoxyphenyl and *N*-phenyl) arranged similarly as rings A (trimethoxyphenyl) and B (3-hydroxy-4-methoxyphenyl) of combretastatin A-4 (Figure 6). Furthermore, with the only exception of compound 12 that binds in the reverse sense, in all cases the 4-methoxyphenyl rings bound at the B-ring site (zone 1) of combretastatin A-4 whereas the *N*-phenyl rings did so at the A-ring site (zone 2), thus reflecting their respective size and shape similarity that translates into the protein cavities that they lodge in. Regarding the protein sites preferred, most of the selected poses bind to sites similar in shape and size to combretastatin A-4 (the most frequent sites being those binding the *b*-lactam analogs of combretastatins, which likely reflects the larger space needed to allocate the sulphonamide bridge compared to the olefin of CA-4 itself). Concerning the conformation of the selected poses (Figure 6 and Supplemental Table 1), a different outcome was observed depending on the positions of the substituents of the phenyl ring occupying zone 2 and the bulkiness of the substituent on the sulphonamide nitrogen. For compounds with a 3,4,5-substituted *N*-phenyl ring such as those of series 1 (e.g. 8a) a *cisoid* conformation of the sulphonamide that results in a very close overlap with CA-4 are observed (Figure 6(A)) unless polar or/and bulky substituents on the sulphonamide nitrogen cause the sulphonamide to adopt a *transoid* confirmation, which is the preferred one in most compounds having 2,3,5- (series 1) or 2,4,5-substituted (series 2-4) *N*-phenyl rings (Figure 6(B–D)). For all the compounds with a substituent *ortho* to the anilide nitrogen, the steric demand increases, therefore favouring a *transoid* disposition (Figure 6(B–D)). In every case, the disposition of the ring aims at fulfilling the pocket for the A-ring, and depending on the substituent *ortho* to the nitrogen atom of the *N*-phenyl ring differences in their binding mode are observed: for the 2-bromo- series 2 (Figure 6(B)) the *N*-substituent projects towards the interfacial surface between the *a* and *b* tubulin subunits, whereas for the 2-methoxy- series 3 (4-bromo-5-methoxy, Figure 6(C)) and 4 (4,5-dimethoxy, Figure 6(D)), except in this later case for the combination with the smaller substituents on the sulphonamide nitrogen (hydrogen or methyl), the *N*-substituent points towards S8–10, thus replacing one of the methoxy groups. This new binding mode explains the high potency observed for the acetonitrile substituent on the sulphonamide nitrogen, which was not observed for *N*-(3,4,5-trimethoxyphenyl)-4-methoxybenzenesulphonamides[41].

Conclusion

A focussed library of 37 new sulphonamides that represents a scan of the substitution of hydrogen atoms on the anilide ring of the basic colchicine-binding site pharmacophore *N*-(5-methoxyphenyl)-4-methoxybenzenesulphonamides with methoxy and/or bromo groups, grouped in 4 structural series, has been successfully prepared. The assessment of the antiproliferative activity of the library members against several human cancer cell lines showed that many compounds outperform analogs carrying the conventional TMP ring. Furthermore, the compounds are not substrates of the MDR-1 protein, as co-treatments with MDR-1 inhibitor verapamil do not enhance the antiproliferative potency against the HT-29 cell line. The structure-activity relationships of the series differ from the TMP analogs, with polar substituents better tolerated on the sulphonamide bridge, and a special susceptibility is observed for the breast cancer cell line MCF7, not paralleled by the TMP analogs. Unexpectedly, the most promising series is the more structurally dissimilar to the TMP, the 4-bromo-2,5-dimethoxyphenyl series 3. The effect of the most potent compounds on the microtubule system was confirmed by *in vitro* tubulin polymerisation inhibition. Compound 25 inhibits microtubule polymerisation *in cells* as shown by confocal microscopy studies and causes a mitotic arrest followed by a dose-dependent induction of apoptosis at later times, accompanied by autophagy induction. Docking experiments agree with binding to the tubulin colchicine-site in a different disposition that accounts for the high potency. In conclusion, the structural modifications provide access to new colchicine-site compounds, and lead compound 25 is a promising new candidate tubulin-binding antitumor drug.

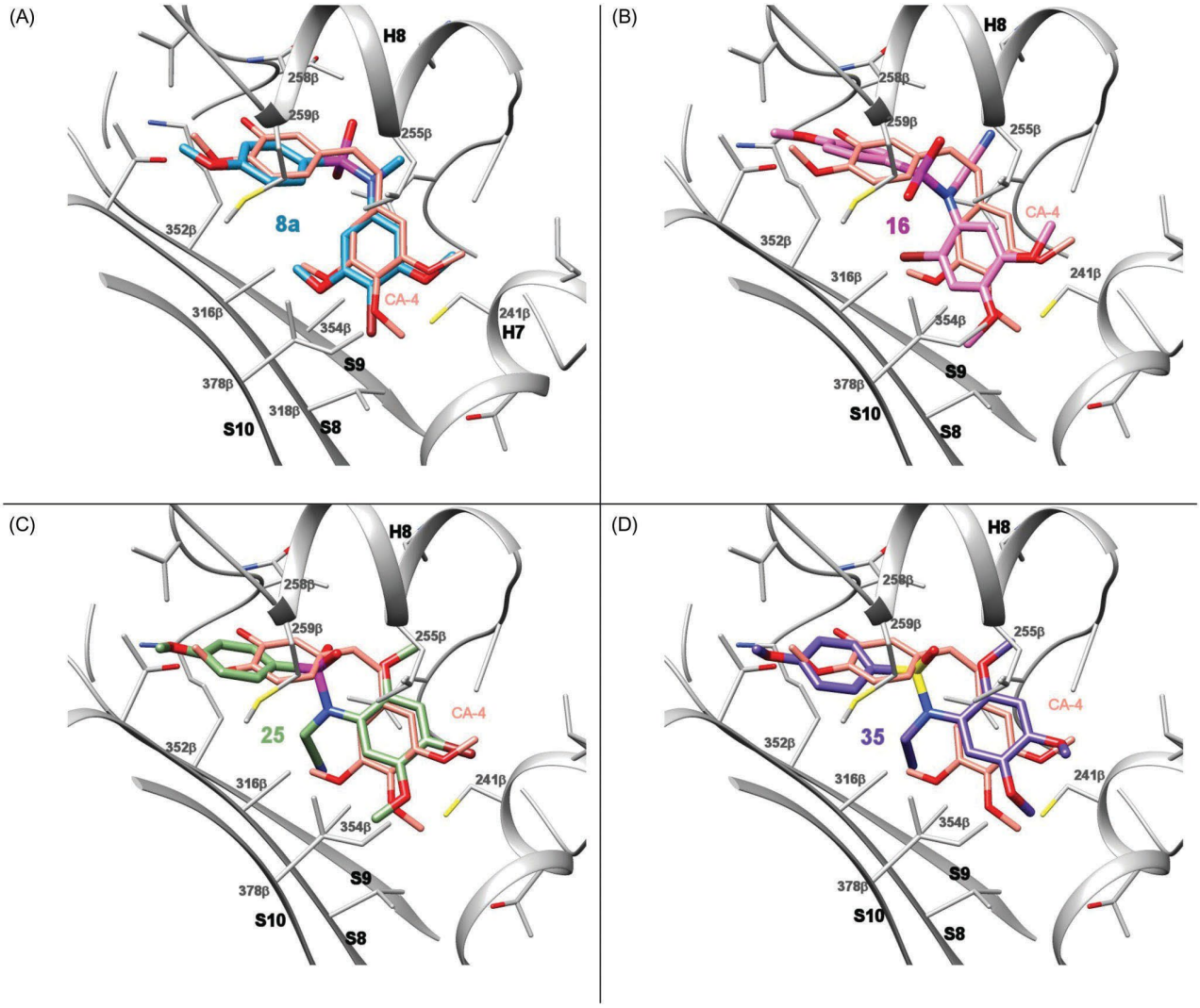

Figure 6. Consensus docking poses for representative compounds of each series: (A) 8a (carbons in dodger blue) of series 1, (B) 16 (carbons in magenta) of series 2, (C) 25 (carbons in yellow-green) of series 3, (D) 35 (carbons in purple) of series 4. The secondary elements of the colchicine site are shown in a silver cartoon representation and labelled. In every panel, the X-ray structure of combretastatin A-4 (CA-4) in thinner sticks with carbons in orange is shown superimposed for comparison. Amino acids within 5 A of the ligands are shown as thin sticks.

Acknowledgements

We thank the people at Frigor ıficos Salamanca S.A. slaughterhouse for providing us with the calf brains, "Servicio General de NMR" and "Servicio General de Espectrometr ıa de Masas" of the University of Salamanca for equipment. M.G. acknowledges a predoctoral fellowship from the Junta de Castilla y Leo n (ORDEN EDU/529/2017 de 26 de junio). M.O.-S. acknowledges a predoctoral fellowship from the IBSAL (IBpredoc17/00010). A.V.-B. acknowledges a predoctoral fellowship from the Spanish Ministerio de Educacio n, Cultura y Deporte (FPU15/02457).

Author contributions

Conceptualisation, M.G., and R.P.; methodology, M.G., and M.O.-S.; software, R.P.; validation, R.P., M.M. and R.G.-S.; formal analysis, M.G., M.O.-S., and A.V.-B.; investigation, M.M., R.G.-S. and R.P.; resources, R.G.-S. and R.P.; data curation, M.G., and R.P.; writing—original draft preparation, M.G.; writing—review and editing, A.V.-B., M.M., R.G.-S., and R.P.; visualisation, M.G. and M.O.-S.; supervision, R.G.-S., and R.P.; project administration, R.G.-S., and R.P.; funding acquisition, R.G.-S., and R.P. All authors have read and agreed to the published version of the manuscript.

Disclosure statement

No potential conflict of interest was reported by the author(s).

Funding

This research was funded by the Consejer ıa de Educacio n de la Junta de Castilla y Leo n (ORDEN EDU/529/2017 de 26 de junio, SA030U16, SA262P18 and SA116P20), co-funded by the EU's European Regional Development Fund-FEDER, the Spanish Ministry of Science, Innovation and Universities (RTI2018-099474-BI00) and the health research program of the Instituto de Salud Carlos III (Spanish Ministry of Economy and Competitiveness) [PI16/01920 and PI20/01569] co-funded with FEDER funds.

Ministerio de Educacio n, Cultura y Deporte [FPU15/02457], IBSAL [IBpredoc17/00010].

References

1. Dumontet C, Jordan MA. Microtubule-binding agents: a dynamic field of cancer therapeutics. Nat Rev Drug Discov 2010;9:790–803.
2. Jordan MA, Wilson L. Microtubules as a target for anticancer drugs. Nat Rev Cancer 2004;4:253–63.
3. Vicente-Bl azquez A, Gonz alez M, A lvarez R, et al. Antitubulin sulphonamides: the successful combination of an established drug class and a multifaceted target. Med Res Rev 2019;39:775–830.
4. Alvarez R, Medarde M, Pelaez R. New Ligands of the tubulin colchicine site based on x-ray structures. Curr Top Med Chem 2014;14:2231–52.
5. Ravelli RBG, Gigant B, Curmi PA, et al. Insight into tubulin regulation from a complex with colchicine and a stathmin-like domain. Nature 2004;428:198–202.
6. Torres F, Garcia-Rubino M, Lozano-Lopez C, et al. Imidazoles and benzimidazoles as tubulin-modulators for anti-cancer therapy. Curr Med Chem 2015;22:1312–23.
7. Tron GC, Pirali T, Sorba G, et al. Medicinal chemistry of combretastatin A4: present and future directions. J Med Chem 2006;49:3033–44.
8. Kavallaris M. Microtubules and resistance to tubulin-binding agents. Nat Rev Cancer 2010;10:194–204
9. Li L, Jiang S, Li X, et al. Recent advances in trimethoxyphenyl (TMP) based tubulin inhibitors targeting the colchicine binding site. Eur J Med Chem 2018;151:482–94.
10. Negi AS, Gautam Y, Alam S, et al. Natural antitubulin agents: importance of 3,4,5-trimethoxyphenyl fragment. Bioorg Med Chem 2015;23:373–89.
11. Aprile S, Del Grosso E, Tron GC, Grosa G. *In vitro* metabolism study of combretastatin A-4 in rat and human liver microsomes. Drug Metab Dispos 2007;35:2252–61.
12. Ghinet A, Rigo B, H enichart JP, et al. Synthesis and biological evaluation of phenstatin metabolites. Bioorg Med Chem 2011;19:6042–54.
13. Le Broc-Ryckewaert D, Pommery N, Pommery J, et al. *In vitro* metabolism of phenstatin: potential pharmacological consequences. Drug Metab Lett 2011;5:209–15.
14. Hamze A, Alami M, Provot O. Developments of isoCombretastatin A-4 derivatives as highly cytotoxic agents. Eur J Med Chem 2020;190:112110.
15. Gonzalez M, Ellahioui Y, Alvarez R, et al. The Masked Polar Group Incorporation (MPGI) strategy in drug design: effects of nitrogen substitutions on combretastatin and isocombretastatin tubulin inhibitors. Molecules 2019;24:4319.
16. Alvarez R, Aramburu L, Puebla P, et al. Pyridine based antitumour compounds acting at the colchicine site. Curr Med Chem 2016;23:1100–30.
17. A lvarez R, Aramburu L, Gajate C, et al. Methylsulfanylpyridine based diheteroaryl isocombretastatin analogs as potent anti-proliferative agents. Eur J Med Chem 2021;209:112933.
18. Lu Y, Shi T, Wang Y, et al. Halogen bonding-a novel interaction for rational drug design? J Med Chem 2009;52: 2854–62.
19. Beale TM, Myers RM, Shearman JW, et al. Antivascular and anticancer activity of dihalogenated A-ring analogues of combretastatin A-4. Med Chem Comm 2010;1:202–8.
20. Loe DW, Deeley RG, Cole SP. Verapamil stimulates glutathione transport by the 190-kDa multidrug resistance protein 1 (MRP1). J Pharmacol Exp Ther 2000;293:530–8.
21. Greene LM, O'Boyle NM, Nolan DP, et al. The vascular targeting agent Combretastatin-A4 directly induces autophagy in adenocarcinoma-derived colon cancer cells. Biochem Pharmacol 2012;84:612–24.
22. Wei RJ, Lin SS, Wu WR, et al. A microtubule inhibitor, ABT-751, induces autophagy and delays apoptosis in Huh-7 cells. Toxicol Appl Pharmacol 2016;311:88–98.
23. Dumortier C, Gorbunoff MJ, Andreu JM, Engelborghs Y. Different kinetic pathways of the binding of two biphenyl analogues of colchicine to tubulin. Biochemistry 1996;35: 4387–95.
24. Shelanski ML, Gaskin F, Cantor CR. Microtubule assembly in the absence of added nucleotides. Proc Nat Acad Sci U.S.A. 1973;70:765–8.
25. Bradford M. A rapid and sensitive method for the quantitation of microgram quantities of protein utilizing the principle of protein-dye binding. Anal Biochem 1976;72:248–54.
26. Alvarez R, Aramburu L, Gajate C, et al. Potent colchicine-site ligands with improved intrinsic solubility by replacement of the 3,4,5-trimethoxyphenyl ring with a 2-methylsulfanyl-6-methoxypyridine ring. Bioorg Chem 2020;98:103755.
27. Korb O, Stu€tzle T, Exner TE. Empirical scoring functions for advanced protein-ligand docking with plants. J Chem Inf Model 2009;49:84–96.
28. Forli S, Huey R, Pique ME, et al. Computational protein-ligand docking and virtual drug screening with the AutoDock suite. Nat Protoc 2016;11:905–19.
29. Berthold MR, Cebron N, Dill F, et al. KNIME: the Konstanz information miner. Studies in classification, data analysis, and knowledge organization. Berlin, Germany: Springer; 2007:319–326.
30. Pettersen EF, Goddard TD, Huang CC, et al. UCSF Chimera-A visualization system for exploratory research and analysis. J Comput Chem 2004;25:1605–12.
31. Marvin 17.8 ChemAxon. 2017 [accessed 2020 May 2]. https://www.chemaxon.com
32. OpenEye Scientific Software, Inc, Santa Fe. 2019 [accessed 2020 May 2]. https://www.eyesopen.com/
33. Garcia-Perez C, Pelaez R, Theron R, Luis Lopez-Perez J. JADOPPT: Java based AutoDock preparing and processing tool. Bioinformatics 2017;33:583–5.
34. Cafici L, Pirali T, Condorelli F, et al. Solution-phase parallel synthesis and biological evaluation of combretatriazoles. J Comb Chem 2008;10:732–40.
35. Liao SY, Qian L, Miao TF, et al. Theoretical studies on QSAR and mechanism of 2-indolinone derivatives as tubulin inhibitors. Int J Quantum Chem 2009;109:999–1008.
36. Mu F, Hamel E, Lee DJ, et al. Synthesis, anticancer activity, and inhibition of tubulin polymerization by conformationally restricted analogues of lavendustin A. J Med Chem 2003;46: 1670–82.
37. Stocker V, Ghinet A, Leman M, et al. On the synthesis and biological properties of isocombretastatins: a case of ketone homologation during Wittig reaction attempts. RSC Adv 2013;3:3683–96.
38. Hu L, Jiang J, Dong Qu J, et al. Novel potent antimitotic heterocyclic ketones: synthesis, antiproliferative activity, and

structure-activity relationships. Bioorg Med Chem Lett 2007; 17:3613–7.
39. Hu L, Li ZR, Li Y, et al. Synthesis and structure-activity relationships of carbazole sulphonamides as a novel class of antimitotic agents against solid tumors. J Med Chem 2006; 49:6273–82.
40. Dohle W, Jourdan FL, Menchon G, et al. Quinazolinone-based anticancer agents: synthesis, antiproliferative SAR, antitubulin activity, and tubulin co-crystal structure. J Med Chem 2018;61:1031–44.
41. Gonz alez M, Ovejero-S anchez M, Vicente-Bl azquez A, et al. Microtubule destabilizing sulphonamides as an alternative to taxane-based chemotherapy. Int J Mol Sci 2021;22:1907.
42. Schobert R, Effenberger-Neidnicht K, Biersack B. Stable combretastatin A-4 analogues with sub-nanomolar efficacy against chemoresistant HT-29 cells. Int J Clin Pharmacol Ther 2011;49:71–2.
43. Cummings J, Zelcer N, Allen JD, et al. Glucuronidation as a mechanism of intrinsic drug resistance in colon cancer cells: contribution of drug transport proteins. Biochem Pharmacol 2004;67:31–9.
44. Nam N-H. Combretastatin A-4 analogues as antimitotic antitumor agents. Curr Med Chem 2003;10:1697–722.
45. Andreu JM, Perez-Ramirez B, Gorbunoff MJ, et al. Role of the colchicine ring A and its methoxy groups in the binding to tubulin and microtubule inhibition. Biochemistry 1998;37: 8356–68.
46. Liu Y, Wu Y, Sun L, et al. Synthesis and structure-activity relationship study of water-soluble carbazole sulphonamide derivatives as new anticancer agents. Eur J Med Chem 2020; 191:112181.
47. Liu J, Liu C, Zhang X, et al. Anticancer sulphonamide hybrids that inhibit bladder cancer cells growth and migration as tubulin polymerisation inhibitors. J Enzyme Inhib Med Chem 2019;34:1380–1387.
48. Sharom FJ. The P-glycoprotein multidrug transporter. Essays in Biochem 2011;50:161–178.
49. Alvarez R, Gajate C, Puebla P, et al. Substitution at the indole 3 position yields highly potent indolecombretastatins against human tumor cells. Eur J Med Chem 2018;158: 167–183.
50. Lee MM, Gao Z, Peterson BR. Synthesis of a fluorescent analogue of paclitaxel that selectively binds microtubules and sensitively detects efflux by P-glycoprotein. Angew Chem Int Ed Engl 2017;56:6927–31
51. J€anicke RU, Sprengart ML, Wati MR, Porter AG. Caspase-3 is required for DNA fragmentation and morphological changes associated with apoptosis. J Biol Chem 1998;273:9357–9360.
52. Yang XH, Sladek TL, Liu X, et al. Reconstitution of caspase 3 sensitizes MCF-7 breast cancer cells to doxorubicin- and etoposide-induced apoptosis. Cancer Res 2001;61:348–354.
53. Mollinedo F, Gajate C. Microtubules, microtubule-interfering agents and apoptosis. Apoptosis 2003;8:413–50.
54. Vakifahmetoglu H, Olsson M, Zhivotovsky B. Death through a tragedy: mitotic catastrophe. Cell Death Differ 2008;15: 1153–62.
55. Castedo M, Perfettini JL, Roumier T, et al. Cell death by mitotic catastrophe: a molecular definition. Oncogene 2004; 23:2825–2837.
56. Klionsky DJ, Abdelmohsen K, Abe A, et al. Guidelines for the use and interpretation of assays for monitoring autophagy (3rd edition). Autophagy 2016;12:1–222.
57. Bitto A, Lerner CA, Nacarelli T, et al. p62/SQSTM1 at the interface of aging, autophagy, and disease. Age 2014;36: 1137–9626.
58. Amaro RE, Baudry J, Chodera J, et al. Ensemble docking in drug discovery. Biophys J 2018;114:2271–78.

MATERIAL SUPLEMENTARIO

El material suplementario del artículo 2 se encuentra disponible *online* en la siguiente dirección:

https://doi.org/10.1080/14756366.2021.1925265

Se compone de los siguientes apartados, lo cuales se desarrollan a continuación de esta página:

Supplemental Figure 1. Tubulin Polymerization Assay data. IC_{50} calculation.

Supplemental Table 1. Results of the docking studies.

^{1}H NMR and ^{13}C NMR spectra. (online and Anexo digital 2.d).

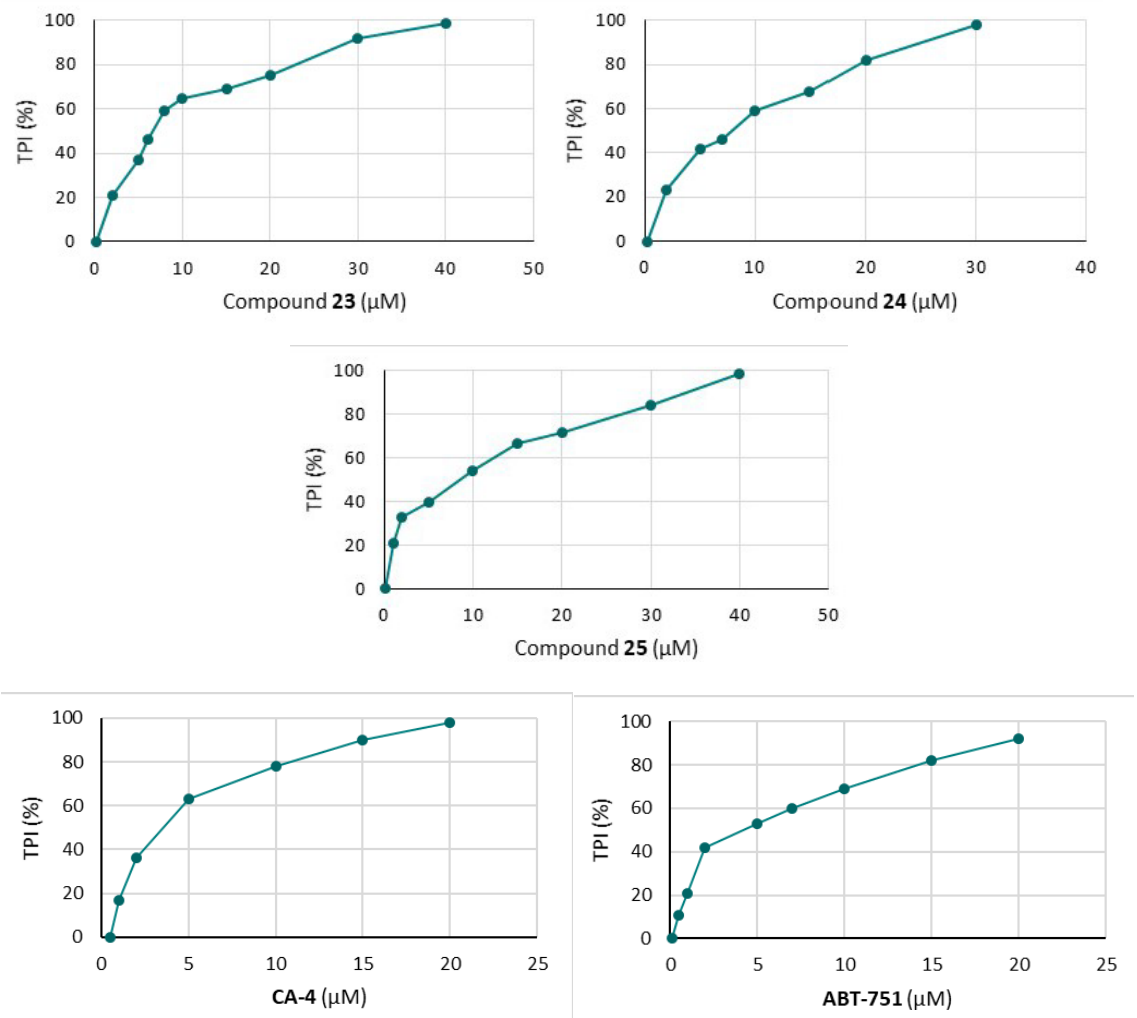

Supplemental Figure 1. Tubulin Polymerization Assay data. IC_{50} calculation. Tubulin Polymerization Inhibition (TPI) percentages are the average of three independent experiments.

Supplemental Table 1. Results of the docking studies.

Series 1	HeLa	MCF-7	HT-29	HT29 Ver	TPI	Conformation	PDB-ID	SITE_OCC	Z-score	PLANTS	E_AD
8a M327	497	99	495	293	>10						
35DM4Br_MeNSO2_4MeOPh_M327_5GON_conf_01						cisoid	5GON	AB	1,0	-85,5	-25,5
35DM4Br_MeNSO2_4MeOPh_M327_5LYJ_90						cisoid	5LYJ	AB	1,0		
8b M327B	>1000	>1000	>1000	-	>10						
35DM2Br_MeNSO2_4MeOPh_M327B_5CB4_conf_02						transoid out	5CB4	AB	1,0	-79,5	-23,4
35DM2Br_MeNSO2_4MeOPh_M327B_5LYJ_78						transoid out	5LYJ	AB	1,0		
9a M335	417	-	610	-	>10						
35DM4Br_EtNSO2_4MeOPh_M335_5GON_conf_01						cisoid out	5GON	AB	1,0	-87,7	-25,2
35DM4Br_EtNSO2_4MeOPh_M335_5LYJ_60						transoid out	5LYJ	AB	1,0		
9b M335B	>1000	>1000	>1000	-	>10						
35DM2Br_EtNSO2_4MeOPh_M335B_5XKH_39						transoid out	5XKH	AB	1,0		
35DM2Br_EtNSO2_4MeOPh_M335B_6GJ4_conf_01						cisoid out	6GJ4	AB	1,0	-81,4	-23,1
10a M326	310	335	450	533	>10						
35DM4Br_BnNSO2_4MeOPh_M326_6BS2_78						transoid out	6BS2	ABC	1,0		
35DM4Br_BnNSO2_4MeOPh_M326_5GON_conf_01						transoid out	5GON	AB	1,0	-94,5	-25,3
10b M326B	>1000	>1000	>1000	>1000	>10						
35DM2Br_BnNSO2_4MeOPh_M326B_5XAF_31						transoid out	5XAF	AB	1,0		
35DM2Br_BnNSO2_4MeOPh_M326B_5GON_conf_01						transoid out	5GON	AB	0,9	-95,6	-25,6
10c M326C	>1000	>1000	>1000	>1000	>10						
35DM24Br2_BnNSO2_4MeOPh_M326C_5GON_conf_01						transoid out	5GON	AB	1,0	-90,3	-23,6
35DM24Br2_BnNSO2_4MeOPh_M326C_5XAF_38						transoid out	5XAF	AB	1,0		

Series 2	HeLa	MCF-7	HT-29	HT29 Ver	TPI	Conformation	PDB-ID	SITE_OCC	Z-score	PLANTS	E_AD
11 M8	>1000	>1000	>1000	>1000	>10						
34DM_HNSO2_4MeOPh_M8_5GON_conf_02						transoid	5GON	AB	0,8	-76,7	-23,1
34DM_HNSO2_4MeOPh_M8_6BS2_47						transoid	6BS2	AB	0,7		
12 M38	>1000	>1000	>1000	>1000	>10						
34DM_MeNSO2_4MeOPh_M38_5GON_conf_01						cisoid reverse	5GON	AB	0,5	-83,1	-25,0
34DM_MeNSO2_4MeOPh_M38_5LYJ_83						cisoid reverse	5LYJ	AB	0,5		
14 M236	557	-	907	-	>10						
34DM6Br_MeNSO2_4MeOPh_M236_6GJ4_conf_01						cisoid	6GJ4	AB	1,0	-75,9	-22,2
34DM6Br_MeNSO2_4MeOPh_M236_5XKF_78						cisoid	5XKF	BC	1,0		
15 M354	313	660	365	500	>10						

34DM6Br_EtNSO2_4MeOPh_M354_5GON_conf_01						cisoid	5GON	AB	1,0	-90,4	-26,1
34DM6Br_EtNSO2_4MeOPh_M354_6D88_86						cisoid	6D88	AB	1,0		
34DM6Br_EtNSO2_4MeOPh_M354_5LYJ_conf_01						transoid	5LYJ	ABC	1,0	-88,7	-25,6
34DM6Br_EtNSO2_4MeOPh_M354_5XKG_6						transoid	5XKG	BC	1,0		
16 M237	407	575	360	750	>10						
34DM6Br_NAcNSO2_4MeOPh_M237_6BRY_55						transoid out	6BRY	AB	1,0		
34DM6Br_NAcNSO2_4MeOPh_M237_5CB4_conf_01						transoid out	5CB4	AB	1,0	-79,6	-21,5
34DM6Br_NAcNSO2_4MeOPh_M237_5XKF_22						transoid in	5XKF	ABC	1,0		
34DM6Br_NAcNSO2_4MeOPh_M237_5XLZ_conf_03						transoid in	5XLZ	AB	1,0	-80,2	-21,7
17 M355	>1000	>1000	>1000	>1000	>10						
34DM6Br_EtOAcNSO2_4MeOPh_M355_5CB4_conf_02						transoid out	5CB4	AB	1,0	-91,2	-23,2
34DM6Br_EtOAcNSO2_4MeOPh_M355_5XKG_79						transoid out	5XKG	AB	1,0		
18 M356	>1000	>1000	>1000	>1000	>10						
34DM6Br_BnNSO2_4MeOPh_M356_6BR1_91						transoid out	6BR1	AB	1,0		
34DM6Br_BnNSO2_4MeOPh_M356_5GON_conf_02						transoid out	5GON	AB	1,0	-101,7	-27,6
21 M76	227	350	187	187	>10						
25DM_HNSO2_4MeOPh_M76_5XLZ_conf_02						transoid	5XLZ	AB	-79,9	-67,9	
25DM_HNSO2_4MeOPh_M76_6BRY_65						transoid	6BRY	AB			-8,0
22 M89	177	153	250	305	>10						
25DM_MeNSO2_4MeOPh_M89_6BRY_4						transoid	6BRY	AB	0,5		
25DM_MeNSO2_4MeOPh_M89_5XLZ_conf_02						transoid	5XLZ	AB	0,5	-76,8	-22,8
23 M98	45	25	72	30	6.9						
25DM4Br_HNSO2_4MeOPh_M98_5GON_conf_03							5GON	AB	0,5	-77,2	-22,9
25DM4Br_HNSO2_4MeOPh_M98_5XAF_22						transoid	5XAF	BC	0,5		
24 M105	33	19	123	160	7,6						
25DM4Br_MeNSO2_4MeOPh_M105_6BS2_conf_01							6BS2	AB	0,7	-76,6	-22,4
25DM4Br_MeNSO2_4MeOPh_M105_5LYJ_59							5LYJ	AB	0,7		
25 M176	36	86	97	85	7,6						
25DM4Br_NAcNSO2_4MeOPh_M176_5XLZ_conf_01						transoid	5XLZ	AB	0,8	-81,1	-22,0
25DM4Br_NAcNSO2_4MeOPh_M176_5LYJ_89						transoid	5LYJ	AB	0,8		
26 M177	577	700	2100	867	>10						
25DM4Br_EtOAcSO2_4MeOPh_M177_5XAF_20						transoid	5XAF	AB	1,0		
25DM4Br_EtOAcSO2_4MeOPh_M177_5CB4_conf_01						transoid	5CB4	AB	1,0	-89,9	-22,8
27 M98	377	220	525	170	>10						
25DM4Br_EtOCONSO2_4MeOPh_M98_5XKF_22						transoid	5XKF	AB	1,0		
25DM4Br_EtOAcNSO2_4MeOPh_M98_5GON_conf_02						transoid	5GON	AB	1,0	-90,0	-23,7

27 M177	377	220	525	170	>10						
25DM4Br_EtOCONSO2_4MeOPh_M179_5XKF_62						transoid	5XKF	AB	1,0		
25DM4Br_EtOCONSO2_4MeOPh_M179_5GON_conf_03						transoid	5GON	AB	0,9	-87,5	-22,9
28 M178R	495	-	860	-	>10						
25DM4Br_OxirMeNSO2_4MeOPh_M178_5XLZ_conf_01						transoid	5XLZ	AB	1,0	-88,5	-24,2
25DM4Br_OxirMeNSO2_4MeOPh_M178_6D88_16						transoid	6D88	AB	1,0		
28 M178S											
25DM4Br_OxirMeNSO2_4MeOPh_M178S_6BRY_57						cisoid	6BRY	AB	1,0		
25DM4Br_OxirMeNSO2_4MeOPh_M178S_5XAF_conf_01						cisoid	5XAF	AB	1,0	-86,4	-23,5
29 M190	>1000	>1000	>1000	>1000	>10						
25DM4Br_HOAcSO2_4MeOPh_M190_6D88_59						transoid	6D88	AB	1,0		
25DM4Br_HOAcSO2_4MeOPh_M190_5XLZ_conf_01						transoid	5XLZ	AB	1,0	-86,7	-22,9
29 M190an											
25DM4Br_OAcSO2_4MeOPh_M190_5LYJ_40						transoid	5LYJ	AB	1,0		
25DM4Br_OAcSO2_4MeOPh_M190_6BS2_conf_01						cisoid	6BS2	AB	1,0	-88,3	-24,1
25DM4Br_OAcSO2_4MeOPh_M190_6BRY_7						cisoid	6BRY	AB	0,9		
25DM4Br_OAcSO2_4MeOPh_M190_5XLZ_conf_02						transoid	5XLZ	AB	0,9	-83,4	-22,5
32 M350	410	580	360	553	>10						
245TM_HNSO2_4MeOPh_M350_5XAF_conf_01						cisoid	5XAF	AB	0,9	-74,6	-21,0
245TM_HNSO2_4MeOPh_M350_6BRY_36						transoid	6BRY	AB	0,9		
33 M361	413	99	500	577	>10						
245TM_MeNSO2_4MeOPh_M361_5XKG_6						transoid	5XKG	ABC	1,0		
245TM_MeNSO2_4MeOPh_M361_5XLZ_conf_02						transoid	5XLZ	AB	1,0	-72,8	-20,1
34 M362	313	715	500	1070	>10						
245TM_EtNSO2_4MeOPh_M362_6D88_54						transoid	6D88	ABC	1,0		
245TM_EtNSO2_4MeOPh_M362_5XLZ_conf_02						transoid	5XLZ	AB	0,9	-79,0	-21,3
35 M365	500	67	365	415	>10						
245TM_NAcNSO2_4MeOPh_M365_5XKG_90						transoid	5XKG	BC	1,0		
245TM_NAcNSO2_4MeOPh_M365_5XLZ_conf_03						transoid	5XLZ	AB	0,9	-78,2	-20,1
36 M364	>1000	>1000	>1000	-	>10						
245TM_EtOAcNSO2_4MeOPh_M364_5CB4_conf_01						cisoid	5CB4	AB	1,0	-86,7	-20,8
245TM_EtOAcNSO2_4MeOPh_M364_5XAF_42						transoid	5XAF	AB	1,0		
37 M363	833	-	1250	-	>10						
245TM_BnNSO2_4MeOPh_M363_6BR1_14						transoid	6BR1	AB	0,99361702		
245TM_BnNSO2_4MeOPh_M363_5GON_conf_01						transoid	5GON	AB	0,92598817	-91,3968	-23,3645

Series 3	HeLa	MCF-7	HT-29	HT29 Ver	TPI	Conformation	PDB-ID	SITE_OCC	Z-score	PLANTS	E_AD
21 M76	227	350	187	187							
25DM_HNSO2_4MeOPh_M76_5XLZ_conf_02						transoid	5XLZ	AB	-79,9		
25DM_HNSO2_4MeOPh_M76_6BRY_65						transoid	6BRY	AB			-8,0
22 M89	177	153	250	305							
25DM_MeNSO2_4MeOPh_M89_6BRY_4						transoid	6BRY	AB	0,5		
25DM_MeNSO2_4MeOPh_M89_5XLZ_conf_02						transoid	5XLZ	AB	0,5		-22,8
23 M98	45	25	72	30							
25DM4Br_HNSO2_4MeOPh_M98_5GON_conf_03							5GON	AB	0,5		-22,9
25DM4Br_HNSO2_4MeOPh_M98_5XAF_22						transoid	5XAF	BC	0,5		
24 M105	33	19	123	160							
25DM4Br_MeNSO2_4MeOPh_M105_6BS2_conf_01							6BS2	AB	0,7		-22,4
25DM4Br_MeNSO2_4MeOPh_M105_5LYJ_59							5LYJ	AB	0,7		
25 M176	36	86	97	85							
25DM4Br_NAcNSO2_4MeOPh_M176_5XLZ_conf_01						transoid	5XLZ	AB	0,8		-22,0
25DM4Br_NAcNSO2_4MeOPh_M176_5LYJ_89						transoid	5LYJ	AB	0,8		
26 M177	577	700	2100	867							
25DM4Br_EtOAcSO2_4MeOPh_M177_5XAF_20						transoid	5XAF	AB	1,0		
25DM4Br_EtOAcSO2_4MeOPh_M177_5CB4_conf_01						transoid	5CB4	AB	1,0		-22,8
27 M98	377	220	525	170							
25DM4Br_EtOCONSO2_4MeOPh_M98_5XKF_22						transoid	5XKF	AB	1,0		
25DM4Br_EtOAcNSO2_4MeOPh_M98_5GON_conf_02						transoid	5GON	AB	1,0		-23,7
27 M177	377	220	525	170							
25DM4Br_EtOCONSO2_4MeOPh_M179_5XKF_62						transoid	5XKF	AB	1,0		
25DM4Br_EtOCONSO2_4MeOPh_M179_5GON_conf_03						transoid	5GON	AB	0,9		-22,9
28 M178R	495	-	860	-							
25DM4Br_OxirMeNSO2_4MeOPh_M178_5XLZ_conf_01						transoid	5XLZ	AB	1,0		-24,2
25DM4Br_OxirMeNSO2_4MeOPh_M178_6D88_16						transoid	6D88	AB	1,0		
28 M178S											
25DM4Br_OxirMeNSO2_4MeOPh_M178S_6BRY_57						cisoid	6BRY	AB	1,0		
25DM4Br_OxirMeNSO2_4MeOPh_M178S_5XAF_conf_01						cisoid	5XAF	AB	1,0		-23,5
29 M190	>1000	>1000	>1000	>1000							
25DM4Br_HOAcSO2_4MeOPh_M190_6D88_59						transoid	6D88	AB	1,0		
25DM4Br_HOAcSO2_4MeOPh_M190_5XLZ_conf_01						transoid	5XLZ	AB	1,0		-22,9
29 M190an											
25DM4Br_OAcSO2_4MeOPh_M190_5LYJ_40						transoid	5LYJ	AB	1,0		

25DM4Br_OAcSO2_4MeOPh_M190_6BS2_conf_01						cisoid	6BS2	AB	1,0	-24,1	
25DM4Br_OAcSO2_4MeOPh_M190_6BRY_7						cisoid	6BRY	AB	0,9		
25DM4Br_OAcSO2_4MeOPh_M190_5XLZ_conf_02						transoid	5XLZ	AB	0,9	-22,5	

Series 4	**HeLa**	**MCF-7**	**HT-29**	**HT29 Ver**	**TPI**	**Conformation**	**PDB-ID**	**SITE_OCC**	**Z-score**	**PLANTS**	**E_AD**
32 M350	410	580	360	553							
245TM_HNSO2_4MeOPh_M350_5XAF_conf_01						cisoid	5XAF	AB	0,9	-21,0	
245TM_HNSO2_4MeOPh_M350_6BRY_36						transoid	6BRY	AB	0,9		
33 M361	413	99	500	577							
245TM_MeNSO2_4MeOPh_M361_5XKG_6						transoid	5XKG	ABC	1,0		
245TM_MeNSO2_4MeOPh_M361_5XLZ_conf_02						transoid	5XLZ	AB	1,0	-20,1	
34 M362	313	715	500	1070							
245TM_EtNSO2_4MeOPh_M362_6D88_54						transoid	6D88	ABC	1,0		
245TM_EtNSO2_4MeOPh_M362_5XLZ_conf_02						transoid	5XLZ	AB	0,9	-21,3	
35 M365	500	67	365	415							
245TM_NAcNSO2_4MeOPh_M365_5XKG_90						transoid	5XKG	BC	1,0		
245TM_NAcNSO2_4MeOPh_M365_5XLZ_conf_03						transoid	5XLZ	AB	0,9	-20,1	
36 M364	>1000	>1000	>1000	-							
245TM_EtOAcNSO2_4MeOPh_M364_5CB4_conf_01						cisoid	5CB4	AB	1,0	-20,8	
245TM_EtOAcNSO2_4MeOPh_M364_5XAF_42						transoid	5XAF	AB	1,0		
37 M363	833	-	1250	-							
245TM_BnNSO2_4MeOPh_M363_6BR1_14						transoid	6BR1	AB	0,99361702		
245TM_BnNSO2_4MeOPh_M363_5GON_conf_01						transoid	5GON	AB	0,92598817	-23,3645	

artículo 3

New diarylsulfonamide inhibitors of Leishmania infantum amastigotes

Myriam González, Pedro José Alcolea, Raquel Álvarez, Manuel Medarde, Vicente Larraga, Rafael Peláez.

Int. J. Parasitol. Drugs Drug Resist. **2021**, 16, 45-64
DOI: 10.1016/j.ijpddr.2021.02.006

RESUMEN

El objetivo de este estudio consiste en la búsqueda de nuevos fármacos contra la leishmaniasis visceral con un mecanismo de acción diferente y con un coste, una estabilidad y unas propiedades adecuadas que mejoren a los limitados tratamientos actuales. Actualmente, no existen en clínica fármacos de unión a tubulina que actúen sobre parásitos de *Leishmania infantum*, el agente causante de la leishmaniasis visceral en la cuenca mediterránea. En este trabajo, se diseña y sintetiza una biblioteca de 350 *N*-fenilbencenosulfonamidas dirigidas contra la tubulina de *Leishmania* spp. basándonos en la relación estructura-actividad de ligandos conocidos y en las diferencias entre las secuencias de la tubulina del mamífero hospedador y el parásito; comprobando a su vez que los compuestos diseñados sean accesibles, estables y con una solubilidad acuosa aceptable. La batería de sulfonamidas sintetizada se ensaya *in vitro* contra promastigotes, amastigotes axénicos y amastigotes intracelulares de *L. infantum*, de donde se obtienen 0, 8 y 16 compuestos activos, respectivamente. 5 de los compuestos activos frente a amastigotes axénicos presentan una potencia similar o incluso mejor que la miltefosina, fármaco utilizado en el tratamiento de la enfermedad. La tasa de éxito contra amastigotes intracelulares, tras descartar los compuestos citotóxicos, es de más del 10%, con 14 compuestos inactivos frente a las formas axénicas, pero sí frente a las intracelulares, lo que sugiere un mecanismo de acción dependiente del huésped que podría ser ventajoso al hacerlos menos susceptibles al desarrollo de resistencias por parte del parásito. Los compuestos activos estructuralmente relacionados se agrupan en cinco familias químicas, favoreciendo el establecimiento de relaciones estructura-actividad y posibilitando el desarrollo de nuevas series de compuestos mejorados. Los estudios de acoplamiento molecular, respaldados por las relaciones estructura-actividad observadas, fueron consistentes con el mecanismo de acción propuesto de unión al dominio de colchicina en tubulina. La similitud de secuencia entre *L. infantum* y otras especies relevantes de *Leishmania* sugiere una posible extensión para su uso frente a otras especies. Por lo tanto, las nuevas diarilsulfonamidas activas frente a amastigotes del parásito *L. infantum* representan una alternativa farmacológica potencial en el tratamiento de la leishmaniasis, con una combinación favorable de estabilidad, accesibilidad, solubilidad acuosa y coste económico.

International Journal for Parasitology: Drugs and Drug Resistance 16 (2021) 45–64

Contents lists available at ScienceDirect

International Journal for Parasitology: Drugs and Drug Resistance

journal homepage: www.elsevier.com/locate/ijpddr

New diarylsulfonamide inhibitors of *Leishmania infantum* amastigotes

Myriam González [a,b,c], Pedro José Alcolea [d], Raquel Álvarez [a,b,c], Manuel Medarde [a,b,c], Vicente Larraga [d], Rafael Peláez [a,b,c,*]

[a] Laboratorio de Química Orga´nica y Farmac´eutica, Departamento de Ciencias Farmac´euticas, Facultad de Farmacia, Universidad de Salamanca, Salamanca, Spain
[b] Instituto de Investigaci´on Biom´edica de Salamanca (IBSAL), Facultad de Farmacia, Universidad de Salamanca, Salamanca, Spain
[c] Centro de Investigaci´on de Enfermedades Tropicales de la Universidad de Salamanca (CIETUS), Facultad de Farmacia, Universidad de Salamanca, Salamanca, Spain
[d] Laboratorio de Parasitología Molecular, Departamento de Biología Celular y Molecular, Centro de Investigaciones Biolo´gicas Margarita Salas, Consejo Superior de Investigaciones Científicas, Madrid, Spain

ARTICLE INFO

Keywords:
Leishmania
Amastigote
Sulfonamides
Tubulin

ABSTRACT

New drugs against visceral leishmaniasis with mechanisms of action differing from existing treatments and with adequate cost, stability, and properties are urgently needed. No antitubulin drug is currently in the clinic against *Leishmania infantum*, the causative agent of visceral leishmaniasis in the Mediterranean area. We have designed and synthesized a focused library of 350 compounds against the *Leishmania* tubulin based on the structure-activity relationship (SAR) and sequence differences between host and parasite. The compounds synthesized are accessible, stable, and appropriately soluble in water. We assayed the library against *Leishmania* promastigotes, axenic, and intracellular amastigotes and found 0, 8, and 16 active compounds, respectively, with a high success rate against intracellular amastigotes of over 10%, not including the cytotoxic compounds. Five compounds have a similar or better potency than the clinically used miltefosine. 14 compounds showed a host-dependent mechanism of action that might be advantageous as it may render them less susceptible to the development of drug resistance. The active compounds cluster in five chemical classes that provide structure-activity relationships for further hit improvement and facilitate series development. Molecular docking is consistent with the proposed mechanism of action, supported by the observed structure-activity relationships, and suggests a potential extension to other *Leishmania* species due to sequence similarities. A new family of diarylsulfonamides designed against the parasite tubulins is active against *Leishmania infantum* and represents a new class of potential drugs with favorable cost, stability, and aqueous solubility for the treatment of visceral leishmaniasis (VL). These results could be extended to other clinically relevant species of *Leishmania* spp.

1. Introduction

Leishmaniasis is a neglected tropical disease caused by protozoan parasites classified into the genus *Leishmania* (Kinetoplastida: Trypanosomatidae). The incidence is 700,000–2,000,000 cases causing 20,000–30,000 annual deaths (Alvar et al., 2012). The main clinical forms are kala-azar or visceral (VL), cutaneous (CL), and mucocutaneous leishmaniasis (MCL). VL is fatal without treatment. Anthroponotic VL (AVL) is caused by *Leishmania donovani* in Southeastern Asia and Western Africa, whereas *Leishmania infantum* causes zoonotic VL (ZVL) and distributes in the Mediterranean basin and South America. Dogs are the main reservoirs of ZVL, whose incidence is limited in humans in developed countries. Nevertheless, about a decade ago, an outbreak in humans was registered in Spain (Arce et al., 2013; Jim´enez et al., 2014; Molina et al., 2012).

The life cycle of *Leishmania* spp. is digenetic and develops in two stages. The promastigote is a motile fusiform extracellular stage. The amastigote is a round intracellular stage whose flagellum does not emerge from the cellular body. Promastigotes undergo a differentiation process known as metacyclogenesis within the sand fly vector (Diptera: Psychodidae) gut. The vector injects highly infective metacyclic promastigotes in the mammalian host's dermis during blood feeding. Metacyclic promastigotes are internalized by phagocytes and differentiate into amastigotes. Amastigotes multiply within infected cells, affecting different tissues depending on the causative species. When a sand fly feeds on an infected host, amastigotes transform into procyclic

* Corresponding author. Laboratorio de Química Orga´nica y Farmac´eutica, Departamento de Ciencias Farmac´euticas, Facultad de Farmacia, Universidad de Salamanca, Salamanca, Spain.
E-mail address: pelaez@usal.es (R. Pela´ez).

https://doi.org/10.1016/j.ijpddr.2021.02.006
Received 13 October 2020; Received in revised form 22 February 2021; Accepted 22 February 2021
Available online 24 March 2021

promastigotes within the peritrophic membrane and begin differentiation into metacyclic forms as they migrate towards the anterior midgut (Alcolea et al., 2016; Escudero-Martínez et al., 2017).

The number of drugs available against the parasite is limited and they present toxicity, side effects, resistance (Jain and Jain, 2018), long-term treatment, and cost limitations [reviewed in (Nagle et al., 2014; Ponte-Sucre et al., 2017; Rama et al., 2015)]. Their efficacy varies depending on the species, the clinical development these species cause, and the host (Tiuman et al., 2011). Combination therapy of current treatments is being explored and slightlys improves (Zulfiqar et al., 2017). Hence, new drugs are required to control this challenging disease (Zhang et al., 2018). The most used drugs during the last 70 years have been pentavalent antimonials, administered by the intramuscular or the intravenous route. The long-term treatments cause serious side effects, including cardiac arrhythmia and acute pancreatitis (Monzote, 2009; Nagle et al., 2014). Resistance has decreased efficacy over time, which is related to multidrug resistance phenotypes (L´egar´e et al., 2001), mutations in the macrophage aquaporin AQP1 gene, and IL10-mediated up-regulation of the macrophage multiple resistance protein MDR1 (Marquis et al., 2005). Amphotericin B is a polyenic macrolide antibiotic with powerful antifungal and antileishmanial activity. This drug also causes several side effects, and is expensive, poorly soluble in water, not stable in the gastric environment, and poorly membrane permeable. Fungizone®, a micellar suspension of sodium deoxycholate, is administered by the intravenous route and the patients must be hospitalized and monitored (Abu Ammar et al., 2019; Monzote, 2009; Nagle et al., 2014). In the 1990s it replaced pentamidine as second-line therapy for refractory VL cases in India (Nagle et al., 2014). High-cost lipid formulations (AmBisome®) allow lower dosages and side effects, and help in VL control in the Indian subcontinent, but are ineffective against other species in other countries (De Rycker et al., 2018). Resistance has emerged associated with changes in ergosterol biosynthesis and oxidative stress prevention (Mbongo et al., 1998). Miltefosine was approved as a first-line drug in 2002 to replace antimonials in several regions (Nagle et al., 2014; Sundar et al., 2002). It initially showed significant antileishmanial activity, but a gradual increase in resistances related to transporters (Mondelaers et al., 2016; P´erez-Victoria et al, 2003, 2006) and relapses have followed (Rijal et al., 2013; Sundar and Murray, 2005). Paromomycin is efficacious as an ointment against CL but not frequently used due to its side effects, such as ototoxicity (Monzote, 2009; Sundar et al., 2007). Several drug classes, such as the aminopyrazoles, the nitroimidazoles, the oxaboroles, the proteasome inhibitors, and the kinase inhibitors, are currently in development against VL, but oral, safe, effective, low cost, and of short course administration new chemotypes acting on alternative targets are still required (Alves et al., 2018).

The sulfonamides are synthetically accessible, stable, drug-like compounds. They have a long history of clinical success (Drews, 2000). Their antiparasitic and antitumor effects are linked to inhibition of the microtubule dynamics (Dumontet and Jordan, 2010; Vicente-Bl´azquez et al., 2019). None of the current antileishmanial drugs in the clinical practice or clinical trials target tubulin. Diarylsulfonamides bind at the colchicine site of tubulin, inhibiting microtubule dynamics, and eliciting antimitotic activity (Vicente-Bla´zquez et al., 2019). They combine being a privileged scaffold for the generation of pharmacological activities with synthetic accessibility and adequate pharmacokinetic profiles, arising from a favorable combination of chemical stability, hydrogen bonding ability, polarity, hydrophilic-lipophilic balance, adjustable pK_a values, solubility, and conformational preferences (Laurence et al., 2009; Perlovich et al., 2014).

The microtubules of eukaryotic cells are made up of αβ-tubulin dimers, and most drugs affecting microtubule dynamics bind to tubulin dimer, microtubule lattice, or microtubule-associated proteins and motors. Tubulins are highly conserved throughout evolution. However, differences between the mammalian and parasitic orthologs suggest sufficient binding selectivity for drug development. These cytoskeletal supramolecular structures are involved in structural support, cell motility, cell division, organelle transport, maintenance of cell morphology, and signal transduction (Jordan et al., 1998). Specifically, *Leishmania* tubulin is an essential component of the flagellum and the subpellicular microtubules. These structures are related to parasite survival (Sinclair and de Graffenried, 2019; Sunter and Gull, 2017). At least seven drug-binding sites have been identified in tubulin and the microtubules, named after their prototypical drugs: the taxanes, the Vinca minor alkaloids, the maytansine, the peloruside/laulimalide, the eribulin, the pironetin, and the colchicine binding sites (Vicente-Bla´zquez et al., 2019). Different parasitic species show sequence variations compared to their hosts which vary depending on the sites, thus making them more or less susceptible to specific drug classes and representatives, thus allowing for specific treatments (Dost´al and Libusova´, 2014). *Leishmania* parasites are not susceptible to colchicine (Luis et al., 2013), the archetypical ligand of the mammalian eponymous domain. Hence, an opportunity for selective ligand development arises like in the treatment of helminth and fungal parasitosis with antimitotic benzimidazoles binding at the colchicine site, such as triclabendazole or albendazole (Lacey, 1990).

2. Materials and methods

2.1. Chemical synthesis

2.1.1. General chemical techniques

Reagents were used as purchased without further purification. Solvents (EtOAc, DMF, CH_2Cl_2, toluene, MeOH and CH_3CN) were stored over molecular sieves. THF was refluxed with sodium/benzophenone and hexane was dried by distillation and stored over $CaCl_2$. TLC was performed on precoated silica gel polyester plates (0.25 mm thickness) with a UV fluorescence indicator 254 (Polychrom SI F254). Chromatographic separations were performed on silica gel columns by flash (Kieselgel 40, 0.040–0.063; Merck) chromatography. Melting points were determined on a Buchi 510 apparatus and are uncorrected. ^1H NMR and ^{13}C NMR spectra were recorded in $CDCl_3$, CD_3OD, DMSO-D_6 or Acetone-D_6 on a Bruker WP 200-SY spectrometer at 200/50 MHz or a Bruker SY spectrometer at 400/100 MHz. Chemical shifts (δ) are given in ppm downfield from tetramethylsilane and coupling constants (*J* values) are in Hertz. IR spectra were run on a Nicolet Impact 410 Spectrophotometer. A hybrid QSTAR XL quadrupole/time of flight spectrometer was used for HRMS analyses. GC-MS spectra were performed using a Hewlett-Packard 5890 series II mass detector. A Helios-α UV-320 from Thermo-Spectronic was used for UV spectra.

2.1.2. 1,4-Dimethoxy-2-nitrobenzene (**74**)

To a solution of 1,4-dimethoxybenzene (2.35 g, 17 mmol) in acetic acid (30 mL) at 0 °C, nitric acid (1.13 mL, 17 mmol) in acetic acid (20 mL) was added dropwise under nitrogen atmosphere. The reaction mixture was stirred at 0 °C for 4 h and then poured onto ice with 5% $NaHCO_3$ and extracted with ethyl acetate. The organic layers were washed to neutrality with brine, dried over anhydrous Na_2SO_4, filtered and concentrated in vacuum to obtain 2.92 g (94%) of **74**. M.p.: 71.8–72.5 °C (CH_2Cl_2/Hexane). IR (KBr): 1528, 874, 763 cm^{-1}. ^1H NMR (400 MHz, $CDCl_3$): δ 3.82 (3H, *s*), 3.92 (3H, *s*), 7.03 (1H, *d*, $J = 9.6$), 7.12 (1H, *dd*, $J = 9.6$ and 3.2), 7.4 (1H, *d*, $J = 3.2$). ^{13}C NMR (100 MHz, $CDCl_3$): δ 55.9 (CH_3), 56.9 (CH_3), 109.9 (CH), 115.0 (CH), 120.8 (CH), 139.3 (C), 147.3 (C), 152.7 (C). GC-MS ($C_8H_9NO_4$): 183 (M^+).

2.1.3. 2,5-Dimethoxyaniline (**75**)

1,4-dimethoxy-2-nitrobenzene (**74**, 2.92 g, 15.95 mmol) was suspended in ethyl acetate (100 mL) and was palladium-catalyzed (Pd (C) 10 mg) reduced under H_2 atmosphere for 48 h. The reaction mixture was filtered through Celite® and the solvent evaporated in vacuum to isolate 2.42 g (99%) of **75**. Crude reaction product was obtained and used without further purification. IR (KBr): 3459, 1519, 839 cm^{-1}. ^1H NMR

(400 MHz, $CDCl_3$): δ 3.72 (3H, *s*), 3.79 (3H, *s*), 6.24 (1H, *dd*, *J* = 9.2 and 3.2), 6.33 (1H, *d*, *J* = 3.2), 6.69 (1H, *d*, *J* = 9.2). ^{13}C NMR (100 MHz, $CDCl_3$): δ 54.5 (CH_3), 55.1 (CH_3), 100.9 (CH), 101.1 (CH), 110.3 (CH), 136.2 (C), 140.9 (C), 153.3 (C). GC-MS ($C_8H_{11}NO_2$): 153 (M^+).

*2.1.4. N-(2,5-dimethoxyphenyl)-4-methoxybenzenesulfonamide (**76**)*

To a solution of **75** (2.42 g, 15.84 mmol) in CH_2Cl_2 (50 mL) and pyridine (2 mL), was slowly added 4-methoxybenzenesulfonyl chloride (3.27 g, 15.84 mmol). The mixture was stirred at room temperature for 4 h. Then the reaction was treated with 2N HCl and 5% $NaHCO_3$, washed with brine, dried over anhydrous Na_2SO_4 and the solvent evaporated to obtain 4.9 g (95%) of **76**. It was purified by crystallization in CH_2Cl_2/Hexane (4.29 g, 84%). M.p.: 114–115 °C (CH_2Cl_2/Hexane). IR (KBr): 3313, 1578, 830 cm^{-1}. ^{1}H NMR (400 MHz, $CDCl_3$): δ 3.62 (3H, *s*), 3.74 (3H, *s*), 3.81 (3H, *s*), 6.53 (1H, *dd*, *J* = 9.2 and 3.2), 6.65 (1H, *d*, *J* = 9.2), 6.86 (2H, *d*, *J* = 9.2), 7.01 (1H, *s*), 7.14 (1H, *d*, *J* = 3.2), 7.72 (2H, *d*, *J* = 9.2). ^{13}C NMR (100 MHz, $CDCl_3$): δ 55.5 (CH_3), 55.7 (CH_3), 56.2 (CH_3), 106.8 (CH), 109.5 (CH), 111.4 (CH), 113.9 (2CH), 126.8 (C), 129.4 (2CH), 130.7 (C), 143.4 (C), 153.8 (C), 163.0 (C). HRMS ($C_{15}H_{17}NO_5S$ + H^+): calcd 324.0900 (M + H^+), found 324.0900.

*2.1.5. N-(2,5-dimethoxy-4-nitrophenyl)-4-methoxybenzenesulfonamide (**96**)*

To a stirred solution at 0 °C of **76** (2.07 g, 6.42 mmol) in acetic acid (30 mL), nitric acid (0.44 mL, 6.42 mmol) in acetic acid (20 mL) was slowly added under nitrogen atmosphere. After 4 h at 0 °C, the reaction mixture was poured onto ice and basified with 5% $NaHCO_3$ solution. Then it was extracted with ethyl acetate. The organic layers were washed with brine, dried over anhydrous Na_2SO_4, filtered and concentrated in vacuum to obtain 2.14 g (90%) of **96**. By crystallization in CH_2Cl_2/Hexane 1.53 g (65%) of purified product were isolated. M.p.: 161–163 °C (CH_2Cl_2/Hexane). IR (KBr): 3277, 1522, 1450, 822 cm^{-1}. ^{1}H NMR (400 MHz, $CDCl_3$): δ 3.76 (3H, *s*), 3.79 (3H, *s*), 3.88 (3H, *s*), 6.9 (2H, *d*, *J* = 9.2), 7.26 (1H, *s*), 7.39 (1H, *s*), 7.56 (1H, *s*), 7.77 (2H, *d*, *J* = 9.2). ^{13}C NMR (100 MHz, $CDCl_3$): δ 55.7 (CH_3), 56.6 (CH_3), 57.0 (CH_3), 103.2 (CH), 108.3 (CH), 114.4 (2CH), 129.4 (2CH), 129.9 (C), 132.8 (C), 133.1 (C), 141.1 (C), 149.2 (C), 163.6 (C). HRMS ($C_{15}H_{16}N_2O_7S$ + H^+): calcd 369.0751 (M + H^+), found 369.0753.

*2.1.6. N-(4-amino-2,5-dimethoxyphenyl)-4-methoxybenzenesulfonamide (**104**)*

The nitro sulfonamide **96** (1.44 g, 3.91 mmol) in ethyl acetate (100 mL) and Pd (C) (10 mg) was stirred at room temperature under H_2 atmosphere for 48 h. By filtration through Celite® and solvent evaporation, hydrogenated sulfonamide **104** (1.28 g, 97%) was obtained. 1.11 g (84%) of **104** were isolated by crystallization in CH_2Cl_2/Hexane. M.p.: 164–166 °C (CH_2Cl_2/Hexane). IR (KBr): 3430, 3291, 1451, 834 cm^{-1}. ^{1}H NMR (400 MHz, $CDCl_3$): δ 3.38 (3H, *s*), 3.79 (3H, *s*), 3.82 (3H, *s*), 6.15 (1H, *s*), 6.54 (1H, *s*), 6.82 (2H, *d*, *J* = 9.2), 7.04 (1H, *s*), 7.58 (2H, *d*, *J* = 9.2). ^{13}C NMR (100 MHz, $CDCl_3$): δ 55.5 (CH_3), 55.9 (CH_3), 56.2 (CH_3), 99.2 (CH), 108.4 (CH), 113.5 (2CH), 115.3 (C), 129.4 (2CH), 130.7 (C), 134.6 (C), 141.0 (C), 145.8 (C), 162.7 (C). HRMS ($C_{15}H_{18}N_2O_5S$ + H^+): calcd 339.1009 (M + H^+), found 339.1012.

*2.1.7. 2-Chloro-N-(2,5-dimethoxy-4-((4-methoxyphenyl)sulfonamido) phenyl)acetamide (**129**)*

To a solution of amine **104** (160 mg, 0.47 mmol) in CH_2Cl_2 (25 mL) 2-chloroacetyl chloride (46.4 μL, 0.57 mmol) was added dropwise under nitrogen atmosphere. After 12 h at room temperature the reaction was washed with water, dried over anhydrous Na_2SO_4 and the solvent evaporated in vacuum to give 171 mg (87%) of **129.** The crude reaction product was purified by crystallization in methanol (55 mg, 28%). M.p.: 175–177 °C (MeOH). IR (KBr): 3372, 3265, 1677, 1598, 829 cm^{-1}. ^{1}H NMR (400 MHz, CD_3OD): δ 3.47 (3H, *s*), 3.81 (3H, *s*), 3.86 (3H, *s*), 4.25 (2H, *s*), 6.94 (2H, *d*, *J* = 8.8), 7.14 (1H, *s*), 7.62 (2H, *d*, *J* = 8.8), 7.74 (1H, *s*). ^{13}C NMR (100 MHz, Acetone-D_6): δ 43.2 (CH_2), 55.1 (CH_3), 55.8 (CH_3), 56.0 (CH_3), 104.1 (CH), 106.9 (CH), 113.8 (2CH), 124.8 (C), 129.3 (2CH), 131.4 (C), 138.1 (C), 142.4 (C), 144.9 (C), 163.0 (C), 164.1 (C). HRMS ($C_{17}H_{19}ClN_2O_6S$ + H^+): calcd 415.0725 (M + H^+), found 415.0700.

*2.1.8. 3-Chloro-N-(2,5-dimethoxy-4-((4-methoxyphenyl)sulfonamido) phenyl)propanamide (**138**)*

To a stirred solution at room temperature of **104** (143 mg, 0.42 mmol) in CH_2Cl_2 (30 mL) 3-chloropropanoyl chloride (49.4 μL, 0.51 mmol) was slowly added under nitrogen atmosphere. After 12 h, the reaction mixture was crystallized in CH_2Cl_2 to obtain 88 mg (48%) of **138**. M.p.: 193–197 °C (CH_2Cl_2). ^{1}H NMR (400 MHz, CD_3OD): δ 2.89 (2H, *t*, *J* = 6.4), 3.47 (3H, *s*), 3.81 (3H, *s*), 3.83 (3H, *s*), 3.83 (2H, *t*, *J* = 6.4), 6.95 (2H, *d*, *J* = 9.2), 7.12 (1H, *s*), 7.63 (2H, *d*, *J* = 9.2), 7.68 (1H, *s*). ^{13}C NMR (100 MHz, Acetone-D_6): δ 39.6 (CH_2), 40.1 (CH_2), 55.1 (CH_3), 55.7 (CH_3), 55.9 (CH_3), 104.4 (CH), 107.1 (CH), 113.7 (2CH), 120.9 (C), 125.7 (C), 129.3 (2CH), 131.7 (C), 142.2 (C), 144.9 (C), 162.9 (C), 167.8 (C). HRMS ($C_{18}H_{21}ClN_2O_6S$ + H^+): calcd 429.0882 (M + H^+), found 429.0879.

*2.1.9. 4-Methoxy-3-nitrobenzonitrile (**250**)*

To a solution of 4-methoxy-3-nitrobenzaldehyde (870 mg, 4.80 mmol) in MeOH (30 mL) hydroxylamine hydrochloride (334 mg, 4.80 mmol) and two drops of pyridine were added. After 24 h at reflux, the solvent was evaporated, the obtained residue was dissolved in CH_2Cl_2 and washed with water, dried over anhydrous Na_2SO_4, evaporated under vacuum, and dissolved in 15 mL of pyridine. Finally, acetic anhydride (1 mL) was added to the mixture. After 9 h at room temperature, the reaction was treated with 2N HCl, extracted with CH_2Cl_2 and the solvent evaporated to obtain 685 mg (80%) of **250**. Crude reaction product was obtained and used without further purification. ^{1}H NMR (400 MHz, $CDCl_3$): δ 4.05 (3H, *s*), 7.20 (1H, *d*, *J* = 8.8), 7.83 (1H, *dd*, *J* = 8.8 and 2), 8.15 (1H, *d*, *J* = 2). GC-MS ($C_8H_6N_2O_3$): 178 (M^+).

*2.1.10. 3-Amino-4-methoxybenzonitrile (**258**)*

To a solution of **250** (685 mg, 3.84 mmol) in ethyl acetate (100 mL) Pd (C) (10 mg) was added and the reaction was stirred at room temperature under H_2 atmosphere for 48 h. By filtration through Celite® and solvent evaporation, 529 mg (93%) of crude reaction **258** was obtained and used without further purification.^{1}H NMR (400 MHz, $CDCl_3$): δ 3.83 (3H, *s*), 6.71 (1H, *d*, *J* = 8), 6.84 (1H, *d*, *J* = 2), 6.87 (1H, *s*), 6.98 (1H, *dd*, *J* = 8 and 2). GC-MS ($C_8H_8N_2O$): 148 (M^+).

*2.1.11. N-(5-cyano-2-methoxyphenyl)-4-methoxybenzenesulfonamide (**276A**) and 4-cyano-2-((4-methoxyphenyl)sulfonamido)phenyl 4-methoxybenzenesulfonate (**276B**)*

To a solution of **258** (529 mg, 3.57 mmol) in CH_2Cl_2 (50 mL) and pyridine (2 mL) 4-methoxybenzenesulfonyl chloride (1.106 g, 5.35 mmol) was slowly added. The mixture was stirred at room temperature for 4 h. Then the reaction was treated with 2N HCl and 5% $NaHCO_3$, washed with brine, dried over anhydrous Na_2SO_4 and the solvent evaporated in vacuum to give a residue that was purified by silica gel chromatography using hexane/EtOAc (7:3) to yield the sulfonamides **276A** (466 mg, 41%) and **276B** (205 mg, 30%). **276A:** ^{1}H NMR (400 MHz, $CDCl_3$): δ 3.80 (3H, *s*), 3.83 (3H, *s*), 6.80 (1H, *d*, *J* = 8), 6.91 (2H, *d*, *J* = 9.2), 7.09 (1H, *s*), 7.33 (1H, *dd*, *J* = 8 and 2), 7.75 (2H, *d*, *J* = 9.2), 7.76 (1H, *d*, *J* = 2). ^{13}C NMR (100 MHz, $CDCl_3$): δ 55.6 (CH_3), 56.1 (CH_3), 104.5 (C), 110.9 (CH), 114.2 (2CH), 118.6 (C), 122.6 (CH), 127.2 (C), 129.4 (2CH), 129.5 (CH), 130.1 (C), 152.1 (C), 163.4 (C). HRMS ($C_{15}H_{14}N_2O_4S$ + Na^+): calcd 341.0569 (M + Na^+), found 341.0566. **276B:** IR (KBr): 2233, 1462, 833, 749 cm^{-1}. ^{1}H NMR (400 MHz, $CDCl_3$): δ 3.83 (3H, *s*), 3.91 (3H, *s*), 6.91 (2H, *d*, *J* = 9.2), 7.01 (2H, *d*, *J* = 8.8), 7.03 (1H, *d*, *J* = 8), 7.15 (1H, *s*), 7.25 (1H, *dd*, *J* = 8 and 2), 7.73 (2H, *d*, *J* = 9.2), 7.75 (2H, *d*, *J* = 8.8), 7.78 (1H, *d*, *J* = 2). ^{13}C NMR (100 MHz, $CDCl_3$): δ 55.6 (CH_3), 55.9 (CH_3), 111.5 (C), 114.5 (2CH), 115.0 (2CH), 117.4 (C), 123.7 (CH), 124.4 (CH), 124.8 (C), 128.4 (CH), 129.4 (2CH),

129.8 (C), 130.8 (2CH), 131.5 (C), 142.4 (C), 163.6 (C), 165.1 (C). HRMS ($C_{21}H_{18}N_2O_7S_2$ + Na^+): calcd 497.0448 (M + Na^+), found 497.0409.

*2.1.12. 4-Methoxy-3-nitrobenzenesulfonyl chloride (**86**)*

To a stirred solution at 0 °C of 4-methoxybenzenesulfonyl chloride (4.41 g, 21.36 mmol) in CH_2Cl_2 (20 mL) and H_2SO_4 (5 mL) nitric acid (0.95 mL, 21.36 mmol) was dropwise added under nitrogen atmosphere. After 4 h, the reaction was poured onto ice and the mixture was kept at 4 °C for 30 min. Then, the precipitate was filtered under vacuum to dryness to obtain 4.97 g (92%) of **86**. ^{1}H NMR (400 MHz, $CDCl_3$): δ 4.11 (3H, *s*), 7.33 (1H, *d, J* = 8.8), 8.20 (1H, *dd, J* = 8.8 and 2.4), 8.48 (1H, *d, J* = 2.4). ^{13}C NMR (100 MHz, $CDCl_3$): δ 57.0 (CH_3), 114.0 (CH), 124.8 (CH), 127.1 (C), 132.2 (CH), 135.0 (C), 157.1 (C). GC-MS ($C_7H_6ClNO_5S$): 251 (M^+).

*2.1.13. N-(2,5-dimethoxyphenyl)-4-methoxy-3-nitrobenzenesulfonamide (**183**)*

To 650 mg of the amine **75** (4.24 mmol) in CH_2Cl_2 (50 mL) and pyridine (2 mL), 1.07 g (4.24 mmol) of the sulfonyl chloride **86** was slowly added and stirred at room temperature for 6 h. The reaction was treated with 2N HCl and 5% $NaHCO_3$, washed with brine, dried over anhydrous Na_2SO_4 and the solvent evaporated to obtain 4.9 g (95%) of **76**. The residue was crystallized in CH_2Cl_2/Hexane to afford the purified compound (4.29 g, 84%). M.p.: 121–123 °C (CH_2Cl_2/Hexane). ^{1}H NMR (400 MHz, $CDCl_3$): δ 3.61 (3H, *s*), 3.72 (3H, *s*), 3.96 (3H, *s*), 6.56 (1H, *dd, J* = 8.8 and 3.2), 6.65 (1H, *d, J* = 8.8), 7.07 (1H, *d, J* = 8.8), 7.09 (1H, *d, J* = 3.2), 7.16 (1H, *s*), 7.88 (1H, *dd, J* = 8.8 and 2.4), 8.22 (1H, *d, J* = 2.4). ^{13}C NMR (100 MHz, $CDCl_3$): δ 55.7 (CH_3), 56.0 (CH_3), 57.0 (CH_3), 108.1 (CH), 110.5 (CH), 111.4 (CH), 113.6 (CH), 125.2 (CH), 125.5 (C), 130.9 (C), 133.1 (CH), 138.8 (C), 143.9 (C), 153.8 (C), 155.8 (C). HRMS ($C_{15}H_{16}N_2O_7S$ + Na^+): calcd 391.0563 (M + Na^+), found 391.0570.

*2.1.14. N-(4-bromo-2,5-dimethoxyphenyl)-4-methoxy-N-methyl-3-nitrobenzenesulfonamide (**204**)*

To a stirred solution of **183** (86 mg, 0.23 mmol) in CH_2Cl_2 (25 mL) *N*-bromosuccinimide (41 mg, 0.23 mmol) was added. After 2 h the solvent was evaporated in vacuum and the residue was re-dissolved in CH_3CN. 25 mg of crushed KOH (0.36 mmol) and 17 μL of methyl iodide (0.27 mmol) were added to the reaction mixture and it was stirred at room temperature for 24 h. Finally, it was concentrated, re-dissolved in CH_2Cl_2, washed with brine, dried over anhydrous Na_2SO_4, filtered and concentrated in vacuum. The residue was purified by silica gel chromatography using toluene/EtOAc (8:2) to afford 87 mg (80%) of **204**. ^{1}H NMR (400 MHz, $CDCl_3$): δ 3.18 (3H, *s*), 3.43 (3H, *s*), 3.88 (3H, *s*) 4.01 (3H, *s*), 6.96 (1H, *s*), 6.99 (1H, *d, J* = 9.2), 7.01 (1H, *s*), 7.68 (1H, *dd, J* = 9.2 and 2.4), 7.72 (1H, *d, J* = 2.4). ^{13}C NMR (100 MHz, $CDCl_3$): δ 37.7 (CH_3), 55.5 (CH_3), 56.6 (CH_3), 56.9 (CH_3), 111.0 (CH), 112.0 (C), 116.1 (CH), 116.6 (CH), 127.2 (CH), 127.9 (C), 130.2 (CH), 131.6 (C), 139.0 (C), 149.9 (C), 150.0 (C), 157.6 (C). HRMS ($C_{16}H_{17}BrN_2O_7S$ + H^+): calcd 462.9877 (M + H^+), found 462.9992.

*2.1.15. N-(2,5-dimethoxyphenyl)-4-nitrobenzenesulfonamide (**130**)*

To a solution of **75** (1.06 g, 6.89 mmol) in CH_2Cl_2 (50 mL) and pyridine (2 mL) was slowly added 4-nitrobenzenesulfonyl chloride (1.53 g, 6.89 mmol). The mixture was stirred at room temperature for 4 h. Then the reaction was treated with 2N HCl and 5% $NaHCO_3$, washed with brine, dried over anhydrous Na_2SO_4 and the solvent evaporated to obtain 2.09 g (90%) of the sulfonamide **130**. The crude reaction product was purified by crystallization in CH_2Cl_2/Hexane (1.274 g, 55%). M.p.: 164–168 °C (CH_2Cl_2/Hexane). ^{1}H NMR (400 MHz, $CDCl_3$): δ 3.57 (3H, *s*), 3.74 (3H, *s*), 6.58 (1H, *dd, J* = 9.2 and 2.8), 6.65 (1H, *d, J* = 9.2), 7.15 (1H, *d, J* = 2.8), 7.93 (2H, *d, J* = 9.2), 8.22 (2H, *d, J* = 9.2). ^{13}C NMR (100 MHz, $CDCl_3$): δ 55.8 (CH_3), 56.0 (CH_3), 108.3 (CH), 110.6 (CH), 111.5 (CH), 123.9 (2CH), 125.3 (C), 128.5 (2CH), 143.8 (C), 144.7 (C), 150.1 (C), 153.8 (C). HRMS ($C_{14}H_{14}N_2O_6S$ + Na^+): calcd 361.0465 (M + Na^+), found 361.0463.

*2.1.16. N-(4-bromo-2,5-dimethoxyphenyl)-4-nitrobenzenesulfonamide (**296**)*

To a stirred solution of **130** (1.95 g, 5.76 mmol) in CH_2Cl_2 (100 mL) *N*-bromosuccinimide (1.23 g, 6.92 mmol) was added. After 4 h at room temperature the reaction was washed with water, dried over anhydrous Na_2SO_4 and the solvent evaporated in vacuum to give 2.35 g (98%) of **296.** The crude reaction product was purified by crystallization in methanol (1.26 g, 52%). M.p.: 190–196 °C (MeOH). ^{1}H NMR (400 MHz, $CDCl_3$): δ 3.57 (3H, *s*), 3.88 (3H, *s*), 6.94 (1H, *s*), 6.97 (1H, *s*), 7.24 (1H, *s*), 7.90 (2H, *d, J* = 8.8), 8.27 (2H, *d, J* = 8.8). ^{13}C NMR (100 MHz, $CDCl_3$): δ 56.8 (CH_3), 57.5 (CH_3), 107.6 (CH), 108.7 (C), 116.6 (CH), 124.6 (2CH), 124.8 (C), 129.0 (2CH), 144.7 (C), 145.1 (C), 150.8 (C), 151.0 (C). HRMS ($C_{14}H_{13}BrN_2O_6S$ + Na^+): calcd 438.9580 and 440.9561 (M + Na^+), found 438.9570 and 440.9549.

*2.1.17. 4-Amino-N-(4-bromo-2,5-dimethoxyphenyl)benzenesulfonamide (**302**)*

To an EtOH/HOAc/H_2O mixture (2:2:1, 12.5 mL) HCl (c) (1 drop), **296** (2.35 g, 5.63 mmol) and Fe (3.15 g, 56.3 mmol) were added and the reaction stirred for 2 h at 100 °C. After extraction with CH_2Cl_2, filtration through Celite® and treatment with 5% $NaHCO_3$, the crude reaction mixture was purified by silica gel chromatography using hexane/EtOAc (7:3) to yield 1.02 g (47%) of **302.** IR (KBr): 3368, 1498, 822 cm^{-1}. ^{1}H NMR (400 MHz, CD_3OD): δ 3.55 (3H, *s*), 3.77 (3H, *s*), 6.57 (2H, *d, J* = 8.8), 7.00 (1H, *s*), 7.11 (1H, *s*), 7.39 (2H, *d, J* = 8.8). ^{13}C NMR (100 MHz, Acetone-d_6): δ 56.2 (CH_3), 56.3 (CH_3), 105.0 (C), 105.9 (CH), 112.9 (2CH), 116.3 (CH), 125.6 (C), 127.4 (C), 129.3 (2CH), 144.5 (C), 150.1 (C), 152.9 (C). HRMS ($C_{14}H_{15}BrN_2O_4S$ + Na^+): calcd 408.9828 and 410.9808 (M + Na^+), found 408.9825 and 410.9793.

*2.1.18. N-(4-(N-(4-bromo-2,5-dimethoxyphenyl)sulfamoyl)phenyl) formamide (**315**)*

690 mg of **302** (1.78 mmol) were dissolved in CH_2Cl_2 (70 mL), pyridine (5 mL) and formic acid (10 mL) and stirred at room temperature. After 24 h, the reaction mixture was poured onto ice and treated with 2N HCl and 5% $NaHCO_3$. The organic layers were washed to neutrality with brine, dried over anhydrous Na_2SO_4, filtered and evaporated to dryness to afford 708 mg (95%) of **315**. The crude reaction product was purified by crystallization in methanol (307 mg, 41%). M.p.: 202–207 °C (MeOH). IR (KBr): 3337, 1702, 1593, 831 cm^{-1}. ^{1}H NMR (400 MHz, CD_3OD): δ 3.49 (3H, *s*), 3.81 (3H, *s*), 7.01 (1H, *s*), 7.15 (1H, *s*), 7.67 (4H, *bs*), 8.30 (1H, *s*). ^{13}C NMR (100 MHz, DMSO-d_6): δ 56.9 (CH_3), 57.0 (CH_3), 107.1 (C), 109.8 (CH), 117.1 (CH), 119.1 (2CH), 126.2 (C), 128.6 (2CH), 134.8 (C), 142.8 (C), 146.9 (C), 149.6 (C), 160.6 (CH). HRMS ($C_{15}H_{14}BrN_2O_5S$ + Na^+): calcd 436.9777 and 438.9757 (M + Na^+), found 436.9772 and 438.9750.

*2.1.19. N-(4-bromo-2,5-dimethoxyphenyl)-4-(methylamino) benzenesulfonamide (**323**)*

To a solution of the formamide **315** (680 mg, 1.64 mmol) and $NaBH_4$ (93 mg, 2.45 mmol) in dry THF (15 mL) at 0 °C, trichloroacetic acid (401 mg, 2.45 mmol) in dry THF (10 mL) was added dropwise under nitrogen atmosphere. The reaction mixture was stirred at 0 °C to room temperature for 24 h and then concentrated and re-dissolved in EtOAc, washed with brine, dried over anhydrous Na_2SO_4, filtered and solvent evaporated in vacuum. The residue was purified by silica gel chromatography using hexane/EtOAc (8:2) to yield 246 mg (37%) of **323**. IR (KBr): 3420, 3251, 1599, 820 cm^{-1}. ^{1}H NMR (400 MHz, CD_3OD): δ 2.76 (3H, *s*), 3.56 (3H, *s*), 3,78 (3H, *s*), 6.51 (2H, *d, J* = 8.8), 7.00 (1H, *s*), 7.13 (1H, *s*), 7,45 (2H, *d, J* = 8.8). ^{13}C NMR (100 MHz, $CDCl_3$): δ 30.0 (CH_3), 56.5 (CH_3), 56.8 (CH_3), 105.3 (CH), 105.5 (C), 111.1 (2CH), 115.8 (CH), 125.0 (C), 126.6 (C), 129.3 (2CH), 143.5 (C), 150.2 (C), 152.7 (C). HRMS ($C_{15}H_{16}BrN_2O_4S$ + Na^+): calcd 422.9985 and 424.9964 (M + Na^+), found 422.9985 and 424.9959.

*2.1.20. N-benzyl-N-(4-bromo-2,5-dimethoxyphenyl)-4-(methylamino) benzenesulfonamide (**332**)*

35 mg (0.25 mmol) of K_2CO_3 were added to a stirred solution of **323** (50 mg, 0.12 mmol) in 3 mL of dry DMF. After 1 h at room temperature 21.7 μL (0.19 mmol) of benzyl chloride were added and stirred for 24 h. The reaction mixture was concentrated, re-dissolved in CH_2Cl_2, washed with brine, dried over anhydrous Na_2SO_4, filtered and concentrated in vacuum to obtain 59 mg (96%) and crystallized in MeOH (23 mg, 38%). M.p.: 177–183 °C (MeOH). ^{1}H NMR (400 MHz, $CDCl_3$): δ 2.79 (3H, *s*), 3.33 (3H, *s*), 3.57 (3H, *s*), 4.64 (2H, *s*), 6.46 (2H, *d, J* = 8.8), 6.52 (1H, *s*), 6.85 (1H, *s*), 7.14 (5H, *m*), 7.44 (2H, *d, J* = 8.8). ^{13}C NMR (100 MHz, $CDCl_3$): δ 30.1 (CH_3), 53.3 (CH_2), 55.7 (CH_3), 56.7 (CH_3), 110.8 (2CH), 111.5 (C), 116.5 (CH), 117.5 (CH), 126.5 (C), 126.9 (C), 127.4 (CH), 128.2 (2CH), 128.7 (2CH), 129.7 (2CH), 136.7 (C), 149.4 (C), 151.0 (C), 152.4 (C). HRMS ($C_{22}H_{23}BrN_2O_4S$ + Na^+): calcd 515.0415 (M + Na^+), found 515.0434.

*2.1.21. 3,4,5-Trimethoxy-2-((4-methoxyphenyl)sulfonamido)benzoic acid (63A) and 3,4,5-trimethoxy-2-(3,4,5-trimethoxy-2-((4-methoxyphenyl) sulfonamido)benzamido)benzoic acid (**63B**)*

To a stirred solution of 2-amino-3,4,5-trimethoxybenzoic acid (300 mg, 1.32 mmol) in CH_2Cl_2 (50 mL) and pyridine (2 mL) 4-methoxybenzenesulfonyl chloride (273 g, 1.32 mmol) was slowly added. After 6 h, the reaction mixture was poured onto a 2N HCl solution and extracted with CH_2Cl_2. The organic layers were washed to neutrality with saturated NaCl, dried over anhydrous Na_2SO_4, filtered and evaporated to dryness. The residue was purified by two successive crystallizations in CH_2Cl_2/hexane, compounds **63A** (40 mg, 8%) and **63B** (17 mg, 4%) were isolated. **63A:** M.p.: 165–167 °C (CH_2Cl_2/Hexane). IR (KBr): 3264, 2939, 1668, 1458, 837 cm^{-1}. ^{1}H NMR (400 MHz, $CDCl_3$): δ 3.45 (3H, *s*), 3.84 (3H, *s*), 3.88 (3H, *s*), 3.91 (3H, *s*), 6.93 (2H, *d, J* = 8.8), 7.28 (1H, *s*), 7.77 (2H, *d, J* = 8.8), 8.7 (1H, *s*). ^{13}C NMR (100 MHz, $CDCl_3$): δ 55.6 (CH_3), 56.1 (CH_3), 60.3 (CH_3), 61.1 (CH_3), 109.0 (CH), 113.7 (2CH), 116.5 (C), 128.0 (C), 129.4 (2CH), 132.0 (C), 147.7 (C), 148.4 (C), 150.5 (C), 162.8 (C), 171.4 (C). HRMS ($C_{17}H_{19}NO_8S$ + H^+): calcd 398.0901 (M + H^+), found 398.0905. **63B:** M.p.: 170–171 °C (CH_2Cl_2/Hexane). ^{1}H NMR (400 MHz, $CDCl_3$): δ 3.35 (3H, *s*), 3.75 (3H, *s*), 3.79 (3H, *s*), 3.84 (3H, *s*), 3.88 (3H, *s*), 3.96 (3H, *s*), 3.99 (3H, *s*), 6.85 (2H, *d, J* = 8.8), 7.20 (1H, *s*), 7.25 (1H, *s*), 7.68 (2H, *d, J* = 8.8), 8.15 (1H, *s*), 9.22 (1H, *s*). ^{13}C NMR (100 MHz, $CDCl_3$): δ 57.1 (CH_3), 59.0 ($2CH_3$), 61.9 (CH_3), 62.4 (CH_3), 62.6 (CH_3), 63.0 (CH_3), 108.9 (CH), 110.2 (CH), 115.2 (2CH), 120.9 (C), 124.1 (C), 126.6 (C), 127.4 (C), 131.3 (2CH), 133.2 (C), 147.0 (C), 148.3 (C), 149.7 (C), 149.9 (C), 152.9 (C), 153.4 (C), 153.9 (C), 165.3 (C), 167.5 (C). HRMS ($C_{27}H_{30}N_2O_{12}S$ + H^+): calcd 607.1599 (M + H^+), found 607.1593.

*2.1.22. N-(3,5-dimethoxyphenyl)-4-methoxybenzenesulfonamide (**259**)*

To a solution of 3,5-dimethoxyaniline (290 mg, 1.89 mmol) in CH_2Cl_2 (50 mL) and pyridine (2 mL), was slowly added 4-methoxybenzenesulfonyl chloride (469 mg, 2.27 mmol). The mixture was stirred at room temperature for 4 h. Then the reaction was treated with 2N HCl and 5% $NaHCO_3$, washed with brine, dried over anhydrous Na_2SO_4 and the solvent evaporated to obtain 596 mg (97%) of the sulfonamide **259**. The crude reaction product was purified by crystallization in CH_2Cl_2/Hexane (438 mg, 71%). M.p.: 115–122 °C (CH_2Cl_2/Hexane). IR (KBr): 3234, 1595, 824 cm^{-1}. ^{1}H NMR (400 MHz, $CDCl_3$): δ 3.66 (6H, *s*), 3.77 (3H, *s*), 6.13 (1H, *t, J* = 2), 6.17 (2H, *d, J* = 2), 6.85 (2H, *d, J* = 8.8), 7.68 (2H, *d, J* = 8.8). ^{13}C NMR (100 MHz, $CDCl_3$): δ 55.3 ($2CH_3$), 55.5 (CH_3), 97.0 (CH), 98.9 (2CH), 114.2 (2CH), 129.5 (2CH), 130.4 (C), 138.6 (C), 161.1 (2C), 163.1 (C). HRMS ($C_{15}H_{17}NO_5S$ + H^+): calcd 324.0909 (M + H^+), found 324.0900.

*2.1.23. N-benzyl-N-(3,5-dimethoxyphenyl)-4-methoxybenzenesulfonamide (**270**)*

To a stirred solution of **259** (90 mg, 0.28 mmol) in dry DMF (3 mL) 78 mg (0.56 mmol) of K_2CO_3 was added. After 1 h at room temperature, 48.5 μL (0.42 mmol) of benzyl chloride was added and stirred for 24 h. The reaction mixture was concentrated, re-dissolved in CH_2Cl_2, washed with brine, dried over anhydrous Na_2SO_4, filtered and concentrated under vacuum to produce 104 mg (90%) of crude reaction product from which 81 mg (70%) of **270** were purified by crystallization. M.p.: 146–150 °C (MeOH). IR (KBr): 3467, 1458, 806 cm^{-1}. ^{1}H NMR (400 MHz, $CDCl_3$): δ 3.62 (6H, *s*), 3.87 (3H, *s*), 4.65 (2H, *s*), 6.12 (2H, *d, J* = 2), 6.28 (1H, *t, J* = 2), 6.94 (2H, *d, J* = 8.8), 7.22 (5H, *m*), 7.63 (2H, *d, J* = 8.8). ^{13}C NMR (100 MHz, $CDCl_3$): δ 54.7 (CH_2), 55.3 ($2CH_3$), 55.6 (CH_3), 100.0 (CH), 107.2 (2CH), 113.9 (2CH), 127.5 (CH), 128.3 (2CH), 128.5 (2CH), 129.8 (2CH), 130.3 (C), 136.1 (C), 140.9 (C), 160.4 (2C), 162.9 (C). HRMS ($C_{22}H_{23}NO_5S$ + H^+): calcd 414.1370 (M + H^+), found 414.1369.

*2.1.24. N-benzyl-N-(4-bromo-3,5-dimethoxyphenyl)-4-methoxybenzenesulfonamide (**326A**), N-benzyl-N-(2-bromo-3,5-dimethoxyphenyl)-4-methoxybenzenesulfonamide (**326B**) and N-benzyl-N-(2,4-dibromo-3,5-dimethoxyphenyl)-4-methoxybenzenesulfonamide (**326C**)*

To a solution of **270** (195 mg, 0.47 mmol) in CH_2Cl_2 (40 mL) *N*-bromosuccinimide (168 mg, 0.94 mmol) was added and stirred for 48 h at room temperature. After that, the reaction was washed with water, dried over anhydrous Na_2SO_4 and the solvent evaporated in vacuum to produce 183 mg. The residue was flash chromatographed on silica gel (hexane/EtOAc 8:2) to afford the purified compounds: **326A** (116 mg, 50%), **326B** (24 mg, 10%) and **326C** (6 mg, 2%). **326A:** M.p.: 199–203 °C (MeOH). IR (KBr): 3435, 1589, 836 cm^{-1}. ^{1}H NMR (200 MHz, $CDCl_3$): δ 3.65 (6H, *s*), 3.88 (3H, *s*), 4.68 (2H, *s*), 6.12 (2H, *s*), 6.97 (2H, *d, J* = 9), 7.22 (5H, *bs*), 7.65 (2H, *d, J* = 9). ^{13}C NMR (100 MHz, $CDCl_3$): δ 54.9 (CH_2), 55.7 (CH_3), 56.4 ($2CH_3$), 100.5 (C), 105.8 (2CH), 114.0 (2CH), 127.8 (CH), 128.4 (2CH), 128.6 (2CH), 129.9 (C), 130.0 (2CH), 135.7 (C), 139.4 (C), 156.7 (2C), 163.1 (C). HRMS ($C_{22}H_{22}BrNO_5S$ + H^+): calcd 492.0475 and 494.0454 (M + H^+), found 492.0473 and 494.0440. **326B:** IR (KBr): 2938, 1593, 831 cm^{-1}. ^{1}H NMR (200 MHz, $CDCl_3$): δ 3.57 (3H, *s*), 3.80 (3H, *s*), 3.87 (3H, *s*), 4.60 (1H, *d, J* = 14.4), 4.89 (1H, *d, J* = 14.4), 6.14 (1H, *d, J* = 2.8), 6.38 (1H, *d, J* = 2.8), 6.94 (2H, *d, J* = 9), 7.20 (5H, *bs*), 7.74 (2H, *d, J* = 9). ^{13}C NMR (100 MHz, $CDCl_3$): δ 54.4 (CH_2), 55.5 (CH_3), 55.6 (CH_3), 56.3 (CH_3), 100.0 (CH), 105.9 (C), 109.4 (CH), 113.9 (2CH), 127.7 (CH), 128.2 (2CH), 129.4 (2CH), 130.1 (2CH), 131.8 (C), 135.7 (C), 138.8 (C), 157.2 (C), 158.9 (C), 163.0 (C). HRMS ($C_{22}H_{22}BrNO_5S$ + H^+): calcd 492.0475 and 494.0454 (M + H^+), found 492.0467 and 494.0447. **326C:** IR (KBr): 2935, 1595, 835 cm^{-1}. ^{1}H NMR (200 MHz, $CDCl_3$): δ 3.60 (3H, *s*), 3.77 (3H, *s*), 3.87 (3H, *s*), 4.55 (1H, *d, J* = 14.4), 4.97 (1H, *d, J* = 14.4), 6.30 (1H, *s*), 6.95 (2H, *d, J* = 9), 7.22 (5H, *m*), 7.73 (2H, *d, J* = 9). ^{13}C NMR (100 MHz, $CDCl_3$): δ 54.2 (CH_2), 55.6 (CH_3), 56.5 (CH_3), 60.5 (CH_3), 108.8 (C), 112.4 (C), 112.8 (CH), 114.0 (2CH), 128.0 (CH), 128.3 (2CH), 129.4 (2CH), 130.0 (2CH), 131.5 (C), 135.4 (C), 137.4 (C), 155.6 (C), 155.7 (C), 163.2 (C). HRMS ($C_{22}H_{21}Br_2NO_5S$ + H): calcd 569.9580 and 571.9559 (M^+ + H), found 569.9577 and 571.9558.

*2.1.25. N-(3,5-dimethoxyphenyl)-4-nitrobenzenesulfonamide (**242**)*

To a solution of 3,5-dimethoxyaniline (1.39 g, 9.98 mmol) in CH_2Cl_2 (50 mL) and pyridine (2 mL), was slowly added 4-nitrobenzenesulfonyl chloride (2.21 g, 9.07 mmol) and stirred at room temperature for 12 h. Then the reaction mixture was treated with 2N HCl and 5% $NaHCO_3$. The organic layers were washed to neutrality with brine, dried over anhydrous Na_2SO_4 and concentrated under vacuum to yield 2.66 g (87%) of the sulfonamide **242**. The crude reaction product was purified by crystallization in CH_2Cl_2/Hexane (2.43 g, 79%). M.p.: 131–139 °C (CH_2Cl_2/Hexane). ^{1}H NMR (400 MHz, $CDCl_3$): δ 3.71 (6H, *s*), 6.22 (1H, *t, J* = 2.4), 6.25 (2H, *d, J* = 2.4), 7.98 (2H, *d, J* = 8.8), 8.28 (2H, *d, J* = 8.8). ^{13}C NMR (100 MHz, $CDCl_3$): δ 55.4 ($2CH_3$), 97.4 (CH), 99.7 (2CH), 124.3 (2CH), 128.6 (2CH), 137.4 (C), 144.4 (C), 150.1 (C), 161.3 (2C). HRMS ($C_{14}H_{14}N_2O_6S$ + H^+): calcd 339.0653 (M + H^+), found 339.0645.

*2.1.26. 4-Amino-N-(3,5-dimethoxyphenyl)benzenesulfonamide (**245**)*

To a solution of **242** (2.60 g, 7.69 mmol) in ethyl acetate (150 mL) and MeOH (5 mL), Pd (C) (10 mg) was added and the reaction was stirred at room temperature under H_2 atmosphere for 24 h. By filtration through Celite® and solvent evaporation, 2.30 g (97%) of **245** was obtained and purified by crystallization in MeOH (1.53 g, 65%). M.p.: 149–155 °C (MeOH). IR (KBr): 3450, 3370, 1458, 821 cm^{-1}. ^1H NMR (400 MHz, CD_3OD): δ 3.67 (6H, *s*), 6.13 (1H, *t, J* = 2.4), 6.25 (2H, *d, J* = 2.4), 6.60 (2H, *d, J* = 8.8), 7.46 (2H, *d, J* = 8.8). ^{13}C NMR (100 MHz, CD_3OD): δ 54.2 ($2CH_3$), 95.6 (CH), 98.2 (2CH), 112.8 (2CH), 125.3 (C), 128.8 (2CH), 139.8 (C), 152.8 (C), 161.1 (2C). HRMS ($C_{14}H_{16}N_2O_4S$ + H^+): calcd 309.0904 (M + H^+), found 309.0915.

*2.1.27. N-(3,5-dimethoxyphenyl)-4-(dimethylamino)benzenesulfonamide (**254**)*

To a solution of *p*-formaldehyde (534 mg, 17.77 mmol) in MeOH (40 mL), 548 mg of **245** (1.77 mmol) were added and stirred for 30 min, then $NaBH_3CN$ (223 mg, 10.62 mmol) was added and the reaction was heated at reflux for 24 h. The reaction mixture was concentrated, poured onto ice and extracted with EtOAc, dried over Na_2SO_4, filtered through Celite® and the solvent evaporated in vacuum to afford 580 mg (97%) of **254**. M.p.: 158–164 °C (MeOH). IR (KBr): 3228, 1498, 812 cm^{-1}. ^1H NMR (400 MHz, CD_3OD): δ 2.99 (6H, *s*), 3.67 (6H, *s*), 6.12 (1H, *t, J* = 2.4), 6.26 (2H, *d, J* = 2.4), 6.68 (2H, *d, J* = 9.2), 7.58 (2H, *d, J* = 9.2). ^{13}C NMR (100 MHz, $CDCl_3$): δ 39.9 ($2CH_3$), 55.3 ($2CH_3$), 96.6 (CH), 98.4 (2CH), 110.8 (2CH), 123.9 (C), 129.1 (2CH), 139.1 (C), 152.9 (C), 161.1 (2C). HRMS ($C_{16}H_{20}N_2O_4S$ + H^+): calcd 337.1217 (M + H^+), found 337.1205.

*2.1.28. N-benzyl-N-(3,5-dimethoxyphenyl)-4-(dimethylamino) benzenesulfonamide (**275**)*

77 mg (0.55 mmol) of K_2CO_3 were added to a stirred solution of **254** (93 mg, 0.27 mmol) in 3 mL of dry DMF. After 1 h at room temperature 48.2 μL (0.41 mmol) of benzyl chloride were added and stirred for 24 h. The reaction mixture was concentrated, re-dissolved in EtOAc, washed with brine, dried over anhydrous Na_2SO_4, filtered and concentrated in vacuum to obtain 112 mg (95%) and crystallized in MeOH (62 mg, 52%). M.p.: 155–160 °C (MeOH). IR (KBr): 3471, 1455, 811 cm^{-1}. ^1H NMR (400 MHz, $CDCl_3$): δ 3.05 (6H, *s*), 3.63 (6H, *s*), 4.63 (2H, *s*), 6.18 (2H, *d, J* = 2.4), 6.26 (1H, *t*, J = 2.4), 6.64 (2H, *d, J* = 8.8), 7.20 (5H, *m*), 7.53 (2H, *d, J* = 8.8). ^{13}C NMR (100 MHz, $CDCl_3$): δ 40.1 ($2CH_3$), 54.5 (CH_2), 55.3 ($2CH_3$), 99.9 (CH), 107.1 (2CH), 110.6 (2CH), 123.9 (C), 127.4 (CH), 128.2 (2CH), 128.5 (2CH), 129.6 (2CH), 136.4 (C), 141.4 (C), 152.8 (C), 160.3 (2C). HRMS ($C_{23}H_{26}N_2O_4S$ + H^+): calcd 427.1686 (M + H^+), found 427.1658.

*2.1.29. N-(6-methoxypyridin-3-yl)-4-nitrobenzenesulfonamide (**283**)*

To a solution of 6-methoxypyridin-3-amine (1.82 g, 14.66 mmol) in CH_2Cl_2 (50 mL) and pyridine (2 mL), was slowly added 4-nitrobenzenesulfonyl chloride (3.9 g, 17.59 mmol). The mixture was stirred at room temperature for 4 h. Then the reaction was treated with 2N HCl and 5% $NaHCO_3$, washed with brine, dried over anhydrous Na_2SO_4 and the solvent evaporated to obtain 3.10 g (68%) of **273**. It was purified by crystallization in MeOH 2.67 g (59%). M.p.: 139–143 °C (MeOH). IR (KBr): 3208, 1610, 1350, 826 cm^{-1}. ^1H NMR (400 MHz, $CDCl_3$): δ 3.88 (3H, *s*), 6.49 (1H, *s*), 6.70 (1H, *d, J* = 8.8), 7.43 (1H, *dd, J* = 8.8 and 2.8), 7.72 (1H, *d, J* = 2.8), 7.88 (2H, *d, J* = 9.2), 8.31 (2H, *d, J* = 9.2). ^{13}C NMR (100 MHz, $CDCl_3$): δ 53.8 (CH_3), 111.5 (CH), 124.4 (2CH), 125.2 (C), 128.6 (2CH), 136.3 (CH), 143.2 (CH), 144.3 (C), 150.3 (C), 163.1 (C). HRMS ($C_{12}H_{11}N_3O_5S$ + H^+): calcd 310.0492 (M + H^+), found 310.0487.

*2.1.30. 4-Amino-N-(6-methoxypyridin-3-yl)benzenesulfonamide (**287**)*

3.00 g of **283** (9.71 mmol) was suspended in ethyl acetate (120 mL) and was palladium-catalyzed (Pd (C) 10 mg) reduced under H_2 atmosphere for 72 h. The reaction mixture was filtered through Celite® and the solvent evaporated in vacuum to isolate 2.67 g (98%) of **287**. Crude reaction product was purified by crystallization in MeOH (539 mg, 20%). M.p.: 176–180 °C (MeOH). IR (KBr): 3485, 3281, 1619, 1500, 794 cm^{-1}. ^1H NMR (400 MHz, CD_3OD): δ 3.82 (3H, *s*), 6.59 (2H, *d, J* = 8.4), 6.68 (1H, *d, J* =8.8), 7.33 (2H, *d, J* =8.4), 7.41 (1H, *dd, J* 8.8 and 2.4), 7.71 (1H, *d, J* = 2.4). ^{13}C NMR (100 MHz, CD_3OD): δ 52.7 (CH_3), 110.1 (CH), 112.8 (2CH), 124.6 (C), 128.4 (C), 128.8 (2CH), 135.2 (CH), 141.2 (CH), 152.9 (C), 161.9 (C). HRMS ($C_{12}H_{13}N_3O_5S$ + H^+): calcd 280.0750 (M + H^+), found 280.0745.

*2.1.31. N-(4-(N-(6-methoxypyridin-3-yl)sulfamoyl)phenyl)formamide (**309**)*

970 mg of **287** (3.57 mmol) were dissolved in CH_2Cl_2 (100 mL), pyridine (5 mL) and formic acid (15 mL) and stirred at room temperature. After 24 h, the reaction mixture was poured onto ice and treated with 2N HCl and 5% $NaHCO_3$. The organic layers were washed to neutrality with brine, dried over anhydrous Na_2SO_4, filtered and evaporated to dryness to afford 555 mg (52%) of **309**. The crude reaction product was purified by crystallization in methanol (368 mg, 34%). M.p.: 189–193 °C (MeOH). IR (KBr): 3349, 3273, 1698, 1592, 823 cm^{-1}. ^1H NMR (400 MHz, CD_3OD): δ 3.82 (3H, *s*), 6.69 (1H, *d, J* = 8.8), 7.42 (1H, *dd, J* = 8.8 and 2.8), 7.62 (2H, *d, J* = 8.8), 7.70 (2H, *d, J* = 8.8), 7.71 (1H, *d, J* = 2.8), 8.31 (1H, *s*). ^{13}C NMR (100 MHz, Acetone-D6): δ 52.8 (CH_3), 110.6 (CH), 118.9 (2CH), 128.0 (C), 128.4 (2CH), 133.9 (C), 134.8 (CH), 141.6 (CH), 142.3 (C), 159.6 (C), 161.9 (CH). HRMS ($C_{13}H_{13}N_3O_4S$ + H^+): calcd 308.0703 (M + H^+), found 308.0700.

*2.1.32. N-(6-methoxypyridin-3-yl)-4-(methylamino)benzenesulfonamide (**316**)*

To a solution of the formamide **309** (485 mg, 1.58 mmol) and $NaBH_4$ (90 mg, 2.37 mmol) in dry THF (15 mL) at 0 °C, trichloroacetic acid (387 mg, 2.37 mmol) in dry THF (10 mL) was added dropwise under nitrogen atmosphere. The reaction mixture was stirred at 0 °C to room temperature for 24 h and then concentrated and re-dissolved in EtOAc, washed with brine, dried over anhydrous Na_2SO_4, filtered and solvent evaporated in vacuum. The crude reaction product (334 mg, 72%) was purified by crystallization in MeOH to yield 137 mg (30%) of **316**. M.p.: 183–186 °C (MeOH). IR (KBr): 3387, 3277, 1500, 821 cm^{-1}. ^1H NMR (400 MHz, CD_3OD): δ 2.76 (3H, *s*), 3.82 (3H, *s*), 6.52 (2H, *d, J* = 8.8), 6.67 (1H, *d, J* = 8.8), 7.38 (2H, *d, J* = 8.8), 7.41 (1H, *dd, J* = 8.8 and 2.8), 7.71 (1H, *d, J* = 2.8). ^{13}C NMR (100 MHz, $CDCl_3$): δ 30.0 (CH_3), 53.6 (CH_3), 111.0 (CH), 111.3 (2CH), 124.8 (C), 127.0 (C), 129.3 (2CH), 135.9 (CH), 142.5 (CH), 152.7 (C), 162.4 (C). HRMS ($C_{13}H_{15}N_3O_3S$ + H^+): calcd 294.0907 (M + H^+), found 294.0907.

*2.1.33. N-(4-(N-(6-methoxypyridin-3-yl)sulfamoyl)phenyl)-N-methylformamide (**320**)*

The compound **316** (88 mg, 0.30 mmol) was stirred in a mixture of CH_2Cl_2 (50 mL), pyridine (2 mL) and formic acid (5 mL) at room temperature for 24 h. The reaction mixture was poured onto ice and treated with 2N HCl and 5% $NaHCO_3$, washed to neutrality with brine, dried over anhydrous Na_2SO_4, filtered and solvent evaporated to produce 33 mg (34%) of **320**, which crystallized in methanol (24 mg, 25%). M.p.: 164–172 °C (MeOH). ^1H NMR (400 MHz, CD_3OD): δ 3.30 (3H, *s*), 3.82 (3H, *s*), 6.69 (1H, *d, J* = 8.8), 7.44 (2H, *d, J* = 8.8), 7.46 (1H, *dd, J* = 8.8 and 2.8), 7.71 (1H, *d, J* = 2.8), 7.74 (2H, *d, J* = 8.8), 8.65 (1H, *s*). ^{13}C NMR (100 MHz, CD_3OD): δ 29.9 (CH_3), 52.8 (CH_3), 110.7 (CH), 120.2 (2CH), 127.9 (C), 128.6 (2CH), 134.8 (CH), 135.6 (C), 141.5 (CH), 146.3 (C), 161.4 (C), 161.9 (CH). HRMS ($C_{14}H_{15}N_3O_4S$ + H^+): calcd 322.0856 (M + H^+), found 322.0855.

*2.1.34. 4-Methoxy-N-(6-methoxypyridin-3-yl)benzenesulfonamide (**240**)*

To a stirred solution of 6-methoxypyridin-3-amine (312 mg, 2.51 mmol) in CH_2Cl_2 (25 mL) and pyridine (1 mL) 4-methoxybenzenesulfonyl chloride (623 mg, 3.02 mmol) was added under nitrogen atmosphere. After 6 h, the reaction mixture was treated with 2N HCl and 5%

$NaHCO_3$ solutions. The organic layers were washed to neutrality with saturated NaCl, dried over anhydrous Na_2SO_4, filtered and evaporated to yield 631 mg (85%) of the sulfonamide **240**. The residue was purified by flash chromatography on silica gel using hexane/EtOAc (6:4) to afford 464 mg (62%). ^{1}H NMR (400 MHz, $CDCl_3$): δ 3.80 (3H, *s*), 3.83 (3H, *s*), 6.62 (1H, *d, J* = 8.8), 6.87 (2H, *d, J* = 8.8), 7.40 (1H, *dd, J* = 8.8 and 2.8), 7.63 (2H, *d, J* = 8.8), 7.75 (1H, *d, J* = 2.8). ^{13}C NMR (100 MHz, $CDCl_3$): δ 54.3 (CH_3), 56.2 (CH_3), 111.6 (CH) 114.9 (2CH), 127.5 (C), 130.1 (2CH), 130.6 (C), 136.3 (CH), 143.1 (CH), 162.9 (C), 163.8 (C). HRMS ($C_{13}H_{14}N_2O_4S + H^+$): calcd 295.0747 (M + H^+), found 295.0761.

*2.1.35. N-benzyl-4-methoxy-N-(6-methoxypyridin-3-yl) benzenesulfonamide (**279**)*

92 mg (0.31 mmol) of **240** dissolved in dry DMF (3 mL) were stirred for 1 h in the presence of K_2CO_3 (97 mg, 0.62 mmol). After that, benzyl chloride (54.5 μL 0.47 mmol) was added and stirred for 24 h. The reaction mixture was concentrated, re-dissolved in EtOAc, washed with brine, dried over anhydrous Na_2SO_4, filtered and concentrated in vacuum to obtain 112 mg (93%) and crystallized in MeOH (77 mg, 64%). M. p.: 144–146 °C (MeOH). IR (KBr): 3435, 1490, 823 cm^{-1}. ^{1}H NMR (400 MHz, CD_3OD): δ 3.81 (3H, *s*), 3.89 (3H, *s*), 4.72 (2H, *s*), 6.61 (1H, *d, J* = 8.8), 7.10 (2H, *d, J* = 8.8), 7.22 (5H, *bs*), 7.23 (1H, *dd, J* = 8.8 and 2.8), 7.62 (2H, *d, J* = 8.8), 7.67 (1H, *d, J* = 2.8). ^{13}C NMR (100 MHz, $CDCl_3$): δ 53.7 (CH_3), 54.9 (CH_2), 55.7 (CH_3), 110.8 (CH), 114.2 (2CH), 127.8 (CH), 128.5 (2CH), 128.6 (2CH), 129.2 (C), 129.7 (2CH), 130.7 (C), 135.4 (C), 139.5 (CH), 147.2 (CH), 163.0 (C), 163.1 (C). HRMS ($C_{20}H_{20}N_2O_4S + H^+$): calcd 385.1217 (M + H^+), found 385.1210.

*2.1.36. N-(3,4-dimethoxyphenyl)-4-methoxybenzenesulfonamide (**8**)*

To 2.49 g of 3,4-dimethoxyaniline (16.26 mmol) in CH_2Cl_2 (50 mL) and pyridine (4 mL), 3.61 g of 4-methoxybenzenesulfonyl chloride was slowly added (16.26 mmol) and stirred at room temperature for 12 h. The reaction was treated with 2N HCl and 5% $NaHCO_3$, washed with brine, dried over anhydrous Na_2SO_4 and the solvent evaporated to obtain 5.29 g (99%) of **8**. The residue was crystallized in CH_2Cl_2/Hexane to afford the purified compound (4.04 g, 75%). M.p.: 101–102 °C (CH_2Cl_2/Hexane). IR (KBr): 3224, 1498, 801 cm^{-1}. ^{1}H NMR (400 MHz, $CDCl_3$): δ 3.75 (3H, *s*), 3.79 (3H, *s*), 3.80 (3H, *s*), 6.53 (1H, *dd, J* = 8.8 and 2.8), 6.66 (1H, *d, J* = 8.8), 6.70 (1H, *d, J* = 2.8), 6.86 (2H, *d, J* = 8.8), 7.66 (2H, *d, J* = 8.8). ^{13}C NMR (100 MHz, $CDCl_3$): δ 55.5 (CH_3), 55.9 (CH_3), 55.9(CH_3), 107.7 (CH), 111.1 (CH), 114.0 (2CH), 115.4 (CH), 129.4 (2CH), 129.5 (C), 130.3 (C), 147.2 (C), 149.1 (C), 163.0 (C). HRMS ($C_{15}H_{17}NO_5S + H^+$): calcd 324.0900 (M + H^+), found 324.0906.

*2.1.37. N-(4,5-dimethoxy-2-nitrophenyl)-4-methoxybenzenesulfonamide (**11**)*

To a solution of **8** (588 mg, 1.82 mmol) in CH_3CN (50 mL) *tert*-butyl nitrite (120 μL, 0.91 mmol) was added and stirred at 45 °C. After 1 h, additional 0.91 mmol *tert*-butyl nitrite was added to the reaction mixture and it was stirred at 45 °C for 24 h. The mixture was poured onto ice and basified with 5% $NaHCO_3$ solution and extracted with EtOAc. The organic layers were washed with brine, dried over Na_2SO_4 and concentrated under vacuum to yield **11** (638 mg, 95%). The residue was purified by crystallization in CH_2Cl_2/Hexane to afford 527 mg (78%). M. p.: 152–154 °C (CH_2Cl_2/Hexane). IR (KBr): 3257, 1521, 1499, 804 cm^{-1}. ^{1}H NMR (400 MHz, $CDCl_3$): δ 3.83 (3H, *s*), 3.87 (3H, *s*), 3.98 (3H, *s*), 6.90 (2H, *d, J* = 9.2), 7.35 (1H, *s*), 7.53 (1H, *s*), 7.73 (2H, *d, J* = 9.2). ^{13}C NMR (100 MHz, $CDCl_3$): δ 55.7 (CH_3), 56.3 (CH_3), 56.7 (CH_3), 103.0 (CH), 107.2 (CH), 114.4 (2CH), 129.4 (2CH), 129.7 (C), 129.9 (C), 130.3 (C), 145.2 (C), 155.4 (C), 163.6 (C). HRMS ($C_{15}H_{16}N_2O_7S + H^+$): calcd 369.0751 (M + H^+), found 369.0752.

*2.1.38. N-(2-amino-4,5-dimethoxyphenyl)-4-methoxybenzenesulfonamide (**12**)*

To a solution of **11** (620 mg, 1.68 mmol) in ethyl acetate (100 mL) Pd (C) (10 mg) was added and the reaction was stirred at room temperature under H_2 atmosphere for 48 h. By filtration through Celite® and solvent evaporation, 550 mg (96%) of crude **12** was obtained. 374 mg (65%) of the purified compound were isolated by crystallization in CH_2Cl_2/Hexane. M.p.: 102–112 °C (CH_2Cl_2/Hexane). IR (KBr): 3265, 1458, 835 cm^{-1}. ^{1}H NMR (400 MHz, $CDCl_3$): δ 3.46 (3H, *s*), 3.74 (3H, *s*), 3.79 (3H, *s*), 5.72 (1H, *s*), 5.88 (1H, *s*), 6.23 (1H, *s*), 6.87 (2H, *d, J* = 8.4), 7.61 (2H, *d, J* = 8.4). ^{13}C NMR (100 MHz, $CDCl_3$): δ 55.6 (CH_3), 55.8 (CH_3), 56.2 (CH_3), 101.0 (CH), 112.4 (C), 112.9 (CH), 114.1 (2CH), 129.8 (2CH), 130.4 (C), 139.0 (C), 141.5 (C), 149.6 (C), 163.1 (C). HRMS ($C_{15}H_{18}N_2O_5S + H^+$): calcd 339.1009 (M + H^+), found 339.1018.

*2.1.39. N-(2-amino-4,5-dimethoxyphenyl)-4-methoxy-N-methylbenzenesulfonamide (**120**)*

To a solution of **12** (167 mg, 0.49 mmol) in CH_3CN (25 mL) 68 mg of crushed KOH (0.98 mmol) and 62 μL of methyl iodide (0.98 mmol) were added and stirred at room temperature for 24 h. Then, the reaction mixture was concentrated, re-dissolved in CH_2Cl_2, washed with brine, dried over anhydrous Na_2SO_4, filtered and concentrated in vacuum to produce 140 mg (80%) of **120**. The crude reaction product was purified by crystallization in MeOH (52 mg, 30%). M.p.: 140–141 °C (MeOH). ^{1}H NMR (400 MHz, $CDCl_3$): δ 3.11 (3H, *s*), 3.46 (3H, *s*), 3.82 (3H, *s*), 3.87 (3H, *s*), 5.80 (1H, *s*), 6.34 (1H, *s*), 6.97 (2H, *d, J* = 8.8), 7.65 (2H, *d, J* 8.8). ^{13}C NMR (100 MHz, $CDCl_3$): δ 40.2 (CH_3), 56.9 (CH_3), 57.0 (CH_3), 57.6 (CH_3), 101.9 (CH), 112.1 (CH), 115.2 (2CH), 119.4 (C), 129.8 (C), 131.6 (2CH), 141.5 (C), 142.2 (C), 151.1 (C), 164.4 (C). HRMS ($C_{16}H_{20}N_2O_5S + H^+$): calcd 353.1166 (M + H^+), found 353.1179.

*2.1.40. N-(4,5-dimethoxy-2-((4-methoxy-N-methylphenyl)sulfonamido) phenyl)acetamide (**124**)*

90 mg of **120** (0.25 mmol) was dissolved in CH_2Cl_2 (45 mL) and pyridine (1 mL). 29 μL of acetic anhydride (0.30 mmol) was added to the solution and stirred at room temperature for 24 h. The reaction mixture was poured onto ice and treated with 2N HCl and 5% $NaHCO_3$. The organic layers were washed to neutrality with brine, dried over anhydrous Na_2SO_4, filtered and evaporated to dryness. The residue was purified by silica preparative TLC (hexane/EtOAc 2:8) to afford **124** (56 mg, 55%). ^{1}H NMR (400 MHz, $CDCl_3$): δ 2.21 (3H, *s*), 3.10 (3H, *s*), 3.44 (3H, *s*), 3.85 (3H, *s*), 3.88 (3H, *s*), 5.75 (1H, *s*), 6.96 (2H, *d, J* = 8.8), 7.55 (2H, *d, J* = 8.8), 7.89 (1H, *s*), 8.21 (1H, *s*). ^{13}C NMR (100 MHz, $CDCl_3$): δ 24.8 (CH_3), 39.5 (CH_3), 55.6 (CH_3), 55.8 (CH_3), 56.0 (CH_3), 105.9 (CH), 108.9 (CH), 114.0 (2CH), 122.5 (C), 127.1 (C), 130.4 (C), 130.8 (2CH), 144.8 (C), 148.8 (C), 163.5 (C), 168.6 (C). HRMS ($C_{18}H_{22}N_2O_6S + H^+$): calcd 395.1271 (M + H^+), found 395.1280.

*2.1.41. N-(3,4-dimethoxyphenyl)-4-nitrobenzenesulfonamide (**23**)*

To a solution of 3,4-dimethoxyaniline (2.82 g, 18.41 mmol) in CH_2Cl_2 (50 mL) and pyridine (4 mL), 4-nitrobenzenesulfonyl chloride was slowly added (4.49 g, 20.25 mmol) and stirred at room temperature. After 4 h, the reaction was treated with 2N HCl and 5% $NaHCO_3$, washed with brine to neutrality, dried over anhydrous Na_2SO_4 and concentrated under vacuum to yield 5.43 g (87%) of the sulfonamide **23**. The residue was crystallized in EtOAc to afford the purified compound (4.40 g, 70%). M.p.: 181–183 °C (EtOAc). IR (KBr): 3251, 1532, 1450, 803 cm^{-1}. ^{1}H NMR (400 MHz, $CDCl_3$): δ 3.83 (3H, *s*), 3.84 (3H, *s*), 6.38 (1H, *s*), 6.43 (1H, *dd, J* = 8.4 and 2.4), 6.69 (1H, *d, J* = 8.4), 6.77 (1H, *d, J* = 2.4), 7.87 (2H, *d, J* = 8.8), 8.28 (2H, *d, J* = 8.8). ^{13}C NMR (100 MHz, Acetone-D_6): δ 55.1 (CH_3), 55.2 (CH_3), 107.6 (CH), 111.9 (CH), 114.9 (CH), 124.1 (2CH), 128.6 (2CH), 129.5 (C), 145.2 (C), 147.6 (C), 149.6 (C), 150.2 (C). HRMS ($C_{14}H_{14}N_2O_6S$ + Na^+): calcd 361.0465 (M + Na^+), found 361.0469.

*2.1.42. N-(4,5-dimethoxy-2-nitrophenyl)-4-nitrobenzenesulfonamide (**334**)*

To a solution of **23** (112 mg, 0.33 mmol) in CH_3CN (50 mL) *tert*-butyl nitrite (21.9 μL, 0.16 mmol) was added and stirred at 45 °C. After 24 h, additional 0.16 mmol of *tert*-butyl nitrite was added to the reaction

mixture and it was stirred at 45 °C for another 24 h. Then, the mixture was concentrated, re-dissolved in EtOAc and treated with 5% $NaHCO_3$ solution. The organic layers were washed with brine, dried over Na_2SO_4 and concentrated under vacuum to yield **334** (109 mg, 86%). The residue was purified by crystallization in MeOH to afford 30 mg (24%). M. p.: 169–172 °C (MeOH). ^{1}H NMR (200 MHz, Acetone-D_6): δ 3.88 (3H, *s*), 3.98 (3H, *s*), 7.28 (1H, *s*), 7.57 (1H, *s*), 8.16 (2H, *d, J* = 9), 8.41 (2H, *d, J* = 9). ^{13}C NMR (100 MHz, Acetone-D_6): δ 55.7 (CH_3), 56.1 (CH_3), 105.3 (CH), 107.7 (CH), 124.6 (2CH), 127.4 (C), 128.9 (2CH), 144.4 (C), 146.5 (C), 150.7 (C), 150.7 (C), 155.3 (C). HRMS ($C_{14}H_{13}N_3O_8S$ + Na^+): calcd 406.0316 (M + Na^+), found 406.0313.

*2.1.43. 4-Amino-N-(3,4-dimethoxyphenyl)benzenesulfonamide (**26**)*

To a solution of **23** (1.96 g, 5.81 mmol) in ethyl acetate (150 mL) and MeOH (5 mL), Pd (C) (10 mg) was added and the reaction was stirred at room temperature under H_2 atmosphere for 48 h. By filtration through Celite® and solvent evaporation, 1.71 g (95%) of **26** was obtained and purified by crystallization in EtOAc (1.39 g, 78%). M.p.: 186–187 °C (EtOAc). IR (KBr): 3449, 3221, 1462, 804 cm^{-1}. ^{1}H NMR (400 MHz, $CDCl_3$): δ 3.73 (3H, *s*), 3.76 (3H, *s*), 4.01 (2H, *s*), 6.02 (1H, *s*), 6.41 (1H, *dd, J* = 8.4 and 2.4), 6.52 (2H, *d, J* = 8.4), 6.61 (1H, *d, J* = 8.4), 6.62 (1H, *d, J* = 2.4), 7.40 (2H, *d, J* = 8.4). ^{13}C NMR (100 MHz, Acetone-D_6): δ 55.0 (CH_3), 55.3 (CH_3), 106.9 (CH), 111.9 (CH), 112.8 (2CH), 113.8 (CH), 126.0 (C), 129.1 (2CH), 131.5 (C), 146.7 (C), 149.4 (C), 152.5 (C). HRMS ($C_{14}H_{16}N_2O_4S$ + Na^+): calcd 331.0723 (M + Na^+), found 331.0733.

*2.1.44. N-(3,4-dimethoxyphenyl)-4-(dimethylamino)benzenesulfonamide (**29**)*

To a solution of *p*-formaldehyde (1.25 g, 41.11 mmol) in MeOH (40 mL) few drops of acetic acid were added to acid pH, then, 1.27 g of **26** (4.11 mmol) were added and stirred for 30 min. Finally, $NaBH_3CN$ (517 mg, 24.66 mmol) was added and the reaction was heated at reflux for 24 h. The reaction mixture was concentrated, re-dissolved in EtOAc and treated with 2N HCl and 5% $NaHCO_3$ solutions. The organic layers were washed with brine to neutrality, dried over Na_2SO_4, filtered through Celite® and the solvent evaporated in vacuum to afford 1.04 g (75%) of **29**. M.p.: 161–163 °C (EtOAc). IR (KBr): 3467, 3255, 1596, 795 cm^{-1}. ^{1}H NMR (400 MHz, $CDCl_3$): δ 3.01 (6H, *s*), 3.79 (3H, *s*), 3.82 (3H, *s*), 6.09 (1H, *s*), 6.48 (1H, *dd, J* = 8.4 and 2.4), 6.57 (2H, *d, J* = 9.2), 6.68 (1H, *d, J* = 8.4), 6.70 (1H, *d, J* = 2.4), 7.51 (2H, *d, J* = 9.2). ^{13}C NMR (100 MHz, $CDCl_3$): δ 39.9 ($2CH_3$), 55.8 (CH_3), 55.9 (CH_3), 107.2 (CH), 110.6 (2CH), 111.1 (CH), 114.9 (CH), 123.7 (C), 129.1 (2CH), 130.2 (C), 146.7 (C), 148.9 (C), 152.8 (C). HRMS ($C_{16}H_{20}N_2O_4S$ + H^+): calcd 337.1217 (M + H^+), found 337.1204.

*2.1.45. N-(4,5-dimethoxy-2-nitrophenyl)-4-(dimethylamino) benzenesulfonamide (**33**)*

To sulfonamide **29** (1.17 g, 3.48 mmol) in CH_3CN (50 mL) *tert*-butyl nitrite was added dropwise by two successive additions (460 μL, 3.48 mmol) and the reaction stirred for 24 h at 45 °C. Then, the mixture was concentrated, re-dissolved in EtOAc and treated with 5% $NaHCO_3$ solution. The organic layers were washed with brine, dried over Na_2SO_4 and concentrated under vacuum to produce 1.22 g of crude reaction product from which 949 mg of **33** (71%) was isolated by crystallization in EtOAc. M.p.: 190–195 °C (EtOAc). IR (KBr): 3255, 1593, 1525, 793 cm^{-1}. ^{1}H NMR (400 MHz, $CDCl_3$): δ 3.01 (6H, *s*), 3.86 (3H, *s*), 3.97 (3H, *s*), 6.57 (2H, *d, J* = 9.2), 7.35 (1H, *s*), 7.54 (1H, *s*), 7.63 (2H, *d, J* = 9.2). ^{13}C NMR (100 MHz, $CDCl_3$): δ 40.0 ($2CH_3$), 56.2 (CH_3), 56.7 (CH_3), 102.4 (CH), 107.1 (CH), 110.8 (2CH), 122.9 (C), 129.1 (C), 129.2 (2CH), 131.2 (C), 144.7 (C), 153.2 (C), 155.4 (C). HRMS ($C_{16}H_{19}N_3O_6S$ + H^+): calcd 382.1067 (M + H^+), found 382.1067.

*2.1.46. N-(2-amino-4,5-dimethoxyphenyl)-4-(dimethylamino) benzenesulfonamide (**35**)*

To nitroderivative **33** (655 mg, 1.72 mmol) in ethyl acetate (100 mL) under H_2 atmosphere, Pd (C) (10 mg) was added and the reaction stirred at room temperature for 48 h. After filtration through Celite® and solvent evaporation 577 mg of **35** (95%) was isolated. M.p.: 153–157 °C (MeOH). IR (KBr): 3403, 1449, 824 cm^{-1}. ^{1}H NMR (400 MHz, $CDCl_3$): δ 3.02 (6H, *s*), 3.49 (3H, *s*), 3.80 (3H, *s*), 5.77 (1H, *s*), 6.00 (1H, *s*), 6.29 (1H, *s*), 6.61 (2H, *d, J* = 9.2), 7.54 (2H, *d, J* = 9.2). ^{13}C NMR (100 MHz, $CDCl_3$): δ 41.2 ($2CH_3$), 56.8 (CH_3), 57.3 (CH_3), 102.1 (CH), 110.0 (CH), 111.8 (2CH), 114.3 (C), 124.9 (C), 130.5 (2CH), 139.9 (C), 142.5 (C), 150.5, (C), 154.1 (C). HRMS ($C_{16}H_{21}N_3O_4S$ + H^+): calcd 352.1326 (M + H^+), found 352.1320.

*2.1.47. N-(2-amino-4,5-dimethoxyphenyl)-4-(dimethylamino)-N-methylbenzenesulfonamide (**118**)*

To a solution of **35** (155 mg, 0.44 mmol) in CH_3CN (25 mL) 61 mg of crushed KOH (0.88 mmol) and 55 μL of methyl iodide (0.88 mmol) were added and stirred at room temperature for 24 h. Then, the reaction mixture was concentrated, re-dissolved in CH_2Cl_2, washed with brine, dried over anhydrous Na_2SO_4, filtered and concentrated in vacuum to produce 144 mg of crude reaction product from which 105 mg of **118** (65%) was isolated by flash chromatography (hexane/EtOAc 4:6). M.p.: 156–157 °C (MeOH). IR (KBr): 3437, 1462, 812 cm^{-1}. ^{1}H NMR (400 MHz, $CDCl_3$): δ 3.04 (6H, *s*), 3.08 (3H, *s*), 3.47 (3H, *s*), 3.82 (3H, *s*), 5.87 (1H, *s*), 6.33 (1H, *s*), 6.65 (2H, *d, J* = 9.2), 7.52 (2H, *d, J* = 9.2). ^{13}C NMR (100 MHz, $CDCl_3$): δ 38.8 (CH_3), 39.9 ($2CH_3$), 55.7 (CH_3), 56.3 (CH_3), 100.5 (CH), 110.5 (2CH), 111.0 (CH), 118.7 (C), 121.8 (C), 129.9 (2CH), 140.3 (C), 140.8 (C), 149.8 (C), 152.9 (C). HRMS ($C_{17}H_{23}N_3O_4S$ + H^+): calcd 366.1482 (M + H^+), found 366.1471.

*2.1.48. N-(2-((4-(dimethylamino)-N-methylphenyl)sulfonamido)-4,5-dimethoxyphenyl) formamide (**132**)*

The compound **118** (60 mg, 0.16 mmol) was stirred in a mixture of CH_2Cl_2 (30 mL), pyridine (1 mL) and formic acid (2 mL) at room temperature for 24 h. Then, the reaction mixture was poured onto ice and treated with 2N HCl and 5% $NaHCO_3$, washed to neutrality with brine, dried over anhydrous Na_2SO_4, filtered and solvent evaporated to produce 51 mg of crude reaction product. The residue was purified by silica preparative TLC (hexane/EtOAc 2:8) to afford **132** (31 mg, 50%). ^{1}H NMR (400 MHz, $CDCl_3$): δ 3.05 (6H, *s*), 3.09 (3H, *s*), 3.48 (3H, *s*), 3.91 (3H, *s*), 5.85 (1H, *s*), 6.65 (2H, *d, J* = 9.2), 7.45 (2H, *d, J* = 9.2), 8.00 (1H, *s*), 8.42 (1H, *s*). ^{13}C NMR (100 MHz, $CDCl_3$): δ 39.4 (CH_3), 40.1 ($2CH_3$), 55.8 (CH_3), 56.0 (CH_3), 105.5 (CH), 109.1 (CH), 110.5 (2CH), 120.2 (C), 123.0 (C), 129.9 (2CH), 130.3 (C), 144.9 (C), 148.6 (C), 153.2 (C), 159.1 (CH). HRMS ($C_{18}H_{23}N_3O_5S$ + Na^+): calcd 416.1251 (M + Na^+), found 416.1250.

*2.1.49. 4-((5,6-Dimethoxy-1H-benzo[d][1,2,3]triazol-1-yl)sulfonyl)-N,N-dimethylaniline (**117**)*

To a solution of **35** (100 mg, 0.28 mmol) in MeOH (20 mL) and H_2O (200 μL) at 0 °C, *tert*-butyl nitrite (33.8 μL, 0.28 mmol) was added and the reaction stirred. After 1 h, acetic acid (20 μL) was added to the reaction mixture and stirred for 24 h to room temperature. Then, the mixture was concentrated, re-dissolved in EtOAc and treated with 5% $NaHCO_3$ solution. The organic layers were washed with brine to neutrality, dried over Na_2SO_4 and concentrated under vacuum. The residue was chromatographed on silica preparative TLC (hexane/EtOAc 1:1) to afford the purified compound **117** (14 mg, 13%). ^{1}H NMR (400 MHz, $CDCl_3$): δ 3.03 (6H, *s*), 3.94 (3H, *s*), 4.04 (3H, *s*), 6.62 (2H, *d, J* = 9.2), 7.34 (1H, *s*), 7.46 (1H, *s*), 7.88 (2H, *d, J* = 9.2). ^{13}C NMR (100 MHz, $CDCl_3$): δ 40.0 ($2CH_3$), 56.2 (CH_3), 56.6 (CH_3), 92.7 (CH), 99.1 (CH), 110.9 (2CH), 120.8 (C), 127.1 (C), 130.0 (2CH), 139.6 (C), 149.2 (C), 152.7 (C), 154.2 (C). HRMS ($C_{16}H_{18}N_4O_4S$ + H^+): calcd 363.1122 (M + H^+), found 363.1127.

*2.1.50. Methyl 3,5-dinitrobenzoate (**80**)*

3.24 g of 3,5-dinitrobenzoic acid (15.28 mmol) was stirred in a mixture of MeOH (100 mL) and H_2SO_4 (1 mL) for 12 h. Then, anhydrous

Na_2CO_3 was added to the reaction mixture, filtered and concentrated in vacuum. The residue was re-dissolved in EtOAc, washed with water to neutrality, dried over Na_2SO_4 and solvent evaporated. 3.22 g (94%) of the crude reaction product was obtained and used without further purification. ^{1}H NMR (400 MHz, $CDCl_3$): δ 4.06 (3H, *s*), 9.18 (2H, *d*, *J* = 2.4), 9.24 (1H, *t*, *J* = 2.4). GC-MS ($C_8H_6N_2O_6$): 226 (M^+).

*2.1.51. Methyl 3,5-diaminobenzoate (**81**)*

The compound **80** (3.23 g, 14.27 mmol) was suspended in ethyl acetate (100 mL) and was palladium-catalyzed (Pd (C) 10 mg) reduced under H_2 atmosphere for 72 h. The reaction mixture was filtered through Celite® and the solvent evaporated in vacuum to isolate 2.18 g (92%) of **81**. Crude reaction product was obtained and used without further purification. ^{1}H NMR (400 MHz, $CDCl_3$): δ 3.85 (3H, *s*), 6.18 (1H, *t*, *J* = 2), 6.77 (2H, *d*, *J* = 2). GC-MS ($C_8H_{10}N_2O_2$): 166 (M^+).

*2.1.52. Methyl 3-amino-5-((4-methoxyphenyl)sulfonamido)benzoate (**84A**) and methyl 3,5-bis((4-methoxyphenyl)sulfonamido)benzoate (**84B**)*

To a solution of **81** (1.52 g, 9.14 mmol) in CH_2Cl_2 (50 mL) and pyridine (1 mL), was dropwise added 4-methoxybenzenesulfonyl chloride (1.89 g, 9.14 mmol) dissolved in CH_2Cl_2 (20 mL). The mixture was stirred at room temperature for 4 h. Then the reaction was treated with 0.5N HCl washed with brine, dried over anhydrous Na_2SO_4 and concentrated in vacuum. The residue was purified by flash chromatography on silica gel with toluene/EtOAc (7:3) to yield compounds **84A** (375 mg, 12%) and **84B** (957 mg, 41%). **84A:** M.p.: 165–166 °C (CH_2Cl_2/Hexane). IR (KBr): 3468, 3377, 1697, 1497, 1176, 803 cm^{-1}. ^{1}H NMR (400 MHz, $CDCl_3$): δ 3.80 (3H, *s*), 3.84 (3H, *s*), 6.82 (1H, *t*, *J* = 2), 6.87 (2H, *d*, *J* = 8.8), 7.01 (1H, *t*, *J* = 2), 7.09 (1H, *t*, *J* = 2), 7.71 (2H, *d*, *J* = 8.8). ^{13}C NMR (100 MHz, CD_3OD): δ 51.1 (CH_3), 54.7 (CH_3), 110.2 (CH), 110.8 (CH), 111.5 (CH), 113.8 (2CH), 128.9 (2CH), 130.9 (C), 131.2 (C), 138.8 (C), 148.9 (C), 163.1 (C), 167.0 (C). HRMS ($C_{15}H_{16}N_2O_5S$ + H^+): calcd 337.0853 (M + H^+), found 337.0855. **84B:** M.p.: 174–178 °C (CH_2Cl_2/Hexane). IR (KBr): 3270, 1724, 1498, 1150, 802 cm^{-1}. ^{1}H NMR (400 MHz, CD_3OD): δ 3.81 (9H, *s*), 6.94 (4H, *d*, *J* = 8.8), 7.31 (2H, *d*, *J* = 2), 7.35 (1H, *t*, *J* = 2), 7.63 (4H, *d*, *J* = 8.8). ^{13}C NMR (100 MHz, CD_3OD): δ 51.5 (CH_3), 54.8 ($2CH_3$), 113.8 (4CH), 115.1 (CH), 116.0 (2CH), 129.0 (4CH), 130.6 (2C), 131.5 (C), 139.1 (2C), 163.2 (2C), 165.9 (C). HRMS ($C_{22}H_{22}N_2O_8S_2$ + Na^+): calcd 529.0710 (M + Na^+), found 529.0749.

*2.1.53. Methyl 3,5-bis((4-methoxy-N-methylphenyl)sulfonamido)benzoate (**147**)*

To a solution of **84B** (132 mg, 0.39 mmol) in acetone (20 mL) K_2CO_3 (542 mg, 3.92 mmol) and $(CH_3)_2SO_4$ (281 μL, 2.94 mmol) were added, heated at reflux and stirred overnight. Then, the reaction mixture was filtered, poured onto ice and extracted with CH_2Cl_2. The organic layers were dried over anhydrous Na_2SO_4, filtered and evaporated to dryness. By crystallization in MeOH compound **147** (73 mg, 51%) was isolated. M.p.: 139–142 °C (MeOH). ^{1}H NMR (400 MHz, $CDCl_3$): δ 3.10 (6H, *s*), 3.84 (6H, *s*), 3.86 (3H, *s*), 6.91 (4H, *d*, *J* = 8.8), 7.21 (1H, *t*, *J* = 2), 7.45 (4H, *d*, *J* = 8.8), 7.66 (2H, *d*, *J* = 2). ^{13}C NMR (100 MHz, $CDCl_3$): δ 38.1 ($2CH_3$), 52.9 (CH_3), 56.1 ($2CH_3$), 114.7 (4CH), 126.0 (2CH), 127.9 (2C), 129.4 (CH), 130.3 (4CH), 131.7 (C), 142.9 (2C), 163.7 (2C), 165.9 (C). HRMS ($C_{24}H_{26}N_2O_8S_2$ + Na^+): calcd 557.1023 (M + Na^+), found 557.1024.

*2.1.54. Methyl 3-amino-5-methoxybenzoate (**78**)*

957 mg of 3-amino-5-methoxybenzoic acid (5.73 mmol) was stirred in a mixture of MeOH (50 mL) and H_2SO_4 (1 mL) for 24 h. Then, anhydrous Na_2CO_3 was added to the reaction mixture, filtered and concentrated in vacuum. The residue was re-dissolved in EtOAc, filtered again and evaporated to dryness. 799 mg (77%) of crude reaction product was obtained and used without further purification. ^{1}H NMR (400 MHz, CD_3OD): δ 3.74 (3H, *s*), 3.83 (3H, *s*), 6.48 (1H, *t*, *J* = 2), 6.84 (1H, *t*, *J* = 2), 6.95 (1H, *t*, *J* = 2). ^{13}C NMR (100 MHz, $CDCl_3$): δ 52.1 (CH_3), 55.3 (CH_3), 104.3 (CH), 105.7 (CH), 109.2 (CH), 132.0 (C), 147.6 (C), 160.6 (C), 167.1 (C). GC-MS ($C_9H_{11}NO_3$): 181 (M^+).

*2.1.55. Methyl 3-methoxy-5-((4-methoxyphenyl)sulfonamido)benzoate (**79**)*

To a solution of **78** (620 mg, 3.42 mmol) in CH_2Cl_2 (50 mL) and pyridine (2 mL), was slowly added 4-methoxybenzenesulfonyl chloride (707 mg, 3.42 mmol). The mixture was stirred at room temperature for 4 h. Then the reaction was treated with 2N HCl and 5% $NaHCO_3$, washed with brine, dried over anhydrous Na_2SO_4 and the solvent evaporated to obtain 1.15 g (95%) of the sulfonamide **79**. The crude reaction product was purified by crystallization in CH_2Cl_2 (529 mg, 44%). M.p.: 176–177 °C (CH_2Cl_2). IR (KBr): 3258, 1700, 1497, 1152, 802 cm^{-1}. ^{1}H NMR (400 MHz, CD_3OD): δ 3.76 (3H, *s*), 3.81 (3H, *s*), 3.85 (3H, *s*), 6.91 (1H, *t*, *J* = 2.4), 6.99 (2H, *d*, *J* = 8.8), 7.20 (1H, *t*, *J* = 2.4), 7.32 (1H, *t*, *J* = 2.4), 7.71 (2H, *d*, *J* = 8.8). ^{1} C NMR (100 MHz, Acetone-D_6): δ 51.6 (CH_3), 54.9 (CH_3), 55.1 (CH_3), 109.6 (CH), 110.2 (CH), 113.1 (CH), 114.2 (2CH), 129.2 (2CH), 131.2 (C), 132.1 (C), 139.6 (C), 160.3 (C), 163.2 (C), 165.6 (C). HRMS ($C_{16}H_{17}NO_6S$ + H^+): calcd 352.0849 (M + H^+), found 352.0842.

*2.1.56. 3-Methoxy-5-((4-methoxy-N-methylphenyl)sulfonamido)benzoic acid (**90**)*

To a solution of **79** (100 mg, 0.28 mmol) in CH_3CN (40 mL) 38 mg of crushed KOH (0.56 mmol) and 36 μL of methyl iodide (0.56 mmol) were added and stirred at room temperature for 24 h. Then, the reaction mixture was concentrated, re-dissolved in CH_2Cl_2, treated with 2N HCl, washed with brine to neutrality, dried over anhydrous Na_2SO_4, filtered and concentrated in vacuum. The residue was purified by silica preparative TLC with CH_2Cl_2 (98:2) yielding compound **90** (69 mg, 66%). M.p.: 186–187 °C (CH_2Cl_2). IR (KBr): 3000, 1689, 1502, 806 cm^{-1}. ^{1}H NMR (400 MHz, CD_3OD): δ 3.16 (3H, *s*), 3.79 (3H, *s*), 3.86 (3H, *s*), 6.94 (1H, *t*, *J* = 2.4), 7.03 (2H, *d*, *J* = 8.8), 7.26 (1H, *t*, *J* = 2.4), 7.46 (1H, *t*, *J* = 2.4), 7.47 (2H, *d*, *J* = 8.8). ^{13}C NMR (100 MHz, $CDCl_3$): δ 37.8 (CH_3), 55.6 (CH_3), 55.7 (CH_3), 113.8 (CH), 114.0 (2CH), 118.7 (CH), 119.3 (CH), 127.7 (C), 129.9 (2CH), 130.9 (C), 143.1 (C), 159.7 (C), 163.2 (C), 170.6 (C). HRMS ($C_{16}H_{17}NO_6S$ + H^+): calcd 352.0849 (M + H^+), found 352.0848.

2.2. Determination of aqueous solubility

The aqueous solubility of the sulfonamides was determined in a Helios Alfa Spectrophotometer using an approach based on the saturation shake-flask method. 1–2 mg of each tested compound was suspended in 300 μL pH 7.0 buffer and stirred for 72 h at room temperature. The resulting mixture was filtered over a 45 μm filter to discard the insoluble residues. Then, a scan between 270 and 400 nm was performed and the three maximum wavelengths were selected for each compound. Calibration curves were performed at these wavelengths and the concentration in the supernatant was measured by UV absorbance.

2.3. Cells and culture conditions

The *L. infantum* strain used in this study was MCAN/ES/MON1/Z001. The myeloid human cell line used, originally obtained from a patient with histiocytic leukemia was U937 (ATCC® CRL1593.2). The human tumor cell lines were HT-29, HeLa, and MCF7, obtained from a patient with colon, cervical, and breast cancer respectively.

Leishmania promastigotes were cultured at 27 °C in RPMI 1640 supplemented with L-glutamine (Lonza-Cambrex, Karlskoga, Sweden), 10% heat-inactivated fetal bovine serum (HIFBS) (Lonza-Cambrex), and 100 μg/mL streptomycin-100 IU/mL penicillin (Lonza-Cambrex) in 25 mL culture flasks. Logarithmic and late stationary promastigotes were obtained after incubation for 3–4 and 6–7 days respectively. The starting inoculum was $4{\cdot}10^6$ parasites/mL.

Leishmania axenic amastigotes were obtained from late stationary

promastigotes. After harvesting promastigotes at 250 g for 10 min, they were centrifuged in Percoll® (Sigma) gradient to select the living population. Then, promastigotes were seeded at $4{\cdot}10^6$ parasites/mL in M199 medium (Invitrogen, Leiden, The Netherlands) supplemented with 10% HIFBS, 1 g/L β-alanine, 100 mg/L L-asparagine, 200 mg/L sucrose, 200 mg/L D-fructose, 50 mg/L sodium pyruvate, 320 mg/L malic acid, 40 mg/L fumaric acid, 70 mg/L succinic acid, 200 mg/L α-ketoglutaric acid, 300 mg/L citric acid, 1.1 g/L sodium bicarbonate, 5 g/L morpholineethanesulfonic acid (MES), 0.4 mg/L hemin, 10 mg/L gentamicin and 100 µg/mL streptomycin-100 IU/mL penicillin; pH 5.4, at 37 °C in a 95% humidity, 5% CO_2 atmosphere. After 24h of incubation, all parasites had a round morphology without an emerging flagellum.

U937 (human lung histiocytic lymphoma) and HT-29 (human colon carcinoma) cells were cultured at 37 °C in complete RPMI 1640 medium (see above) in a 95% humidity, 5% CO_2 atmosphere. HeLa (human cervical carcinoma) and MCF7 (human breast carcinoma) cell lines were cultured in DMEM medium containing 10% (v/v) HIFBS, 2 mM L-glutamine and 100 µg/mL streptomycin-100 IU/mL penicillin at 37 °C in 95% humidity, 5% CO_2 atmosphere.

2.4. Cytotoxicity assays

The effect of the different compounds on the proliferation of human tumor cell lines was determined by using the XTT (sodium 3,39-[1(phenylaminocarbonyl)-3,4-tetrazolium]-bis(4-methoxy-6-nitro)benzene sulfonic acid hydrate) cell proliferation kit (Roche Molecular Biochemicals, Mannheim, Germany) as previously described (Scudiero et al., 1988). Briefly, a freshly prepared mixture solution of XTT labeling reagent and PMS (N-methyl-dibenzopyrazine methyl sulfate) electron coupling reagent was added to cells and were incubated during the corresponding time according to each cell line (6 h for U937 and HT-29 and 4 h for HeLa and MCF7 cells), in a humidified atmosphere (37 °C, 5% CO_2), and the absorbance of the formazan product generated was measured at a test wavelength of 450 nm. A positive control is formed by cells without compounds at 72 h and a negative control is formed by cells without compounds at 0 h of incubation. Measurements were performed in triplicate, and each experiment was repeated three times. Cell viability was evaluated seeding 100 µL of cells in exponential growth phase with appropriate cell line concentration ($1{\cdot}10^5$ U937 cells/mL, $3{\cdot}10^4$ HT-29 cells/mL, $1.5{\cdot}10^4$ HeLa cells/mL and $1.5{\cdot}10^4$ MCF7 cells/mL) in complete RPMI 1640 or DMEM medium in 96-well plates at 37 °C and 5% CO_2. The tested sulfonamides were added at 10 µM after 24 h of incubation, to attached U937 cells and 1 µM to HT-29, HeLa, and MCF7 cells. The effect on proliferation was evaluated 72 h post-treatment. The compounds were dissolved in dimethyl sulfoxide (DMSO) and the final solvent concentrations never exceeded 0.5% (v/v).

2.5. Leishmanicidal assays

The leishmanial growth inhibition assays in promastigotes and axenic amastigotes were performed by using the XTT method described above.

2.5.1. In vitro promastigote assay

The *in vitro* promastigote susceptibility assay was performed with logarithmic and late stationary promastigotes including two independent replicates. 100 µL of promastigotes in complete RPMI 1640 medium were seeded at $4{\cdot}10^6$ parasites/mL in 96-well plates at 27 °C, in the absence and the presence of 10 µM concentration of the corresponding sulfonamides. The compounds were dissolved in DMSO. The final solvent concentrations never exceeded 0.5% (v/v). After 24 h incubation, each plate-well was examined by light microscopy to detect changes in parasite morphology or motility. 72 h after treatment, 50 µL of XTT solution were added to each well, and the cells were incubated for 7 h at 27 °C. Thereafter, absorbance was measured at 450 nm with a MicroPlate Reader 680 spectrophotometer and MicroPlate Manager 5.2.1. software (BioRad). Measurements were done in triplicate, and each experiment was repeated three times.

2.5.2. Axenic amastigote assay

Axenic amastigote viability assays were performed following a similar method. Promastigotes were differentiated into axenic amastigotes as previously described. 100 µL of late stationary promastigotes were seeded at $4{\cdot}10^6$ parasites/mL in complete M199 medium in 96-well plates at 37 °C. After 24 h incubation sulfonamides at different concentrations (a first screening using 10 µM and then 15, 10, 9, 7, 6, 4, 2, and 1 µM of active compounds) were added to axenic amastigotes. Then, the XTT solution was added 48 h post-treatment and incubated for 7 h at 37 °C. The efficacy of each compound was estimated by calculating the IC_{50} (half maximal inhibitory concentration). Measurements were done in triplicate, and each experiment was repeated three times.

2.5.3. In vitro macrophage infection and intracellular amastigote assay

The *in vitro* infection of the human U937 myeloid cell line with *L. infantum* promastigotes was carried out to evaluate the antileishmanial activity of new sulfonamides. U937 cells were centrifuged at 250 g for 10 min. Then, 400 µL of cells in complete RPMI 1640 medium were seeded at $3.75{\cdot}10^5$ cells/mL in 8-well chambers slides (LabTek, New York, NY) at 37 °C and were differentiated by stimulation with 20 ng/ml phorbol 12-myristate 13-acetate (PMA) (Sigma, Saint Louis, MO) for 72 h. The cultures were rinsed three times with complete RPMI medium to remove nondifferentiated unattached cells. Then, cells were infected with stationary *L. infantum* promastigotes at 37 °C at a 5:1 promastigote:macrophage ratio in 400 µL complete RPMI medium in an atmosphere of 5% CO_2 for 2 h. Noninternalized promastigotes were removed by 3–4 successive washes with complete RPMI medium. Then, infected macrophages were incubated in complete medium with sulfonamides at different concentrations (first screening using 20 µM, then 20, 15, 10, 7, and 5 µM for active compounds) for 48 h. The compounds were dissolved in DMSO and the final solvent concentrations never exceeded 0.5% (v/v). Finally, fixation and staining were performed. For this purpose, the wells were first washed three times with fresh complete medium. Then, the cells were treated with hypotonic solution (complete medium:water 9:11) for 5 min and were fixed with 150 µL ethanol:acetic acid 3:1 for 10 min (step repeated three times). The preparations were allowed to air dry and the wells were removed from the slide. Modified Giemsa staining was carried out with Diff-Quick® Stain Solution I and II (Dade Behring, Marburg, Germany). The preparations were washed with distilled water, air-dried, and mounted with Entellan® Neu (Merck, Darmstadt, Germany). The number of amastigotes per infected cell was estimated by counting 100 cells per biological replicate randomly. The experiment was performed in triplicate and the statistical analysis was based on Student's paired *t*-test.

2.6. Docking studies

The sequences of α and β tubulins from *Leishmania* with sizes larger than 400 amino acids were retrieved from UniProt (Bateman, 2019). Sequences were aligned with each other and with the sheep tubulin sequence of the pdbID 3HKC X-ray structure from the Protein Data Bank (Berman et al., 2003) using ClustalX (Larkin et al., 2007). The amino acids forming the colchicine domain were defined and selected as those closer than 6 Å to the ligands in the colchicine site of the tubulin-colchicine site ligand complex X-ray structures published in PDB. The comparison of 20 *Leishmania* sequences with the sheep sequence indicated changes at 11 amino acid residues with sidechains contacting colchicine site ligands. Eight of them were conserved in the *Leishmania* sequences and all three that changed (i.e. N167β, K254β, and I347β) could be represented by just four sequence combinations used for building the homology models. The sheep 3HKC X-ray structure was used as a template for the generation of the homology models for two

reasons: i) the ABT-751 ligand is one of the very few ligands binding to the 3 zones (1–3) of the colchicine site; and ii) said ligand has an *N*-aryl-methoxybenzenesulfonamide structure in common to the compounds in our library. Hence, it provides the most favorable starting point for the docking studies, as confirmed by successful cross-dockings of other ligands with known X-ray structures binding at zones 1, 2, or 3, like combretastatin A-4 (sites 1 and 2) or nocodazole (sites 2 and 3). 5 homology models were generated with Modeller 9.15 (S˘ali and Blundell, 1993) for each sequence combination, for a total of 20 homology models for the *Leishmania* proteins. The models were curated manually to avoid the colchicine binding site collapse previous to the docking experiments. Docking studies of the ligands in the mammalian proteins and the *Leishmania* homology models were carried out as described (Álvarez et al., 2013). Additionally, representative ligands binding at zones 1, 2, and/or 3 of the colchicine site were docked and compared with their X-ray complex structures to validate the selection of 3HKC as a template. Docking runs were performed with PLANTS with default settings (Korb et al., 2009) and generated 10 runs per ligand. AutoDock 4.2 (Forli et al., 2016) runs applied the Lamarckian genetic algorithm (LGA) 100–300 times for a maximum of 2.5×10^6 energy evaluations, 150 individuals, and 27000 generations maximum. The poses were automatically assigned to zones 1–3, and the results tabulated using in-house KNIME pipelines (Berthold et al., 2007). Z-scores were generated from the programs' scores. The results were analyzed with Chimera (Pettersen et al., 2004), Marvin ("Marvin 17.8 ChemAxon," 2017), OpenEye ("OpenEye Scientific Software, Inc, Santa Fe," 2019), and JADOPPT (Garcia-Perez et al., 2017).

3. Results and discussion

3.1. Chemical library design

The search for new antiparasitic drugs, including antileishmanial compounds has followed two distinct approaches: i) the blind screening of large compound libraries (HTS) that impair parasite viability, the so-called phenotypic assays; or ii) or target-based screenings where ligands acting on a particular target of interest are sought (Zulfiqar et al., 2017). The first approach has the advantage of guaranteeing effects on the whole organism and therefore fulfilling pharmacokinetic and pharmacodynamic requirements and finds drugs active against unforeseen targets. However, it has the disadvantage of requiringing challenging target deconvolution in the following drug development process. Target-based screens, on the other hand, have the advantage of facilitating later stages of drug development, although the compounds do not always have

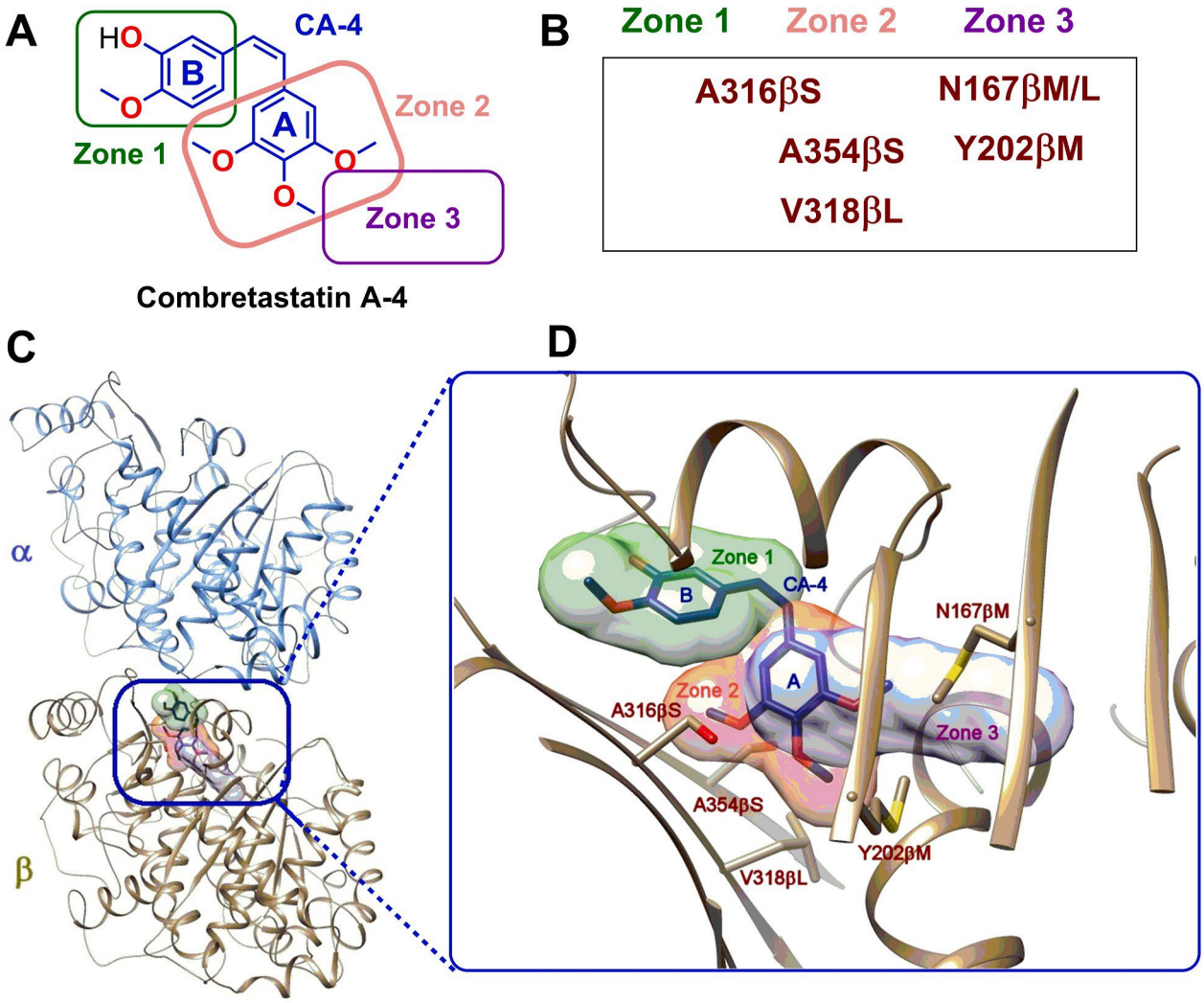

Fig. 1. The tubulin colchicine site and differences between mammals and *Leishmanias*. (**A**) Chemical structure of combretastatin A-4 with the interaction zones indicated by colored rectangles. (**B**) Amino acid substitutions in trypanosomatids compared to mammals. (**C**) Ribbon model of the tubulin dimer with combretastatin A-4 bound in the colchicine site, indicated by a blue rectangle. (**D**) Detail of the colchicine-binding site with the three binding zones indicated as colored volumes and with the amino acids of the *Leishmania* sequences which vary from humans shown. (For interpretation of the references to color in this figure legend, the reader is referred to the Web version of this article.)

adequate pharmacokinetic properties, or the target turns out to be non-essential and lacks activity in the whole organism. Herein, an intermediate approach has been adopted by designing a focused library against the well validated target tubulin and assaying the compounds in a phenotypic screen against several stages of the parasite life cycle. As a result, both pharmacokinetic and pharmacodynamic issues were simultaneously assessed to achieve a basis of the mechanism of action.

Trypanosomatid microtubules present up to 11 different amino acid substitutions in the colchicine-binding site relative to mammalian orthologs (Luis et al., 2013). To determine sequence differences from humans to *Leishmania* potentially affecting the binding of colchicine site ligands, the colchicine site was defined as any set of tubulin amino acid residues whose sidechain is less than 6 Å away from the ligand complexed at said site. More than 50 colchicine site ligands complexed with tubulin retrieved from Protein Data Bank (PDB) (Berman et al., 2003; Vicente-Bla´zquez et al., 2019) were considered. The study determined sequence differences between the human and the *Leishmania* ortholog affecting ligand binding to the colchicine site. Clustal X (Larkin et al., 2007) alignment of the X-ray structure sequences with the *Leishmania* sequences retrieved from UniProt (Bateman, 2019) and comparison of the amino acids assigned to the colchicine site allowed for identifying mutated residues (Fig. 1). The colchicine domain in tubulin has been subdivided into three sub-pockets (1-3). Zzones 1–3 bind several moieties of typical colchicine site ligands, such as combretastatin A-4 (Fig. 1) and nocodazole. Zone 1 (Massarotti et al., 2012) is the pocket for combretastatin A-4 ring B. Sequence conservation between leishmanial and human tubulin is high in this pocket. The sole exception is the A316βS replacement, located at the inner edge of the V-shaped A and B rings of combretastatin A-4. It makes the gap smaller but more polar due to the presence of the serine side chain hydroxyl group. Therefore, small modifications were envisaged for B-rings, except for the introduction of non-bulky hydrogen bond acceptors and donors such as small amine or formamide groups. *Leishmania* tubulin sequences show an A250βS change compared to the sheep ortholog in the pocket accommodating the bridge connecting zones 1 and 2, located in a flexible loop at the interface between tubulin subunits. The hydroxyl group in this region suggested the introduction of a sulfonamide to bridge the A and B rings. *Leishmania* tubulin sequences contain the substitutions A316βS, A354βS, C241βT, and V318βL in zone 2. These changes configure a smaller and more polar pocket compared to the mammalian protein due to three additional hydroxyl groups. This suggested the possibility of removing some of the methoxyl groups from the classical trimetoxyphenyl A ring of combretastatin A-4 and the introduction of additional hydrogen bonding groups. These modifications may also probably reduce activity against human tubulin, thus conferring selectivity. Finally, zone 3 contains the N167βI and the Y202βM substitutions. This zone would become smaller and less polar, thus leaving the negatively charged D200β in a very hydrophobic environment. However, mutations in zone 3 have been described in parasites resistant to benzimidazoles. Hence, this zone was not pursued (Furtado et al., 2016).

Considering these sequence differences between the tubulin of Leishmania and the mammalian hosts at the colchicine site, a focused library of 350 compounds was designed by a combination of several substitutions on a diarylsulfonamide scaffold and later synthesized. The

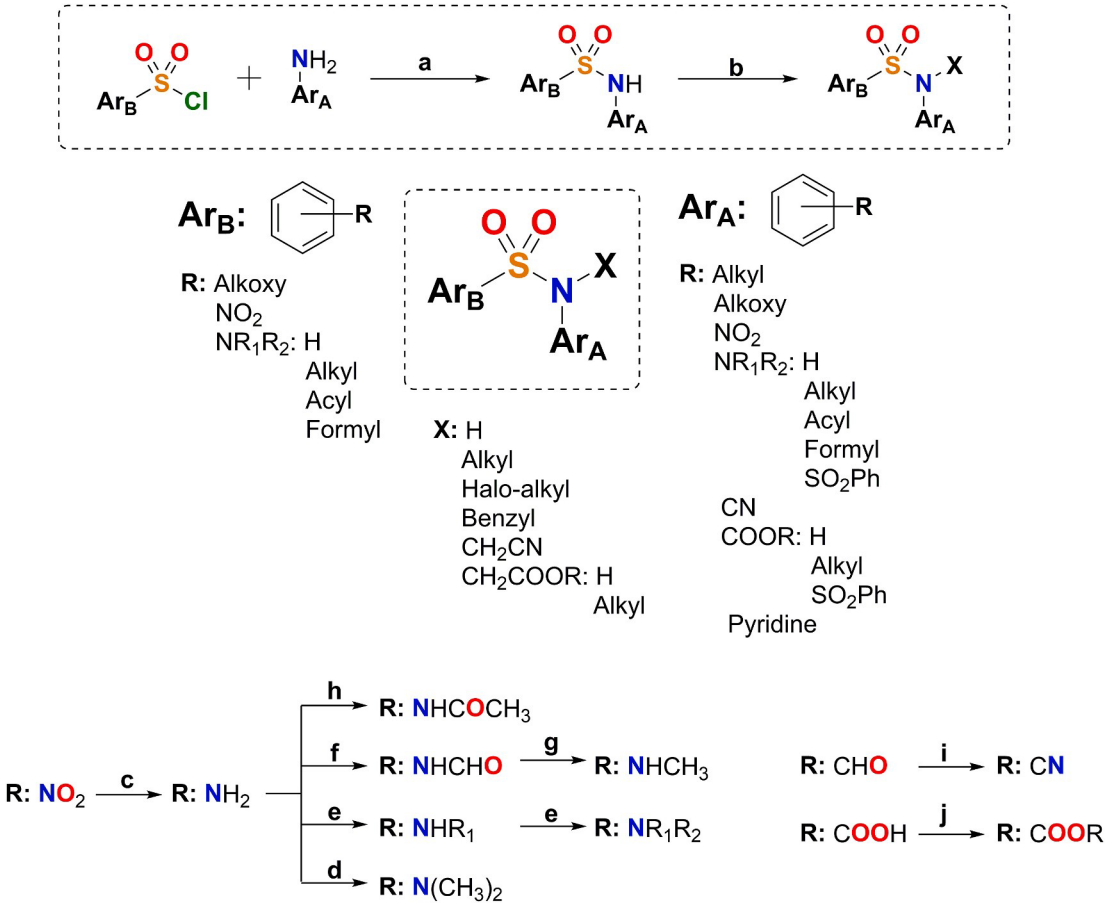

Fig. 2. General structure of diarylsulfonamide library. General chemical synthetic route for the chemical library of 350 diarylsulfonamides: (a) Pyridine, CH_2Cl_2, rt, 1 h. (b) X-Halogen, K_2CO_3, DMF, rt, 12 h. (**B**) Some of the most frequent modifications carried out in aromatic ring B (Ar_B) and/or aromatic ring A (Ar_A) substituents. Structural variations in the library and main functional group modifications: (c) H_2, Pd/C, EtOAc, rt, 48 h. (d) *p*-formaldehyde, $NaBH_3CN$, AcOH, MeOH, reflux, 2 h. (e) R-Halogen, CH_2Cl_2, rt, 1–12 h. (f) Formic acid, CH_2Cl_2, rt, 24 h. (g) Trichloroacetic acid, $NaBH_4$, THF, rt, 12 h. (h) Acetic anhydride, CH_2Cl_2, rt, 30 min. (i) 1) $NH_2OH{\cdot}HCl$, pyridine, MeOH, reflux 24 h. 2) Acetic anhydride, pyridine, reflux, 48 h. (j) R–OH, H_2SO_4, rt, 3 h.

substitutions were selected with two purposes: i) fitting the structural requirements of the parasite tubulins; and ii) avoiding binding to the mammalian counterparts. These substitutions are schematically shown in Fig. 2, altogether with the general synthetic route applied to build the library. According to the observed sequence differences for zone 2, the trimethoxyphenyl ring of mammalian anti-tubulin ligands has been replaced with dimethoxyphenyl rings bearing the methoxy groups in different positions, methoxypyridines, carboxyanilines, and others. All the compounds were isolated, purified, and chemically characterized. Herein, the synthetic details described in the Methods section and below for the active compounds are described. The synthesized compounds are readily available, chemically stable, and possess drug-like properties (Supp Mat Table 1) (Daina et al., 2017), in good agreement with the requests for new antileishmanial therapies.

3.2. Chemical synthesis

The construction of the diarylsulfonamide scaffolds was performed through the reaction between sulfonyl chlorides and primary amines (Fig. 2). The reactions occurred in good yields (85–98%) and could be easily prepared in large amounts for later modifications. Non-commercial amines required for the synthesis of the sulfonamide bridge were obtained by the nitration of the correspondent aromatic rings, and subsequent palladium-catalyzed reduction. When further substituent modifications on the ring were required, they were carried out before the introduction of the amine groups. Occasionally, for aryls with two amino groups or with an amino group and a carboxylic acid group simultaneously, products with three aromatic rings were also obtained (e.g. **63B, 147**). Diarylsulfonamides with amine or amine derivative substituents were prepared after sulfonamide assembly from nitro groups and later functional group modification. Substitutions on the sulfonamide nitrogen were introduced by alkylation reactions. Bromination reactions were performed when necessary. Detailed chemical synthesis of compounds that showed antileishmanial activity can be found in materials and methods and the structures of all the synthesized compounds are available from the authors upon request.

3.3. Solubility and chemical stability

The low stability and low aqueous solubility of 1 µg/mL (Vandermeulen et al., 2006) are the main pharmacokinetic drawbacks of Amphotericin B. This drug is generally administered in sodium deoxycholate or liposomal formulations and needs special storing and transport conditions. This increases the cost and treatment difficulty. All the prepared compounds remained stable for more than 48 h in solution at room temperature, as determined by ^{1}H-NMR. Most of them are crystalline solids that remain unaltered for weeks at room temperature. The solubility of representative active compounds of the series in phosphate buffer at pH 7.0 was determined as follows: i) shaking in pH 7.0 phosphate buffer for 72 h; ii) microfiltration; and iii) identification and quantification by UV absorbance at three different wavelengths. Compounds **26**, **35**, and **63B** showed thermodynamic solubilities of 55 µg/mL, 118 µg/mL; and, 1889 µg/mL, respectively. These are moderate to good aqueous solubilities, which is an important parameter for the oral administration of drugs.

3.4. Cytotoxicity in human cells

The effect of the synthesized sulfonamides on the cellular proliferation of four human tumor cell lines: U937 (human lung histiocytic lymphoma), HT-29 (human colon carcinoma), HeLa (human cervical carcinoma), and MCF7 (human breast adenocarcinoma), was studied as a surrogate of human toxicity and to select the least cytotoxic compounds against human cells for the *in vitro* leishmanicidal assays (Table 1). The compounds were tested at concentrations of 10 µM for the U937 and 1 µM for HT-29, HeLa, and MCF7 cell lines. Most compounds did not show antiproliferative effects at the concentrations studied, which might be due to the structural modifications introduced to reduce binding to mammalian tubulin. The more cytotoxic compounds were those with bulky substituents on the sulfonamide nitrogen, such as a benzyl group in the 3,5-dimethoxyaniline series (e.g. compounds **332, 326B,** and **275**) and/or a bromine atom on the 2,5-dimethoxyaniline series (for example, **204, 332** and **326B**) (Table 1, Fig. 3). After evaluating antileishmanial activity (see below), the IC_{50} values of antiproliferative activity against the human cancer cell line HeLa were determined, and selectivity indexes were calculated (Supplemental Table S1). The best selectivity indexes correspond to compound **276B**, with values of 11.5 for axenic amastigotes and 3.45 for intracellular amastigotes.

3.5. Activity in leishmania promastigotes

The 350 sulfonamides under study were tested for their antiprotozoal activity against logarithmic and late stationary cultured *L. infantum* promastigotes (MCAN/ES/MON1/Z001). Cell proliferation was assessed 72 h after drug treatment at 10 µM using the XTT method and compared with untreated cells taken as 100% of proliferation. None of the compounds was active against this parasite stage at the tested concentration. However, this is not a requirement for treatment. Promastigotes are not the mammalian stage, unlike intracellular amastigotes. Noticeable differences in gene expression profiles have been found between them (Almeida et al., 2004; Leifso et al., 2007). Hence, active compounds should target amastigotes.

3.6. Activity in axenic amastigotes

Since *Leishmania* spp amastigotes are responsible for all clinical manifestations in humans and studying intracellular amastigotes is challenging, the compounds were first tested against axennic amastigotes. This allowed for selecting the best candidates for subsequent assays with intracellular amastigotes. *L. infantum* axenic amastigotes were differentiated from late stationary promastigotes by temperature, pH, and culture medium shift. All compounds were tested using the XTT method after 48 h of treatment initially at 10 µM. Those significantly active were selected for IC_{50} calculation. Measurements were done in triplicate, and each experiment was repeated three times. Eight compounds out of 350 (2.3%) showed potencies better than 10 µM against axenic amastigotes (Table 1). Three of them (**129, 204,** and **332**) behaved like or better than miltefosine. Compound **129** was the most potent of the series with sub-micromolar potency and did not show cytotoxicity against the human cancer cell lines. Five additional compounds had satisfactory IC_{50} values between 5 and 12 µM (**326B, 275, 279, 334** and **276B**) (Table 1). Series including several active compounds are phenyl sulfonamides of 2,5-dimethoxy- (**129, 204** and **332**) and 3,5-dimethoxy- (**275**, **326B**) anilines. The first series includes all three most potent compounds. The introduction of a bromo substituent in this series renders the compounds (**204**, **326B,** and **332**) cytotoxic. Nevertheless, the most potent compound of the series (**129**) is not cytotoxic at the tested concentrations. The allowed substituents on the phenylsulfonamide include the methoxy groups and both monomethyl and dimethylamines. Additional substituents on the ring are also tolerated. These results indicate a more permissive binding pocket of the target for these moieties. Interestingly, the larger triaryl compound **276B** is also active against axenic amastigotes but not cytotoxic. These results show that small structural changes can result in selective activity against axenic amastigotes without affecting the host cells. These non-cytotoxic compounds are considered ideal candidates for further development as leishmanicidal drugs.

3.7. Activity against intracellular amastigotes

Intracellular amastigotes are the clinically relevant infective stage of

Table 1
Leishmanicidal and cytotoxic activities of sulfonamides that showed antileishmanial activity in any of the parasite stages.

Compound	*Leishmania infantum*			U937	HT-29	HeLa	MC7
	Promastigotes	Axenic amastigotes	Intracellular amastigotes	10 µM	1 µM	1 µM	1 µM
	10 µM	IC_{50} (µM)	20 µM				
129	NA	0.93	A	NC	NC	NC	NC
138	NA	NA	A	NC	NC	NC	NC
204	NA	2.2	ND	C	C	C	C
183	NA	NA	A	NC	NC	NC	NC
332	NA	4.3	ND	C	C	C	C
326B	NA	8.2	ND	C	C	C	C
275	NA	8.1	ND	C	NC	NC	NC
242	NA	NA	A	NC	NC	NC	NC
320	NA	NA	A	NC	NC	NC	NC
316	NA	NA	A	NC	NC	NC	NC
279	NA	12	NA	NC	NC	NC	NC
334	NA	5.75	NA	NC	NC	NC	NC
124	NA	NA	A	NC	NC	NC	NC
132	NA	NA	A	NC	NC	NC	NC
117	NA	NA	A	NC	NC	NC	NC
35	NA	NA	A	NC	NC	NC	NC
26	NA	NA	A	NC	NC	NC	NC
84	NA	NA	A	NC	NC	NC	NC
90	NA	NA	A	NC	NC	NC	NC
147	NA	NA	A	NC	NC	NC	NC
63B	NA	NA	A	NC	NC	NC	NC
276B	NA	6.7	A	NC	NC	NC	NC
Miltefosine	A	4.4	A	NC	ND	ND	ND

Leishmanicidal activities of sulfonamides on *L. infantum* promastigotes and axenic amastigotes at 10 µM and IC_{50} calculation; on intracellular amastigotes at 20 µM and cytotoxicity on human tumor cell lines U937 at 10 µM and HT-29, HeLa and MCF7 at 1 µM. NA, Inactive at tested concentration. A, Active at tested concentration. NC, Not Cytotoxic at tested concentration. C, Cytotoxic at tested concentration. ND, Undetermined. Assays are described in Materials and Methods.

Leishmania spp. in mammals. They frequently show different drug sensitivities from promastigotes or axenic amastigotes (Zulfiqar et al., 2017). The intracellular leishmanicidal activity was assayed in amastigote-infected U937 cells. Infection was performed by incubation with stationary *L. infantum* promastigotes. Then, infected macrophages were incubated with treatment compounds for 48 h. After fixation and staining of the samples, activity was determined by randomly counting the number of amastigotes per infected cell. Activity against intracellular amastigotes at 20 µM was evaluated for all compounds in the library not inducing cytotoxicity in U937 cells used for infection at 10 µM (157 compounds). 16 compounds showed activity against intracellular amastigotes (Table 1), 10% of the tested compounds and 5% of the total: very high success rates. More compounds were active against intracellular than axenic amastigotes. Promastigotes are usually more sensitive than amastigotes to most compounds tested elsewhere (De Muylder et al., 2011). The diarylsulfonamide inhibitors detailed above are an exception.

Among the eight active compounds against axenic amastigotes (Table 1), four are cytotoxic to U937 cells and two are inactive against intracellular amastigotes (i.e. **279** and **334**). Just two, i.e. **129** and **276B** (Fig. 4), are active against both amastigote forms and not cytotoxic. Box Plot data analysis of the number of amastigotes per cell (Fig. 4A) showed that the infection progress is inversely proportional to the ligand concentration compared with untreated control cells. 75% of the analyzed cells host 0–1 amastigote per cell when treated with active compounds (Fig. 4B). The same percentage of untreated cells accommodate 0–4 amastigotes per cell. The maximum reached 6–9 amastigotes per cell under different treatments and 15 in the untreated control. Hence, late stationary *L. infantum* promastigotes infected the U937 macrophages and subsequently differentiated into intracellular amastigotes, divided into the host cell, and infected other cells in the untreated control, whereas the evidence shown in Table 1 and Figs. 4 and 5 suggests that at least one of these steps may have been partially blocked in treated cells by a few compounds. Compound **129** leads to the most remarkable decrease in the infection measured in terms of the percentage of infected cells and the number of amastigotes per infected cell. Sulfonamides **279** and **334** with activity against axenic amastigotes did not show activity against intracellular amastigotes. The reason could be differences in cellular uptake or to the reported biochemical differences between both amastigote forms (Alcolea et al, 2010, 2014; Rochette et al., 2009).

Interestingly, a high proportion of compounds (14 out of 16) showed activity against intracellular amastigotes but not against axenic amastigotes (Table 1 and Fig. 6). This discrepancy could be due to the different threshold applied for considering positives, but the number of examples suggests a more probable host-cell-dependent mechanism of action (De Muylder et al., 2011). These results and the subtle differences between mammalian and parasitic tubulins suggest the possibility of an action on the host tubulin at sub-cytotoxic concentrations, which has been previously shown in the treatment of eukaryotic cells with tubulin inhibitors, contributing to the antileishmanial activity. The well-known capability of tubulins of different origins, specifically mammalian and leishmanial, to co-assemble and exchange dimer subunits would support the possibility of a tubulin-mix based mechanism (Montecinos-Franjola et al., 2019). Aside from compounds only active against intracellular amastigotes (**138** and **183** from the 2,5-dimethoxyphenyl, **242** from the 3,5-dimethoxyphenyl, and **316** and **320** from the 6-methoxy-3-pyridyl series) (Fig. 3 and Table 1), new structural types of phenyl sulfonamides are also active against intracellular amastigotes: i) 3,4-dimethoxyanilines (**26**, **35**, **117**, **124**, **132**, and **334**, the latter also active against axenic amastigotes); ii) 3-carboxy-5-aminoanilines (**84A**, **90**, and **147**); and the triaryl **63B**.

3.8. Docking studies

To obtain insights into tubulin-binding of the active compounds, we have performed flexible docking studies with mammalian and leishmanial tubulins. Protein flexibility was accounted for by using several structures with different binding-site configurations. For the mammalian proteins, we used 50 X-Ray crystal structures of complexes with different ligands bound to the colchicine domain available in PDB and five more representative models from a molecular dynamics simulation, as described (Álvarez et al., 2013). For the leishmanial tubulin, 5

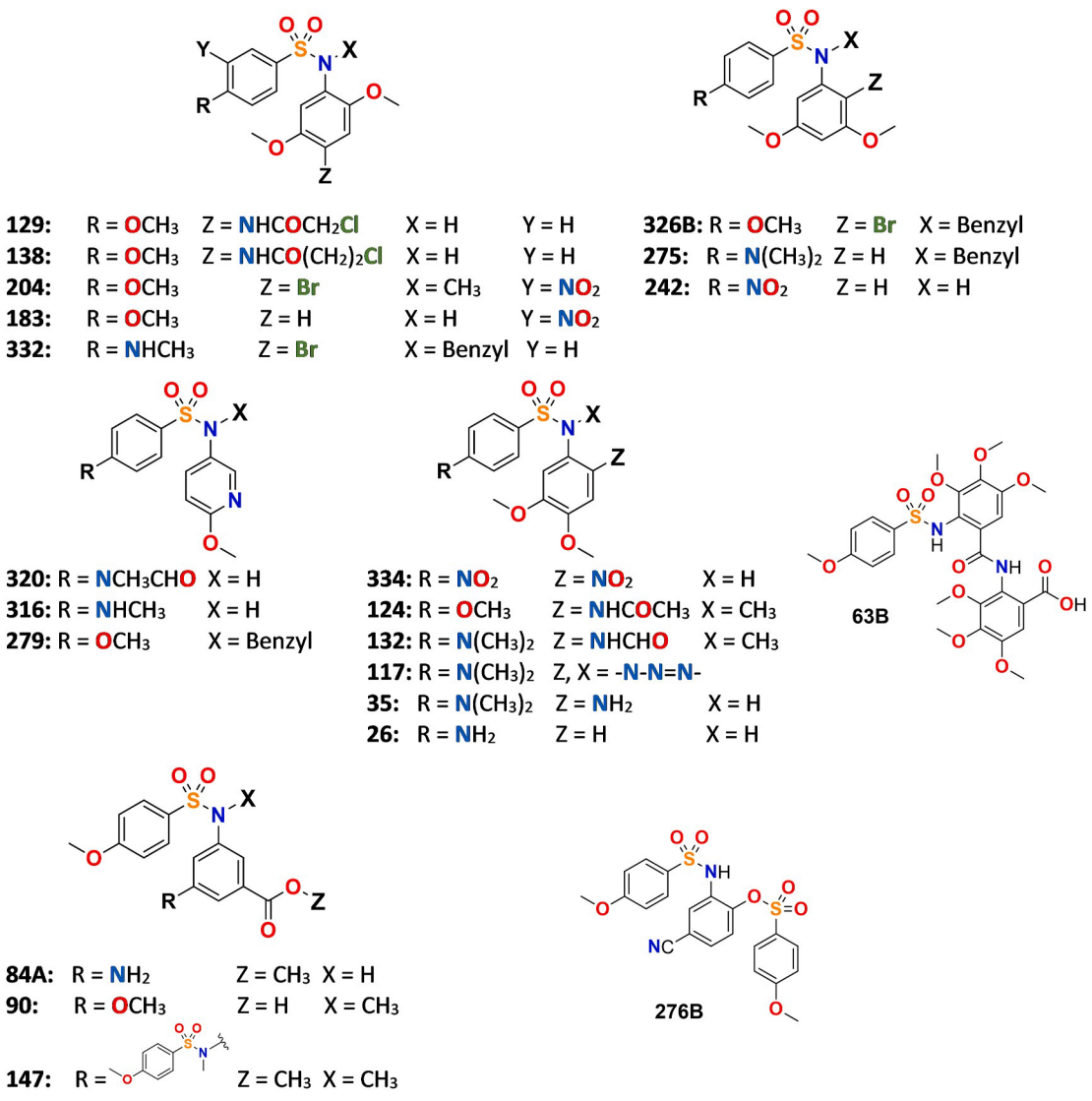

Fig. 3. Structures of the tested sulfonamides that showed leishmanicidal activity.

homology models were generated with Modeler (Šali and Blundell, 1993) for each unique combination of amino acids in the colchicine site present in the leishmanial sequences retrieved from UniProt. As a result, 20 models of leishmanial tubulin were used for the docking studies. These studies were performed with two frequently used docking programs that use very different scoring functions. For each ligand, several thousand poses were generated bound to each of the protein sets. The poses were automatically assigned to the occupied zones (A-D) of the binding domain. Those showing the best consensus scores returned by both programs were selected as the binding poses (Fig. 7) (Supp Mat Table 2).

Most ligands bind in similar ways to the mammalian and the leishmanial protein, occupying sites A and B (Fig. 7). Even the apparently large ligand **276B** for a colchicine-site ligand binds similarly to ABT-751 (Supplemental Fig SF1. The phenyl rings with the larger substituents are always located in zone 2, while the other ring binds at zone 1. The size reduction from the trimethoxyphenyl ring of combretastatin A-4 to those used herein (2,5- (**129**), 3,4- (**124**), and 3,5-dimethoxyphenyl and 3-carboxy-5-aminophenyl (**84**)) are a better fit for the smaller and more polar zone 2 of the parasite orthologs. For the sulfonamides with a 6-methoxy-3-pyridyl ring, such as **320**, the pyridine ring is in zone 1. This fact confirms the importance of filling the available space in zone 2. The unoccupied space left by the smaller rings in zone 2 is responsible for the selectivity of the ligands, which are apparently associated with a affinity reduction for the host protein. The similar binding to host's and parasite's tubulin is consistent with the observed host-cell-dependent action.

The compounds stack an aromatic ring at zone 1 between Asn258β of helix H8 and the sidechain methylenes of Ser316β and Lys or Arg352β of sheets S8 and S9, respectively, making additional hydrophobic contacts along the ring plane with the sidechains of Val181α, Leu255β, Met259β, and Thr314β. The other aromatic ring is inserted edgewise towards the surface of sheets S8 and S9 boxed between the sidechains of Ser316β and Val318 (S8) or Lys or Arg352β, and Ser354β (S9). They are overlaid by helices H7 and H8 and the loop between them and interact with the sidechains of Cys241β, Leu242β, Leu248β, Ala250β, and Leu255β. These residues are highly conserved amongst the different *Leishmania* species. Therefore, the activity of the compounds might extend to other members of the genus.

4. Conclusions

A focused library of diarylsulfonamides has been designed to target the colchicine site of leishmanial but not mammalian tubulin, based on known structure-activity relationships (SAR), on the differences in amino acids between the two organisms, and the presumed favorable cost, stability, and solubility profiles. 350 new sulfonamides have been

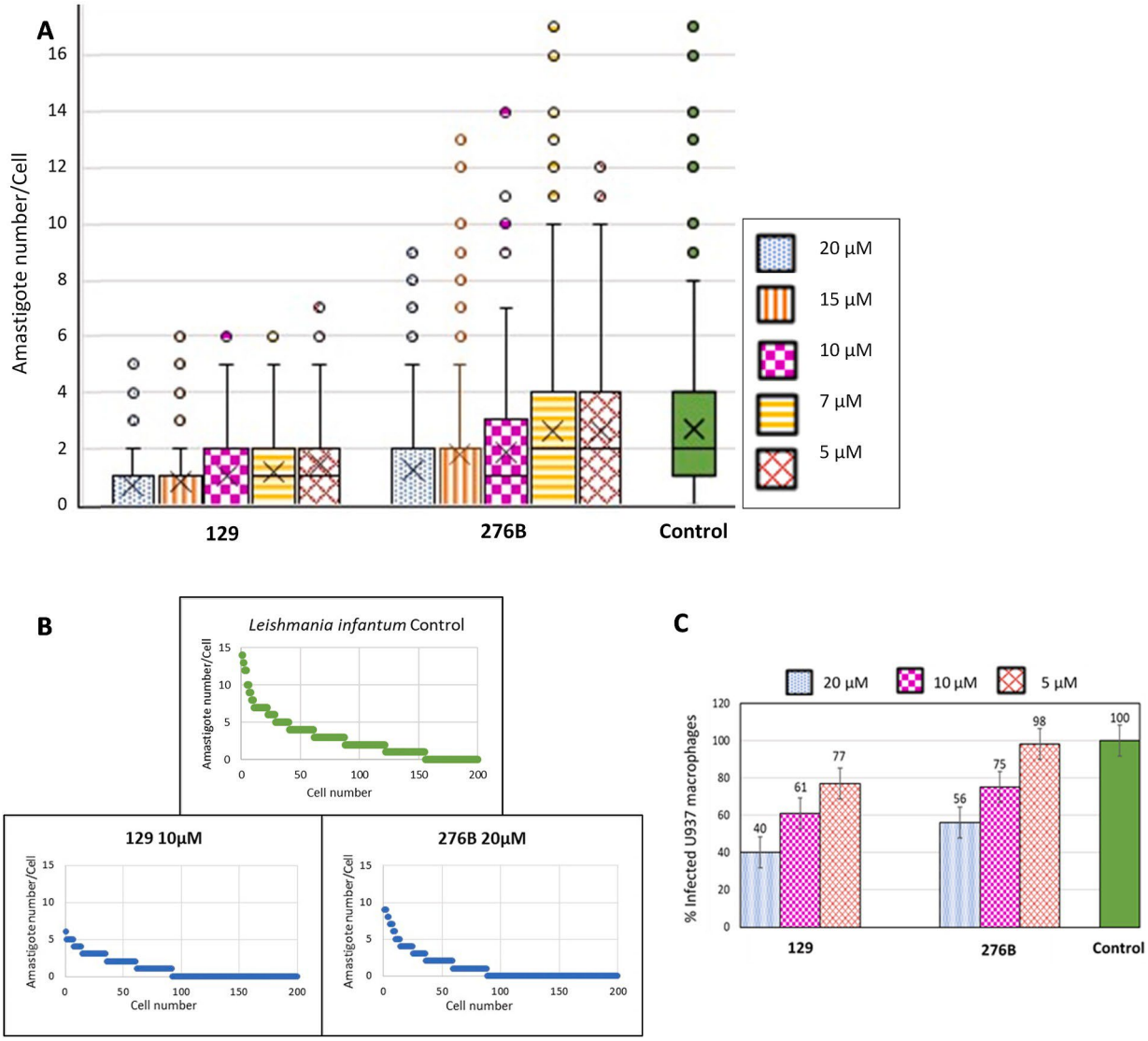

Fig. 4. Dose-response study against *L. infantum* intracellular amastigotes of non-cytotoxic sulfonamides with axenic activity. (**A**) Intracellular amastigote number per infected macrophage in the range of concentrations 20-5 µM of non-cytotoxic compounds that showed activity against both, axenic and intracellular *L. infantum* amastigotes, **129** and **276B**. Untreated control cells were run in parallel. Results shown by Box Plot data analysis are representative of three independent experiments. (**B**) Number of amastigotes accommodated per counted macrophage sorted in decreasing order in a representative sample of 200 macrophages for untreated sample (control), **129** and **276B** treatments. (**C**) Percentage of infected U937 macrophages treated with sulfonamides **129** or **276B** in a 20-5 µM concentration range normalized to the percentage of infected macrophages in untreated controls (usually about 70%), taken as 100%.

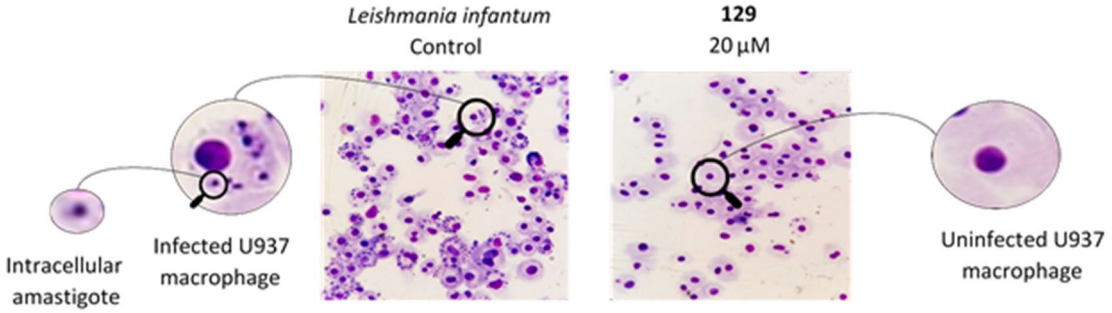

Fig. 5. Light microscopy image of modified Giemsa-stained preparations of *in vitro* macrophage infections. Left: control cells without treatment, U937 macrophages infected with *L. infantum* amastigotes. Right: Treated cells with the compound **129** at 20 µM, infection clearly interrupted.

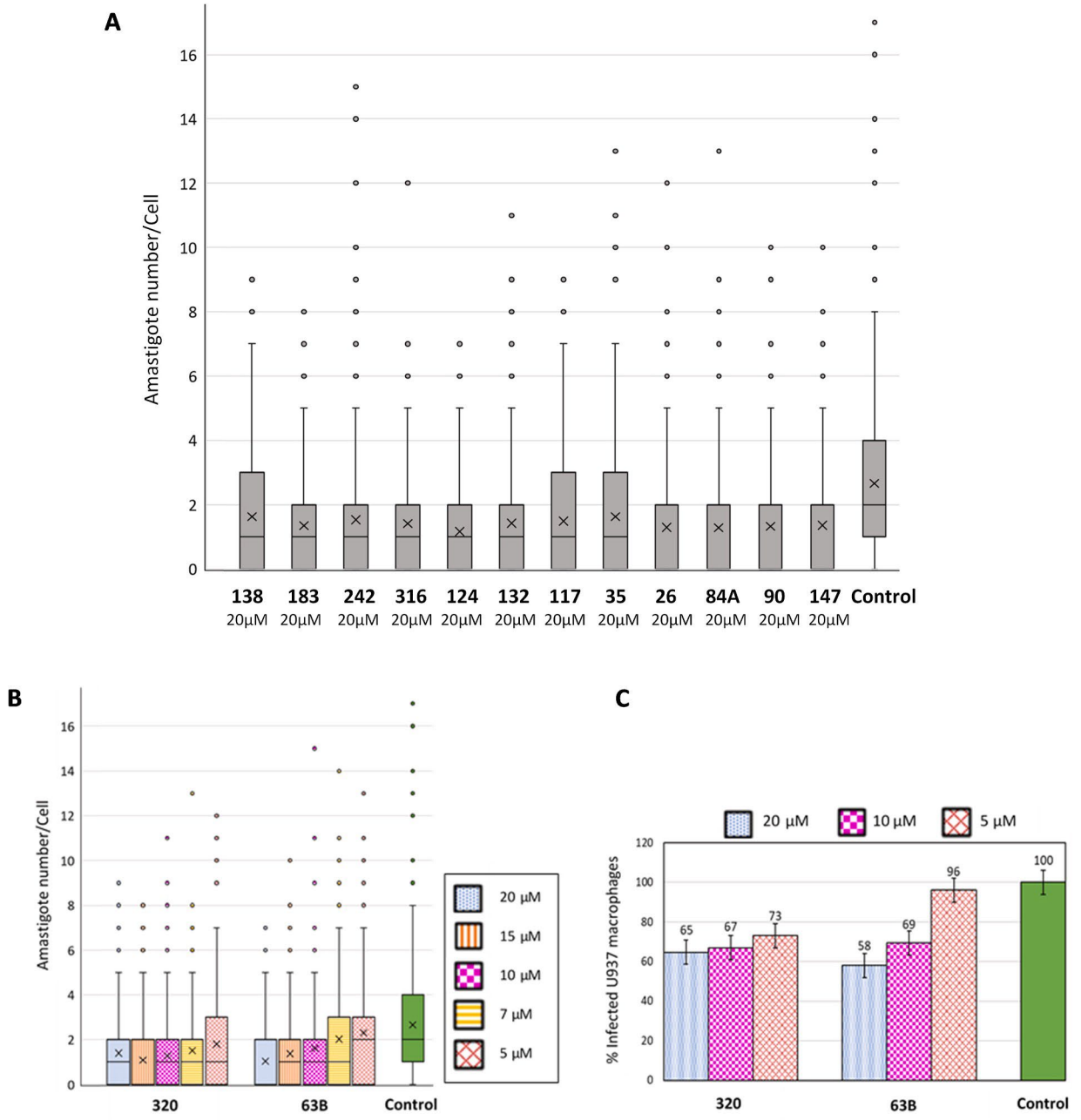

Fig. 6. Dose-response study against *L. infantum* intracellular amastigotes of non-cytotoxic sulfonamides without axenic activity. (**A**) Effect on the *L. infantum* intracellular amastigotes activity in cells treated with non-cytotoxic and non-active sulfonamides on axenic amastigotes at 10 µM, but which showed a significant *in vitro* infection decrease at 20 µM. Depicted data are representative of three independent experiments. (**B**) Box Plot data analysis of the number of intracellular amastigotes per infected cell in the 20-5 µM range of most potent non-cytotoxic sulfonamides without axenic activity that were more deeply studied, **320** and **63B**. (**C**) Percentage of infected treated cells normalized to the percentage of infected macrophages in untreated controls (usually about 70% and taken as 100%), at 20, 10, and 5 µM of compounds **320** and **63B**.

synthesized, characterized, and shown to have adequate solubility, stability, and cost compared with current antileishmanial treatments. A compound library was evaluated *in vitro* against different parasite life cycle stages using a human host cell line, leading to new compounds against the ZVL-causing agent *L. infantum*. None showed activity against promastigotes. However, eight sulfonamides (**129, 204, 332, 326B, 275, 279, 334,** and **276B**) are active against axenic amastigotes. The IC_{50} values are comprised between 0.9 and 12 µM, similar or even better than the reference drug miltefosine. The structural requirements for activity against axenic amastigotes include dimethoxyphenyl rings substituted at the 2,5-, 2,3- or 3,4-position. These requirements are not very different from those for interaction with human tubulin because 50% are also cytotoxic against cancer human cell lines. 157 compounds lacking cytotoxic activity were assayed in intracellular amastigotes. As a result, 16 severely reduced the number of axenic amastigotes found in treated infected macrophages compared to the untreated controls. The high success rate of 10% validates the design approach in a phenotypic assay reproducing the clinically relevant form in the mammalian host. Sulfonamides **129** and **276B** efficiently interrupted the course of the U937 macrophage infection in the micromolar range. These compounds constitute an starting point for development of new antileishmanial drugs. Their target is different from those of drugs under clinical trials or already implemented in clinical practice. Hence, combination therapies might be favorable. 14 of the 16 new sulfonamides active against

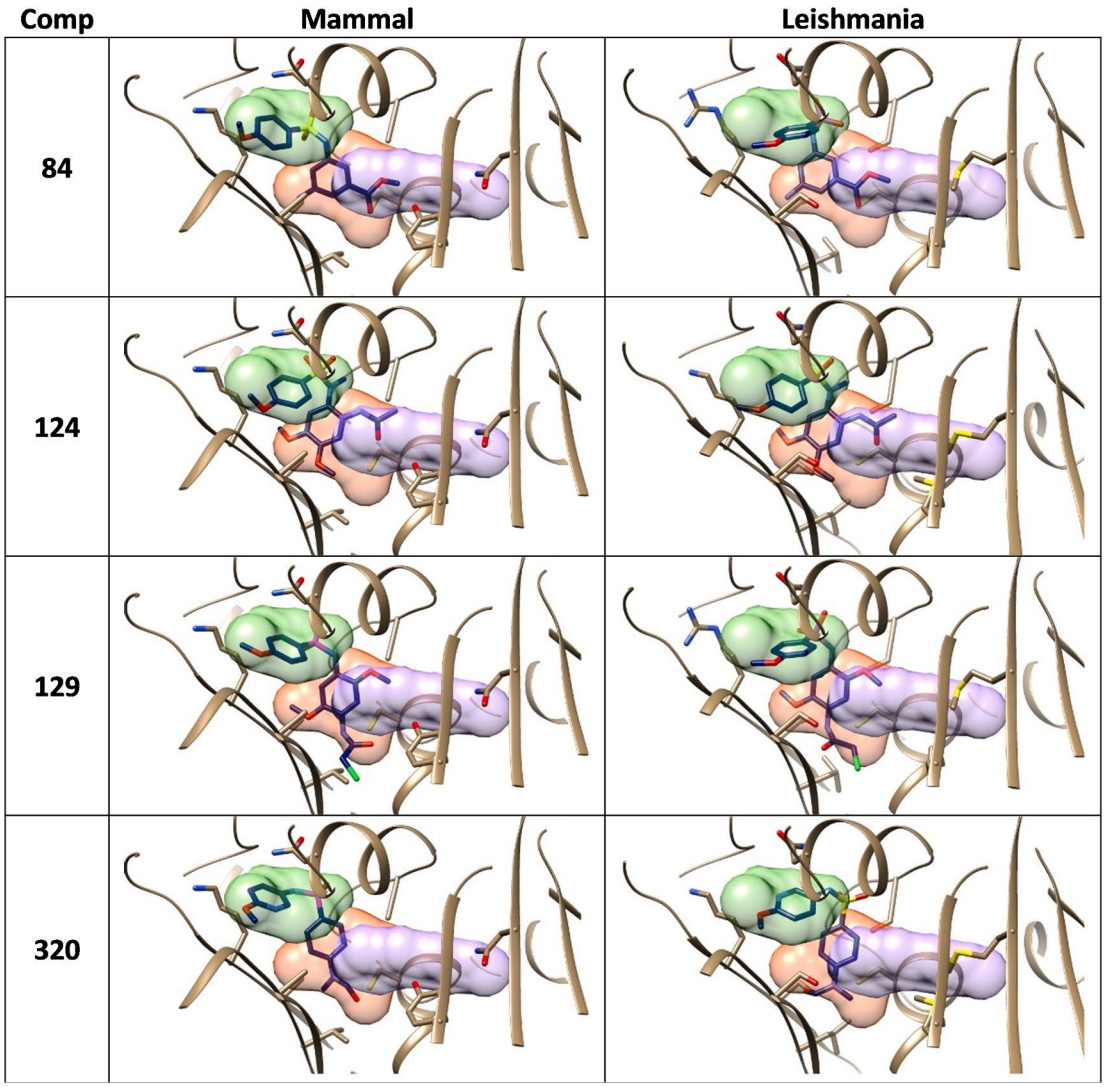

Fig. 7. Docking poses for compounds 84, 124, 129, and 320. The left column corresponds to docking in the colchicine-site of mammalian proteins and the right column to homology models for the *Leishmania* orthologs. The proteins are shown as gray cartoons. Relevant amino acid sidechains and the ligands are shown as sticks. The three zones of the colchicine-binding site are indicated as volumes colored in the same way as Fig. 1.

intracellular amastigotes lacked activity against axenic amastigotes, thus indicating a host-dependent mechanism of action devoid of toxicity which could be an advantage as an added barrier to the development of resistance by the parasite. The consistency of the biological activity found is reinforced by clustering of the active compounds in five chemical classes that also provide preliminary structure-activity relationships for further development. Molecular docking experiments support binding to the colchicine site of tubulin of the parasites, provide good agreement with the structure-activity relationship trends and suggest that the activity might extend to other *Leishmania* species. The appropriate combination of accessibility, antileishmanial activity, mechanism, parasite selectivity, and favorable solubility properties make the herein presented sulfonamides promising. The next step in development is proof-of-concept assays using animal models.

Declaration of competing interest

All authors declare no conflict of interest.

Acknowledgments

This work was supported by Consejería de Educacio´n de la Junta de Castilla y Leo´n (SA030U16 and SA262P189) and the Spanish Ministry of Science, Innovation and Universities (RTI2018-099474-BI00) co-funded by the EU's European Regional Development Fund-FEDER, the EUROLISH NET project (Marie Sklodowska Curie ITN-ETN, EU H2020) and Fundacio´n Ramo´n Areces (2017–2019). MG acknowledges a predoctoral grant EDU/602/2016 from Consejería de Educacio´n de la Junta de Castilla y Leo´n.

Appendix A. Supplementary data

Supplementary data to this article can be found online at https://doi.org/10.1016/j.ijpddr.2021.02.006.

References

Abu Ammar, A., Nasereddin, A., Ereqat, S., Dan-Goor, M., Jaffe, C.L., Zussman, E., Abdeen, Z., 2019. Amphotericin B-loaded nanoparticles for local treatment of cutaneous leishmaniasis. Drug Deliv. Transl. Res. 9, 76–84. https://doi.org/10.1007/s13346-018-00603-0.

Alcolea, P.J., Alonso, A., Go´mez, M.J., Moreno, I., Domínguez, M., Parro, V., Larraga, V., 2010. Transcriptomics throughout the life cycle of Leishmania infantum: high down-regulation rate in the amastigote stage. Int. J. Parasitol. 40, 1497–1516. https://doi.org/10.1016/j.ijpara.2010.05.013.

Alcolea, P.J., Alonso, A., Go´mez, M.J., Postigo, M., Molina, R., Jim´enez, M., Larraga, V., 2014. Stage-specific differential gene expression in Leishmania infantum: from the foregut of Phlebotomus perniciosus to the human phagocyte. BMC Genom. 15 https://doi.org/10.1186/1471-2164-15-849.

Alcolea, P.J., Tun˜o´n, G.I.L., Alonso, A., García-Tabares, F., Ciordia, S., Mena, M.C., Campos, R.N.S., Almeida, R.P., Larraga, V., 2016. Differential protein abundance in promastigotes of nitric oxide-sensitive and resistant Leishmania chagasi strains. Proteonomics Clin. Appl. 10, 1132–1146. https://doi.org/10.1002/prca.201600054.

Almeida, R., Gilmartin, B.J., McCann, S.H., Norrish, A., Ivens, A.C., Lawson, D., Levick, M.P., Smith, D.F., Dyall, S.D., Vetrie, D., Freeman, T.C., Coulson, R.M., Sampaio, I., Schneider, H., Blackwell, J.M., 2004. Expression profiling of the Leishmania life cycle: cDNA arrays identify developmentally regulated genes present but not annotated in the genome. Mol. Biochem. Parasitol. 136, 87–100. https://doi.org/10.1016/j.molbiopara.2004.03.004.

Alvar, J., V´elez, I.D., Bern, C., Herrero, M., Desjeux, P., Cano, J., Jannin, J., de Boer, M., 2012. Leishmaniasis worldwide and global estimates of its incidence. PloS One. https://doi.org/10.1371/journal.pone.0035671.

A´lvarez, R., Puebla, P., Díaz, J.F., Bento, A.C., García-Navas, R., De La Iglesia-Vicente, J., Mollinedo, F., Andreu, J.M., Medarde, M., Pel´aez, R., 2013. Endowing indole-based tubulin inhibitors with an anchor for derivatization: highly potent 3-substituted indolephenstatins and indoleisocombretastatins. J. Med. Chem. 56, 2813–2827. https://doi.org/10.1021/jm3015603.

Alves, F., Bilbe, G., Blesson, S., Goyal, V., Monnerat, S., Mowbray, C., Muthoni Ouattara, G., P´ecoul, B., Rijal, S., Rode, J., Solomos, A., Strub-Wourgaft, N., Wasunna, M., Wells, S., Zijlstra, E.E., Arana, B., Alvar, J., 2018. Recent development of visceral leishmaniasis treatments: successes, pitfalls, and perspectives. Clin. Microbiol. Rev. https://doi.org/10.1128/CMR.00048-18.

Arce, A., Estirado, A., Ordobas, M., Sevilla, S., García, N., Moratilla, L., de la Fuente, S., Martínez, A.M., P´erez, A.M., Ara´nguez, E., Iriso, A., Sevillano, O., Bernal, J., Vilas, F., 2013. Re-emergence of Leishmaniasis in Spain: Community Outbreak in Madrid, Spain, 2009 TO 2012. https://doi.org/10.2807/1560-7917.ES2013.18.30.20546. Eurosurveillance 18.

Bateman, A., 2019. UniProt: a worldwide hub of protein knowledge. Nucleic Acids Res. 47, D506–D515. https://doi.org/10.1093/nar/gky1049.

Berman, H., Henrick, K., Nakamura, H., 2003. Announcing the worldwide protein Data Bank. Nat. Struct. Biol. https://doi.org/10.1038/nsb1203-980.

Berthold, M.R., Cebron, N., Dill, F., Gabriel, T.R., Ko¨tter, T., Meinl, T., Ohl, P., Sieb, C., Thiel, K., Wiswedel, B., 2007. KNIME: the konstanz information miner. Studies in Classification, Data Analysis, and Knowledge Organization. Springer Berlin, Ger, pp. 319–326.

Daina, A., Michielin, O., Zoete, V., 2017. SwissADME: a free web tool to evaluate pharmacokinetics, drug-likeness and medicinal chemistry friendliness of small molecules. Sci. Rep. 7 https://doi.org/10.1038/srep42717.

De Muylder, G., Ang, K.K.H., Chen, S., Arkin, M.R., Engel, J.C., McKerrow, J.H., 2011. A screen against leishmania intracellular amastigotes: comparison to a promastigote screen and identification of a host cell-specific hit. PLoS Neglected Trop. Dis. 5 https://doi.org/10.1371/journal.pntd.0001253.

De Rycker, M., Baragan˜a, B., Duce, S.L., Gilbert, I.H., 2018. Challenges and recent progress in drug discovery for tropical diseases. Nature. https://doi.org/10.1038/s41586-018-0327-4.

Dost´al, V., Libusova´, L., 2014. Microtubule Drugs: Action, Selectivity, and Resistance across the Kingdoms of Life. Protoplasma. https://doi.org/10.1007/s00709-014-0633-0.

Drews, J., 2000. Drug discovery: a historical perspective. Science 80–. https://doi.org/10.1126/science.287.5460.1960.

Dumontet, C., Jordan, M.A., 2010. Microtubule-binding agents: a dynamic field of cancer therapeutics. Nat. Rev. Drug Discov. https://doi.org/10.1038/nrd3253.

Escudero-Martínez, J.M., P´erez-Pertejo, Y., Reguera, R.M., Castro, M.A´., Rojo, M.V., Santiago, C., Abad, A., García, P.A., Lo´pez-P´erez, J.L., San Feliciano, A., Balan˜a-Fouce, R., 2017. Antileishmanial activity and tubulin polymerization inhibition of podophyllotoxin derivatives on Leishmania infantum. Int. J. Parasitol. Drugs Drug Resist. 7, 272–285. https://doi.org/10.1016/j.ijpddr.2017.06.003.

Forli, S., Huey, R., Pique, M.E., Sanner, M.F., Goodsell, D.S., Olson, A.J., 2016. Computational protein-ligand docking and virtual drug screening with the AutoDock suite. Nat. Protoc. 11, 905–919. https://doi.org/10.1038/nprot.2016.051.

Furtado, L.F.V., de Paiva Bello, A.C.P., Rabelo, E´.M.L., 2016. Benzimidazole resistance in helminths: from problem to diagnosis. Acta Trop. https://doi.org/10.1016/j.actatropica.2016.06.021.

Garcia-Perez, C., Pelaez, R., Theron, R., Luis Lopez-Perez, J., 2017. JADOPPT: java based AutoDock preparing and processing tool. Bioinformatics 33, 583–585. https://doi.org/10.1093/bioinformatics/btw677.

Jain, V., Jain, K., 2018. Molecular targets and pathways for the treatment of visceral leishmaniasis. Drug Discov. Today. https://doi.org/10.1016/j.drudis.2017.09.006.

Jim´enez, M., Gonz´alez, E., Martín-Martín, I., Hern´andez, S., Molina, R., 2014. Could wild rabbits (Oryctolagus cuniculus) be reservoirs for Leishmania infantum in the focus of Madrid, Spain? Vet. Parasitol. 202, 296–300. https://doi.org/10.1016/j.vetpar.2014.03.027.

Jordan, A., Hadfield, J.A., Lawrence, N.J., McGown, A.T., 1998. Tubulin as a target for anticancer drugs: agents which interact with the mitotic spindle. Med. Res. Rev. 18, 259–296. https://doi.org/10.1002/(SICI)1098-1128.

Korb, O., Stützle, T., Exner, T.E., 2009. Empirical scoring functions for advanced Protein-Ligand docking with PLANTS. J. Chem. Inf. Model. 49, 84–96. https://doi.org/10.1021/ci800298z.

Lacey, E., 1990. Mode of action of benzimidazoles. Parasitol. Today 6, 112–115. https://doi.org/10.1016/0169-4758(90)90227-U.

Larkin, M.A., Blackshields, G., Brown, N.P., Chenna, R., Mcgettigan, P.A., McWilliam, H., Valentin, F., Wallace, I.M., Wilm, A., Lopez, R., Thompson, J.D., Gibson, T.J., Higgins, D.G., 2007. Clustal W and clustal X version 2.0. Bioinformatics 23, 2947–2948. https://doi.org/10.1093/bioinformatics/btm404.

Laurence, C., Brameld, K.A., Graton, J., Le Questel, J.Y., Renault, E., 2009. The pKBHX database: toward a better understanding of hydrogen-bond basicity for medicinal chemists. J. Med. Chem. https://doi.org/10.1021/jm801331y.

L´egar´e, D., Richard, D., Mukhopadhyay, R., Stierhof, Y.D., Rosen, B.P., Haimeur, A., Papadopoulou, B., Ouellette, M., 2001. The leishmania ATP-binding cassette protein PGPA is an intracellular metal-thiol transporter ATPase. J. Biol. Chem. 276, 26301–26307. https://doi.org/10.1074/jbc.M102351200.

Leifso, K., Cohen-Freue, G., Dogra, N., Murray, A., McMaster, W.R., 2007. Genomic and proteomic expression analysis of Leishmania promastigote and amastigote life stages: the Leishmania genome is constitutively expressed. Mol. Biochem. Parasitol. 152, 35–46. https://doi.org/10.1016/j.molbiopara.2006.11.009.

Luis, L., Serrano, M.L., Hidalgo, M., Mendoza-Leo´n, A., 2013. Comparative analyses of the β-tubulin gene and molecular modeling reveal molecular insight into the colchicine resistance in kinetoplastids organisms. BioMed Res. Int. 843748. https://doi.org/10.1155/2013/843748.

Marquis, N., Gourbal, B., Rosen, B.P., Mukhopadhyay, R., Ouellette, M., 2005. Modulation in aquaglyceroporin AQP1 gene transcript levels in drug-resistant Leishmania. Mol. Microbiol. 57, 1690–1699. https://doi.org/10.1111/j.1365-2958.2005.04782.x.

Marvin, 2017. ChemAxon [WWW Document]. URL, vol. 8. accessed 5.2.20. https://www.chemaxon.com.

Massarotti, A., Coluccia, A., Silvestri, R., Sorba, G., Brancale, A., 2012. The tubulin colchicine domain: a molecular modeling perspective. ChemMedChem. https://doi.org/10.1002/cmdc.201100361.

Mbongo, N., Loiseau, P.M., Billion, M.A., Robert-Gero, M., 1998. Mechanism of amphotericin B resistance in Leishmania donovani promastigotes. Antimicrob. Agents Chemother. 42, 352–357. https://doi.org/10.1128/AAC.00030-11.

Molina, R., Jim´enez, M.I., Cruz, I., Iriso, A., Martín-Martín, I., Sevillano, O., Melero, S., Bernal, J., 2012. The hare (Lepus granatensis) as potential sylvatic reservoir of Leishmania infantum in Spain. Vet. Parasitol. 190, 268–271. https://doi.org/10.1016/j.vetpar.2012.05.006.

Mondelaers, A., Sanchez-Can˜ete, M.P., Hendrickx, S., Eberhardt, E., Garcia-Hernandez, R., Lachaud, L., Cotton, J., Sanders, M., Cuypers, B., Imamura, H., Dujardin, J.-C., Delputte, P., Cos, P., Caljon, G., Gamarro, F., Castanys, S., Maes, L., 2016. Genomic and molecular characterization of miltefosine resistance in leishmania infantum strains with either natural or acquired resistance through experimental selection of intracellular amastigotes. PloS One 11, e0154101. https://doi.org/10.1371/journal.pone.0154101.

Montecinos-Franjola, F., Chaturvedi, S.K., Schuck, P., Sackett, D.L., 2019. All tubulins are not alike: heterodimer dissociation differs among different biological sources. J. Biol. Chem. 294, 10315–10324. https://doi.org/10.1074/jbc.RA119.007973.

Monzote, L., 2009. Current treatment of leishmaniasis: a review. Open Antimicrob. Agents J. https://doi.org/10.2174/1876518100901010009.

Nagle, A.S., Khare, S., Kumar, A.B., Supek, F., Buchynskyy, A., Mathison, C.J.N., Chennamaneni, N.K., Pendem, N., Buckner, F.S., Gelb, M.H., Molteni, V., 2014. Recent developments in drug discovery for leishmaniasis and human african trypanosomiasis. Chem. Rev. https://doi.org/10.1021/cr500365f.

OpenEye Scientific Software, 2019. [WWW Document]. URL. Inc, Santa Fe. accessed 5.2.20. https://www.eyesopen.com/.

P´erez-Victoria, F.J., Gamarro, F., Ouellette, M., Castanys, S., 2003. Functional cloning of the miltefosine transporter: a novel p-type phospholipid translocase from leishmania involved in drug resistance. J. Biol. Chem. 278, 49965–49971. https://doi.org/10.1074/jbc.M308352200.

P´erez-Victoria, F.J., S´anchez-Can˜ete, M.P., Seifert, K., Croft, S.L., Sundar, S., Castanys, S., Gamarro, F., 2006. Mechanisms of experimental resistance of Leishmania to miltefosine: implications for clinical use. Drug Resist. Updates 9, 26–39. https://doi.org/10.1016/j.drup.2006.04.001.

Perlovich, G.L., Kazachenko, V.P., Strakhova, N.N., Raevsky, O.A., 2014. Impact of sulfonamide structure on solubility and transfer processes in biologically relevant solvents. J. Chem. Eng. Data 59, 4217–4226. https://doi.org/10.1021/je500918t.

Pettersen, E.F., Goddard, T.D., Huang, C.C., Couch, G.S., Greenblatt, D.M., Meng, E.C., Ferrin, T.E., 2004. UCSF Chimera-A visualization system for exploratory research and analysis. J. Comput. Chem. 25, 1605–1612. https://doi.org/10.1002/jcc.20084.

Ponte-Sucre, A., Gamarro, F., Dujardin, J.C., Barrett, M.P., Lo´pez-V´elez, R., García-Herna´ndez, R., Pountain, A.W., Mwenechanya, R., Papadopoulou, B., 2017. Drug resistance and treatment failure in leishmaniasis: a 21st century challenge. PLoS Neglected Trop. Dis. https://doi.org/10.1371/journal.pntd.0006052.

Rama, M., Kumar, N.V., enkates, A., Balaji, S., 2015. A comprehensive review of patented antileishmanial agents. Pharm. Pat. Anal. https://doi.org/10.4155/ppa.14.55.

Rijal, S., Ostyn, B., Uranw, S., Rai, K., Bhattarai, N.R., Dorlo, T.P.C., Beijnen, J.H., Vanaerschot, M., Decuypere, S., Dhakal, S.S., Das, M.L., Karki, P., Singh, R., Boelaert, M., Dujardin, J.-C., 2013. Increasing failure of miltefosine in the treatment of Kala-azar in Nepal and the potential role of parasite drug resistance, reinfection, or noncompliance. Clin. Infect. Dis. 56, 1530–1538. https://doi.org/10.1093/cid/cit102.

Rochette, A., Raymond, F., Corbeil, J., Ouellette, M., Papadopoulou, B., 2009. Whole-genome comparative RNA expression profiling of axenic and intracellular amastigote forms of Leishmania infantum. Mol. Biochem. Parasitol. 165, 32–47. https://doi.org/10.1016/j.molbiopara.2008.12.012.

S˘ali, A., Blundell, T.L., 1993. Comparative protein modelling by satisfaction of spatial restraints. J. Mol. Biol. 234, 779–815. https://doi.org/10.1006/jmbi.1993.1626.

Scudiero, D.A., Shoemaker, R.H., Paull, K.D., Monks, A., Tierney, S., Nofziger, T.H., Currens, M.J., Seniff, D., Boyd, M.R., 1988. Evaluation of a soluble tetrazolium/formazan assay for cell growth and drug sensitivity in culture using human and other tumor cell lines. Canc. Res. 48, 4827–4833.

Sinclair, A.N., de Graffenried, C.L., 2019. More than microtubules: the structure and function of the subpellicular array in trypanosomatids. Trends Parasitol. https://doi.org/10.1016/j.pt.2019.07.008.

Sundar, S., Jha, T.K., Thakur, C.P., Engel, J., Sindermann, H., Fischer, C., Junge, K., Bryceson, A., Berman, J., 2002. Oral miltefosine for Indian visceral leishmaniasis. N. Engl. J. Med. 347, 1739–1746. https://doi.org/10.1056/NEJMoa021556.

Sundar, S., Jha, T.K., Thakur, C.P., Sinha, P.K., Bhattacharya, S.K., 2007. Injectable paromomycin for visceral leishmaniasis in India. N. Engl. J. Med. 356, 2571–2581. https://doi.org/10.1056/NEJMoa066536.

Sundar, S., Murray, H.W., 2005. Availability of miltefosine for the treatment of kala-azar in India. Bull. World Health Organ. 83, 394–395. https://doi.org/10.1590/S0042-96862005000500018.

Sunter, J., Gull, K., 2017. Shape, form, function and Leishmania pathogenicity: from textbook descriptions to biological understanding. Open Biol. https://doi.org/10.1098/rsob.170165.

Tiuman, T.S., Santos, A.O., Ueda-Nakamura, T., Filho, B.P.D., Nakamura, C.V., 2011. Recent advances in leishmaniasis treatment. Int. J. Infect. Dis. https://doi.org/10.1016/j.ijid.2011.03.021.

Vandermeulen, G., Rouxhet, L., Arien, A., Brewster, M.E., Pr´eat, V., 2006. Encapsulation of amphotericin B in poly(ethylene glycol)-block-poly(ε- caprolactone-co-trimethylenecarbonate) polymeric micelles. Int. J. Pharm. 309, 234–240. https://doi.org/10.1016/j.ijpharm.2005.11.031.

Vicente-Bla´zquez, A., Gonza´lez, M., A´lvarez, R., del Mazo, S., Medarde, M., Pel´aez, R., 2019. Antitubulin sulfonamides: the successful combination of an established drug class and a multifaceted target. Med. Res. Rev. 39, 775–830. https://doi.org/10.1002/med.21541.

Zhang, C., Bourgeade Delmas, S., Fern´andez A´lvarez, A´., Valentin, A., Hemmert, C., Gornitzka, H., 2018. Synthesis, characterization, and antileishmanial activity of neutral N-heterocyclic carbenes gold(I) complexes. Eur. J. Med. Chem. 143, 1635–1643. https://doi.org/10.1016/j.ejmech.2017.10.060.

Zulfiqar, B., Shelper, T.B., Avery, V.M., 2017. Leishmaniasis drug discovery: recent progress and challenges in assay development. Drug Discov. Today. https://doi.org/10.1016/j.drudis.2017.06.004.

MATERIAL SUPLEMENTARIO

El material suplementario del artículo 3 se encuentra disponible *online* en la siguiente dirección:

https://doi.org/10.1016/j.ijpddr.2021.02.006

Se compone de los siguientes apartados, lo cuales se desarrollan a continuación de esta página:

Table S1. Cellular cytotoxicity and selectivity index.

Supp S1. Materials and methods. Cellular cytotoxicity. IC_{50} calculation.

Table S2. Calculated properties for the active compounds.

Table S3. Docking results for the active compounds.

Figure SF1. Binding pose of compound **276B**.

Supp S2. Raw cytotoxicity data (online).

Table S1. Cellular cytotoxicity and selectivity index

Compound	Cellular cytotoxicity HeLa IC_{50} (µM)	Selectivity index[a]	
		Axenic amastigotes	Intracellular amastigotes[b]
129	2.4	2.6	0.16
276B	77	11.5	3.45
138	16	-	0.27
183	>100	-	-
242	>100	-	>1.9
316	>100	-	>1.8
124	51	-	1.3
132	9.4	-	0.22
117	55	-	1.6
35	>100	-	>1.2
26	>100	-	>1.5
84A	20	-	0.5
90	>100	-	>2.7
147	>100	-	>1.7
320	>100	-	>2.3
63B	95	-	3.5
Miltefosine	6.5	1.5	-

[a]The selectivity index was calculated: IC_{50}-cellular cytotoxicity/IC_{50}-antileishmanial activity. [b]IC_{50} values of antileishmanial activity against intracellular amastigotes were approximately calculated from % of infected U937 macrophages data.

Supp S1. Materials and methods. Cellular cytotoxicity. IC_{50} calculation

HeLa cell proliferation, when treated with the corresponding compounds, was determined using the XTT method as described in materials and methods. To determine cell viability, HeLa cells in exponential growth phase were seeded (100 µL/well in 96-well plates) at $1.5 \cdot 10^4$ cells/mL in complete DMEM medium at 37 °C and 5% CO_2 atmosphere. After 24 h incubation, to allow cells attach to the plates, all tested compounds were added at 100 µM concentration and the effect on the proliferation was evaluated 72 h post-treatment. Compounds showing antiproliferative effects at tested concentration were selected for IC_{50} calculation (50% inhibitory concentration with respect to the untreated controls) at 100, 50, 20 10 and 1 µM concentration. Non-linear curves fitting the experimental data were carried out for each compound. Compounds were dissolved in DMSO and the final solvent concentrations never exceeded 0.5% (v/v). The control wells included treated cells with 0.5% (v/v) DMSO and the positive control. Measurements were performed in triplicate, and each experiment was repeated two or three times.

Table S2. Calculated properties for the active compounds.

Mol	TPSA	iLOGP	XLOGP3	WLOGP	MLOGP	ESOL Class	Ali Class	Silicos-IT class	GI absorption	BBB permeant	Pgp substrate	CYP 1A2 inhibitor	CYP 2C19 inh	CYP 2C9 inh	CYP 2D6 inh	CYP 3A4 inh	log Kp (cm/s)	Lipinski #violations	Ghose #violations	Veber #violations	Egan #violations	Muegge #violations	Bioavailability Score	PAINS #alerts	Brenk #alerts	Leadlikeness #violations	Synthetic Accessibility
129	111.3	3.0	2.2	3.4	1.0	Soluble	Moderately soluble	Poorly soluble	High	No	No	No	Yes	Yes	Yes	Yes	-7.3	0	0	0	0	0	0.6	0	1	2	3.1
138	111.3	3.0	2.1	3.8	1.3	Soluble	Moderately soluble	Poorly soluble	High	No	No	No	Yes	Yes	Yes	Yes	-7.5	0	0	0	0	0	0.6	0	1	2	3.2
204	119.3	3.0	3.1	4.3	1.3	Moderately soluble	Moderately soluble	Moderately soluble	High	No	Yes	No	Yes	Yes	Yes	Yes	-6.9	0	0	0	0	0	0.6	0	2	1	3.5
183	128.1	2.3	2.2	3.3	0.4	Soluble	Moderately soluble	Moderately soluble	High	No	Yes	No	Yes	Yes	Yes	Yes	-7.0	0	0	0	0	0	0.6	0	2	1	3.3
332	76.3	3.4	4.7	5.6	3.3	Moderately soluble	Poorly soluble	Poorly soluble	High	No	Yes	No	Yes	Yes	Yes	Yes	-5.9	0	2	0	0	0	0.6	0	0	3	3.4
326 B	73.5	3.7	4.7	5.8	3.3	Moderately soluble	Poorly soluble	Poorly soluble	High	No	No	No	Yes	Yes	Yes	Yes	-6.0	0	2	0	0	0	0.6	0	0	3	3.3
275	67.5	3.7	4.2	5.1	2.9	Moderately soluble	Moderately soluble	Poorly soluble	High	No	Yes	No	Yes	Yes	Yes	Yes	-5.9	0	0	0	0	0	0.6	0	0	3	3.3
242	110.0	3.1	3.9	4.9	2.1	Moderately soluble	Moderately soluble	Poorly soluble	High	No	Yes	No	Yes	Yes	Yes	Yes	-6.2	0	0	0	0	0	0.6	0	2	3	3.2
320	97.0	2.0	1.6	2.4	0.7	Soluble	Soluble	Moderately soluble	High	No	No	No	No	Yes	No	No	-7.1	0	0	0	0	0	0.6	0	1	0	2.7
316	88.7	2.1	2.3	2.6	0.5	Soluble	Soluble	Moderately soluble	High	No	No	Yes	No	No	No	No	-6.5	0	0	0	0	0	0.6	0	0	0	2.7
279	77.1	3.5	3.3	4.4	2.0	Moderately soluble	Moderately soluble	Poorly soluble	High	No	No	Yes	Yes	Yes	Yes	Yes	-6.3	0	0	0	0	0	0.6	0	0	1	3.2
84A	116.1	2.2	1.6	2.8	1.0	Soluble	Soluble	Moderately soluble	High	No	No	No	No	Yes	No	No	-7.2	0	0	0	0	0	0.6	0	1	0	2.6
90	113.1	1.8	1.7	2.9	-0.2	Soluble	Soluble	Moderately soluble	High	No	No	No	No	Yes	No	No	-7.1	0	0	0	0	0	0.6	0	0	0	2.6
147	136.3	3.5	3.1	5.3	1.7	Moderately soluble	Moderately soluble	Poorly soluble	Low	No	Yes	No	Yes	Yes	No	Yes	-7.3	1	2	0	1	0	0.6	0	0	2	3.5
276 B	148.6	3.5	3.2	5.1	1.8	Moderately soluble	Poorly soluble	Poorly soluble	Low	No	Yes	No	Yes	Yes	No	Yes	-6.9	0	0	1	1	0	0.6	0	1	2	3.6
63B	185.6	3.3	3.7	4.2	0.3	Moderately soluble	Poorly soluble	Poorly soluble	Low	No	No	No	No	Yes	Yes	No	-7.4	2	3	2	1	3	0.1	0	0	3	4.2
334	164.7	1.8	2.6	3.2	-0.2	Soluble	Moderately soluble	Soluble	Low	No	Yes	No	Yes	Yes	Yes	Yes	-6.8	1	0	1	1	1	0.6	0	2	1	3.2
124	102.6	2.7	1.7	3.0	1.2	Soluble	Soluble	Moderately soluble	High	No	No	No	Yes	Yes	Yes	Yes	-7.4	0	0	0	0	0	0.6	0	1	2	3.2
132	96.6	2.7	1.9	3.1	1.4	Soluble	Soluble	Moderately soluble	High	No	Yes	No	Yes	Yes	Yes	Yes	-7.4	0	0	0	0	0	0.6	0	1	2	3.3
117	94.9	2.5	2.4	2.8	2.4	Soluble	Moderately soluble	Moderately soluble	High	No	No	Yes	Yes	Yes	No	No	-6.8	0	0	0	0	0	0.6	0	0	1	3.4
26	99.0	2.0	1.5	3.0	1.0	Soluble	Soluble	Moderately soluble	High	No	No	No	No	Yes	No	Yes	-7.1	0	0	0	0	0	0.6	0	1	0	2.6

Table S3. Docking Results.

Compound DokingProg_Ligand_pdbID_(conf)_number	**pdBID/ Homol**	**Site**	**Zscore**	**PLANTS score**	**AD4 score**
M204A1					
AD4_M204A1_5LYJ_29	5LYJ	AB	1.0		-7.6
PLANTS_M204A1_5XAF_conf_01	5XAF	AB	0.9	-74.6	
AD4_M204A1_Lmaj_MKL_4H_52	4H	AB	0.7		-5.7
M332					
AD4_M332_5LYJ_67	5LYJ	AB	1.0		-10.9
PLANTS_M332_5GON_conf_01	5GON	AB	1.0	-99.0	
AD4_M332_Lbr_IKI_4H_85	4H	AB	0.8		-8.3
PLANTS_M332_Lmaj_MKL_4H_conf_02	4H	AB	0.8	-87.4	
M129					
PLANTS_M129_5GON_conf_01	5GON	AB	1.0	-88.2	
AD4_M129_5XAF_55	5XAF	AB	1.0		-9.0
AD4_M129_Lmaj_MKL_4H_78	4H	AB	1.0		-8.3
PLANTS_M129_Lmaj_MKL_4H_conf_02	4H	AB	0.9	-80.5	
M326B					
PLANTS_M326B_5CB4_conf_01	5CB4	AB	1.0	-99.2	
AD4_M326B_5XAF_31	5XAF	AB	1.0		-10.4

AD4_M326B_Lbr_IKI_2H_82	2H	AB	1.0		-8.7
PLANTS_M326B_Lsp_MKI_4H_conf_01	4H	AB	0.7	-74.3	
M275					
PLANTS_M275_5CB4_conf_01	5CB4	AB	1.0	-110.2	
AD4_M275_5YLJ_75	5YLJ	AB	0.9		-9.2
PLANTS_M275_Lbr_IKI_4H_conf_03	4H	AB	0.8	-93.5	
AD4_M275_Lsp_MKI_4H_41	4H	AB	0.8		-7.7
M334					
PLANTS_M334_5XAF_conf_02	5XAF	AB	0.9	-75.4	
AD4_M334_5XAF_20	5XAF	AB	0.7		-5.6
AD4_M334_Lgu_MMI_2H_68	2H	AB	0.7		-5.0
PLANTS_M334_Lmaj_MKI_3H_conf_02	3H	AB	0.5	-57.2	
PLANTS_M334_Lbr_IKI_2H_conf_01	2H	ACD	1.0	-69.2	
AD4_M334_Lbr_IKI_2H_43	2H	ACD	0.8		-5.4
M279					
AD4_M279_5LYJ_78	5LYJ	AB	0.8		-7.1
PLANTS_M279_5LYJ_conf_01	5LYJ	AB	0.7	-87.4	
AD4_M279_Lsp_MKI_1H_51	1H	AB	0.9		-6.4
PLANTS_M279_Lmaj_MKL_4H_conf_04	4H	AB	0.6	-78.1	
M320					
AD4_M320_5LYJ_51	5LYJ	Aba	0.8		-7.2

PLANTS_M320_5LYJ_conf_01	5LYJ	ABa	0.8	-87.4	
PLANTS_M320_5XAF_conf_03	5XAF	ABb	0.8	-87.8	
AD4_M320_5LYJ_7	5LYJ	ABb	0.7		-6.8
AD4_M320_Lmaj_MKI_1H_80	1H	AB	0.8		-6.3
M84					
AD4_M84_5XKG_24	5XKG	AB	0.8		-10.0
PLANTS_M84_5CB4_conf_01	5CB4	AB	0.8	-92.4	
AD4_M84_Lgu_MMI_2H_51	2H	AB	0.7		-8.5
PLANTS_M84_Lmaj_MKL_4H_conf_02	4H	AB	0.6	-81.9	
M183					
PLANTS_M183_6H9B_conf_01	6H9B	AB	0.9	-79.5	
AD4_M183_6BRY_4	6BRY	AB	0.9		-7.0
AD4_M183_Lmaj_MKI_1H_54	1H	AB	0.8		-6.2
PLANTS_M183_Lmaj_MKL_2H_conf_06	2H	AB	0.5	-61.1	
M138					
PLANTS_M138_5XAF_conf_01	5XAF	AB	1.0	-86.5	
AD4_M138_5XAG_2	5XAG	AB	1.0		-9.5
AD4_M138_Lbr_IKI_3H_65	3H	AB	0.9		-7.5
PLANTS_M138_Lmaj_MKL_2H_conf_02	2H	AB	0.7	-75.1	
M26					

AD4_M26_6BRY_89	6BRY	AB	0.9		-8.0
PLANTS_M26_5XAG_conf_01	5XAG	AB	0.8	-81.6	
AD4_M26_Lmaj_MKI_1H_17	1H	AB	0.8		-7.3
PLANTS_M26_Lmaj_MKI_1H_conf_01	1H	AB	0.5	-70.5	
M132					
AD4_M132_5XAG_56	5XAG	AB	1.0		-7.7
PLANTS_M132_5CB4_conf_01	5CB4	AB	0.9	-87.0	
AD4_M132_Lmaj_MKI_3H_65	3H	AB	0.8		-5.7
PLANTS_M132_Lmaj_MKL_4H_conf_01	4H	AB	0.8	-77.0	
M124					
AD4_M124_3HKC_67	3HKC	AB	0.9		-8.2
PLANTS_M124_6GJ4_conf_01	6GJ4	AB	0.9	-83.5	
AD4_M124_Lmaj_MKI_1H_5	1H	AB	0.9		-7.2
PLANTS_M124_Lmaj_MKL_4H_conf_02	4H	AB	0.8	-74.6	
M117					
PLANTS_M117_5GON_conf_01	5GON	Aba	1.0	-85.5	
AD4_M117_5LYJ_40	5LYJ	ABa	0.9		-8.4
PLANTS_M117_6GJ4_conf_02	6GJ4	ABb	0.9	-83.0	
AD4_M117_5LYJ_72	5LYJ	ABb	0.9		-8.3
AD4_M117_Lsp_MKI_5H_24	5H	AB	0.9		-7.0
PLANTS_M117_Lbr_IKI_3H_conf_01	3H	AB	0.9	-72.1	

M90					
AD4_M90_5JVD_21	5JVD	AB	0.8		-8.9
PLANTS_M90_5NFZ_conf_04	5NFZ	AB	0.7	-72.5	
AD4_M90_Lsp_MKI_5H_7	5H	AB	0.7		-8.1
PLANTS_M90_Lmaj_MKI_4H_conf_01	4H	AB	0.5	-61.6	
M90a					
AD4_M90a_5JVD_4	5JVD	ABa	0.9		-8.3
PLANTS_4MeOPh_M90a_5NFZ_conf_01	5NFZ	ABa	0.8	-75.8	
AD4_M90a_5JVD_62	5JVD	ABb	0.8		-8.1
PLANTS_M90a_5JVD_conf_01	5JVD	ABb	0.8	-73.5	
PLANTS_M90a_Lmaj_MKI_3H_conf_01	3H	AB	0.8	-67.2	
AD4_M90a_Lsp_MKI_5H_12	5H	AB	0.7		-6.9
M147					
AD4_M147_3HKD_76	3HKD	ABC	1.0		-10.8
AD4_M147_Lmaj_MKL_2H_14	2H	ABC	0.8		-7.6
M242					
AD4_M242_6BRY_50	6BRY	AB	0.6		-6.5
PLANTS_M242_5GON_conf_01	5GON	AB	0.6	-80.0	
PLANTS_M242_Lmaj_MKI_3H_conf_01	3H	AB	0.7	-71.1	
AD4_M242_Lmaj_MKI_5H_9	5H	AB	0.6		-5.8

M316					
AD4_M316_5LYJ_23	5LYJ	AB	0.8		-7.4
PLANTS_M316_5GON_conf_01	5GON	AB	0.7	-84.9	
PLANTS_M316_Lbr_IKI_2H_conf_04	2H	AB	0.5	-75.5	
AD4_M316_Lbr_IKI_3H_69	3H	AB	0.4		-5.8
M35					
AD4_M35_5XAF_5	5XAF	AB	1.0		-8.3
PLANTS_M35_5GON_conf_01	5GON	AB	0.9	-59.1	
AD4_M35_Lmaj_MKI_3H_5	3H	AB	1.0		-7.1
PLANTS_M35_Lmaj_MKI_3H_conf_02	3H	AB	0.7	-48.3	

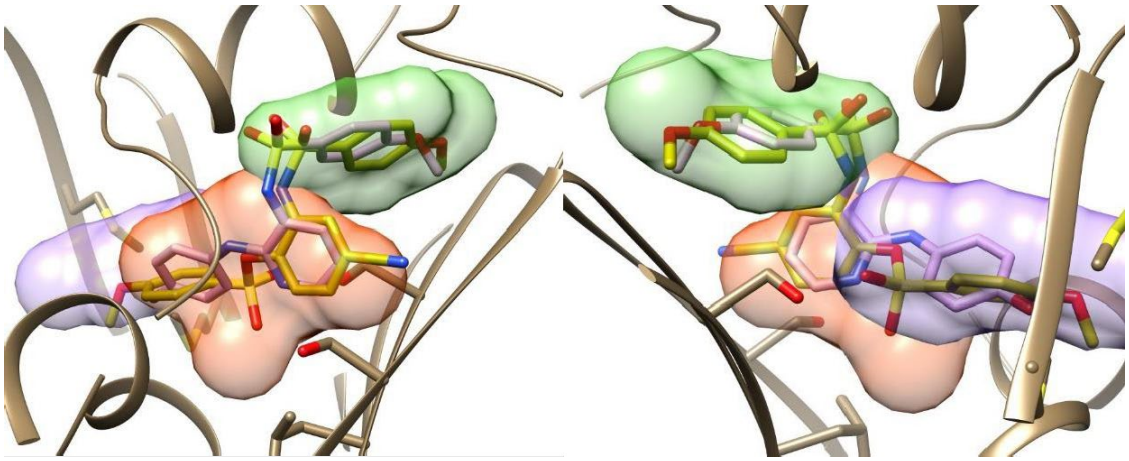

Figure SF1. Binding mode of **276B** superposed to the X-ray structure of ABT-751 at the colchicine site, showing a fair adjustment to the colchicine site. ABT-751 is shown with carbons in light pink and **276B** with carbons in yellow. The protein secondary structure elements are shown as gray cartoons and the binding zones volumes colored.

conclusiones

"Cuando crees que conoces todas las respuestas, llega el Universo y te cambia todas las preguntas."

Jorge F. Pinto

En este trabajo de Tesis Doctoral se ha llevado a cabo el diseño, la síntesis y la evaluación de nuevas *N*-fenilbencenosulfonamidas en las que se han explorado numerosas modificaciones estructurales en los sustituyentes sobre ambos anillos aromáticos y el nitrógeno de la sulfonamida. Se han obtenido y caracterizado 350 compuestos que se han evaluado como agentes citotóxicos frente a varias líneas celulares de tumores humanos y diferentes estadios del protozoo parásito *Leishmania infantum*, el agente causal de la leishmaniasis visceral en la cuenca mediterránea. Finalmente, se ha estudiado el mecanismo de acción de los compuestos más prometedores de cada familia y se ha planteado un modo de unión a la diana propuesta, la tubulina.

De los resultados obtenidos se pueden extraer las siguientes conclusiones:

- El elevado porcentaje de compuestos sintetizados que presentan actividad antitumoral y/o leishmanicida valida la estrategia de diseño utilizada.
- Las diferencias en las secuencias de aminoácidos entre la tubulina de mamíferos y la de *Leishmania* spp. posibilitan encontrar ligandos activos frente a una u otra especie. Aunque, debido a la sutileza de estas diferencias, también se encuentran compuestos activos frente a ambas especies.
- La metodología sintética empleada es adecuada para obtener los esqueletos de *N*-fenilbencenosulfonamida en cantidades y pureza suficientes. La modificación posterior de los esqueletos permite introducir variabilidad en las familias con muy buenos rendimientos en la mayoría de los casos.
- La sustitución del puente olefínico de las combretastatinas por un puente de sulfonamida, conservando el Ar_A convencional de 3,4,5-trimetoxifenilo (TMP), mantiene la actividad antiproliferativa sobre líneas celulares de tumores humanos y mejora en muchos casos la presentada por la sulfonamida de referencia ABT-751.
- La sustitución del grupo hidroxilo del Ar_B de la CA-4, metabólicamente inestable, por grupos solubilizadores, tales como aminas primarias, o el reemplazo del metoxilo de la posición 4 por aminas secundarias, conlleva al aumento de la potencia citotóxica de las nuevas sulfonamidas.
- Los estudios de relación estructura-actividad sobre líneas celulares tumorales humanas muestran que un Ar_A de TMP puede conferir potencias comparables a las de los taxanos.
- El "*scan*" estructural con grupos metoxilo y/o bromo permite descubrir alternativas al anillo de TMP, habiendo resultado muy favorable la agrupación 4-bromo-2,5-dimetoxifenilo, especialmente frente a la línea tumoral de cáncer de mama MCF7.
- La metilación del nitrógeno de la sulfonamida, independientemente de los sustituyentes presentes en ambos anillos aromáticos, incrementa la potencia antitumoral, dando lugar en la mayoría de los casos a los derivados más potentes. La introducción de sustituyentes muy voluminosos lleva a la disminución o incluso a la pérdida de la actividad antiproliferativa. Sin embargo, sustituyentes solubilizadores como grupos nitrilo, que puedan contrarrestar la pérdida del hidrógeno de la sulfonamida sin sustituir, mantienen la potencia e incluso en algunos caso la mejoran.
- La gran mayoría de los compuestos ensayados no son sustratos de las proteínas de membrana MDR, principal causa de resistencias frente a fármacos antitumorales, puesto que el co-tratamiento con verapamilo (inhibidor de MDR) no aumenta la potencia antiproliferativa en la línea celular HT-29.

- Los estudios de mecanismo de acción antitumoral llevados a cabo sobre los compuestos seleccionados confirman que ejercen su acción gracias a la interferencia con el sistema de microtúbulos, ya que: i) los ligandos inhiben la polimerización de proteína microtubular *in vitro*, ii) desencadenan parada mitótica bloqueando el ciclo celular en G_2/M, iii) producen un incremento en las poblaciones de células que sufren apoptosis y iv) desestabilizan la red de microtúbulos afectando también a la organización de la cromatina en los núcleos celulares.
- La biblioteca de sulfonamidas sintetizada no presenta efecto leishmanicida sobre formas extracelulares del estadio de promastigote del parásito *L. infantum*. Sin embargo, un total de 8 compuestos son activos frente a amastigotes axénicos, el estadio clínicamente relevante en el huésped mamífero.
- El 10% de las sulfonamidas no citotóxicas ensayadas frente a amastigotes intracelulares impiden el avance de la infección en macrófagos infectados por *L. infantum*.
- Los estudios de relación estructura-actividad sobre parásitos establecen que de entre todas las modificaciones realizadas en el Ar_A, anillos de 3,4-, 3,5- y 2,5-dimetoxifenilo, 6-metoxi-3-piridilo o 3-carboxi-5-aminofenilo, así como sulfonamidas tricíclicas favorecen la actividad leishmanicida al tiempo que reducen la citotoxicidad frente a células de mamífero.
- Los compuestos con Ar_A de 2,5-dimetoxifenilo presentan actividad leishmanicida y antiproliferativa, confiriéndoles el sustituyente en la posición 4 la selectividad entre especies: un bromo proporciona actividad antitumoral, mientras que una urea los hace antiparasitarios.
- La ausencia de sustitución sobre el nitrógeno de la sulfonamida favorece la actividad leishmanicida frente a la citotóxica.
- Los estudios de *docking* realizados sobre las tubulinas de mamífero y de *Leishmania* sugieren una interacción de unión muy favorable con la proteína, consistente con los modos de unión de otros fármacos conocidos del dominio de la colchicina.
- La solubilidad acuosa de las nuevas sulfonamidas antimitóticas es apreciablemente mayor que la de los ligandos de referencia CA-4 y Anfotericina B.

CONCLUSIONS

In this Ph.D. thesis, we have designed, synthesized, and evaluated novel *N*-phenylbenzenesulfonamides in which numerous structural modifications have been explored in the substituents on both aromatic rings and the sulfonamide nitrogen. 350 compounds have been obtained and characterized as cytotoxic agents against several human tumor cell lines and different stages of the parasitic protozoan *Leishmania infantum*, the causative agent of visceral leishmaniasis in the Mediterranean area. Finally, the mechanism of action of the most promising compounds of each family has been studied and a way of binding to the proposed target, tubulin, has been proposed.

The following conclusions can be drawn from the results obtained:

- The high percentage of compounds synthesized that present antitumor and/or antileishmanial activity validates the design strategy used.
- Differences in amino acid sequences between mammalian and *Leishmania* spp. tubulins allow to find active ligands against one or another species. Although, due to the subtlety of these differences, active compounds are also found against both species.
- The synthetic procedures used in this work are adequate to obtain the *N*-phenylbenzenesulfonamide scaffolds in sufficient quantities and purity. The subsequent modifications allow to introduce family variability in good yields in most cases.
- The replacement of the olefinic bridge of the combretastatins by a sulfonamide bridge, preserving the conventional 3,4,5-trimethoxyphenyl (TMP) Ar_A, maintains the antiproliferative activity against human tumor cell lines, and in many cases, improves that of the reference sulfonamide ABT-751.
- The replacement of the metabolically unstable hydroxyl group of the CA-4 Ar_B by solubilizing groups such as primary amines, or the 4-position methoxy group by secondary amines leads to an increase in the potency of the novel sulfonamides.
- Structure-activity relationship studies on human tumor cell lines establish that the TMP Ar_A confers comparable potencies to those of taxanes.
- The structural scan with methoxy and/or bromine groups allows us to discover alternatives to the TMP ring, being the 4-bromo-2,5-dimethoxyphenyl residue very favorable, especially against the MCF7 breast cancer cell line.
- The methylation of the sulfonamide nitrogen, independently of aromatic rings substitution pattern, increases the antitumor potency, leading in most cases to the most potent derivatives. The introduction of bulky substituents leads to a decrease or even loss of antiproliferative activity. However, solubilizing substituents such as nitrile groups, which can counteract the loss of the hydrogen from the unsubstituted sulfonamide, maintain potency and even in some cases improve it.
- Most of the tested ligands are not substrates of the MDR membrane proteins, the main cause of resistance against antitumor drugs, since co-treatment with verapamil (MDR inhibitor) does not increase the antiproliferative potency in the HT-29 cell line.
- The studies of antitumor mechanism of action, carried out with selected compounds, confirm that they exert their action through the interference with the microtubule system, since: i) the ligands inhibit the polymerization of microtubular protein *in vitro*, ii) they trigger mitotic arrest by blocking the cell cycle in G_2/M, iii) they increase cell populations that undergo apoptosis and, iv) they destabilize the microtubule network, also affecting the chromatin organization in cell nuclei.

- The synthesized sulfonamide library does not show antileishmanial effect on extracellular forms of the promastigote stage of the *L. infantum* parasite. However, a total of 8 compounds are active against axenic amastigotes, the clinically relevant stage in the mammalian host.
- 10% of the non-cytotoxic sulfonamides tested against intracellular amastigotes prevent the progression of infection in infected macrophages by *L. infantum*.
- Structure-activity relationship studies on parasites establish that, within all modifications made in Ar_A, rings of 3,4-, 3,5- and 2,5-dimethoxyphenyl, 6-methoxy-3-pyridyl or 3-carboxy-5-aminophenyl, as well as tricyclic sulfonamides, promote antileishmanial activity while reducing cytotoxicity against mammalian cells.
- Compounds with 2,5-dimethoxyphenyl Ar_A show antileishmanial and antiproliferative activity, with the substituent in position 4 conferring selectivity between species: a bromine provides antitumor activity, while a urea makes them antiparasitic.
- The absence of substituents on the sulfonamide nitrogen favors the antileishmanial activity over the cytotoxic one.
- Docking studies performed on mammalian and *Leishmania* tubulins suggest a very favorable binding interaction with the protein, consistent with the binding modes of other known colchicine-domain binding drugs.
- The aqueous solubility of the new antimitotic sulfonamides is appreciably greater than that of the reference ligands CA-4 and Amphotericin B.

bibliografía

"Lee y conducirás,
no leas y serás conducido."

Santa Teresa de Jesús

(1) Schafer, K. A. The Cell Cycle: A Review. *Vet. Pathol.* **1998**, *35* (6), 461–478. https://doi.org/10.1177/030098589803500601.

(2) Schmidt, M.; Bastians, H. Mitotic Drug Targets and the Development of Novel Anti-Mitotic Anticancer Drugs. *Drug Resist. Updat.* **2007**, *10* (4–5), 162–181. https://doi.org/10.1016/j.drup.2007.06.003.

(3) Kastan, M. B.; Bartek, J. Cell-Cycle Checkpoints and Cancer. *Nature* **2004**, *432* (7015), 316–323. https://doi.org/10.1038/nature03097.

(4) Musacchio, A.; Salmon, E. D. The Spindle-Assembly Checkpoint in Space and Time. *Nat. Rev. Mol. Cell Biol.* **2007**, *8* (5), 379–393. https://doi.org/10.1038/nrm2163.

(5) Castedo, M.; Perfettini, J. L.; Roumier, T.; Andreau, K.; Medema, R.; Kroemer, G. Cell Death by Mitotic Catastrophe: A Molecular Definition. *Oncogene* **2004**, 2825–2837. https://doi.org/10.1038/sj.onc.1207528.

(6) Vakifahmetoglu, H.; Olsson, M.; Zhivotovsky, B. Death through a Tragedy: Mitotic Catastrophe. *Cell Death Differ.* **2008**, *15* (7), 1153–1162. https://doi.org/10.1038/cdd.2008.47.

(7) Bates, D.; Eastman, A. Microtubule Destabilising Agents: Far More than Just Antimitotic Anticancer Drugs. *Br. J. Clin. Pharmacol.* **2017**, *83* (2), 255–268. https://doi.org/10.1111/bcp.13126.

(8) Dumontet, C.; Jordan, M. A. Microtubule-Binding Agents: A Dynamic Field of Cancer Therapeutics. *Nat. Rev. Drug Discov.* **2010**, *9* (10), 790–803. https://doi.org/10.1038/nrd3253.

(9) Sakurikar, N.; Eichhorn, J. M.; Chambers, T. C. Cyclin-Dependent Kinase-1 (Cdk1)/Cyclin B1 Dictates Cell Fate after Mitotic Arrest via Phosphoregulation of Antiapoptotic Bcl-2 Proteins. *J. Biol. Chem.* **2012**, *287* (46), 39193–39204. https://doi.org/10.1074/jbc.M112.391854.

(10) Zhou, L.; Cai, X.; Han, X.; Xu, N.; Chang, D. C. CDK1 Switches Mitotic Arrest to Apoptosis by Phosphorylating Bcl-2/Bax Family Proteins during Treatment with Microtubule Interfering Agents. *Cell Biol. Int.* **2014**, *38* (6), 737–746. https://doi.org/10.1002/cbin.10259.

(11) Mollinedo, F.; Gajate, C. Microtubules, Microtubule-Interfering Agents and Apoptosis. *Apoptosis* **2003**, *8* (5), 413–450. https://doi.org/10.1023/A:1025513106330.

(12) Nagle, A.; Hur, W.; Gray, N. Antimitotic Agents of Natural Origin. *Curr. Drug Targets* **2006**, *7* (3), 305–326. https://doi.org/10.2174/138945006776054933.

(13) Jackson, J. R.; Patrick, D. R.; Dar, M. M.; Huang, P. S. Targeted Anti-Mitotic Therapies: Can We Improve on Tubulin Agents? *Nat. Rev. Cancer* **2007**, *7* (2), 107–117. https://doi.org/10.1038/nrc2049.

(14) Penna, L. S.; Henriques, J. A. P.; Bonatto, D. Anti-Mitotic Agents: Are They Emerging Molecules for Cancer Treatment? *Pharmacol. Ther.* **2017**, *173*, 67–82. https://doi.org/10.1016/j.pharmthera.2017.02.007.

(15) Olziersky, A. M.; Labidi-Galy, S. I. Clinical Development of Anti-Mitotic Drugs in Cancer. *Adv. Exp. Med. Biol.* **2017**, *1002*, 125–152. https://doi.org/10.1007/978-3-319-57127-0_6.

(16) Paclitaxel - National Cancer Institute https://www.cancer.gov/about-cancer/treatment/drugs/paclitaxel (accessed Mar 10, 2021).

(17) Prostate Cancer Treatment (PDQ®)–Health Professional Version - National Cancer Institute https://www.cancer.gov/types/prostate/hp/prostate-treatment-pdq#_71 (accessed Mar 10, 2021).

(18) Treatment for Cancer - National Cancer Institute https://www.cancer.gov/about-cancer/treatment (accessed Mar 10, 2021).

(19) Dempsey, E.; Prudêncio, M.; Fennell, B. J.; Gomes-Santos, C. S.; Barlow, J. W.; Bell, A. Antimitotic Herbicides Bind to an Unidentified Site on Malarial Parasite Tubulin and Block Development of Liver-Stage Plasmodium Parasites. *Mol. Biochem. Parasitol.* **2013**, *188* (2), 116–127. https://doi.org/10.1016/j.molbiopara.2013.03.001.

(20) Blume, Y. B.; Nyporko, A. Y.; Yemets, A. I.; Baird, W. V. Structural Modeling of the Interaction of Plant α-Tubulin with Dinitroaniline and Phosphoroamidate Herbicides. *Cell Biol. Int.* **2003**, *27* (3), 171–174. https://doi.org/10.1016/S1065-6995(02)00298-6.

(21) Stanton, R. A.; Gernert, K. M.; Nettles, J. H.; Aneja, R. Drugs That Target Dynamic Microtubules: A New Molecular Perspective. *Med. Res. Rev.* **2011**, *31* (3), 443–481. https://doi.org/10.1002/med.20242.

(22) Benzimidazoles - an overview | ScienceDirect Topics https://www.sciencedirect.com/topics/neuroscience/benzimidazoles (accessed Mar 10, 2021).

(23) Kiselyov, A.; Balakin, K.; Tkachenko, S.; Savchuk, N.; Ivachtchenko, A. Recent Progress in Discovery and Development of Antimitotic Agents. *Anticancer. Agents Med. Chem.* **2008**, *7* (2), 189–208. https://doi.org/10.2174/187152007780058650.

(24) Čermák, V.; Dostál, V.; Jelínek, M.; Libusová, L.; Kovář, J.; Rösel, D.; Brábek, J. Microtubule-Targeting Agents and Their Impact on Cancer Treatment. *Eur. J. Cell Biol.* **2020**, *99* (4), 151075. https://doi.org/10.1016/j.ejcb.2020.151075.

(25) Dumontet, C.; Jordan, M. A. Microtubule-Binding Agents: A Dynamic Field of Cancer Therapeutics. *Nat. Rev. Drug Discov.* **2010**, 790–803. https://doi.org/10.1038/nrd3253.

(26) Jordan, M. A.; Wilson, L. Microtubules As a Target for Anticancer Drugs. *Nat. Rev. Cancer* **2004**, *4*, 253–263. https://doi.org/10.1038/nr1317.

(27) Escudero-Martínez, J. M.; Pérez-Pertejo, Y.; Reguera, R. M.; Castro, M. Á.; Rojo, M. V.; Santiago, C.; Abad, A.; García, P. A.; López-Pérez, J. L.; San Feliciano, A.; Balaña-Fouce, R. Antileishmanial Activity and Tubulin Polymerization Inhibition of Podophyllotoxin Derivatives on Leishmania Infantum. *Int. J. Parasitol. Drugs Drug Resist.* **2017**, *7* (3), 272–285. https://doi.org/10.1016/j.ijpddr.2017.06.003.

(28) Jordan, M. A.; Wilson, L. Microtubules as a Target for Anticancer Drugs. *Nat. Rev. Cancer* **2004**, *4* (4), 253–265. https://doi.org/10.1038/nrc1317.

(29) Sinclair, A. N.; de Graffenried, C. L. More than Microtubules: The Structure and Function of the Subpellicular Array in Trypanosomatids. *Trends Parasitol.* **2019**, *35* (10), 760–777. https://doi.org/10.1016/j.pt.2019.07.008.

(30) Sunter, J.; Gull, K. Shape, Form, Function and Leishmania Pathogenicity: From Textbook Descriptions to Biological Understanding. *Open Biol.* **2017**, *7* (9). https://doi.org/10.1098/rsob.170165.

(31) Nogales, E.; Wolf, S. G.; Downing, K. H. Structure of the Aβ Tubulin Dimer by Electron Crystallography. *Nature* **1998**, *391* (6663), 199–203. https://doi.org/10.1038/34465.

(32) Ludueña, R. F. Multiple Forms of Tubulin: Different Gene Products and Covalent Modifications. *Int. Rev. Cytol.* **1998**, *178*, 207–275. https://doi.org/10.1016/s0074-7696(08)62138-5.

(33) Prassanawar, S. S.; Panda, D. Tubulin Heterogeneity Regulates Functions and Dynamics of Microtubules and Plays a Role in the Development of Drug Resistance in Cancer. *Biochem. J.* **2019**, *476* (9), 1359–1376. https://doi.org/10.1042/BCJ20190123.

(34) Leandro-García, L. J.; Leskelä, S.; Landa, I.; Montero-Conde, C.; López-Jiménez, E.; Letón, R.; Cascón, A.; Robledo, M.; Rodríguez-Antona, C. Tumoral and Tissue-Specific Expression of the Major Human β-Tubulin Isotypes. *Cytoskeleton* **2010**, *67*, 214–223. https://doi.org/10.1002/cm.20436.

(35) Lewis, S. A.; Gu, W.; Cowan, N. J. Free Intermingling of Mammalian β-Tubulin Isotypes among Functionally Distinct Microtubules. *Cell* **1987**, *49*, 539–548. https://doi.org/10.1016/0092-8674(87)90456-9.

(36) Löwe, J.; Li, H.; Downing, K. H.; Nogales, E. Refined Structure of Aβ-Tubulin at 3.5 Å Resolution. *J. Mol. Biol.* **2001**, *313* (5), 1045–1057. https://doi.org/10.1006/jmbi.2001.5077.

(37) Wilson, L.; Jordan, M. A. Microtubule Dynamics: Taking Aim at a Moving Target. *Chem. Biol.* **1995**, *2* (9), 569–573. https://doi.org/10.1016/1074-5521(95)90119-1.

(38) Brouhard, G. J.; Rice, L. M. Microtubule Dynamics: An Interplay of Biochemistry and Mechanics. *Nat. Rev. Mol. Cell Biol.* **2018**, *19* (7), 451–463. https://doi.org/10.1038/s41580-018-0009-y.

(39) Heald, R.; Nogales, E. Microtubule Dynamics. *J. Cell Sci.* **2002**, *115* (1).

(40) Jordan, A.; Hadfield, J. A.; Lawrence, N. J.; McGown, A. T. Tubulin as a Target for Anticancer Drugs: Agents Which Interact with the Mitotic Spindle. *Med. Res. Rev.* **1998**, *18* (4), 259–296. https://doi.org/10.1002/(SICI)1098-1128(199807)18:4<259::AID-MED3>3.0.CO;2-U.

(41) Horwitz, S. B.; Lothstein, L.; Manfredi, J. J.; Mellado, W.; Parness, J.; Roy, S. N.; Schiff, P. B.; Sorbara, L.; Zeheb, R. Taxol: Mechanisms of Action and Resistance. *Ann. N. Y. Acad. Sci.* **1986**, *466* (1), 733–744. https://doi.org/10.1111/j.1749-6632.1986.tb38455.x.

(42) Schiff, P. B.; Fant, J.; Horwitz, S. B. Promotion of Microtubule Assembly *in Vitro* by Taxol. *Nature* **1979**, *277* (5698), 665–667. https://doi.org/10.1038/277665a0.

(43) Ravelli, R. B. G.; Gigant, B.; Curmi, P. A.; Jourdain, I.; Lachkar, S.; Sobel, A.; Knossow, M. Insight into Tubulin Regulation from a Complex with Colchicine and a Stathmin-like Domain. *Nature* **2004**, *428* (6979), 198–202. https://doi.org/10.1038/nature02393.

(44) Massarotti, A.; Coluccia, A.; Silvestri, R.; Sorba, G.; Brancale, A. The Tubulin Colchicine Domain: A Molecular Modeling Perspective. *ChemMedChem* **2012**, *7* (1), 33–42. https://doi.org/10.1002/cmdc.201100361.

(45) Pérez-Pérez, M. J.; Priego, E. M.; Bueno, O.; Martins, M. S.; Canela, M. D.; Liekens, S. Blocking Blood Flow to Solid Tumors by Destabilizing Tubulin: An Approach to Targeting Tumor Growth. *J. Med. Chem.* **2016**, *59* (19), 8685–8711. https://doi.org/10.1021/acs.jmedchem.6b00463.

(46) Jane Lunt, S.; Akerman, S.; Hill, S. A.; Fisher, M.; Wright, V. J.; Reyes-Aldasoro, C. C.; Tozer, G. M.; Kanthou, C. Vascular Effects Dominate Solid Tumor Response to Treatment with Combretastatin A-4-Phosphate. *Int. J. Cancer* **2011**, *129* (8), 1979–1989. https://doi.org/10.1002/ijc.25848.

(47) McLoughlin, E. C.; O'boyle, N. M. Colchicine-Binding Site Inhibitors from Chemistry to Clinic: A Review. *Pharmaceuticals* **2020**, *13*, E8. https://doi.org/10.3390/ph13010008.

(48) EU/3/13/1154 | European Medicines Agency https://www.ema.europa.eu/en/medicines/human/orphan-designations/eu3131154 (accessed Mar 25, 2021).

(49) Ambudkar, S. V.; Kimchi-Sarfaty, C.; Sauna, Z. E.; Gottesman, M. M. P-Glycoprotein: From Genomics to Mechanism. *Oncogene* **2003**, *22*, 7468–7485. https://doi.org/10.1038/sj.onc.1206948.

(50) Kanthou, C.; Tozer, G. M. Microtubule Depolymerizing Vascular Disrupting Agents: Novel Therapeutic Agents for Oncology and Other Pathologies. *Int. J. Exp. Pathol.* **2009**, *90*, 284–294. https://doi.org/10.1111/j.1365-2613.2009.00651.x.

(51) Dark, G. G.; Hill, S. A.; Prise, V. E.; Tozer, G. M.; Pettit, G. R.; Chaplin, D. J. Combretastatin A-4, an Agent That Displays Potent and Selective Toxicity toward Tumor Vasculature. *Cancer Res.* **1997**, *57*, 1829–1834.

(52) Samarin, J.; Rehm, M.; Krueger, B.; Waschke, J.; Goppelt-Struebe, M. Up-Regulation of Connective Tissue Growth Factor in Endothelial Cells by the Microtubule-Destabilizing Agent Combretastatin A-4. *Mol. Cancer Res.* **2009**, *7*, 180–188. https://doi.org/10.1158/1541-7786.MCR-08-0292.

(53) Pollock, J. K.; Verma, N. K.; O'Boyle, N. M.; Carr, M.; Meegan, M. J.; Zisterer, D. M. Combretastatin (CA)-4 and Its Novel Analogue CA-432 Impair T-Cell Migration through the Rho/ROCK Signalling Pathway. *Biochem. Pharmacol.* **2014**, *92* (4), 544–557. https://doi.org/10.1016/j.bcp.2014.10.002.

(54) Williams, L. J.; Mukherjee, D.; Fisher, M.; Reyes-Aldasoro, C. C.; Akerman, S.; Kanthou, C.; Tozer, G. M. An in Vivo Role for Rho Kinase Activation in the Tumour Vascular Disrupting Activity of Combretastatin A-4 3-O-Phosphate. *Br. J. Pharmacol.* **2014**, *171* (21), 4902–4913. https://doi.org/10.1111/bph.12817.

(55) Kanthou, C.; Tozer, G. M. Tumour Targeting by Microtubule-Depolymerising Vascular Disrupting Agents. *Expert Opin. Ther. Targets* **2007**, *11*, 1443–1457. https://doi.org/10.1517/14728222.11.11.1443.

(56) Chaplin, D. J.; Hill, S. A. The Development of Combretastatin A4 Phosphate as a Vascular Targeting Agent. *Int. J. Radiat. Oncol. Biol. Phys.* **2002**, *54*, 1491–1496. https://doi.org/10.1016/S0360-3016(02)03924-X.

(57) Alvarez, R.; Medarde, M.; Pelaez, R. New Ligands of the Tubulin Colchicine Site Based on X-Ray Structures. *Curr. Top. Med. Chem.* **2014**, *14* (20), 2231–2252. https://doi.org/10.2174/1568026614666141130092637.

(58) Lu, Y.; Chen, J.; Xiao, M.; Li, W.; Miller, D. D. An Overview of Tubulin Inhibitors That Interact with the Colchicine Binding Site. *Pharm. Res.* **2012**, *29* (11), 2943–2971. https://doi.org/10.1007/s11095-012-0828-z.

(59) Sapra, S.; Bhalla, Y.; Nandani; Sharma, S.; Singh, G.; Nepali, K.; Budhiraja, A.; Dhar, K. L. Colchicine and Its Various Physicochemical and Biological Aspects. *Med. Chem. Res.* **2013**, *22*, 531–547. https://doi.org/10.1007/s00044-012-0077-z.

(60) Tron, G. C.; Pirali, T.; Sorba, G.; Pagliai, F.; Busacca, S.; Genazzani, A. A. Medicinal Chemistry of Combretastatin A4: Present and Future Directions. *J. Med. Chem.* **2006**, *49* (11), 3033–3044. https://doi.org/10.1021/jm0512903.

(61) Hamze, A.; Alami, M.; Provot, O. Developments of IsoCombretastatin A-4 Derivatives as Highly Cytotoxic Agents. *Eur. J. Med. Chem.* **2020**, *190*, 112110. https://doi.org/10.1016/j.ejmech.2020.112110.

(62) Álvarez, R.; Álvarez, C.; Mollinedo, F.; Sierra, B. G.; Medarde, M.; Peláez, R. Isocombretastatins A: 1,1-Diarylethenes as Potent Inhibitors of Tubulin Polymerization and Cytotoxic Compounds. *Bioorganic Med. Chem.* **2009**, *17* (17), 6422–6431. https://doi.org/10.1016/j.bmc.2009.07.012.

(63) Álvarez, R.; Puebla, P.; Díaz, J. F.; Bento, A. C.; García-Navas, R.; De La Iglesia-Vicente, J.; Mollinedo, F.; Andreu, J. M.; Medarde, M.; Peláez, R. Endowing Indole-Based Tubulin Inhibitors with an Anchor for Derivatization: Highly Potent 3-Substituted Indolephenstatins and Indoleisocombretastatins. *J. Med. Chem.* **2013**, *56* (7), 2813–2827. https://doi.org/10.1021/jm3015603.

(64) Chen, X.; Wang, S.-M.; Kumar, G. B.; Bare, G. A. L.; Leng, J.; Bukhari, S. N. A.; Qin, H.-L. Recent Developments on Phenstatins as Potent Antimitotic Agents. *Curr. Med. Chem.* **2018**, *25* (20), 2329–2352. https://doi.org/10.2174/0929867324666171106162048.

(65) Álvarez, R.; Aramburu, L.; Puebla, P.; Caballero, E.; González, M.; Vicente, A.; Medarde, M.; Peláez, R. Pyridine Based Antitumour Compounds Acting at the Colchicine Site. *Curr. Med. Chem.* **2016**, *23* (11), 1100–1130. https://doi.org/10.2174/0929867323111604201048 23.

(66) Chamberlain, M. C.; Grimm, S.; Phuphanich, S.; Recht, L.; Zhu, J. Z.; Kim, L.; Rosenfeld, S.; Fadul, C. E. A Phase 2 Trial of Verubulin for Recurrent Glioblastoma: A Prospective Study by the Brain Tumor Investigational Consortium (BTIC). *J. Neurooncol.* **2014**, *118* (2), 335–343. https://doi.org/10.1007/s11060-014-1437-y.

(67) Cirla, A.; Mann, J. Combretastatins: From Natural Products to Drug Discovery. *Nat. Prod. Rep.* **2003**, *20* (6), 558–564. https://doi.org/10.1039/b306797c.

(68) Vicente-Blázquez, A.; González, M.; Álvarez, R.; del Mazo, S.; Medarde, M.; Peláez, R. Antitubulin Sulfonamides: The Successful Combination of an Established Drug Class and a Multifaceted Target. *Med. Res. Rev.* **2019**, *39* (3), 775–830. https://doi.org/10.1002/med.21541.

(69) Zhou, P.; Liu, Y.; Zhou, L.; Zhu, K.; Feng, K.; Zhang, H.; Liang, Y.; Jiang, H.; Luo, C.; Liu, M.; Wang, Y. Potent Antitumor Activities and Structure Basis of the Chiral β-Lactam Bridged Analogue of Combretastatin A-4 Binding to Tubulin. *J. Med. Chem.* **2016**, *59* (22), 10329–10334.https://doi.org/10.1021/acs.jmedchem.6b01268.

(70) Zhou, P.; Liang, Y.; Zhang, H.; Jiang, H.; Feng, K.; Xu, P.; Wang, J.; Wang, X.; Ding, K.; Luo, C.; et al. Design, Synthesis, Biological Evaluation and Cocrystal Structures with Tubulin of Chiral β-Lactam Bridged Combretastatin A-4 Analogues as Potent Antitumor Agents. *Eur. J. Med. Chem.* **2018**, *144*, 817–842. https://doi.org/10.1016/j.ejmech.2017.12.004.

(71) Edwards, M. L.; Stemerick, D. M.; Sunkara, P. S. Chalcones: A New Class of Antimitotic Agents. *J. Med. Chem.* **1990**, *33* (7), 1948–1954. https://doi.org/10.1021/jm00169a021.

(72) Kumar, D.; Patel, G.; Johnson, E. O.; Shah, K. Synthesis and Anticancer Activities of Novel 3,5-Disubstituted-1,2,4-Oxadiazoles. *Bioorganic Med. Chem. Lett.* **2009**, *19* (10), 2739–2741. https://doi.org/10.1016/j.bmcl.2009.03.158.

(73) Chen, J.; Li, C. M.; Wang, J.; Ahn, S.; Wang, Z.; Lu, Y.; Dalton, J. T.; Miller, D. D.; Li, W. Synthesis and Antiproliferative Activity of Novel 2-Aryl-4-Benzoyl- Imidazole Derivatives Targeting Tubulin Polymerization. *Bioorganic Med. Chem.* **2011**, *19* (16), 4782–4795. https://doi.org/10.1016/j.bmc.2011.06.084.

(74) Wang, L.; Woods, K. W.; Li, Q.; Barr, K. J.; McCroskey, R. W.; Hannick, S. M.; Gherke, L.; Credo, R. B.; Hui, Y. H.; Marsh, K.; et al. Potent, Orally Active Heterocycle-Based Combretastatin A-4 Analogues: Synthesis, Structure - Activity Relationship, Pharmacokinetics, and in Vivo Antitumor Activity Evaluation. *J. Med. Chem.* **2002**, *45* (8), 1697–1711. https://doi.org/10.1021/jm010523x.

(75) Shan, B.; Medina, J. C.; Santha, E.; Frankmoelle, W. P.; Chou, T. C.; Learned, R. M.; Narbut, M. R.; Stott, D.; Wu, P.; Jaen, J. C.; et al. Selective, Covalent Modification of β-Tubulin Residue Cys-239 by T138067, an Antitumor Agent with in Vivo Efficacy against Multidrug-Resistant Tumors. *Proc. Natl. Acad. Sci. U. S. A.* **1999**, *96* (10), 5686–5691. https://doi.org/10.1073/pnas.96.10.5686.

(76) Dorléans, A.; Gigant, B.; Ravelli, R. B. G.; Mailliet, P.; Mikol, V.; Knossow, M. Variations in the Colchicine-Binding Domain Provide Insight into the Structural Switch of Tubulin. *Proc. Natl. Acad. Sci. U. S. A.* **2009**, *106* (33), 13775–13779. https://doi.org/10.1073/pnas.0904223106.

(77) Singh, J.; Petter, R. C.; Baillie, T. A.; Whitty, A. The Resurgence of Covalent Drugs. *Nat. Rev. Drug Discov.* **2011**, *10*, 307–317. https://doi.org/10.1038/nrd3410.

(78) McNamara, D. E.; Senese, S.; Yeates, T. O.; Torres, J. Z. Structures of Potent Anticancer Compounds Bound to Tubulin. *Protein Sci.* **2015**, *24* (7), 1164–1172. https://doi.org/10.1002/pro.2704.

(79) Wang, Y.; Zhang, H.; Gigant, B.; Yu, Y.; Wu, Y.; Chen, X.; Lai, Q.; Yang, Z.; Chen, Q.; Yang, J. Structures of a Diverse Set of Colchicine Binding Site Inhibitors in Complex with Tubulin Provide a Rationale for Drug Discovery. *FEBS J.* **2016**, *283* (1), 102–111. https://doi.org/10.1111/febs.13555.

(80) Li, Z.; Ma, L.; Wu, C.; Meng, T.; Ma, L.; Zheng, W.; Yu, Y.; Chen, Q.; Yang, J.; Shen, J. The Structure of MT189-Tubulin Complex Provides Insights into Drug Design. *Lett. Drug Des. Discov.* **2018**, *16* (9), 1069–1073. https://doi.org/10.2174/1570180816666181122122655.

(81) Yoshimatsu, K.; Yamaguchi, A.; Yoshino, H.; Koyanagi, N.; Kitoh, K. Mechanism of Action of E7010, an Orally Active Sulfonamide Antitumor Agent: Inhibition of Mitosis by Binding to the Colchicine Site of Tubulin. *Cancer Res.* **1997**, *57*, 3208–3213.

(82) Search of: AVE 8062 - List Results - ClinicalTrials.gov https://clinicaltrials.gov/ct2/results?term=AVE+8062 (accessed Feb 15, 2021).

(83) Eskens, F. A. L. M.; Tresca, P.; Tosi, D.; Van Doorn, L.; Fontaine, H.; Van Der Gaast, A.; Veyrat-Follet, C.; Oprea, C.; Hospitel, M.; Dieras, V. A Phase i Pharmacokinetic Study of the Vascular Disrupting Agent Ombrabulin (AVE8062) and Docetaxel in Advanced Solid Tumours. *Br. J. Cancer* **2014**, *110* (9), 2170–2177. https://doi.org/10.1038/bjc.2014.137.

(84) Search of: Fosbretabulin - List Results - ClinicalTrials.gov https://clinicaltrials.gov/ct2/results?recrs=&cond=&term=Fosbretabulin&cntry=&state=&city=&dist= (accessed Feb 15, 2021).

(85) Zweifel, M.; Jayson, G. C.; Reed, N. S.; Osborne, R.; Hassan, B.; Ledermann, J.; Shreeves, G.; Poupard, L.; Lu, S. P.; Balkissoon, J.; Chaplin, D. J.; Rustin, G. J. S. Phase II Trial of Combretastatin A4 Phosphate, Carboplatin, and Paclitaxel in Patients with Platinum-Resistant Ovarian Cancer. *Ann. Oncol.* **2011**, *22* (9), 2036–2041. https://doi.org/10.1093/annonc/mdq708.

(86) EU/3/16/1633 | European Medicines Agency https://www.ema.europa.eu/en/medicines/human/orphan-designations/eu3161633 (accessed Mar 25, 2021).

(87) Lacey, E. Mode of Action of Benzimidazoles. *Parasitol. Today* **1990**, *6* (4), 112–115. https://doi.org/10.1016/0169-4758(90)90227-U.

(88) Kavallaris, M. Microtubules and Resistance to Tubulin-Binding Agents. *Nat. Rev. Cancer* **2010**, *10* (3), 194–204. https://doi.org/10.1038/nrc2803.

(89) Liang, W.; Ni, Y.; Chen, F. Tumor Resistance to Vascular Disrupting Agents: Mechanisms, Imaging, and Solutions. *Oncotarget* **2016**, *7* (13), 15444–15459. https://doi.org/10.18632/oncotarget.6999.

(90) Werbovetz, K. A.; Morgan, R. E. Selective Lead Compounds against Kinetoplastid Tubulin. *Adv. Exp. Med. Biol.* **2008**, *625*, 33–47. https://doi.org/10.1007/978-0-387-77570-8_4.

(91) Werbovetz, K. A.; Brendle, J. J.; Sackett, D. L. Purification, Characterization, and Drug Susceptibility of Tubulin from Leishmania. *Mol. Biochem. Parasitol.* **1999**, *98* (1), 53–65. https://doi.org/10.1016/S0166-6851(98)00146-7.

(92) Fennell, B. J.; Naughton, J. A.; Barlow, J.; Brennan, G.; Fairweather, I.; Hoey, E.; McFerran, N.; Trudgett, A.; Bell, A. Microtubules as Antiparasitic Drug Targets. *Expert Opin. Drug Discov.* **2008**, *3* (5), 501–518. https://doi.org/10.1517/17460441.3.5.501.

(93) Luis, L.; Serrano, M. L.; Hidalgo, M.; Mendoza-León, A. Comparative Analyses of the β -Tubulin Gene and Molecular Modeling Reveal Molecular Insight into the Colchicine Resistance in Kinetoplastids Organisms. *Biomed Res. Int.* **2013**, *2013*. https://doi.org/10.1155/2013/843748.

(94) Luis, L.; Serrano, M. L.; Hidalgo, M.; Mendoza-León, A. Comparative Analyses of the β-Tubulin Gene and Molecular Modeling Reveal Molecular Insight into the Colchicine Resistance in Kinetoplastids Organisms. *Biomed Res. Int.* **2013**, *2013*, 843748. https://doi.org/10.1155/2013/843748.

(95) Drews, J. Drug Discovery: A Historical Perspective. *Science (80-.).* **2000**, *287* (5460), 1960–1964. https://doi.org/10.1126/science.287.5460.1960.

(96) Apaydın, S.; Török, M. Sulfonamide Derivatives as Multi-Target Agents for Complex Diseases. *Bioorganic Med. Chem. Lett.* **2019**, *29* (16), 2042–2050. https://doi.org/10.1016/j.bmcl.2019.06.041.

(97) Laurence, C.; Brameld, K. A.; Graton, J.; Le Questel, J. Y.; Renault, E. The PKBHX Database: Toward a Better Understanding of Hydrogen-Bond Basicity for Medicinal Chemists. *J. Med. Chem.* **2009**, *52* (14), 4073–4086. https://doi.org/10.1021/jm801331y.

(98) Perlovich, G. L.; Kazachenko, V. P.; Strakhova, N. N.; Raevsky, O. A. Impact of Sulfonamide Structure on Solubility and Transfer Processes in Biologically Relevant Solvents. *J. Chem. Eng. Data* **2014**, *59* (12), 4217–4226. https://doi.org/10.1021/je500918t.

(99) ClinicalTrials.gov https://clinicaltrials.gov/ (accessed Jul 28, 2020).

(100) Li, L.; Jiang, S.; Li, X.; Liu, Y.; Su, J.; Chen, J. Recent Advances in Trimethoxyphenyl (TMP) Based Tubulin Inhibitors Targeting the Colchicine Binding Site. *Eur. J. Med. Chem.* **2018**, *151*, 482–494. https://doi.org/10.1016/j.ejmech.2018.04.011.

(101) Negi, A. S.; Gautam, Y.; Alam, S.; Chanda, D.; Luqman, S.; Sarkar, J.; Khan, F.; Konwar, R. Natural Antitubulin Agents: Importance of 3,4,5-Trimethoxyphenyl Fragment. *Bioorganic Med. Chem.* **2015**, *23* (3), 373–389. https://doi.org/10.1016/j.bmc.2014.12.027.

(102) Bray, F.; Ferlay, J.; Soerjomataram, I.; Siegel, R. L.; Torre, L. A.; Jemal, A. Global Cancer Statistics 2018: GLOBOCAN Estimates of Incidence and Mortality Worldwide for 36 Cancers in 185 Countries. *CA. Cancer J. Clin.* **2018**, *68* (6), 394–424. https://doi.org/10.3322/caac.21492.

(103) El cáncer - Instituto Nacional del Cáncer https://www.cancer.gov/espanol/cancer (accessed Feb 15, 2021).

(104) Hanahan, D.; Weinberg, R. A. The Hallmarks of Cancer. *Cell* **2000**, *100* (1), 57–70. https://doi.org/10.1016/S0092-8674(00)81683-9.

(105) Stacker, S. A.; Achen, M. G.; Jussila, L.; Baldwin, M. E.; Alitalo, K. Lymphangiogenesis and Cancer Metastasis. *Nat. Rev. Cancer* **2002**, *2* (8), 573–583. https://doi.org/10.1038/nrc863.

(106) Alcolea, P. J.; Alonso, A.; Degayón, M. A.; Moreno-Paz, M.; Jiménez, M.; Molina, R.; Larraga, V. *In Vitro* Infectivity and Differential Gene Expression of Leishmania Infantum Metacyclic Promastigotes: Negative Selection with Peanut Agglutinin in Culture versus Isolation from the Stomodeal Valve of Phlebotomus Perniciosus. *BMC Genomics* **2016**, *17* (1), 375. https://doi.org/10.1186/s12864-016-2672-8.

(107) Leishmaniasis https://www.who.int/es/news-room/fact-sheets/detail/leishmaniasis (accessed Nov 19, 2020).

(108) Bray, F.; Jemal, A.; Grey, N.; Ferlay, J.; Forman, D. Global Cancer Transitions According to the Human Development Index (2008-2030): A Population-Based Study. *Lancet Oncol.* **2012**, *13* (8), 790–801. https://doi.org/10.1016/S1470-2045(12)70211-5.

(109) Galmarini, D.; Galmarini, C. M.; Galmarini, F. C. Cancer Chemotherapy: A Critical Analysis of Its 60 Years of History. *Crit. Rev. Oncol. Hematol.* **2012**, *84* (2), 181–199. https://doi.org/10.1016/j.critrevonc.2012.03.002.

(110) Cao, Y.; Depinho, R. A.; Ernst, M.; Vousden, K. Cancer Research: Past, Present and Future. *Nat. Rev. Cancer* **2011**, *11* (10), 749–754. https://doi.org/10.1038/nrc3138.

(111) Berger, A. C.; Korkut, A.; Kanchi, R. S.; Hegde, A. M.; Lenoir, W.; Liu, W.; Liu, Y.; Fan, H.; Shen, H.; Ravikumar, V.; et al. Comprehensive Pan-Cancer Molecular Study of Gynecologic and Breast Cancers. *Cancer Cell* **2018**, *33* (4), 690-705.e9. https://doi.org/10.1016/j.ccell.2018.03.014.

(112) Jayson, G. C.; Kohn, E. C.; Kitchener, H. C.; Ledermann, J. A. Ovarian Cancer. *Lancet* **2014**, *384* (9951), 1376–1388. https://doi.org/10.1016/S0140-6736(13)62146-7.

(113) Ghersi, D.; Wilcken, N.; Simes, R. J. A Systematic Review of Taxane-Containing Regimens for Metastatic Breast Cancer. *Br. J. Cancer* **2005**, *93*, 293–301. https://doi.org/10.1038/sj.bjc.6602680.

(114) Friedrichs, K.; Hölzel, F.; Jänicke, F. Combination of Taxanes and Anthracyclines in First-Line Chemotherapy of Metastatic Breast Cancer: An Interim Report. *Eur. J. Cancer* **2002**, *38* (13), 1730–1738. https://doi.org/10.1016/S0959-8049(02)00144-2.

(115) Telli, M. L.; Carlson, R. W. First-Line Chemotherapy for Metastatic Breast Cancer. *Clin. Breast Cancer* **2009**, *9* (SUPPL.2), S66–S72. https://doi.org/10.3816/CBC.2009.s.007.

(116) Piccart-Gebhart, M. J.; Burzykowski, T.; Buyse, M.; Sledge, G.; Carmichael, J.; Lück, H. J.; Mackey, J. R.; Nabholtz, J. M.; Paridaens, R.; Biganzoli, L.; et al. Taxanes Alone or in Combination with Anthracyclines as First-Line Therapy of Patients with Metastatic Breast Cancer. *J. Clin. Oncol.* **2008**, *26* (12), 1980–1986. https://doi.org/10.1200/JCO.2007.10.8399.

(117) Ozols, R. F.; Bundy, B. N.; Greer, B. E.; Fowler, J. M.; Clarke-Pearson, D.; Burger, R. A.; Mannel, R. S.; DeGeest, K.; Hartenbach, E. M.; Baergen, R.; et al. Phase III Trial of Carboplatin and Paclitaxel Compared with Cisplatin and Paclitaxel in Patients with Optimally Resected Stage III Ovarian Cancer: A Gynecologic Oncology Group Study. *J. Clin. Oncol.* **2003**, *21* (17), 3194–3200. https://doi.org/10.1200/JCO.2003.02.153.

(118) McGuire, W. P.; Markman, M. Primary Ovarian Cancer Chemotherapy: Current Standards of Care. *Br. J. Cancer* **2003**, *89* (SUPPL. 3). https://doi.org/10.1038/sj.bjc.6601494.

(119) Bicaku, E.; Xiong, Y.; Marchion, D. C.; Chon, H. S.; Stickles, X. B.; Chen, N.; Judson, P. L.; Hakam, A.; Gonzalez-Bosquet, J.; Wenham, R. M.; et al. *In Vitro* Analysis of Ovarian Cancer Response to Cisplatin, Carboplatin, and Paclitaxel Identifies Common Pathways That Are Also Associated with Overall Patient Survival. *Br. J. Cancer* **2012**, *106* (12), 1967–1975. https://doi.org/10.1038/bjc.2012.207.

(120) Pectasides, D.; Pectasides, E.; Economopoulos, T. Systemic Therapy in Metastatic or Recurrent Endometrial Cancer. *Cancer Treat. Rev.* **2007**, *33* (2), 177–190. https://doi.org/10.1016/j.ctrv.2006.10.007.

(121) Moxley, K. M.; McMeekin, D. S. Endometrial Carcinoma: A Review of Chemotherapy, Drug Resistance, and the Search for New Agents. *Oncologist* **2010**, *15* (10), 1026–1033. https://doi.org/10.1634/theoncologist.2010-0087.

(122) Serkies, K.; Jassem, J. Systemic Therapy for Cervical Carcinoma – Current Status. *Chinese J. Cancer Res.* **2018**, *30* (2), 209–221. https://doi.org/10.21147/j.issn.1000-9604.2018.02.04.

(123) Boussios, S.; Seraj, E.; Zarkavelis, G.; Petrakis, D.; Kollas, A.; Kafantari, A.; Assi, A.; Tatsi, K.; Pavlidis, N.; Pentheroudakis, G. Management of Patients with Recurrent/Advanced Cervical Cancer beyond First Line Platinum Regimens: Where Do We Stand? A Literature Review. *Crit. Rev. Oncol. Hematol.* **2016**, *108*, 164–174. https://doi.org/10.1016/j.critrevonc.2016.11.006.

(124) Hennenfent, K. L.; Govindan, & R. Review Novel Formulations of Taxanes: A Review. Old Wine in a New Bottle? *Ann. Oncol.* **2006**, *17*, 735–749. https://doi.org/10.1093/annonc/mdj100.

(125) Ten Tije, A. J.; Verweij, J.; Loos, W. J.; Sparreboom, A. Pharmacological Effects of Formulation Vehicles: Implications for Cancer Chemotherapy. *Clin. Pharmacokinet.* **2003**, *42* (7), 665–685. https://doi.org/10.2165/00003088-200342070-00005.

(126) Weiss, R. B. Hypersensitivity Reactions from Taxol. *J. Clin. Oncol.* **1990**, *8* (7), 1263–1268. https://doi.org/10.1200/JCO.1990.8.7.1263.

(127) Gligorov, J.; Lotz, J. P. Preclinical Pharmacology of the Taxanes: Implications of the Differences. *Oncologist* **2004**, *9* (S2), 3–8. https://doi.org/10.1634/theoncologist.9-suppl_2-3.

(128) Holohan, C.; Van Schaeybroeck, S.; Longley, D. B.; Johnston, P. G. Cancer Drug Resistance: An Evolving Paradigm. *Nat. Rev. Cancer* **2013**, *13* (10), 714–726. https://doi.org/10.1038/nrc3599.

(129) Rivera, E.; Gomez, H. Chemotherapy Resistance in Metastatic Breast Cancer: The Evolving Role of Ixabepilone. *Breast Cancer Res.* **2010**, *12* (SUPPL. 2), S2. https://doi.org/10.1186/bcr2573.

(130) Gonzalez-Angulo, A. M.; Morales-Vasquez, F.; Hortobagyi, G. N. Overview of Resistance to Systemic Therapy in Patients with Breast Cancer. *Madame Curie Biosci. Database* **2013**.

(131) Agarwal, R.; Kaye, S. B. Ovarian Cancer: Strategies for Overcoming Resistance to Chemotherapy. *Nat. Rev. Cancer* **2003**, *3* (7), 502–516. https://doi.org/10.1038/nrc1123.

(132) Pokhriyal, R.; Hariprasad, R.; Kumar, L.; Hariprasad, G. Chemotherapy Resistance in Advanced Ovarian Cancer Patients. *Biomark. Cancer* **2019**, *11*, 1179299X1986081. https://doi.org/10.1177/1179299x19860815.

(133) Chaudhry, P.; Asselin, E. Resistance to Chemotherapy and Hormone Therapy in Endometrial Cancer. *Endocr. Relat. Cancer* **2009**, *16* (2), 363–380. https://doi.org/10.1677/ERC-08-0266.

(134) Alfarouk, K. O.; Stock, C. M.; Taylor, S.; Walsh, M.; Muddathir, A. K.; Verduzco, D.; Bashir, A. H. H.; Mohammed, O. Y.; Elhassan, G. O.; Harguindey, S.; et al. Resistance to Cancer Chemotherapy: Failure in Drug Response from ADME to P-Gp. *Cancer Cell Int.* **2015**, *15*, 71. https://doi.org/10.1186/s12935-015-0221-1.

(135) Orr, G. A.; Verdier-Pinard, P.; McDaid, H.; Horwitz, S. B. Mechanisms of Taxol Resistance Related to Microtubules. *Oncogene* **2003**, *22* (47 REV. ISS. 6), 7280–7295. https://doi.org/10.1038/sj.onc.1206934.

(136) Yusuf, R.; Duan, Z.; Lamendola, D.; Penson, R.; Seiden, M. Paclitaxel Resistance: Molecular Mechanisms and Pharmacologic Manipulation. *Curr. Cancer Drug Targets* **2003**, *3* (1), 1–19. https://doi.org/10.2174/1568009033333754.

(137) Murray, S.; Briasoulis, E.; Linardou, H.; Bafaloukos, D.; Papadimitriou, C. Taxane Resistance in Breast Cancer: Mechanisms, Predictive Biomarkers and Circumvention Strategies. *Cancer Treat. Rev.* **2012**, *38* (7), 890–903. https://doi.org/10.1016/j.ctrv.2012.02.011.

(138) Tommasi, S.; Mangia, A.; Lacalamita, R.; Bellizzi, A.; Fedele, V.; Chiriatti, A.; Thomssen, C.; Kendzierski, N.; Latorre, A.; Lorusso, V.; et al. Cytoskeleton and Paclitaxel Sensitivity in Breast Cancer: The Role of β-Tubulins. *Int. J. Cancer* **2007**, *120* (10), 2078–2085. https://doi.org/10.1002/ijc.22557.

(139) Chong, T.; Sarac, A.; Yao, C. Q.; Liao, L.; Lyttle, N.; Boutros, P. C.; Bartlett, J. M. S.; Spears, M. Deregulation of the Spindle Assembly Checkpoint Is Associated with Paclitaxel Resistance in Ovarian Cancer. *J. Ovarian Res.* **2018**, *11*, 27. https://doi.org/10.1186/s13048-018-0399-7.

(140) Kavallaris, M.; Kuo, D. Y. S.; Burkhart, C. A.; Regl, D. L.; Norris, M. D.; Haber, M.; Horwitz, S. B. Taxol-Resistant Epithelial Ovarian Tumors Are Associated with Altered Expression of Specific β-Tubulin Isotypes. *J. Clin. Invest.* **1997**, *100* (5), 1282–1293. https://doi.org/10.1172/JCI119642.

(141) Peng, X.; Gong, F.; Chen, Y.; Jiang, Y.; Liu, J.; Yu, M.; Zhang, S.; Wang, M.; Xiao, G.; Liao, H. Autophagy Promotes Paclitaxel Resistance of Cervical Cancer Cells: Involvement of Warburg Effect Activated Hypoxia-Induced Factor 1-α-Mediated Signaling. *Cell Death Dis.* **2014**, *5* (8), 1–11. https://doi.org/10.1038/cddis.2014.297.

(142) WHO | Leishmaniasis https://www.who.int/neglected_diseases/resources/leishmaniasis/en/ (accessed Apr 8, 2020).

(143) Alvar, J.; Vélez, I. D.; Bern, C.; Herrero, M.; Desjeux, P.; Cano, J.; Jannin, J.; de Boer, M. Leishmaniasis Worldwide and Global Estimates of Its Incidence. *PLoS One* **2012**, *7* (5), 1–6. https://doi.org/10.1371/journal.pone.0035671.

(144) Chappuis, F.; Sundar, S.; Hailu, A.; Ghalib, H.; Rijal, S.; Peeling, R. W.; Alvar, J.; Boelaert, M. Visceral Leishmaniasis: What Are the Needs for Diagnosis, Treatment and Control? *Nat. Rev. Microbiol.* **2007**, *5* (11), 873–882. https://doi.org/10.1038/nrmicro1748.

(145) Reithinger, R.; Dujardin, J. C.; Louzir, H.; Pirmez, C.; Alexander, B.; Brooker, S. Cutaneous Leishmaniasis. *Lancet Infect. Dis.* **2007**, *7* (9), 581–596. https://doi.org/10.1016/S1473-3099(07)70209-8.

(146) Arce, A.; Estirado, A.; Ordobas, M.; Sevilla, S.; García, N.; Moratilla, L.; de la Fuente, S.; Martínez, A. M.; Pérez, A. M.; Aránguez, E.; et al. Re-Emergence of Leishmaniasis in Spain: Community Outbreak in Madrid, Spain, 2009 TO 2012. *Eurosurveillance* **2013**, *18* (30). https://doi.org/10.2807/1560-7917.ES2013.18.30.20546.

(147) Molina, R.; Jiménez, M. I.; Cruz, I.; Iriso, A.; Martín-Martín, I.; Sevillano, O.; Melero, S.; Bernal, J. The Hare (Lepus Granatensis) as Potential Sylvatic Reservoir of Leishmania Infantum in Spain. *Vet. Parasitol.* **2012**, *190* (1–2), 268–271. https://doi.org/10.1016/j.vetpar.2012.05.006.

(148) Jiménez, M.; González, E.; Martín-Martín, I.; Hernández, S.; Molina, R. Could Wild Rabbits (Oryctolagus Cuniculus) Be Reservoirs for Leishmania Infantum in the Focus of Madrid, Spain? *Vet. Parasitol.* **2014**, *202* (3–4), 296–300. https://doi.org/10.1016/j.vetpar.2014.03.027.

(149) Alcolea, P. J.; Tuñón, G. I. L.; Alonso, A.; García-Tabares, F.; Ciordia, S.; Mena, M. C.; Campos, R. N. S.; Almeida, R. P.; Larraga, V. Differential Protein Abundance in Promastigotes of Nitric Oxide-Sensitive and Resistant Leishmania Chagasi Strains. *Proteomics - Clin. Appl.* **2016**, *10* (11), 1132–1146. https://doi.org/10.1002/prca.201600054.

(150) Jain, V.; Jain, K. Molecular Targets and Pathways for the Treatment of Visceral Leishmaniasis. *Drug Discov. Today* **2018**, *23* (1), 161–170. https://doi.org/10.1016/j.drudis.2017.09.006.

(151) Ponte-Sucre, A.; Gamarro, F.; Dujardin, J. C.; Barrett, M. P.; López-Vélez, R.; García-Hernández, R.; Pountain, A. W.; Mwenechanya, R.; Papadopoulou, B. Drug Resistance and Treatment Failure in Leishmaniasis: A 21st Century Challenge. *PLoS Negl. Trop. Dis.* **2017**, *11* (12). https://doi.org/10.1371/journal.pntd.0006052.

(152) Nagle, A. S.; Khare, S.; Kumar, A. B.; Supek, F.; Buchynskyy, A.; Mathison, C. J. N.; Chennamaneni, N. K.; Pendem, N.; Buckner, F. S.; Gelb, M. H.; Molteni, V. Recent Developments in Drug Discovery for Leishmaniasis and Human African Trypanosomiasis. *Chem. Rev.* **2014**, *114* (22), 11305–11347. https://doi.org/10.1021/cr500365f.

(153) Rama, M.; Kumar, N. V. enkates. A.; Balaji, S. A Comprehensive Review of Patented Antileishmanial Agents. *Pharm. Pat. Anal.* **2015**, *4* (1), 37–56. https://doi.org/10.4155/ppa.14.55.

(154) Tiuman, T. S.; Santos, A. O.; Ueda-Nakamura, T.; Filho, B. P. D.; Nakamura, C. V. Recent Advances in Leishmaniasis Treatment. *Int. J. Infect. Dis.* **2011**, *15* (8), e525-32. https://doi.org/10.1016/j.ijid.2011.03.021.

(155) Monzote, L. Current Treatment of Leishmaniasis: A Review. *Open Antimicrob. Agents J.* **2009**, 1.

(156) Thakur, C. P.; Narayan, S.; Ranjan, A. Epidemiological, Clinical & Pharmacological Study of Antimony-Resistant Visceral Leishmaniasis in Bihar, India. *Indian J. Med. Res.* **2004**, *120* (3), 166–172.

(157) Légaré, D.; Richard, D.; Mukhopadhyay, R.; Stierhof, Y. D.; Rosen, B. P.; Haimeur, A.; Papadopoulou, B.; Ouellette, M. The Leishmania ATP-Binding Cassette Protein PGPA Is an Intracellular Metal-Thiol Transporter ATPase. *J. Biol. Chem.* **2001**, *276* (28), 26301–26307. https://doi.org/10.1074/jbc.M102351200.

(158) Marquis, N.; Gourbal, B.; Rosen, B. P.; Mukhopadhyay, R.; Ouellette, M. Modulation in Aquaglyceroporin AQP1 Gene Transcript Levels in Drug-Resistant Leishmania. *Mol. Microbiol.* **2005**, *57* (6), 1690–1699. https://doi.org/10.1111/j.1365-2958.2005.04782.x.

(159) Javed, I.; Hussain, S. Z.; Ullah, I.; Khan, I.; Ateeq, M.; Shahnaz, G.; Rehman, H. U.; Razi, M. T.; Shah, M. R.; Hussain, I. Synthesis, Characterization and Evaluation of Lecithin-Based Nanocarriers for the Enhanced Pharmacological and Oral Pharmacokinetic Profile of Amphotericin B. *J. Mater. Chem. B* **2015**, *3* (42), 8359–8365. https://doi.org/10.1039/c5tb01258a.

(160) Lemke, A.; Kiderlen, A. F.; Kayser, O. Amphotericin B. *Appl. Microbiol. Biotechnol.* **2005**, *68* (2), 151–162. https://doi.org/10.1007/s00253-005-1955-9.

(161) Abu Ammar, A.; Nasereddin, A.; Ereqat, S.; Dan-Goor, M.; Jaffe, C. L.; Zussman, E.; Abdeen, Z. Amphotericin B-Loaded Nanoparticles for Local Treatment of Cutaneous Leishmaniasis. *Drug Deliv. Transl. Res.* **2019**, *9* (1), 76–84. https://doi.org/10.1007/s13346-018-00603-0.

(162) De Rycker, M.; Baragaña, B.; Duce, S. L.; Gilbert, I. H. Challenges and Recent Progress in Drug Discovery for Tropical Diseases. *Nature* **2018**, *559* (7715), 498–506. https://doi.org/10.1038/s41586-018-0327-4.

(163) Mbongo, N.; Loiseau, P. M.; Billion, M. A.; Robert-Gero, M. Mechanism of Amphotericin B Resistance in Leishmania Donovani Promastigotes. *Antimicrob. Agents Chemother.* **1998**, *42* (2), 352–357.

(164) Sundar, S.; Jha, T. K.; Thakur, C. P.; Engel, J.; Sindermann, H.; Fischer, C.; Junge, K.; Bryceson, A.; Berman, J. Oral Miltefosine for Indian Visceral Leishmaniasis. *N. Engl. J. Med.* **2002**, *347* (22), 1739–1746. https://doi.org/10.1056/NEJMoa021556.

(165) Sundar, S.; Murray, H. W. Availability of Miltefosine for the Treatment of Kala-Azar in India. *Bull. World Health Organ.* **2005**, *83* (5), 394–395. https://doi.org//S0042-96862005000500018.

(166) Rijal, S.; Ostyn, B.; Uranw, S.; Rai, K.; Bhattarai, N. R.; Dorlo, T. P. C.; Beijnen, J. H.; Vanaerschot, M.; Decuypere, S.; Dhakal, S. S.; et al. Increasing Failure of Miltefosine in the Treatment of Kala-Azar in Nepal and the Potential Role of Parasite Drug Resistance, Reinfection, or Noncompliance. *Clin. Infect. Dis.* **2013**, *56* (11), 1530–1538. https://doi.org/10.1093/cid/cit102.

(167) Pérez-Victoria, F. J.; Sánchez-Cañete, M. P.; Seifert, K.; Croft, S. L.; Sundar, S.; Castanys, S.; Gamarro, F. Mechanisms of Experimental Resistance of Leishmania to Miltefosine: Implications for Clinical Use. *Drug Resist. Updat.* **2006**, *9* (1–2), 26–39. https://doi.org/10.1016/j.drup.2006.04.001.

(168) Pérez-Victoria, F. J.; Gamarro, F.; Ouellette, M.; Castanys, S. Functional Cloning of the Miltefosine Transporter: A Novel p-Type Phospholipid Translocase from Leishmania Involved in Drug Resistance. *J. Biol. Chem.* **2003**, *278* (50), 49965–49971. https://doi.org/10.1074/jbc.M308352200.

(169) Mondelaers, A.; Sanchez-Cañete, M. P.; Hendrickx, S.; Eberhardt, E.; Garcia-Hernandez, R.; Lachaud, L.; Cotton, J.; Sanders, M.; Cuypers, B.; Imamura, H.; et al. Genomic and Molecular Characterization of Miltefosine Resistance in Leishmania Infantum Strains with Either Natural or Acquired Resistance through Experimental Selection of Intracellular Amastigotes. *PLoS One* **2016**, *11* (4), e0154101. https://doi.org/10.1371/journal.pone.0154101.

(170) Coelho, A. C.; Beverley, S. M.; Cotrim, P. C. Functional Genetic Identification of PRP1, an ABC Transporter Superfamily Member Conferring Pentamidine Resistance in Leishmania Major. *Mol. Biochem. Parasitol.* **2003**, *130* (2), 83–90. https://doi.org/10.1016/s0166-6851(03)00162-2.

(171) Sundar, S.; Jha, T. K.; Thakur, C. P.; Sinha, P. K.; Bhattacharya, S. K. Injectable Paromomycin for Visceral Leishmaniasis in India. *N. Engl. J. Med.* **2007**, *356* (25), 2571–2581. https://doi.org/10.1056/NEJMoa066536.

(172) Alves, F.; Bilbe, G.; Blesson, S.; Goyal, V.; Monnerat, S.; Mowbray, C.; Muthoni Ouattara, G.; Pécoul, B.; Rijal, S.; Rode, J.; et al. Recent Development of Visceral Leishmaniasis Treatments: Successes, Pitfalls, and Perspectives. *Clin. Microbiol. Rev.* **2018**, *31* (4). https://doi.org/10.1128/CMR.00048-18.

(173) Nguyen, T. L.; McGrath, C.; Hermone, A. R.; Burnett, J. C.; Zaharevitz, D. W.; Day, B. W.; Wipf, P.; Hamel, E.; Gussio, R. A Common Pharmacophore for a Diverse Set of Colchicine Site Inhibitors Using a Structure-Based Approach. *J. Med. Chem.* **2005**, *48* (19), 6107–6116. https://doi.org/10.1021/jm050502t.

(174) Alkadi, H.; Khubeiz, M. J. Colchicine: A Review About Chemical Structure and Clinical Using. *Infect. Disord. - Drug Targets* **2017**, *17*. https://doi.org/10.2174/1871526517666171017114901.

(175) Siemann, D. W.; Chaplin, D. J.; Walicke, P. A. A Review and Update of the Current Status of the Vasculature-Disabling Agent Combretastatin-A4 Phosphate (CA4P). *Expert Opin. Investig. Drugs* **2009**, *18*, 189–197. https://doi.org/10.1517/13543780802691068.

(176) Delmonte, A.; Sessa, C. AVE8062: A New Combretastatin Derivative Vascular Disrupting Agent. *Expert Opin. Investig. Drugs* **2009**, *18*, 1541–1548. https://doi.org/10.1517/13543780903213697.

(177) Aprile, S.; Del Grosso, E.; Tron, G. C.; Grosa, G. *In Vitro* Metabolism Study of Combretastatin A-4 in Rat and Human Liver Microsomes. *Drug Metab. Dispos.* **2007**, *35* (12), 2252–2261. https://doi.org/10.1124/dmd.107.016998.

(178) Gaukroger, K.; Hadfield, J. A.; Lawrence, N. J.; Nolan, S.; McGown, A. T. Structural Requirements for the Interaction of Combretastatins with Tubulin: How Important Is the Trimethoxy Unit? *Org. Biomol. Chem.* **2003**, *1* (17), 3033–3037. https://doi.org/10.1039/b306878a.

(179) Chen, J.; Liu, T.; Dong, X.; Hu, Y. Recent Development and SAR Analysis of Colchicine Binding Site Inhibitors. *Mini-Reviews Med. Chem.* **2009**, *9* (10), 1174–1190. https://doi.org/10.2174/138955709789055234.

(180) Nam, N.-H. Combretastatin A-4 Analogues as Antimitotic Antitumor Agents. *Curr. Med. Chem.* **2003**, *10* (17), 1697–1722. https://doi.org/10.2174/0929867033457151.

(181) Ghinet, A.; Rigo, B.; Hénichart, J. P.; Le Broc-Ryckewaert, D.; Pommery, J.; Pommery, N.; Thuru, X.; Quesnel, B.; Gautret, P. Synthesis and Biological Evaluation of Phenstatin Metabolites. *Bioorganic Med. Chem.* **2011**, *19* (20), 6042–6054. https://doi.org/10.1016/j.bmc.2011.08.047.

(182) Le Broc-Ryckewaert, D.; Pommery, N.; Pommery, J.; Ghinet, A.; Farce, A.; Wiart, J.-F.; Gautret, P.; Rigo, B.; Henichart, J.-P. *In Vitro* Metabolism of Phenstatin: Potential Pharmacological Consequences. *Drug Metab. Lett.* **2011**, *5* (3), 209–215. https://doi.org/10.2174/187231211796904973.

(183) Greene, L. M.; O'Boyle, N. M.; Nolan, D. P.; Meegan, M. J.; Zisterer, D. M. The Vascular Targeting Agent Combretastatin-A4 Directly Induces Autophagy in Adenocarcinoma-Derived Colon Cancer Cells. *Biochem. Pharmacol.* **2012**, *84* (5), 612–624. https://doi.org/10.1016/j.bcp.2012.06.005.

(184) Cummings, J.; Zelcer, N.; Allen, J. D.; Yao, D.; Boyd, G.; Maliepaard, M.; Friedberg, T. H.; Smyth, J. F.; Jodrell, D. I. Glucuronidation as a Mechanism of Intrinsic Drug Resistance in Colon Cancer Cells: Contribution of Drug Transport Proteins. *Biochem. Pharmacol.* **2004**, *67* (1), 31–39. https://doi.org/10.1016/j.bcp.2003.07.019.

(185) Jiménez, C.; Ellahioui, Y.; Álvarez, R.; Aramburu, L.; Riesco, A.; González, M.; Vicente, A.; Dahdouh, A.; Ibn Mansour, A.; Jiménez, C.; et al. Exploring the Size Adaptability of the B Ring Binding Zone of the Colchicine Site of Tubulin with Para -Nitrogen Substituted Isocombretastatins. *Eur. J. Med. Chem.* **2015**, *100*, 210–222. https://doi.org/10.1016/j.ejmech.2015.05.047.

(186) Álvarez, R.; Álvarez, C.; Mollinedo, F.; Sierra, B. G.; Medarde, M.; Peláez, R. Isocombretastatins A: 1,1-Diarylethenes as Potent Inhibitors of Tubulin Polymerization and Cytotoxic Compounds. *Bioorganic Med. Chem.* **2009**, *17* (17), 6422–6431. https://doi.org/10.1016/j.bmc.2009.07.012.

(187) González, M.; Ellahioui, Y.; Álvarez, R.; Gallego-Yerga, L.; Caballero, E.; Vicente-Blázquez, A.; Ramudo, L.; Marín, M.; Sanz, C.; Medarde, M.; Pelaéz, R. The Masked Polar Group Incorporation (MPGI) Strategy in Drug Design: Effects of Nitrogen Substitutions on Combretastatin and Isocombretastatin Tubulin Inhibitors. *Molecules* **2019**, *24* (23), 4319. https://doi.org/10.3390/molecules24234319.

(188) Gaspari, R.; Prota, A. E.; Bargsten, K.; Cavalli, A.; Steinmetz, M. O. Structural Basis of Cis- and Trans-Combretastatin Binding to Tubulin. *Chem* **2017**, *2* (1), 102–113. https://doi.org/10.1016/j.chempr.2016.12.005.

(189) Chaudhary, A.; Pandeya, S.; Kumar, P.; Sharma, P.; Gupta, S.; Soni, N.; Verma, K.; Bhardwaj, G. Combretastatin A-4 Analogs as Anticancer Agents. *Mini-Reviews Med. Chem.* **2007**, *7* (12), 1186–1205. https://doi.org/10.2174/138955707782795647.

(190) Seddigi, Z. S.; Malik, M. S.; Saraswati, A. P.; Ahmed, S. A.; Babalghith, A. O.; Lamfon, H. A.; Kamal, A. Recent Advances in Combretastatin Based Derivatives and Prodrugs as Antimitotic Agents. *Medchemcomm* **2017**, *8* (8), 1592–1603. https://doi.org/10.1039/c7md00227k.

(191) Dong, M.; Liu, F.; Zhou, H.; Zhai, S.; Yan, B. Novel Natural Product-and Privileged Scaffold-Based Tubulin Inhibitors Targeting the Colchicine Binding Site. *Molecules* **2016**, *21* (10), 1375–1483. https://doi.org/10.3390/molecules21101375.

(192) Li, W.; Sun, H.; Xu, S.; Zhu, Z.; Xu, J. Tubulin Inhibitors Targeting the Colchicine Binding Site: A Perspective of Privileged Structures. *Future Med. Chem.* **2017**, *9* (15), 1765–1794. https://doi.org/10.4155/fmc-2017-0100.

(193) Gill, R.; Kaur, R.; Kaur, G.; Rawal, R.; Shah, A.; Bariwal, J. A Comprehensive Review on Combretastatin Analogues as Tubulin Binding Agents. *Curr. Org. Chem.* **2014**, *18* (19), 2462–2512. https://doi.org/10.2174/1385272818191410281144428.

(194) Patil, P.; Patil, A.; Rane, R.; Patil, P.; Deshmukh, P.; Bari, S.; Patil, D.; Naphade, S. Recent Advancement in Discovery and Development of Natural Product Combretastatin-Inspired Anticancer Agents. *Anticancer. Agents Med. Chem.* **2015**, *15* (8), 955–969. https://doi.org/10.2174/1871520615666150526141259.

(195) Kaur, R.; Kaur, G.; Gill, R. K.; Soni, R.; Bariwal, J. Recent Developments in Tubulin Polymerization Inhibitors: An Overview. *Eur. J. Med. Chem.* **2014**, *87*, 89–124. https://doi.org/10.1016/j.ejmech.2014.09.051.

(196) Soussi, M. A.; Provot, O.; Bernadat, G.; Bignon, J.; Desravines, D.; Dubois, J.; Brion, J. D.; Messaoudi, S.; Alami, M. IsoCombretaQuinazolines: Potent Cytotoxic Agents with Antitubulin Activity. *ChemMedChem* **2015**, *10* (8), 1392–1402. https://doi.org/10.1002/cmdc.201500069.

(197) Khelifi, I.; Naret, T.; Renko, D.; Hamze, A.; Bernadat, G.; Bignon, J.; Lenoir, C.; Dubois, J.; Brion, J.-D.; Provot, O.; Alami, M. Design, Synthesis and Anticancer Properties of IsoCombretaQuinolines as Potent Tubulin Assembly Inhibitors. *Eur. J. Med. Chem.* **2017**, *127*, 1025–1034. https://doi.org/10.1016/j.ejmech.2016.11.012.

(198) Shuai, W.; Li, X.; Li, W.; Xu, F.; Lu, L.; Yao, H.; Yang, L.; Zhu, H.; Xu, S.; Zhu, Z.; Xu, J. Design, Synthesis and Anticancer Properties of Isocombretapyridines as Potent Colchicine Binding Site Inhibitors. *Eur. J. Med. Chem.* **2020**, *197*, 112308. https://doi.org/10.1016/j.ejmech.2020.112308.

(199) Álvarez, R.; Aramburu, L.; Gajate, C.; Vicente-Blázquez, A.; Mollinedo, F.; Medarde, M.; Peláez, R. Potent Colchicine-Site Ligands with Improved Intrinsic Solubility by Replacement of the 3,4,5-Trimethoxyphenyl Ring with a 2-Methylsulfanyl-6-Methoxypyridine Ring. *Bioorg. Chem.* **2020**, *98*, 103755. https://doi.org/10.1016/j.bioorg.2020.103755.

(200) Álvarez, R.; Aramburu, L.; Gajate, C.; Vicente-Blázquez, A.; Mollinedo, F.; Medarde, M.; Peláez, R. Methylsulfanylpyridine Based Diheteroaryl Isocombretastatin Analogs as Potent Anti-Proliferative Agents. *Eur. J. Med. Chem.* **2021**, *209*. https://doi.org/10.1016/j.ejmech.2020.112933.

(201) Dohle, W.; Jourdan, F. L.; Menchon, G.; Prota, A. E.; Foster, P. A.; Mannion, P.; Hamel, E.; Thomas, M. P.; Kasprzyk, P. G.; Ferrandis, E.; et al. Quinazolinone-Based Anticancer Agents: Synthesis, Antiproliferative SAR, Antitubulin Activity, and Tubulin Co-Crystal Structure. *J. Med. Chem.* **2018**, *61* (3), 1031–1044. https://doi.org/10.1021/acs.jmedchem.7b01474.

(202) Wang, Q.; Arnst, K. E.; Wang, Y.; Kumar, G.; Ma, D.; Chen, H.; Wu, Z.; Yang, J.; White, S. W.; Miller, D. D.; Li, W. Structural Modification of the 3,4,5-Trimethoxyphenyl Moiety in the Tubulin Inhibitor VERU-111 Leads to Improved Antiproliferative Activities. *J. Med. Chem.* **2018**, *61* (17), 7877–7891. https://doi.org/10.1021/acs.jmedchem.8b00827.

(203) Hu, L.; Li, Z. R.; Li, Y.; Qu, J.; Ling, Y. H.; Jiang, J. D.; Boykin, D. W. Synthesis and Structure-Activity Relationships of Carbazole Sulfonamides as a Novel Class of Antimitotic Agents against Solid Tumors. *J. Med. Chem.* **2006**, *49* (21), 6273–6282. https://doi.org/10.1021/jm060546h.

(204) CDC - Leishmaniasis - Biology https://www.cdc.gov/parasites/leishmaniasis/biology.html (accessed Mar 26, 2021).

anexos

"Cualquier momento es perfecto
para aprender algo nuevo."
Albert Einstein

anexo 1

Artículo de revisión de las sulfonamidas antimitóticas:

Antitubulin sulfonamides: The successful combination of an established drug class and a multifaceted target.

Vicente-Blázquez, A.; **González, M.**; Álvarez, R.; del Mazo, S.; Medarde, M.; Peláez, R.

Med. Res. Rev. **2019**, 39, 775–830.
DOI: 10.1002/med.21541

Received: 8 June 2018 | Revised: 2 September 2018 | Accepted: 6 September 2018

DOI: 10.1002/med.21541

REVIEW ARTICLE

WILEY

Antitubulin sulfonamides: The successful combination of an established drug class and a multifaceted target

Alba Vicente-Blázquez[1,2,3,4] | Myriam González[1,2,3] | Raquel Álvarez[1,2,3] | Sara del Mazo[1,2,3] | Manuel Medarde[1,2,3] | Rafael Peláez[1,2,3]

[1]Laboratorio de Química Orgánica y Farmacéutica, Departamento de Ciencias Farmacéuticas, Universidad de Salamanca, Campus Miguel de Unamuno, Salamanca, Spain

[2]Facultad de Farmacia, Instituto de Investigación Biomédica de Salamanca (IBSAL), Universidad de Salamanca, Campus Miguel de Unamuno, Salamanca, Spain

[3]Facultad de Farmacia, Centro de Investigación de Enfermedades Tropicales de la Universidad de Salamanca (CIETUS), Universidad de Salamanca, Campus Miguel de Unamuno, Salamanca, Spain

[4]Laboratory of Cell Death and Cancer Therapy, Department of Molecular Biomedicine, Centro de Investigaciones Biológicas, Consejo Superior de Investigaciones Científicas (CSIC), Madrid, Spain

Correspondence
Rafael Peláez, Laboratorio de Química Orgánica y Farmacéutica, Departamento de Ciencias Farmacéuticas, Universidad de Salamanca, Campus Miguel de Unamuno, E-37007 Salamanca, Spain.
Email: pelaez@usal.es

Funding information
Consejería de Educación de la Junta de Castilla y León. Cofunded by the EU's European Regional Development Fund - FEDER, Grant/Award Number: SA030U16

Abstract

Tubulin, the microtubules and their dynamic behavior are amongst the most successful antitumor, antifungal, antiparasitic, and herbicidal drug targets. Sulfonamides are exemplary drugs with applications in the clinic, in veterinary and in the agrochemical industry. This review summarizes the actual state and recent progress of both fields looking from the double point of view of the target and its drugs, with special focus onto the structural aspects. The article starts with a brief description of tubulin structure and its dynamic assembly and disassembly into microtubules and other polymers. Posttranslational modifications and the many cellular means of regulating and modulating tubulin's biology are briefly presented in the tubulin code. Next, the structurally characterized drug binding sites, their occupying drugs and the effects they induce are described, emphasizing on the structural requirements for high potency, selectivity, and low toxicity. The second part starts with a summary of the favorable and highly tunable combination of physical–chemical and biological properties that render sulfonamides a prototypical example of privileged scaffolds with representatives in many therapeutic areas. A complete description of tubulin-binding sulfonamides is provided, covering the different species and drug sites. Some of the antimitotic sulfonamides have met with very successful

applications and others less so, thus illustrating the advances, limitations, and future perspectives of the field. All of them combine in a mechanism of action and a clinical outcome that conform efficient drugs.

KEYWORDS
molecular mechanisms, sulfonamides, tubulin binding drugs, tubulin binding sites

1 | INTRODUCTION

Drugs targeting tubulin and the microtubules (tubulin binding drugs [TBDs]) are amongst the most successful antitumor, antifungal, antiparasitic, and herbicidal agents with applications in the clinic, in veterinary and in the agrochemical industry. Recently, the combination of computational methods, medicinal chemistry, biochemistry, structural biology, and cell biology is starting to unravel the intricacies of tubulin binding drugs and of the microtubules themselves, thus paving the way towards new and better TBDs. New methodological advances such as the high resolution cryo-electron microscopy, the imaging of individual microtubule dynamics, and the achievement of recombinant tubulin, altogether with more established methodologies for the study of the microtubules have combined to provide a sharper view of the structure and function of these essential cell components and their interactions with clinically important drugs.

The sulfonamides are a prototypical example of privileged scaffolds, with representatives in many therapeutic areas, due to a combination of favorable and highly tunable physical–chemical and biological properties. The early discovery of the dinitroaniline herbicides, and mainly the seminal discovery of ABT-751 and its limited success as an oral antitumor drug in the clinic led the path to an intense research for new antimitotic sulfonamides with better profiles, which has flourished in recent years with hundreds of new analogs. Antimitotic sulfonamides have provided exemplary cases of TBDs, binding to different tubulin species and sites, some are very successful and others less so, thus illustrating advances, limitations, and future perspectives of the field.

2 | TUBULIN AS A TARGET

Tubulin is a heterodimer of two globular subunits called α and β tubulin, which share a 40% amino acid sequence identity and a common fold, characterized by a compact aggregate of two globular domains with one β sheet each flanked by α helices and separated by a central helix (H7) running along with the longitudinal axis of the dimer (Figure 1). The larger globular domain is formed by the N-terminal 205 amino acids and contains a six β-strand parallel sheet (B1-B6) with two helices on one side (H1 and H2) and three on the other (H3–H5), known as the Rossmann fold characteristic of a family of dinucleotide binding proteins. Both tubulin subunits bind a guanine nucleotide in a region close to the longitudinal intradimer for α and interdimer for β contacts, in which α tubulin is always GTP and is nonexchangeable (N site) whereas in β tubulin can be GTP, GDP + P_i or GDP and exchange can readily occur in the free dimers (E site). The core of the subunit and the second globular domain is formed by the intermediate domain composed of residues 206 to 381 arranged as a four β-strand mixed sheet (B7-B10) flanked on one side by helices H9 and H10 and H8 on the other. The C-terminal domain folds as two helices (H11 and H12) connected by a U-turn and ends up in a negatively charged acidic unstructured tail where most of the isoform sequence variations and posttranslational modifications occur.[1–4]

Tubulin polymerize to form microtubules and other polymeric structures depending on the conditions such as the nucleation factors, the isotypes, and the posttranslational modifications.[5] Tubulin dimers associate

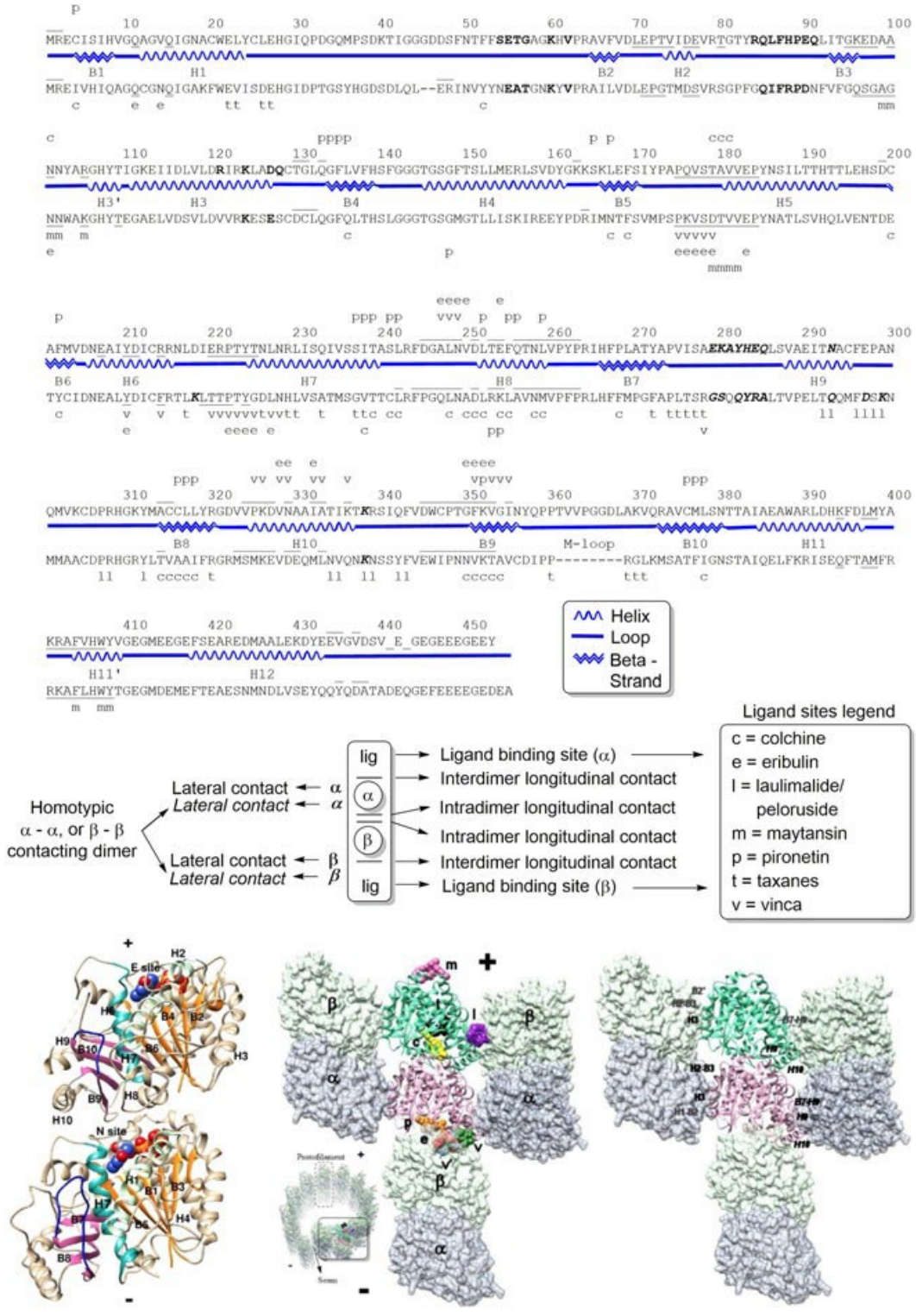

FIGURE 1 Continued.

longitudinally head to tail to form protofilaments. When the α subunit of a dimer stacks on the β subunit at the plus end of a protofilament it places the H7-H8 loop and the helix H8 close to the phosphates of the nucleotide at the E site and activates the GTPase activity by means of E254α.[1,6,7] The GDP bound dimer is inactive for polymerization[8,9] due to its higher reluctance to adopt a straight conformation than GTP-bound tubulin,[10] and it stores potential energy while trapped in the straight conformation in a microtubule or protofilament lattice until depolymerization releases the energy,[11,12] which is important for the separation of the sister chromatids during anaphase.[13] The plus end of the microtubule contains a cap of GTP or GDP + P_i bound dimers, which promotes polymerization and prevents depolymerization.[14–16] The exchangeable nucleotide site becomes protected and nonexchangeable in the protofilament until the dimer dissociates. In vivo microtubules are formed by 13 protofilaments except for particular functions or in particular cell types, usually associated with specific tubulin isotypes.[5,17,18] Lateral contacts between protofilaments form sheets that roll to form microtubules with a slight staggering between successive protofilaments. The subunits are disposed in shallow helices covering the walls of a cylinder and forming slender hollow tubes with important structural, motile, and intracellular-trafficking roles. The 13 protofilament B lattice imposes a 3 start helix with the protofilaments aligned parallel to the microtubule lattice (an arrangement which is probably important for the trafficking along them of bulky cargoes) and making homotypic (α-α or β-β) lateral contacts between them except for the so called seam between the 13th and the 1st protofilaments where heterotypic (α-β or vice versa) contacts are observed.[19–21] The lateral contacts are made between the end of H6 and H9, and the B7-H9 loop of one protofilament and the H1-B2 and H2-B3 loops and H3 of the other.[16]

2.1 | Microtubule dynamics

The microtubules rather than static, are very dynamic cellular structures involved in continuous fast reactions of addition and withdrawal of tubulin dimers mainly at the ends of the polymer, which results in microtubule formation or net growing, shrinking, and maintenance or disappearance.[22–24] The first step in microtubule formation is nucleation of a number of tubulin dimers, an energetically and kinetically unfavorable process facilitated in cells by nucleation factors, such as the γ–tubulin ring complex (γ-TuRC) involved in the assembly of 13 protofilament microtubules at microtubule organizing centers and other nucleation pathways, XMAP215 and TPX2.[17,25–28] Once formed, microtubules grow by addition of dimers at the plus or minus ends. The plus ends are intrinsically more dynamic than minus end, and grow and shrink faster. Formed microtubules experience two additional dynamic processes: dynamic instability and poleward flux. Poleward flux refers to the continuous flow of dimers from the plus to the minus end caused by growing at the plus end and shortening at the minus end and plays an important role in maintaining the tension of the mitotic spindle, which in turn is important for passing through the spindle checkpoint.[29,30] Dynamic instability is the most characteristic dynamic behavior of microtubules and consists on stochastic sudden changes at either microtubule end from net growing to shrinking (called catastrophes) or from shrinking to growing (called rescues) or to lag periods where no net length changes take

◀

FIGURE 1 Top: One letter code amino acid sequences and common numbering of α (up) and β (down) tubulins. The common secondary structure elements and their names (B for β-strands and H for helices) are indicated between the two sequences. The ligand binding sites of each subunit are indicated by letters above the α or below the β sequences, respectively. Longitudinal intradimer (α-β) contacts are indicated by underlined residues for the α sequence and overlined for the β sequence. Longitudinal interdimer (β-α or α-β) contacts are indicated by overlined residues for the α sequence and underlined for the β sequence. Residues making lateral contacts in the microtubule are bolded or bolded and italicized depending on the direction of the advance of the lattice helix. Bottom: Structure of the isolated tubulin dimer with the β subunit on top (plus end) and an indication of the secondary structure elements and the nucleotide binding sites and in the context of a microtubule (shown as a small insert with the boxed zone enlarged) with the structurally characterized tubulin binding sites indicated by their ligands (shown as Corey–Pauling–Koltun [CPK]) and the lateral contacts on the right

place (pauses), that are independent of the net growth or shrinkage.[14,31] Again, the higher dynamism of plus end results in larger effects than at the minus end, whose dynamism in cells is often suppressed by associated proteins. This dynamic behavior is of paramount importance to their biological functions and is therefore highly regulated in cells by an intricate combination of the tubulin isotypes and posttranslational modifications, the chemical state of the nucleotide at the E site, the conformations of the tubulin dimer, the microtubule lattice, and many proteins binding to the dimers and to the microtubule itself. The dynamic behavior of tubulin and microtubules and its relationship to mechanical and biochemical processes[22] have been studied by means of a variety of computational methods due to the vast range of timescales (from nanoseconds to minutes or even hours) and resolutions (from atomistic to coarse-grained models) covered.[32] These studies are providing an understanding of the mechanisms underlying microtubule behavior, from GTP hydrolysis[10] to microtubule growth, shrinkage, and dynamic instability[33–36] and the effects and functioning of associated proteins[37–39] or drug binding.[40–44] Microtubule targeting drugs at concentrations lower than those affecting microtubule polymer mass presumably exert their action altering this dynamic behavior by binding to their putative sites on tubulin.[14,22,31,45–49] The mitotic microtubules turn over 4 to 100 times faster than interphase microtubules and are therefore expected to be more sensitive to drugs, although other mechanisms have been proposed.[50–52]

2.2 | The tubulin code

The diversity of functions exerted by microtubules and their dynamics have to be carefully tuned in cells, which is achieved by controlling tubulin isotype expression (in humans there are eight α and eight β isotypes)[48] and introducing posttranslational modifications of tubulin.[53] Their combination makes possible the specification of multiple microtubule states with regard to structure, dynamics, protein, and drug binding, further modification, assembly formation, and eventually function in what has been called the "tubulin code."[3,53–59] Different tubulin isotypes can copolymerize forming mosaic microtubules, but specialized microtubules, such as those of neurons or axonemes, are enriched in individual β isotypes which could in part be responsible for their specific functions (eg TubB1 in mammals is exclusive of platelets and megakaryocytes, TubB3 is enriched in neurons, TubB4 in axonemes of cilia and flagella or in the nematode *Caenorhabditis elegans*, and the α tubulin MEC-12 and the β tubulin MEC-7 form 15 protofilament microtubules in the touch neurons).[48,60] Changes in isotype expression have been observed in cancer cells in response to treatment with TBDs.[61–63] Much less is known about α isotypes. Tubulin posttranslational modifications are mainly found at the unstructured, microtubule protruding, acidic C-terminus of both subunits. α Tubulin can lose its C-terminal tyrosine (detyrosination) in the microtubule and is retyrosinated after dimer release, giving rise to patterns of detyrosinated tubulin in stable microtubules and tyrosinated in more recent ones, which are important for correct development, neuronal differentiation, and also in tumorigenesis amongst others. Detyrosinated α tubulin can irreversibly lose additional amino acids from the C-terminus. Acetylation of tubulin occurs mainly on lysine K40 of α tubulin at the microtubule lumen by αTAT and deacetylation is catalyzed by histone deacetylase 6 (HDAC-6) or sirtuins, but its functional role remains to be determined. Additional acetylation sites have been recently described, such as K252 of β tubulin. Glutamate sidechains of α and β tubulin are (poly)glutamylated or (poly)glycylated by enzymes with different preferences for branching points or chain extension-reduction. Polyglutamylated microtubules are more often severed by spastin until a certain length, and thereafter they stabilize microtubules instead. Other posttranslational modifications of tubulin include methylation (competing with acetylation), phosphorylation, palmitoylation, ubiquitylation, sumoylation, and more. The effects of these posttranslational modifications are still mostly unknown.

2.3 | Tubulin binding sites

Tubulin is the molecular target of many successful drugs used for the treatment of different types of cancer,[45,47] several parasitic diseases,[64] and also as some herbicides.[65,66] Drugs targeting the microtubules are

TABLE 1 Structurally characterized ligand sites. PDB IDs of the complexes of tubulin with ligands binding to the different sites. For covalently binding ligands the modified residue is indicated

PDB[70] ID	Ligand(s)	Res	Tubulin	Effect	Covalent	Ref
Taxoids						
5NG1	Zampanolide. MTC	2.2	Curved	MSA. MDA	HIS229β	[71]
5EZY	Taccalonolide AJ	2.05	Curved	MSA	ASP226β	[72]
5LXS	KS-1-199-32	2.2	Curved	MSA	-	[73]
5LXT	Discodermolide	1.9	Curved	MSA	-	[73]
5MF4	Dictyostatin	2.3	Curved	MSA	-	[74]
5SYE	Paclitaxel. Peloruside	3.5	Straight	MSA. MSA	-	[75]
5SYF	Paclitaxel	3.5	Straight	MSA	-	[75]
5SYG	Zampanolide	3.5	Straight	MSA	HIS229β	[75]
3J6G	Paclitaxel	5.5	Straight	MSA	-	[16]
4I4T	Zampanolide	1.8	Curved	MSA	HIS229β	[76]
4I50	Epothilone A	2.3	Curved	MSA	-	[76]
1TVK	Epothilone A	2.89	Straight	MSA	-	[77]
1JFF	Paclitaxel	3.5	Straight	MSA	-	[1]
1TUB	Paclitaxel	3.7	Straight	MSA	-	[6]
Laulimalide/Peloruside						
4O4H	Laulimalide	2.1	Curved	MSA	-	[41]
4O4I	Laulimalide. Epothilone A	2.4	Curved	MSA. MSA	-	[41]
4O4J	Peloruside A	2.2	Curved	MSA	-	[41]
4O4L	Peloruside A. Epothilone A	2.2	Curved	MSA. MSA	-	[41]
Vinca						
1Z2B	COL. VLB	4.10	Curved	MDA. MDA	-	[78]
3DU7	COL. Phomopsin A	4.10	Curved	MDA. MDA	-	[79]
3E22	COL. Soblidotin	3.80	Curved	MDA. MDA	-	[79]
3UT5	COL. Ustiloxin	2.73	Curved	MDA. MDA	-	[80]
4EB6	VLB	3.47	Curved	MDA	-	[80]
4X1I	Dolastatin 10 analog	3.11	Curved	MDA	-	[81]
4X1K	Dolastatin 10 analog	3.50	Curved	MDA	-	[81]
4X1Y	Dolastatin 10 analog	3.19	Curved	MDA	-	[81]
4X20	Dolastatin 10 analog	3.50	Curved	MDA	-	[81]
4ZHQ	MMAE	2.55	Curved	MDA	-	[82]
4ZI7	HTI286	2.51	Curved	MDA	-	[82]
4ZOL	Tubulysin M	2.50	Curved	MDA	-	[82]
5BMV	VLB	2.50	Curved	MDA	-	[82]
5H74	14b complex	2.60	Curved	MDA	-	-
5IYZ	MMAE	1.80	Curved	MDA	-	[83]
5J2T	VLB	2.20	Curved	MDA	-	[83]
5J2U	MMAF	2.50	Curved	MDA	-	[83]

(Continues)

TABLE 1 (Continued)

PDB[70] ID	Ligand(s)	Res	Tubulin	Effect	Covalent	Ref
5KX5	Tubulysin 11	2.50	Curved	MDA	-	[84]
5LOV	DZ-2384	2.40	Curved	MDA	-	[85]
5NJH	Triazolopyrimidine	2.39	Curved	MSA	-	[86]
Eribulin						
5JH7	Eribulin	2.25	Curved	MDA	-	[87]
Maytansin						
4TUY	Rhizoxin	2.10	Curved	MDA	-	[88]
4TV8	Maytansin	2.10	Curved	MDA	-	[88]
4TV9	PM060184	2.00	Curved	MDA	-	[88]
Pironetin						
5FNV	α-β unsaturated lactone	2.61	Curved	MDA	C316α	[89]
5LA6	Pironetin	2.10	Curved	MDA	C316α	[90]
Colchicine						
1SA0	DAMA-Colchicine	3.58	Curved	MDA	-	[91]
1SA1	Podophyllotoxin	4.20	Curved	MDA	-	[91]
3HKC	ABT-751	3.80	Curved	MDA	-	[92]
3HKD	TN-16	3.70	Curved	MDA	-	[92]
3HKE	T-138067	3.60	Curved	MDA	C241β	[92]
3N2G	NSC 613863	4.00	Curved	MDA	-	[93]
3N2K	NSC 613862	4.00	Curved	MDA	-	[93]
4O2A	BAL-27862	2.50	Curved	MDA	-	[94]
4O2B	Colchicine	2.30	Curved	MDA	-	[94]
4YJ2	MI-181	2.60	Curved	MDA	-	[95]
4YJ3	Triazolothiadiazine	3.75	Curved	MDA	-	[95]
5C8Y	Plinabulin	2.59	Curved	MDA	-	[96]
5CA0	Lexibulin	2.50	Curved	MDA	-	[96]
5CA1	Nocodazole	2.40	Curved	MDA	-	[96]
5CB4	Tivantinib	2.19	Curved	MDA	-	[96]
5GON	CA-4 β-lactam	2.48	Curved	MDA	-	[97]
5H7O	Imidazopyridine	2.80	Curved	MDA	-	[98]
5JCB	YJTSF1	2.30	Curved	MDA	-	[99]
5JVD	TUB092	2.39	Curved	MDA	-	[100]
5LP6	Thiocolchicine	2.90	Curved	MDA	-	[101]
5LYJ	Combretastatin A-4	2.40	Curved	MDA	-	[102]
5M7E	BKM120	2.05	Curved	MDA	-	[103]
5M7G	MTD147	2.25	Curved	MDA	-	[103]
5M8D	MTD265R1	2.25	Curved	MDA	-	[103]
5M8G	MTD265	2.15	Curved	MDA	-	[103]
5NFZ	MTC	2.1	Curved	MDA	-	[71]

(Continues)

TABLE 1 (Continued)

PDB[70] ID	Ligand(s)	Res	Tubulin	Effect	Covalent	Ref
5O7A	Quinolin-6-yloxyacetamide	2.49	Curved	MDA	-	104
5OSK	Quinazolinone	2.11	Curved	MDA	-	105
5OV7	Rigosertib	2.40	Curved	MDA	-	106
5XAF	CA-4 β-lactam Z1	2.55	Curved	MDA	-	107
5XAG	CA-4 β-lactam Z2	2.56	Curved	MDA	-	107
5XHC	PO10	2.75	Curved	MDA	-	-
5XI5	PO5	2.81	Curved	MDA	-	-
5XI7	PO7	2.99	Curved	MDA	-	-
5XLT	4′-Demethylepipodophyllotoxin	2.81	Curved	MDA	-	108
5XLZ	9(10 H)-Anthracenone	2.30	Curved	MDA	-	109
5YL4	Plinabulin 8WR	2.64	Curved	MDA	-	-
6BR1	Pyrido[2,3-d]pyrimidine	2.30	Curved	MDA	-	110
6BRF	Pyrido[3,2-d]pyrimidine	2.5	Curved	MDA	-	110
6BRY	Furo[3,2-d]pyrimidine	2.7	Curved	MDA	-	110
6BS2	Oxazolo[5,4-d]pyrimidin	2.65	Curved	MDA	-	110
6FKJ	TUB075	2.15	Curved	MDA	-	111
6FKL	TUB015	2.10	Curved	MDA	-	111

Abbreviations: MDA, microtubule–destabilizing agents; MSA, microtubule–stabilizing agents; PDB, Protein Data Bank
PDB IDs of the complexes of tubulin with ligands binding to the different sites. For covalently binding ligands the modified residue is indicated.

often classified as microtubule–destabilizing agents (MDAs) or microtubule–stabilizing agents (MSAs) according to the effect they have on polymer mass at high concentrations: MDAs promote depolymerization and prevent polymerization, whereas MSAs promote formation and stabilize preformed microtubules, and prevent depolymerization.[45,47,67] The changes in polymer mass result from the thermodynamic linkage of the tubulin polymerization–depolymerization equilibria and the preferential binding of drugs to either the dimer (MDAs) or to the polymers (MSAs). When a drug binds preferentially to the dimer it behaves as an MDA while the reversal is true for MSAs.[68]

Irrespective of their effect on polymer mass at high concentrations or their binding site on tubulin, at the clinically relevant lower concentrations MSAs and MDAs perturb the dynamic behavior of the microtubules,[47,69] which is considered to lie behind the effects observed in cells, including the mitotic arrest associated with their antimitotic activity.

Currently, the two well-structurally defined binding sites for MSAs (Table 1) have been located on the β subunit: the taxoid site at the microtubule lumen and the laulimalide and peloruside binding site located on the exterior of the microtubule.[112] Additionally, an external type pore I site associated with initial low-affinity taxane binding, and mutually exclusive with the taxoid luminal site has been proposed[113] and identified as the site where the MSA cyclostreptin covalently binds.[114] All these MSAs binding sites are close to protein regions involved in lateral contacts between protofilaments. Recently, a new class of MSA has been added from a classical MDA site, the vinca alkaloids.[86] MDAs (Table 1) bind to at least five well structurally characterized sites on either α (the pironetin binding site), or the α-β interface (the vinca alkaloid), or β tubulin, (colchicine, rhizoxin/maytansin, and eribulin binding sites).

2.3.1 | The taxoids site

The taxoids binding site is a hydrophobic pocket located on the intermediate region of the β subunit close to the interprotofilament interface at the internal lumen of the microtubule (Figure 2B). It extends along H7 (the core helix of the intermediate domain) towards the C-terminus of H1, the H6-H7 loop, B7 and the B7-H9 loop, and the M-loop (B9-B10).[1,6] The site on α tubulin is occupied by the eight additional amino acids present in the B9-B10 loop (Figure 2B), which have a stabilizing effect on the M-loop that is mimicked by the binding of MSAs to the taxoids site of the β subunit.[76]

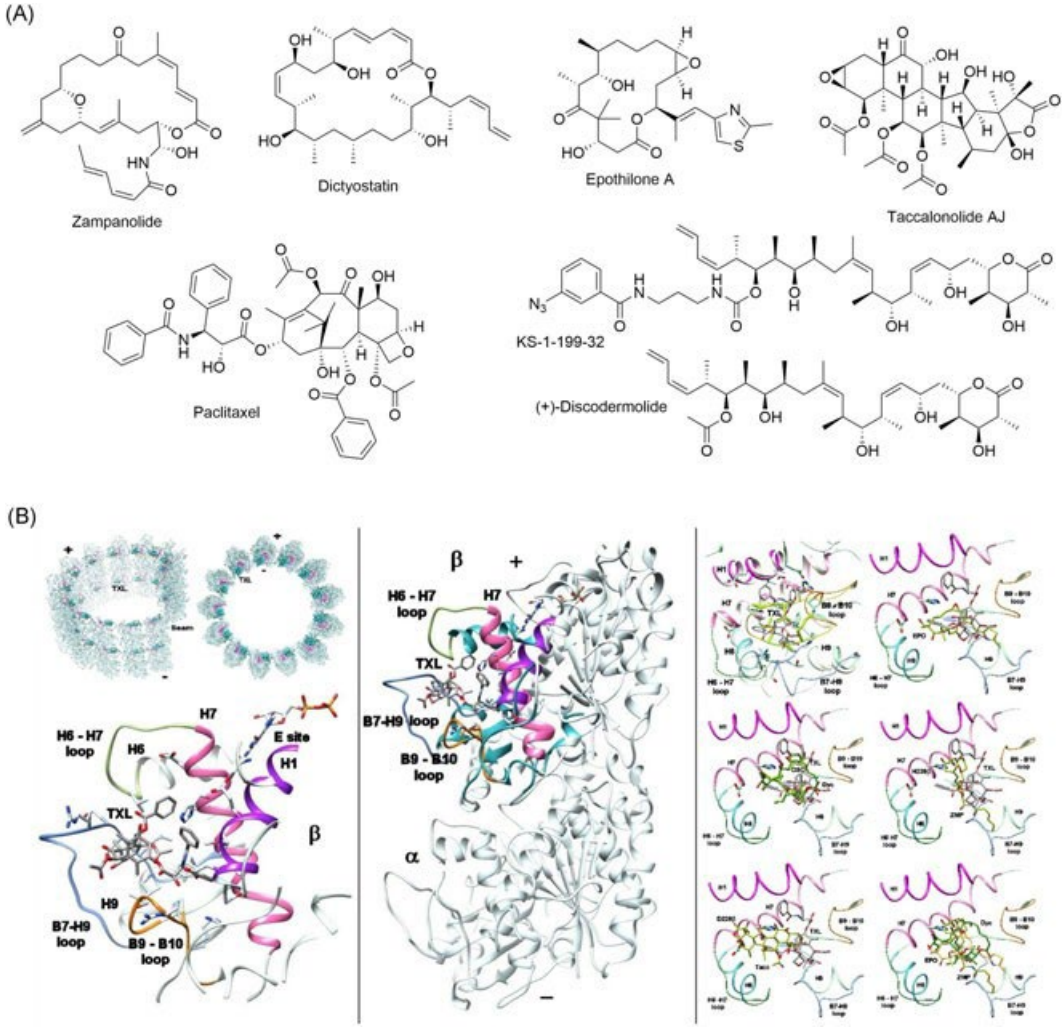

FIGURE 2 A, Taxoid site ligands. B, The taxoids binding site. Left: location of the paclitaxel (Corey–Pauling–Koltun [CPK]) binding site (H7 is highlighted) at the inner luminal surface of the microtubule (up) and detail of the taxoid binding site. Center: tubulin dimer with paclitaxel (sticks) in the T conformation bound to the β subunit. Right: the taxoids ligands in their site (paclitaxel [TXL], is always shown as gray sticks for comparison). From left to right and from up to down: 1) a superposition of β and α tubulin at the taxoid site, showing that TXL replaces the extended B9–B10 loop of the α subunit, 2) the complex with epothilone A (EPO), 3) the complex with dictyostatin (Dyc) and discodermolide (DSC), 4) the covalent complex with zampanolide (ZMP), 5) the covalent complex with taccalonolide AJ (Tacc), and 6) superposition of epothilone A (EPO), dictyostatin (Dyc), and zampanolide (ZMP)

After the initial finding of paclitaxel many taxoid site ligands Figure 2A[115] have been discovered in the research for improved aqueous solubility, reduced susceptibility to resistance by transport proteins or tubulin isotype changes,[63] and improved toxicity profiles. Most of them are complex natural products or semisynthetically derived analogs, although many efforts have been devoted to more accessible simplified analogs.[116] Apart from the taxanes (paclitaxel, docetaxel, and cabazitaxel, and an albumin bound paclitaxel nano-droplet formulation [Abraxane®]) only the aza-epothilone B analog ixabepilone has been approved.[117] Recently, drugs covalently binding to the taxoid site of tubulin (in particular to aminoacids H229β, N228β, and D226β lining one side of H7) such as zampanolide,[71,76] dactylolide, and taccalonolide AJ[72] have also appeared,[112,118] but despite the potential benefits of a different mechanism of action, longer lifetimes, and less clearance,[119] they have not yet reached the clinic.

Even if they bind to the same pocket of β tubulin, the structures of the complexes show that there is no evident common pharmacophore and that each ligand adapts in a distinct pose to the structural elements of the site (Figure 2B). However, the available structural information allows for the design of combinations of structural moieties of different series.

2.3.2 | The laulimalide/peroluside site

Laulimalide[120] and peloruside A[121] (Figure 3) are two macrocyclic lactones from marine sponges. They bind to an external site of the β subunit formed by H9, H10, and the H9-B8 and H10-B9 loops, making hydrophobic contacts and structure-specific hydrogen bonds.[41] The side chains of both compounds occupy a common hydrophobic pocket at the C-terminus of helices H9 and H10 and the macrocyclic cores passing by the side of H9 with their main planes slightly rotated with respect to each other: laulimalide extending along H9 and peloruside crossing perpendicular to H9, presenting the more similarly occupied zone towards the protofilament side, where it contacts H3 of the contiguous protofilament, thus stabilizing the microtubule. Furthermore, a cross talk between the laulimalide/peloruside site and the taxoids site has been observed, which results in the structuring of the M-loop

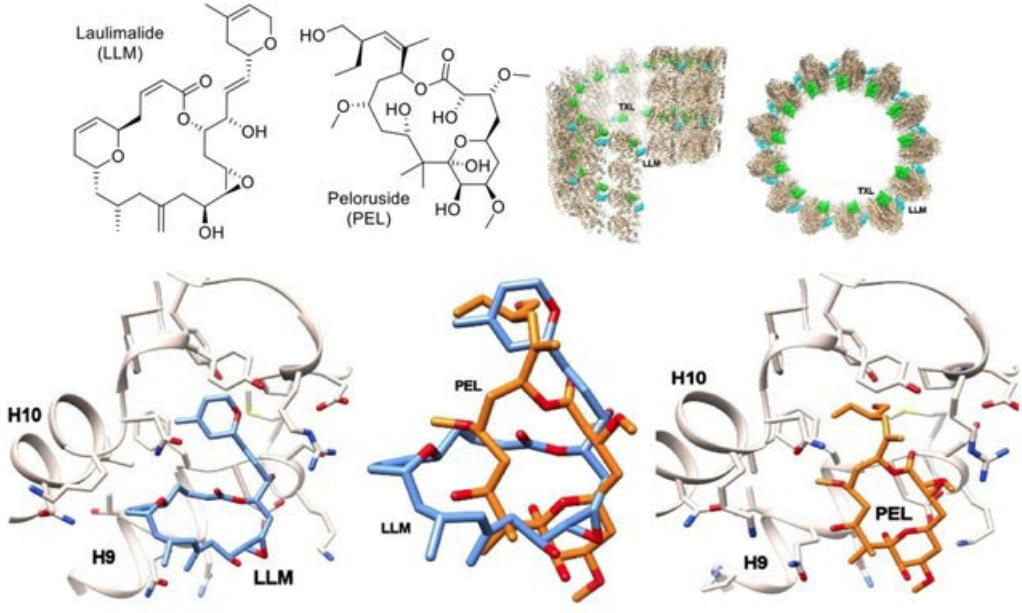

FIGURE 3 Structure of laulimalide (LLM) and peloruside A (PEL), binding sites on β tubulin (lower row) and a superposition of both ligands. A microtubule model indicating the location of the binding site at the external surface of the microtubule is shown, with paclitaxel (TXL) in the inner luminal space indicated for comparison

(considered important in the stabilization of lateral protofilament contacts in the microtubule) *via* Gln294β.

High resolution cryo-electron microscopy structural studies of microtubules formed in the presence of peloruside show a regularization of the microtubule lattice by means of a reinforcement of the lateral contacts between protofilaments which results in more homogeneous nonseam (homologous α-α and β-β) and seam (heterologous α-β) interactions that increase the helical symmetry of the microtubule.[75] This effect is opposed to that observed for taxoid site ligands.

2.3.3 | The vinca alkaloids domain

The vinca alkaloids (eg vinblastine) bind at the interface between two tubulins, contacting almost equally the β subunit of one dimer and the α subunit of the incoming one, thus acting as a wedge. They prevent the formation of straight protofilaments as required for the microtubules and thus promote microtubule depolymerization and the formation of curved polymers. The site is located at the longitudinal interface between two tubulin dimers, close to the exchangeable nucleotide site (E site) and between the helices H6, H7 and the H6-H7 and the B5-H5 loops of the β subunit of one dimer and along B9, H10 and the loop connecting them of the α subunit of the incoming tubulin dimer at the plus end.[78]

Several ligands (Figure 4A), natural peptides, or analogs (eg dolastatins,[81] auristatins,[82,83] and tubulysins[84]), have subsequently been structurally characterized bound to the vinca site. They climb H7 and extend towards H1 and contact the β subunit further than vinblastine, thus leading to very potent tubulin polymerization inhibitory activity and cytotoxicity. This high potency has been clinically exploited in the form of antibody-drug conjugates (ADCs). The vinca peptides share binding modes that have been summarized in a common pharmacophore model,[82] which also represents the binding of several macrocyclic peptides, such as ustiloxin[80] and phomopsin A.[79]

The great structural plasticity of the vinca site, currently unparalleled amongst the microtubule targeting agents, has been recently exposed by two structurally different chemical classes, the diazonamides[85] and the triazolopyrimidines.[86] The diazonamides bind to the vinca site but due to their reduced size and distinct shape, they behave as a smaller wedge between the tubulin dimers than the classical vinca alkaloids or the vinca peptides. Therefore, they cause a significant effect on the dynamic behavior of the microtubule, but only a reduced effect on the microtubule polymer mass. These properties have been linked to a reduced toxicity profile due to preferential action on mitotic over interphase microtubules.[85] A further improvement in the versatility of the vinca site ligands has come from a family of synthetic triazolopyrimidines that behave as MSAs as a result of their small size and flat structure. They cause a stabilization of the longitudinal contacts along with a straightening of the tubulin dimers, thus facilitating microtubule polymerization.[86]

2.3.4 | The eribulin site

Eribulin binds to a mixed-character site of β tubulin between the helices H1, H6, and H7 and the B3-H3, H6-H7, and B5-H5 loops, which partially overlaps with the amino terminus of the vinca peptides (Figure 5) but extends towards the opposite side of Y224β and the nucleotide of the exchangeable nucleotide site (E site) of the β subunit recognized by the C-terminus of the vinca peptides: the phenolic end of Y224β and the ribose of the nucleotide. Eribulin capping of the microtubule plus end is incompatible with straight protofilament extension, thus stalling protofilament elongation and favoring catastrophe and depolymerization.[87]

2.3.5 | The maytansin site

The maytansin site is located close to the nucleotide E site of the β subunit, boxed by the helices H3′ and H11′ and the loops B3-H3 and B5-H5. Maytansin and rhizoxin F share a common pharmacophore making hydrophobic contacts with the lower surface of the macrocycles to the sidechains of F404β, W407β, and Y408β (H11′), with the oxirane rings to V181β and V182β (B5-H5) and making hydrogen bonds with the carbamate or the six–membered lactone to the sidechains of N102β and K105β of H3′ and with the amide or ketone carbonyls to the backbone of

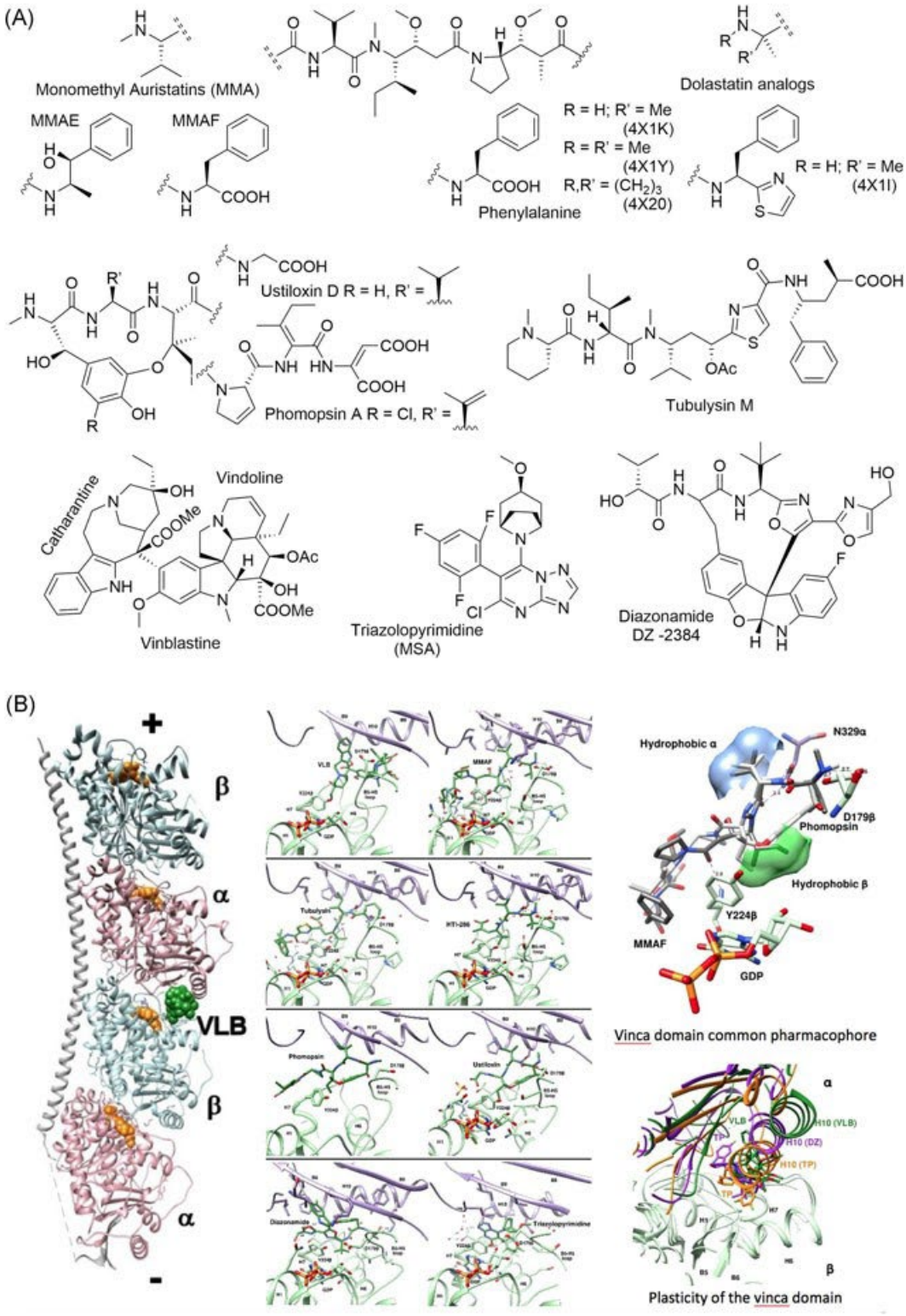

FIGURE 4 Continued.

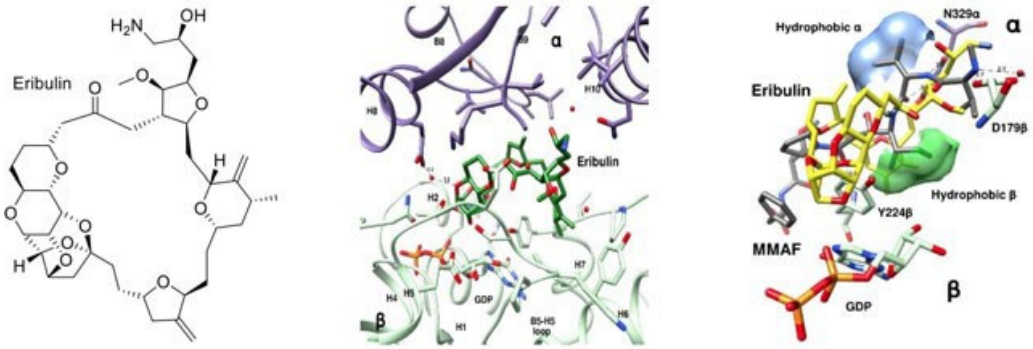

FIGURE 5 The eribulin site. Structure of eribulin and of the eribulin–tubulin complex at the interdimer interfacial surface between β and α tubulins, partially overlapping with the vinca domain, as shown on the right hand side by a superposition of eribulin and monomethyl auristatin F on the pharmacophore of the vinca domain ligands (Figure 4)

V181β (B5-H5). PM060184 binds in a similar way, adapting itself quite closely to the upper region of maytansin that connects the two hydrogen bonded carbonyls.[88]

Maytansin site ligands and vinblastine show mutual inhibition of tubulin binding, despite binding to different sites (Figure 6): the former bind exclusively at the β subunit and block longitudinal interdimer interactions due to steric clashes with H8 of α tubulin, while vinblastine requires the formation of the interdimer interface as it binds almost equally to both subunits.

2.3.6 | The pironetin site

Pironetin binds covalently to C316 of the α subunit and adopts an extended conformation in a hydrophobic cavity formed between helix H7 and the β sheets B7, B8, B9, and B10 and B1, B2, B4, and B5 by displacement upon binding of the N terminus of helix H8 and the H7-H8 loop (Figure 7). As a result, H8 and the H7-H8 loop protrude towards the interdimer space and collide with the β subunit, thus perturbing the longitudinal interdimer contacts and resulting in microtubule depolymerization.[89,90]

2.3.7 | The colchicine domain

The colchicine site is a hydrophobic pocket located at the interdimer interface (Figure 8), close to the nonexchangeable nucleotide site (N site).[91] Ligand binding shifts H7, distorts loop H7-H8, and impedes the curved to straight transition due to steric clashes along the longitudinal interdimer interface, thus causing microtubule depolymerization.

Many colchicine site ligands (Figure 9) have been discovered, both natural and synthetic, and the structural interactions of many of them with tubulin have been described in recent years (Table 1). The colchicine binding

◀

FIGURE 4 A, Structure of vinca domain site ligands. B, The vinca domain at the interdimer interfacial surface between β and α tubulins. Left: location of VLB between two consecutive dimers. Center: detail of the vinca binding domain in complex with VLB, MMAF, tubulysin M, HTI-286, phomopsin A, ustiloxin, DZ, and TP. Right: on top, the common pharmacophore of the vinca peptide ligands represented by MMAF and phomopsin A and at the bottom the plasticity of the vinca domain is shown by means of a superposition of the complex with the microtubule–stabilizing agents TP, the polymer mass nonmodifying DZ, and the microtubule–destabilizing agents VLB showing the progressive displacement of helix 10 implicated in lateral interprotofilament contacts (Figure 1).
DZ, diazonamide; MMAF, monomethyl auristatin F; TP, triazolopyrimidines; VLB, vinblastine

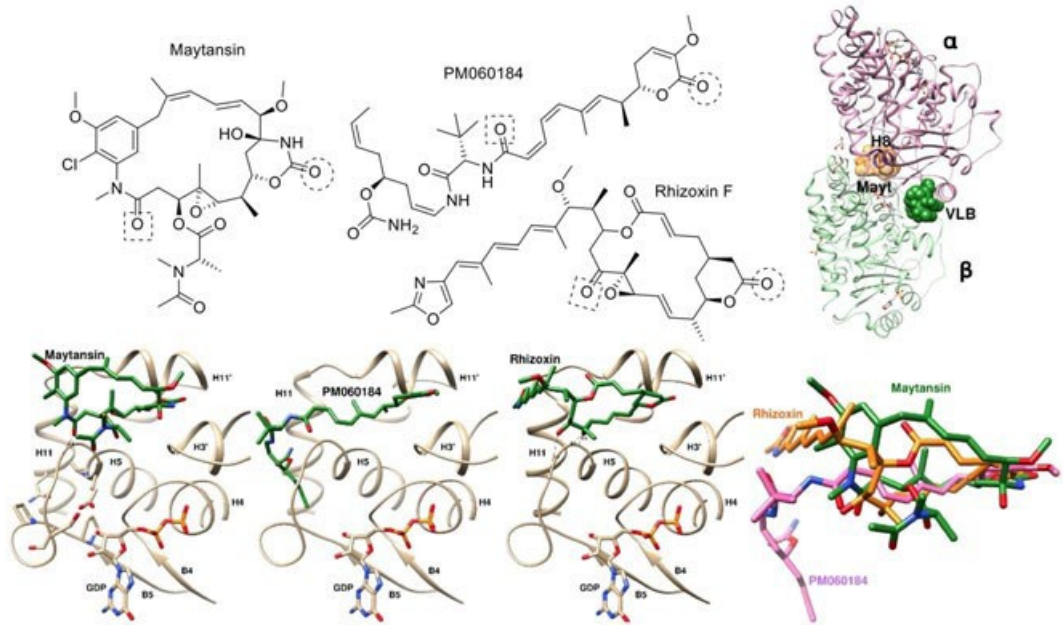

FIGURE 6 The maytansin site at β tubulin longitudinal interdimer surface. Structures of maytansin, PM060184, rhizoxin F and their complexes with tubulin. The tubulin dimer on the upper right side shows the steric clash of maytansin site ligands (white transparent surface) with helix H8α in the conformation needed to complete the vinblastine (Corey–Pauling–Koltun [CPK]) site at the interface that explains their mutual exclusion

domain includes an ensemble of at least three distinct pockets disposed in a sequential arrangement.[122,123] The first pocket contacts both the α (B5-H5 loop) and β subunits (H10-B9 loop, H8, and B9), the central one is located at the C-terminus of the central H7, over B8, B9 ,and B10 and covered by the displaced H10-B9 loop and H8, while the third pocket is more buried in the β subunit, passing behind H8 towards the sheet formed by B1, B4, B5, and B6 and covered by H1 and the middle part of H7. Currently, most of the colchicine-domain drugs structurally characterized bind only to two contiguous pockets out of the available three, with the exception of the sulfonamide

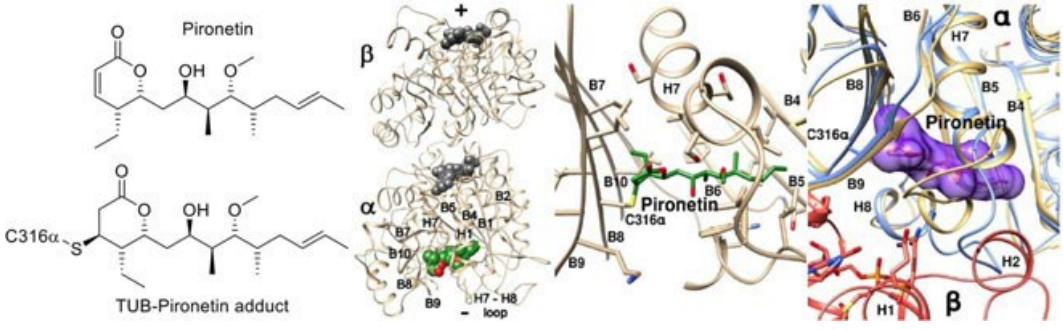

FIGURE 7 The pironetin site on α tubulin at the longitudinal intradimer surface. Structures of pironetin and its covalent adduct with C316α. The location of the pironetin binding site of tubulin and detail of the binding site is shown in the middle. On the right-hand side the steric clash of pironetin (transparent surface) in the tubulin complex (blue) with H8 in a straight dimer disposition (wheat) and the resulting displacement of H7-H8 explains the microtubule disrupting action due to steric clash with the β subunit

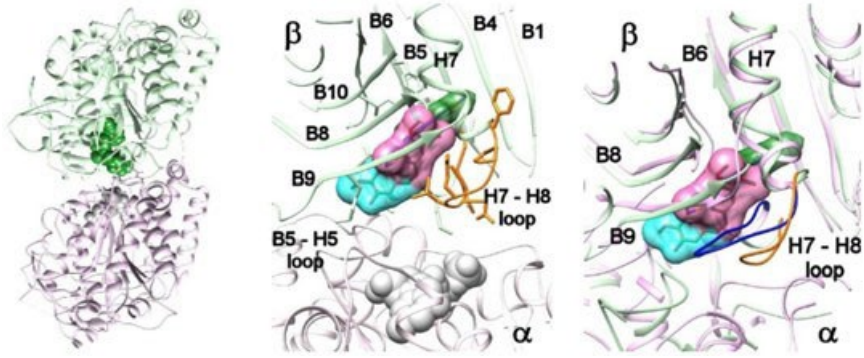

FIGURE 8 The colchicine domain on β tubulin at the longitudinal intradimer surface. The location of the colchicine domain (left) within the dimer, a detailed view of the three zones (center) and a superposition (right) of the site with the straight dimer showing the displacement of H7-H8 of the β subunit that prevents straightening

ABT-751 and the pyrimidine lexibulin which binds completely to two of them but also partially occupy the third one.[105,124]

3 | THE SULFONAMIDES

Sulfonamides are the amides of sulfonic acids, with a general formula of $RSO_2NR^1R^2$ (Figure 10). Depending on the number of substituents on the nitrogen, they are referred to as primary (R^1 and R^2 equal to H), secondary (R^1 or R^2 equal to H) or tertiary (R^1 and R^2 different from H) sulfonamides. The sulfonamide moiety is considered a privileged scaffold in medicinal chemistry due to its frequent appearance in drugs and to the large number of biological activities presented by sulfonamide containing drugs. Following the initial discovery of prontosil and the antibacterial sulfa drugs, for example sulfamethoxazole, new activities were described for the sulfonamide scaffold, including the hypoglycemic effects of sulfonylureas, for example tolbutamide, used for the treatment of non-insulin-dependent diabetes mellitus, and the inhibition of carbonic anhydrases by sulfanilamide which led to the discovery of diuretics such as acetazolamide, hydrochlorothiazide, and furosemide, used for the treatment of hypertension, glaucoma, and edema. Subsequent structural variations led to the uncovering of diverse biological effects such as anti-inflammatory, anticonvulsant, antithyroid, herbicidal, antiviral, and anticancer.[125] As a reflection of their perceived privileged scaffold in medicinal chemistry, more sulfonamides are continuously being approved for different applications, like the kinase inhibitor Omipalisib© approved on 2015,[126] and the first in class inhibitor of the apoptosis regulator B-cell lymphoma-2 (Bcl-2) Venetoclax© approved on 2016[127] (Figure 10).

The high occurrence of sulfonamide moieties in drugs is evidenced by their ranking as the 22nd most frequent side chain in the classic analysis of the structural elements present in known drugs by Bemis and Murcko.[128,129] Out of 11542 new chemical entities that have historically entered clinical trials the sulfonamide moiety is present in 455 (3.9%), out of which 102 have primary, 247 have secondary, and 108 have tertiary sulfonamides.[130]

Sulfonamides have been defined as molecular chimeras able to make hydrogen bonds and interact with unipolar environments.[131] A study on the binding preference of ligand fragments for protein amino acids present in the Protein Data Bank (PDB) found that the sulfonamide group as part of 4 out of the 315 fragments, with a sufficient number of contacts.[132] Mirroring the chimeric character of the sulfonamides, the preferred amino acids belong to different property classes: histidines are the most frequent partners for primary sulfonamides (probably biased by the sulfonamide anions of many carbonic anhydrase representatives complexed to Zn cations surrounded by histidine ligands), whereas the hydrophobic amino acids (eg glycine, valine, or leucine) are preferred for others.

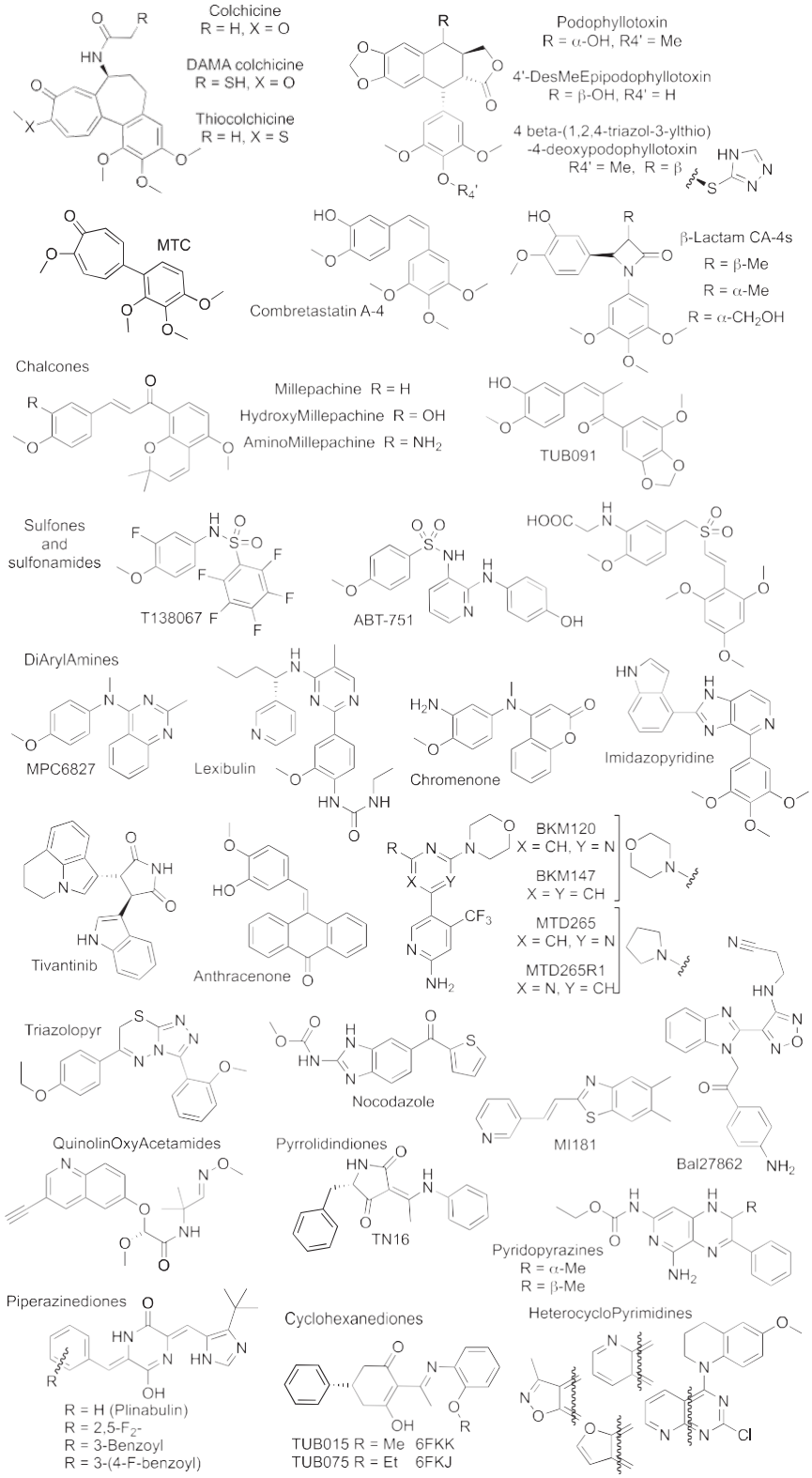

FIGURE 9 Structure of colchicine site ligands with X-ray structures in complex with tubulin

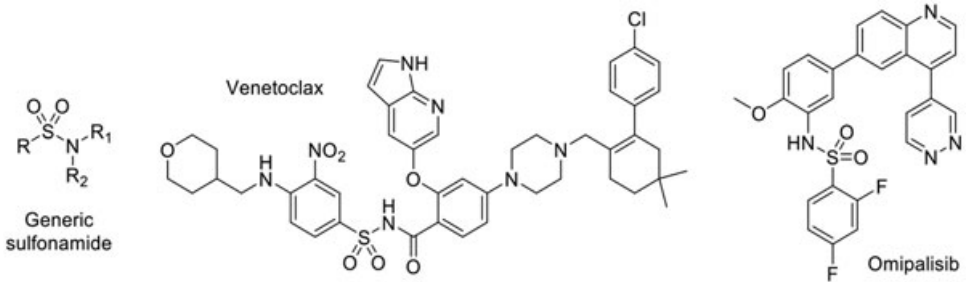

FIGURE 10 Generic structure of a sulfonamide and two recently FDA approved examples of sulfonamide drugs

3.1 | Medicinal chemistry of the sulfonamides

The favorable properties that make sulfonamides a frequent pick in the design of drug–like molecules include a suitable combination of accessibility, stability, hydrogen-bonding capability, polarity, hydrophobic–hydrophilic balance, and conformational preferences, among others.

3.1.1 | Conformations

The sulfur atoms of sulfonamides are tetrahedral and the nitrogen atoms are pyramidal, generally slightly less so than tertiary aliphatic amines.[133,134] Compared to the favored ϖ dihedral angle of 180° for the planar amides the sulfonamides have favored angles of 90° or less and the long S-N bond lowers the rotation barriers as compared to the carboxamides.[135–137]

The preferred conformations of aryl sulfonamides are those in which the π orbital of the *ipso* carbon to the sulfur bisects the O-S-O angle, as evidenced by X-ray crystallographic studies,[133,138] theoretical calculations,[139,140] and by searches and statistical analysis of the Cambridge Structural Database (CSD) and the PDB,[139] and the C-S-N-C dihedral adopts a staggered conformation with the lone pair of the nitrogen bisecting the O-S-O angle.[139]

3.1.2 | Hydrogen bonding

The sulfonamide oxygen atoms are weak hydrogen bond acceptors.[141] A recent search for hydrogen bonds to strong donors (O-H and N-H) of aryl sulfonamides and aryl sulfones found 6617 sulfonamides forming a single hydrogen bond out of 7856 hits in the CSD and 847 out of 1410 in the PDB, while two hydrogen bonds were only found in 37 and 496 hits, respectively.[139] The median O–X distances for hydrogen-bonded sulfonamide oxygen atoms to oxygen or nitrogen hydrogen-bond donors (in the CSD) ranged 2.85–3 Å, with shorter distances for oxygen (0.19 Å shorter than the sum of the van der Waals radii) than for nitrogen (0.06 Å shorter than the sum of the van der Waals radii) hydrogen bond donors.[131] There is a slight preference for a linear arrangement of the sulfur–oxygen bond and the hydrogen bond donor atom over the direction of the free lone pairs of the oxygen atom, which in turn show a preference for the *syn* (towards the other oxygen) than *anti* direction.[131,139]

Primary and secondary sulfonamides are hydrogen bond donors and as a result of the more acidic character as compared to amides and carbamates, they are expected to be better hydrogen bond donors.[142] Hydrogen bonding of the sulfonamide N-H to protein acceptors is often an important binding contribution, after which the hydrogen-bond donor strength can be rationally exploited for affinity improvement.[143]

3.1.3 | pK_a

Primary and secondary sulfonamides are weak acids with varying pK_a values depending on the substitutions.[144–147] Different therapeutic applications of sulfonamides possess distinct optimal acidity ranges, for instance carbonic anhydrase antiglaucoma sulfonamides present higher acidity than anticancer ones, whereas for bacteriostatic activity reduced acidity is usually preferred.[146] The acidic strength of sulfonamide moieties in drugs affects drug binding to the targets and in some cases the active species is the conjugated base, like in the important class of carbonic anhydrase inhibitors where it displaces a hydroxy group bound to a Zn cation, whereas in others it is the neutral form which binds to the target. Acidity and (de)protonation are also related to permeability and solubility and therefore are important factors affecting sulfonamide activity.[148]

3.1.4 | Solubility and permeability

Sulfonamides in general are high melting point solids poorly soluble in water, but ionization due to its acidic pK_a can greatly improve solubility. Therefore, electron-withdrawing moieties can significantly improve the aqueous solubility of sulfonamides.[148,149]

3.1.5 | Tautomerism (*N*-heterocyclic)

N-Heterocyclic sulfonamides are in equilibria with the tautomeric sulfonimides, a property that has been exploited in synthetic organic chemistry, which underlies the phenomena of tautomeric polymorphism.[150,151] In the solid state, the environment favors in some cases the sulfonimides, which also become stabilized in polar solvents.[152,153] The two tautomeric forms could presumably be important for therapeutic action.

3.1.6 | Synthesis

One of the reasons for the application of sulfonamides to different therapeutic purposes is their easy access. There are several general synthetic approaches to sulfonamides (Figure 11), although the most widespread is the use of sulfur derivatives in the proper oxidation state (represented within the doted framework in Figure 11), including assembly from sulfonic acid derivatives and amines (Routes 1), and the conversion of one sulfonamide into another (Routes 2).

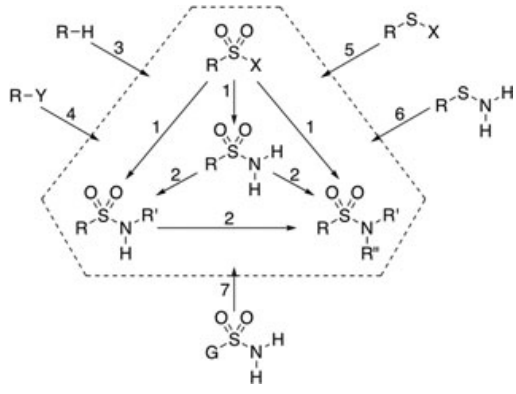

FIGURE 11 General approaches to sulfonamide synthesis

Sulfonamides are usually prepared by treatment of a sulfonyl chloride with ammonia or amines (Figure 11; Routes 1, X=Cl).[154] A wide range of conditions have been applied, among which the use of triethylamine or *N*,*N*-dimethyl-4-aminopyridine as bases are the most frequent. Metal catalysts[155] have been used for less harsh conditions[156] or for chemoselective sulfonylation of aminoalcohols.[157] Chlorosulfonation of amines in water,[158] and even solvent-free, have also been used.[159] Evolution of HCl and formation of disulfonylation products[160] are suppressed using other sulfonyl derivatives, such as sulfonyl pyridinium (X=pyr$^+$)[161] or DBN (X=DBN$^+$)[162] salts, pentafluorophenyl (X=OC_6F_5), 2,4,6-trichlorophenyl (X=$OC_6H_2Cl_3$)[163] and benzotriazole (X=$OC_6H_5N_3$)[164] sulfonates or sulfonyl hydrazides.[165] An alternative is the reduction of sulfonyl azides or other nitrogenated derivatives.[166] In many cases, the conversion of the sulfonic acids into their highly reactive and unstable chloro derivatives is required (Figure 11; Route 1, X=OH to X=Cl), a reaction that is accomplished with phosphorus/sulfur halides or other halogenating reagents.[167] For all these reasons, and due to their high stability, the sulfonamides are introduced in initial stages of the synthetic process.

Primary sulfonamides can be easily converted into secondary sulfonamides, and these into tertiary sulfonamides (Figure 11. Routes 2). The most common strategies are treatment with bases to subtract the proton followed by alkylation with alkyl halides, Mitsunobu reaction,[168] use of other alkylating agents under thermal conditions,[169] and metal-mediated (Cu,[170] Pd,[171,172] and Ru[173]) coupling of various types of reagents, especially for *N*-arylation purposes. Olefins have also been used for intermolecular or intramolecular alkylations of sulfonamides.[174]

A preliminary step in the preparation of sulfonamides or their precursors (eg sulfonic acids, sulfonyl halides, or activated sulfonates) is the introduction of sulfur-containing groups in nonfunctionalized (Figure 11; Route 3) or functionalized positions (Figure 11; Route 4). Examples of route 3 are the chlorosulfonation of aromatic systems by means of chlorosulfonic acid[175] or the lithiation followed by treatment with sulfur and chlorine.[176] The conversion of aryl halides into Grignard reagents followed by treatment with sulfur reagents[177] or the oxidative substitution of diazonium salts are route 4 representatives.[178]

Oxidation of less oxidized sulfur derivatives with nitrogen (Figure 11; Route 6) or without nitrogen (Figure 11; Route 5) also produces sulfonamides and sulfonic acid derivatives. Route 5 includes thiols or disulfides,[179] sulfinates,[180] sulfamoyl salts,[181] sulfonyl azides,[182] or silyl sulfides[183] that have been oxidized in halogenating[180,184] and non-halogenating conditions.[185] Example of route 6 is the direct oxidation of sulfenamides to sulfonamides with permanganate[186] or *meta*-chloroperoxybenzoic acid (MCPBA).[187]

Routes 1 to 6 cover the synthetic approaches to sulfonamides based on the formation of the sulfonamide group on a starting alkyl or aryl moiety (Figure 11; R = alkyl or aryl). Alternatively, route 7 represents the exchange of different groups attached to the sulfur atom by the alkyl or aryl moieties of the required sulfonamide (Figure 11; G-SO_2Z to R-SO_2Z). Within this methodology, the lithiation of the carbon atom attached to the sulfur followed by alkylation[188] or arylation of sulfamoyl chlorides[189] has been successfully applied.

3.2 | Antimitotic sulfonamides

Many sulfonamides with anticancer and antiparasitic activities have been described. Primary sulfonamides have been mostly developed as carbonic anhydrase inhibitors[190] and secondary and tertiary sulfonamides are inhibitors of multiple kinases or tubulin inhibitors binding to the colchicine domain.[191] All the antimitotic sulfonamides are aromatic or heteroaromatic sulfonamides with additional aromatic substitutions on the sulfonamide nitrogen. Taking into account the division of the colchicine domain in three different subpockets,[122,123] the antimitotic sulfonamides have been classified accordingly (Figure 12) based on their structural similarity to combretastatin A-4 (binding to sites I and II) or to ABT-751 (binding to sites I, II and III).

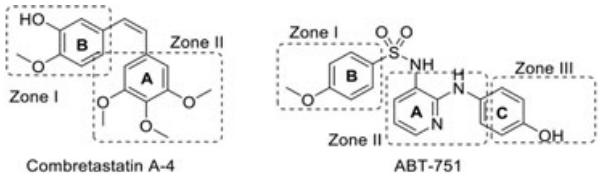

FIGURE 12 Structure of combretastatin A-4 and ABT-751 used as reference compounds for classification of antimitotic sulfonamides based on the colchicine domain zones indicated by dotted squares

3.2.1 | Antimitotic sulfonamides related to combretastatin A-4 (CA-4)

Sulfonamides related to CA-4 have been in turn classified according to the complexity of their aromatic sulfur and nitrogen substituents as shown in Figure 13. In most cases, sulfonamide reversal results in only minor structural and biological effects and therefore they are included in the same group.

Monocyclic antimitotic sulfonamides

Replacement of the olefinic bridge of CA-4 by a sulfonamide leads to diarylsulfonamide analogs with submicromolar potency and improved water solubility (Figure 14). Bridge reversal has modest effects but sulfonamide nitrogen methylation enhances potency.[192] Simultaneous removal of the methoxy groups on both rings results in dramatic potency losses.[193] Replacement of the hydroxy group at the 3 position of the B ring by an amino group maintains the potency, but substitution of the *p*-methoxy group by methyl, amino, or acetamido groups decreases cytotoxicity.[194] The trimethoxyphenyl ring is required in combretastatins for high cytotoxicity but for diarylsulfonamides it can be successfully replaced by 2-acetamido- or 2-ethylureido-phenyl groups, structurally more akin to ABT-751.[195]

Trimethoxyphenyl ring substitution with a pentafluorophenyl led to a family of pentafluorobenzenesulfonamides. T138067 with a combination of a pentafluorophenyl ring and a 3-fluoro-4-methoxyphenyl moiety displays in vitro cytotoxicity against sensitive and multidrug resistant (MDR) tumor cells,[196,197] and in nude mouse tumor xenografts models by inhibiting tubulin polymerization by irreversible covalently binding to β-tubulin isoforms 1, 2, and 4 at residue C241β of H7 (Figure 14).[198] Currently, T138067 is in phase III clinical trials (Table 2).

The replacement of the methoxy group of T138067 with either methyl or dimethylamino groups decreases growth inhibitory activity.[197] Nevertheless, dimethylamino derivatives, besides TPI activity, are also able to activate low-density lipoprotein receptor (LDLR) gene transcription.[209] Consistent with the proposed mechanism of action, the fluorine at 4 position is absolutely essential and its replacement by chlorine or bromine or the suppression of fluorine atoms at the 5 and 6 positions leads to a significant loss of antitumor activity.[197]

Due to its high lipophilicity T138067 might cross the hematoencephalic barrier and cause central neurotoxicity. Less lipophilic derivatives carrying different amino or amido substituents at the 3 position of the *p*-methoxyphenyl ring show similar in vivo efficacy and no detectable signs of blood brain barrier crossing.[210] The ureido derivative T900607 has advanced to phase II clinical trials.[211] (Figure 14)

One-polycycle antimitotic sulfonamides

The polycycles (Figure 15) are mostly benzo-fused nitrogenated heterocycles such as indoles, indazoles, carbazoles, or carbolines that can either substitute the methoxyphenyl B ring or the trimethoxyphenyl A ring. Taking the indole ring as the minimal possible aromatic polycycle, the rest can be considered as aza analogs (benzimidazoles and indazoles), benzo-enlarged analogs (carbazoles) and their aza analogs (carbolines).

Replacement of the trimethoxyphenyl ring is best achieved by 7-indolyl moieties. Interestingly, the indole substitution pattern leads to the compounds that differ in the mechanism of action. Substitution at the indole 3 position favors blockade of the cell cycle at the G_1 phase rather than inhibition of tubulin polymerization.[212] The

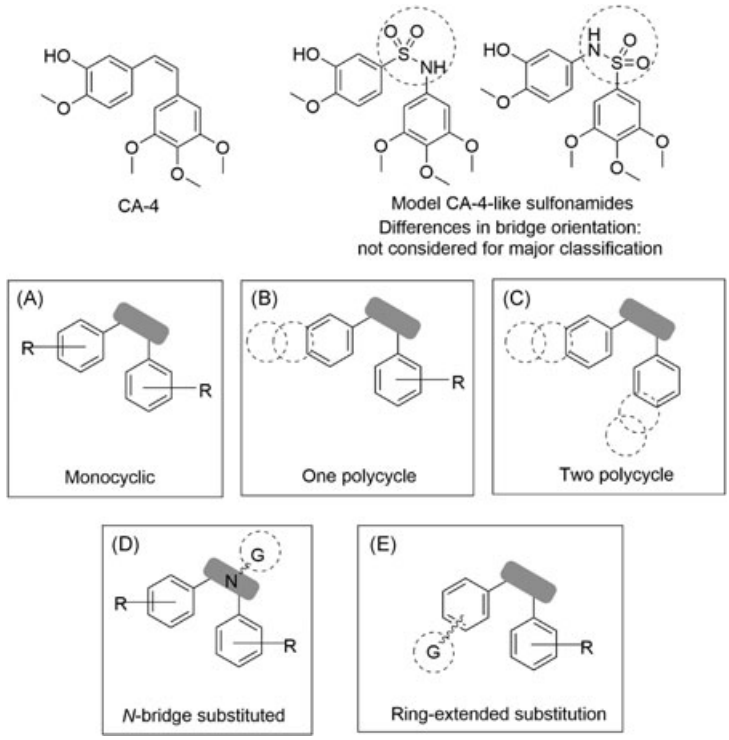

FIGURE 13 Structural classification for combretastatin A-4-like antimitotic sulfonamides

different mechanism of action also arises from different B ring substitution patterns, as shown by the lead compound E7070 currently in phase II clinical trials.[212–215] On the other hand, 2-substituted indoles in combination with *p*-methoxy or *p*-methylphenyl B rings lead to the compounds that induce G_2/M cycle arrest, alter microtubule dynamics, and mitotic spindle organization.[216] The most promising compounds of this series have either a chlorine (ER68378) or hydroxy group at indole 2-position.[217–220] Indazoles bound through the 4 or 7 positions lead to submicromolar cytotoxic compounds,[221,222] preferentially unsubstituted at indazole nitrogen, with a chlorine group at the indazole 3 position and a *p*-methoxy or *p*-methylphenyl as the B ring.

N-Methyl-5-indolyl moieties replace the B ring leading to potent TPI and cytotoxic compounds when combined with trimethoxyphenyl rings. A-293620 is cytotoxic at nanomolar concentrations, even against MDR over-expressing cells, and its prodrug A-318315 has shown in vivo tumor-selective antivascular effects.[223] A replacement of the trimethoxyphenyl ring with a 2,6-dimethoxypyridin-3-yl ring or by 4-fluorophenyl, 4-chlorophenyl, or 4-nitrophenyl rings reduces significantly or suppresses antitumor activity.[211,224–226] Changes on bridge orientation also decrease growth inhibitory activity.[192,223] Pentafluorobenzene sulfonamides with a 5-indolyl moiety or a 6-benzodioxine ring are as potent as T136087 against both sensitive and resistance cancer cell lines.[197] 7-Benzimidazolyl, 5- and 6-indazolyl derivatives are significantly less potent.[221,224,227,228] *N*-alkylated carbazole sulfonamides display low nanomolar cytotoxic values showing a prolonged G_2/M cell cycle arrest with Bcl-2 upregulation and apoptosis. Changes on bridge orientation or replacement of the carbazole by dibenzofurane decrease potency.[211,229] Carbazole derivatives with substituted pyridines as A ring replacements such as IG-105 with a 2,6-dimethoxypyrid-3-yl moiety are slightly less potent, but show promising in vivo profiles in terms of activity, bioavailability, and toxicity on two human xenograft models (MCF-7 and Bel-7402).[226,230,231] Hydroxy or amino groups at carbazole 6 or 7 position improve aqueous solubility and cytotoxicity down to nanomolar range due to a proposed additional hydrogen bond with the protein, whereas the corresponding carbolines[232] and other polycycles such as benzothiazole, 2,3-dihydroindene, and anthracene have lower potency.[224]

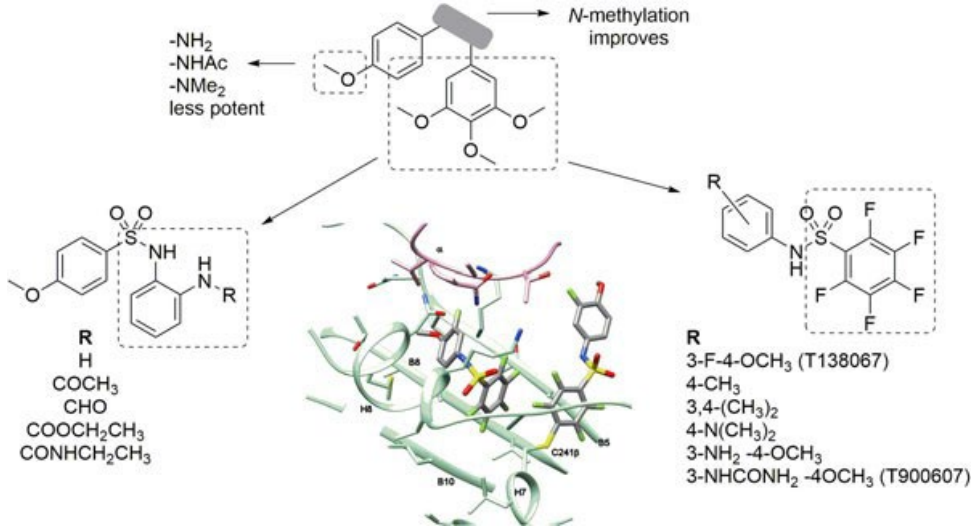

FIGURE 14 Monocyclic sulfonamide scaffolds related to combretastatin A-4 (CA-4). (Right) Pentafluorobenzenesulfonamides related to CA-4 and (center) structure of the covalently bound adduct of T138067 with C241 of β tubulin in complex with a second T138067 unit

Two-polycycle antimitotic sulfonamides

Naphthalene and quinoline moieties linked through sulfonamide bridges to isoquinoline, quinoxalin, tetrahydronaphthalene, benzothiazole, indazole, indole, and indene rings have been synthesized and assayed against several cancer cell lines (Figure 16). However, only indole-naphthalene combinations are cytotoxic with values from 0.091 to 17 μM. They promote a severe G_2/M cell cycle arrest, cellular senescence, and caspase-mediated apoptosis.[224]

N-Bridge substituted antimitotic sulfonamides

The introduction of small hydrophobic groups on the sulfonamide nitrogen (Figure 13d) such as methyl or ethyl groups improve the potency. Changes in the mechanism of action have also been observed for less-potent series.[232] Larger more polar substitutions showed reduced potencies.[193,233]

Ring-extended substituted antimitotic sulfonamides

The introduction of small heterocycles as phenyl ring substituents in diarylsulfonamides (Figure 17) provides increased interacting surfaces while preserving some flexibility compared to polycyclic systems, and could serve to modulate the biological activity. Substitution of the B ring methoxy group in phenyl 4-(2-oxoimidazolidin-1-yl) benzenesulfonamides (PIB-SAs) results in highly cytotoxic compounds with potencies from 0.018 to 1 μM that arrest the cell cycle at G2/M phase and exhibit promising antiangiogenic profiles.[234] Replacement of the 2-oxoimidazolidin ring by potential precursor chloroethyl- or chloropropyl- ureas or ethyl groups decreased antiproliferative potential.[235]

A high throughput screening campaign on more than 1 million simple synthetic lead compounds identified benzenesulfonamide scaffolds able to bind to tubulin such as CID20959075 (Figure 17), with a half maximal inhibitory concentration (IC_{50}) against the HCT116 cell line of 0.049 μM.[236] Ring contraction to an indoline is well tolerated (0.055-0.105 μM), with electron-donating groups at indoline 5-position improving and electron-withdrawing groups at indoline 6-position maintaining the potency.[237] Further lead modification of the tetrahydroquinoline to benzothiazepine, benzodiazepine, benzoxazepine, benzoxazine, or benzothiazine, found that the benzoxazepine derivatives to be the most potent (IC_{50} = 0.040 μM, HCT116), especially those with a fluorine atom at 7 position (0.007-0.036 μM).[238]

TABLE 2 Current status of sulfonamides in clinical trials[199]

Compound/structure	Status	Phases	Routes	Administration
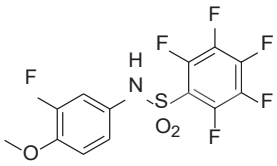 T138067 T67 batabulin	Completed	Phase I for advanced refractory cancer[200,201]	iv	Over 3 h every 4 wk during 6 mo
	Unknown	Phase II for locally advanced or metastatic NSCL cancer that failed taxane therapy[200,201]	iv	Over 3 h for days 1, 8, and 15, every 21 d
	Terminated	Phase II/III for hepatocellular carcinoma vs doxorubicin	iv	NA
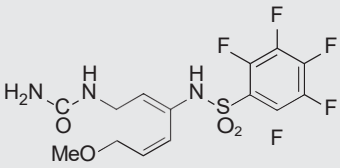 T900607 T607	Completed	Phase II for gastroesophageal junction cancer	iv	Over 1 h once a week
	Completed	Phase II for unresectable liver cancer	iv	Over 1 h once a week
	Unknown	Phase II for ovarian cancer	iv	NA
	Terminated	Phase II for non-Hodgkin's lymphoma	iv	NA
	Unknown	Phase II for hepatocellular carcinoma	iv	NA
	Suspended	Phase II for gastric cancer and esophagus adenocarcinoma	iv	NA
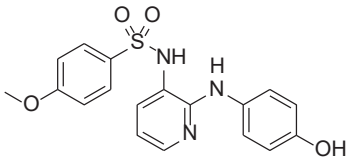 ABT-751 E7010	Terminated	Phase I/II for hormone-refractory metastatic prostate cancer.[202] *Lack of effectiveness*	po	Twice daily on days 1-7 and 15-21, every 28 d. 125 mg for phase II
	Terminated	Phase I/II in combination with carboplatin for advanced NSCL cancer.[203] *Terminated based on lack of effectiveness showed in a similar clinical trial*	po	Administered twice on day 1 of each cycle for 7 d. Dose escalation 100-200 mg
	Active, not recruiting	Phase II for children with neuroblastoma	po	Once daily on days 1-7 every 21 d for 52 courses
	Terminated	Phase I/II in combination with docetaxel for advanced of metastatic NSCL cancer	po	200 mg daily for 14 d every 21 d
	Completed	Phase II for refractory colorectal carcinoma	po	Daily for 21 d with 7 d off before the next cycle
	Completed	Phase II for renal cell cancer	po	Daily for 21 d with 7 d off before the next cycle
	Completed	Phase II for taxane-refractory NSCL cancer	po	Daily for 21 d with 7 d off before the next cycle
	Completed	Phase I for refractory hematological malignancies	NA	NA

(Continues)

TABLE 2 (Continued)

Compound/structure	Status	Phases	Routes	Administration
	Completed	Phase II for taxane-refractory breast cancer	po	Daily for 21 d with 7 d off before the next cycle
	Completed	Phase I for refractory solid tumors in young patients[204–207]	po	Once daily for 7 d every 21 d or for 21 d every 28 d
	Completed	Phase I/II in combination with pemetrexed for advanced or metastatic NSCL cancer[208]	po	200 mg for 14 d every 21 d
	Terminated	Phase I/II in combination for acute lymphoblastic leukemia	po	Daily for 21 d

Abbreviations: iv, intravenous; NA, not available; NSCL, nonsmall cell lung; po, oral.

3.2.2 | ABT-like sulfonamides

This group includes compounds structurally related to ABT-751 with three distinct ring systems, and has been divided in two classes (Figure 18): compounds preserving the three–ring (B, A, C)–two-bridges (BA, AC) scaffold, and those in which any of the bridges has been cyclized onto any of the rings (Figure 18). In the first subgroup, structural modifications (SM1-5) affect exclusively individual rings or bridges and retain high similarity with ABT-751. The second subgroup gathers conformationally restricted ABT-751 analogs (CR1-3), where a ring-closing strategy has occurred, thus fixing a preferential geometry.

Modifications on the ABT-751 scaffold (SM1-5)

Several structural modifications (SM1-5) affecting different parts of the ABT-751 scaffold have been described (Figure 19): (SM1) changes of the B-ring substituents; (SM2) sulfonamide nitrogen substitution and occasional bond reversal; (SM3) A-ring modifications including changes of the pyridine moiety, of the 2,3-disubstitution pattern, and even the introduction of additional substituents; (SM4) changes involving the amino linker between A-C rings; and (SM5) C-ring variations, including additional substituents or its replacement by alternative heteroaromatic rings. Several of these structural modifications often occur simultaneously and SM4 has been selected as the classification criteria for this group as it entails the main skeletal variation: amines (1.1), extension to amides (1.2) or olefins (1.4), or the altogether removal of the spacer (1.3).

Highly related ABT-751 analogs keeping the amino linker E7010[239] (renamed ABT-751 after its acquisition by Abbott Laboratories) emerged from modifications of a lead sulfonamide discovered by the Eisai Co Ltd[240] (Figure 20) while searching for new molecules for oral cancer treatment.[241–245] 1 to 2 atoms alkyl, alkoxy, or amino groups were explored at the *p*-position of the B ring (SM1). The methoxy group gave optimal antiproliferative activity against KB cells and was retained throughout.[239,240] Methylation of the sulfonamide bridge resulted in a four-fold potency increase (SM2).[240]

The role of *ortho*-phenylenediamine (A ring) has also been explored. Replacement of the benzene by a pyridine (SM3) improved in vitro potency and in vivo tumor growth inhibition,[239] whereas replacement by a 4-methoxypyrimidine-5,6-diamine or the introduction of methoxy or methyl groups, or fluorine atoms (SM3) led to remarkable potency decreases.[240]

The antiproliferative activity greatly varies with the structure of C ring (SM5).[239,240] Benzenes with different substitution patterns result in variable outcomes. Methyl, methoxy, or phenoxy groups produced unfavorable effects, and only the 4-ethoxy substituent retained the potency. Hydroxy groups are important for the in vivo activity and phosphate prodrugs, ethers, and aromatic and aliphatic ester groups have been prepared with good results for the

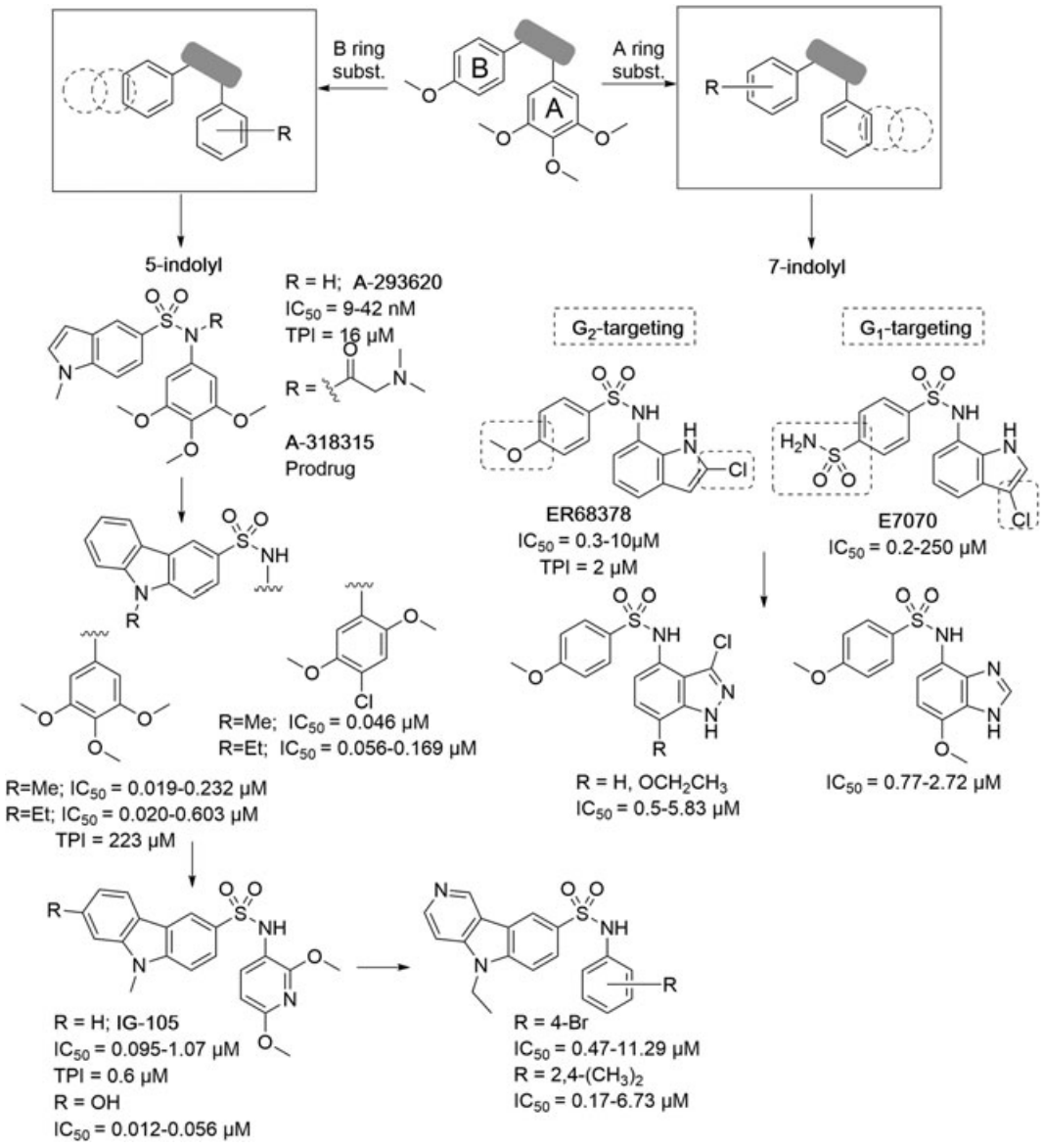

FIGURE 15 One-polycycle sulfonamides related to combretastatin A-4 and representative cytotoxicity IC_{50}s

bulkier ones, such as tertiary butyl or aromatic esters. Fluorine but not chlorine atoms are well tolerated at any position. The replacement of the C ring by heterocycles has been also studied (SM5). Combined with a 2,3-diaminopyridine A ring, a 2-pyridine caused a four-fold decrease in antiproliferative activity whereas a combination with of a 1,2-phenylenediamine with heterocycles such as 2-pyridine or 2-pyridimidine showed an average of eight-fold higher potency.

ABT-751 binds at the colchicine site[246] showing preference for the βIII isoform[247] and induces mitotic arrest and mitochondria-dependent apoptosis even in MDR resistant cells, eliciting vascular disrupting activity.[248,249] Autophagy induction was also observed in Huh-7 cell line.[250]

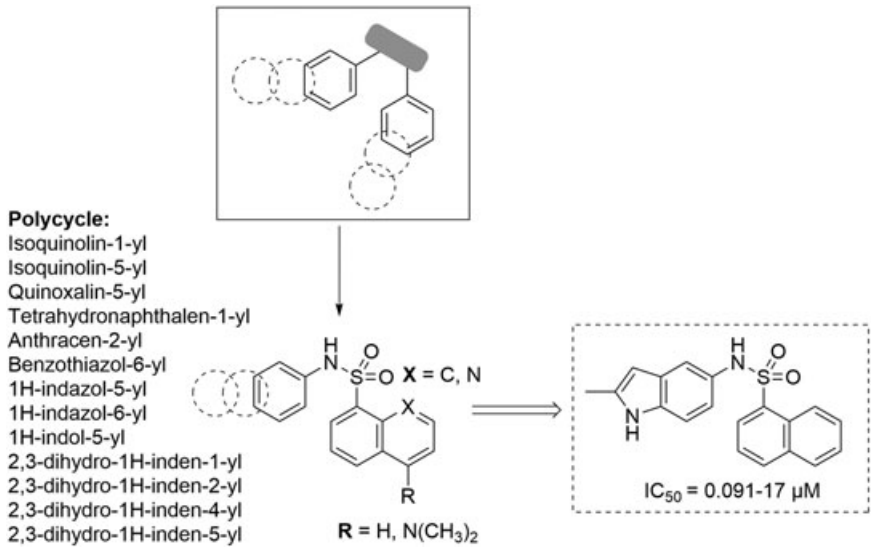

FIGURE 16 Two-polycycle sulfonamides related to combretastatin A-4

ABT-751 underwent clinical trials (Table 2) in humans[202–206,208,251–257] and dogs suffering from lymphoma,[258] being currently at phase II either alone or in combination regimens, although results are not as expected probably due to insufficient effect.

ABT-like compounds with amido spacer The replacement of the amino linker between the A-C rings with amides (SM4) led to greater potencies against the KB cell line and less so for thioamides. The replacement of the C ring with heterocycles showed higher potencies (tenths of nM) than substituted benzene rings, which is in agreement with SAR observed for amino linker containing analogs.[240]

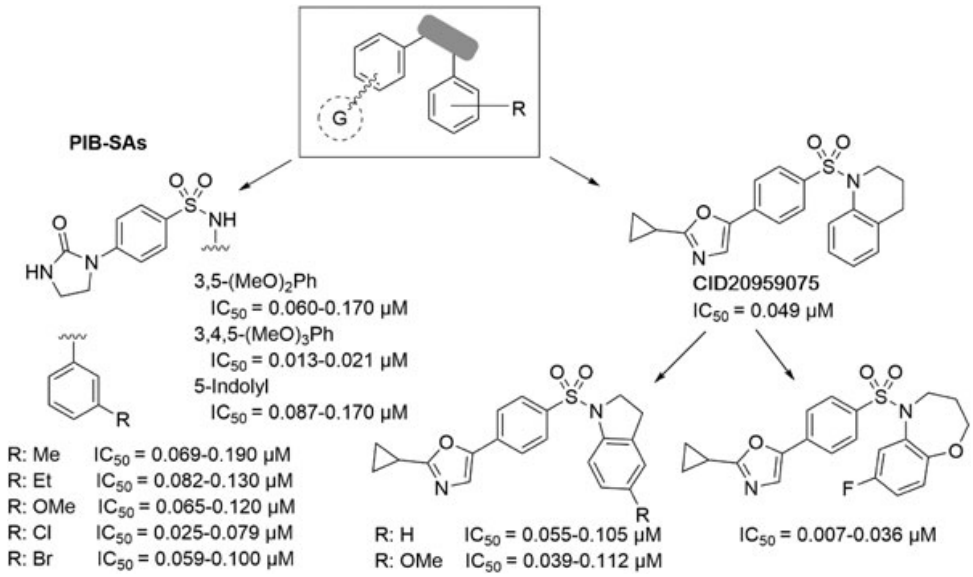

FIGURE 17 Ring-extended substituted sulfonamides related to combretastatin A-4

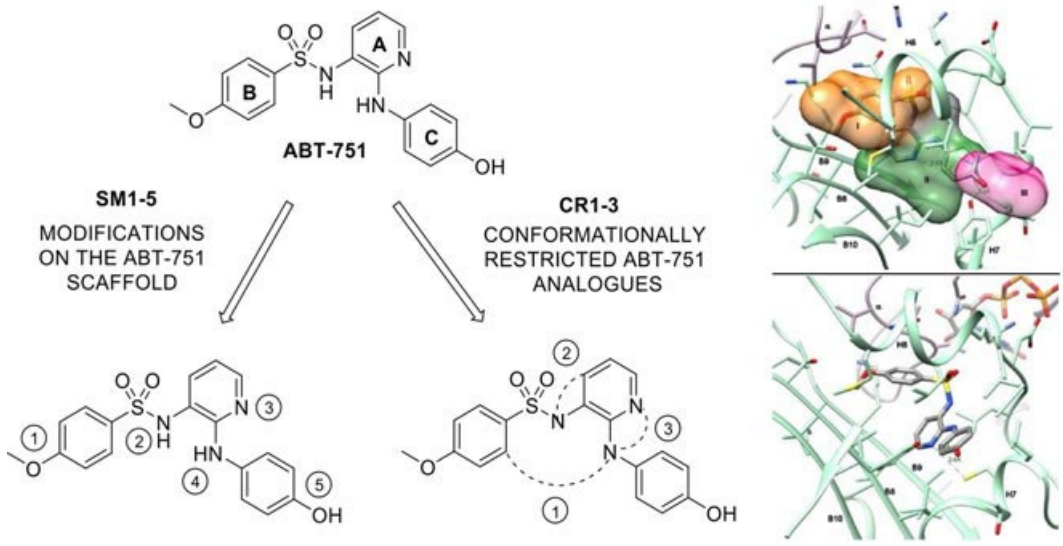

FIGURE 18 Scheme of structural modifications (SM) included in this classification: modifications on the ABT-751 scaffold (SM1-5) and conformationally restricting cyclizations (CR1-3). The three zones of the colchicine domain partially occupied by ABT-751 are shown on the right-hand side to assist in the assessment of the effects of the structural modifications on the activity

Derivatives lacking the amino spacer The amino linker between the A-C rings confers some shape adaptability to the molecule, and its suppression in *N*-benzenesulfonylaminobiaryls (SM4) has been explored (Figure 20 bottom left and center).

MTP0G066 with a non-substituted biaryl[259,260] represents a slight improvement with respect to ABT-751. Halogenation at position 4 of the C ring leads to a two to three-fold improvement (SM5), and is preferred over the 3 position.[260] The highest (ten-fold increase) antiproliferative in vitro cytotoxic activity (0.03 μM against AsPC-1) was achieved for LTP-1 with a 4′ nitrile.[260,261] A replacement with heterocyclic rings, such as pyridine or furan, led to worse biological results.

These compounds bind at the colchicine site and cause mitotic arrest.[259–261] In addition to dose-dependent TPI, compounds with a nitrile group on the C ring inhibit STAT3 phosphorylation.[260,261]

The replacement of ABT-751's phenolic ring with a thiophene bioisoster (SM5) while migrating it to the 3 position (SM3) led to ELR510444, a colchicine domain tubulin inhibitor with potent cytotoxic profile against different tumor cell lines (9-31 nM), overcoming P-glycoprotein and βIII isoform overexpression mediated resistances.[262,263] Microtubule disruption leads to apoptotic cell death and vascular disrupting activity.[262] ERL510444 also has antiangiogenic properties and downregulates HIF-1α and HIF-2α.[263]

Stilbene-related sulfonamides Replacement of the ABT-751 amino spacer (SM4) with an ethylene gives stilbene-sulfonamides, mitotic arrest inducers with mechanisms different from tubulin binding (Figure 20 bottom right).[264–267] HMN-214 is a prodrug that produces the active metabolite HMN-176 by carboxylesterases hydrolysis.[266] HMN-214 is currently in phase I clinical trials as an orally-administered treatment of advanced solid tumors.[268]

Conformationally-restricted ABT-751 analogs (CR1-3)

Three types of ring closures can be distinguished (Figure 21): (CR1) formation of a cycle between the B ring and the amino spacer connecting the A and C rings, thus forming fused tricyclic sulfonamide analogs; (CR2) ring formation

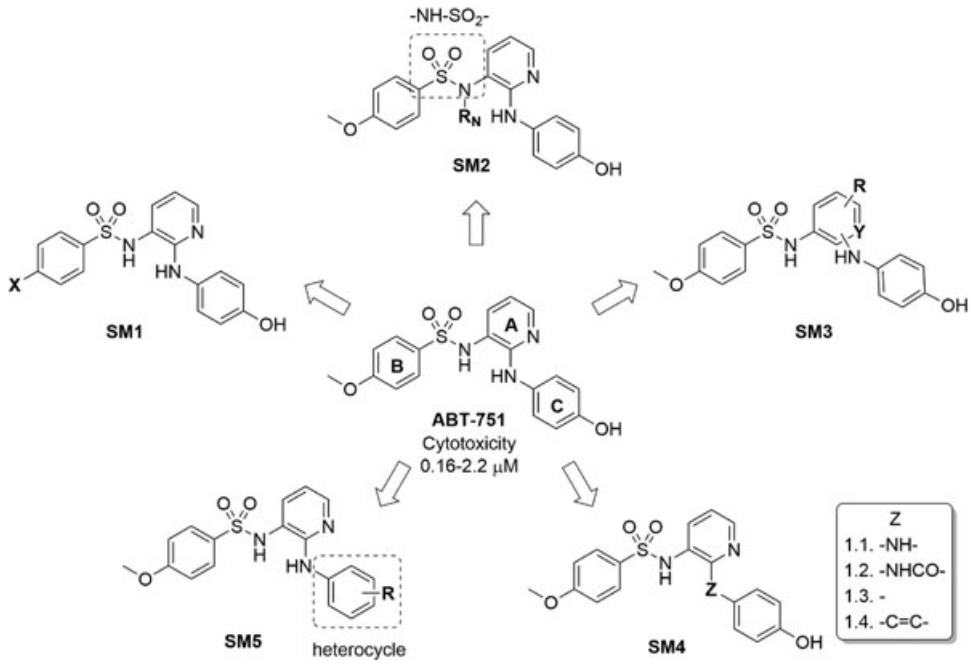

FIGURE 19 Breakdown of modification strategies over the ABT-751 scaffold structural modifications-5 (SM1-5)

by incorporating the sulfonamide nitrogen and the A ring into a benzenesulfonyl(aza)indol(in)e; and (CR3) ring closure between the A ring and the amino linker between the A and C rings giving *N*-indole-7-ylsulfonamides.

Fused tricyclic sulfonamide analogs (CR1) Tricyclic thiadiazepine ABT-751 analogs (Figure 22) with the arylalkyl side chain linked to the central thiadiazepine ring showed no cell proliferation inhibition,[269,270] which was recovered (0.3-9 μM IC_{50} values) when the side chain was moved to the pyridine nitrogen after tautomerization.[270] The optimal length for the spacer between the pendant ring and the tricyclic system is two carbons. A *p*-methoxy group on the pendant ring was optimal, whereas 3,4,5-trimethoxy, benzyloxy, hydroxy, or dimethylaminoethoxy groups rendered the compounds inactive. Any substitution on the 2 or 3 positions of the fused benzene, such as chlorine, methyl, trifluoromethyl or methoxy groups, resulted in reduced potencies.[270] Reversal of the sulfonamide orientation gave similar results. The replacement of the methyl group on the sulfonamide nitrogen by bulkier aminoalkyl chains or aromatic containing derivatives led to loss of activity, whereas the unsubstituted sulfonamide nitrogen led to a three-fold decreased potency.

In vivo results were disappointing due to lack of chemical and metabolic stability, since they show good oral bioavailability.[270] The fused pyridine ring was substituted by pyrrolidine or piperidine rings (Figure 22 bottom right, n = 0 and n = 1).[271] The piperidine analogs with a *p*-methoxyphenethyl chain showed modest cytotoxic activity against the HT-29 human colon adenocarcinoma cell line (0.2 μM), but very potent tubulin polymerization inhibition. Docking studies suggest an interaction between the sulfonamide and the thiol group of tubulin Cys241β, with the *p*-methoxyphenethyl replacing the *p*-methoxybenzenesulfonamide of ABT-751.

Benzenesulfonyl(aza)indol(in)es (CR2) *N*-Benzenesulfonyl-azaindolines,[272–275] -indoles[274,276] or -6-azaindoles[273] resulting from the linkage between the sulfonamide nitrogen and the A ring (CR2) are conformationally restricted ABT-751 analogs with similar antiproliferative activities (Figure 23).

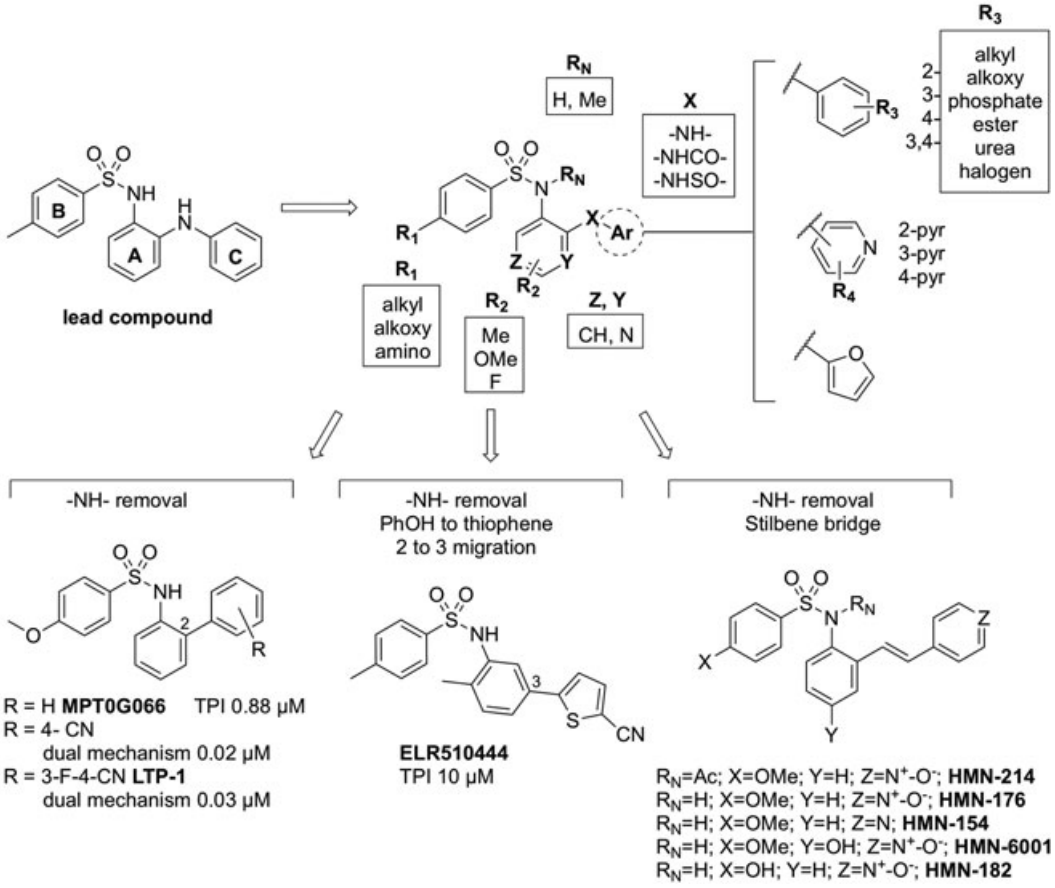

FIGURE 20 Top, Evolution of the lead compound by structural modifications on the ABT-like scaffold. Bottom left and center, Biaryl ABT-derivatives lacking the amino A-C linker. Bottom right, Stilbene-sulfonamides

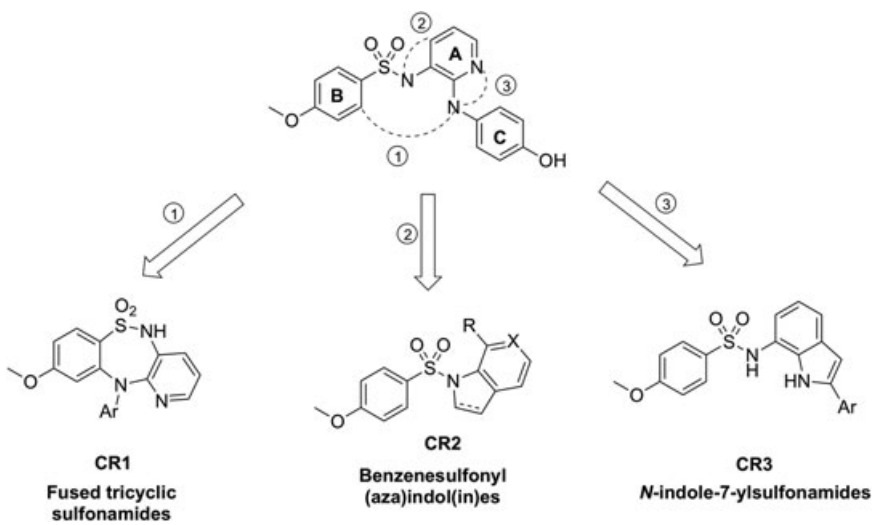

FIGURE 21 Types of conformationally restricted analogs of ABT-751

N-Benzenesulfonyl(aza)indolines The replacement of the amino spacer to the pendant ring with methylamine, *N*-methylurea or carbamate led to complete loss of cytotoxic activity.[275] However, its removal provided the most potent compounds,[274] and amides and other amine derivatives also displayed good IC_{50} values.[272,275] Regarding the pendant aromatic ring (Figure 24 top), unsubstituted benzene showed lower potency compared to the hydroxy-substituted ring. Electron-withdrawing substituents such as 4-F, 3,4-F_2, 4-NO_2, 4-CN or 4-COOMe, yielded an improvement in cytotoxicity with IC_{50} values ranging from 45.0 to 98.0 nM against KB cell line.[274] The best potency within amine, amido, or no-spacer families, was found in the 4-cyanophenyl derivative.[272,274]

The conversion of the pendant benzene to unsubstituted 3- or 4-pyridines proved acceptable, showing a slight improvement in cytotoxic activity for the family with no spacer (95.9-96.0 nM).[274] Pyridine substitution by a 2-furan ring also slightly improved the in vitro inhibitory effect when bound directly to indoline, while a 2-thiophene one showed a potency depletion. For the amide series, 4-pyridine (J30)[277] displayed a 31-fold improvement in IC_{50} (9.6 nM) compared to the benzene derivative[275] (297 nM), which is in agreement with the SAR of amido spacer ABT-like sulfonamides. Even the corresponding *N*-oxide is a successful replacement (MPT0B271).[278] Similar results were obtained in this series with the introduction of a 2-furan ring (9.6 nM, 31-fold improvement) and a thiophene ring (47 nM, 6-fold improvement).[275] Substitutions at the 5-position of the indoline ring (Z) led to a 10-fold decrease in potency.[275]

The two most potent compounds (Figure 24), J30 and its counterpart with a 2-furyl ring, displayed strong cytotoxic activity, even against MDR-overexpressing cell lines, and vascular disrupting activity due to binding at the colchicine site (TPI IC_{50} is 1.1 μM).[272,274,275,277] In addition, J30 has potential as PET probe[279] and MPT0B271 has shown an additional mechanism of action through STAT3 phosphorylation inhibition.[280]

Indole and 6-azaindole-containing sulfonamides Indole derivatives have been synthesized as aromatic analogs of the indoline series.[274] While the indoline allows certain flexibility, aromatization renders them plane and more rigid, and results in a lower (2-5 fold) in vitro potency (Figure 24 middle).[274] Replacement of the pendant phenyl ring by heteroaromatic rings causes tubulin disassembly and STAT3 phosphorylation inhibition but not higher

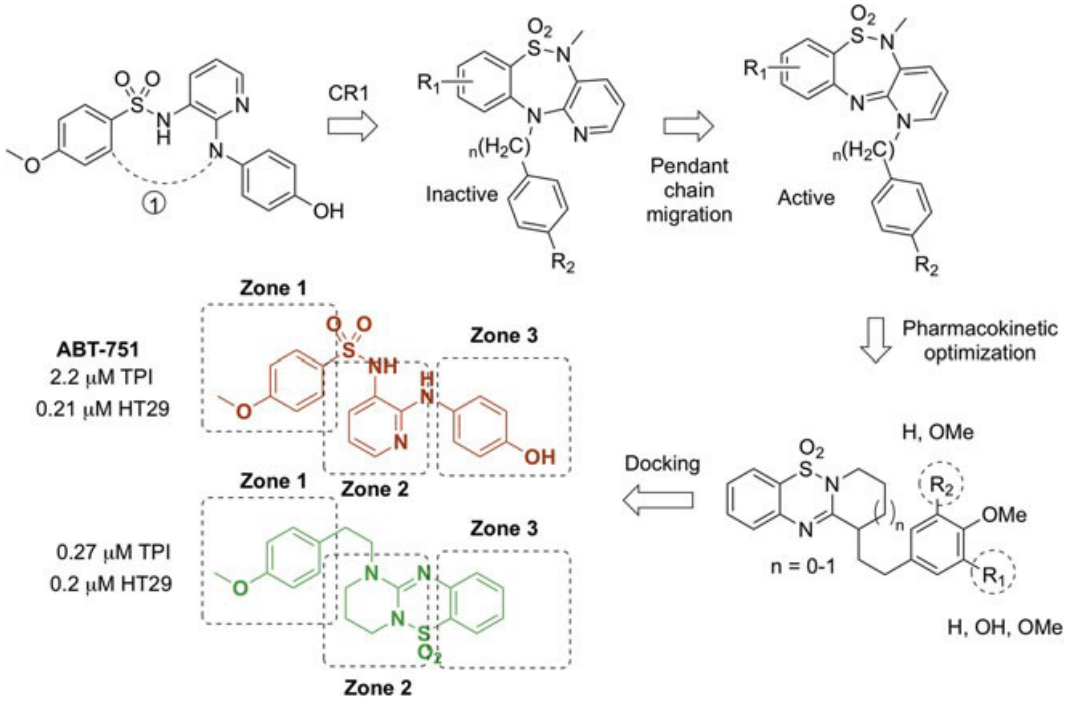

FIGURE 22 ABT-751 derivatives with a fused tricyclic scaffold

potencies.[276]

Benzenesulfonyl-6-azaindole derivatives (Figure 24 bottom) with the pending phenol directly bound (no linker) yielded better results (3-fold improvement) than those with an amino spacer.[273] Substituents on the phenyl ring such as hydroxy or methoxy do not improve the antiproliferative profile the same way electron withdrawing groups such as 4-F or 4-NO_2 do. Once more, replacement of the phenyl ring by isosteric heterocycles such as 4-pyridine, 2-thiophene or 2-furan enhances cytotoxic potency. The most potent compound among the 6-azaindole family turned out to be the one with a furylazaindole scaffold (21.1 nM for KB). Docking experiments superimposed it quite well with the X-Ray structure of ABT-751 (3HKC complex) in good agreement with a tubulin polymerization inhibition of 50% at 2.0 μM, due to colchicine site binding and microtubule disruption leading to G_2/M arrest. Additionally, these ligands are also able to act through a vascular disrupting mechanism, keeping off the tumor growth in in vivo cancer xenografts.[273]

N-indole sulfonamide derivatives (CR3) A series of E7070-ABT hybrids containing a 2-phenyl-3-substituted-indol-7-yl substituent on the *p*-methoxybenzenesulfonamido nitrogen (Figure 25) showed activity against PC-3 prostate cancer cell line, with the most active member having an IC_{50} value of 0.11 μM due to colchicine site binding with a TPI IC_{50} of 3.59 μM, followed by caspase-dependent cell death.[281] Neither R_2 nor R_3 modifications improved the in vitro antiproliferative effect, and the methoxy group at the *para* position of the B ring conferred 8-fold higher activity against PC-3 than the methyl counterpart,[281] which is in agreement with the ABT-751 SAR.[239,281] Indazole analogs linked to the sulfonamide by the 6 or 7 positions showed significantly lower in vitro potencies.[222,227,282]

3.2.3 | Sulfonamides not related to CA-4 nor ABT-751

This group includes miscellaneous scaffolds that do not fit neither as CA-4 related compounds nor as ABT-like derivatives. Polycyclic cores whose binding mode is not yet well established are included.

Dinitroaniline herbicides

The dinitroaniline sulfonamide oryzalin (Figure 26 top) is an antimitotic herbicide discovered in 1960 by scientists at Eli Lilly.[283] Oryzalin is mainly used as a contact non-systemic herbicide in pre-emergent control of a broad

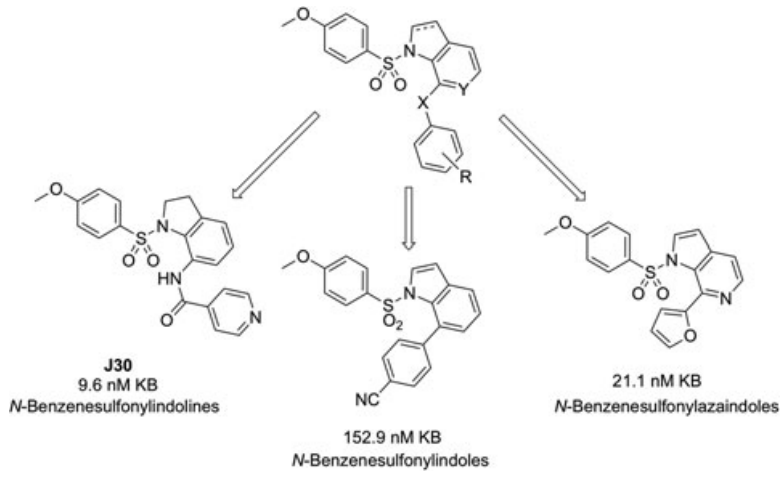

FIGURE 23 Main scaffold of benzenesulfonyl(aza)indol(in)e sulfonamides. The most potent indoline, indole and 6-azaindole derivatives are represented

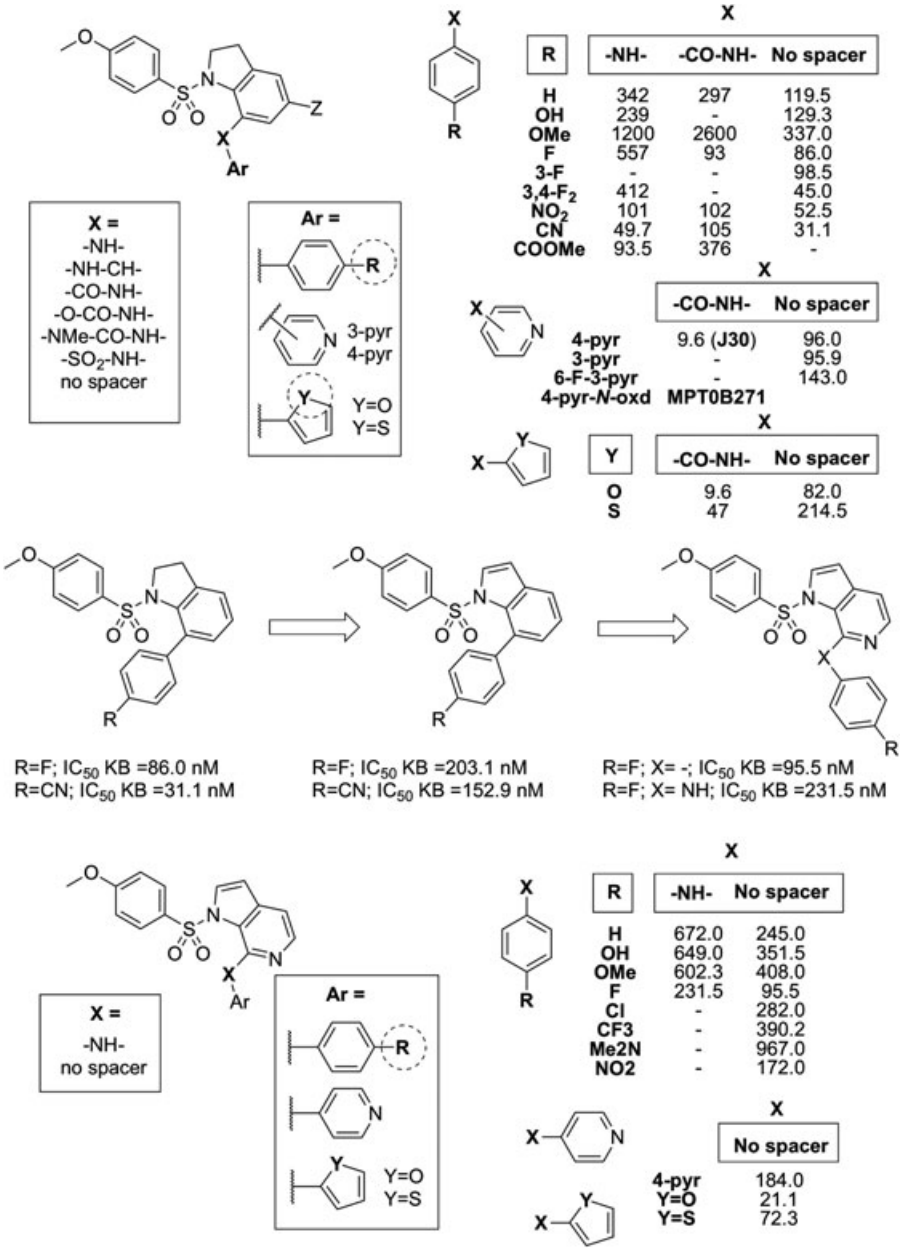

R	-NH-	-CO-NH-	No spacer
H	342	297	119.5
OH	239	-	129.3
OMe	1200	2600	337.0
F	557	93	86.0
3-F	-	-	98.5
3,4-F_2	412	-	45.0
NO_2	101	102	52.5
CN	49.7	105	31.1
COOMe	93.5	376	-

	-CO-NH-	No spacer
4-pyr	9.6 (J30)	96.0
3-pyr	-	95.9
6-F-3-pyr	-	143.0
4-pyr-*N*-oxd	MPT0B271	

Y	-CO-NH-	No spacer
O	9.6	82.0
S	47	214.5

R	-NH-	No spacer
H	672.0	245.0
OH	649.0	351.5
OMe	602.3	408.0
F	231.5	95.5
Cl	-	282.0
CF3	-	390.2
Me2N	-	967.0
NO2	-	172.0

	No spacer
4-pyr	184.0
Y=O	21.1
Y=S	72.3

FIGURE 24 Top) Selected modifications of the benzenesulfonylindoline scaffold and their effect on the activity (IC_{50}s in nM). Middle) Changes on the in vitro activity regarding indoline, indole and 6-azaindole rings. Bottom) Modifications over the 6-azaindole-containing sulfonamide scaffold and structure-activity relationships (IC_{50}s in nM)

spectrum of weeds, both grasses and broad-leaved. Oryzalin binds to tubulin of sensitive plant species and inhibits meristematic growth in roots and shoots. Dinitroaniline herbicides also disrupt microtubules of both free-living and parasitic protozoa without affecting tubulin from fungi or vertebrates.[284–286] This selectivity has suggested the possibility of finding novel antiparasitic agents.[287] There are differences in sensitivity among the human parasites species, and *Plasmodium* and *Toxoplasma* are more affected while others such as *Trypanosome*, *Leishmania* and

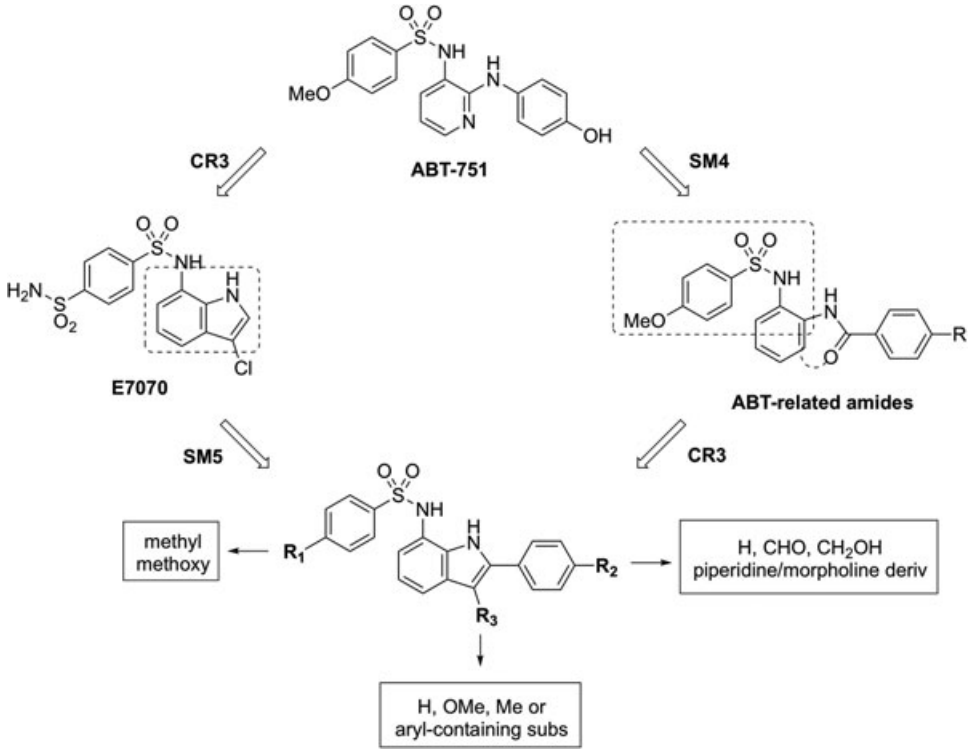

FIGURE 25 Hybrid structure of *N*-(2-aryl-1*H*-indol-7-yl)benzenesulfonamides

Entamoeba are less sensitive.[288–291] Substantial effort has been devoted towards establishing the tubulin binding site of dinitroaniline herbicides and their mechanism of action. Development of resistances in dinitroaniline sensitive organisms has often been linked to common point mutations of the α–tubulin genes and the implied amino acids have therefore been implicated in enhancing microtubule stability and/or in herbicide binding. As a result, two close binding sites have been proposed in the vicinity of the *N* terminus of α tubulin (Figure 26).[287,292–295] The primary sulfonamide is not an essential trait, as trifluralin and pendimethalin have it replaced by a trifluoromethyl and a methyl group respectively (Figure 26). Many primary sulfonamides are carbonic anhydrase inhibitors,[296] and oryzalin has been also found to inhibit human carbonic anhydrase.[293]

The introduction of a phenyl ring on the sulfonamide nitrogen (Figure 26 bottom left) increases antileishmanial potency,[295] and the replacement of one of the alkyl groups of the aniline by a phosphocholine yielded compound TC95 (Figure 26 bottom center) with improved potency with respect to miltefosine by combination of multiple cellular effects.[294] The nitro groups are the most favorable, and only cyano groups maintain potency, while ketones, acids, or acid derivatives result in potency reduction.[297,298] Enhancement of the potency against *Toxoplasma gondii* was achieved by replacing the sulfonamide with a trifluoromethyl and the introduction of an amino substituent on the phenyl ring (Figure 26 bottom right).

Triazole-containing sulfonamide scaffold

This family with an aryl sulfonamide moiety, a 1,2,3-triazole and one phenyl ring at least (Figure 27 left) has emerged as the result of a hybridization strategy between privileged groups in medicinal chemistry.[299] Despite the lack of structural analogy with other colchicine site ligands, the antitubulin profile was made evident with a micromolar in vitro PC-3 proliferation inhibition.

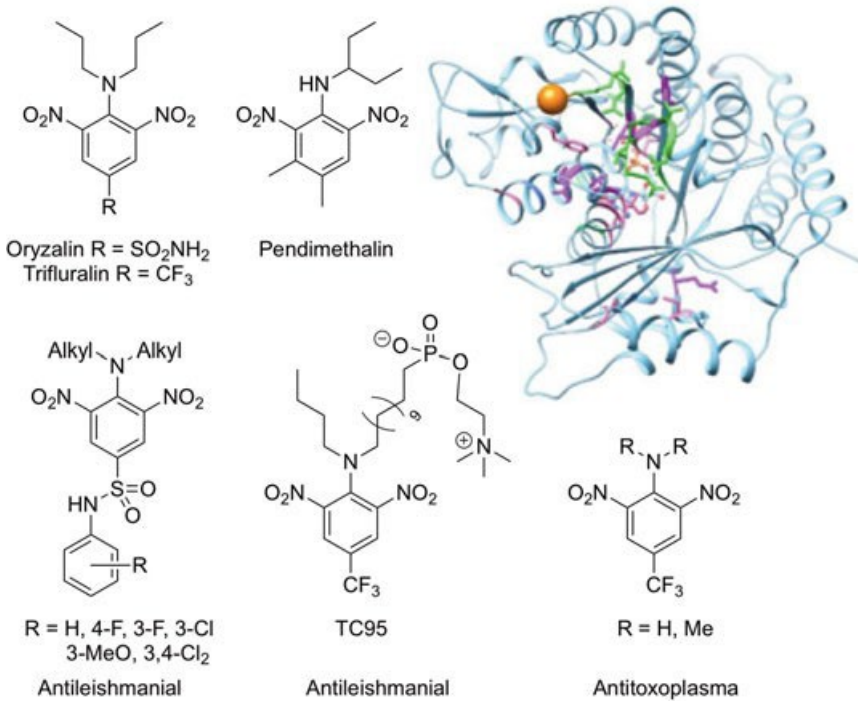

FIGURE 26 Top) Structure of the dinitroaniline herbicides. View of the structure α tubulin along the longitudinal axis (from the minus end) of the microtubule with the proposed binding pockets (in green and in magenta) in the proximity of the *N* terminus (indicated as an orange ball) proposed after the mutations (light pink) responsible for the development of resistance to the dinitroaniline herbicide. Bottom) Oryzalin derivatives with enhanced antiparasitic potency

Sulfonylurea derivatives

Originally conceived as sulofenur (LY186641) analogs, some sulfonylurea derivatives showed antitubulin properties (Figure 27). For instance, DW2282[300–306] displayed 0.012 μM as IC_{50} against HCT116 cell line, with a quite high correlation with TPI activity (1.5 μM).

4 | BIOLOGICAL ACTIVITY OF ANTITUBULIN SULFONAMIDES

4.1 | Clinical trials

The number of sulfonamide drugs that have undergone clinical trials is quite large,[199,307–309] and also a large number of tubulin binding drugs, often classified as vascular disrupting agents,[199,307–310] have reached the clinic.[190,191,199,307–309] Three sulfonamides binding to tubulin have undergone clinical trials, ABT-751, T138067, and T900607 (Table 2). ABT-751 was the pioneer compound of the class but has unfortunately shown low efficacy, probably associated with insufficient potency. More recently, two pentafluorophenylsulfonamides (T138067 and T900607), which are putative covalent modifiers and therefore less likely to suffer from lack of efficacy,[119] have entered clinical trials.[111,199,307,309]

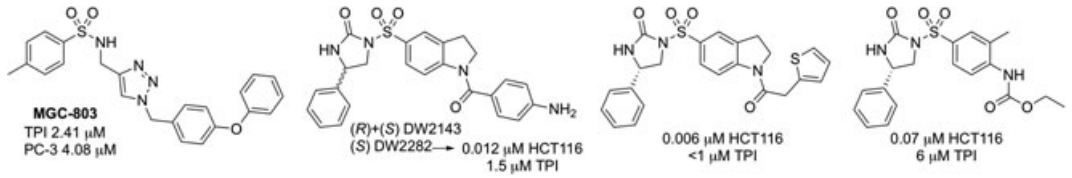

FIGURE 27 Representative of the triazole-sulfonamide hybrid family (left) and sulfonylurea-related compounds

4.2 | Molecular mechanisms and downstream events beneath TBDs treatment

Microtubule interfering agents' mechanisms of action have been extensively studied although the complete tale has not yet been elucidated, just a few highlights are known so far.[311] The most common explanation of how this kind of selective chemotherapy is preferentially targeted against neoplastic cells is based on their higher proliferation rate compared to normal cells, mainly backed up by the increased toxicity manifested for high-turnover tissues. Recently, some controversy has emerged about the basis of this selectivity, gathered in the strengthened "proliferation rate paradox" theory.[52] According to this theory tumor regression caused by drugs that affect dividing cells is doubtfully based on the enhanced proliferation, as many clinical neoplasms responding to chemotherapy show low dividing rates.

Several actions have been attributed to TBDs, grouped in two main categories: mitosis-dependent cell death and mitosis-independent tumor regression. Indeed, the "proliferation rate paradox" is supported by data suggesting that mitosis-independent actions after disturbance of interphase events are key components of the clinical response.[312,313] Cytotoxic concentrations of TBDs hinder proper cell division due to mitotic spindle disruption,[311] which is a common characteristic among tubulin ligands, irrespective of the binding site they are embraced by. A second mechanism of action has emerged, mainly for colchicine binding site analogs that behave as vascular disrupting agents (VDAs).[314–320] This duality confers them an advantage, since the antivascular profile is achieved at lower concentrations than those needed to kill proliferating cells, possibly avoiding some of the toxic side effects linked to conventional chemotherapy.[320–322]

Some colchicine site ligands such as CA-4 have an antiangiogenic profile that is also achieved at low concentrations too.[323–325] The impairment of new sprout formation is related to Rho/ROCK-dependent connective tissue growth factor (CTFG) upregulation, and VE-cadherin/β-catenin pathway interference,[323,326] thus affecting adhesion, chemotaxis, and migration of the endothelial cells required to constitute novel tubes,[323,327,328] although some other molecules have been related to the antiangiogenic profile such as Rac1, Cdc42, Hsp90 and PKC.[329–331] In addition, metastasis prevention has been reported through matrix metalloproteinases transport alterations,[332–334] which are proteolytic enzymes associated to the cleavage of extracellular matrix, allowing neoplastic cells to enter the blood system to settle a secondary tumor mass. Beside these widespread mechanisms, some sulfonamide based inhibitors have been reported to target other proteins or pathways such as STAT3 or HIF, as mentioned before.[260–262,276,280] In this review, we have focused on the molecular mechanisms leading to both mitosis inhibition and vascular disrupting activity, those that have been more widely explored.

4.2.1 | Mitosis inhibition dependent cell death

The molecular consequences following in vitro treatment with TBDs have been extensively studied in most cases for some representative TBDs such as paclitaxel, nocodazole and vinca alkaloids. Despite the structural diversity of TBDs and their opposing effect on microtubules (MSAs stabilize and MDAs destabilize) they exert a common action: microtubule dynamics disruption.[311] Therefore, the main molecular mechanisms beneath TBDs treatment might be extendable to all of them. Indeed, reports regarding molecular pathways following treatment with sulfonamide-including tubulin inhibitors are in agreement with that observed for classical TBDs.

The primary target of TBDs is the tubulin cytoskeleton of rapidly proliferating cells, thus affecting processes where tubulin polymers take part such as spindle-mediated cell division, thereby leading to a mitosis progression blockage.[335] Spindle assembly disruption manifested after treatment with TBDs causes a prolonged mitotic arrest that can be followed by either apoptotic-related cell death (mitotic catastrophe)[336] or slippage, a situation in which the cell exits mitosis reaching G_1 phase but skipping the division due to overcoming of checkpoint controls.[337,338]

During metaphase the chromosomes line up along cell equator being the DNA content organized in sister chromatids whose cohesion is guaranteed by a multimeric ring-shaped protein called cohesin.[339,340] Previously to chromosome segregation, emerging tubulin polymers from microtubule-organizing centers (MTOCs) try to establish proper attachments with chromosomes through sister chromatid binding by dynamic shrinkage and elongation until they reach the kinetochores.[341,342] To prevent chromosome missegregation, the presence of a single unattached kinetochore is enough[343] to activate the spindle assembly checkpoint (SAC) whose purpose is to delay the anaphase onset until insurance of accurate attachments is guaranteed.[344–347] Microtubule dynamics play a paramount role in these processes.[22]

Checkpoint activation occurs temporally at the early stages of metaphase and after TBDs treatment also. The difference is that the temporal checkpoint-induced arrest is alleviated after establishment of every single kinetochore attachment,[344,348] but not after treatment with tubulin disruptors. This checkpoint works by recruitment of proteins from Mad (mitotic-arrest deficient) and Bub (budding uninhibited by benzimidazole) families at the kinetochores[349] to constitute the MCC (mitotic checkpoint complex) formed by Mad2, Bub3, BubR1 and Cdc20.[350] The "template model" suggests that the key step in the formation of the MCC is the recruitment of an open-Mad2 by a Mad1-close-Mad2 dimer at the kinetochore, changing its conformational state into a close one.[346,351,352]

The MCC is responsible for the inhibition of the E3 ubiquitin ligase APC/C^{Cdc20} (anaphase promoting complex or cyclosome)[353–357] by changing its conformational state into a locked one.[358,359] The role of APC/C^{Cdc20} is to target substrates such as cyclin B1[353] and securin[360] for ubiquitination. The inactivated APC/$C^{Cdc20\text{-}MCC}$ is no longer able to label its substrates for proteasome 26S-dependent degradation (Figure 28).[361] APC/C inhibition has two main consequences: on one hand, cyclin B1/Cdk1 complex (MPF, maturation promoting factor) is permanently activated what means that anaphase entrance can't be triggered because it needs a drop in cyclin B1 levels. On the other hand, securin upregulation prevents separase, a proteolytic enzyme, from targeting cohesin for degradation,[362] keeping the integrity of sister chromatid cohesion.[360] At the end, there is a sustained G_2/M arrest that can last even for days.

The link between G_2/M arrest and cell death remains unclear. Indeed, it has been reported that prolonged cell arrest is not enough for the cell to die, presumably explained by another mechanism connecting mitotic arrest and apoptotic cell death,[363] through the mitochondria-dependent pathway.[364,365] Experimental data suggest that sustained Cdk1 levels switch cell fate from mitotic arrest to caspase-mediated cell death through a phosphorylation cascade. The intrinsic apoptotic pathway is tightly regulated by members from Bcl-2 family with proapoptotic and antiapoptotic roles,[366–368] in the second case ensuring the integrity of the mitochondria membrane. Many Bcl-2 protein family members, such as Bad, Bcl-xL, Bcl-2[369] and Mcl-1[370–372] are phosphorylated by sustained Cdk1 activation among other kinases,[373–380] eliciting substantially different consequences. Although Bad has an inherent proapoptotic role[373] and Bcl-xL, Mcl-1 and Bcl-2 are antiapoptotic proteins,[381,382] phosphorylation of Bcl-xL and Bad promotes apoptosis[374,376,380] as well as phosphorylation of Mcl-1,[380,383] although the relevance of Bcl-2 phosphorylation generates controversy as some authors attribute an apoptotic effect[352,369,374] but some others are in agreement with Cdk1 having a dual role due to the enhancement of cytoprotection after Bcl-2 phosphorylation.[380,384]

It has been reported that Mcl-1 is the main Bcl-2 family member involved in the linkage between mitotic arrest and cell death,[349,385,386] because unlike the other Bcl-2 members, Cdk1-mediated Mcl-1 phosphorylation favors its ubiquitination and subsequent degradation.[377,383] As Mcl-1 is an antiapoptotic protein, downregulation of Mcl-1 levels preferentially impair Bak sequestration,[377] another proapoptotic Bcl-2 protein responsible for the creation of

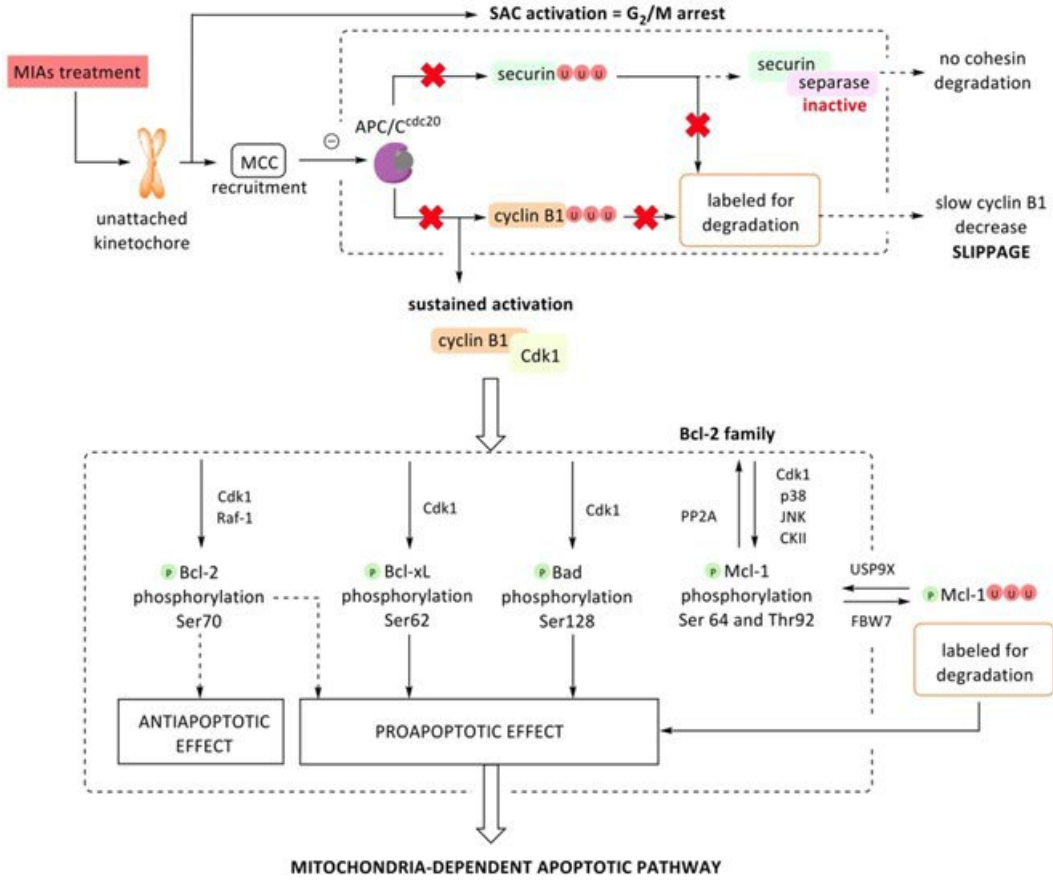

FIGURE 28 Microtubule dynamics inhibition leads to spindle assembly checkpoint activation, causing a prolonged metaphase arrest. The sustained activation of Cdk1 is responsible for a phosphorylation cascade that ends in intrinsic apoptotic cell death

pores at the mitochondria leading to MOMP (mitochondria outer membrane permeabilization).[387] Alteration of mitochondria membrane integrity allows cytochrome c to be released and the subsequent activation of the caspase machinery.

Although some other theories have emerged,[388,389] there is a growing evidence that whether cell fate undergoes apoptosis or slippage[387–390] depends on an imbalance between cyclin B1 and Mcl-1 degradation rates.[349,386] During an active SAC, the MCC prevents APC/C to label cyclin B1 for ultimate degradation but the inhibition is not total, being a very slow gradual drop in cyclin B1 levels.[391] If cyclin B1 degradation overcomes the threshold needed to anaphase onset before Mcl-1 does, cell would undergo slippage, meaning anaphase entrance with no DNA content division, becoming a tetraploid cell. However, if Mcl-1 decreases below the level required to prevent MOMP cell would trigger a caspase-mediated PARP cleavage undergoing apoptosis cell death with membrane blebbing.[392]

4.2.2 | TBDs as vascular disrupting agents (VDAs)

Antivascular therapies have emerged as highly promising strategies against solid tumors taking advantage of the fact that the tumor mass cannot surpass beyond 1 to 2 mm^3 [337,393] unless a whole blood microvessel network is settled to guarantee oxygen and nutrient supplies.[394,395] In addition, vascular targeted approaches offer a great

opportunity compared to conventional chemotherapy as these new vessels are constituted by non-tumor cells that are less prone to mutations than cancerous cells.[396,397] Due to the greater genetic stability of healthy endothelial cells, the mutation rate is quite low, what would presumably minimize the acquired resistance.[398] Besides, chemotherapy failure is likely related to the awkward access to the tumor itself in some cases and therefore targeting easily accessible tumor microvessels would favor the success of anticancer therapy.

Vascular targeted therapies include both the antiangiogenesis approach[399–401] and vascular disrupting agents.[402–404] The main difference lies in the target, which in turn conditions the schedules and the susceptible stages of the disease.[394,403,405] Antiangiogenic strategies impair the establishment of the blood vessel network by blocking the formation of new vessels, while vascular disruptors target the already established tumor vessels, halting the blood flow which causes ischemia and a massive necrosis of the tumor core.[402,406,407] Thus, angiogenesis inhibitors are useful in early stages of solid neoplasms[403] and require chronic administration schedules to prevent the growth of the tumor mass.[408] Nevertheless, vascular disrupting agents cause an almost immediately collapse in advanced cancers acutely administered.[409]

Despite VDAs target healthy non-tumor cells, the effects after treatment are almost completely selective[318,322,410] towards microvessels in the tumor microenvironment due to the physiological differences between normal blood vessels and the neovasculature that crosses the tumor mass.[409,411–413] Just a mild transient depletion in blood flow is observed in healthy tissues.[318,414] Quiescent normal vasculature is built by a well-structured network of hierarched branches. The luminal space is covered by a monolayer of non-proliferating planar endothelial cells tightly close one from the other through cell-to-cell junctions to ensure the stability of the blood vessel and avoid the basement membrane to be exposed, providing a non-thrombogenic surface. The presence of smooth muscle pericytes reinforces and stabilizes the architecture of the vessel. On the contrary, microvessels irrigating solid tumors are fragile, thin-walled and chaotically arranged[415,416] in a tangled and tortuous branch system lacking hierarchy with even blind sprouts.[417] The immatureness of tumor vessels[418] along with the high proliferation rate of their endothelial cells[417] is the consequence of overexpression of proangiogenic molecules in the tumor microenvironment. The defective cell junctions increase vessel permeability compared to normal vessels. Besides, the almost lack of pericytes and the weakened basement membrane contribute to the fragility of tumor microvessels,[409,410,418,419] being cytoskeleton-dependent endothelial cell shape the feature holding the vessel integrity that can be easily compromised by VDAs.[420,421] These differences altogether justify the susceptibility of the neovessel network to vascular disruptors.

Tubulin ligands as VDAs selectively target the interphase cytoskeleton of proliferating endothelial cells from tumor irrigating microvessels.[402,422,423] The activation of the Rho/ROCK pathway is involved in the subtle dynamic alterations of the F-actin and tubulin network at such low concentrations.[402,420,424,425] However, high concentrations are toxic for rapidly proliferating endothelial cells that suffer a caspase-dependent apoptosis[426] after a manifested mitotic arrest.[335] The induction of the Rho GTPase activity unchains a downstream cascade that ends in rapid collapse[427] of the vascular system where hemorrhage and clotting processes take place, finally leading to stress-oxidative hypoxia and ischemia (Figure 29).[428] The widespread network failure is responsible for the tumor regression as the inner core can't be provided with nutrients and oxygen,[429] therefore undergoing necrotic cell death.[52,320] The main disadvantage is that a thin layer of outer rim cells at the periphery of the tumor mass remains undamaged due to the covered supplies by normal surrounding non tumor vessels.[409,430,431] These viable cells are able to easily restore the inner tumor mass, what can be prevented through combination with conventional chemotherapy, radiotherapy or even antiangiogenic drugs, arising as really promising in clinical trials.[432–434]

Among other kinases, Rho kinase is responsible for the phosphorylation of myosin light chain (MLC),[435,436] subsequently enhancing the assembly of actin-myosin fibers and therefore the contractility.[402,437] The increased contraction/retraction dynamic enhances cellular tension leading to membrane blebbing[402,427] and cell shape alterations[421,423,438] that offer geometric resistance to blood flow.[423,439] In addition, Rho activation pathway is related to the stress-activated protein kinase 2 (SAPK2) activation,[402,440] with stress-fibers misassembly at the periphery of the cell.[275] Those fibers, along with F-actin accumulation around the cytoplasm are associated to the

FIGURE 29 Downstream events occurring after cytoskeleton alteration in proliferating endothelial cells

round-shaped cell phenotype and the presence of superficial blebs.[402] The FAK-dependent formation of focal adhesions[441] as well as the disassembly of cell-to-cell junctions through interference with vascular endothelial-cadherin/β-catenin/Akt pathway[421,442,443] contribute to a drop in cell adherence and a weakening of the vessel wall.[444] Rho-dependent morphology changes of the discontinuous endothelial layer trigger dramatic osmotic forces alterations that contribute to the shutdown of the blood flow.[445,446] A raise in vascular permeability,[447] which is already higher for tumor vessels[419,448] elicits the leakage of macromolecules to the nearby tissue with the probably subsequent increase in interstitial pressure.[449,450] The raise in erythrocyte concentration given by the loss of plasma impairs blood flow increasing viscous resistance[322] what might cause stagnation and rouleaux formation due to red cells clumping.[451] The thrombogenic situation is aggravated by the exposure of the basement membrane after adherence disturbance and loss of cells, inducing the clotting cascade and recruitment of platelets with vasoconstrictor serotonin release. Widespread collapse of the damaged vascular network with occlusive and hemorrhagic processes[318,414] cuts the flow to and from the tumor core that undergoes a necrotic cell death.[322]

5 | CONCLUSSIONS AND FUTURE PERSPECTIVE

Tubulin has remained as one of the most successful chemotherapeutic targets in the last decades. The toxicity expected for drugs altering such a fundamental protein and the development of resistances questioned their sustainability as a first line anticancer therapy and promoted the search for alternatives. Unfortunately, the clinical response to the so called antimitotic targeted drugs has so far been unsatisfactory. On the other hand, TBDs have shown more tricks than mere mitosis disruption. The complex tubulin biochemistry and the versatility offered by many different drug binding sites is unveiling new therapeutic opportunities and strategies at the same time as they are helping to disentangle the biological intricacies of their functioning within cells. In particular, advances in structural studies combined with TBDs are providing key insights into the microtubules structure, regulation, and biology and fueling on the way drug discovery efforts. These advancements in the field foresees a promising future for TBDs and as more information becomes available the chances of successful outcomes increase.

The application of antimitotic agents to parasitic diseases has however not advanced as much. The development of resistances has significantly impacted on their use, and there are few new candidates in the pipeline, even if the other disadvantages for anticancer therapy (ie disruption of a fundamental cytoskeletal protein) turn into advantages in this case. The judicious exploitation of the many drug binding sites, of tubulin particularities and of species differences might in the future restore this therapeutic opportunity.

The antimitotic sulfonamides are a good reflection of both worlds. They have been explored as antitumor, as antiparasitic and as herbicides. In this search, both a well characterized site (the colchicine domain) and an ill-defined site on α tubulin have been uncovered. Both sites have yielded useful drugs and helped to establish the basis for future design. In this regard, the structurally characterized colchicine domain has experienced a much more active development of drugs for anticancer and antiparasitic applications, whereas the other site remains less exploited. This illustrates the impact of structural information on drug design. New sulfonamides are expected in the future to fill these gaps and exploit their favorable drug-like properties to make possible an access to the clinic.

ACKNOWLEDGEMENTS

Financial support from a Project from the Consejería de Educación de la Junta de Castilla y León and FEDER Funds (SA030U16) is aknowledged. MG and SM thank the Consejería de Educación de la Junta de Castilla y León for a predoctoral fellowship and AV the Spanish Ministerio de Educación, Cultura y Deporte for a predoctoral FPU fellowship.

ORCID

Raquel Álvarez http://orcid.org/0000-0002-6890-8416
Manuel Medarde http://orcid.org/0000-0002-3311-5846
Rafael Peláez http://orcid.org/0000-0003-1433-1612

REFERENCES

1. Löwe J, Li H, Downing KH, Nogales E. Refined structure of alpha beta-tubulin at 3.5 A resolution. *J Mol Biol*. 2001;313 (5):1045-1057.
2. Gigant B, Curmi PA, Martin-Barbey C, et al. The 4 A X-ray structure of a tubulin:stathmin-like domain complex. *Cell*. 2000;102(6):809-816.
3. Roll-Mecak A. Intrinsically disordered tubulin tails: complex tuners of microtubule functions?. *Semin Cell Dev Biol*. 2015;37:11-19.
4. Amos LA, Schlieper D. Microtubules and maps. *Adv Protein Chem*. 2005;71:257-298.

5. Chaaban S, Brouhard GJ. A microtubule bestiary: structural diversity in tubulin polymers. *Mol Biol Cell*. 2017;28 (22):2924-2931.
6. Nogales E, Wolf SG, Downing KH. Structure of the alpha beta tubulin dimer by electron crystallography. *Nature*. 1998;391(6663):199-203.
7. Nogales E, Whittaker M, Milligan RA, Downing KH. High-resolution model of the microtubule. *Cell*. 1999;96(1):79-88.
8. Buey RM, Díaz JF, Andreu JM. The nucleotide switch of tubulin and microtubule assembly: a polymerization-driven structural change. *Biochemistry*. 2006;45(19):5933-5938.
9. Wang HW, Nogales E. Nucleotide-dependent bending flexibility of tubulin regulates microtubule assembly. *Nature*. 2005;435(7044):911-915.
10. Igaev M, Grubmüller H. Microtubule assembly governed by tubulin allosteric gain in flexibility and lattice induced fit. *eLife*. 2018;7:e34353.
11. Driver JW, Geyer EA, Bailey ME, Rice LM, Asbury CL. Direct measurement of conformational strain energy in protofilaments curling outward from disassembling microtubule tips. *eLife*. 2017;6:e28433.
12. Geyer EA, Burns A, Lalonde BA, et al. A mutation uncouples the tubulin conformational and GTPase cycles, revealing allosteric control of microtubule dynamics. *eLife*. 2015;4:e10113.
13. Asbury C. Anaphase A: disassembling microtubules move chromosomes toward spindle poles. *Biology*. 2017;6(1):15.
14. Zhang R, Alushin GM, Brown A, Nogales E. Mechanistic origin of microtubule dynamic instability and its modulation by EB proteins. *Cell*. 2015;162(4):849-859.
15. Maurer SP, Fourniol FJ, Bohner G, Moores CA, Surrey T. EBs recognize a nucleotide-dependent structural cap at growing microtubule ends. *Cell*. 2012;149(2):371-382.
16. Alushin GM, Lander GC, Kellogg EH, Zhang R, Baker D, Nogales E. High-resolution microtubule structures reveal the structural transitions in alphabeta-tubulin upon GTP hydrolysis. *Cell*. 2014;157(5):1117-1129.
17. Kollman JM, Polka JK, Zelter A, Davis TN, Agard DA. Microtubule nucleating gamma-TuSC assembles structures with 13-fold microtubule-like symmetry. *Nature*. 2010;466(7308):879-882.
18. Evans L, Mitchison T, Kirschner M. Influence of the centrosome on the structure of nucleated microtubules. *J Cell Biol*. 1985;100(4):1185-1191.
19. McIntosh JR, Morphew MK, Grissom PM, Gilbert SP, Hoenger A. Lattice structure of cytoplasmic microtubules in a cultured Mammalian cell. *J Mol Biol*. 2009;394(2):177-182.
20. Amos L, Klug A. Arrangement of subunits in flagellar microtubules. *J Cell Sci*. 1974;14(3):523-549.
21. Zhang R, Nogales E. A new protocol to accurately determine microtubule lattice seam location. *J Struct Biol*. 2015;192 (2):245-254.
22. Brouhard GJ, Rice LM. Microtubule dynamics: an interplay of biochemistry and mechanics. *Nat Rev Mol Cell Biol*. 2018;19(7):451-463.
23. Akhmanova A, Steinmetz MO. Control of microtubule organization and dynamics: two ends in the limelight. *Nat Rev Mol Cell Biol*. 2015;16(12):711-726.
24. Ohi R, Zanic M. Ahead of the curve: new insights into microtubule dynamics. *F1000Research*. 2016;5:314.
25. Zhang R, Roostalu J, Surrey T, Nogales E. Structural insight into TPX2-stimulated microtubule assembly. *eLife*. 2017;6: e30959.
26. Roostalu J, Surrey T. Microtubule nucleation: beyond the template. *Nat Rev Mol Cell Biol*. 2017;18(11):702-710.
27. Kollman JM, Merdes A, Mourey L, Agard DA. Microtubule nucleation by gamma-tubulin complexes. *Nat Rev Mol Cell Biol*. 2011;12(11):709-721.
28. Popov AV, Severin F, Karsenti E. XMAP215 is required for the microtubule-nucleating activity of centrosomes. *Curr Biol*. 2002;12(15):1326-1330.
29. Fernandez N, Chang Q, Buster DW, Sharp DJ, Ma A. A model for the regulatory network controlling the dynamics of kinetochore microtubule plus-ends and poleward flux in metaphase. *Proc Natl Acad Sci U S A*. 2009;106 (19):7846-7851.
30. Rogers GC, Rogers SL, Sharp DJ. Spindle microtubules in flux. *J Cell Sci*. 2005;118(Pt 6):1105-1116.
31. Brouhard GJ. Dynamic instability 30 years later: complexities in microtubule growth and catastrophe. *Mol Biol Cell*. 2015;26(7):1207-1210.
32. Hemmat M, Castle BT, Odde DJ. Microtubule dynamics: moving toward a multi-scale approach. *Curr Opin Cell Biol*. 2018;50:8-13.
33. Bowne-Anderson H, Hibbel A, Howard J. Regulation of microtubule growth and catastrophe: unifying theory and experiment. *Trends Cell Biol*. 2015;25(12):769-779.
34. Gardner MK, Charlebois BD, Jánosi IM, Howard J, Hunt AJ, Odde DJ. Rapid microtubule self-assembly kinetics. *Cell*. 2014;159(1):215.
35. Margolin G, Gregoretti IV, Cickovski TM, et al. The mechanisms of microtubule catastrophe and rescue: implications from analysis of a dimer-scale computational model. *Mol Biol Cell*. 2012;23(4):642-656.

36. Gardner MK, Charlebois BD, Jánosi IM, Howard J, Hunt AJ, Odde DJ. Rapid microtubule self-assembly kinetics. *Cell*. 2011;146(4):582-592.
37. Zhang Z, Goldtzvik Y, Thirumalai D. Parsing the roles of neck-linker docking and tethered head diffusion in the stepping dynamics of kinesin. *Proc Natl Acad Sci U S A*. 2017;114(46):E9838-E9845.
38. Kellogg EH, Howes S, Ti SC, et al. Near-atomic cryo-EM structure of PRC1 bound to the microtubule. *Proc Natl Acad Sci U S A*. 2016;113(34):9430-9439.
39. Gupta KK, Li C, Duan A, et al. Mechanism for the catastrophe-promoting activity of the microtubule destabilizer Op18/stathmin. *Proc Natl Acad Sci U S A*. 2013;110(51):20449-20454.
40. Kumbhar BV, Borogaon A, Panda D, Kunwar A. Exploring the origin of differential binding affinities of human tubulin isotypes alphabetaII, alphabetaIII and alphabetaIV for DAMA-colchicine using homology modelling, molecular docking and molecular dynamics simulations. *PLOS One*. 2016;11(5):e0156048.
41. Prota AE, Bargsten K, Northcote PT, et al. Structural basis of microtubule stabilization by laulimalide and peloruside A. *Angew Chem*. 2014;53(6):1621-1625.
42. Garzoni M, Okuro K, Ishii N, Aida T, Pavan GM. Structure and shape effects of molecular glue on supramolecular tubulin assemblies. *ACS Nano*. 2014;8(1):904-914.
43. Álvarez R, Puebla P, Díaz JF, et al. Endowing indole-based tubulin inhibitors with an anchor for derivatization: highly potent 3-substituted indolephenstatins and indoleisocombretastatins. *J Med Chem*. 2013;56(7):2813-2827.
44. Natarajan K, Senapati S. Understanding the basis of drug resistance of the mutants of alphabeta-tubulin dimer via molecular dynamics simulations. *PLOS One*. 2012;7(8):e42351.
45. Dumontet C, Jordan MA. Microtubule-binding agents: a dynamic field of cancer therapeutics. *Nat Rev Drug Discov*. 2010;9(10):790-803.
46. Jordan M, Kamath K. How do microtubule-targeted drugs work? An overview. *Curr Cancer Drug Targets*. 2007;7 (8):730-742.
47. Jordan MA, Wilson L. Microtubules as a target for anticancer drugs. *Nat Rev Cancer*. 2004;4(4):253-265.
48. Vemu A, Atherton J, Spector JO, Moores CA, Roll-Mecak A. Tubulin isoform composition tunes microtubule dynamics. *Mol Biol Cell*. 2017;28(25):3564-3572.
49. Kueh HY, Mitchison TJ. Structural plasticity in actin and tubulin polymer dynamics. *Science*. 2009;325(5943):960-963.
50. Bates D, Eastman A. Microtubule destabilising agents: far more than just antimitotic anticancer drugs. *Br J Clin Pharmacol*. 2017;83(2):255-268.
51. Florian S, Mitchison TJ. Anti-microtubule drugs. *Methods Mol Biol*. 2016;1413:403-421.
52. Mitchison TJ. The proliferation rate paradox in antimitotic chemotherapy. *Mol Biol Cell*. 2012;23(1):1-6.
53. Wloga D, Joachimiak E, Louka P, Gaertig J. Posttranslational modifications of tubulin and cilia. *Cold Spring Harbor Perspect Biol*. 2017;9(6):a028159.
54. Gadadhar S, Bodakuntla S, Natarajan K, Janke C. The tubulin code at a glance. *J Cell Sci*. 2017;130(8):1347-1353.
55. Barisic M, Maiato H. The tubulin code: a navigation system for chromosomes during mitosis. *Trends Cell Biol*. 2016;26 (10):766-775.
56. Yu I, Garnham CP, Roll-Mecak A. Writing and reading the tubulin code. *J Biol Chem*. 2015;290(28):17163-17172.
57. Raunser S, Gatsogiannis C. Deciphering the tubulin code. *Cell*. 2015;161(5):960-961.
58. Barisic M, Maiato H. Cracking the (tubulin) code of mitosis. *Oncotarget*. 2015;6(23):19356-19357.
59. Wehenkel A, Janke C. Towards elucidating the tubulin code. *Nature Cell Biol*. 2014;16(4):303-305.
60. Rezania V, Azarenko O, Jordan MA, et al. Microtubule assembly of isotypically purified tubulin and its mixtures. *Biophys J*. 2008;95(4):1993-2008.
61. Parker AL, Kavallaris M, McCarroll JA. Microtubules and their role in cellular stress in cancer. *Front Oncol*. 2014;4:153.
62. Stengel C, Newman SP, Leese MP, Potter BVL, Reed MJ, Purohit A. Class III beta-tubulin expression and in vitro resistance to microtubule targeting agents. *Br J Cancer*. 2010;102(2):316-324.
63. Kavallaris M. Microtubules and resistance to tubulin-binding agents. *Nat Rev Cancer*. 2010;10(3):194-204.
64. Dostál V, Libusová L. Microtubule drugs: action, selectivity, and resistance across the kingdoms of life. *Protoplasma*. 2014;251(5):991-1005.
65. Dempsey E, Prudêncio M, Fennell BJ, Gomes-Santos CS, Barlow JW, Bell A. Antimitotic herbicides bind to an unidentified site on malarial parasite tubulin and block development of liver-stage Plasmodium parasites. *Mol Biochem Parasitol*. 2013;188(2):116-127.
66. Blume YB, Nyporko AY, Yemets AI, Baird WV. Structural modeling of the interaction of plant alpha-tubulin with dinitroaniline and phosphoroamidate herbicides. *Cell Biol Int*. 2003;27(3):171-174.
67. Jordan M. Mechanism of action of antitumor drugs that interact with microtubules and tubulin. *Curr Med Chem Anticancer Agents*. 2002;2(1):1-17.
68. Diaz JF, Menendez M, Andreu JM. Thermodynamics of ligand-induced assembly of tubulin. *Biochemistry*. 1993;32 (38):10067-10077.

69. Nogales E. Structural insights into microtubule function. *Annu Rev Biochem*. 2000;69:277-302.
70. Berman H, Henrick K, Nakamura H. Announcing the worldwide Protein Data Bank. *Nature Struct Biol*. 2003;10:980-980.
71. Field JJ, Pera B, Gallego JE, et al. Zampanolide binding to tubulin indicates cross-talk of taxane site with colchicine and nucleotide sites. *J Nat Prod*. 2018;81(3):494-505.
72. Wang Y, Yu Y, Li GB, et al. Mechanism of microtubule stabilization by taccalonolide AJ. *Nat Commun*. 2017;8:15787.
73. Prota AE, Bargsten K, Redondo-Horcajo M, et al. Structural basis of microtubule stabilization by discodermolide. *Chembiochem*. 2017;18(10):905-909.
74. Trigili C, Barasoain I, Sánchez-Murcia PA, et al. Structural determinants of the dictyostatin chemotype for tubulin binding affinity and antitumor activity against taxane- and epothilone-resistant cancer cells. *ACS Omega*. 2016;1 (6):1192-1204.
75. Kellogg EH, Hejab NMA, Howes S, et al. Insights into the distinct mechanisms of action of taxane and non-taxane microtubule stabilizers from cryo-EM structures. *J Mol Biol*. 2017;429(5):633-646.
76. Prota AE, Bargsten K, Zurwerra D, et al. Molecular mechanism of action of microtubule-stabilizing anticancer agents. *Science*. 2013;339(6119):587-590.
77. Nettles JH, Li H, Cornett B, Krahn JM, Snyder JP, Downing KH. The binding mode of epothilone A on alpha,beta-tubulin by electron crystallography. *Science*. 2004;305(5685):866-869.
78. Gigant B, Wang C, Ravelli RBG, et al. Structural basis for the regulation of tubulin by vinblastine. *Nature*. 2005;435 (7041):519-522.
79. Cormier A, Marchand M, Ravelli RBG, Knossow M, Gigant B. Structural insight into the inhibition of tubulin by vinca domain peptide ligands. *EMBO Rep*. 2008;9(11):1101-1106.
80. Ranaivoson FM, Gigant B, Berritt S, Joullié M, Knossow M. Structural plasticity of tubulin assembly probed by vinca-domain ligands. *Acta Crystallogr D Biol Crystallogr*. 2012;68(Pt 8):927-934.
81. Maderna A, Doroski M, Subramanyam C, et al. Discovery of cytotoxic dolastatin 10 analogues with N-terminal modifications. *J Med Chem*. 2014;57(24):10527-10543.
82. Wang Y, Benz FW, Wu Y, et al. Structural insights into the pharmacophore of vinca domain inhibitors of microtubules. *Mol Pharmacol*. 2016;89(2):233-242.
83. Waight AB, Bargsten K, Doronina S, Steinmetz MO, Sussman D, Prota AE. Structural basis of microtubule destabilization by potent auristatin anti-mitotics. *PLOS One*. 2016;11(8):e0160890.
84. Leverett CA, Sukuru SCK, Vetelino BC, et al. Design, synthesis, and cytotoxic evaluation of novel tubulysin analogues as ADC payloads. *ACS Med Chem Lett*. 2016;7(11):999-1004.
85. Wieczorek M, Tcherkezian J, Bernier C, et al. The synthetic diazonamide DZ-2384 has distinct effects on microtubule curvature and dynamics without neurotoxicity. *Sci Transl Med*. 2016;8(365):365ra159-365ra159.
86. Sáez-Calvo G, Sharma A, Balaguer FA, et al. Triazolopyrimidines are microtubule-stabilizing agents that bind the vinca inhibitor site of tubulin. *Cell chemical biology*. 2017;24(6):737-750. e736
87. Doodhi H, Prota AE, Rodríguez-García R, et al. Termination of protofilament elongation by eribulin induces lattice defects that promote microtubule catastrophes. *Current biology: CB*. 2016;26(13):1713-1721.
88. Prota AE, Bargsten K, Diaz JF, et al. A new tubulin-binding site and pharmacophore for microtubule-destabilizing anticancer drugs. *Proc Natl Acad Sci U S A*. 2014;111(38):13817-13821.
89. Yang J, Wang Y, Wang T, et al. Pironetin reacts covalently with cysteine-316 of alpha-tubulin to destabilize microtubule. *Nat Commun*. 2016;7:12103.
90. Prota AE, Setter J, Waight AB, et al. Pironetin binds covalently to alphaCys316 and perturbs a major loop and helix of alpha-tubulin to inhibit microtubule formation. *J Mol Biol*. 2016;428(15):2981-2988.
91. Ravelli RBG, Gigant B, Curmi PA, et al. Insight into tubulin regulation from a complex with colchicine and a stathmin-like domain. *Nature*. 2004;428(6979):198-202.
92. Dorleans A, Gigant B, Ravelli RBG, Mailliet P, Mikol V, Knossow M. Variations in the colchicine-binding domain provide insight into the structural switch of tubulin. *Proc Natl Acad Sci U S A*. 2009;106(33):13775-13779.
93. Barbier P, Dorléans A, Devred F, et al. Stathmin and interfacial microtubule inhibitors recognize a naturally curved conformation of tubulin dimers. *J Biol Chem*. 2010;285(41):31672-31681.
94. Prota AE, Danel F, Bachmann F, et al. The novel microtubule-destabilizing drug BAL27862 binds to the colchicine site of tubulin with distinct effects on microtubule organization. *J Mol Biol*. 2014;426(8):1848-1860.
95. McNamara DE, Senese S, Yeates TO, Torres JZ. Structures of potent anticancer compounds bound to tubulin. *Protein Sci*. 2015;24(7):1164-1172.
96. Wang Y, Zhang H, Gigant B, et al. Structures of a diverse set of colchicine binding site inhibitors in complex with tubulin provide a rationale for drug discovery. *FEBS J*. 2016;283(1):102-111.
97. Zhou P, Liu Y, Zhou L, et al. Potent antitumor activities and structure basis of the chiral beta-lactam bridged analogue of combretastatin A-4 binding to tubulin. *J Med Chem*. 2016;59(22):10329-10334.

98. Arnst KE, Wang Y, Hwang DJ, et al. A potent, metabolically stable tubulin inhibitor targets the colchicine binding site and overcomes taxane resistance. *Cancer Res*. 2018;78(1):265-277.
99. Zhao W, Zhou C, Guan ZY, Yin P, Chen F, Tang YJ. Structural insights into the inhibition of tubulin by the antitumor agent 4beta-(1,2,4-triazol-3-ylthio)-4-deoxypodophyllotoxin. *ACS Chem Biol*. 2017;12(3):746-752.
100. Canela MD, Noppen S, Bueno O, et al. Antivascular and antitumor properties of the tubulin-binding chalcone TUB091. *Oncotarget*. 2017;8(9):14325-14342.
101. Marangon J, Christodoulou MS, Casagrande FVM, et al. Tools for the rational design of bivalent microtubule-targeting drugs. *Biochem Biophys Res Commun*. 2016;479(1):48-53.
102. Gaspari R, Prota AE, Bargsten K, Cavalli A, Steinmetz MO. Structural basis of cis- and trans-combretastatin binding to tubulin. *Chem*. 2017;2(1):102-113.
103. Bohnacker T, Prota AE, Beaufils F, et al. Deconvolution of Buparlisib's mechanism of action defines specific PI3K and tubulin inhibitors for therapeutic intervention. *Nat Commun*. 2017;8:14683.
104. Field J, Northcote P, Paterson I, Altmann KH, Díaz J, Miller J. Zampanolide, a microtubule-stabilizing agent, is active in resistant cancer cells and inhibits cell migration. *Int J Mol Sci*. 2017;18(5):971-989.
105. Dohle W, Jourdan FL, Menchon G, et al. Quinazolinone-based anticancer agents: synthesis, antiproliferative SAR, antitubulin activity, and tubulin co-crystal structure. *J Med Chem*. 2018;61(3):1031-1044.
106. Jost M, Chen Y, Gilbert LA, et al. Combined CRISPRi/a-based chemical genetic screens reveal that rigosertib is a microtubule-destabilizing agent. *Mol Cell*. 2017;68(1):210-223. e216
107. Zhou P, Liang Y, Zhang H, et al. Design, synthesis, biological evaluation and cocrystal structures with tubulin of chiral beta-lactam bridged combretastatin A-4 analogues as potent antitumor agents. *Eur J Med Chem*. 2018;144:817-842.
108. Niu L, Wang Y, Wang C, et al. Structure of 4′-demethylepipodophyllotoxin in complex with tubulin provides a rationale for drug design. *Biochem Biophys Res Commun*. 2017;493(1):718-722.
109. Cheng J, Wu Y, Wang Y, et al. Structure of a benzylidene derivative of 9(10H)-anthracenone in complex with tubulin provides a rationale for drug design. *Biochem Biophys Res Commun*. 2018;495(1):185-188.
110. Banerjee S, Arnst KE, Wang Y, et al. Heterocyclic-fused pyrimidines as novel tubulin polymerization inhibitors targeting the colchicine binding site: structural basis and antitumor efficacy. *J Med Chem*. 2018;61(4):1704-1718.
111. Bueno O, Estévez gallego J, Martins S, et al. High-affinity ligands of the colchicine domain in tubulin based on a structure-guided design. *Sci Rep*. 2018;8(1):4242.
112. Field JJ, Díaz JF, Miller JH. The binding sites of microtubule-stabilizing agents. *Chem Biol*. 2013;20(3):301-315.
113. Magnani M, Maccari G, Andreu JM, Díaz JF, Botta M. Possible binding site for paclitaxel at microtubule pores. *FEBS J*. 2009;276(10):2701-2712.
114. Buey RM, Calvo E, Barasoain I, et al. Cyclostreptin binds covalently to microtubule pores and lumenal taxoid binding sites. *Nat Chem Biol*. 2007;3(2):117-125.
115. Zhao Y, Mu X, Du G. Microtubule-stabilizing agents: New drug discovery and cancer therapy. *Pharmacol Ther*. 2016;162:134-143.
116. Kingston DGI, Snyder JP. The quest for a simple bioactive analog of paclitaxel as a potential anticancer agent. *Acc Chem Res*. 2014;47(8):2682-2691.
117. Ojima I, Lichtenthal B, Lee S, Wang C, Wang X. Taxane anticancer agents: a patent perspective. *Expert Opin Ther Pat*. 2016;26(1):1-20.
118. Sackett DL. Antimicrotubule Agents That Bind Covalently to Tubulin. In: Fojo T, ed. *The Role of Microtubules in Cell Biology, Neurobiology, and Oncology*. Totowa, NJ: Humana Press; 2008:pp. 281-306.
119. Singh J, Petter RC, Baillie TA, Whitty A. The resurgence of covalent drugs. *Nat Rev Drug Discov*. 2011;10(4):307-317.
120. Mooberry SL, Tien G, Hernandez AH, Plubrukarn A, Davidson BS. Laulimalide and isolaulimalide, new paclitaxel-like microtubule-stabilizing agents. *Cancer Res*. 1999;59(3):653-660.
121. West LM, Northcote PT, Battershill CN. Peloruside A: a potent cytotoxic macrolide isolated from the New Zealand marine sponge Mycale sp. *J Org Chem*. 2000;65(2):445-449.
122. Alvarez R, Medarde M, Pelaez R. New ligands of the tubulin colchicine site based on X-ray structures. *Curr Top Med Chem*. 2014;14(20):2231-2252.
123. Massarotti A, Coluccia A, Silvestri R, Sorba G, Brancale A. The tubulin colchicine domain: a molecular modeling perspective. *ChemMedChem*. 2012;7(1):33-42.
124. Álvarez R, Aramburu L, Puebla P, et al. Pyridine based antitumour compounds acting at the colchicine site. *Curr Med Chem*. 2016;23(11):1100-1130.
125. Drews J. Drug discovery: a historical perspective. *Science*. 2000;287(5460):1960-1964.
126. Mullard A. 2015 FDA drug approvals. *Nat Rev Drug Discov*. 2016;15(2):73-76.
127. Mullard A. 2016 FDA drug approvals. *Nat Rev Drug Discov*. 2017;16(2):73-76.
128. Bemis GW, Murcko MA. Properties of known drugs. 2. Side chains. *J Med Chem*. 1999;42(25):5095-5099.
129. Bemis GW, Murcko MA. The properties of known drugs. 1. Molecular frameworks. *J Med Chem*. 1996;39(15):2887-2893.

130. (EBI) EBI. https://www.ebi.ac.uk/chembl/drugstore. Accessed 15-03-2018, 2018.
131. Bissantz C, Kuhn B, Stahl M. A medicinal chemist's guide to molecular interactions. *J Med Chem*. 2010;53 (14):5061-5084.
132. Wang L, Xie Z, Wipf P, Xie XQ. Residue preference mapping of ligand fragments in the Protein Data Bank. *J Chem Inf Model*. 2011;51(4):807-815.
133. Brameld KA, Kuhn B, Reuter DC, Stahl M. Small molecule conformational preferences derived from crystal structure data. A medicinal chemistry focused analysis. *J Chem Inf Model*. 2008;48(1):1-24.
134. Radkiewicz JL, McAllister MA, Goldstein E, Houk KN. A theoretical investigation of phosphonamidates and sulfonamides as protease transition state isosteres. *J Org Chem*. 1998;63(5):1419-1428.
135. Vijayadas KN, Davis HC, Kotmale AS, et al. An unusual conformational similarity of two peptide folds featuring sulfonamide and carboxamide on the backbone. *Chem Commun*. 2012;48(78):9747-9749.
136. Parkin A, Collins A, Gilmore CJ, Wilson CC. Using small molecule crystal structure data to obtain information about sulfonamide conformation. *Acta Crystallogr B*. 2008;64(1):66-71.
137. Gennari C, Salom B, Potenza D, et al. Conformational studies of chiral vinylogous sulfonamidopeptides. *Chem—Eur J*. 1996;2(6):644-655.
138. Beddoes RL, Dalton L, Joule JA, Mills OS, Street JD, Watt CIF. The geometry at nitrogen in *N*-phenylsulphonylpyrroles and -indoles. The geometry of sulphonamides. *J Chem Soc Perkin Trans 2*. 1986;6:787-797.
139. Schwertz G, Frei MS, Witschel MC, et al. Conformational aspects in the design of inhibitors for serine hydroxymethyltransferase (SHMT): biphenyl, aryl sulfonamide, and aryl sulfone motifs. *Chemistry*. 2017;23 (57):14345-14357.
140. Hof F, Schütz A, Fäh C, et al. Starving the malaria parasite: inhibitors active against the aspartic proteases plasmepsins I, II, and IV. *Angew Chem*. 2006;45(13):2138-2141.
141. Laurence C, Brameld KA, Graton J, Le Questel JY, Renault E. The pK(BHX) database: toward a better understanding of hydrogen-bond basicity for medicinal chemists. *J Med Chem*. 2009;52(14):4073-4086.
142. Gennari C, Gude M, Potenza D, Piarulli U. Hydrogen-bonding donor/acceptor scales in β-sulfonamidopeptides. *Chem —Eur J*. 1998;4(10):1924-1931.
143. Lawhorn BG, Philp J, Graves AP, Holt DA, Gatto GJ, Jr., Kallander LS. Substituent effects on drug-receptor H-bond interactions: correlations useful for the design of kinase inhibitors. *J Med Chem*. 2016;59(23):10629-10641.
144. Aidas K, Lanevskij K, Kubilius R, Juška L, Petkevičius D, Japertas P. Aqueous acidities of primary benzenesulfonamides: quantum chemical predictions based on density functional theory and SMD. *J Comput Chem*. 2015;36 (29):2158-2167.
145. Remko M. Molecular structure, pKa, lipophilicity, solubility and absorption of biologically active aromatic and heterocyclic sulfonamides. *J Mol Struct THEOCHEM*. 2010;944(1):34-42.
146. Remko M, von der Lieth C-W. Theoretical study of gas-phase acidity, pKa, lipophilicity, and solubility of some biologically active sulfonamides. *Bioorg Med Chem*. 2004;12(20):5395-5403.
147. Remko M. Theoretical study of molecular structure and gas-phase acidity of some biologically active sulfonamides. *J Phys Chem A*. 2003;107(5):720-725.
148. Perlovich GL, Kazachenko VP, Strakhova NN, Raevsky OA. Impact of sulfonamide structure on solubility and transfer processes in biologically relevant solvents. *J Chem Eng Data*. 2014;59(12):4217-4226.
149. Raevsky OA, Perlovich GL, Kazachenko VP, Strakhova NN, Schaper K-J. Octanol/water partition coefficients of sulfonamides: experimental determination and calculation using physicochemical descriptors. *J Chem Eng Data*. 2009;54(11):3121-3124.
150. Mukherjee A, Desiraju GR. Polymorphism: the same and not quite the same. *Cryst Growth Des*. 2008;8(1):3-5.
151. Apperley DC, Fletton RA, Harris RK, Lancaster RW, Tavener S, Threlfall TL. Sulfathiazole polymorphism studied by magic-angle spinning NMR. *J Pharm Sci*. 2000;88(12):1275-1280.
152. Chourasiya SS, Patel DR, Nagaraja CM, Chakraborti AK, Bharatam PV. Sulfonamide vs. sulfonimide: tautomerism and electronic structure analysis of *N*-heterocyclic arenesulfonamides. *New J Chem*. 2017;41(16):8118-8129.
153. Nilsson Lill SO, Broo A. Molecule VI: sulfonimide or sulfonamide?. *Cryst Growth Des*. 2014;14(8):3704-3710.
154. Anderson KK. Sulfonic acids and their derivatives. In: Barton DHR, Ollis WD, Jones DN, eds. *Comprehensive Organic Chemistry*. Vol 3. Oxford: Pergamon Press; 1979:pp. 331-350.
155. Kim J-G, Jang D. Mild and efficient indium metal catalyzed synthesis of sulfonamides and sulfonic esters. *Synlett*. 2007;2007(16):2501-2504.
156. Meshram GA, Patil VD. A simple and efficient method for sulfonylation of amines, alcohols and phenols with cupric oxide under mild conditions. *Tetrahedron Lett*. 2009;50(10):1117-1121.
157. Kang HH, Rho HS, Kim DH, Oh S-G. Metal oxide in aqueous organic solution promoted chemoselective *N*-sulfonylation of hydrophilic amino alcohols. *Tetrahedron Lett*. 2003;44(38):7225-7227.
158. Sridhar R, Srinivas B, Kumar VP, Narender M, Rao KR. β-Cyclodextrin-catalyzed monosulfonylation of amines and amino acids in water. *Adv Synth Catal*. 2007;349(11-12):1873-1876.

159. Massah A, Kazemi F, Azadi D, et al. A mild and chemoselective solvent-free method for the synthesis of *N*-aryl and *N*-alkylsulfonamides. *Lett Org Chem*. 2006;3(3):235-241.
160. Yasuhara A, Kameda M, Sakamoto T. Selective monodesulfonylation of *N,N*-disulfonylarylamines with tetrabutylammonium fluoride. *Chem Pharm Bull*. 1999;47(6):809-812.
161. Dhonthulachitty C, Kothakapu SR, Neella CK. An efficient practical tosylation of phenols, amines, and alcohols employing mild reagent [DMAPTs]+Cl−. *Tetrahedron Lett*. 2016;57(41):4620-4623.
162. Jones CS, Bull SD, Williams JM. DBN hexafluorophosphate salts as convenient sulfonylating and phosphonylating agents. *Org Biomol Chem*. 2016;14(36):8452-8456.
163. Wilden JD, Geldeard L, Lee CC, Judd DB, Caddick S. Trichlorophenol (TCP) sulfonate esters: A selective alternative to pentafluorophenol (PFP) esters and sulfonyl chlorides for the preparation of sulfonamides. *Chem Commun*. 2007;10:1074-1076.
164. Palakurthy NB, Mandal B. Sulfonamide synthesis using *N*-hydroxybenzotriazole sulfonate: an alternative to pentafluorophenyl (PFP) and trichlorophenyl (TCP) esters of sulfonic acids. *Tetrahedron Lett*. 2011;52(52):7132-7134.
165. Parumala SKR, Peddinti RK. Metal-free synthesis of sulfonamides via iodine-catalyzed oxidative coupling of sulfonyl hydrazides and amines. *Tetrahedron Lett*. 2016;57(11):1232-1235.
166. Suthagar K, Fairbanks AJ. A new way to do an old reaction: highly efficient reduction of organic azides by sodium iodide in the presence of acidic ion exchange resin. *Chem Commun*. 2017;53(4):713-715.
167. Blotny G. A new, mild preparation of sulfonyl chlorides. *Tetrahedron Lett*. 2003;44(7):1499-1501.
168. Tsunoda T, Yamamoto H, Goda K, Itô S. Mitsunobu-type alkylation of *p*-toluenesulfonamide. A convenient new route to primary and secondary amines. *Tetrahedron Lett*. 1996;37(14):2457-2458.
169. Wallach DR, Chisholm JD. Alkylation of sulfonamides with trichloroacetimidates under thermal conditions. *J Org Chem*. 2016;81(17):8035-8042.
170. Chan DMT, Monaco KL, Wang R-P, Winters MP. New *N*- and *O*-arylations with phenylboronic acids and cupric acetate. *Tetrahedron Lett*. 1998;39(19):2933-2936.
171. Yin J, Buchwald SL. Palladium-catalyzed intermolecular coupling of aryl halides and amides. *Org Lett*. 2000;2(8):1101-1104.
172. Burton G, Cao P, Li G, Rivero R. Palladium-catalyzed intermolecular coupling of aryl chlorides and sulfonamides under microwave irradiation. *Org Lett*. 2003;5(23):4373-4376.
173. Hamid MHSA, Allen CL, Lamb GW, et al. Ruthenium-catalyzed *N*-alkylation of amines and sulfonamides using borrowing hydrogen methodology. *J Am Chem Soc*. 2009;131(5):1766-1774.
174. Komeyama K, Morimoto T, Takaki K. A simple and efficient iron-catalyzed intramolecular hydroamination of unactivated olefins. *Angew Chem Int Ed*. 2006;45(18):2938-2941.
175. Huntress EH, Carten FH. Identification of organic compounds. I. Chlorosulfonic acid as a reagent for the identification of aryl halides. *J Am Chem Soc*. 1940;62(3):511-514.
176. Gonzalez MA, Gorman DB, Hamilton CT, Roth GA. Process development for the sulfonamide herbicide pyroxsulam. *Organ Process Res Dev*. 2008;12(2):301-303.
177. Bhattacharya SN, Eaborn C, Walton DRM. Preparation of arenesulphonyl chlorides from Grignard reagents. *J Chem Soc C: Organ*. 1968;0:1265-1267.
178. Májek M, Neumeier M, Jacobi von wangelin A. Aromatic chlorosulfonylation by photoredox catalysis. *ChemSusChem*. 2016;10(1):151-155.
179. Bahrami K, Khodaei MM, Abbasi J. Synthesis of sulfonamides and sulfonic esters via reaction of amines and phenols with thiols using H2O2–POCl3 system. *Tetrahedron*. 2012;68(25):5095-5101.
180. Fu L, Bao X, Li S, et al. Synthesis of sulfonamides from azoles and sodium sulfinates at ambient temperature. *Tetrahedron*. 2017;73(17):2504-2511.
181. Young JM, Lee AG, Chandrasekaran RY, Tucker JW. The synthesis of alkyl and (hetero)aryl sulfonamides from sulfamoyl inner salts. *J Org Chem*. 2015;80(16):8417-8423.
182. Chow SY, Stevens MY, Odell LR. Sulfonyl azides as precursors in ligand-free palladium-catalyzed synthesis of sulfonyl carbamates and sulfonyl ureas and synthesis of sulfonamides. *J Org Chem*. 2016;81(7):2681-2691.
183. Gareau Y, Pellicelli J, Laliberté S, Gauvreau D. Oxidation of aromatic and aliphatic triisopropylsilanylsulfanyls to sulfonyl chlorides: preparation of sulfonamides. *Tetrahedron Lett*. 2003;44(42):7821-7824.
184. Schwenkkraus P, Merkle S, Otto HH. Properties and reactions of substituted 1,2-thiazetidine 1,1-dioxides: 3-acetoxy-1,2-thiazetidine 1,1-dioxide, synthesis and reactions with C-nucleophiles. *Liebigs Ann*. 2006;1997(6):1261-1266.
185. Jiang Y, Wang Q-Q, Liang S, Hu L-M, Little RD, Zeng C-C. Electrochemical oxidative amination of sodium sulfinates: synthesis of sulfonamides mediated by NH4I as a redox catalyst. *J Org Chem*. 2016;81(11):4713-4719.
186. Greenbaum SB. Potential metabolic antagonists of orotic acid: 6-uracilsulfonamide and 6-uracil methyl sulfone1. *J Am Chem Soc*. 1954;76(23):6052-6054.

187. Ramasamy K, Imamura N, Hanna NB, et al. Synthesis and antitumor evaluation in mice of certain 7-deazapurine (pyrrolo[2,3-d]pyrimidine) and 3-deazapurine (imidazo[4,5-c]pyridine) nucleosides structurally related to sulfenosine, sulfinosine, and sulfonosine. *J Med Chem*. 1990;33(4):1220-1225.
188. Corey EJ, Chaykovsky M. Methylsulfinyl carbanion (CH3-SO-CH2-). Formation and applications to organic synthesis. *J Am Chem Soc*. 1965;87(6):1345-1353.
189. Frost CG, Hartley JP, Griffin D. Catalytic arylation of sulfamoyl chlorides: a practical synthesis of sulfonamides. *Synlett*. 2002;2002(11):1928-1930.
190. Carta F, Scozzafava A, Supuran CT. Sulfonamides: a patent review (2008 – 2012). *Expert Opin Ther Pat*. 2012;22 (7):747-758.
191. Scozzafava A, Carta F, Supuran CT. Secondary and tertiary sulfonamides: a patent review (2008–2012). *Expert Opin Ther Pat*. 2013;23(2):203-213.
192. Li Q, Sham HL. Discovery and development of antimitotic agents that inhibit tubulin polymerisation for the treatment of cancer. *Expert Opin Ther Pat*. 2002;12(11):1663-1702.
193. Liu Z, Zhou Z, Tian W, et al. Discovery of novel 2-*N*-aryl-substituted benzenesulfonamidoacetamides: orally bioavailable tubulin polymerization inhibitors with marked antitumor activities. *ChemMedChem*. 2012;7(4):680-693.
194. Salum LB, Mascarello A, Canevarolo RR, et al. *N*-(1′-naphthyl)-3,4,5-trimethoxybenzohydrazide as microtubule destabilizer: synthesis, cytotoxicity, inhibition of cell migration and in vivo activity against acute lymphoblastic leukemia. *Eur J Med Chem*. 2015;96:504-518.
195. Yoshino H, Ueda N, Sugumi H, et al., inventors; Eisai Co., Ltd., Japan, assignee. Preparation of *N*-[(2-arylamino)aryl] benzenesulfonamides as antitumor agents. US patent EP472053A21992.
196. Medina JC, Roche D, Shan B, et al. Novel halogenated sulfonamides inhibit the growth of multidrug resistant MCF-7/ ADR cancer cells. *Bioorgan Med Chem Lett*. 1999;9(13):1843-1846.
197. Medina JC, Shan B, Beckmann H, et al. Novel antineoplastic agents with efficacy against multidrug resistant tumor cells. *Bioorgan Med Chem Lett*. 1998;8(19):2653-2656.
198. Shan B, Medina JC, Santha E, et al. Selective, covalent modification of beta-tubulin residue Cys-239 by T138067, an antitumor agent with in vivo efficacy against multidrug-resistant tumors. *Proc Natl Acad Sci U S A*. 1999;96 (10):5686-5691.
199. https://clinicaltrials.gov/. 2018. Accessed 1 May, 2018.
200. Berlin JD, Venook A, Bergsland E, Rothenberg M, Lockhart AC, Rosen L. Phase II trial of T138067, a novel microtubule inhibitor, in patients with metastatic, refractory colorectal carcinoma. *Clin Colorectal Cancer*. 2008;7 (1):44-47.
201. Kirby S, Gertler SZ, Mason W, et al. Phase 2 study of T138067-sodium in patients with malignant glioma: trial of the National Cancer Institute of Canada Clinical Trials Group. *Neuro-Oncology*. 2005;7(2):183-188.
202. Michels J, Ellard SL, Le L, et al. A phase IB study of ABT-751 in combination with docetaxel in patients with advanced castration-resistant prostate cancer. *Ann Oncol*. ;21(2):305-311.
203. Ma T, Fuld AD, Rigas JR, et al. A phase I trial and in vitro studies combining ABT-751 with carboplatin in previously treated non-small cell lung cancer patients. *Chemotherapy*. 2012;58(4):321-329.
204. Fox E, Maris JM, Cohn SL, et al. Pharmacokinetics of orally administered ABT-751 in children with neuroblastoma and other solid tumors. *Cancer Chemother Pharmacol*. 2010;66(4):737-743.
205. Fox E, Maris JM, Widemann BC, et al. A phase I study of ABT-751, an orally bioavailable tubulin inhibitor, administered daily for 21 days every 28 days in pediatric patients with solid tumors. *Clin Cancer Res*. 2008;14 (4):1111-1115.
206. Hande KR, Hagey A, Berlin J, et al. The pharmacokinetics and safety of ABT-751, a novel, orally bioavailable sulfonamide antimitotic agent: results of a phase 1 study. *Clin Cancer Res*. 2006;12(9):2834-2840.
207. Fox E, Maris JM, Widemann BC, et al. A phase 1 study of ABT-751, an orally bioavailable tubulin inhibitor, administered daily for 7 days every 21 days in pediatric patients with solid tumors. *Clinical cancer research: an official journal of the American Association for Cancer Research*. 2006;12(16):4882-4887.
208. Rudin CM, Mauer A, Smakal M, et al. Phase I/II study of pemetrexed with or without ABT-751 in advanced or metastatic non-small-cell lung cancer. *J Clin Oncol*. 2011;29(8):1075-1082.
209. Ziegelbauer J, Shan B, Yager D, Larabell C, Hoffmann B, Tjian R. Transcription factor MIZ-1 is regulated via microtubule association. *Mol Cell*. 2001;8(2):339-349.
210. Rubenstein SM, Baichwal V, Beckmann H, et al. Hydrophilic, pro-drug analogues of T138067 are efficacious in controlling tumor growth in vivo and show a decreased ability to cross the blood brain barrier. *J Med Chem*. 2001;44 (22):3599-3605.
211. Hu L, Li Z, Jiang J, Boykin D. Novel diaryl or heterocyclic sulfonamides as antimitotic agents. *Anti Cancer Agents Med Chem*. 2008;8(7):739-745.
212. Fukuoka K, Usuda J, Iwamoto Y, et al. Mechanisms of action of the novel sulfonamide anticancer agent E7070 on cell cycle progression in human non-small cell lung cancer cells. *Invest New Drugs*. 2001;19(3):219-227.

213. Han T, Goralski M, Gaskill N, et al. Anticancer sulfonamides target splicing by inducing RBM39 degradation via recruitment to DCAF15. *Science*. 2017;356(6336):eaal3755.
214. Abbate F, Casini A, Owa T, Scozzafava A, Supuran CT. Carbonic anhydrase inhibitors: E7070, a sulfonamide anticancer agent, potently inhibits cytosolic isozymes I and II, and transmembrane, tumor-associated isozyme IX. *Bioorganic & medicinal chemistry letters*. 2004;14(1):217-223.
215. Ozawa Y, Sugi NH, Nagasu T, et al. E7070, a novel sulphonamide agent with potent antitumour activity in vitro and in vivo. *Eur J Cancer*. 2001;37(17):2275-2282.
216. Mohan R, Banerjee M, Ray A, et al. Antimitotic sulfonamides inhibit microtubule assembly dynamics and cancer cell proliferation. *Biochemistry*. 2006;45(17):5440-5449.
217. Owa T, Okauchi T, Yoshimatsu K, et al. A focused compound library of novel N-(7-indolyl)benzenesulfonamides for the discovery of potent cell cycle inhibitors. *Bioorganic & medicinal chemistry letters*. 2000;10(11):1223-1226.
218. Owa T, Yokoi A, Yamazaki K, Yoshimatsu K, Yamori T, Nagasu T. Array-based structure and gene expression relationship study of antitumor sulfonamides including N-[2-[(4-hydroxyphenyl)amino]-3-pyridinyl]-4-methoxybenzenesulfonamide and N-(3-chloro-7-indolyl)-1,4-benzenedisulfonamide. *J Med Chem*. 2002;45(22):4913-4922.
219. Yokoi A, Kuromitsu J, Kawai T, et al. Profiling novel sulfonamide antitumor agents with cell-based phenotypic screens and array-based gene expression analysis. *Mol Cancer Ther*. 2002;1(4):275-286.
220. Banerjee M, Poddar A, Mitra G, Surolia A, Owa T, Bhattacharyya B. Sulfonamide drugs binding to the colchicine site of tubulin: thermodynamic analysis of the drug-tubulin interactions by isothermal titration calorimetry. *J Med Chem*. 2005;48(2):547-555.
221. Abbassi N, Chicha H, Rakib EM, et al. Synthesis, antiproliferative and apoptotic activities of N-(6(4)-indazolyl)-benzenesulfonamide derivatives as potential anticancer agents. *Eur J Med Chem*. 2012;57:240-249.
222. Bouissane L, El Kazzouli S, Léonce S, et al. Synthesis and biological evaluation of N-(7-indazolyl)benzenesulfonamide derivatives as potent cell cycle inhibitors. *Bioorg Med Chem*. 2006;14(4):1078-1088.
223. Segreti JA, Brooks KA, Marsh KC, et al. Tumour-selective antivascular effects of the novel anti-mitotic compound A-318315: An in vivo rat regional haemodynamic study. *Clinical and experimental pharmacology & physiology*. 2010;37(5-6):636-640.
224. Aceves-Luquero C, Galiana-Roselló C, Ramis G, et al. N-(2-methyl-indol-1H-5-yl)-1-naphthalenesulfonamide: A novel reversible antimitotic agent inhibiting cancer cell motility. *Biochem Pharmacol*. 2016;115:28-42.
225. Patil SA, Patil R, Miller DD. Indole molecules as inhibitors of tubulin polymerization: potential new anticancer agents. *Future Med Chem*. 2012;4(16):2085-2115.
226. Hu L, Li ZR, Wang YM, Wu Y, Jiang JD, Boykin DW. Novel pyridinyl and pyrimidinylcarbazole sulfonamides as antiproliferative agents. *Bioorganic & medicinal chemistry letters*. 2007;17(5):1193-1196.
227. Abbassi N, Rakib EM, Chicha H, et al. Synthesis and antitumor activity of some substituted indazole derivatives. *Arch Pharm*. 2014;347(6):423-431.
228. Zhou J, Zhang Y, Cui YW, et al. Synthesis and cytotoxic evaluation of N-(4-methoxy-1H-benzo[d]imidazol-7-yl)-arylsulfonamide and N-aryl-(4-methoxy-1H-benzo[d]imidazol)-7-sulfonamide analogs of combretastatin A-4. *J Asian Nat Prod Res*. 2011;13(4):330-340.
229. Hu L, Li Z, Li Y, et al. Synthesis and structure-activity relationships of carbazole sulfonamides as a novel class of antimitotic agents against solid tumors. *J Med Chem*. 2006;49(21):6273-6282.
230. Wang YM, Hu LX, Liu ZM, et al. N-(2,6-dimethoxypyridine-3-yl)-9-methylcarbazole-3-sulfonamide as a novel tubulin ligand against human cancer. *Clinical cancer research: an official journal of the American Association for Cancer Research*. 2008;14(19):6218-6227.
231. Hu L, Jiang JD, Qu J, et al. Novel potent antimitotic heterocyclic ketones: synthesis, antiproliferative activity, and structure-activity relationships. *Bioorganic & medicinal chemistry letters*. 2007;17(13):3613-3617.
232. Chen J, Liu T, Wu R, et al. Design, synthesis, and biological evaluation of novel N-gamma-carboline arylsulfonamides as anticancer agents. *Bioorg Med Chem*. 2010;18(24):8478-8484.
233. Liu Z, Tian W, Wang Y, Kuang S, Luo X, Yu Q. A novel sulfonamide agent, MPSP-001, exhibits potent activity against human cancer cells in vitro through disruption of microtubule. *Acta Pharmacol Sin*. 2012;33(2):261-270.
234. Fortin S, Wei L, Moreau E, et al. Substituted phenyl 4-(2-oxoimidazolidin-1-yl)benzenesulfonamides as antimitotics. Antiproliferative, antiangiogenic and antitumoral activity, and quantitative structure-activity relationships. *Eur J Med Chem*. 2011;46(11):5327-5342.
235. Turcotte V, Fortin S, Vevey F, et al. Synthesis, biological evaluation, and structure-activity relationships of novel substituted N-phenyl ureidobenzenesulfonate derivatives blocking cell cycle progression in S-phase and inducing DNA double-strand breaks. *J Med Chem*. 2012;55(13):6194-6208.
236. Yang WS, Shimada K, Delva D, et al. Identification of Simple Compounds with Microtubule-Binding Activity That Inhibit Cancer Cell Growth with High Potency. *ACS Med Chem Lett*. 2012;3(1):35-38.
237. Yang J, Zhou S, Ji L, et al. Synthesis and structure-activity relationship of 4-azaheterocycle benzenesulfonamide derivatives as new microtubule-targeting agents. *Bioorganic & medicinal chemistry letters*. 2014;24(21):5055-5058.

238. Yang J, Yang S, Zhou S, et al. Synthesis, anti-cancer evaluation of benzenesulfonamide derivatives as potent tubulin-targeting agents. *Eur J Med Chem*. 2016;122:488-496.
239. Yoshino H, Ueda N, Niijima J, et al. Novel sulfonamides as potential, systemically active antitumor agents. *J Med Chem*. 1992;35(13):2496-2497.
240. Yoshino H, UedaHirovuki N, Niijima S, et al., Inventors; Eisai Co Ltd assignee. Sulfonamide phenyl substituted compounds. 1997.
241. Shoemaker RH. New approaches to antitumor drug screening: the human tumor colony-forming assay. *Cancer Treat Rep*. 1986;70:9-12.
242. Louie KG, Hamilton TC, Shoemaker RH, Young RC, Ozols RF. Evaluation of in vitro drug screening leads using experimental models of human ovarian cancer. *Invest New Drugs*. 1992;10(2):73-78.
243. Masters JRW, Jenkins WEA, Shoemaker RH. Screening of new anticancer agents in vitro using panels of human cell lines derived from non-seminomatous germ cell tumours and transitional cell carcinomas of the bladder. *Eur J Cancer*. 1992;28A(10):1617-1622.
244. Branda RF, Moore AL, McCormack JJ. Immunosuppressive properties of chloroquinoxaline sulfonamide. *Biochem Pharmacol*. 1989;38(20):3521-3526.
245. Branda RF, McCormack JJ, Perlmutter CA. Cellular pharmacology of chloroquinoxaline sulfonamide and a related compound in murine B16 melanoma cells. *Biochem Pharmacol*. 1988;37(23):4557-4564.
246. Yoshimatsu K, Yamaguchi A, Yoshino H, Koyanagi N, Kitoh K. Mechanism of action of E7010, an orally active sulfonamide antitumor agent: inhibition of mitosis by binding to the colchicine site of tubulin. *Cancer Res*. 1997;57 (15):3208-3213.
247. Iwamoto Y, Nishio K, Fukumoto H, Yoshimatsu K, Yamakido M, Saijo N. Preferential binding of E7010 to murine beta 3-tubulin and decreased beta 3-tubulin in E7010-resistant cell lines. *Japanese journal of cancer research: Gann*. 1998;89 (9):954-962.
248. Luo Y, Hradil VP, Frost DJ, et al. ABT-751, a novel tubulin-binding agent, decreases tumor perfusion and disrupts tumor vasculature. *Anticancer Drugs*. 2009;20(6):483-492.
249. Segreti J, Polakowski J, Koch K, et al. Tumor selective antivascular effects of the novel antimitotic compound ABT-751: an in vivo rat regional hemodynamic study. *Cancer Chemother Pharmacol*. 2004;54(3):273-281.
250. Wei RJ, Lin SS, Wu WR, et al. A microtubule inhibitor, ABT-751, induces autophagy and delays apoptosis in Huh-7 cells. *Toxicol Appl Pharmacol*. 2016;311:88-98.
251. Rudek MA, Dasari A, Laheru D, et al. Phase 1 Study of ABT-751 in Combination With CAPIRI (Capecitabine and Irinotecan) and Bevacizumab in Patients With Advanced Colorectal Cancer. *J Clin Pharmacol*. 2016;56(8):966-973.
252. Fox E, Mosse' YP, Meany HM, et al. Time to disease progression in children with relapsed or refractory neuroblastoma treated with ABT-751: a report from the Children's Oncology Group (ANBL0621). *Pediatr Blood Cancer*. 2014;61(6):990-996.
253. Gaynon PS, Harned TM, Therapeutic Advances in Childhood Leukemia/Lymphoma C. ABT-751 in relapsed childhood acute lymphoblastic leukemia. *J Pediatr Hematol Oncol*. 2012;34(7):583-584.
254. Meany HJ, Sackett DL, Maris JM, et al. Clinical outcome in children with recurrent neuroblastoma treated with ABT-751 and effect of ABT-751 on proliferation of neuroblastoma cell lines and on tubulin polymerization in vitro. *Pediatr Blood Cancer*. 2010;54(1):47-54.
255. Mauer AM, Cohen EEW, Ma PC, et al. A phase II study of ABT-751 in patients with advanced non-small cell lung cancer. *Journal of thoracic oncology: official publication of the International Association for the Study of Lung Cancer*. 2008;3(6):631-636.
256. Yee KW, Hagey A, Verstovsek S, et al. Phase 1 study of ABT-751, a novel microtubule inhibitor, in patients with refractory hematologic malignancies. *Clinical cancer research: an official journal of the American Association for Cancer Research*. 2005;11(18):6615-6624.
257. Yamamoto K, Noda K, Yoshimura A, Fukuoka M, Furuse K, Niitani H. Phase I study of E7010. *Cancer Chemother Pharmacol*. 1998;42(2):127-134.
258. Silver M, Rusk A, Phillips B, et al. Evaluation of the oral antimitotic agent (ABT-751) in dogs with lymphoma. *J Vet Intern Med*. 2012;26(2):349-354.
259. Huang HL, Chao MW, Li YC, et al. MPT0G066, a novel anti-mitotic drug, induces JNK-independent mitotic arrest, JNK-mediated apoptosis, and potentiates antineoplastic effect of cisplatin in ovarian cancer. *Sci Rep*. 2016;6:31664.
260. Lai MJ, Lee HY, Chuang HY, et al. N-Sulfonyl-aminobiaryls as Antitubulin Agents and Inhibitors of Signal Transducers and Activators of Transcription 3 (STAT3) Signaling. *J Med Chem*. 2015;58(16):6549-6558.
261. Huang HL, Chao MW, Chen CC, et al. LTP-1, a novel antimitotic agent and Stat3 inhibitor, inhibits human pancreatic carcinomas in vitro and in vivo. *Sci Rep*. 2016;6:27794.
262. Carew JS, Esquivel JA, 2nd, Espitia CM, et al. ELR510444 inhibits tumor growth and angiogenesis by abrogating HIF activity and disrupting microtubules in renal cell carcinoma. *PLOS One*. 2012;7(1):e31120.

263. Risinger AL, Westbrook CD, Encinas A, et al. ELR510444, a novel microtubule disruptor with multiple mechanisms of action. *J Pharmacol Exp Ther*. 2011;336(3):652-660.
264. DiMaio MA, Mikhailov A, Rieder CL, Von Hoff DD, Palazzo RE. The small organic compound HMN-176 delays satisfaction of the spindle assembly checkpoint by inhibiting centrosome-dependent microtubule nucleation. *Mol Cancer Ther*. 2009;8(3):592-601.
265. Medina-Gundrum L, Cerna C, Gomez L, Izbicka E. Investigation of HMN-176 anticancer activity in human tumor specimens in vitro and the effects of HMN-176 on differential gene expression. *Invest New Drugs*. 2005;23(1):3-9.
266. Takagi M, Honmura T, Watanabe S, et al. In vivo antitumor activity of a novel sulfonamide, HMN-214, against human tumor xenografts in mice and the spectrum of cytotoxicity of its active metabolite, HMN-176. *Invest New Drugs*. 2003;21(4):387-399.
267. Tanaka H, Ohshima N, Ikenoya M, Komori K, Katoh F, Hidaka H. HMN-176, an active metabolite of the synthetic antitumor agent HMN-214, restores chemosensitivity to multidrug-resistant cells by targeting the transcription factor NF-Y. *Cancer Res*. 2003;63(20):6942-6947.
268. Garland LL, Taylor C, Pilkington DL, Cohen JL, Von Hoff DD. A phase I pharmacokinetic study of HMN-214, a novel oral stilbene derivative with polo-like kinase-1-interacting properties, in patients with advanced solid tumors. *Clin Cancer Res*. 2006;12(17):5182-5189.
269. Gallet S, Flouquet N, Carato P, et al. Benzopyridooxathiazepine derivatives as novel potent antimitotic agents. *Bioorg Med Chem*. 2009;17(3):1132-1138.
270. Lebegue N, Gallet S, Flouquet N, et al. Novel benzopyridothiadiazepines as potential active antitumor agents. *J Med Chem*. 2005;48(23):7363-7373.
271. Segaoula Z, Leclercq J, Verones V, et al. Synthesis and biological evaluation of N-[2-(4-hydroxyphenylamino)-pyridin-3-yl]-4-methoxy-benzenesulfonamide (ABT-751) tricyclic analogues as antimitotic and antivascular agents with potent in vivo antitumor activity. *J Med Chem*. 2016;59(18):8422-8440.
272. Mehndiratta S, Chiang YF, Lai MJ, et al. Concise syntheses of 7-anilino-indoline-N-benzenesulfonamides as antimitotic and vascular disrupting agents. *Bioorg Med Chem*. 2014;22(17):4917-4923.
273. Lee HY, Pan SL, Su MC, et al. Furanylazaindoles: potent anticancer agents in vitro and in vivo. *J Med Chem*. 2013;56 (20):8008-8018.
274. Chang J-Y, Lai M-J, Chang Y-T, et al. Synthesis and biological evaluation of 7-arylindoline-1-benzenesulfonamides as a novel class of potent anticancer agents. *Med Chem Comm*. 2010;1(2):152-155.
275. Chang JY, Hsieh HP, Chang CY, et al. 7-Aroyl-aminoindoline-1-sulfonamides as a novel class of potent antitubulin agents. *J Med Chem*. 2006;49(23):6656-6659.
276. Zhou Q, Zhu J, Chen J, Ji P, Qiao C. N-Arylsulfonylsubstituted-1H indole derivatives as small molecule dual inhibitors of signal transducer and activator of transcription 3 (STAT3) and tubulin. *Bioorg Med Chem*. 2018;26(1):96-106.
277. Liou JP, Hsu KS, Kuo CC, Chang CY, Chang JY. A novel oral indoline-sulfonamide agent, N-[1-(4-methoxybenzenesulfonyl)-2,3-dihydro-1H-indol-7-yl]-isonicotinamide (J30), exhibits potent activity against human cancer cells in vitro and in vivo through the disruption of microtubule. *J Pharmacol Exp Ther*. 2007;323(1):398-405.
278. Tsai AC, Wang CY, Liou JP, et al. Orally active microtubule-targeting agent, MPT0B271, for the treatment of human non-small cell lung cancer, alone and in combination with erlotinib. *Cell Death Dis*. 2014;5:e1162.
279. Wang M, Gao M, Miller KD, Sledge GW, Hutchins GD, Zheng QH. Synthesis of new carbon-11-labeled 7-aroyl-aminoindoline-1-sulfonamides as potential PET agents for imaging of tubulin polymerization in cancers. *J Labelled Compd Radiopharm*. 2008;51(1):6-11.
280. Wu TY, Cho TY, Lu CK, Liou JP, Chen MC. Identification of 7-(4′-Cyanophenyl)indoline-1-benzenesulfonamide as a mitotic inhibitor to induce apoptotic cell death and inhibit autophagy in human colorectal cancer cells. *Sci Rep*. 2017;7 (1):017-12795.
281. Chiou CT, Chen GS, Chen ML, et al. Synthesis of anti-microtubule N-(2-Arylindol-7-yl)benzenesulfonamide derivatives and their antitumor mechanisms. *Chem Med Chem*. 2010;5(9):1489-1497.
282. Rakib EM, Oulemda B, Abouricha S, Bouissane L, Mouse HA, Zyad A. In Vitro Cytotoxicity Evaluation of Some Substituted Indazole Derivatives. *Lett Drug Des Discov*. 2007;4(7):467-470.
283. Alder EF, Wright WL, Soper QF. Control of seedling grasses in turf with diphenylacetonitrile and a substituted dinitroaniline. *In*: Proceedings 17th Nth. Cent. Weed Control Conf. 1960:23-24.
284. Morrissette N, Sept D Dinitroaniline Interactions with Tubulin: Genetic and Computational Approaches to Define the Mechanisms of Action and Resistance. In: Blume Y.B., Baird W.V., Yemets A.I., Breviario D. (eds), *The Plant Cytoskeleton: a Key Tool for Agro-Biotechnology. NATO Science for Peace and Security Series C: Environmental Security*. Dordrecht: Springer;2008.
285. Morgan RE, Werbovetz KA. Selective lead compounds against kinetoplastid tubulin. *Adv Exp Med Biol*. 2008;625:33-47.
286. Werbovetz K. Tubulin as an antiprotozoal drug target. *Mini Rev Med Chem*. 2002;2(6):519-529.

287. Lyons-Abbott S, Sackett DL, Wloga D, et al. Alpha-Tubulin mutations alter oryzalin affinity and microtubule assembly properties to confer dinitroaniline resistance. *Eukaryot Cell*. 2010;9(12):1825-1834.
288. Morrissette NS, Mitra A, Sept D, Sibley LD. Dinitroanilines bind α-tubulin to disrupt microtubules. *Mol Biol Cell*. 2004;15(4):1960-1968.
289. Traub-Cseko YM, Ramalho-Ortigão JM, Dantas AP, De Castro SL, Barbosa HS, Downing KH. Dinitroaniline herbicides against protozoan parasites: the case of Trypanosoma cruzi. *Trends Parasitol*. 2001;17(3):136-141.
290. Stokkermans TJW, Schwartzman JD, Keenan K, Morrissette NS, Tilney LG, Roos DS. Inhibition of toxoplasma gondii replication by dinitroaniline herbicides. *Exp Parasitol*. 1996;84(3):355-370.
291. Witschel M, Rottmann M, Kaiser M, Brun R. Agrochemicals against malaria, sleeping sickness, leishmaniasis, and Chagas disease. *PLOS Negl Trop Dis*. 2012;6(10):e1805.
292. Mitra A, Sept D. Binding and interaction of dinitroanilines with apicomplexan and kinetoplastid alpha-tubulin. *J Med Chem*. 2006;49(17):5226-5231.
293. Baranauskiene L, Matulis D. Herbicide oryzalin inhibits human carbonic anhydrases in vitro. *J Biochem Mol Toxicol*. 2017;31(6):e21894.
294. Godinho JLP, Georgikopoulou K, Calogeropoulou T, de Souza W, Rodrigues JCF. A novel alkyl phosphocholine-dinitroaniline hybrid molecule exhibits biological activity in vitro against Leishmania amazonensis. *Exp Parasitol*. 2013;135(1):153-165.
295. Goodarzi M, da Cunha EFF, Freitas MP, Ramalho TC. QSAR and docking studies of novel antileishmanial diaryl sulfides and sulfonamides. *Eur J Med Chem*. 2010;45(11):4879-4889.
296. Supuran CT. Carbonic anhydrases: novel therapeutic applications for inhibitors and activators. *Nat Rev Drug Discov*. 2008;7:168-181.
297. George TG, Endeshaw MM, Morgan RE, et al. Synthesis, biological evaluation, and molecular modeling of. *Bioorg Med Chem*. 2007;15(18):6071-6079.
298. Bhattacharya G, Salem MM, Werbovetz KA. Antileishmanial dinitroaniline sulfonamides with activity against parasite tubulin. *Bioorg Med Chem Lett*. 2002;12(17):2395-2398.
299. Fu DJ, Liu JF, Zhao RH, Li JH, Zhang SY, Zhang YB. Design and antiproliferative evaluation of novel sulfanilamide derivatives as potential tubulin polymerization inhibitors. *Molecules*. 2017;22(9):e1470.
300. Lee KC, Venkateswararao E, Sharma VK, Jung SH. Investigation of amino acid conjugates of (S)-1-[1-(4-aminobenzoyl)-2,3-dihydro-1H-indol-6-sulfonyl]-4-phenyl-imidazolidin- 2-one (DW2282) as water soluble anticancer prodrugs. *Eur J Med Chem*. 2014;80:439-446.
301. Kim S, Park JH, Koo SY, et al. Novel diarylsulfonylurea derivatives as potent antimitotic agents. *Bioorg Med Chem Lett*. 2004;14(24):6075-6078.
302. Lee CW, Hong DH, Han SB, et al. A novel stereo-selective sulfonylurea, 1-[1-(4-aminobenzoyl)-2,3-dihydro-1H-indol-6-sulfonyl]-4-phenyl-imidazolidin-2-on e, has antitumor efficacy in in vitro and in vivo tumor models. *Biochem Pharmacol*. 2002;64(3):473-480.
303. Piao W, Yoo J, Lee DK, Hwang HJ, Kim JH. Induction of G2/M phase arrest and apoptosis by a new synthetic anti-cancer agent, DW2282, in promyelocytic leukemia (HL-60) cells11Abbreviations: FBS, fetal bovine serum; PARP, poly (ADP-ribose) polymerase; and MTT, 3-(4,5-dimethylthiazol-2-yl)-2,5-diphenyltetrazolium bromide. *Biochem Pharmacol*. 2001;62(11):1439-1447.
304. Moon EY, Seong SK, Jung SH, et al. Antitumor activity of 4-phenyl-1-arylsulfonylimidazolidinone, DW2143. *Cancer Lett*. 1999;140(1-2):177-187.
305. Moon EY, Hwang HS, Choi CH, Jung SH, Yoon SJ. Effect of DW2282 on the induction of methemoglobinemia, hypoglycemia or WBC count and hematological changes. *Arch Pharmacal Res*. 1999;22(6):565-570.
306. Hwang HS, Moon EY, Seong SK, et al. Characterization of the anticancer activity of DW2282, a new anticancer agent. *Anticancer Res*. 1999;19(6B):5087-5093.
307. Wishart DS, Feunang YD, Guo AC, et al. DrugBank 5.0: a major update to the DrugBank database for 2018. *Nucleic Acids Res*. 2018;46(D1):D1074-D1082.
308. Li YH, Yu CY, Li XX, et al. Therapeutic target database update 2018: enriched resource for facilitating bench-to-clinic research of targeted therapeutics. *Nucleic Acids Res*. 2018;46(D1):D1121-D1127.
309. ChEMBL. Accessed 15/07/2018.
310. Chase DM, Chaplin DJ, Monk BJ. The development and use of vascular targeted therapy in ovarian cancer. *Gynecol Oncol*. 2017;145(2):393-406.
311. Mollinedo F, Gajate C. Microtubules, microtubule-interfering agents and apoptosis. *Apoptosis*. 2003;8(5):413-450.
312. Fürst R, Vollmar AM. A new perspective on old drugs: non-mitotic actions of tubulin-binding drugs play a major role in cancer treatment. *Pharmazie*. 2013;68(7):478-483.
313. Komlodi-Pasztor E, Sackett D, Wilkerson J, Fojo T. Mitosis is not a key target of microtubule agents in patient tumors. *Nat Rev Clin Oncol*. 2011;8(4):244-250.

314. Jane Iunt S, Akerman S, Hill SA, et al. Vascular effects dominate solid tumor response to treatment with combretastatin A-4-phosphate. *Int J Cancer*. 2011;129(8):1979-1989.
315. Chaplin DJ, Hill SA. The development of combretastatin A4 phosphate as a vascular targeting agent. *Int J Radiat Oncol*Biol*Phys*. 2002;54(5):1491-1496.
316. Blakey DC, Westwood FR, Walker M, et al. Antitumor activity of the novel vascular targeting agent ZD6126 in a panel of tumor models. *Clin Cancer Res*. 2002;8(6):1974-1983.
317. Otani M, Natsume T, Watanabe J, et al. TZT-1027, an antimicrotubule agent, attacks tumor vasculature and induces tumor cell death. *Jpn J Cancer Res*. 2000;91(8):837-844.
318. Tozer GM, Prise VE, Wilson J, et al. Combretastatin A-4 phosphate as a tumor vascular-targeting agent: early effects in tumors and normal tissues. *Cancer Res*. 1999;59(7):1626-1634.
319. Chaplin DJ, Pettit GR, Hill SA. Anti-vascular approaches to solid tumour therapy: evaluation of combretastatin A4 phosphate. *Anticancer Res*. 1999;19(1A):189-195.
320. Dark GG, Hill SA, Prise VE, Tozer GM, Pettit GR, Chaplin DJ. Combretastatin A-4, an agent that displays potent and selective toxicity toward tumor vasculature. *Cancer Res*. 1997;57(10):1829-1834.
321. Kanthou C, Tozer GM. Tumour targeting by microtubule-depolymerizing vascular disrupting agents. *Expert Opin Ther Targets*. 2007;11(11):1443-1457.
322. Tozer GM, Kanthou C, Baguley BC. Disrupting tumour blood vessels. *Nat Rev Cancer*. 2005;5(6):423-435.
323. Porcù E, Viola G, Bortolozzi R, et al. TR-644 a novel potent tubulin binding agent induces impairment of endothelial cells function and inhibits angiogenesis. *Angiogenesis*. 2013;16(3):647-662.
324. Pasquier E, Honore S, Braguer D. Microtubule-targeting agents in angiogenesis: where do we stand?. *Drug Resist Updat*. 2006;9(1-2):74-86.
325. Ahmed B, Van Eijk LI, Bouma-Ter Steege JCA, et al. Vascular targeting effect of combretastatin A-4 phosphate dominates the inherent angiogenesis inhibitory activity. *Int J Cancer*. 2003;105(1):20-25.
326. Samarin J, Rehm M, Krueger B, Waschke J, Goppelt-Struebe M. Up-regulation of connective tissue growth factor in endothelial cells by the microtubule-destabilizing agent combretastatin A-4. *Molecular cancer research: MCR*. 2009;7 (2):180-188.
327. Pollock JK, Verma NK, O'boyle NM, Carr M, Meegan MJ, Zisterer DM. Combretastatin (CA)-4 and its novel analogue CA-432 impair T-cell migration through the Rho/ROCK signalling pathway. *Biochem Pharmacol*. 2014;92(4):544-557.
328. Shen CH, Shee JJ, Wu JY, Lin YW, Wu JD, Liu YW. Combretastatin A-4 inhibits cell growth and metastasis in bladder cancer cells and retards tumour growth in a murine orthotopic bladder tumour model. *Br J Pharmacol*. 2010;160 (8):2008-2027.
329. Rothmeier AS, Ischenko I, Joore J, et al. Investigation of the marine compound spongistatin 1 links the inhibition of PKCalpha translocation to nonmitotic effects of tubulin antagonism in angiogenesis. *FASEB J*. 2009;23(4):1127-1137.
330. Bijman MN, van Nieuw Amerongen GP, Victor NL, van Hinsbergh WM, Boven VW, E. Microtubule-targeting agents inhibit angiogenesis at subtoxic concentrations, a process associated with inhibition of Rac1 and Cdc42 activity and changes in the endothelial cytoskeleton. *Mol Cancer Ther*. 2006;5(9):2348-2357.
331. Murtagh J, Lu H, Schwartz EL. Taxotere-induced inhibition of human endothelial cell migration is a result of heat shock protein 90 degradation. *Cancer Res*. 2006;66(16):8192-8199.
332. Herrmann J, Elnakady YA, Wiedmann RM, et al. Pretubulysin: from hypothetical biosynthetic intermediate to potential lead in tumor therapy. *PLOS One*. 2012;7(5):17.
333. Lin HL, Chiou SH, Wu CW, et al. Combretastatin A4-induced differential cytotoxicity and reduced metastatic ability by inhibition of AKT function in human gastric cancer cells. *J Pharmacol Exp Ther*. 2007;323(1):365-373.
334. Schnaeker EM, Ossig R, Ludwig T, et al. Microtubule-dependent matrix metalloproteinase-2/matrix metalloproteinase-9 exocytosis: prerequisite in human melanoma cell invasion. *Cancer Res*. 2004;64(24):8924-8931.
335. Kanthou C, Greco O, Stratford A, et al. The tubulin-binding agent combretastatin A-4-phosphate arrests endothelial cells. *Am J Pathol*. 2004;165(4):1401-1411.
336. Castedo M, Perfettini JL, Roumier T, Andreau K, Medema R, Kroemer G. Cell death by mitotic catastrophe: a molecular definition. *Oncogene*. 2004;23(16):2825-2837.
337. Brito DA, Rieder CL. Mitotic checkpoint slippage in humans occurs via cyclin B destruction in the presence of an active checkpoint. *Current biology: CB*. 2006;16(12):1194-1200.
338. Rieder CL, Maiato H. Stuck in division or passing through: what happens when cells cannot satisfy the spindle assembly checkpoint. *Dev Cell*. 2004;7(5):637-651.
339. Losada A. Cohesin in cancer: chromosome segregation and beyond. *Nat Rev Cancer*. 2014;14(6):389-393.
340. Nasmyth K, Haering CH. Cohesin: its roles and mechanisms. *Annu Rev Genet*. 2009;43:525-558.
341. Santaguida S, Musacchio A. The life and miracles of kinetochores. *EMBO J*. 2009;28(17):2511-2531.
342. Cheeseman IM, Desai A. Molecular architecture of the kinetochore-microtubule interface. *Nat Rev Mol Cell Biol*. 2008;9(1):33-46.

343. Rieder CL, Cole RW, Khodjakov A, Sluder G. The checkpoint delaying anaphase in response to chromosome monoorientation is mediated by an inhibitory signal produced by unattached kinetochores. *J Cell Biol*. 1995;130 (4):941-948.
344. Musacchio A. The molecular biology of spindle assembly checkpoint signaling dynamics. *Curr biol*. 2015;25(20): R1002-R1018.
345. Giannotta M, Trani M, Dejana E. VE-cadherin and endothelial adherens junctions: active guardians of vascular integrity. *Dev Cell*. 2013;26(5):441-454.
346. Lara-Gonzalez P, Westhorpe FG, Taylor SS. The spindle assembly checkpoint. *Curr Biol*. 2012;22(22):R966-R980.
347. Millán J, Cain RJ, Reglero-Real N, et al. Adherens junctions connect stress fibres between adjacent endothelial cells. *BMC Biol*. 2010;8(11):1741-7007.
348. Varetti G, Musacchio A. The spindle assembly checkpoint. *Curr Biology*. 2008;18(14):R591-R595.
349. Musacchio A, Salmon ED. The spindle-assembly checkpoint in space and time. *Nat Rev Mol Cell Biol*. 2007;8 (5):379-393.
350. Pines J, Clute P. Temporal and spatial control of cyclin B1 destruction in metaphase. *Nat Cell Biol*. 1999;1(2):82-87.
351. Matson DR, Stukenberg PT. Spindle poisons and cell fate: a tale of two pathways. *Mol Interv*. 2011;11(2):141-150.
352. Sudakin V, Chan GKT, Yen TJ. Checkpoint inhibition of the APC/C in HeLa cells is mediated by a complex of BUBR1, BUB3, CDC20, and MAD2. *J Cell Biol*. 2001;154(5):925-936.
353. Chang L, Zhang Z, Yang J, McLaughlin SH, Barford D. Molecular architecture and mechanism of the anaphase-promoting complex. *Nature*. 2014;513(7518):388-393.
354. Kruse T, Larsen MSY, Sedgwick GG, et al. A direct role of Mad1 in the spindle assembly checkpoint beyond Mad2 kinetochore recruitment. *EMBO Rep*. 2014;15(3):282-290.
355. Primorac I, Musacchio A. Panta rhei: the APC/C at steady state. *J Cell Biol*. 2013;201(2):177-189.
356. Pines J. Cubism and the cell cycle: the many faces of the APC/C. *Nat Rev Mol Cell Biol*. 2011;12(7):427-438.
357. Yu H. Structural activation of Mad2 in the mitotic spindle checkpoint: the two-state Mad2 model versus the Mad2 template model. *J Cell Biol*. 2006;173(2):153-157.
358. Peters JM. The anaphase promoting complex/cyclosome: a machine designed to destroy. *Nat Rev Mol Cell Biol*. 2006;7 (9):644-656.
359. Acquaviva C, Pines J. The anaphase-promoting complex/cyclosome: APC/C. *J Cell Sci*. 2006;119(Pt 12):2401-2404.
360. Alfieri C, Chang L, Zhang Z, et al. Molecular basis of APC/C regulation by the spindle assembly checkpoint. *Nature*. 2016;536(7617):431-436.
361. Herzog F, Primorac I, Dube P, et al. Structure of the anaphase-promoting complex/cyclosome interacting with a mitotic checkpoint complex. *Science*. 2009;323(5920):1477-1481.
362. Nasmyth K, Peters JM, Uhlmann F. Splitting the chromosome: cutting the ties that bind sister chromatids. *Science*. 2000;288(5470):1379-1385.
363. Clarke PR, Allan LA. Cell-cycle control in the face of damage--a matter of life or death. *Trends Cell Biol*. 2009;19 (3):89-98.
364. Hornig NCD, Knowles PP, McDonald NQ, Uhlmann F. The dual mechanism of separase regulation by securin. *Current biology: CB*. 2002;12(12):973-982.
365. Zimmermann KC, Green DR. How cells die: apoptosis pathways. *J Allergy Clin Immunol*. 2001;108(4 Suppl):S99-S103.
366. Xiong S, Mu T, Wang G, Jiang X. Mitochondria-mediated apoptosis in mammals. *Protein & cell*. 2014;5(10):737-749.
367. Youle RJ, Strasser A. The BCL-2 protein family: opposing activities that mediate cell death. *Nat Rev Mol Cell Biol*. 2008;9(1):47-59.
368. Jiang X, Wang X. Cytochrome C-mediated apoptosis. *Annu Rev Biochem*. 2004;73:87-106.
369. Hardwick JM, Soane L. Multiple functions of BCL-2 family proteins. *Cold Spring Harbor Perspect Biol*. 2013;5(2): a008722-a008722.
370. Rolland SG, Conradt B. New role of the BCL2 family of proteins in the regulation of mitochondrial dynamics. *Curr Opin Cell Biol*. 2010;22(6):852-858.
371. Akgul C. Mcl-1 is a potential therapeutic target in multiple types of cancer. *Cellular and molecular life sciences: CMLS*. 2009;66(8):1326-1336.
372. Haldar S, Basu A, Croce CM. Bcl2 is the guardian of microtubule integrity. *Cancer Res*. 1997;57(2):229-233.
373. Zhou L, Cai X, Han X, Xu N, Chang DC. CDK1 switches mitotic arrest to apoptosis by phosphorylating Bcl-2/Bax family proteins during treatment with microtubule interfering agents. *Cell Biol Int*. 2014;38(6):737-746.
374. Sakurikar N, Eichhorn JM, Chambers TC. Cyclin-dependent kinase-1 (Cdk1)/cyclin B1 dictates cell fate after mitotic arrest via phosphoregulation of antiapoptotic Bcl-2 proteins. *J Biol Chem*. 2012;287(46):39193-39204.
375. Chu R, Terrano DT, Chambers TC. Cdk1/cyclin B plays a key role in mitotic arrest-induced apoptosis by phosphorylation of Mcl-1, promoting its degradation and freeing Bak from sequestration. *Biochem Pharmacol*. 2012;83(2):199-206.

376. Terrano DT, Upreti M, Chambers TC. Cyclin-dependent kinase 1-mediated Bcl-xL/Bcl-2 phosphorylation acts as a functional link coupling mitotic arrest and apoptosis. *Mol Cell Biol*. 2010;30(3):640-656.
377. Thomas LW, Lam C, Edwards SW. Mcl-1; the molecular regulation of protein function. *FEBS Lett*. 2010;584 (14):2981-2989.
378. Michels J, Johnson PW, Packham G. Mcl-1. *Int J Biochem Cell Biol*. 2005;37(2):267-271.
379. Berndtsson M, Konishi Y, Bonni A, et al. Phosphorylation of BAD at Ser-128 during mitosis and paclitaxel-induced apoptosis. *FEBS Lett*. 2005;579(14):3090-3094.
380. Basu A, Haldar S. Identification of a novel Bcl-xL phosphorylation site regulating the sensitivity of taxol- or 2-methoxyestradiol-induced apoptosis. *FEBS Lett*. 2003;538(1-3):41-47.
381. Westermann S, Avila-Sakar A, Wang HW, et al. Formation of a dynamic kinetochore- microtubule interface through assembly of the Dam1 ring complex. *Mol Cell*. 2005;17(2):277-290.
382. Yang E, Zha J, Jockel J, Boise LH, Thompson CB, Korsmeyer SJ. Bad, a heterodimeric partner for Bcl-XL and Bcl-2, displaces Bax and promotes cell death. *Cell*. 1995;80(2):285-291.
383. Cheng EHYA, Wei MC, Weiler S, et al. BCL-2, BCL-X(L) sequester BH3 domain-only molecules preventing BAX- and BAK-mediated mitochondrial apoptosis. *Mol Cell*. 2001;8(3):705-711.
384. Kim R. Unknotting the roles of Bcl-2 and Bcl-xL in cell death. *Biochem Biophys Res Commun*. 2005;333(2):336-343.
385. Harley ME, Allan LA, Sanderson HS, Clarke PR. Phosphorylation of Mcl-1 by CDK1-cyclin B1 initiates its Cdc20-dependent destruction during mitotic arrest. *EMBO J*. 2010;29(14):2407-2420.
386. Ito T, Deng X, Carr B, May WS. Bcl-2 phosphorylation required for anti-apoptosis function. *J Biol Chem*. 1997;272 (18):11671-11673.
387. Wertz IE, Kusam S, Lam C, et al. Sensitivity to antitubulin chemotherapeutics is regulated by MCL1 and FBW7. *Nature*. 2011;471(7336):110-114.
388. Sloss O, Topham C, Diez M, Taylor S. Mcl-1 dynamics influence mitotic slippage and death in mitosis. *Oncotarget*. 2016;7(5):5176-5192.
389. Upreti M, Chu R, Galitovskaya E, Smart SK, Chambers TC. Key role for Bak activation and Bak-Bax interaction in the apoptotic response to vinblastine. *Mol Cancer Ther*. 2008;7(7):2224-2232.
390. Galán-Malo P, Vela L, Gonzalo O, et al. Cell fate after mitotic arrest in different tumor cells is determined by the balance between slippage and apoptotic threshold. *Toxicol Appl Pharmacol*. 2012;258(3):384-393.
391. Topham CH, Taylor SS. Mitosis and apoptosis: how is the balance set?. *Curr Opin Cell Biol*. 2013;25(6):780-785.
392. Cheng B, Crasta K. Consequences of mitotic slippage for antimicrotubule drug therapy. *Endocr Relat Cancer*. 2017;24 (9):T97-T106.
393. Dulaney C, Marcrom S, Stanley J, Yang ES. Poly(ADP-ribose) polymerase activity and inhibition in cancer. *Semin Cell Dev Biol*. 2017;63:144-153.
394. Hahnfeldt P, Panigrahy D, Folkman J, Hlatky L. Tumor development under angiogenic signaling: a dynamical theory of tumor growth, treatment response, and postvascular dormancy. *Cancer Res*. 1999;59(19):4770-4775.
395. Folkman J. How is blood vessel growth regulated in normal and neoplastic tissue? G.H.A. Clowes memorial Award lecture. *Cancer Res*. 1986;46(2):467-473.
396. Denekamp J. Review article: angiogenesis, neovascular proliferation and vascular pathophysiology as targets for cancer therapy. *Br J Radiol*. 1993;66(783):181-196.
397. Folkman J. What is the evidence that tumors are angiogenesis dependent?. *J Natl Cancer Inst*. 1990;82(1):4-6. FAU - Folkman, J
398. Close A. Antiangiogenesis and vascular disrupting agents in cancer: circumventing resistance and augmenting their therapeutic utility. *Future Med Chem*. 2016;8(4):443-462.
399. Potente M, Gerhardt H, Carmeliet P. Basic and therapeutic aspects of angiogenesis. *Cell*. 2011;146(6):873-887.
400. Kanthou C, Tozer GM. Selective destruction of the tumour vasculature by targeting the endothelial cytoskeleton. *Drug Discovery Today: Therapeutic Strategies*. 2007;4(4):237-243.
401. Marme D. The impact of anti-angiogenic agents on cancer therapy. *J Cancer Res Clin Oncol*. 2003;129(11):607-620.
402. Vasudev NS, Reynolds AR. Anti-angiogenic therapy for cancer: current progress, unresolved questions and future directions. *Angiogenesis*. 2014;17(3):471-494.
403. Ferrara N, Kerbel RS. Angiogenesis as a therapeutic target. *Nature*. 2005;438(7070):967-974.
404. Thorpe PE. Vascular targeting agents as cancer therapeutics. *Clinical cancer research: an official journal of the American Association for Cancer Research*. 2004;10(2):415-427.
405. Siemann DW, Bibby MC, Dark GG, et al. Differentiation and definition of vascular-targeted therapies. *Clinical cancer research: an official journal of the American Association for Cancer Research*. 2005;11(2 Pt 1):416-420.
406. Kanthou C, Tozer GM. The tumor vascular targeting agent combretastatin A-4-phosphate induces reorganization of the actin cytoskeleton and early membrane blebbing in human endothelial cells. *Blood*. 2002;99(6):2060-2069.
407. Folkman J. Seminars in Medicine of the Beth Israel Hospital, Boston. Clinical applications of research on angiogenesis. *N Engl J Med*. 1995;333(26):1757-1763.

408. Shi W, Siemann DW. Preclinical studies of the novel vascular disrupting agent MN-029. *Anticancer Res*. 2005;25 (6B):3899-3904.
409. Kim TJ, Ravoori M, Landen CN, et al. Antitumor and antivascular effects of AVE8062 in ovarian carcinoma. *Cancer Res*. 2007;67(19):9337-9345.
410. Cai W, Rao J, Fau - Gambhir SS, Gambhir Ss, Fau - Chen X, Chen X. How molecular imaging is speeding up antiangiogenic drug development. *Mol Cancer Ther*. 2006;5(11):2624-2633.
411. Siemann DW. The unique characteristics of tumor vasculature and preclinical evidence for its selective disruption by Tumor-Vascular Disrupting Agents. *Cancer Treat Rev*. 2011;37(1):63-74.
412. Tozer GM, Akerman S, Cross NA, et al. Blood vessel maturation and response to vascular-disrupting therapy in single vascular endothelial growth factor-A isoform-producing tumors. *Cancer Res*. 2008;68(7):2301-2311.
413. Denekamp J. Endothelial cell proliferation as a novel approach to targeting tumour therapy. *Br J Cancer*. 1982;45 (1):136-139. FAU - Denekamp, J
414. Dvorak HF, Nagy JA, Dvorak JT, Dvorak AM. Identification and characterization of the blood vessels of solid tumors that are leaky to circulating macromolecules. *Am J Pathol*. 1988;133(1):95-109.
415. Siemann DW, Horsman MR. Modulation of the tumor vasculature and oxygenation to improve therapy. *Pharmacol Ther*. 2015;153:107-124.
416. Prise V, Honess D, Stratford M, Wilson J, Tozer G. The vascular response of tumor and normal tissues in the rat to the vascular targeting agent, combretastatin A-4-phosphate, at clinically relevant doses. *Int J Oncol*. 2002;21(4):717-726.
417. Konerding MA, Fait E, Gaumann A. 3D microvascular architecture of pre-cancerous lesions and invasive carcinomas of the colon. *Br J Cancer*. 2001;84(10):1354-1362.
418. McDonald DM, Choyke PL. Imaging of angiogenesis: from microscope to clinic. *Nature Med*. 2003;9(6):713-725.
419. Eberhard A, Kahlert S, Goede V, Hemmerlein B, Plate KH, Augustin HG. Heterogeneity of angiogenesis and blood vessel maturation in human tumors: implications for antiangiogenic tumor therapies. *Cancer Res*. 2000;60 (5):1388-1393.
420. Baluk P, Hashizume H, Mcdonald DM. Cellular abnormalities of blood vessels as targets in cancer. *Curr Opin Genet Dev*. 2005;15(1):102-111.
421. Hashizume H, Baluk P, Morikawa S, et al. Openings between defective endothelial cells explain tumor vessel leakiness. *Am J Pathol*. 2000;156(4):1363-1380.
422. Vincent L, Kermani P, Young LM, et al. Combretastatin A4 phosphate induces rapid regression of tumor neovessels and growth through interference with vascular endothelial-cadherin signaling. *J Clin Invest*. 2005;115(11):2992-3006.
423. Bayless KJ, Davis GE. Microtubule depolymerization rapidly collapses capillary tube networks in vitro and angiogenic vessels in vivo through the small GTPase Rho. *J Biol Chem*. 2004;279(12):11686-11695.
424. Tozer GM, Kanthou C, Parkins CS, Hill SA. The biology of the combretastatins as tumour vascular targeting agents. *Int J Exp Pathol*. 2002;83(1):21-38.
425. Galbraith SM, Chaplin DJ, Lee F, et al. Effects of combretastatin A4 phosphate on endothelial cell morphology in vitro and relationship to tumour vascular targeting activity in vivo. *Anticancer Res*. 2001;21(1A):93-102.
426. Ding X, Zhang Z, Li S, Wang A. Combretastatin A4 phosphate induces programmed cell death in vascular endothelial cells. *Oncol Res*. 2011;19(7):303-309.
427. Williams LJ, Mukherjee D, Fisher M, et al. An in vivo role for Rho kinase activation in the tumour vascular disrupting activity of combretastatin A-4 3-O-phosphate. *Br J Pharmacol*. 2014;171(21):4902-4913.
428. Tozer GM, Prise VE, Wilson J, et al. Mechanisms associated with tumor vascular shut-down induced by combretastatin A-4 phosphate: intravital microscopy and measurement of vascular permeability. *Cancer Res*. 2001;61(17):6413-6422.
429. Kanthou C, Tozer GM. Microtubule depolymerizing vascular disrupting agents: novel therapeutic agents for oncology and other pathologies. *Int J Exp Pathol*. 2009;90(3):284-294.
430. Wojciak-Stothard B, Tsang LYF, Haworth SG. Rac and Rho play opposing roles in the regulation of hypoxia/ reoxygenation-induced permeability changes in pulmonary artery endothelial cells. *Am J Physiol: Lung Cell Mol Physiol*. 2005;288(4):L749-L760.
431. Vaupel P, Hockel M. Blood supply, oxygenation status and metabolic micromilieu of breast cancers: characterization and therapeutic relevance. *Int J Oncol*. 2000;17(5):869-879.
432. Heath VL, Bicknell R. Anticancer strategies involving the vasculature. *Nat Rev Clin Oncol*. 2009;6(7):395-404.
433. Horsman MR, Siemann DW. Pathophysiologic effects of vascular-targeting agents and the implications for combination with conventional therapies. *Cancer Res*. 2006;66(24):11520-11539.
434. Rojiani AM, Li L, Rise L, Siemann DW. Activity of the vascular targeting agent combretastatin A-4 disodium phosphate in a xenograft model of AIDS-associated Kaposi's sarcoma. *Acta Oncol*. 2002;41(1):98-105.
435. Pérez-Pérez MJ, Priego EM, Bueno O, Martins MS, Canela MD, Liekens S. Blocking Blood Flow to Solid Tumors by Destabilizing Tubulin: An Approach to Targeting Tumor Growth. *J Med Chem*. 2016;59(19):8685-8711.

436. Cesca M, Bizzaro F, Zucchetti M, Giavazzi R. Tumor delivery of chemotherapy combined with inhibitors of angiogenesis and vascular targeting agents. *Front Oncol*. 2013;3:259.
437. Amano M, Ito M, Kimura K, et al. Phosphorylation and activation of myosin by Rho-associated kinase (Rho-kinase). *J Biol Chem*. 1996;271(34):20246-20249.
438. Verin AD, Birukova A, Wang P, et al. Microtubule disassembly increases endothelial cell barrier dysfunction: role of MLC phosphorylation. *Am J Physiol: Lung Cell Mol Physiol*. 2001;281(3):L565-L574.
439. Ridley AJ. Rho GTPase signalling in cell migration. *Curr Opin Cell Biol*. 2015;36:103-112. LID - 110.1016/j.ceb.2015.1008.1005 [doi] LID - S0955-0674(1015)00110-00116 [pii]
440. Hori K, Saito S. Microvascular mechanisms by which the combretastatin A-4 derivative AC7700 (AVE8062) induces tumour blood flow stasis. *Br J Cancer*. 2003;89(7):1334-1344.
441. Griggs J, Metcalfe JC, Hesketh R. Targeting tumour vasculature: the development of combretastatin A4. *Lancet Oncol*. 2001;2(2):82-87.
442. Zhao X, Guan JL. Focal adhesion kinase and its signaling pathways in cell migration and angiogenesis. *Adv Drug Deliv Rev*. 2011;63(8):610-615.
443. Houle F, Huot J. Dysregulation of the endothelial cellular response to oxidative stress in cancer. *Mol Carcinog*. 2006;45(6):362-367.
444. Nelson CM, Pirone DM, Tan JL, Chen CS. Vascular endothelial-cadherin regulates cytoskeletal tension, cell spreading, and focal adhesions by stimulating RhoA. *Mol Biol Cell*. 2004;15(6):2943-2953.
445. Wojciak-Stothard B, Ridley AJ. Rho GTPases and the regulation of endothelial permeability. *Vascul Pharmacol*. 2002;39(4-5):187-199.
446. Vaupel P, Fortmeyer HP, Runkel S, Kallinowski F. Blood flow, oxygen consumption, and tissue oxygenation of human breast cancer xenografts in nude rats. *Cancer Res*. 1987;47(13):3496-3503.
447. Reyes-Aldasoro CC, Wilson I, Prise VE, et al. Estimation of apparent tumor vascular permeability from multiphoton fluorescence. *Microcirculation*. 2008;15(1):65-79.
448. Baluk P, Morikawa S, Haskell A, Mancuso M, McDonald DM. Abnormalities of basement membrane on blood vessels and endothelial sprouts in tumors. *Am J Pathol*. 2003;163(5):1801-1815.
449. Ley CD, Horsman MR, Kristjansen PEG. Early effects of combretastatin-A4 disodium phosphate on tumor perfusion and interstitial fluid pressure. *Neoplasia*. 2007;9(2):108-112.
450. Milosevic MF, Fyles AW, Hill RP. The relationship between elevated interstitial fluid pressure and blood flow in. *Int J Radiat Oncol Biol Phys*. 1999;43(5):1111-1123.
451. Lominadze D, McHedlishvili G. Red blood cell behavior at low flow rate in microvessels. *Microvasc Res*. 1999;58(2):187-189.

How to cite this article: Vicente-Blázquez A, González M, Álvarez R, del Mazo S, Medarde M and Peláez R. Antitubulin sulfonamides: The successful combination of an established drug class and a multifaceted target. *Med Res Rev*. 2018;1-56. https://doi.org/10.1002/med.21541

anexo 2

Anexo metodológico al artículo 3: "The Sulfonamide Library".

Anexo 2.a. Chemical structure of the designed and synthesized sulfonamide library.

Anexo 2.b. Chemical synthesis of the sulfonamide library.

Anexo 2.c. Biological evaluation of the synthesized sulfonamide library.

Anexo digital 2.d. ^{1}H and ^{13}C NMR spectra of the synthesized sulfonamide library.

Anexo 2.a. Chemical structure of the designed and synthesized sulfonamide library.

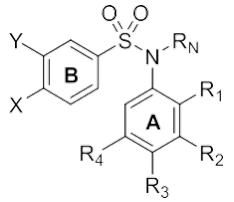

								Artículos invest.	
Y	**X**	**R_N**	**R_1**	**R_2**	**R_3**	**R_4**	**Nº Comp.**	**Nº Art.**	**Nº Comp.**
H	OCH_3	H	H	OCH_3	OCH_3	OCH_3	**1a**	1	**1a**
H	OCH_3	SO_2-4-OCH_3Ph	H	OCH_3	OCH_3	OCH_3	**1b**	1	**1b**
H	OCH_3	CH_3	H	OCH_3	OCH_3	OCH_3	**2a**	1	**2a**
H	OCH_3	CH_2-Dim	H	OCH_3	OCH_3	OCH_3	**2b**	1	**2b**
H	OCH_3	Et	H	OCH_3	OCH_3	OCH_3	**3**	1	**3**
H	OCH_3	EtBr	H	OCH_3	OCH_3	OCH_3	**4**	1	**4**
H	OCH_3	Ac	H	OCH_3	OCH_3	OCH_3	**5**	1	**5**
H	OCH_3	CH_2CN	H	OCH_3	OCH_3	OCH_3	**6**	1	**6**
H	OCH_3	CH_2COOEt	H	OCH_3	OCH_3	OCH_3	**7**	1	**7**
H	OCH_3	CH_2COOH	H	OCH_3	OCH_3	OCH_3	**8**	1	**8**
H	OCH_3	Benzyl	H	OCH_3	OCH_3	OCH_3	**9**	1	**9**
H	OCH_3	COOBenzyl	H	OCH_3	OCH_3	OCH_3	**10**	1	**10**
H	OCH_3	H	NO_2	OCH_3	OCH_3	OCH_3	**11**	1	**11**
H	OCH_3	H	NH_2	OCH_3	OCH_3	OCH_3	**12**	1	**12**
H	OCH_3	CH_3	NH_2	OCH_3	OCH_3	OCH_3	**13**	1	**13**
H	OCH_3	CH_2-Dim	NH_2	OCH_3	OCH_3	OCH_3	**14**	1	**14**
H	OCH_3	H	NHAc	OCH_3	OCH_3	OCH_3	**15**	1	**15**
H	OCH_3	CH_3	NHAc	OCH_3	OCH_3	OCH_3	**16**	1	**16**
H	OCH_3	H	NHCHO	OCH_3	OCH_3	OCH_3	**17**	1	**17**
H	OCH_3	H	$N(CH_3)_2$	OCH_3	OCH_3	OCH_3	**18**	1	**18**
H	OCH_3	CH_3	$N(CH_3)_2$	OCH_3	OCH_3	OCH_3	**19**	1	**19**
H	OCH_3	H	Br	OCH_3	OCH_3	OCH_3	**20**	1	**20**
H	OCH_3	H	Gly-*t*BOC	OCH_3	OCH_3	OCH_3	**21**	1	**21**
H	OCH_3	H	Succinic	OCH_3	OCH_3	OCH_3	**22**	1	**22**

								Artículos invest.	
Y	**X**	**R_N**	**R_1**	**R_2**	**R_3**	**R_4**	**Nº Comp.**	**Nº Art.**	**Nº Comp.**
H	OCH_3	-N=N-		OCH_3	OCH_3	OCH_3	**23**	1	**23**
H	OCH_3	-CH=N-		OCH_3	OCH_3	OCH_3	**24**	1	**24**
H	NO_2	H	H	OCH_3	OCH_3	OCH_3	**25**	1	**25**
H	NH_2	H	H	OCH_3	OCH_3	OCH_3	**26**	1	**26**
H	NH_2	CH_3	H	OCH_3	OCH_3	OCH_3	**27**	1	**27**
H	$N(CH_3)_2$	H	H	OCH_3	OCH_3	OCH_3	**28**	1	**28**
H	$N(CH_3)_2$	CH_3	H	OCH_3	OCH_3	OCH_3	**29a**	1	**29a**
H	$N(CH_3)_2$	CH_2-Dim	H	OCH_3	OCH_3	OCH_3	**29b**	1	**29b**
H	$N(CH_3)_2$	Et	H	OCH_3	OCH_3	OCH_3	**30**	1	**30**
H	$N(CH_3)_2$	Ac	H	OCH_3	OCH_3	OCH_3	**31**	1	**31**
H	$N(CH_3)_2$	CH_2CN	H	OCH_3	OCH_3	OCH_3	**32**	1	**32**
H	$N(CH_3)_2$	CH_2COOEt	H	OCH_3	OCH_3	OCH_3	**33**	1	**33**
H	$N(CH_3)_2$	CH_2COOH	H	OCH_3	OCH_3	OCH_3	**34**	1	**34**
H	$N(CH_3)_2$	Benzyl	H	OCH_3	OCH_3	OCH_3	**35a**	1	**35a**
H	$N(CH_3)_2$	COOBenzyl	H	OCH_3	OCH_3	OCH_3	**35b**	1	**35b**
H	$N(CH_3)_2$	H	NO_2	OCH_3	OCH_3	OCH_3	**36**		
H	NHCHO	H	H	OCH_3	OCH_3	OCH_3	**37**	1	**36**
H	$NHCH_3$	H	H	OCH_3	OCH_3	OCH_3	**38**	1	**37**
H	$NHCH_3$	CH_3	H	OCH_3	OCH_3	OCH_3	**39**	1	**38**
H	$NHCH_3$	Et	H	OCH_3	OCH_3	OCH_3	**40**		
H	$NHCH_3$	CH_2CN	H	OCH_3	OCH_3	OCH_3	**41**		
H	$NHCH_3$	CH_2COOEt	H	OCH_3	OCH_3	OCH_3	**42**		
H	$NHCH_3$	Benzyl	H	OCH_3	OCH_3	OCH_3	**43**		
H	NHAc	H	H	OCH_3	OCH_3	OCH_3	**44a**		
H	NHAc	Ac	H	OCH_3	OCH_3	OCH_3	**44b**		
H	NHAc	CH_3	H	OCH_3	OCH_3	OCH_3	**45**		
H	$NHCH_2CH_3$	CH_3	H	OCH_3	OCH_3	OCH_3	**46**		
H	$NHCH(CH_3)_2$	H	H	OCH_3	OCH_3	OCH_3	**47**		
H	$NHCH(CH_3)_2$	CH_3	H	OCH_3	OCH_3	OCH_3	**48**		
H	$NHCH(CH_3)_2$	Et	H	OCH_3	OCH_3	OCH_3	**49**		
H	$NHCH(CH_3)_2$	CH_2CN	H	OCH_3	OCH_3	OCH_3	**50**		
H	$NHCH(CH_3)_2$	Benzyl	H	OCH_3	OCH_3	OCH_3	**51**		

Y	X	R_N	R_1	R_2	R_3	R_4	Nº Comp.	Artículos invest. Nº Art.	Nº Comp.
H	Succinic	CH_3	H	OCH_3	OCH_3	OCH_3	**52**		
NO_2	OCH_3	H	H	OCH_3	OCH_3	OCH_3	**54**	1	**40**
NH_2	OCH_3	H	H	OCH_3	OCH_3	OCH_3	**55**	1	**41**
NH_2	OCH_3	CH_3	H	OCH_3	OCH_3	OCH_3	**56**	1	**42**
NH_2	OCH_3	Et	H	OCH_3	OCH_3	OCH_3	**57**	1	**43**
NH_2	OCH_3	CH_2CN	H	OCH_3	OCH_3	OCH_3	**58**	1	**44**
NH_2	OCH_3	Benzyl	H	OCH_3	OCH_3	OCH_3	**59**	1	**45**
$NHCH_2COOEt$	OCH_3	CH_3	H	OCH_3	OCH_3	OCH_3	**60**	1	**46**
$NHCH_2COOEt$	OCH_3	CH_2COOEt	H	OCH_3	OCH_3	OCH_3	**61**	1	**47**
$NHCH_3$	OCH_3	CH_3	H	OCH_3	OCH_3	OCH_3	**62**	1	**48a**
$N(CH_3)_2$	OCH_3	CH_3	H	OCH_3	OCH_3	OCH_3	**63**	1	**48b**
H	OCH_3	H	NO_2	OCH_3	OH	OCH_3	**64a**		
H	OCH_3	H	NH_2	OCH_3	OH	OCH_3	**65**		
H	OCH_3	H	NHAc	OCH_3	OH	OCH_3	**66a**		
H	OCH_3	Ac	NHAc	OCH_3	OH	OCH_3	**66b**		
H	OCH_3	CH_3	NH_2	OCH_3	OH	OCH_3	**67**		
H	OCH_3	-CH=N-		OCH_3	OH	OCH_3	**68**		
H	OCH_3	H	H	OCH_3	H	OCH_3	**69**	2	**1**
								3	**259**
H	OCH_3	CH_3	H	OCH_3	H	OCH_3	**70**	2	**2**
H	OCH_3	Et	H	OCH_3	H	OCH_3	**71**	2	**3**
H	OCH_3	CH_2CN	H	OCH_3	H	OCH_3	**72**	2	**4**
H	OCH_3	CH_2COOEt	H	OCH_3	H	OCH_3	**73**	2	**5**
H	OCH_3	Benzyl	H	OCH_3	H	OCH_3	**74**	2	**6**
								3	**270**
H	OCH_3	COOBenzyl	H	OCH_3	H	OCH_3	**75**	2	**7**
H	NO_2	H	H	OCH_3	H	OCH_3	**76**	3	**242**
H	NH_2	H	H	OCH_3	H	OCH_3	**77**	3	**245**
H	$N(CH_3)_2$	H	H	OCH_3	H	OCH_3	**78**	3	**254**
H	$N(CH_3)_2$	CH_3	H	OCH_3	H	OCH_3	**79**		
H	$N(CH_3)_2$	Et	H	OCH_3	H	OCH_3	**80**		
H	$N(CH_3)_2$	CH_2CN	H	OCH_3	H	OCH_3	**81**		

								Artículos invest.	
Y	**X**	**R_N**	**R_1**	**R_2**	**R_3**	**R_4**	**Nº Comp.**	**Nº Art.**	**Nº Comp.**
H	$N(CH_3)_2$	CH_2COOEt	H	OCH_3	H	OCH_3	**82**		
H	$N(CH_3)_2$	Benzyl	H	OCH_3	H	OCH_3	**83**	3	**275**
H	NHCHO	H	H	OCH_3	H	OCH_3	**84**		
H	$NHCH_3$	H	H	OCH_3	H	OCH_3	**85**		
H	$NHCH_3$	CH_3	H	OCH_3	H	OCH_3	**86**		
H	$NHCH_3$	Et	H	OCH_3	H	OCH_3	**87**		
H	$NHCH_3$	CH_2COOEt	H	OCH_3	H	OCH_3	**88**		
H	NCH_3CHO	H	H	OCH_3	H	OCH_3	**89**		
NO_2	OCH_3	H	H	OCH_3	H	OCH_3	**90**		
NH_2	OCH_3	H	H	OCH_3	H	OCH_3	**91**		
NH_2	OCH_3	CH_3	H	OCH_3	H	OCH_3	**92**		
NH_2	OCH_3	Et	H	OCH_3	H	OCH_3	**93**		
NH_2	OCH_3	CH_2CN	H	OCH_3	H	OCH_3	**94**		
NH_2	OCH_3	CH_2COOEt	H	OCH_3	H	OCH_3	**95a**		
NH_2	OCH_3	Benzyl	H	OCH_3	H	OCH_3	**96**		
$NHCH_2COOEt$	OCH_3	CH_2COOEt	H	OCH_3	H	OCH_3	**95b**		
H	OCH_3	CH_3	H	OCH_3	Br	OCH_3	**97a**	2	**8a**
H	OCH_3	CH_3	Br	OCH_3	H	OCH_3	**97b**	2	**8b**
H	OCH_3	Et	H	OCH_3	Br	OCH_3	**98a**	2	**9a**
H	OCH_3	Et	Br	OCH_3	H	OCH_3	**98b**	2	**9b**
H	OCH_3	Benzyl	H	OCH_3	Br	OCH_3	**99a**	2	**10a**
								3	**326A**
H	OCH_3	Benzyl	Br	OCH_3	H	OCH_3	**99b**	2	**10b**
								3	**326B**
H	OCH_3	Benzyl	Br	OCH_3	Br	OCH_3	**99c**	2	**10c**
								3	**326C**
H	OCH_3	H	H	$COOCH_3$	H	OCH_3	**101**	3	**79**
H	OCH_3	CH_3	H	$COOCH_3$	H	OCH_3	**102**		
H	OCH_3	CH_3	H	COOH	H	OCH_3	**103**	3	**90**
H	NO_2	H	H	$COOCH_3$	H	OCH_3	**104**		
H	NH_2	H	H	$COOCH_3$	H	OCH_3	**105**		
H	$N(CH_3)_2$	H	H	$COOCH_3$	H	OCH_3	**106**		

Y	X	R_N	R_1	R_2	R_3	R_4	Nº Comp.	Artículos invest. Nº Art.	Artículos invest. Nº Comp.
H	$N(CH_3)_2$	CH_3	H	$COOCH_3$	H	OCH_3	**107**		
H	$N(CH_3)_2$	Et	H	$COOCH_3$	H	OCH_3	**108**		
H	NHCHO	H	H	$COOCH_3$	H	OCH_3	**109**		
H	$NHCH_3$	H	H	$COOCH_3$	H	OCH_3	**110**		
H	$NHCH_3$	CH_3	H	$COOCH_3$	H	OCH_3	**111**		
H	NCH_3CHO	H	H	$COOCH_3$	H	OCH_3	**112**		
H	OCH_3	H	H	$COOCH_3$	H	NH_2	**115a**	3	**84A**
H	OCH_3	H	H	$COOCH_3$	H	$NHSO_2$-4-OCH_3Ph	**115b**	3	**84B**
H	OCH_3	H	H	$COOCH_3$	H	NHCHO	**116**		
H	OCH_3	H	H	$COOCH_3$	H	$NHCH_3$	**117**		
H	OCH_3	CH_3	H	$COOCH_3$	H	NCH_3SO_2-4-OCH_3Ph	**118**	3	**147**
NO_2	OCH_3	H	H	$COOCH_3$	H	$NHSO_2$-3-NO_2-4-OCH_3Ph	**119**		
H	OCH_3	H	H	H	OCH_3	OCH_3	**120**	2	**11**
								3	**8**
H	OCH_3	CH_3	H	H	OCH_3	OCH_3	**121a**	2	**12**
H	OCH_3	CH_2-Dim	H	H	OCH_3	OCH_3	**121b**		
H	OCH_3	H	NO_2	H	OCH_3	OCH_3	**122**	3	**11**
H	OCH_3	H	NH_2	H	OCH_3	OCH_3	**123**	3	**12**
H	OCH_3	CH_3	NH_2	H	OCH_3	OCH_3	**124**	3	**120**
H	OCH_3	H	NHAc	H	OCH_3	OCH_3	**125a**		
H	OCH_3	CH_3	NHAc	H	OCH_3	OCH_3	**126**	3	**124**
H	OCH_3	Ac	NHAc	H	OCH_3	OCH_3	**125b**		
H	OCH_3	H	NHCHO	H	OCH_3	OCH_3	**127**		
H	OCH_3	H	$NHCH_3$	H	OCH_3	OCH_3	**128**		
H	OCH_3	H	$N(CH_3)_2$	H	OCH_3	OCH_3	**129**		
H	OCH_3	H	NHCO-4-NO_2Ph	H	OCH_3	OCH_3	**130**		
H	OCH_3	H	Gly-*t*Boc	H	OCH_3	OCH_3	**131**		
H	OCH_3	H	Succinic	H	OCH_3	OCH_3	**132**		
H	OCH_3	-N=N-		H	OCH_3	OCH_3	**133**		
H	OCH_3	-CH=N-		H	OCH_3	OCH_3	**134**		
H	OCH_3	H	Br	H	OCH_3	OCH_3	**135**	2	**13**
H	OCH_3	CH_3	Br	H	OCH_3	OCH_3	**136**	2	**14**

								Artículos invest.	
Y	**X**	**R_N**	**R_1**	**R_2**	**R_3**	**R_4**	**Nº Comp.**	**Nº Art.**	**Nº Comp.**
H	OCH_3	Et	Br	H	OCH_3	OCH_3	**137**	2	**15**
H	OCH_3	CH_2CN	Br	H	OCH_3	OCH_3	**138**	2	**16**
H	OCH_3	CH_2COOEt	Br	H	OCH_3	OCH_3	**139**	2	**17**
H	OCH_3	Benzyl	Br	H	OCH_3	OCH_3	**140**	2	**18**
H	NO_2	H	H	H	OCH_3	OCH_3	**141**	3	**23**
H	NO_2	H	NO_2	H	OCH_3	OCH_3	**142**	3	**334**
H	NO_2	H	Br	H	OCH_3	OCH_3	**143**		
H	NH_2	H	H	H	OCH_3	OCH_3	**144**	3	**26**
H	NH_2	H	Br	H	OCH_3	OCH_3	**145**		
H	$N(CH_3)_2$	H	H	H	OCH_3	OCH_3	**146**	3	**29**
H	$N(CH_3)_2$	CH_3	H	H	OCH_3	OCH_3	**147a**		
H	$N(CH_3)_2$	CH_2-Dim	H	H	OCH_3	OCH_3	**147b**		
H	$N(CH_3)_2$	H	NO_2	H	OCH_3	OCH_3	**148**	3	**33**
H	$N(CH_3)_2$	H	NH_2	H	OCH_3	OCH_3	**149**	3	**35**
H	$N(CH_3)_2$	CH_3	NH_2	H	OCH_3	OCH_3	**150**	3	**118**
H	$N(CH_3)_2$	CH_3	NHCHO	H	OCH_3	OCH_3	**151**	3	**132**
H	$N(CH_3)_2$	CH_3	$NHCH_3$	H	OCH_3	OCH_3	**152a**		
H	$N(CH_3)_2$	CH_3	$N(CH_3)_2$	H	OCH_3	OCH_3	**152b**		
H	$N(CH_3)_2$	-N=N-		H	OCH_3	OCH_3	**153**	3	**117**
H	$N(CH_3)_2$	H	Br	H	OCH_3	OCH_3	**154**		
H	$N(CH_3)_2$	CH_3	Br	H	OCH_3	OCH_3	**155**		
H	$N(CH_3)_2$	CH_2CN	Br	H	OCH_3	OCH_3	**156**		
H	NHCHO	H	H	H	OCH_3	OCH_3	**157**		
H	NHCHO	H	Br	H	OCH_3	OCH_3	**158**		
H	$NHCH_3$	H	H	H	OCH_3	OCH_3	**159**		
H	$NHCH_3$	CH_3	H	H	OCH_3	OCH_3	**160**		
H	$NHCH_3$	Et	H	H	OCH_3	OCH_3	**161**		
H	$NHCH_3$	CH_2CN	H	H	OCH_3	OCH_3	**162**		
H	$NHCH_3$	CH_2COOEt	H	H	OCH_3	OCH_3	**163**		
H	$NHCH_3$	H	Br	H	OCH_3	OCH_3	**164**		
H	$NHCH_3$	CH_3	Br	H	OCH_3	OCH_3	**165**		
H	$NHCH_3$	Et	Br	H	OCH_3	OCH_3	**166**		

								Artículos invest.	
Y	**X**	**R_N**	**R_1**	**R_2**	**R_3**	**R_4**	**Nº Comp.**	**Nº Art.**	**Nº Comp.**
H	$NHCH_3$	CH_2CN	Br	H	OCH_3	OCH_3	**167**		
H	NCH_3CHO	H	H	H	OCH_3	OCH_3	**168**		
H	OCH_3	H	H	NH_2	OCH_3	OCH_3	**172**		
H	OCH_3	CH_3	H	NH_2	OCH_3	OCH_3	**173**		
H	OCH_3	H	H	NHCHO	OCH_3	OCH_3	**174**		
H	OCH_3	H	H	$NHCH_3$	OCH_3	OCH_3	**175**		
H	OCH_3	CH_3	H	$NHCH_3$	OCH_3	OCH_3	**176**		
H	OCH_3	CH_3	H	$N(CH_3)_2$	OCH_3	OCH_3	**177**		
H	OCH_3	H	H	CN	OCH_3	OCH_3	**181**		
H	OCH_3	CH_3	H	CN	OCH_3	OCH_3	**182**		
H	OCH_3	Et	H	CN	OCH_3	OCH_3	**183**		
H	OCH_3	CH_2CN	H	CN	OCH_3	OCH_3	**184**		
H	OCH_3	CH_2COOEt	H	CN	OCH_3	OCH_3	**185**		
H	OCH_3	H	OCH_3	H	H	OCH_3	**188**	2	**21**
								3	**76**
H	OCH_3	CH_3	OCH_3	H	H	OCH_3	**189**	2	**22**
H	OCH_3	H	OCH_3	H	NO_2	OCH_3	**190**	3	**96**
H	OCH_3	H	OCH_3	H	NH_2	OCH_3	**191**	3	**104**
H	OCH_3	H	OCH_3	H	NHCHO	OCH_3	**192**		
H	OCH_3	H	OCH_3	H	$NHCH_3$	OCH_3	**193**		
H	OCH_3	CH_3	OCH_3	H	$NHCH_3$	OCH_3	**194**		
H	OCH_3	H	OCH_3	H	NHAc	OCH_3	**195**		
H	OCH_3	CH_3	OCH_3	H	NCH_3Ac	OCH_3	**196**		
H	OCH_3	H	OCH_3	H	$NHCOCH_2Cl$	OCH_3	**197**	3	**129**
H	OCH_3	H	OCH_3	H	$NHCO(CH_2)_2Cl$	OCH_3	**198**	3	**138**
H	OCH_3	H	OCH_3	H	Ethylurea	OCH_3	**199**		
H	OCH_3	CH_3	OCH_3	H	CH_3Ethylurea	OCH_3	**200**		
H	OCH_3	H	OCH_3	H	Br	OCH_3	**201**	2	**23**
H	OCH_3	CH_3	OCH_3	H	Br	OCH_3	**202**	2	**24**
H	OCH_3	CH_2CN	OCH_3	H	Br	OCH_3	**203**	2	**25**
H	OCH_3	CH_2COOEt	OCH_3	H	Br	OCH_3	**204**	2	**26**
H	OCH_3	CH_2COOH	OCH_3	H	Br	OCH_3	**205**	2	**29**

Y	X	R_N	R_1	R_2	R_3	R_4	Nº Comp.	Artículos invest. Nº Art.	Artículos invest. Nº Comp.
H	OCH_3	COOEt	OCH_3	H	Br	OCH_3	**206**	2	**27**
H	OCH_3	CH_2-oxirane	OCH_3	H	Br	OCH_3	**207**	2	**28**
H	NO_2	H	OCH_3	H	H	OCH_3	**208**	3	**130**
H	NO_2	H	OCH_3	H	Br	OCH_3	**209**	3	**296**
H	NH_2	H	OCH_3	H	H	OCH_3	**210**		
H	NH_2	H	OCH_3	H	Br	OCH_3	**211**	3	**302**
H	$N(CH_3)_2$	H	OCH_3	H	H	OCH_3	**212**		
H	$N(CH_3)_2$	CH_3	OCH_3	H	H	OCH_3	**213**		
H	$N(CH_3)_2$	H	OCH_3	H	Br	OCH_3	**214**		
H	$N(CH_3)_2$	CH_3	OCH_3	H	Br	OCH_3	**215**		
H	$N(CH_3)_2$	Et	OCH_3	H	Br	OCH_3	**216**		
H	$N(CH_3)_2$	CH_2CN	OCH_3	H	Br	OCH_3	**217**		
H	$N(CH_3)_2$	CH_2COOEt	OCH_3	H	Br	OCH_3	**218**		
H	$N(CH_3)_2$	Benzyl	OCH_3	H	Br	OCH_3	**219**		
H	NHCHO	H	OCH_3	H	H	OCH_3	**220**		
H	NHCHO	H	OCH_3	H	Br	OCH_3	**221**	3	**315**
H	$NHCH_3$	H	OCH_3	H	H	OCH_3	**222**		
H	$NHCH_3$	CH_3	OCH_3	H	H	OCH_3	**223**		
H	$NHCH_3$	H	OCH_3	H	Br	OCH_3	**224**	3	**323**
H	$NHCH_3$	CH_3	OCH_3	H	Br	OCH_3	**225**		
H	$NHCH_3$	CH_2CN	OCH_3	H	Br	OCH_3	**226**		
H	$NHCH_3$	Benzyl	OCH_3	H	Br	OCH_3	**227**	3	**332**
Br	$NHCH_3$	CH_3	OCH_3	H	H	OCH_3	**228a**		
Br	$NHCH_3$	CH_3	OCH_3	H	Br	OCH_3	**228b**		
Br	$NHCH_3$	H	OCH_3	H	Br	OCH_3	**229**		
NO_2	OCH_3	H	OCH_3	H	H	OCH_3	**230**	3	**183**
NO_2	OCH_3	CH_3	OCH_3	H	Br	OCH_3	**231**	3	**204**
NH_2	OCH_3	H	OCH_3	H	H	OCH_3	**232**		
NH_2	OCH_3	H	OCH_3	H	Br	OCH_3	**233**		
NH_2	OCH_3	CH_3	OCH_3	H	Br	OCH_3	**234**		
NH_2	OCH_3	CH_2CN	OCH_3	H	Br	OCH_3	**235**		
NHCOOEt	OCH_3	CH_3	OCH_3	H	Br	OCH_3	**236**		

								Artículos invest.	
Y	**X**	**R_N**	**R_1**	**R_2**	**R_3**	**R_4**	**Nº Comp.**	**Nº Art.**	**Nº Comp.**
H	OCH_3	H	OCH_3	H	OCH_3	OCH_3	**239**	2	**32**
H	OCH_3	CH_3	OCH_3	H	OCH_3	OCH_3	**240**	2	**33**
H	OCH_3	Et	OCH_3	H	OCH_3	OCH_3	**241**	2	**34**
H	OCH_3	CH_2CN	OCH_3	H	OCH_3	OCH_3	**242**	2	**35**
H	OCH_3	CH_2COOEt	OCH_3	H	OCH_3	OCH_3	**243**	2	**36**
H	OCH_3	Benzyl	OCH_3	H	OCH_3	OCH_3	**244**	2	**37**
H	NO_2	H	OCH_3	H	OCH_3	OCH_3	**245**		
H	NH_2	H	OCH_3	H	OCH_3	OCH_3	**246**		
H	$N(CH_3)_2$	H	OCH_3	H	OCH_3	OCH_3	**247**		
H	$N(CH_3)_2$	CH_3	OCH_3	H	OCH_3	OCH_3	**248**		
H	$N(CH_3)_2$	Et	OCH_3	H	OCH_3	OCH_3	**249**		
H	$N(CH_3)_2$	CH_2CN	OCH_3	H	OCH_3	OCH_3	**250**		
H	$N(CH_3)_2$	CH_2COOEt	OCH_3	H	OCH_3	OCH_3	**251**		
H	$N(CH_3)_2$	Benzyl	OCH_3	H	OCH_3	OCH_3	**252**		
H	NHCHO	H	OCH_3	H	OCH_3	OCH_3	**253**		
H	$NHCH_3$	H	OCH_3	H	OCH_3	OCH_3	**254**		
H	$NHCH_3$	CH_3	OCH_3	H	OCH_3	OCH_3	**255**		
H	$NHCH_3$	CH_2CN	OCH_3	H	OCH_3	OCH_3	**256**		
H	$NHCH_3$	CH_2COOEt	OCH_3	H	OCH_3	OCH_3	**257**		
NO_2	OCH_3	H	OCH_3	H	OCH_3	OCH_3	**258**		
NH_2	OCH_3	H	OCH_3	H	OCH_3	OCH_3	**259**		
NH_2	OCH_3	CH_3	OCH_3	H	OCH_3	OCH_3	**260**		
NH_2	OCH_3	Et	OCH_3	H	OCH_3	OCH_3	**261**		
NH_2	OCH_3	CH_2CN	OCH_3	H	OCH_3	OCH_3	**262**		
NH_2	OCH_3	CH_2COOEt	OCH_3	H	OCH_3	OCH_3	**263a**		
NH_2	OCH_3	Benzyl	OCH_3	H	OCH_3	OCH_3	**264**		
$NHCH_2COOEt$	OCH_3	CH_2COOEt	OCH_3	H	OCH_3	OCH_3	**263b**		
H	OCH_3	H	OCH_3	H	OCH_3	Cl	**265**		
H	OCH_3	CH_3	OCH_3	H	OCH_3	Cl	**266**		
H	OCH_3	H	H	Br	OCH_3	Br	**270**		
H	OCH_3	CH_3	H	Br	OCH_3	Br	**271**		
H	OCH_3	Et	H	Br	OCH_3	Br	**272**		

								Artículos invest.	
Y	**X**	**R_N**	**R_1**	**R_2**	**R_3**	**R_4**	**Nº Comp.**	**Nº Art.**	**Nº Comp.**
H	OCH_3	CH_2COOEt	H	Br	OCH_3	Br	**273**		
H	OCH_3	H	OCH_3	H	H	CN	**276a**	3	**276A**
H	OCH_3	H	OSO_2-4-OCH_3Ph	H	H	CN	**276b**	3	**276B**
H	OCH_3	CH_3	OCH_3	H	H	CN	**277**		
H	OCH_3	H	H	H	Br	H	**278**		
H	OCH_3	CH_3	H	H	Br	H	**279**		
H	NO_2	H	H	OH	OCH_3	H	**281**		
H	OCH_3	H	OCH_3	H	H	CF_3	**282**		
H	OCH_3	CH_3	OCH_3	H	H	CF_3	**283**		
H	OCH_3	Benzyl	OCH_3	H	H	CF_3	**284**		
H	OCH_3	H	H	CF_3	Br	H	**285**		
H	OCH_3	CH_3	H	CF_3	Br	H	**286**		
H	OCH_3	H	H	CF_3	H	H	**287**		
H	OCH_3	CH_3	H	CF_3	H	H	**288**		
H	OCH_3	Benzyl	H	CF_3	H	H	**289**		
H	OCH_3	H	H	H	CF_3	H	**290**		
H	OCH_3	CH_3	H	H	CF_3	H	**291**		
H	OCH_3	Benzyl	H	H	CF_3	H	**292**		

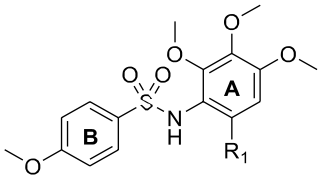

		Artículos invest.	
R_1	Nº Comp.	Nº Art.	Nº Comp.
COOH	**293a**	3	**63A**
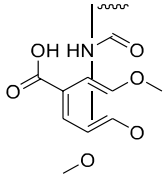	**293b**	3	**63B**
$COOCH_3$	**295**		

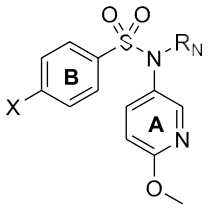

			Artículos invest.	
X	R_N	Nº Comp.	Nº Art.	Nº Art.
OCH_3	H	**296**	3	**240**
OCH_3	CH_3	**297**		
OCH_3	CH_2CN	**298**		
OCH_3	Benzyl	**299**	3	**279**
NO_2	H	**300**	3	**283**
NH_2	H	**301**	3	**287**
$N(CH_3)_2$	H	**302**		
$N(CH_3)_2$	CH_3	**303**		
$N(CH_3)_2$	Et	**304**		
$N(CH_3)_2$	CH_2CN	**305**		
$N(CH_3)_2$	CH_2COOEt	**306**		
NHCHO	H	**307**	3	**309**
$NHCH_3$	H	**308**	3	**316**
$NHCH_3$	CH_3	**309**		
$NHCH_3$	CH_2CN	**310**		
CH_3NCHO	H	**311**	3	**320**

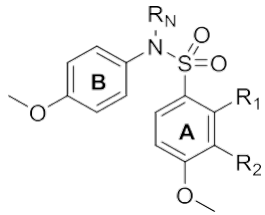

R_N	R_1	R_2	Nº Comp.
H	OCH_3	OCH_3	**313**
CH_3	OCH_3	OCH_3	**314**
CH_2CN	OCH_3	OCH_3	**315**
H	OCH_3	H	**316**
CH_3	OCH_3	H	**317**
CH_2CN	OCH_3	H	**318**
Benzyl	OCH_3	H	**319**
H	H	OCH_3	**320**
CH_3	H	OCH_3	**321**
CH_2CN	H	OCH_3	**322**
Benzyl	H	OCH_3	**323**

Anexo 2.b. Chemical synthesis of the sulfonamide library.

General chemical techniques

Reagents were used as purchased without further purification. Solvents (EtOAc, DMF, CH_2Cl_2, MeOH, CH_3CN, toluene) were stored over molecular sieves. THF was refluxed with sodium/benzophenone, and hexane was dried by distillation and stored over $CaCl_2$. TLC was performed on precoated silica gel polyester plates (0.25 mm thickness) with a UV fluorescence indicator 254 (Polychrom SI F254). Chromatographic separations were performed on silica gel columns by flash (Kieselgel 40, 0.040-0.063; Merck) chromatography. Melting points were determined on a Buchi 510 apparatus and are uncorrected. ^{1}H NMR and ^{13}C NMR spectra were recorded in $CDCl_3$, CD_3OD, DMSO-D_6, or acetone-D_6 on a Bruker WP 200-SY spectrometer operating at 200/50 MHz, or a Bruker SY spectrometer at 400/100 MHz. Chemical shifts (δ) are given in ppm downfield from tetramethylsilane and coupling constants (*J* values) are given in Hz. IR spectra in KBr disk were run on a Nicolet Impact 410 Spectrophotometer. A hybrid QSTAR XL quadrupole/time of flight spectrometer was used for HRMS analyses. GC-MS spectra were performed using a Hewlett-Packard 5890 series II mass detector. A Helios-α UV-320 from Thermo-Spectronic was used for UV spectra.

Chemical synthesis

4-Methoxy-*N*-(3,4,5-trimethoxyphenyl)benzenesulfonamide (**1a**) and 4-methoxy-*N*-((4-methoxyphenyl)sulfonyl)-*N*-(3,4,5-trimethoxyphenyl)benzenesulfonamide (**1b**).

*Compounds **1a** and **1b** article 1. Available at Supplementary Material, Methods SP1.*

4-Methoxy-*N*-methyl-*N*-(3,4,5-trimethoxyphenyl)benzenesulfonamide (**2a**) and *N*,*N*'-methylenebis(4-methoxy-*N*-(3,4,5-trimethoxyphenyl)benzenesulfonamide) (**2b**).

*Compounds **2a** and **2b** article 1. Available at Supplementary Material, Methods SP1.*

N-ethyl-4-methoxy-*N*-(3,4,5-trimethoxyphenyl)benzenesulfonamide (**3**).

*Compound **3** article 1. Available at Supplementary Material, Methods SP1.*

N-(2-bromoethyl)-4-methoxy-*N*-(3,4,5-trimethoxyphenyl)benzenesulfonamide (**4**).

*Compound **4** article 1. Available at Supplementary Material, Methods SP1.*

N-((4-methoxyphenyl)sulfonyl)-*N*-(3,4,5-trimethoxyphenyl)acetamide (**5**).

*Compound **5** article 1. Available at Supplementary Material, Methods SP1.*

N-(cyanomethyl)-4-methoxy-*N*-(3,4,5-trimethoxyphenyl)benzenesulfonamide (**6**).

*Compound **6** article 1. Available at Supplementary Material, Methods SP1.*

Ethyl *N*-((4-methoxyphenyl)sulfonyl)-*N*-(3,4,5-trimethoxyphenyl)glycinate (**7**).

*Compound **7** article 1. Available at Supplementary Material, Methods SP1.*

N-((4-methoxyphenyl)sulfonyl)-*N*-(3,4,5-trimethoxyphenyl)glycine (**8**).

*Compound **8** article 1. Available at Supplementary Material, Methods SP1.*

N-benzyl-4-methoxy-*N*-(3,4,5-trimethoxyphenyl)benzenesulfonamide (**9**).

*Compound **9** article 1. Available at Supplementary Material, Methods SP1.*

Benzyl ((4-methoxyphenyl)sulfonyl)(3,4,5-trimethoxyphenyl)carbamate (**10**).

*Compound **10** article 1. Available at Supplementary Material, Methods SP1.*

4-Methoxy-*N*-(3,4,5-trimethoxy-2-nitrophenyl)benzenesulfonamide (**11**).

*Compound **11** article 1. Available at Supplementary Material, Methods SP1.*

N-(2-amino-3,4,5-trimethoxyphenyl)-4-methoxybenzenesulfonamide (**12**).

*Compound **12** article 1. Available at Supplementary Material, Methods SP1.*

N-(2-amino-3,4,5-trimethoxyphenyl)-4-methoxy-*N*-methylbenzenesulfonamide (**13**).

*Compound **13** article 1. Available at Supplementary Material, Methods SP1.*

N-(2-amino-3,4,5-trimethoxyphenyl)-4-methoxy-*N*-(((2,3,4-trimethoxy-6-((4-methoxyphenyl)sulfonamido)phenyl)amino)methyl)benzenesulfonamide (**14**).

*Compound **14** article 1. Available at Supplementary Material, Methods SP1.*

N-(2,3,4-trimethoxy-6-((4-methoxyphenyl)sulfonamido)phenyl)acetamide (**15**).

*Compound **15** article 1. Available at Supplementary Material, Methods SP1.*

N-(2,3,4-trimethoxy-6-((4-methoxy-*N*-methylphenyl)sulfonamido)phenyl)acetamide (**16**).

*Compound **16** article 1. Available at Supplementary Material, Methods SP1.*

N-(2,3,4-trimethoxy-6-((4-methoxyphenyl)sulfonamido)phenyl)formamide (**17**).

*Compound **17** article 1. Available at Supplementary Material, Methods SP1.*

N-(2-(dimethylamino)-3,4,5-trimethoxyphenyl)-4-methoxybenzenesulfonamide (**18**).

*Compound **18** article 1. Available at Supplementary Material, Methods SP1.*

N-(2-(dimethylamino)-3,4,5-trimethoxyphenyl)-4-methoxy-*N*-methylbenzenesulfonamide (**19**).

*Compound **19** article 1. Available at Supplementary Material, Methods SP1.*

N-(2-bromo-3,4,5-trimethoxyphenyl)-4-methoxybenzenesulfonamide (**20**).

*Compound **20** article 1. Available at Supplementary Material, Methods SP1.*

Tert-butyl (2-oxo-2-((2,3,4-trimethoxy-6-((4-methoxyphenyl)sulfonamido)phenyl)amino) ethyl)carbamate (**21**).

*Compound **21** article 1. Available at Supplementary Material, Methods SP1.*

4-Oxo-4-((2,3,4-trimethoxy-6-((4-methoxyphenyl)sulfonamido)phenyl)amino)butanoicacid(**22**).

*Compound **22** article 1. Available at Supplementary Material, Methods SP1.*

4,5,6-Trimethoxy-1-((4-methoxyphenyl)sulfonyl)-1*H*-benzo[d][1,2,3]triazole (**23**).

*Compound **23** article 1. Available at Supplementary Material, Methods SP1.*

4,5,6-Trimethoxy-1-((4-methoxyphenyl)sulfonyl)-1*H*-benzo[d]imidazole (**24**).

*Compound **24** article 1. Available at Supplementary Material, Methods SP1.*

4-Nitro-*N*-(3,4,5-trimethoxyphenyl)benzenesulfonamide (**25**).

*Compound **25** article 1. Available at Supplementary Material, Methods SP1.*

4-Amino-*N*-(3,4,5-trimethoxyphenyl)benzenesulfonamide (**26**).

*Compound **26** article 1. Available at Supplementary Material, Methods SP1.*

4-Amino-*N*-methyl-*N*-(3,4,5-trimethoxyphenyl)benzenesulfonamide (**27**).

*Compound **27** article 1. Available at Supplementary Material, Methods SP1.*

4-(Dimethylamino)-*N*-(3,4,5-trimethoxyphenyl)benzenesulfonamide (**28**).

*Compound **28** article 1. Available at Supplementary Material, Methods SP1.*

4-(Dimethylamino)-*N*-methyl-*N*-(3,4,5-trimethoxyphenyl)benzenesulfonamide (**29a**) and *N*,*N*'-methylenebis(4-(dimethylamino)-*N*-(3,4,5-trimethoxyphenyl)benzenesulfonamide) (**29b**).

*Compounds **29a** and **29b** article 1. Available at Supplementary Material, Methods SP1.*

4-(Dimethylamino)-*N*-ethyl-*N*-(3,4,5-trimethoxyphenyl)benzenesulfonamide (**30**).

*Compound **30** article 1. Available at Supplementary Material, Methods SP1.*

N-((4-(dimethylamino)phenyl)sulfonyl)-*N*-(3,4,5-trimethoxyphenyl)acetamide (**31**).

*Compound **31** article 1. Available at Supplementary Material, Methods SP1.*

N-(cyanomethyl)-4-(dimethylamino)-*N*-(3,4,5-trimethoxyphenyl)benzenesulfonamide (**32**).

*Compound **32** article 1. Available at Supplementary Material, Methods SP1.*

Ethyl *N*-((4-(dimethylamino)phenyl)sulfonyl)-*N*-(3,4,5-trimethoxyphenyl)glycinate (**33**).

*Compound **33** article 1. Available at Supplementary Material, Methods SP1.*

N-((4-(dimethylamino)phenyl)sulfonyl)-*N*-(3,4,5-trimethoxyphenyl)glycine (**34**).

*Compound **34** article 1. Available at Supplementary Material, Methods SP1.*

N-benzyl-4-(dimethylamino)-*N*-(3,4,5-trimethoxyphenyl)benzenesulfonamide (**35a**) and benzyl ((4-(dimethylamino)phenyl)sulfonyl)(3,4,5-trimethoxyphenyl)carbamate (**35b**).

*Compounds **35a** and **35b** article 1. Available at Supplementary Material, Methods SP1.*

4-(Dimethylamino)-*N*-(3,4,5-trimethoxy-2-nitrophenyl)benzenesulfonamide (**36**). To a solution of **28** (100 mg, 0.28 mmol) in CH_3CN (50 mL), *tert*-butyl nitrite (19 µL, 0.14 mmol) was added and stirred at 45 °C. After 1 h, additional 0.14 mmol *tert*-butyl nitrite was added to the reaction mixture and it was stirred at 45 °C for 24 h. The mixture was poured into ice and basified with 5% $NaHCO_3$ solution and extracted with EtOAc. The organic layers were washed with brine, dried over Na_2SO_4 and concentrated under vacuum. The residue was purified by preparative TLC (hexane/EtOAc 4:6) to give pure product **36** (55 mg, 0.13 mmol, 48%). IR (KBr): 3278, 1594, 1498, 861 cm^{-1}. ^1H NMR (400 MHz, $CDCl_3$): δ 2.95 (6H, *s*), 3.74 (3H, *s*), 3.77 (3H, *s*), 3.82 (3H, *s*), 6.49 (2H, *d, J* = 8.8), 6.98 (1H, *s*), 7.42 (2H, *d, J* = 8.8), 8.07 (1H, *s*). ^{13}C NMR (100 MHz, $CDCl_3$): δ 40.0 ($2CH_3$), 56.4 (CH_3), 61.1 (CH_3), 62.3 (CH_3), 101.6 (CH), 110.9 (2CH), 122.7 (C), 128.7 (2CH), 128.8 (C), 139.7 (C), 148.3 (C), 153.3 (C), 156.8 (2C). HRMS ($C_{17}H_{21}N_3O_7S + H^+$): calcd 412.1173 ($M + H^+$), found 412.1134.

N-(4-(*N*-(3,4,5-trimethoxyphenyl)sulfamoyl)phenyl)formamide (**37**).

*Compound **36** article 1. Available at Supplementary Material, Methods SP1.*

4-(Methylamino)-*N*-(3,4,5-trimethoxyphenyl)benzenesulfonamide (**38**).

*Compound **37** article 1. Available at Supplementary Material, Methods SP1.*

N-methyl-4-(methylamino)-*N*-(3,4,5-trimethoxyphenyl)benzenesulfonamide (**39**).

*Compound **38** article 1. Available at Supplementary Material, Methods SP1.*

N-ethyl-4-(methylamino)-*N*-(3,4,5-trimethoxyphenyl)benzenesulfonamide (**40**). 77 mg (0.22 mmol) of compound **38** were dissolved in dry DMF (3 mL) and 61 mg (0.44 mmol) of crushed K_2CO_3 were added. After 30 min stirring at room temperature, 72.6 µL (0.97 mmol) of bromoethane were added to the solution. The reaction mixture was stirred at room temperature for 48 h. The solution was concentrated in vacuo and re-dissolved with EtOAc. Then, it was washed with brine, dried over Na_2SO_4 and evaporated to dryness to give 70 mg (0.18 mmol, 84%) of **40**. The crude product was crystallized from methanol to give 39 mg (0.10 mmol, 47%) of the purified compound **40**. M.p.: 120-122 °C (MeOH). ^{1}H NMR (200 MHz, CD_3OD): δ 1.04 (3H, *t, J* = 7), 2.80 (3H, *s*), 3.53 (2H, *q, J* = 7), 3.70 (6H, *s*), 3.74 (3H, *s*), 6.27 (2H, *s*), 6.60 (2H, *d, J* = 8.8), 7.34 (2H, *d, J* = 8.8). ^{13}C NMR (100 MHz, CD_3OD): δ 12.9 (CH_3), 28.4 (CH_3), 45.3 (CH_2), 55.1 ($2CH_3$), 59.7 (CH_3), 106.5 (2CH), 110.2 (2CH), 122.6 (C), 129.5 (2CH), 135.1 (C), 137.5 (C), 152.9 (C), 153.8 (2C). HRMS ($C_{18}H_{24}N_2O_5S + H^+$): calcd 381.1479 ($M + H^+$), found 381.1482.

N-(cyanomethyl)-4-(methylamino)-*N*-(3,4,5-trimethoxyphenyl)benzenesulfonamide (**41**). 2-chloroacetonitrile (26.6 µL, 0.42 mmol) was added after 30 min to a stirred solution of **38** (74 mg, 0.21 mmol) and K_2CO_3 (58 mg, 0.42 mmol) in dry DMF (5 mL). After 24 h, the reaction mixture was dried under vacuum, re-dissolved in EtOAc and washed with brine. After drying over Na_2SO_4 and removal of the solvent, crude product **41** was obtained (77 mg, 0.20 mmol, 94%) and it was purified by crystallization in methanol (29 mg, 0.07 mmol, 35%). M.p.: 134-136 °C (MeOH). ^{1}H NMR (200 MHz, CD_3OD): δ 2.81 (3H, *s*), 3.70 (6H, *s*), 3.75 (3H, *s*), 4.65 (2H, *s*), 6.42 (2H, *s*), 6.61 (2H, *d, J* = 8.8), 7.40 (2H, *d, J* = 8.8). ^{13}C NMR (100 MHz, $CDCl_3$): δ 29.9 (CH_3), 39.6 (CH_2), 56.1 ($2CH_3$), 60.8 (CH_3), 105.9 (2CH), 111.1 (2CH), 115.4 (C), 122.9 (C), 130.3 (2CH), 134.3 (C), 138.4 (C), 153.3 (C), 153.3 (2C). HRMS ($C_{18}H_{21}N_3O_5S + H^+$): calcd 392.1275 ($M + H^+$), found 392.1272.

Ethyl *N*-((4-(methylamino)phenyl)sulfonyl)-*N*-(3,4,5-trimethoxyphenyl)glycinate (**42**). To a solution of **38** (74 mg, 0.21 mmol) in dry DMF (5 mL) K_2CO_3 (58 mg, 0.42 mmol) was added and the resulting mixture was stirred for 30 min. Then, ethyl 2-bromoacetate (46.7 µL, 0.42 mmol) was added. After 48 h, the solvent was evaporated to dryness and the residue was dissolved in brine and extracted with EtOAc. The organics were dried over Na_2SO_4 before concentration under reduced pressure to yield the compound **42** (87 mg, 0.20 mmol, 95%). The crude reaction product was purified by crystallization in methanol (32 mg, 0.07 mmol, 35%). M.p.: 111-112 °C (MeOH). ^{1}H NMR (200 MHz, CD_3OD): δ 1.23 (3H, *t, J* = 7), 2.80 (3H, *s*), 3.68 (6H, *s*), 3.72 (3H, *s*), 4.16 (2H, *q, J* = 7), 4.36 (2H, *s*), 6.43 (2H, *s*), 6.59 (2H, *d, J* = 8.8), 7.40 (2H, *d, J* = 8.8). ^{13}C NMR (100 MHz, $CDCl_3$): δ 14.3 (CH_3), 30.2 (CH_3), 53.1 (CH_2), 56.4 ($2CH_3$), 61.0 (CH_3), 61.5 (CH_2), 106.6 (2CH), 111.0 (2CH), 125.1 (C), 130.2 (2CH), 136.1 (C), 137.9 (C), 153.0 (C), 153.2 (2C), 169.3 (C). HRMS ($C_{20}H_{26}N_2O_7S + H^+$): calcd 439.1533 ($M + H^+$), found 439.1531.

N-benzyl-4-(methylamino)-*N*-(3,4,5-trimethoxyphenyl)benzenesulfonamide (**43**). A solution of **38** (78 mg, 0.22 mmol) and K_2CO_3 (60 mg, 0.44 mmol) in dry DMF (5 mL) was stirred at room temperature for 30 min, then 66.4 µL (0.57 mmol) of benzyl chloride were added and mixture stirred for 48 h. When completed, solvent was removed under vacuum and the residue was washed with brine, extracted with EtOAc, dried (Na_2SO_4), filtered and evaporated to dryness to afford 88 mg (0.20 mmol, 90%) of **43.** The crude reaction product was purified by crystallization in methanol (61 mg, 0.14 mmol, 62%). M.p.: 159-162 °C (MeOH). ^{1}H NMR (200 MHz, CD_3OD): δ 2.82 (3H, *s*), 3.59 (6H, *s*), 3.67 (3H, *s*), 4.67 (2H, *s*), 6.19 (2H, *s*), 6.64 (2H, *d, J* = 9), 7.23 (5H, *bs*), 7.43 (2H, *d, J* = 9). ^{13}C NMR (100 MHz, $CDCl_3$): δ 30.1 (CH_3), 55.0 (CH_2), 56.0 ($2CH_3$), 60.8 (CH_3), 106.7 (2CH), 111.0 (2CH), 125.2 (C), 127.5 (CH), 128.2 (2CH), 128.6 (2CH), 129.9 (2CH), 135.1 (C), 136.4 (C), 137.5 (C), 152.5 (C), 152.7 (2C). HRMS ($C_{23}H_{26}N_2O_5S + H^+$): calcd 443.1635 ($M + H^+$), found 443.1627.

N-(4-(*N*-(3,4,5-trimethoxyphenyl)sulfamoyl)phenyl)acetamide (**44a**) and *N*-((4-acetamidophenyl)sulfonyl)-*N*-(3,4,5-trimethoxyphenyl)acetamide (**44b**). A mixture of **26** (104 mg, 0.31 mmol) and acetic anhydride (58 µL, 0.62 mmol) in CH_2Cl_2 (50 mL) and pyridine (1 mL) was stirred at room temperature. After 48 h, the reaction mixture was poured onto ice and extracted with CH_2Cl_2, the organics were washed with 2N HCl, 5% $NaHCO_3$ and brine, dried over Na_2SO_4, filtered, and concentrated under vacuum. The residue was purified by preparative TLC (CH_2Cl_2/MeOH 95:5) to afford compounds **44a** (37 mg, 0.10 mmol, 31%) and **44b** (61 mg, 0.14 mmol, 47%). **44a:** ^{1}H NMR (400 MHz, CD_3OD): δ 2.12 (3H, *s*), 3.66 (3H, *s*), 3.71 (6H, *s*), 6.36 (2H, *s*), 7.68 (4H, *s*). ^{13}C NMR (100 MHz, $CDCl_3$): δ 29.6 (CH_3), 56.1 ($2CH_3$), 60.9 (CH_3), 100.0 (2CH), 119.1 (2CH), 128.6 (2CH), 132.2 (C), 133.6 (C), 135.8 (C), 142.1 (C), 153.5 (2C), 168.7 (C). HRMS ($C_{17}H_{20}N_2O_6S$ + H^+): calcd 381.1115 (M + H^+), found 381.1098. **44b:** M.p.: 255-258 °C (CH_2Cl_2/hexane). ^{1}H NMR (400 MHz, $CDCl_3$): δ 1.93 (3H, *s*), 2.23 (3H, *s*), 3.84 (6H, *s*), 3.90 (3H, *s*), 6.45 (2H, *s*), 7.7 (2H, *d, J* = 8.8), 8.02 (2H, *d, J* = 8.8). ^{13}C NMR (100 MHz, acetone-D_6): δ 24.6 (CH_3), 24.9 (CH_3), 56.6 ($2CH_3$), 60.5 (CH_3), 108.2 (2CH), 118.7 (2CH), 130.5 (2CH), 132.4 (C), 132.5 (C), 138.8 (C), 144.6 (C), 153.5 (2C), 169.6 (C), 170.3 (C). HRMS ($C_{19}H_{22}N_2O_7S$ + H^+): calcd 423.1220 (M + H^+), found 423.1211.

N-(4-(*N*-methyl-*N*-(3,4,5-trimethoxyphenyl)sulfamoyl)phenyl)acetamide (**45**). A solution of **27** (45 mg, 0.13 mmol) and acetic anhydride (14.5 µL, 0.15 mmol) in CH_2Cl_2 (25 mL) and pyridine (1 mL) was stirred overnight at room temperature. The reaction mixture was poured onto ice, extracted with CH_2Cl_2 and washed with 2N HCl, 5% $NaHCO_3$ and brine. After drying (Na_2SO_4), the crude reaction product was concentrated and recrystallized from CH_2Cl_2/hexane to give the pure product **45** (33 mg, 0.08 mmol, 66%). M.p.: 175-177 °C (CH_2Cl_2/hexane). IR (KBr): 3373, 1704, 1594, 1503, 805 cm^{-1}. ^{1}H NMR (400 MHz, $CDCl_3$): δ 2.22 (3H, *s*), 3.14 (3H, *s*), 3.73 (6H, *s*), 3.83 (3H, *s*), 6.28 (2H, *s*), 7.34 (1H, *s*), 7.57 (2H, *d, J* = 8.8), 7.62 (2H, *d, J* = 8.8). ^{13}C NMR (100 MHz, $CDCl_3$): δ 24.4 (CH_3), 38.4 (CH_3), 55.9 ($2CH_3$), 60.7 (CH_3), 104.3 (2CH), 118.7 (2CH), 128.9 (2CH), 130.6 (C), 136.9 (C), 137.1 (C), 142.3 (C), 152.8 (2C), 168.9 (C). HRMS ($C_{18}H_{22}N_2O_6S$ + H^+): calcd 395.1271 (M + H^+), found 395.1281.

4-(Ethylamino)-*N*-(3,4,5-trimethoxyphenyl)benzenesulfonamide (**46**). To a solution of **45** (72 mg, 0.18 mmol) in dry THF (20 mL), $LiAlH_4$ (34.6 mg, 0.91 mmol) was slowly added and stirred at room temperature for 48 h. The reaction was quenched by addition a mixture of EtOAc, MeOH and Na_2SO_4 to the solution. Then, the mixture was filtered and evaporated to dryness. The residue was re-dissolved in EtOAc, washed with brine, dried over Na_2SO_4, filtered, concentrated under vacuum, and recrystallized from MeOH to give pure product **46** (23 mg, 0.06 mmol, 33%). M.p.: 126-134 °C (MeOH). IR (KBr): 3374, 1504, 805 cm^{-1}. ^{1}H NMR (400 MHz, $CDCl_3$): δ 1.27 (3H, *t, J* = 7.2), 3.10 (3H, *s*), 3.19 (2H, *q, J* = 7.2), 3.73 (6H, *s*), 3.82 (3H, *s*), 6.31 (2H, *s*), 6.52 (2H, *d, J* = 8.8), 7.38 (2H, *d, J* = 8.8). ^{13}C NMR (100 MHz, $CDCl_3$): δ 14.4 (CH_3), 37.9 (CH_2), 38.4 (CH_3), 56.1 ($2CH_3$), 60.8 (CH_3), 104.7 (2CH), 111.1 (2CH), 122.9 (C), 130.1 (2CH), 137.2 (C), 137.8 (C), 151.7 (C), 152.8 (2C). HRMS ($C_{18}H_{24}N_2O_5S$ + H^+): calcd 381.1479 (M + H^+), found 381.1477.

4-(Isopropylamino)-*N*-(3,4,5-trimethoxyphenyl)benzenesulfonamide (**47**). 490 mg (1.45 mmol) of **26** were dissolved in dry THF (30 mL). Acetone (1.07 mL, 14.5 mmol) and trichloroacetic acid (355 mg, 2.17 mmol) diluted in dry THF (10 mL) were slowly added and the reaction mixture was stirred at room temperature for 2 h. Then, $NaBH_4$ (548 mg, 14.5 mmol) was added and stirred overnight. The reaction mixture was concentrated and re-dissolved in EtOAc, washed with brine, dried over anhydrous Na_2SO_4, filtered and solvent evaporated in vacuum. The residue was purified by flash column chromatography (hexane/EtOAc 8:2) to afford the compound **47** (165 mg, 0.43 mmol, 30%). IR (KBr): 3362, 1598, 1505, 830 cm^{-1}. ^{1}H NMR (400 MHz, CD_3OD): δ 1.17 (6H, *d, J* = 6.4), 3.63 (1H, *m*), 3.66 (3H, *s*), 3.71 (6H, *s*), 6.35 (2H, *s*), 6.55 (2H, *d, J* = 8.8), 7.45 (2H, *d, J* = 8.8). ^{13}C NMR (100 MHz, acetone-D_6): δ 21.6 ($2CH_3$), 43.4 (CH), 55.4 ($2CH_3$), 59.6 (CH_3), 98.4 (2CH), 111.2 (2CH), 125.0 (C), 129.2 (2CH), 134.5 (C), 134.9 (C), 151.6 (C), 153.5 (2C). HRMS ($C_{18}H_{24}N_2O_5S$ + H^+): calcd 381.1479 (M + H^+), found 381.1483.

4-(Isopropylamino)-*N*-methyl-*N*-(3,4,5-trimethoxyphenyl)benzenesulfonamide (**48**). To a solution of **47** (88 mg, 0.23 mmol) in CH_3CN (40 mL) KOH (26 mg, 0.46 mmol) was added and stirred for 30 min. Then, CH_3I (29 µL, 0.46 mmol) was added. The reaction mixture was stirred at room temperature for 24 h and evaporated to dryness. The residue was dissolved in EtOAc, washed with brine, and dried over Na_2SO_4. After concentration, the residue was purified by preparative TLC (CH_2Cl_2/MeOH 97:3) to give 72 mg (0.18 mmol, 79%) of **48**. ^{1}H NMR (200 MHz, CD_3OD): δ 1.19 (6H, *d, J* = 7.8), 3.08 (3H, *s*), 3.65 (1H, *m*), 3.70 (6H, *s*), 3.73 (3H, *s*), 6.32 (2H, *s*), 6.59 (2H, *d, J* = 9), 7.27 (2H, *d, J* = 9). ^{13}C NMR (100 MHz, $CDCl_3$): δ 22.5 ($2CH_3$), 38.4 (CH_3), 43.9 (CH), 56.0 ($2CH_3$), 60.8 (CH_3), 104.6 (2CH), 111.4 (2CH), 122.2 (C), 130.1 (2CH), 137.1 (C), 137.9 (C), 151.0 (C), 152.8 (2C). HRMS ($C_{19}H_{26}N_2O_5S + H^+$): calcd 395.1635 ($M + H^+$), found 395.1634.

N-ethyl-4-(isopropylamino)-*N*-(3,4,5-trimethoxyphenyl)benzenesulfonamide (**49**). A solution of **47** (83 mg, 0.22 mmol) and K_2CO_3 (61 mg, 0.44 mmol) in DMF (5 mL) was stirred for 30 min. Then, 2-bromoethane (32.6 µL, 0.44 mmol) was added to the solution and was stirred for 24 h. The solution was concentrated in vacuo and re-dissolved with EtOAc. Then, it was washed with brine, dried over Na_2SO_4 and evaporated to dryness to give 81 mg (0.20 mmol, 91%) of **49**. Crude product was purified by crystallization in methanol (53 mg, 0.13 mmol, 59%). M.p.: 157-163 °C (MeOH). ^{1}H NMR (400 MHz, $CDCl_3$): δ 1.05 (3H, *t, J* = 7.2), 1.21 (2H, *d, J* = 6.4), 3.50 (2H, *q, J* = 7.2), 3.65 (1H, *m*), 3.72 (6H, *s*), 3.82 (3H, *s*), 6.24 (2H, *s*), 6.49 (2H, *d, J* = 8.8), 7.40 (2H, *d, J* = 8.8). ^{13}C NMR (100 MHz, $CDCl_3$): δ 14.0 (CH_3), 22.6 ($2CH_3$), 43.9 (CH), 45.6 (CH_2), 56.0 ($2CH_3$), 60.8 (CH_3), 106.5 (2CH), 111.4 (2CH), 124.3 (C), 130.0 (2CH), 135.0 (C), 137.5 (C), 150.7 (C), 152.9 (2C). HRMS ($C_{20}H_{28}N_2O_5S + H^+$): calcd 409.1792 ($M + H^+$), found 409.1790.

N-(cyanomethyl)-4-(isopropylamino)-*N*-(3,4,5-trimethoxyphenyl)benzenesulfonamide (**50**). 75 mg (0.19 mmol) of **47** were dissolved in DMF (5 mL) and K_2CO_3 (54 mg, 0.39 mmol) was added. After 30 min stirring at room temperature 2-chloroacetonitrile (25 µL, 0.39 mmol) was added to the solution and stirred for 48 h. The solvent was removed under reduced pressure. The residue was dissolved in EtOAc and washed with brine, dried (Na_2SO_4) and concentrated in vacuo to afford 65 mg (0.15 mmol, 78%) of **50**. The crude product was purified by crystallization in methanol (51 mg, 0.12 mmol, 61%). M.p.: 140-146 °C (MeOH). IR (KBr): 3389, 1901, 1592, 1503, 831 cm^{-1}. ^{1}H NMR (200 MHz, CD_3OD): δ 1.20 (6H, *d, J* = 6.6), 3.70 (1H, *m*), 3.71 (6H, *s*), 3.75 (3H, *s*), 4.64 (2H, *s*), 6.41 (2H, *s*), 6.62 (2H, *d, J* = 9), 7.37 (2H, *d, J* = 9). ^{13}C NMR (100 MHz, $CDCl_3$): δ 22.5 ($2CH_3$), 39.6 (CH_2), 43.9 (CH), 56.1 ($2CH_3$), 60.8 (CH_3), 106.0 (2CH), 111.6 (2CH), 115.3 (C), 122.7 (C), 130.4 (2CH), 134.3 (C), 138.5 (C), 151.5 (C), 153.3 (2C). HRMS ($C_{20}H_{25}N_3O_5S + H^+$): calcd 420.1588 ($M + H^+$), found 420.1584.

N-benzyl-4-(isopropylamino)-*N*-(3,4,5-trimethoxyphenyl)benzenesulfonamide (**51**). **47** (70 mg, 0.18 mmol) was dissolved in DMF (5 mL), K_2CO_3 (50 mg, 0.36 mmol) was added and the resulting mixture was stirred for 30 min. Then, benzyl chloride (42.7 µL, 0.36 mmol) was added. After 24 h, the reaction mixture was concentrated under reduced pressure, diluted with EtOAc, washed with brine, dried over Na_2SO_4, filtered, and concentrated in vacuo to give 73 mg (0.15 mmol, 84%) of **51**. The crude was crystallized from methanol to give pure product (36 mg, 0.08 mmol, 41%). M.p.: 131-138 °C (MeOH). ^{1}H NMR (400 MHz, $CDCl_3$): δ 1.23 (6H, *d, J* = 6.8), 3.61 (6H, *s*), 3.69 (1H, *m*), 3.77 (3H, *s*), 4.63 (2H, *s*), 6.15 (2H, *s*), 6.53 (2H, *d, J* = 9.2) 7.22 (5H, *bs*), 7.47 (2H, *d, J* = 9.2). ^{13}C NMR (100 MHz, $CDCl_3$): δ 22.6 ($2CH_3$), 43.9 (CH), 55.0 (CH_2), 55.9 ($2CH_3$), 60.8 (CH_3), 106.7 (2CH), 111.6 (2CH), 124.7 (C), 127.5 (CH), 128.2 (2CH), 128.6 (2CH), 130.0 (2CH), 135.2 (C), 136.4 (C), 137.5 (C), 150.9 (C), 152.7 (2C). HRMS ($C_{25}H_{30}N_2O_5S + H^+$): calcd 471.1948 ($M + H^+$), found 471.1942.

4-((4-(*N*-methyl-*N*-(3,4,5-trimethoxyphenyl)sulfamoyl)phenyl)amino)-4-oxobutanoic acid (**52**). A mixture of **27** (99 mg, 0.28 mmol), succinic anhydride (46.7 mg, 0.47 mmol) and pyridine (drops) in CH_2Cl_2 (50 mL) was heated at reflux for 72 h. After cooling, the mixture was washed with 2N HCl and brine, dried over anhydrous Na_2SO_4 and filtered. The solution was evaporated

to dryness and the residue was purified by preparative TLC (CH_2Cl_2/MeOH 9:1) to give **52** (45 mg, 0.10 mmol, 35%). IR (KBr): 3385, 2925, 1708, 1592, 830 cm^{-1}. ^1H NMR (400 MHz, CD_3OD): δ 2.63 (2H, *m*), 2.66 (2H, *m*), 3.18 (3H, *s*), 3.68 (6H, *s*), 3.73 (3H, *s*), 6.31 (2H, *s*), 7.51 (2H, *d, J* = 8.4), 7.74 (2H, *d, J* = 8.4). ^{13}C NMR (50 MHz, acetone-D_6): δ 28.9 (CH_2), 30.8 (CH_2), 38.7 (CH_3), 56.2 ($2CH_3$), 60.5 (CH_3), 105.6 (2CH), 119.2 (2CH), 129.9 (C), 130.0 (2CH), 131.3 (C), 138.3 (C), 153.9 (3C), 154.8 (C), 171.5 (C). HRMS ($C_{20}H_{24}N_2O_8S$ + Na^+): calcd 475.1143 (M + Na^+), found 475.1163.

4-Methoxy-3-nitrobenzenesulfonyl chloride (**53**).

*Compound **39** article 1. Available at Supplementary Material, Methods SP1.*
*Compound **86** article 3. Available at Materials and methods, chemical synthesis (2.1).*

4-Methoxy-3-nitro-*N*-(3,4,5-trimethoxyphenyl)benzenesulfonamide (**54**).

*Compound **40** article 1. Available at Supplementary Material, Methods SP1.*

3-Amino-4-methoxy-*N*-(3,4,5-trimethoxyphenyl)benzenesulfonamide (**55**).

*Compound **41** article 1. Available at Supplementary Material, Methods SP1.*

3-Amino-4-methoxy-*N*-methyl-*N*-(3,4,5-trimethoxyphenyl)benzenesulfonamide (**56**).

*Compound **42** article 1. Available at Supplementary Material, Methods SP1.*

3-Amino-*N*-ethyl-4-methoxy-*N*-(3,4,5-trimethoxyphenyl)benzenesulfonamide (**57**).

*Compound **43** article 1. Available at Supplementary Material, Methods SP1.*

3-Amino-*N*-(cyanomethyl)-4-methoxy-*N*-(3,4,5-trimethoxyphenyl)benzenesulfonamide (**58**).

*Compound **44** article 1. Available at Supplementary Material, Methods SP1.*

3-Amino-*N*-benzyl-4-methoxy-*N*-(3,4,5-trimethoxyphenyl)benzenesulfonamide (**59**).

*Compound **45** article 1. Available at Supplementary Material, Methods SP1.*

Ethyl (2-methoxy-5-(*N*-methyl-*N*-(3,4,5-trimethoxyphenyl)sulfamoyl)phenyl)glycinate (**60**).

*Compound **46** article 1. Available at Supplementary Material, Methods SP1.*

Ethyl (5-(*N*-(2-ethoxy-2-oxoethyl)-*N*-(3,4,5-trimethoxyphenyl)sulfamoyl)-2-methoxyphenyl) glycinate (**61**).

*Compound **47** article 1. Available at Supplementary Material, Methods SP1.*

4-Methoxy-*N*-methyl-3-(methylamino)-*N*-(3,4,5-trimethoxyphenyl)benzenesulfonamide (**62**) and 3-(dimethylamino)-4-methoxy-*N*-methyl-*N*-(3,4,5-trimethoxyphenyl) benzenesulfonamide (**63**).

*Compounds **48a** and **48b** article 1. Available at Supplementary Material, Methods SP1.*

N-(4-hydroxy-3,5-dimethoxy-2-nitrophenyl)-4-methoxybenzenesulfonamide (**64a**) and *N*-(3,5-dimethoxy-4-oxocyclohexa-2,5-dien-1-ylidene)-4-methoxybenzenesulfonamide (**64b**). To a solution of **1a** (2.23 g, 6.33 mmol) in CH_3CN (50 mL), *tert*-butyl nitrite (418 µL, 3.16 mmol) was added and stirred at 45 °C. After 1 h, additional 3.16 mmol *tert*-butyl nitrite was added to the reaction mixture and it was stirred at 45 °C for 24 h. The mixture was poured into ice and basified with 5% $NaHCO_3$ solution and extracted with EtOAc. The organic layers were washed with brine, dried over Na_2SO_4 and concentrated under vacuum. The residue was purified by silica gel column chromatography (hexane/EtOAc 6:4) to afford compounds **11** (907 mg, 2.28 mmol, 36%), **64a**

(260 mg, 0.68 mmol, 11%) and **64b** (719 mg, 2.13 mmol, 34%). **64a**: IR (KBr): 3435, 1595, 1508, 1154, 823 cm^{-1}. ^1H NMR (400 MHz, $CDCl_3$): δ 3.82 (3H, *s*), 3.90 (3H, *s*), 4.14 (3H, *s*), 6.93 (2H, *d*, *J* = 9.2), 7.15 (1H, *s*), 7.79 (2H, *d*, *J* = 9.2). ^{13}C NMR (100 MHz, $CDCl_3$): δ 55.7 (CH_3), 57.5 (CH_3), 61.6 (CH_3), 99.0 (CH), 114.3 (2CH), 129.6 (2CH), 131.1 (C), 145.4 (C), 155.5 (C), 156.1 (C), 163.7 (C), 176.2 (C). HRMS ($C_{15}H_{16}N_2O_8S + H^+$): calcd 385.0700 ($M + H^+$), found 385.0691. **64b**: M.p.: 170-171 °C (CH_2Cl_2/hexane). IR (KBr): 3435, 1693, 1639, 1586, 1251 cm^{-1}. ^1H NMR (400 MHz, $CDCl_3$): δ 3.80 (3H, *s*), 3.88 (3H, *s*), 3.93 (3H, *s*), 6.01 (1H, *d*, *J* = 2.4), 7.02 (2H, *d*, *J* = 9.2), 7.29 (1H, *d*, *J* = 2.4), 7.94 (2H, *d*, *J* = 9.2). ^{13}C NMR (100 MHz, $CDCl_3$): δ 55.7 (CH_3), 56.5 (CH_3), 56.9 (CH_3), 101.0 (CH), 110.5 (CH), 114.3 (2CH), 129.5 (2CH), 132.4 (C), 156.1 (C), 163.4 (2C), 165.0 (C), 175.5 (C). HRMS ($C_{15}H_{15}NO_6S + H^+$): calcd 338.0693 ($M + H^+$), found 338.0691.

N-(2-amino-4-hydroxy-3,5-dimethoxyphenyl)-4-methoxybenzenesulfonamide (**65**). The sulfonamide **64a** (1.18 g, 3.07 mmol) in ethyl acetate (100 mL) and Pd (C) (10 mg) was stirred at room temperature under H_2 atmosphere for 72 h. The reaction mixture was filtered through Celite®, and the filtrate was evaporated to dryness to give the title compound (**65,** 815 mg, 2.30 mmol, 75%). The crude reaction product was purified by crystallization in CH_2Cl_2 (430 mg, 1.21 mmol, 40%). M.p.: 165-168 °C (CH_2Cl_2). IR (KBr): 3429, 3334, 3256, 1598, 1476, 830 cm^{-1}. ^1H NMR (400 MHz, CD_3OD): δ 3.43 (3H, *s*), 3.76 (3H, *s*), 3.84 (3H, *s*), 5.75 (1H, *s*), 7.02 (2H, *d*, *J* = 8.8), 7.62 (2H, *d*, *J* = 8.8). ^{13}C NMR (100 MHz, CD_3OD): δ 54.8 (CH_3), 55.6 (CH_3), 58.7 (CH_3), 107.9 (CH), 112.7 (C), 113.6 (2CH), 129.5 (2CH), 130.6 (C), 133.2 (C), 136.4 (C), 139.7 (C), 140.2 (C), 163.2 (C). HRMS ($C_{15}H_{18}N_2O_6S + H^+$): calcd 355.0958 ($M + H^+$), found 355.0951.

N-(3-hydroxy-2,4-dimethoxy-6-((4-methoxyphenyl)sulfonamido)phenyl)acetamide (**66a**) and *N*-(2-acetamido-4-hydroxy-3,5-dimethoxyphenyl)-*N*-((4-methoxyphenyl)sulfonyl)acetamide (**66b**). A mixture of **65** (278 mg, 0.78 mmol) and acetic anhydride (89 µL, 0.94 mmol) in CH_2Cl_2 (50 mL) and pyridine (1 mL) was stirred at room temperature. After 24 h, the reaction mixture was poured onto ice and extracted with CH_2Cl_2, the organics were washed with 2N HCl, 5% $NaHCO_3$ and brine, dried over Na_2SO_4, filtered, and concentrated under vacuum. The residue (229 mg) was purified by flash column chromatography (hexane/EtOAc 7:3) to afford compounds **66a** (77 mg, 0.19 mmol, 25%) and **66b** (92 mg, 0.21 mmol, 27%). **66a**: M.p.: 159-160 °C (CH_2Cl_2/hexane). IR (KBr): 3304, 1651, 1596, 1499, 834 cm^{-1}. ^1H NMR (400 MHz, $CDCl_3$): δ 2.00 (3H, *s*), 3.79 (3H, *s*), 3.84 (3H, *s*), 3.90 (3H, *s*), 5.55 (1H, *s*), 6.82 (2H, *bs*), 6.85 (2H, *d*, *J* = 8.8), 7.52 (2H, *d*, *J* = 8.8), 8.03 (1H, *bs*). ^{13}C NMR (100 MHz, $CDCl_3$): δ 24.7 (CH_3), 56.7 (CH_3), 57.5 (CH_3), 61.9 (CH_3), 108.2 (CH), 114.9 (2CH), 120.9 (C), 123.2 (C), 130.1 (2CH), 133.4 (C), 138.4 (C), 140.0 (C), 146.9 (C), 163.9 (C), 170.6 (C). HRMS ($C_{17}H_{20}N_2O_7S + H^+$): calcd 397.1064 ($M + H^+$), found 397.1049. **66b**: M.p.: 169-170 °C (CH_2Cl_2/hexane). ^1H NMR (400 MHz, $CDCl_3$): δ 2.06 (3H, *s*), 2.33 (3H, *s*), 3.70 (3H, *s*), 3.79 (3H, *s*), 3.84 (3H, *s*), 6.87 (2H, *d*, *J* = 9.2), 6.89 (1H, *s*), 7.61 (2H, *d*, *J* = 9.2), 8.22 (1H, *bs*). ^{13}C NMR (100 MHz, $CDCl_3$): δ 20.4 (CH_3), 23.5 (CH_3), 55.6 (CH_3), 56.3 (CH_3), 61.3 (CH_3), 106.1 (CH), 113.9 (2CH), 118.3 (C), 129.0 (2CH), 129.1 (C), 132.1 (C), 140.4 (C), 145.4 (C), 150.6 (C), 163.7 (C), 169.7 (C), 170.9 (C). HRMS ($C_{19}H_{22}N_2O_8S + H^+$): calcd 439.1170 ($M + H^+$), found 439.1168.

N-(2-amino-4-hydroxy-3,5-dimethoxyphenyl)-4-methoxy-*N*-methylbenzenesulfonamide (**67**). To a mixture of **65** (200 mg, 0.56 mmol), NaOH (26 mg, 1.12 mmol) and $nBu_4N^+HSO_4^-$ (224 mg, 1.12 mmol) in CH_2Cl_2 (100 mL), CH_3I (71 µL, 1.12 mmol) was added. The reaction was stirred at room temperature under nitrogen atmosphere for 72 h. The solution was poured onto brine, extracted with CH_2Cl_2, and then dried over Na_2SO_4. After concentration, the residue (211 mg) was purified by preparative TLC (CH_2Cl_2/MeOH, 97:3) to give **67** (112 mg, 0.30 mmol, 54%). IR (KBr): 3460, 1595, 1499, 1154, 911 cm^{-1}. ^1H NMR (400 MHz, $CDCl_3$): δ 3.08 (3H, *s*), 3.47 (3H, *s*),

3.84 (3H, *s*), 3.85 (3H, *s*), 5.66 (1H, *s*), 6.95 (2H, *d*, *J* = 8.8), 7.63 (2H, *d*, *J* = 8.8). ^{13}C NMR (100 MHz, $CDCl_3$): δ 38.9 (CH_3), 55.6 (CH_3), 56.5 (CH_3), 59.9 (CH_3), 105.7 (CH), 113.9 (2CH), 117.9 (C), 128.7 (C), 130.3 (2CH), 134.9 (C), 135.4 (C), 139.0 (C), 139.4 (C), 163.1 (C). HRMS ($C_{16}H_{20}N_2O_6S$ + H^+): calcd 369.1115 (M + H^+), found 369.1108.

4,6-Dimethoxy-1-((4-methoxyphenyl)sulfonyl)-1*H*-benzo[*d*]imidazol-5-ol (**68**). A mixture of **65** (160 mg, 0.45 mmol) and triethyl orthoformate (92 µL, 0.54 mmol) in CH_3CN (25 mL) was heated at reflux for 24 h. The CH_3CN was removed under reduced pressure and the residue was washed with brine, extracted with EtOAc, and dried over Na_2SO_4. After concentration, the residue (170 mg) was purified by flash column chromatography (hexane/EtOAc 6:4) to isolate compound **68** (115 mg, 0.31 mmol, 70%). ^{1}H NMR (400 MHz, $CDCl_3$): δ 3.79 (3H, *s*), 3.93 (3H, *s*), 4.26 (3H, *s*), 6.92 (2H, *d*, *J* = 8.8), 7.04 (1H, *s*), 7.85 (2H, *d*, *J* = 8.8), 8.14 (1H, *s*). ^{13}C NMR (100 MHz, $CDCl_3$): δ 55.8 (CH_3), 56.7 (CH_3), 61.1 (CH_3), 89.4 (CH), 114.8 (2CH), 124.8 (C), 128.6 (C), 129.3 (2CH), 129.9 (C), 134.6 (C), 137.7 (C), 138.7 (CH), 147.2 (C), 164.5 (C). HRMS ($C_{16}H_{16}N_2O_6S$ + H^+): calcd 365.0802 (M + H^+), found 365.0799.

N-(3,5-dimethoxyphenyl)-4-methoxybenzenesulfonamide (**69**).

*Compound **1** article 2. Available at Materials and methods, chemical synthesis.*
*Compound **259** article 3. Available at Materials and methods, chemical synthesis (2.1).*

N-(3,5-dimethoxyphenyl)-4-methoxy-*N*-methylbenzenesulfonamide (**70**).

*Compound **2** article 2. Available at Materials and methods, chemical synthesis.*

N-(3,5-dimethoxyphenyl)-*N*-ethyl-4-methoxybenzenesulfonamide (**71**).

*Compound **3** article 2. Available at Materials and methods, chemical synthesis.*

N-(cyanomethyl)-*N*-(3,5-dimethoxyphenyl)-4-methoxybenzenesulfonamide (**72**).

*Compound **4** article 2. Available at Materials and methods, chemical synthesis.*

Ethyl *N*-(3,5-dimethoxyphenyl)-*N*-((4-methoxyphenyl)sulfonyl)glycinate (**73**).

*Compound **5** article 2. Available at Materials and methods, chemical synthesis.*

N-benzyl-*N*-(3,5-dimethoxyphenyl)-4-methoxybenzenesulfonamide (**74**).

*Compound **6** article 2. Available at Materials and methods, chemical synthesis.*
*Compound **270** article 3. Available at Materials and methods, chemical synthesis (2.1).*

Benzyl (3,5-dimethoxyphenyl)((4-methoxyphenyl)sulfonyl)carbamate (**75**).

*Compound **7** article 2. Available at Materials and methods, chemical synthesis.*

N-(3,5-dimethoxyphenyl)-4-nitrobenzenesulfonamide (**76**).

*Compound **242** article 3. Available at Materials and methods, chemical synthesis (2.1).*

4-amino-*N*-(3,5-dimethoxyphenyl)benzenesulfonamide (**77**).

*Compound **245** article 3. Available at Materials and methods, chemical synthesis (2.1).*

N-(3,5-dimethoxyphenyl)-4-(dimethylamino)benzenesulfonamide (**254**).

*Compound **254** article 3. Available at Materials and methods, chemical synthesis (2.1).*

N-(3,5-dimethoxyphenyl)-4-(dimethylamino)-*N*-methylbenzenesulfonamide (**79**). To a solution of **78** (100 mg, 0.29 mmol) in CH_3CN (25 mL), crushed KOH (33 mg, 0.59 mmol) was added and stirred for 30 min. Then, CH_3I (37 µL, 0.59 mmol) was added. After 24 h, CH_3CN was evaporated and the residue was re-dissolved in EtOAc. The solution was washed with brine, dried over Na_2SO_4, filtered, and evaporated to dryness to afford crude product **79** (96 mg, 0.27 mmol, 92%). Compound **79** was purified by preparative TLC in hexane/EtOAc 1:1 (63 mg, 0.18 mmol, 61%).^{1}H NMR (400 MHz, $CDCl_3$): δ 3.01 (6H, *s*), 3.08 (3H, *s*), 3.71 (6H, *s*), 6.29 (2H, *d*, *J* = 2.4), 6.33 (1H, *t*, *J* = 2.4), 6.59 (2H, *d*, *J* = 9.2), 7.40 (2H, *d*, *J* = 9.2). ^{13}C NMR (100 MHz, $CDCl_3$): δ 38.0 (CH_3), 40.0 ($2CH_3$), 55.4 ($2CH_3$), 99.2 (CH), 104.9 (2CH), 110.5 (2CH), 121.7 (C), 129.6 (2CH), 144.0 (C), 152.9 (C), 160.4 (2C). HRMS ($C_{17}H_{22}N_2O_4S + H^+$): calcd 351.1373 ($M + H^+$), found 351.1372.

N-(3,5-dimethoxyphenyl)-4-(dimethylamino)-*N*-ethylbenzenesulfonamide (**80**). A solution of **78** (90 mg, 0.27 mmol) and K_2CO_3 (73 mg, 0.54 mmol) in DMF (3 mL) was stirred for 30 min. Then, 2-bromoethano (40 µL, 0.54 mmol) was added to the solution and was stirred for 24 h. The solution was concentrated in vacuo and re-dissolved with EtOAc. Then, it was washed with brine, dried over Na_2SO_4 and evaporated to dryness to give 92 mg (0.25 mmol, 94%) of **80**. Crude product was purified by crystallization in methanol (56 mg, 0.15 mmol, 57%). M.p.: 114-117 °C (MeOH). IR (KBr): 3435, 1595, 1194, 825 cm^{-1}. ^{1}H NMR (400 MHz, $CDCl_3$): δ 1.05 (3H, *t*, *J* = 7.2), 3.02 (6H, *s*), 3.50 (2H, *q*, *J* = 7.2), 3.71 (6H, *s*), 6.24 (2H, *d*, *J* = 2.4), 6.38 (1H, *t*, *J* = 2.4), 6.61 (2H, *d*, *J* = 9.2), 7.47 (2H, *d*, *J* = 9.2). ^{13}C NMR (100 MHz, $CDCl_3$): δ 13.9 (CH_3), 40.0 ($2CH_3$), 45.3 (CH_2), 55.4 ($2CH_3$), 100.0 (CH), 107.1 (2CH), 110.5 (2CH), 123.8 (C), 129.5 (2CH), 141.3 (C), 152.7 (C), 160.5 (2C). HRMS ($C_{18}H_{24}N_2O_4S + H^+$): calcd 365.1530 ($M + H^+$), found 365.1525.

N-(cyanomethyl)-*N*-(3,5-dimethoxyphenyl)-4-(dimethylamino)benzenesulfonamide (**81**). A mixture of **78** (90 mg, 0.27 mmol) and K_2CO_3 (73 mg, 0.54 mmol) in dry DMF (3 mL) was stirred at room temperature for 30 min. Then, 2-chloroacetonitrile (34 µL, 0.54 mmol) was added. After 24 h, the solvent was evaporated under reduced pressure. The residue was dissolved in EtOAc and washed with brine, dried (Na_2SO_4) and concentrated in vacuo to afford 62 mg. Compound **81** was isolated by preparative TLC (CH_2Cl_2/MeOH 98:2) (20 mg, 0.05 mmol, 20%). ^{1}H NMR (400 MHz, $CDCl_3$): δ 3.04 (6H, *s*), 3.71 (6H, *s*), 4.49 (2H, *s*), 6.38 (2H, *d*, *J* = 2.4), 6.41 (1H, *t*, *J* = 2.4), 6.62 (2H, *d*, *J* = 9.6), 7.53 (2H, *d*, *J* = 9.6). ^{13}C NMR (100 MHz, $CDCl_3$): δ 39.3 (CH_2), 40.0 ($2CH_3$), 55.5 ($2CH_3$), 101.1 (CH), 106.0 (2CH), 110.6 (2CH), 115.2 (C), 122.0 (C), 129.9 (2CH), 140.7 (C), 153.3 (C), 160.9 (2C). HRMS ($C_{18}H_{21}N_3O_4S + H^+$): calcd 376.1326 ($M + H^+$), found 376.1320.

Ethyl *N*-(3,5-dimethoxyphenyl)-*N*-((4-(dimethylamino)phenyl)sulfonyl)glycinate (**82**). Ethyl 2-bromoacetate (66 µL, 0.60 mmol) was added, after 30 min, to a stirred mixture of compound **78** (100 mg, 0.30 mmol) and K_2CO_3 (83 mg, 0.60 mmol) in dry DMF (3 mL). After 24 h, the solvent was evaporated under reduced pressure and the residue was dissolved in EtOAc, washed with brine, dried over anhydrous Na_2SO_4, filtered and concentrated in vacuum to afford 123 mg (0.29 mmol, 98%) of crude reaction product **82**, from which, 66 mg (0.16 mmol, 52%) were purified by crystallization in methanol. M.p.: 96-97 °C (MeOH). ^{1}H NMR (400 MHz, $CDCl_3$): δ 1.21 (3H, *t*, *J* = 7.2), 3.00 (6H, *s*), 3.68 (6H, *s*), 4.14 (2H, *q*, *J* = 7.2), 4.32 (2H, *s*), 6.33 (1H, *t*, *J* = 2), 6.37 (2H, *d*, *J* = 2), 6.58 (2H, *d*, *J* = 9.2), 7.53 (2H, *d*, *J* = 9.2). ^{13}C NMR (100 MHz, $CDCl_3$): δ 14.0 (CH_3), 40.0 ($2CH_3$), 52.5 (CH_2), 55.4 ($2CH_3$), 61.3 (CH_2), 100.1 (CH), 106.2 (2CH), 110.5 (2CH), 123.8 (C), 129.7 (2CH), 142.2 (C), 152.9 (C), 160.6 (2C), 168.9 (C). HRMS ($C_{20}H_{26}N_2O_6S + H^+$): calcd 423.1584 ($M + H^+$), found 423.1582.

N-benzyl-*N*-(3,5-dimethoxyphenyl)-4-(dimethylamino)benzenesulfonamide (**83**).

*Compound **275** article 3. Available at Materials and methods, chemical synthesis (2.1).*

N-(4-(*N*-(3,5-dimethoxyphenyl)sulfamoyl)phenyl)formamide (**84**). Sulfonamide **77** (855 mg, 2.77 mmol) was dissolved in CH_2Cl_2 (50 mL) and pyridine (1 mL). 10 mL of formic acid were added and stirred at room temperature for 48 h. The reaction mixture was washed with 2N HCl, 5% $NaHCO_3$

and brine, dried over anhydrous Na_2SO_4 and concentrated in vacuo to afford 780 mg (2.32 mmol, 83%) of **84**. Crude reaction product was purified by column chromatography in hexane/EtOAc 6:4 (624 mg, 1.86 mmol, 67%). IR (KBr): 2923, 1708, 1596, 1155, 835 cm^{-1}. ^1H NMR (400 MHz, CD_3OD): δ 3.66 (6H, *s*), 6.15 (1H, *t*, *J* = 2), 6.26 (2H, *d*, *J* = 2), 6.68 (2H, *d*, *J* = 9.2), 7.73 (2H, *d*, *J* = 9.2), 8.28 (1H, *s*). ^{13}C NMR (100 MHz, acetone-D_6): δ 54.7 ($2CH_3$), 95.7 (CH), 98.4 (2CH), 119.0 (2CH), 128.4 (2CH), 134.4 (C), 139.7 (C), 142.2 (C), 159.6 (CH), 161.3 (2C). HRMS ($C_{15}H_{16}N_2O_5S$ + H^+): calcd 337.0853 (M + H^+), found 337.0854.

N-(3,5-dimethoxyphenyl)-4-(methylamino)benzenesulfonamide (**85**). To a solution of **84** (560 mg, 1.66 mmol) and $NaBH_4$ (94 mg, 2.49 mmol) in dry THF (10 mL) at 0 °C, trichloroacetic acid (408 mg, 2.49 mmol) diluted in dry THF (2 mL) was dropwise added under nitrogen atmosphere. The reaction mixture was stirred at 0 °C to room temperature for 24 h, concentrated and re-dissolved in EtOAc, washed with brine, dried over anhydrous Na_2SO_4, filtered and solvent evaporated in vacuum to afford 516 mg (1.60 mmol, 96%) of crude reaction product. Compound **85** was then purified by flash column chromatography (toluene/EtOAc 8:2) (345 mg, 1.07 mmol, 64%). ^1H NMR (400 MHz, $CDCl_3$): δ 2.85 (3H, *s*), 3.71 (6H, *s*), 4.23 (1H, *bs*), 6.16 (1H, *t*, *J* = 2), 6.22 (2H, *d*, *J* = 2), 6.46 (1H, *bs*), 6.50 (2H, *d*, *J* = 8.8), 7.60 (2H, *d*, *J* = 8.8). ^{13}C NMR (100 MHz, CD_3OD): δ 28.4 (CH_3), 54.3 ($2CH_3$), 95.5 (CH), 98.1 (2CH), 110.3 (2CH), 124.3 (C), 128.8 (2CH), 139.9 (C), 153.5 (C), 161.1 (2C). HRMS ($C_{15}H_{18}N_2O_4S$ + H^+): calcd 323.1060 (M + H^+), found 323.1063.

N-(3,5-dimethoxyphenyl)-*N*-methyl-4-(methylamino)benzenesulfonamide (**86**). To a stirred solution of **85** (80 mg, 0.25 mmol) in CH_3CN (40 mL), 28 mg (0.50 mmol) of KOH were added. After 30 min at room temperature, CH_3I (31 µL, 0.50 mmol) was added. The solution was stirred for 24 h; then the mixture was evaporated to dryness. The residue was dissolved with EtOAc and washed with brine, dried over Na_2SO_4, filtered, and evaporated to dryness. The residue (80 mg) was purified by preparative TLC (CH_2Cl_2/MeOH 98:2) to isolate compound **86** (60 mg, 0.18 mmol, 72%). ^1H NMR (400 MHz, CD_3OD): δ 2.79 (3H, *s*), 3.07 (3H, *s*), 3.68 (6H, *s*), 6.23 (2H, *d*, *J* = 2), 6.37 (1H, *t*, *J* = 2), 6.56 (2H, *d*, *J* = 8.4), 7.28 (2H, *d*, *J* = 8.4). ^{13}C NMR (100 MHz, $CDCl_3$): δ 29.9 (CH_3), 38.0 (CH_3), 55.4 ($2CH_3$), 99.2 (CH), 104.9 (2CH), 110.9 (2CH), 122.5 (C), 129.8 (2CH), 143.9 (C), 152.7 (C), 160.4 (2C). HRMS ($C_{16}H_{20}N_2O_4S$ + Na^+): calcd 359.1036 (M + Na^+), found 359.1031.

N-(3,5-dimethoxyphenyl)-*N*-ethyl-4-(methylamino)benzenesulfonamide (**87**). 50 mg (0.15 mmol) of compound **85** were dissolved in CH_3CN (50 mL) and 21 mg (0.30 mmol) of crushed KOH were added. After 30 min stirring at room temperature, 46.3 µL (0.60 mmol) of bromoethane were added to the solution. The reaction mixture was stirred at room temperature for 72 h. The mixture was evaporated to dryness. The residue was diluted with water, and the solution was extracted with EtOAc. The extract was dried over Na_2SO_4 and evaporated to dryness. The residue (43 mg) was purified by preparative TLC (CH_2Cl_2/MeOH 98:2) to give 16 mg (0.05 mmol, 29%) of compound **87**. ^1H NMR (400 MHz, CD_3OD): δ 1.02 (3H, *t*, *J* = 7.2), 2.80 (3H, *s*), 3.51 (2H, *q*, *J* = 7.2), 3.67 (6H, *s*), 6.17 (2H, *d*, *J* = 2.4), 6.41 (1H, *t*, *J* = 2.4), 6.58 (2H, *d*, *J* = 8.4), 7.33 (2H, *d*, *J* = 8.4). ^{13}C NMR (100 MHz, $CDCl_3$): δ 13.9 (CH_3), 30.1 (CH_3), 45.3 (CH_2), 55.4 ($2CH_3$), 100.0 (CH), 107.1 (2CH), 111.0 (2CH), 124.9 (C), 129.8 (2CH), 141.2 (C), 152.4 (C), 160.5 (2C). HRMS ($C_{17}H_{22}N_2O_4S$ + H^+): calcd 351.1373 (M + H^+), found 351.1367.

Ethyl *N*-(3,5-dimethoxyphenyl)-*N*-((4-(methylamino)phenyl)sulfonyl)glycinate (**88**). A mixture of **85** (70 mg, 0.21 mmol) and K_2CO_3 (59 mg, 0.43 mmol) in dry DMF (3 mL), was stirred for 1 h. Then, ethyl 2-bromoacetate (48 µL, 0.43 mmol) was added. After 24 h, the reaction mixture was concentrated under reduced pressure, diluted with EtOAc, washed with brine, dried (Na_2SO_4), filtered, and concentrated in vacuo. Crude residue (82 mg) was purified by preparative TLC (hexane/EtOAc 1:1) (**88**, 61 mg, 0.15 mmol, 68%). ^1H NMR (400 MHz, CD_3OD): δ 1.22 (3H, *t*, *J* = 7.2), 2.79 (3H, *s*), 3.65 (6H, *s*), 4.14 (2H, *q*, *J* = 7.2), 4.35 (2H, *s*), 6.32 (2H, *d*, *J* = 2.4), 6.37 (1H, *t*, *J* = 2.4), 6.57 (2H, *d*, *J* = 9.2), 7.41 (2H, *d*, *J* = 9.2). ^{13}C NMR (100 MHz, $CDCl_3$): δ 14.1 (CH_3), 30.0 (CH_3), 52.5 (CH_2), 55.4 ($2CH_3$), 61.3 (CH_2), 100.1 (CH), 106.2 (2CH), 110.9 (2CH), 125.0 (C), 129.9

(2CH), 142.1 (C), 152.7 (C), 160.6 (2C), 168.9 (C). HRMS ($C_{19}H_{24}N_2O_6S + H^+$): calcd 409.1428 (M + H^+), found 409.1427.

N-(4-(*N*-(3,5-dimethoxyphenyl)sulfamoyl)phenyl)-*N*-methylformamide (**89**). 124 mg of **85** (0.38 mmol) were dissolved in CH_2Cl_2 (50 mL), pyridine (1 mL) and formic acid (5 mL) and stirred at room temperature. After 48 h, the reaction mixture was poured onto ice and treated with 2N HCl and 5% $NaHCO_3$. Organic layers were washed to neutrality with brine, dried over anhydrous Na_2SO_4, filtered, and evaporated to dryness to afford 109 mg (0.31 mmol, 81%) of **89**. The crude reaction product was purified by crystallization in methanol (55 mg, 0.16 mmol, 41%). M.p.: 151-153 °C (MeOH). ^{1}H NMR (400 MHz, CD_3OD): δ 3.30 (3H, *s*), 3.67 (6H, *s*), 6.16 (1H, *t*, *J* = 2.4), 6.28 (2H, *d*, *J* = 2.4), 7.43 (2H, *d*, *J* = 8.8), 7.85 (2H, *d*, *J* = 8.8), 8.63 (1H, *s*). ^{13}C NMR (100 MHz, $CDCl_3$): δ 31.4 (CH_3), 55.4 ($2CH_3$), 97.0 (CH), 99.1 (2CH), 120.8 (2CH), 129.0 (2CH), 136.1 (C), 138.2 (C), 145.9 (C), 161.2 (2C), 161.9 (CH). HRMS ($C_{16}H_{18}N_2O_5S + Na^+$): calcd 373.0829 (M + Na^+), found 373.0820.

N-(3,5-dimethoxyphenyl)-4-methoxy-3-nitrobenzenesulfonamide (**90**). To 291 mg of 3,5-dimethoxyaniline (1.89 mmol) in CH_2Cl_2 (50 mL) and pyridine (2 mL), 525 mg of the sulfonyl chloride **53** was slowly added (2.08 mmol) and stirred at room temperature for 6 h. The reaction was treated with 2N HCl and 5% $NaHCO_3$, washed with brine, dried over anhydrous Na_2SO_4 and the solvent evaporated to obtain 590 mg (1.60 mmol, 84%) of **90**. Crude reaction product was then purified by flash column chromatography (hexane/EtOAc 1:1) to afford 551 mg (1.49 mmol, 79%). ^{1}H NMR (400 MHz, $CDCl_3$): δ 3.69 (6H, *s*), 3.97 (3H, *s*), 6.18 (1H, *t*, *J* = 2.4), 6.29 (2H, *d*, *J* = 2.4), 7.12 (1H, *d*, *J* = 9.2), 7.51 (1H, *bs*), 7.97 (1H, *dd*, *J* = 9.2 and 2.4), 8.31 (1H, *d*, *J* = 2.4). ^{13}C NMR (100 MHz, $CDCl_3$): δ 55.4 ($2CH_3$), 57.1 (CH_3), 97.5 (CH), 99.4 (2CH), 114.0 (CH), 125.4 (CH), 130.7 (C), 133.1 (CH), 137.7 (C), 138.8 (C), 156.1 (C), 161.3 (2C). HRMS ($C_{15}H_{16}N_2O_7S + H^+$): calcd 369.0751 (M + H^+), found 369.0759.

3-Amino-*N*-(3,5-dimethoxyphenyl)-4-methoxybenzenesulfonamide (**91**). The nitro sulfonamide **90** (500 mg, 1.36 mmol) in ethyl acetate (125 mL) and Pd (C) (10 mg) was stirred at room temperature under H_2 atmosphere for 72 h. The reaction mixture was filtered through Celite® and the filtrate was evaporated to dryness to afford the amine sulfonamide **91** (446 mg, 1.31 mmol, 97%), which was purified by column chromatography (hexane/EtOAc 1:1) (416 mg, 1.23 mmol, 90%). IR (KBr): 3479, 3259, 1602, 1506, 1145, 830 cm^{-1}. ^{1}H NMR (200 MHz, $CDCl_3$): δ 3.69 (6H, *s*), 3.86 (3H, *s*), 6.16 (1H, *t*, *J* = 2.4), 6.25 (2H, *d*, *J* = 2.4), 6.73 (1H, *d*, *J* = 8.6), 6.81 (1H, *bs*), 7.13 (1H, *d*, *J* = 2.2), 7.21 (1H, *dd*, *J* = 8.6 and 2.2). ^{13}C NMR (100 MHz, $CDCl_3$): δ 55.3 ($2CH_3$), 55.6 (CH_3), 96.8 (CH), 98.6 (2CH), 109.4 (CH), 112.5 (CH), 118.7 (CH), 130.6 (C), 136.8 (C), 138.8 (C), 150.6 (C), 161.0 (2C). HRMS ($C_{15}H_{18}N_2O_5S + H^+$): calcd 339.1009 (M + H^+), found 339.1005.

3-Amino-*N*-(3,5-dimethoxyphenyl)-4-methoxy-*N*-methylbenzenesulfonamide (**92**). A mixture of **91** (88 mg, 0.26 mmol) and KOH (29 mg, 0.52 mmol) in CH_3CN (50 mL) was stirred for 30 min. Then, CH_3I (32.5 µL, 0.52 mmol) was added and stirred overnight at room temperature. The solvent was removed under reduced pressure. The residue was dissolved in EtOAc and washed with brine, dried (Na_2SO_4) and concentrated in vacuum to afford 74 mg (0.21 mmol, 80%) of **92**. The crude product was purified by crystallization in methanol (52 mg, 0.15 mmol, 56%). M.p.: 134-138 °C (MeOH). ^{1}H NMR (200 MHz, $CDCl_3$): δ 3.11 (3H, *s*), 3.73 (3H, *s*), 3.90 (3H, *s*), 6.30 (2H, *d*, *J* = 2.4), 6.35 (1H, *t*, *J* = 2.4), 6.77 (1H, *d*, *J* = 8.2), 6.90 (1H, *d*, *J* = 2.4), 6.98 (1H, *dd*, *J* = 8.2 and 2.4). ^{13}C NMR (100 MHz, $CDCl_3$): δ 38.2 (CH_3), 55.4 ($2CH_3$), 55.7 (CH_3), 99.4 (CH), 105.0 (2CH), 109.3 (CH), 113.3 (CH), 118.9 (CH), 128.4 (C), 136.4 (C), 143.7 (C), 150.3 (C), 160.4 (2C). HRMS ($C_{16}H_{20}N_2O_5S + H^+$): calcd 353.1166 (M + H^+), found 353.1162.

3-Amino-*N*-(3,5-dimethoxyphenyl)-*N*-ethyl-4-methoxybenzenesulfonamide (**93**). 81 mg (0.24 mmol) of **91** and 66 mg (0.48 mmol) of K_2CO_3 were mixed in dry DMF (3 mL). After 30 min stirring at room temperature, bromoethane (36 µL, 0.48 mmol) was added to the mixture and stirred 48 h. The reaction mixture was concentrated, re-dissolved in EtOAc, washed with brine, dried

over anhydrous Na_2SO_4, filtered, and concentrated in vacuum to obtain 72 mg (0.19 mmol, 82%) of **93** and crystalized in methanol (53 mg, 0.14 mmol, 60%). M.p.: 129-134 °C (MeOH). ^{1}H NMR (200 MHz, $CDCl_3$): δ 1.06 (3H, *t*, *J* = 7.2), 3.52 (2H, *q*, *J* = 7.2), 3.72 (6H, *s*), 3.90 (3H, *s*), 6.24 (2H, *d*, *J* = 2.2), 6.39 (1H, *t*, *J* = 2.2), 6.78 (1H, *d*, *J* = 8.4), 6.97 (1H, *d*, *J* = 2.2), 7.06 (1H, *dd*, *J* = 8.4 and 2.2). ^{13}C NMR (100 MHz, $CDCl_3$): δ 13.9 (CH_3), 45.5 (CH_2), 55.3 ($2CH_3$), 55.7 (CH_3), 100.2 (CH), 107.1 (2CH), 109.3 (CH), 113.2 (CH), 118.7 (CH), 130.2 (C), 136.4 (C), 140.9 (C), 150.2 (C), 160.5 (2C). HRMS ($C_{17}H_{22}N_2O_5S + H^+$): calcd 367.1322 ($M + H^+$), found 367.1320.

3-Amino-*N*-(cyanomethyl)-*N*-(3,5-dimethoxyphenyl)-4-methoxybenzenesulfonamide (**94**). A mixture of **91** (69 mg, 0.20 mmol) and K_2CO_3 (56 mg, 0.41 mmol) in dry DMF (3 mL) was stirred at room temperature for 30 min. Then, 2-chloroacetonitrile (26 µL, 0.41 mmol) was added. After 24 h, the solvent was evaporated under reduced pressure. The residue was dissolved in EtOAc and washed with brine, dried (Na_2SO_4) and concentrated in vacuo to afford 74 mg (0.19 mmol, 96%) of **94**. The title compound was purified by preparative TLC (hexane/EtOAc 1:1) (59 mg, 0.16 mmol, 76%). ^{1}H NMR (200 MHz, $CDCl_3$): δ 3.71 (6H, *s*), 3.89 (3H, *s*), 4.49 (2H, *s*), 6.35 (2H, *d*, *J* = 2.4), 6.42 (1H, *t*, *J* = 2.4), 6.79 (1H, *d*, *J* = 8.6), 6.99 (1H, *d*, *J* = 2.4), 7.10 (1H, *dd*, *J* = 8.6 and 2.4). ^{13}C NMR (100 MHz, $CDCl_3$): δ 39.5 (CH_2), 55.5 ($2CH_3$), 55.8 (CH_3), 101.3 (CH), 106.1 (2CH), 109.5 (CH), 112.8 (CH), 115.1 (C), 119.0 (CH), 128.9 (C), 136.9 (C), 140.3 (C), 150.9 (C), 161.0 (2C). HRMS ($C_{17}H_{19}N_3O_5S + H^+$): calcd 378.1118 ($M + H^+$), found 378.1113.

Ethyl *N*-((3-amino-4-methoxyphenyl)sulfonyl)-*N*-(3,5-dimethoxyphenyl)glycinate (**95a**) and ethyl *N*-(3,5-dimethoxyphenyl)-*N*-((3-((2-ethoxy-2-oxoethyl)amino)-4-methoxyphenyl)sulfonyl)glycinate (**95b**). A mixture of **91** (87 mg, 0.25 mmol) and K_2CO_3 (70 mg, 0.51 mmol) in dry DMF (3 mL), was stirred for 1 h. Then, ethyl 2-bromoacetate (57 µL, 0.51 mmol) was added. After 24 h, the reaction mixture was concentrated under reduced pressure, diluted with EtOAc, washed with brine, dried (Na_2SO_4), filtered, and concentrated in vacuo. The residue (108 mg) was then purified by preparative TLC (CH_2Cl_2/MeOH 98:2) to afford compounds **95a** (63 mg, 0.15 mmol, 58%) and **95b** (20 mg, 0.04 mmol, 15%). **95a**: ^{1}H NMR (200 MHz, $CDCl_3$): δ 1.22 (3H, *t*, *J* = 7), 3.70 (6H, *s*), 3.90 (3H, *s*), 4.15 (2H, *q*, *J* = 7), 4.32 (2H, *s*), 6.37 (3H, *bs*), 6.76 (1H, *d*, *J* = 8.2), 7.03 (1H, *d*, *J* = 2.4), 7.10 (1H, *dd*, *J* = 8.2 and 2.4). ^{13}C NMR (100 MHz, $CDCl_3$): δ 14.1 (CH_3), 52.5 (CH_2), 55.4 ($2CH_3$), 55.7 (CH_3), 61.3 (CH_2), 100.3 (CH), 106.4 (2CH), 109.3 (CH), 113.1 (CH), 118.9 (CH), 130.4 (C), 136.5 (C), 141.8 (C), 150.4 (C), 160.6 (2C), 168.8 (C). HRMS ($C_{19}H_{24}N_2O_7S + H^+$): calcd 425.1377 ($M + H^+$), found 425.1370. **95b**: IR (KBr): 3421, 1736, 1590, 1022, 843 cm^{-1}. ^{1}H NMR (200 MHz, $CDCl_3$): δ 1.22 (3H, *t*, *J* = 7.2), 1.30 (3H, *t*, *J* = 7.2), 3.70 (6H, *s*), 3.84 (2H, *s*), 3.91 (3H, *s*), 4.15 (2H, *q*, *J* = 7.2), 4.25 (2H, *q*, *J* = 7.2), 4.32 (2H, *s*), 6.36 (3H, *bs*), 6.73 (1H, *d*, *J* = 2.4), 6.75 (1H, *d*, *J* = 8.6), 7.11 (1H, *dd*, *J* = 8.6 and 2.4). ^{13}C NMR (100 MHz, $CDCl_3$): δ 14.0 (CH_3), 14.1 (CH_3), 45.1 (CH_2), 52.5 (CH_2), 55.4 ($2CH_3$), 55.7 (CH_3), 61.3 (CH_2), 61.4 (CH_2), 100.3 (CH), 106.4 (2CH), 108.3 (2CH), 118.2 (CH), 130.6 (C), 137.1 (C), 141.9 (C), 150.2 (C), 160.6 (2C), 168.7 (C), 170.4 (C). HRMS ($C_{23}H_{30}N_2O_9S + H^+$): calcd 511.1745 ($M + H^+$), found 511.1738.

3-Amino-*N*-benzyl-*N*-(3,5-dimethoxyphenyl)-4-methoxybenzenesulfonamide (**96**). A solution of **91** (78 mg, 0.23 mmol) and K_2CO_3 (63 mg, 0.46 mmol) in dry DMF (3 mL) was stirred for 30 min. Benzyl chloride (80 µL, 0.69 mmol) was added to the solution and stirred for 48 h. Reaction mixture was concentrated under vacuum, re-dissolved in EtOAc and washed with brine, dried (Na_2SO_4), filtered, and evaporated to dryness to give **96** (76 mg, 0.18 mmol, 77%). Crude reaction product was purified by crystallization in methanol (51 mg, 0.12 mmol, 51%). M.p.: 166-170 °C (MeOH). ^{1}H NMR (400 MHz, $CDCl_3$): δ 3.62 (6H, *s*), 3.90 (3H, *s*), 4.65 (2H, *s*), 6.16 (2H, *d*, *J* = 2.4), 6.28 (1H, *t*, *J* = 2.4), 6.80 (1H, *d*, *J* = 8), 7.00 (1H, *d*, *J* = 2), 7.09 (1H, *dd*, *J* = 8 and 2), 7.21 (5H, *m*). ^{13}C NMR (100 MHz, $CDCl_3$): δ 54.7 (CH_2), 55.3 ($2CH_3$), 55.7 (CH_3), 100.1 (CH), 107.1 (2CH), 109.4 (CH), 113.1 (CH), 118.8 (CH), 127.4 (CH), 128.2 (2CH), 128.5 (2CH), 130.5 (C), 136.2 (C), 136.5 (C), 141.1 (C), 150.3 (C), 160.3 (2C). HRMS ($C_{22}H_{24}N_2O_5S + H^+$): calcd 429.1479 ($M + H^+$), found 429.1476.

N-(4-bromo-3,5-dimethoxyphenyl)-4-methoxy-*N*-methylbenzenesulfonamide (**97a**) and *N*-(2-bromo-3,5-dimethoxyphenyl)-4-methoxy-*N*-methylbenzenesulfonamide (**97b**).

*Compounds **8a** and **8b** article 2. Available at Materials and methods, chemical synthesis.*

N-(4-bromo-3,5-dimethoxyphenyl)-*N*-ethyl-4-methoxybenzenesulfonamide (**98a**) and *N*-(2-bromo-3,5-dimethoxyphenyl)-*N*-ethyl-4-methoxybenzenesulfonamide (**98b**).

*Compounds **9a** and **9b** article 2. Available at Materials and methods, chemical synthesis.*

N-benzyl-*N*-(4-bromo-3,5-dimethoxyphenyl)-4-methoxybenzenesulfonamide (**99a**), *N*-benzyl-*N*-(2-bromo-3,5-dimethoxyphenyl)-4-methoxybenzenesulfonamide (**99b**) and *N*-benzyl-*N*-(2,4-dibromo-3,5-dimethoxyphenyl)-4-methoxybenzenesulfonamide (**99c**).

*Compounds **10a**, **10b** and **10c** article 2. Available at Materials and methods, chemical synthesis. Compounds **326A**, **326B** and **326C** article 3. Available at Materials and methods, chemical synthesis (2.1).*

Methyl 3-amino-5-methoxybenzoate (**100**).

*Compound **78** article 3. Available at Materials and methods, chemical synthesis (2.1).*

Methyl 3-methoxy-5-((4-methoxyphenyl)sulfonamido)benzoate (**101**).

*Compound **79** article 3. Available at Materials and methods, chemical synthesis (2.1).*

Methyl 3-methoxy-5-((4-methoxy-*N*-methylphenyl)sulfonamido)benzoate (**102**). To a solution of **101** (110 mg, 0.31 mmol) in acetone (20 mL), K_2CO_3 (433 mg, 3.13 mmol) and $(CH_3)_2SO_4$ (112 µL, 1.17 mmol) were added, heated at reflux, and stirred overnight. Then, the reaction mixture was filtered, poured onto ice, and extracted with CH_2Cl_2. The organic layers were dried over anhydrous Na_2SO_4, filtered, and evaporated to dryness. The residue (84 mg) was purified by preparative TLC (hexane/EtOAc 6:4) to yield compound **102** (56 mg, 0.15 mmol, 49%). ^{1}H NMR (400 MHz, $CDCl_3$): δ 3.10 (3H, *s*), 3.77 (3H, *s*), 3.81 (3H, *s*), 3.83 (3H, *s*), 6.87 (2H, *d*, *J* = 9.2), 6.95 (1H, *t*, *J* = 2.4), 7.23 (1H, *t*, *J* = 1.6), 7.41 (1H, *dd*, *J* = 2.4 and 1.6), 7.44 (2H, *d*, *J* = 9.2). ^{13}C NMR (100 MHz, $CDCl_3$): δ 37.8 (CH_3), 52.2 (CH_3), 55.4 (CH_3), 55.6 (CH_3), 113.2 (CH), 114.0 (2CH), 117.8 (CH), 118.9 (CH), 127.8 (C), 129.8 (2CH), 131.5 (C), 143.0 (C), 159.6 (C), 163.1 (C), 166.1 (C). HRMS ($C_{17}H_{19}NO_6S$ + H^+): calcd 366.1006 (M + H^+), found 366.1001.

3-Methoxy-5-((4-methoxy-*N*-methylphenyl)sulfonamido)benzoic acid (**103**).

*Compound **90** article 3. Available at Materials and methods, chemical synthesis (2.1).*

Methyl 3-methoxy-5-((4-nitrophenyl)sulfonamido)benzoate (**104**). To 800 mg of aniline **100** (4.42 mmol) in CH_2Cl_2 (50 mL) and pyridine (2 mL), 979 mg of 4-nitrobenzenesulfonyl chloride (4.42 mmol) were slowly added and stirred at room temperature overnight. The reaction was treated with 2N HCl and 5% $NaHCO_3$, washed with brine, dried over anhydrous Na_2SO_4 and the solvent evaporated to obtain 1.36 g (3.72 mmol, 84%) of **104** which was purified by crystallization (710 mg, 1.94 mmol, 44%). M.p.: 171-173 °C (MeOH/acetone). IR (KBr): 3231, 1697, 1540, 1147, 852 cm^{-1}. ^{1}H NMR (400 MHz, acetone-D_6): δ 3.81 (3H, *s*), 3.85 (3H, *s*), 7.08 (1H, *t*, *J* = 2.4), 7.26 (1H, *dd*, *J* = 2.4 and 1.2), 7.48 (1H, *t*, *J* = 1.2), 8.11 (2H, *d*, *J* = 9.2), 8.40 (2H, *d*, *J* = 9.2). ^{13}C NMR (100 MHz, acetone-D_6): δ 51.7 (CH_3), 55.1 (CH_3), 110.6 (CH), 111.0 (CH), 113.7 (CH), 124.4 (2CH), 128.6 (2CH), 132.4 (C), 138.5 (C), 145.0 (C), 150.4 (C), 160.4 (C), 165.4 (C). HRMS ($C_{15}H_{14}N_2O_7S$ + Na^+): calcd 389.0414 (M + Na^+), found 389.0405.

Methyl 3-((4-aminophenyl)sulfonamido)-5-methoxybenzoate (**105**). The nitro sulfonamide **104** (1.25 g, 3.41 mmol) in ethyl acetate (125 mL) and Pd (C) (10 mg) was stirred at room temperature under H_2 atmosphere for 48 h. The reaction mixture was filtered through Celite® and the filtrate

was evaporated to dryness to afford **105** (1.08 g, 3.21 mmol, 94%), which was purified by crystallization in methanol (662 mg, 1.97 mmol, 58%). M.p.: 170-172 °C (MeOH). ^{1}H NMR (400 MHz, CD_3OD): δ 3.74 (3H, *s*), 3.85 (3H, *s*), 6.59 (2H, *d*, *J* = 8.4), 6.89 (1H, *t*, *J* = 2.4), 7.18 (1H, *dd*, *J* = 2.4 and 1.6), 7.32 (1H, *t*, *J* = 1.6), 7.45 (2H, *d*, *J* = 8.4). ^{13}C NMR (100 MHz, acetone-D_6): δ 51.6 (CH_3), 54.9 (CH_3), 109.1 (CH), 109.9 (CH), 112.9 (CH), 113.0 (2CH), 125.6 (C), 129.1 (2CH), 132.0 (C), 140.2 (C), 152.9 (C), 160.2 (C), 165.8 (C). HRMS ($C_{15}H_{16}N_2O_5S$ + Na^+): calcd 359.0672 (M + Na^+), found 359.0665.

Methyl 3-((4-(dimethylamino)phenyl)sulfonamido)-5-methoxybenzoate (**106**). A solution of paraformaldehyde (268 mg, 8.92 mmol), acetic acid (400 µL) and **105** (300 mg, 0.89 mmol) in MeOH (50 mL) was stirred at room temperature for 1 h. Sodium cyanoborohydride (112 mg, 1.78 mmol) was added to the solution and stirred at reflux for 24 h. Reaction mixture was concentrated under vacuum, poured onto ice, and extracted with EtOAc. Organic layers were washed with 5% $NaHCO_3$ and brine, dried (Na_2SO_4), filtered, and evaporated to dryness to give **106** (303 mg, 0.83 mmol, 93%). Crude reaction product was purified by crystallization in methanol (219 mg, 0.60 mmol, 67%). M.p.: 159-166 °C (MeOH). IR (KBr): 3278, 1700, 1505, 1147, 855 cm^{-1}. ^{1}H NMR (400 MHz, CD_3OD): δ 2.98 (6H, *s*), 3.75 (3H, *s*), 3.85 (3H, *s*), 6.68 (2H, *d*, *J* = 8.8), 6.90 (1H, *t*, *J* = 2.4), 7.17 (1H, *dd*, *J* = 2.4 and 1.6), 7.32 (1H, *t*, *J* = 1.6), 7.57 (2H, *d*, *J* = 8.8). ^{13}C NMR (100 MHz, $CDCl_3$): δ 39.9 ($2CH_3$), 52.3 (CH_3), 55.6 (CH_3), 110.4 (CH), 110.6 (CH), 110.8 (2CH), 113.6 (CH), 123.7 (C), 129.1 (2CH), 131.9 (C), 138.8 (C), 153.0 (C), 160.2 (C), 166.5 (C). HRMS ($C_{17}H_{20}N_2O_5S$ + Na^+): calcd 387.0985 (M + Na^+), found 387.0972.

Methyl 3-((4-(dimethylamino)-*N*-methylphenyl)sulfonamido)-5-methoxybenzoate (**107**). 85 mg (0.23 mmol) of **106** and 63 mg (0.46 mmol) of K_2CO_3 were mixed in dry DMF (3 mL). After 30 min stirring at room temperature, CH_3I (29 µL, 0.46 mmol) was added to the mixture and stirred 24 h. The reaction mixture was concentrated, re-dissolved in EtOAc, washed with brine, dried over anhydrous Na_2SO_4, filtered, and concentrated in vacuum to obtain 85 mg (0.22 mmol, 96%) of **107**, which was purified by preparative TLC in CH_2Cl_2/MeOH 98:2 (44 mg, 0.11 mmol, 50%). IR (KBr): 1719, 1458, 787 cm^{-1}. ^{1}H NMR (400 MHz, $CDCl_3$): δ 3.01 (6H, *s*), 3.11 (3H, *s*), 3.81 (3H, *s*), 3.86 (3H, *s*), 6.58 (2H, *d*, *J* = 9.2), 7.02 (1H, *t*, *J* = 2.4), 7.31 (1H, *t*, *J* = 1.6), 7.36 (2H, *d*, *J* = 9.2), 7.43 (1H, *dd*, *J* = 2.4 and 1.6). ^{13}C NMR (100 MHz, $CDCl_3$): δ 37.7 (CH_3), 40.0 ($2CH_3$), 52.2 (CH_3), 55.6 (CH_3), 110.6 (2CH), 113.0 (CH), 117.7 (CH), 119.0 (CH), 121.4 (C), 129.6 (2CH), 131.4 (C), 143.5 (C), 152.9 (C), 159.5 (C), 166.3 (C). HRMS ($C_{18}H_{22}N_2O_5S$ + Na^+): calcd 401.1142 (M + Na^+), found 401.1140.

Methyl 3-((4-(dimethylamino)-*N*-ethylphenyl)sulfonamido)-5-methoxybenzoate (**108**). A mixture of **106** (66 mg, 0.18 mmol) and K_2CO_3 (49 mg, 0.36 mmol) in dry DMF (3 mL) was stirred at room temperature for 30 min. Then, bromoethane (54 µL, 0.72 mmol) was added. After 48 h, the solvent was evaporated under reduced pressure. The residue was dissolved in EtOAc and washed with brine, dried (Na_2SO_4), and concentrated in vacuo to afford 62 mg (0.16 mmol, 87%) of **108**. The title compound was purified by crystallization (37 mg, 0.09 mmol, 52%). M.p.: 145-147 °C (MeOH). IR (KBr): 1723, 1458, 1160, 770 cm^{-1}. ^{1}H NMR (400 MHz, $CDCl_3$): δ 1.03 (3H, *t*, *J* = 7.2), 3.03 (6H, *s*), 3.54 (2H, *q*, *J* = 7.2), 3.80 (3H, *s*), 3.87 (3H, *s*), 6.60 (2H, *d*, *J* = 8.8), 6.91 (1H, *t*, *J* = 2.4), 7.31 (1H, *t*, *J* = 1.6), 7.42 (2H, *d*, *J* = 8.8), 7.48 (1H, *dd*, *J* = 2.4 and 1.6). ^{13}C NMR (100 MHz, $CDCl_3$): δ 13.8 (CH_3), 40.0 ($2CH_3$), 44.9 (CH_2), 52.2 (CH_3), 55.6 (CH_3), 110.7 (2CH), 113.6 (CH), 120.1 (CH), 121.6 (CH), 123.3 (C), 129.4 (2CH), 131.5 (C), 140.9 (C), 152.8 (C), 159.7 (C), 166.3 (C). HRMS ($C_{19}H_{24}N_2O_5S$ + H^+): calcd 393.1479 (M + H^+), found 393.1480.

Methyl 3-((4-formamidophenyl)sulfonamido)-5-methoxybenzoate (**109**). Sulfonamide **105** (400 mg, 1.19 mmol) was dissolved in CH_2Cl_2 (50 mL) and pyridine (1 mL). 5 mL of formic acid were added and stirred at room temperature for 24 h. The reaction mixture was washed with 2N HCl, 5% $NaHCO_3$ and brine, dried over anhydrous Na_2SO_4 and concentrated in vacuo to afford 341 mg (0.94 mmol, 79%) of **109**. Crude reaction product was purified by preparative TLC in

CH_2Cl_2/MeOH 95:5 (289 mg, 0.79 mmol, 67%). ^{1}H NMR (400 MHz, CD_3OD): δ 3.76 (3H, *s*), 3.85 (3H, *s*), 6.91 (1H, *t*, *J* = 2.4), 7.21 (1H, *dd*, *J* = 2.4 and 1.6), 7.32 (1H, *t*, *J* = 1.6), 7.68 (2H, *d*, *J* = 9.6), 7.73 (2H, *d*, *J* = 9.6). ^{13}C NMR (100 MHz, acetone-D_6): δ 51.6 (CH_3), 55.0 (CH_3), 109.7 (CH), 110.4 (CH), 113.2 (CH), 119.0 (2CH), 128.4 (2CH), 128.9 (C), 132.2 (C), 139.4 (C), 142.3 (C), 159.5 (C), 160.3 (CH), 165.6 (C). HRMS ($C_{16}H_{16}N_2O_6S$ + Na^+): calcd 387.0621 (M + Na^+), found 387.0608.

Methyl 3-methoxy-5-((4-(methylamino)phenyl)sulfonamido)benzoate (**110**). To a solution of **109** (250 mg, 0.68 mmol) and $NaBH_4$ (39 mg, 1.03 mmol) in dry THF (10 mL) at 0 °C, trichloroacetic acid (168 mg, 1.03 mmol) diluted in dry THF (2 mL) was dropwise added under nitrogen atmosphere. The reaction mixture was stirred at 0 °C to room temperature for 48 h, concentrated and re-dissolved in EtOAc, washed with brine, dried over anhydrous Na_2SO_4, filtered and solvent evaporated in vacuum to afford 236 mg of crude reaction. Compound **110** (130 mg, 0.37 mmol, 54%) was isolated by flash column chromatography (toluene/EtOAc 8:2). ^{1}H NMR (400 MHz, CD_3OD): δ 2.74 (3H ,*s*), 3.74 (3H, *s*), 3.84 (3H, *s*), 6.52 (2H, *d*, *J* = 8.4), 6.89 (1H, *t*, *J* = 2.4), 7.17 (1H, *dd*, *J* = 2.4 and 1.6), 7.32 (1H, *t*, *J* = 1.6), 7.50 (2H, *d*, *J* = 8.4). ^{13}C NMR (100 MHz, acetone-D_6): δ 29.7 (CH_3), 51.6 (CH_3), 54.9 (CH_3), 109.0 (CH), 109.8 (CH), 110.7 (2CH), 112.8 (CH), 124.9 (C), 129.0 (2CH), 132.0 (C), 140.2 (C), 153.5 (C), 160.3 (C), 165.7 (C). HRMS ($C_{16}H_{18}N_2O_5S$ + Na^+): calcd 373.0829 (M + Na^+), found 373.0825.

Methyl 3-methoxy-5-((*N*-methyl-4-(methylamino)phenyl)sulfonamido)benzoate (**111**). A mixture of **110** (25 mg, 0.07 mmol) and K_2CO_3 (19 mg, 0.14 mmol) in dry DMF (2 mL), was stirred for 1 h. Then, methyl iodide (9 µL, 0.14 mmol) was added. After 24 h, the reaction mixture was concentrated under reduced pressure, diluted with EtOAc, washed with brine, dried (Na_2SO_4), filtered, and concentrated in vacuo. Crude residue (27 mg) was purified by preparative TLC (toluene/EtOAc 1:1) (**111**, 12 mg, 0.03 mmol, 46%). IR (KBr): 3407, 1723, 1600, 1520, 1161, 734 cm^{-1}. ^{1}H NMR (400 MHz, $CDCl_3$): δ 2.87 (3H, *s*), 3.12 (3H, *s*), 3.82 (3H, *s*), 3.87 (3H, *s*), 6.51 (2H, *d*, *J* = 8.8), 7.03 (1H, *t*, *J* = 2.4), 7.32 (1H, *t*, *J* = 1.6), 7.34 (2H, *d*, *J* = 8.8), 7.44 (1H, *dd*, *J* = 2.4 and 1.6). ^{13}C NMR (100 MHz, $CDCl_3$): δ 30.0 (CH_3), 37.7 (CH_3), 52.2 (CH_3), 55.6 (CH_3), 111.1 (2CH), 113.1 (CH), 117.7 (CH), 119.0 (CH), 122.7 (C), 129.8 (2CH), 131.4 (C), 143.5 (C), 152.6 (C), 159.6 (C), 166.3 (C). HRMS ($C_{17}H_{20}N_2O_5S$ + H^+): calcd 365.1166 (M + H^+), found 365.1158.

Methyl 3-methoxy-5-((4-(*N*-methylformamido)phenyl)sulfonamido)benzoate (**112**). A solution of **110** (65 mg, 0.18 mmol) and formic acid (5 mL) in pyridine (2 mL) and CH_2Cl_2 (48 mL) was stirred at room temperature for 48 h. The reaction mixture was poured onto ice and extracted with CH_2Cl_2. Organics layers were washed with 2N HCl, 5% $NaHCO_3$ and brine, dried over Na_2SO_4, filtered, and evaporated to dryness. 58 mg (0.15 mmol, 83%) of **112** was obtained and purified by crystallization in methanol (35 mg, 0.09 mmol, 50%). M.p.: 176-182 °C (MeOH). IR (KBr): 3233, 1724, 1670, 1588, 1327, 1154, 876 cm^{-1}. ^{1}H NMR (400 MHz, CD_3OD): δ 3.28 (3H, *s*), 3.76 (3H, *s*), 3.85 (3H, *s*), 6.94 (1H, *t*, *J* = 2.4), 7.21 (1H, *dd*, *J* = 2.4 and 1.6), 7.34 (1H, *t*, *J* = 1.6), 7.44 (2H, *d*, *J* = 8.8), 7.84 (2H, *d*, *J* = 8.8), 8.63 (1H, *s*). ^{13}C NMR (100 MHz, acetone-D_6): δ 29.9 (CH_3), 51.6 (CH_3), 55.0 (CH_3), 109.8 (CH), 110.4 (CH), 113.1 (CH), 120.3 (2CH), 128.6 (2CH), 132.3 (C), 135.7 (C), 139.3 (C), 146.4 (C), 160.4 (C), 161.4 (CH), 165.6 (C). HRMS ($C_{17}H_{18}N_2O_6S$ + Na^+): calcd 401.0778 (M + Na^+), found 401.0769.

Methyl 3,5-dinitrobenzoate (**113**).

*Compound **80** article 3. Available at Materials and methods, chemical synthesis (2.1).*

Methyl 3,5-diaminobenzoate (**114**).

*Compound **81** article 3. Available at Materials and methods, chemical synthesis (2.1).*

Methyl 3-amino-5-((4-methoxyphenyl)sulfonamido)benzoate (**115a**) and methyl 3,5-bis((4-methoxyphenyl)sulfonamido)benzoate (**115b**).

*Compounds **84A** and **84B** article 3. Available at Materials and methods, chemical synthesis (2.1).*

Methyl 3-formamido-5-((4-methoxyphenyl)sulfonamido)benzoate (**116**). A solution of **115a** (195 mg, 0.58 mmol) and formic acid (3 mL) in CH_2Cl_2 (50 mL) was stirred at room temperature for 48 h. The reaction mixture was poured onto ice and extracted with CH_2Cl_2. Organics layers were washed with 5% $NaHCO_3$ and brine, dried over Na_2SO_4, filtered and evaporated to dryness. 190 mg (0.52 mmol, 90%) of **116** was obtained and purified by crystallization in methanol (128 mg, 0.35 mmol, 60%). M.p.: 221-226 °C (MeOH). IR (KBr): 3325, 3104, 1713, 1640, 1611, 1562, 1161, 889 cm^{-1}. ^1H NMR (400 MHz, CD_3OD): δ 3.81 (3H, *s*), 3.86 (3H, *s*), 6.98 (2H, *d*, *J* = 8.8), 7.47 (1H, *dd*, *J* = 2.4 and 1.6), 7.75 (2H, *d*, *J* = 8.8), 7.77 (1H, *t*, *J* = 2.4), 7.85 (1H, *t*, *J* = 1.6), 8.25 (1H, *s*). ^{13}C NMR (100 MHz, DMSO-D_6): δ 52.8 (CH_3), 56.1 (CH_3), 114.4 (CH), 114.9 (2CH), 115.3 (CH), 115.4 (CH), 129.3 (2CH), 131.1 (C), 131.3 (C), 139.4 (C), 139.6 (C), 160.3 (CH), 163.0 (C), 165.9 (C). HRMS ($C_{16}H_{16}N_2O_6S + Na^+$): calcd 387.0621 ($M + Na^+$), found 387.0617.

Methyl 3-((4-methoxyphenyl)sulfonamido)-5-(methylamino)benzoate (**117**). Formamide **116** (104 mg, 0.28 mmol) was dissolved in dry THF (10 mL). After it was cooled to 0°C, $NaBH_4$ (16 mg, 0.43 mmol) was added, followed by the dropwise addition of trichloroacetic acid (70 mg, 0.43 mmol) dissolved in dry THF (10 mL). The reaction mixture was stirred from 0°C to room temperature for 48 h, then, it was concentrated, poured into ice, and extracted with EtOAc. The organics layers were dried (Na_2SO_4), filtered, and concentrated in vacuo to afford 87 mg (0.25 mmol, 87%) of the desired compound, **117**. The residue was crystallized in CH_2Cl_2/MeOH (24 mg, 0.07 mmol, 24%). M.p.: 217-221 °C (CH_2Cl_2/MeOH). ^1H NMR (400 MHz, CD_3OD): δ 2.70 (3H, *s*), 3.81 (3H, *s*), 3.82 (3H, *s*), 6.57 (1H, *t*, *J* = 2), 6.91 (1H, *dd*, *J* = 2 and 1.6), 6.96 (1H, *t*, *J* = 1.6), 6.97 (2H ,*d*, *J* = 8.8), 7.70 (2H, *d*, *J* = 8.8). ^{13}C NMR (100 MHz, acetone-D_6): δ 39.9 (CH_3), 52.1 (CH_3), 55.9 (CH_3), 108.0 (CH), 109.3 (CH), 109.5 (CH), 114.9 (2CH), 130.1 (2CH), 132.4 (C), 132.4 (C), 140.0 (C), 151.6 (C), 163.9 (C), 167.2 (C). HRMS ($C_{16}H_{18}N_2O_5S + H^+$): calcd 351.1009 ($M + H^+$), found 351.1003.

Methyl 3,5-bis((4-methoxy-*N*-methylphenyl)sulfonamido)benzoate (**118**).

*Compound **147** article 3. Available at Materials and methods, chemical synthesis (2.1).*

Methyl 3,5-bis((4-methoxy-3-nitrophenyl)sulfonamido)benzoate (**119**). To a solution of **114** (675 mg, 4.06 mmol) in CH_2Cl_2 (50 mL) and pyridine (0.5 mL), the benzenesulfonyl chloride **53** (1.02 g, 4.06 mmol) was dropwise added dissolved in CH_2Cl_2 (20 mL). The mixture was stirred at room temperature for 24 h. Then the reaction was treated with 0.5N HCl washed with brine, dried over anhydrous Na_2SO_4 and concentrated in vacuum. The residue (934 mg) was purified by flash chromatography on silica gel with toluene/EtOAc (6:4) to yield compound **119** (449 mg, 0.75 mmol, 37%). M.p.: 155-156 °C (CH_2Cl_2). IR (KBr): 3253, 1708, 1533, 1491, 1166, 895 cm^{-1}. ^1H NMR (400 MHz, CD_3OD): δ 3.82 (3H, *s*), 3.99 (6H, *s*), 7.35 (2H, *d*, *J* = 2), 7.37 (2H, *d*, *J* = 8.8), 7.38 (1H, *t*, *J* = 2), 7.91 (2H, *dd*, *J* = 8.8 and 2.4), 8.10 (2H, *d*, *J* = 2.4). ^{13}C NMR (100 MHz, CD_3OD): δ 51.5 (CH_3), 56.4 ($2CH_3$), 114.3 (2CH), 115.7 (CH), 116.7 (2CH), 124.3 (2CH), 130.8 (2C), 132.0 (C), 132.4 (2CH), 138.7 (2C), 138.9 (2C), 155.7 (2C), 165.5 (C). HRMS ($C_{22}H_{20}N_4O_{12}S_2 + Na^+$): calcd 619.0411 ($M + Na^+$), found 619.0421.

N-(3,4-dimethoxyphenyl)-4-methoxybenzenesulfonamide (**120**).

*Compound **11** article 2. Available at Materials and methods, chemical synthesis.*
*Compound **8** article 3. Available at Materials and methods, chemical synthesis (2.1).*

N-(3,4-dimethoxyphenyl)-4-methoxy-*N*-methylbenzenesulfonamide (**121a**) and *N,N'*-methylenebis(*N*-(3,4-dimethoxyphenyl)-4-methoxybenzenesulfonamide) (**121b**). To a mixture of **120** (205 mg, 0.63 mmol), NaOH (29 mg, 1.26 mmol) and $nBu_4N^+HSO_4^-$ (252 mg, 1.26 mmol) in CH_2Cl_2 (100 mL) CH_3I (80 µL, 1.26 mmol) was added. The reaction was stirred at room temperature under nitrogen atmosphere for 3 days. The solution was poured onto brine,

extracted with CH_2Cl_2, and then dried over Na_2SO_4. After concentration, the residue (340 mg) was purified by silica gel column chromatography (hexane/EtOAc, 6:4) to give **121a** (105 mg, 0.31 mmol, 49%) and **121b** (41 mg, 0.06 mmol, 19%). **121a**: IR (KBr): 3435, 1595, 1508, 823 cm^{-1}. ^1H NMR (400 MHz, $CDCl_3$): δ 3.06 (3H, *s*), 3.72 (3H, *s*), 3.80 (3H, *s*), 6.46 (1H, *dd*, *J* = 8.8 and 2), 6.62 (1H, *d*, *J* = 2), 6.69 (1H, *d*, *J* = 8.8), 6.87 (2H, *d*, *J* = 9.2), 7.44 (2H, *d*, *J* = 9.2). ^{13}C NMR (100 MHz, $CDCl_3$): δ 38.5 (CH_3), 55.6 (CH_3), 55.8 (CH_3), 55.9 (CH_3), 110.5 (CH), 111.1 (CH), 113.8 (2CH), 118.5 (CH), 127.8 (C), 130.0 (2CH), 134.5 (C), 148.2 (C), 148.6 (C), 162.9 (C). HRMS ($C_{16}H_{19}NO_5S$ + H^+): calcd 338.1057 (M + H^+), found 338.1058. **121b**: ^1H NMR (400 MHz, $CDCl_3$): δ 3.62 (6H, *s*), 3.78 (6H, *s*), 3.81 (6H, *s*), 5.44 (2H, *s*), 6.37 (2H, *d*, *J* = 2.4), 6.46 (2H, *dd*, *J* = 8.8 and 2.4), 6.67 (2H, *d*, *J* = 8.8), 6.73 (4H, *d*, *J* = 8.8), 7.24 (4H, *d*, *J* = 8.8). ^{13}C NMR (100 MHz, $CDCl_3$): δ 55.6 ($2CH_3$), 55.8 ($2CH_3$), 55.9 ($2CH_3$), 66.2 (CH_2), 110.6 (2CH), 113.2 (2CH), 113.7 (2CH), 122.0 (4CH), 129.6 (4CH), 130.1 (2C), 130.6 (2C), 148.8 (2C), 149.0 (2C), 162.8 (2C). HRMS ($C_{31}H_{34}N_2O_{10}S_2$ + Na^+): calcd 681.1547 (M + Na^+), found 681.1559.

N-(4,5-dimethoxy-2-nitrophenyl)-4-methoxybenzenesulfonamide (**122**).

*Compound **11** article 3. Available at Materials and methods, chemical synthesis (2.1).*

N-(2-amino-4,5-dimethoxyphenyl)-4-methoxybenzenesulfonamide (**123**).

*Compound **12** article 3. Available at Materials and methods, chemical synthesis (2.1).*

N-(2-amino-4,5-dimethoxyphenyl)-4-methoxy-*N*-methylbenzenesulfonamide (**124**).

*Compound **120** article 3. Available at Materials and methods, chemical synthesis (2.1).*

N-(4,5-dimethoxy-2-((4-methoxyphenyl)sulfonamido)phenyl)acetamide (**125a**) and *N*-(2-acetamido-4,5-dimethoxyphenyl)-*N*-((4-methoxyphenyl)sulfonyl)acetamide (**125b**). To a solution of **123** (200 mg, 0.59 mmol) in pyridine (1 mL), 555 µL of acetic anhydride (5.90 mmol) were added. The reaction mixture was stirred for 30 min. The mixture was poured onto ice and extracted with EtOAc. The organic layer was washed with 2N HCl, 5% $NaHCO_3$ and brine, dried (Na_2SO_4), filtered and concentrated in vacuo to yield 198 mg of crude reaction residue. The residue was purified by preparative TLC (CH_2Cl_2/MeOH 95:5) to afford compounds **125a** (31 mg, 0.08 mmol, 14%) and **125b** (44 mg, 0.10 mmol, 18%). **125a**: ^1H NMR (400 MHz, $CDCl_3$): δ 2.07 (3H, *s*), 3.52 (3H, *s*), 3.79 (6H, *s*), 6.29 (1H, *s*), 6.85 (2H, *d*, *J* = 8.8), 7.34 (1H, *s*), 7.54 (2H, *d*, *J* = 8.8), 7.67 (1H, *bs*). ^{13}C NMR (100 MHz, $CDCl_3$): δ 24.2 (CH_3), 55.7 (CH_3), 55.9 (CH_3), 56.0 (CH_3), 106.4 (CH), 111.5 (CH), 114.1 (2CH), 118.6 (C), 128.3 (C), 129.7 (2CH), 130.1 (C), 145.8 (C), 148.5 (C), 163.3 (C), 169.0 (C). HRMS ($C_{17}H_{20}N_2O_6S$ + H^+): calcd 381.1115 (M + H^+), found 381.1124. **125b**: ^1H NMR (400 MHz, $CDCl_3$): δ 1.86 (3H, *s*), 2.17 (3H, *s*), 3.78 (3H, *s*), 3.90 (3H, *s*), 3.94 (3H, *s*), 6.40 (1H, *s*), 7.02 (2H, *d*, *J* = 8.8), 7.46 (1H, *s*), 7.79 (1H, *s*), 7.99 (2H, *d*, *J* = 8.8). ^{13}C NMR (100 MHz, $CDCl_3$): δ 24.4 (CH_3), 24.5 (CH_3), 55.8 (CH_3), 56.2 (CH_3), 56.3 (CH_3), 107.5 (CH), 111.5 (CH), 114.1 (2CH), 119.4 (C), 129.3 (C), 130.9 (C), 131.7 (2CH), 146.4 (C), 150.5 (C), 164.3 (C), 168.9 (C), 171.0 (C). HRMS ($C_{19}H_{22}N_2O_7S$ + H^+): calcd 423.1220 (M + H^+), found 423.1225.

N-(4,5-dimethoxy-2-((4-methoxy-*N*-methylphenyl)sulfonamido)phenyl)acetamide (**126**).

*Compound **124** article 3. Available at Materials and methods, chemical synthesis (2.1).*

N-(4,5-dimethoxy-2-((4-methoxyphenyl)sulfonamido)phenyl)formamide (**127**). A solution of **123** (100 mg, 0.29 mmol) and formic acid (16 µL, 0.35 mmol) in CH_2Cl_2 (10 mL) was stirred at room temperature for 72 h. The reaction mixture was washed with brine, dried, and concentrated under vacuum to produce 95 mg (0.26 mmol, 88%) of crude reaction product **127**, which was purified by crystallization in CH_2Cl_2/hexane (61 mg, 0.17 mmol, 56%). M.p.: 130-132 °C (CH_2Cl_2/hexane). IR (KBr): 3391, 1664, 1598, 1457 cm^{-1}. ^1H NMR (400 MHz, $CDCl_3$): δ 3.52 (3H,

s), 3.84 (3H, *s*), 3.86 (3H, *s*), 6.03 (1H, *s*), 6.20 (1H, *s*), 6.92 (2H, *d*, *J* =8.8), 7.59 (1H, *s*), 7.62 (2H, *d*, *J* = 8.8), 7.98 (1H, *bs*), 8.29 (1H, *s*). ^{13}C NMR (100 MHz, $CDCl_3$): δ 55.4 (CH_3), 55.5 (CH_3), 55.7 (CH_3), 106.0 (CH), 111.0 (CH), 113.9 (2CH), 117.7 (C), 127.7 (C), 129.3 (C), 129.6 (2CH), 145.4 (C), 148.2 (C), 159.5 (C), 163.1 (CH). HRMS ($C_{16}H_{18}N_2O_6S$ + H^+): calcd 367.0958 (M + H^+), found 367.0966.

N-(4,5-dimethoxy-2-(methylamino)phenyl)-4-methoxybenzenesulfonamide (**128**). To a solution of **127** (85 mg, 0.23 mmol) and $NaBH_4$ (13 mg, 0.35 mmol) in dry THF (5 mL) at 0°C, trichloroacetic acid (57 mg, 0.35 mmol) diluted in dry THF (5 mL) was added dropwise under nitrogen atmosphere. The reaction mixture was stirred at 0°C to room temperature for 24 h, concentrated and re-dissolved in EtOAc, washed with brine, dried over anhydrous Na_2SO_4, filtered, and solvent evaporated in vacuum. The residue (76 mg) was purified by preparative TLC (hexane/EtOAc 3:7) to afford compound **128** (28 mg, 0.08 mmol, 34%). ^{1}H NMR (400 MHz, $CDCl_3$): δ 2.72 (3H, *s*), 3.39 (3H, *s*), 3.78 (3H, *s*), 3.79 (3H, *s*), 5.89 (1H, *s*); 6.17 (1H, *s*), 6.86 (2H, *d*, *J* = 8.8), 7.60 (2H, *d*, *J* = 8.8). ^{13}C NMR (100 MHz, $CDCl_3$): δ 31.1 (CH_3), 55.6 (CH_3), 55.7 (CH_3), 55.9 (CH_3), 96.5 (CH), 111.6 (CH), 113.9 (2CH), 129.6 (C), 129.8 (2CH), 130.4 (C), 131.2 (C), 142.5 (C), 142.6 (C), 163.1 (C). HRMS ($C_{16}H_{20}N_2O_5S$ + H^+): calcd 353.1166 (M + H^+), found 353.1175.

N-(2-(dimethylamino)-4,5-dimethoxyphenyl)-4-methoxybenzenesulfonamide (**129**). Compound **123** (149 mg, 0.44 mmol) was dissolved in MeOH (30 mL) with paraformaldehyde (50 mg, 1.66 mmol) and acetic acid (one drop). After 1 h stirring at room temperature sodium cyanoborohydride (28 mg, 0.44 mmol) was added to the solution. The reaction mixture was allowed to react for 4 days. Crude reaction product was purified by flash chromatography in hexane/EtOAc 6:4 to afford **129** (65 mg, 0.18 mmol, 40%). M.p.: 165-169 °C (MeOH). IR (KBr): 3436, 1594, 1515, 835 cm^{-1}. ^{1}H NMR (400 MHz, $CDCl_3$): δ 2.23 (6H, *s*), 3.73 (6H, *s*), 3.81 (3H, *s*), 6.56 (1H, *s*), 6.78 (2H, *d*, *J* = 8.8), 7.62 (2H, *d*, *J* = 8.8), 7.83 (1H, *bs*). ^{13}C NMR (100 MHz, $CDCl_3$): δ 45.5 ($2CH_3$), 55.5 ($2CH_3$), 56.1 (CH_3), 103.3 (CH), 105.1 (CH), 113.9 (2CH), 126.6 (C), 129.2 (2CH), 130.9 (C), 136.1 (C), 145.8 (C), 146.8 (C), 162.9 (C). HRMS ($C_{17}H_{22}N_2O_5S$ + H^+): calcd 367.1322 (M + H^+), found 367.1328.

N-(4,5-dimethoxy-2-((4-methoxyphenyl)sulfonamido)phenyl)-4-nitrobenzamide (**130**). A mixture of compound **123** (300 mg, 0.89 mmol), 4-nitrobenzoic acid (193 mg, 1.15 mmol), EDC (221 mg, 1.15 mmol) and 4-(dimethylamino)pyridine (70 mg, 0.57 mmol) was heated at 130 °C in microwave conditions for 3 min. The reaction mixture was diluted in CH_2Cl_2 and washed with 0.5N HCl, 5% $NaHCO_3$ and brine, dried over Na_2SO_4, filtered, and concentrated under vacuum. The residue (373 mg) was purified by column chromatography (hexane/EtOAc 7:3) to afford compound **130** (222 mg, 0.45 mmol, 51%). M.p.: 219-220 °C (CH_2Cl_2/hexane). IR (KBr): 3356, 1653, 1599, 1522 cm^{-1}. ^{1}H NMR (400 MHz, $CDCl_3$): δ 3.50 (3H, *s*), 3.85 (3H, *s*), 3.93 (3H, *s*), 5.91 (1H, *s*), 6.10 (1H, *s*), 6.93 (2H, *d*, *J* = 8.8), 7.62 (2H, *d*, *J* = 8.8), 7.93 (1H, *s*), 8.16 (2H, *d*, *J* = 8.4), 8.37 (2H, *d*, *J* = 8.4), 9.30 (1H, *bs*). ^{13}C NMR (100 MHz, $CDCl_3$): δ 55.7 (CH_3), 55.9 (CH_3), 56.1 (CH_3), 106.1 (CH), 111.4 (CH), 114.2 (2CH), 117.5 (C), 124.0 (2CH), 128.5 (2CH), 128.7 (C), 129.3 (C), 129.9 (2CH), 139.8 (C), 145.8 (C), 148.9 (C), 149.8 (C), 163.4 (C), 163.6 (C). HRMS ($C_{22}H_{21}N_3O_8S$ + H^+): calcd 488.1122 (M + H^+), found 488.1162.

4-((4,5-Dimethoxy-2-((4-methoxyphenyl)sulfonamido)phenyl)amino)-4-oxobutanoic acid (**131**). A mixture of **123** (132 mg, 0.39 mmol), succinic anhydride (47 mg, 0.47 mmol) and pyridine drops in CH_2Cl_2 (50 mL) was stirred at room temperature. After 24 h, the precipitate formed was filtered to afford 100 mg (0.23 mmol, 59%) of **131**. IR (KBr): 3365, 3273, 1707, 1689, 1597 cm^{-1}. ^{1}H NMR (400 MHz, CD_3OD): δ 2.53 (2H, *t*, *J* = 6.4), 2.63 (2H, *t*, *J* = 6.4), 3.67 (3H, *s*), 3.76 (3H, *s*), 3.84 (3H, *s*), 6.61 (1H, *s*), 6.99 (2H, *d*, *J* = 9.2), 7.01 (1H, *s*), 7.56 (2H, *d*, *J* = 9.2). ^{13}C NMR (100

MHz, CD_3OD): δ 28.4 (CH_2), 30.5 (CH_2), 54.7 (CH_3), 55.0 (CH_3), 55.1 (CH_3), 107.1 (CH), 111.2 (CH), 113.7 (2CH), 121.0 (C), 126.7 (C), 129.1 (2CH), 130.7 (C), 146.5 (C), 147.9 (C), 163.3 (C), 171.5 (C), 174.8 (C). HRMS ($C_{19}H_{22}N_2O_8S + H^+$): calcd 439.1170 ($M + H^+$), found 439.1184.

Tert-butyl (2-((4,5-dimethoxy-2-((4-methoxyphenyl)sulfonamido)phenyl)amino)-2-oxoethyl)carbamate (**132**). A solution of (*tert*-butoxycarbonyl)glycine (135 mg, 0.77 mmol), EDCI (138 mg, 0.89 mmol) and DMAP (36 mg, 0.29 mmol) in CH_2Cl_2 (20 mL) was stirred for 10 min. Then, to this solution was added the compound **123** (200 mg, 0.59 mmol) and the reaction mixture was stirred at room temperature for 24 h. The solution was washed with 2N HCl, 5% $NaHCO_3$ and brine. After drying (Na_2SO_4) and removal of the solvent (207 mg), compound **132** was isolated by flash column chromatography using as eluent CH_2Cl_2/EtOAc 8:2 (88 mg, 0.18 mmol, 30%). ^{1}H NMR (400 MHz, $CDCl_3$): δ 1.51 (9H, *s*), 3.59 (3H, *s*), 3.85 (6H, *s*), 3.89 (2H, *d*, *J* = 6.4), 6.21 (1H, *s*), 6.49 (1H, *s*), 6.92 (2H, *d*, *J* = 8.8), 7.42 (1H, *s*), 7.60 (2H, *d*, *J* = 8.8). ^{13}C NMR (100 MHz, $CDCl_3$): δ 28.7 ($3CH_3$), 45.1 (CH_2), 56.0 (CH_3), 56.2 (CH_3), 56.3 (CH_3), 80.9 (C), 106.9 (CH), 111.5 (CH), 114.4 (2CH), 119.6 (C), 127.8 (C), 130.1 (2CH), 130.5 (C), 146.3 (C), 148.5 (C), 156.7 (C), 163.6 (C), 168.9 (C). HRMS ($C_{22}H_{29}N_3O_8S + H^+$): calcd 496.1748 ($M + H^+$), found 496.1746.

5,6-Dimethoxy-1-((4-methoxyphenyl)sulfonyl)-1*H*-benzo[*d*][1,2,3]triazole (**133**). To a solution of **123** (57 mg, 0.17 mmol) in CH_3CN (10 mL) and H_2O (100 µL) at 0 °C, *tert*butyl nitrite (22.5 µL, 0.17 mmol) was added and the reaction stirred. After 1 h, acetic acid (10 µL) was added to the reaction mixture and stirred for 24 h to room temperature. Then, the mixture was concentrated, re-dissolved in EtOAc and treated with 5% $NaHCO_3$ solution. The organic layers were washed with brine to neutrality, dried over Na_2SO_4 and concentrated under vacuum. The residue (58 mg) was chromatographed by preparative TLC (CH_2Cl_2/EtOAc 9:1) to afford the purified compound **133** (17 mg, 0.05 mmol, 29%). ^{1}H NMR (400 MHz, $CDCl_3$): δ 3.83 (3H, *s*), 3.94 (3H, *s*), 4.05 (3H, *s*), 6.96 (2H, *d*, *J* = 8.8), 7.34 (1H, *s*), 7.44 (1H, *s*), 8.02 (2H, *d*, *J* = 8.8). ^{13}C NMR (100 MHz, $CDCl_3$): δ 55.8 (CH_3), 56.3 (CH_3), 56.6 (CH_3), 92.5 (CH), 99.3 (CH), 114.8 (2CH), 127.2 (C), 128.2 (C), 130.3 (2CH), 139.7 (C), 149.4 (C), 153.1 (C), 164.9 (C). HRMS ($C_{15}H_{15}N_3O_5S + H^+$): calcd 350.0805 ($M + H^+$), found 350.0796.

5,6-Dimethoxy-1-((4-methoxyphenyl)sulfonyl)-1*H*-benzo[*d*]imidazole (**134**). A mixture of **123** (100 mg, 0.29 mmol) and triethyl orthoformate (60 µL, 0.35 mmol) in CH_3CN (10 mL) was heated at reflux for 12 h. The CH_3CN was removed under reduced pressure and the residue was washed with brine, extracted with EtOAc and dried over Na_2SO_4. After concentration, crude reaction product **134** (100 mg, 0.29 mmol, 97%) was purified by crystallization (81 mg, 0.23 mmol, 79%). M.p.: 175-177 °C (CH_2Cl_2/hexane). IR (KBr): 1633, 1617, 1592 cm^{-1}. ^{1}H NMR (400 MHz, $CDCl_3$): δ 3.83 (3H, *s*), 3.90 (3H, *s*), 3.97 (3H, *s*), 6.94 (2H, *d*, *J* = 9.2), 7.20 (1H, *s*), 7.33 (1H, *s*), 6.88 (2H, *d*, *J* = 9.2), 8.21 (1H, *s*). ^{13}C NMR (100 MHz, $CDCl_3$): δ 55.8 (CH_3), 56.2 (CH_3), 56.5 (CH_3), 95.2 (CH), 102.5 (CH), 114.8 (2CH), 124.5 (C), 128.9 (C), 129.3 (2CH), 137.5 (C), 139.8 (CH), 148.1 (C), 148.7 (C), 164.4 (C). HRMS ($C_{16}H_{16}N_2O_5S + H^+$): calcd 349.0853 ($M + H^+$), found 349.0841.

N-(2-bromo-4,5-dimethoxyphenyl)-4-methoxybenzenesulfonamide (**135**).

*Compound **13** article 2. Available at Materials and methods, chemical synthesis.*

N-(2-bromo-4,5-dimethoxyphenyl)-4-methoxy-*N*-methylbenzenesulfonamide (**136**).

*Compound **14** article 2. Available at Materials and methods, chemical synthesis.*

N-(2-bromo-4,5-dimethoxyphenyl)-*N*-ethyl-4-methoxybenzenesulfonamide (**137**).

*Compound **15** article 2. Available at Materials and methods, chemical synthesis.*

N-(2-bromo-4,5-dimethoxyphenyl)-*N*-(cyanomethyl)-4-methoxybenzenesulfonamide (**138**).

*Compound **16** article 2. Available at Materials and methods, chemical synthesis.*

Ethyl *N*-(2-bromo-4,5-dimethoxyphenyl)-*N*-((4-methoxyphenyl)sulfonyl)glycinate (**139**).

*Compound **17** article 2. Available at Materials and methods, chemical synthesis.*

N-benzyl-*N*-(2-bromo-4,5-dimethoxyphenyl)-4-methoxybenzenesulfonamide (**140**).

*Compound **18** article 2. Available at Materials and methods, chemical synthesis.*

N-(3,4-dimethoxyphenyl)-4-nitrobenzenesulfonamide (**141**).

*Compound **23** article 3. Available at Materials and methods, chemical synthesis (2.1).*

N-(4,5-dimethoxy-2-nitrophenyl)-4-nitrobenzenesulfonamide (**142**).

*Compound **334** article 3. Available at Materials and methods, chemical synthesis (2.1).*

N-(2-bromo-4,5-dimethoxyphenyl)-4-nitrobenzenesulfonamide (**143**). To a solution of **141** (900 mg, 2.66 mmol) in CH_2Cl_2 (50 mL) and CH_3CN (50 mL), *N*-bromosuccinimide (568 mg, 3.19 mmol) was added. The reaction was stirred at room temperature for 24 h. The reaction mixture was concentrated, re-dissolved in EtOAc, washed with brine, dried over anhydrous Na_2SO_4, filtered, and concentrated under vacuum to produced 1.037 g (2.48 mmol, 93%) of crude reaction product from which 540 mg (1.29 mmol, 48%) of **143** were purified by crystallization. M.p.: 205-211 °C (MeOH). ^{1}H NMR (400 MHz, CD_3OD): δ 3.76 (3H, *s*), 3.81 (3H, *s*), 6.97 (1H, *s*), 7.08 (1H, *s*), 7.89 (2H, *d*, *J* = 8.8), 8.31 (2H, *d*, *J* = 8.8). ^{13}C NMR (100 MHz, DMSO-D_6): δ 56.1 (CH_3), 56.4 (CH_3), 112.4 (C), 113.2 (CH), 115.7 (CH), 124.9 (2CH), 126.8 (C), 128.9 (2CH), 146.4 (C), 148.5 (C), 149.0 (C), 150.2 (C). HRMS ($C_{14}H_{13}BrN_2O_6S$ + Na^+): calcd 438.9570 and 440.9549 (M + Na^+), found 438.9583 and 440.9549.

4-Amino-*N*-(3,4-dimethoxyphenyl)benzenesulfonamide (**144**).

*Compound **26** article 3. Available at Materials and methods, chemical synthesis (2.1).*

4-Amino-*N*-(2-bromo-4,5-dimethoxyphenyl)benzenesulfonamide (**145**). To an EtOH/AcOH/H_2O mixture (2:2:1, 12.5 mL) HCl (c) (1 drop), **143** (900 mg, 2.16 mmol) and Fe (1.20 g, 21.6 mmol) were added and the reaction was stirred for 3 h at 100°C. Crude residue was filtered through Celite®, diluted in CH_2Cl_2 and treated with 5% $NaHCO_3$. The organic layers were washed with brine, dried over anhydrous Na_2SO_4, filtered and concentrated under vacuum to afford 600 mg (1.55 mmol, 0.62 mmol, 72%) of compound **145**. Crude reaction product was purified by crystallization in methanol (242 mg, 0.63 mmol, 29%). M.p.: 184-188 °C (MeOH). ^{1}H NMR (400 MHz, CD_3OD): δ 3.74 (3H, *s*), 3.75 (3H, *s*), 6.58 (2H, *d*, *J* = 8.8), 6.94 (1H, *s*), 6.98 (1H, *s*), 7.35 (2H, *d*, *J* = 8.8). ^{13}C NMR (100 MHz, $CDCl_3$): δ 56.2 ($2CH_3$), 106.8 (C), 107.8 (CH), 113.8(2CH), 114.3 (CH), 126.6 (C), 128.1 (C), 129.5 (2CH), 147.2 (C), 148.9 (C), 150.9 (C). HRMS ($C_{14}H_{15}BrN_2O_4S$ + Na^+): calcd 408.9828 and 410.9808 (M + Na^+), found 408.9821 and 410.9787.

N-(3,4-dimethoxyphenyl)-4-(dimethylamino)benzenesulfonamide (**146**).

*Compound **29** article 3. Available at Materials and methods, chemical synthesis (2.1).*

N-(3,4-dimethoxyphenyl)-4-(dimethylamino)-*N*-methylbenzenesulfonamide (**147a**) and *N,N'*-methylenebis(*N*-(3,4-dimethoxyphenyl)-4-(dimethylamino)benzenesulfonamide) (**147b**). To a mixture of **146** (109 mg, 0.32 mmol), NaOH (15 mg, 0.64 mmol) and nBu$_4$N$^+$HSO$_4^-$ (128 mg, 0.64 mmol) in CH_2Cl_2 (50 mL), CH_3I (40 µL, 0.64 mmol) was added. The reaction was stirred at room temperature under nitrogen atmosphere for 2 days. The solution was poured onto brine, extracted with CH_2Cl_2, and then dried over Na_2SO_4. After concentration, the residue was purified

by silica gel column chromatography (hexane/EtOAc, 6:4) to give **147a** (27 mg, 0.07 mmol, 23%) and **147b** (83 mg, 0.12 mmol, 75%). **147a**: ^{1}H NMR (400 MHz, $CDCl_3$): δ 3.03 (6H, *s*), 3.09 (3H, *s*), 3.77 (3H, *s*), 3.85 (3H, *s*), 6.55 (1H, *dd*, *J* = 8.4 and 2.8), 6.60 (2H, *d*, *J* = 8.8), 6.69 (1H, *d*, *J* = 2.8), 6.73 (1H, *d*, *J* = 8.4), 7.39 (2H, *d*, *J* = 8.8). ^{13}C NMR (100 MHz, $CDCl_3$): δ 38.4 (CH_3), 40.0 ($2CH_3$), 55.9 (CH_3), 55.9 (CH_3), 110.4 (2CH), 111.2 (CH), 111.2 (CH), 118.6 (CH), 121.6 (C), 129.8 (2CH), 135.1 (C), 148.0 (C), 148.5 (C), 152.8 (C). HRMS ($C_{17}H_{22}N_2O_4S$ + H^+): calcd 351.1373 (M + H^+), found 351.1372. **147b**: IR (KBr): 3467, 1513, 1150, 812 cm^{-1}. ^{1}H NMR (400 MHz, $CDCl_3$): δ 2.93 (12H, *s*), 3.59 (6H, *s*), 3.80 (6H, *s*), 5.38 (2H, *s*), 6.35 (2H, *d*, *J* = 2), 6.41 (4H, *d*, *J* =8.8), 6.49 (2H, *dd*, *J* = 8.4 and 2), 6.66 (2H, *d*, *J* = 8.4), 7.12 (4H, *d*, *J* = 8.8). ^{13}C NMR (100 MHz, $CDCl_3$): δ 40.3 ($4CH_3$), 56.0 ($2CH_3$), 56.2 ($2CH_3$), 66.1 (CH_2), 110.7 (4CH), 110.8 (2CH), 113.5 (2CH), 122.3 (2CH), 124.4 (2C), 129.6 (4CH), 130.9 (2C), 148.8 (2C), 149.9 (2C), 152.9 (2C). HRMS ($C_{33}H_{40}N_4O_8S_2$ + Na^+): calcd 707.2180 (M + Na^+), found 707.2178.

N-(4,5-dimethoxy-2-nitrophenyl)-4-(dimethylamino)benzenesulfonamide (**148**).

*Compound **33** article 3. Available at Materials and methods, chemical synthesis (2.1).*

N-(2-amino-4,5-dimethoxyphenyl)-4-(dimethylamino)benzenesulfonamide (**149**).

*Compound **35** article 3. Available at Materials and methods, chemical synthesis (2.1).*

N-(2-amino-4,5-dimethoxyphenyl)-4-(dimethylamino)-*N*-methylbenzenesulfonamide (**150**).

*Compound **118** article 3. Available at Materials and methods, chemical synthesis (2.1).*

N-(2-((4-(dimethylamino)-*N*-methylphenyl)sulfonamido)-4,5-dimethoxyphenyl) formamide (**151**).

*Compound **132** article 3. Available at Materials and methods, chemical synthesis (2.1).*

N-(4,5-dimethoxy-2-(methylamino)phenyl)-4-(dimethylamino)-*N*-methylbenzenesulfonamide (**152a**) and 4-(dimethylamino)-*N*-(2-(dimethylamino)-4,5-dimethoxyphenyl)-*N*-methylbenzenesulfonamide (**152b**). To a solution of **149** (110 mg, 0.31 mmol) and K_2CO_3 (433 mg, 3.13 mmol) in acetone (25 mL), $(CH_3)_2SO_4$ (224 µL, 2.35 mmol) was dropwise added and heated at reflux overnight. Then, the reaction mixture was filtered, poured onto ice, and extracted with CH_2Cl_2. The organic layers were dried over anhydrous Na_2SO_4, filtered, and evaporated to dryness. Compounds **152a** (15 mg, 0.04 mmol, 13%) and **152b** (19 mg, 0.05 mmol, 15%) were isolated by preparative TLC (CH_2Cl_2/EtOAc 1:1). **152a**: ^{1}H NMR (400 MHz, $CDCl_3$): δ 2.86 (3H, *s*), 3.03 (6H, *s*), 3.04 (3H, *s*), 3.47 (3H, *s*), 3.87 (3H, *s*), 5.90 (1H, *s*), 6.26 (1H, *s*), 6.64 (2H, *d*, *J* = 9.2), 7.51 (2H, *d*, *J* = 9.2). ^{13}C NMR (100 MHz, $CDCl_3$): δ 31.0 (CH_3), 39.1 (CH_3), 40.1 ($2CH_3$), 55.7 (CH_3), 56.7 (CH_3), 95.9 (CH), 110.5 (2CH), 111.9 (CH), 118.4 (C), 121.9 (C), 130.1 (2CH), 139.2 (C), 143.3 (C), 150.0 (C), 152.9 (C). HRMS ($C_{18}H_{25}N_3O_4S$ + H^+): calcd 380.1639 (M + H^+), found 380.1632. **152b**: ^{1}H NMR (400 MHz, $CDCl_3$): δ 2.82 (6H, *s*), 3.03 (6H, *s*), 3.11 (3H, *s*), 3.60 (3H, *s*), 3.85 (3H, *s*), 6.28 (1H, *s*), 6.56 (1H, *bs*), 6.66 (2H, *d*, *J* = 8.8), 7.63 (2H, *d*, *J* = 8.8). ^{13}C NMR (100 MHz, $CDCl_3$): δ 38.6 (CH_3), 40.0 ($2CH_3$), 44.2 ($2CH_3$), 55.9 (CH_3), 56.0 (CH_3), 104.1 (CH), 109.5 (C), 110.6 (2CH), 111.6 (CH), 126.4 (C), 129.9 (2CH), 140.0 (C), 141.8 (C), 148.8 (C), 152.8 (C). HRMS ($C_{19}H_{27}N_3O_4S$ + H^+): calcd 394.1795 (M + H^+), found 394.1580.

4-((5,6-Dimethoxy-1*H*-benzo[*d*][1,2,3]triazol-1-yl)sulfonyl)-*N*,*N*-dimethylaniline (**153**).

*Compound **117** article 3. Available at Materials and methods, chemical synthesis (2.1).*

N-(2-bromo-4,5-dimethoxyphenyl)-4-(dimethylamino)benzenesulfonamide (**154**). Compound **145** (200 mg, 0.52 mmol) was dissolved in MeOH (50 mL) with paraformaldehyde (155 mg, 5.16 mmol) and acetic acid (one drop). After 1 h stirring at room temperature sodium cyanoborohydride (65 mg, 1.03 mmol) was added to the solution and it was heated at reflux.

The reaction mixture was allowed to react for 3 days. The methanol solution was concentrated under reduced pressure, the residue was dissolved in EtOAc and washed with 5% $NaHCO_3$ and brine. The organics were dried over sodium sulphate and evaporated to afford **154** (201 mg, 0.48 mmol, 94%). The residue was purified by crystallization in methanol (123 mg, 0.29 mmol, 57%). M.p.: 170-178 °C (MeOH). ^{1}H NMR (400 MHz, CD_3OD): δ 3.01 (6H, *s*), 3.75 (3H, *s*), 3.75 (3H, *s*), 6.68 (2H, *d*, *J* = 8.8), 6.97 (1H, *s*), 6.99 (1H, *s*), 7.47 (2H, *d*, *J* = 8.8). ^{13}C NMR (100 MHz, $CDCl_3$): δ 39.9 (CH_3), 56.2 (CH_3), 56.2 (CH_3), 106.3 (C), 107.3 (CH), 110.6 (2CH), 114.3 (CH), 123.6 (C), 128.4 (C), 129.2 (2CH), 146.9 (C), 148.8 (C), 153.1 (C). HRMS ($C_{16}H_{19}BrN_2O_4S$ + Na^+): calcd 437.0141 and 439.0121 (M + Na^+), found 437.0136 and 439.0109.

N-(2-bromo-4,5-dimethoxyphenyl)-4-(dimethylamino)-*N*-methylbenzenesulfonamide (**155**). To a solution of **154** (74 mg, 0.18 mmol) in CH_3CN (40 mL) KOH (20 mg, 0.36 mmol) was added and stirred for 30 min. Then, CH_3I (22 µL, 0.36 mmol) was added. The reaction mixture was stirred at room temperature for 24 h and evaporated to dryness. The residue was dissolved in EtOAc, washed with brine, and dried over Na_2SO_4. After concentration, the residue (70 mg) was purified by preparative TLC (toluene/EtOAc 1:1) to give 35 mg (0.08 mmol, 46%) of **155**. ^{1}H NMR (400 MHz, CD_3OD): δ 3.06 (6H, *s*), 3.07 (3H, *s*), 3.61 (3H, *s*), 3.81 (3H, *s*), 6.46 (1H, *s*), 6.80 (2H, *d*, *J* = 8.8), 7.15 (1H, *s*), 7.56 (2H, *d*, *J* = 8.8). ^{13}C NMR (100 MHz, CD_3OD): δ 37.6 (CH_3), 38.7 ($2CH_3$), 54.9 (CH_3), 55.3 (CH_3), 110.5 (2CH), 112.1 (CH), 115.1 (C), 115.5 (CH), 122.9 (C), 129.5 (2CH), 132.8 (C), 148.5 (C), 149.6 (C), 153.4 (C). HRMS ($C_{17}H_{21}BrN_2O_4S$ + H^+): calcd 429.0478 and 431.0458 (M + H^+), found 429.0514 and 431.0493.

N-(2-bromo-4,5-dimethoxyphenyl)-*N*-(cyanomethyl)-4-(dimethylamino)benzenesulfonamide (**156**). A solution of **154** (82 mg, 0.20 mmol) and K_2CO_3 (55 mg, 0.40 mmol) in dry DMF (5 mL) was stirred at room temperature for 1 h. To this solution 2-chloroacetonitrile (25 µL, 0.40 mmol) was added and the reaction mixture was stirred for 24 h. The solvent was removed under reduced pressure. The residue was dissolved in EtOAc and washed with brine, dried (Na_2SO_4) and concentrated in vacuo to afford 86 mg (0.19 mmol, 95%) of **156**. The crude product was purified by crystallization in methanol (48 mg, 0.11 mmol, 53%). M.p.: 196-202 °C (MeOH). ^{1}H NMR (400 MHz, $CDCl_3$): δ 3.04 (6H, *s*), 3.69 (3H, *s*), 3.85 (3H, *s*), 4.17 (1H, *d*, *J* = 17.2), 4.87 (1H, *d*, *J* = 17.2), 6.64 (2H, *d*, *J* = 8.8), 6.73 (1H, *s*), 7.03 (1H, *s*), 7.60 (2H, *d*, *J* = 8.8). ^{13}C NMR (100 MHz, $CDCl_3$): δ 38.7 (CH_2), 40.0 ($2CH_3$), 56.0 (CH_3), 56.3 (CH_3), 110.7 (2CH), 113.8 (CH), 115.3 (C), 115.4 (C), 115.5 (CH), 123.0 (C), 129.0 (C), 130.0 (2CH), 148.5 (C), 150.2 (C), 153.4 (C). HRMS ($C_{18}H_{20}BrN_3O_4S$ + Na^+): calcd 476.0250 and 478.0230 (M + Na^+), found 476.0239 and 478.0220.

N-(4-(*N*-(3,4-dimethoxyphenyl)sulfamoyl)phenyl)formamide (**157**). A solution of **144** (990 mg, 3.21 mmol) and formic acid (1.2 mL, 32.14 mmol) in pyridine (1 mL) and CH_2Cl_2 (100 mL) was stirred at room temperature for 48 h. Then, the reaction mixture was washed with 2N HCl, 5% $NaHCO_3$ and brine, dried over Na_2SO_4, filtered and evaporated to dryness to afford 815 mg (2.42 mmol, 76%) of **157**, which was purified by preparative TLC (CH_2Cl_2/MeOH 95:5) (648 mg, 1.93 mmol, 60%).^{1}H NMR (400 MHz, CD_3OD): δ 3.71 (3H, *s*), 3.74 (3H, *s*), 6.56 (1H, *dd*, *J* = 8.4 and 2.4), 6.67 (1H, *d*, *J* = 2.4), 6.77 (1H, *d*, *J* = 8.4), 7.63 (2H, *d*, *J* = 8.8), 7.67 (2H, *d*, *J* = 8.8). ^{13}C NMR (100 MHz, acetone-D_6): δ 55.1 (CH_3), 55.3 (CH_3), 107.3 (CH), 112.0 (CH), 114.3 (CH), 118.9 (2CH), 128.4 (2CH), 130.7 (C), 134.4 (C), 142.0 (C), 147.1 (C), 149.5 (C), 159.6 (CH). HRMS ($C_{15}H_{16}N_2O_5S$ + Na^+): calcd 359.0672 (M + Na^+), found 359.0664.

N-(4-(*N*-(2-bromo-4,5-dimethoxyphenyl)sulfamoyl)phenyl)formamide (**158**). A solution of **145** (400 mg, 1.03 mmol) and formic acid (400 µL, 10.33 mmol) in pyridine (1 mL) and CH_2Cl_2 (50 mL) was stirred for 48 h. Then, the reaction mixture was washed with 2N HCl, 5% $NaHCO_3$ and brine, dried over Na_2SO_4, filtered, and evaporated to dryness to afford 397 mg (0.96 mmol, 93%) of **158**. The crude reaction product was purified by crystallization in methanol (171 mg, 0.41 mmol, 40%). M.p.: 199-203 °C (MeOH). ^{1}H NMR (400 MHz, CD_3OD): δ 3.76 (3H, *s*), 3.77 (3H, *s*), 6.98 (1H,

s), 7.01 (1H, *s*), 7.63 (2H, *d*, *J* = 8.8), 7.68 (2H, *d*, *J* = 8.8), 8.31 (1H, *s*). ^{13}C NMR (100 MHz, acetone-D_6): δ 55.4 (CH_3), 55.6 (CH_3), 110.8 (CH), 115.1 (CH), 116.7 (C), 118.8 (2CH), 127.7 (C), 128.6 (2CH), 134.6 (C), 142.4 (C), 148.5 (C), 149.0 (C), 159.5 (CH). HRMS ($C_{15}H_{15}BrN_2O_5S$ + Na^+): calcd 436.9777 (M + Na^+), found 436.9779.

N-(3,4-dimethoxyphenyl)-4-(methylamino)benzenesulfonamide (**159**). To a solution of **157** (610 mg, 1.81 mmol) and $NaBH_4$ (103 mg, 2.72 mmol) in dry THF (15 mL) at 0°C, trichloroacetic acid (444 mg, 2.72 mmol) diluted in dry THF (10 mL) was added dropwise under nitrogen atmosphere. The reaction mixture was stirred at 0°C to room temperature for 48 h, concentrated and re-dissolved in EtOAc, washed with brine, dried over anhydrous Na_2SO_4, filtered and solvent evaporated in vacuum. The residue (534 mg) was purified by flash column chromatography (hexane/EtOAc 1:1) to afford the compound **159** (293 mg, 0.91 mmol, 50%).^{1}H NMR (400 MHz, CD_3OD): δ 2.76 (3H, *s*), 3.70 (3H, *s*), 3.74 (3H, *s*), 6.51 (2H, *d*, *J* = 8.8), 6.56 (1H, *dd*, *J* = 8.4 and 2.4), 6.66 (1H, *d*, *J* = 2.4), 6.76 (1H, *d*, *J* = 8.4), 7.41 (2H, *d*, *J* = 8.8). ^{13}C NMR (100 MHz, $CDCl_3$): δ 30.0 (CH_3), 55.8 (CH_3), 55.9 (CH_3), 107.7 (CH), 111.1 (CH), 111.1 (2CH), 115.3 (CH), 125.2 (C), 129.3 (2CH), 129.9 (C), 147.0 (C), 149.0 (C), 152.5 (C). HRMS ($C_{15}H_{18}N_2O_4S$ + Na^+): calcd 345.0879 (M + Na^+), found 345.0871.

N-(3,4-dimethoxyphenyl)-*N*-methyl-4-(methylamino)benzenesulfonamide (**160**). To 70 mg (0.22 mmol) of **159** and 24 mg (0.43 mmol) of KOH in CH_3CN (40 mL), 27 µL of CH_3I (0.43 mmol) were added and it was stirred for 24 h. The CH_3CN solution was concentrated under reduced pressure, the residue dissolved in EtOAc and washed with brine. The organics were dried over Na_2SO_4, filtered and evaporated. The crude residue (72 mg) was purified by preparative TLC using toluene/EtOAc 1:1 as eluant to give 68 mg (0.20 mmol, 93%) of **160**.^{1}H NMR (400 MHz, $CDCl_3$): δ 2.81 (3H, *s*), 3.07 (3H, *s*), 3.74 (3H, *s*), 3.82 (3H, *s*), 6.48 (2H, *d*, *J* = 8.4), 6.53 (1H, *dd*, *J* = 8.8 and 2.8), 6.65 (1H, *d*, *J* = 2.8), 6.70 (1H, *d*, *J* = 8.8), 7.31 (2H, *d*, *J* = 8.4). ^{13}C NMR (100 MHz, $CDCl_3$): δ 29.9 (CH_3), 38.4 (CH_3), 55.8 (CH_3), 55.9 (CH_3), 110.5 (CH), 110.8 (2CH), 111.2 (CH), 118.7 (CH), 122.6 (C), 129.9 (2CH), 135.1 (C), 148.1 (C), 148.6 (C), 152.6 (C). HRMS ($C_{16}H_{20}N_2O_4S$ + Na^+): calcd 359.1036 (M + Na^+), found 359.1041.

N-(3,4-dimethoxyphenyl)-*N*-ethyl-4-(methylamino)benzenesulfonamide (**161**). A solution of **159** (60 mg, 0.19 mmol) and KOH (20 mg, 0.37 mmol) in CH_3CN (40 mL) was stirred for 30 min. Then, bromoethane (28 µL, 0.37 mmol) was added. After 24 h, the solvent was evaporated to dryness and the crude residue was re-dissolved in EtOAc, washed with brine, dried over Na_2SO_4, filtered, and concentrated in vacuo. The residue (63 mg) was purified by preparative TLC in CH_2Cl_2/MeOH 98:2 to afford 34 mg (0.10 mmol, 52%) of compound **161**. ^{1}H NMR (400 MHz, CD_3OD): δ 1.01 (3H, *t*, *J* = 7.6), 2.79 (3H, *s*), 3.52 (2H, *q*, *J* = 7.6), 3.67 (3H, *s*), 3.80 (3H, *s*), 6.52 (1H, *d*, *J* = 2.4), 6.58 (2H, *d*, *J* = 9.2), 6.59 (1H, *dd*, *J* = 8.8 and 2.4), 6.86 (1H, *d*, *J* = 8.8), 7.31 (2H, *d*, *J* = 9.2). ^{13}C NMR (100 MHz, $CDCl_3$): δ 13.9 (CH_3), 30.1 (CH_3), 45.5 (CH_2), 55.8 (CH_3), 55.9 (CH_3), 110.5 (CH), 110.9 (2CH), 112.6 (CH), 121.1 (CH), 124.7 (C), 129.8 (2CH), 132.1 (C), 148.4 (C), 148.7 (C), 152.4 (C). HRMS ($C_{17}H_{22}N_2O_4S$ + Na^+): calcd 373.1192 (M + Na^+), found 373.1192.

N-(cyanomethyl)-*N*-(3,4-dimethoxyphenyl)-4-(methylamino)benzenesulfonamide (**162**). 2-chloroacetonitrile (20 µL, 0.31 mmol) was added after 30 min to a stirred solution of **159** (50 mg, 0.15 mmol) and K_2CO_3 (42 mg, 0.31 mmol) in DMF (3 mL). After 24 h, the reaction mixture was dried under vacuum, re-dissolved in EtOAc and washed with brine. After drying over Na_2SO_4 and removal of the solvent, the residue (54 mg) was purified by preparative TLC (CH_2Cl_2/MeOH 98:2) to give **162** (41 mg, 0.11 mmol, 73%). ^{1}H NMR (400 MHz, CD_3OD): δ 2.80 (3H, *s*), 3.68 (3H, *s*), 3.82 (3H, *s*), 4.62 (2H, *s*), 6.59 (2H, *d*, *J* = 8.8), 6.66 (1H, *d*, *J* = 2.8), 6.74 (1H, *dd*, *J* = 8.8 and 2.8), 6.90 (1H, *d*, *J* = 8.8), 7.37 (2H, *d*, *J* = 8.8). ^{13}C NMR (100 MHz, $CDCl_3$): δ 30.0 (CH_3), 39.7 (CH_2), 55.9 (CH_3), 55.9 (CH_3), 110.9 (CH), 111.1 (2CH), 112.1 (CH), 115.4 (C), 120.8 (CH), 123.3 (C), 130.2

(2CH), 131.4 (C), 149.1 (C), 149.4 (C), 153.1 (C). HRMS ($C_{17}H_{19}N_3O_4S + Na^+$): calcd 384.0988 (M + Na^+), found 384.0981.

Ethyl *N*-(3,4-dimethoxyphenyl)-*N*-((4-(methylamino)phenyl)sulfonyl)glycinate (**163**). To a solution of **159** (70 mg, 0.22 mmol) and K_2CO_3 (59 mg, 0.43 mmol) in dry DMF (3 mL), ethyl 2-bromoacetate (48 µL, 0.43 mmol) was added after 30 min stirring. The reaction mixture was then stirred for 48 h, concentrated under vacuum, re-dissolved in EtOAc, washed with brine, dried (Na_2SO_4) and evaporated to dryness. The residue (84 mg) was purified by preparative TLC (toluene/EtOAc 1:1) to give **163** (66 mg, 0.16 mmol, 74%). ^{1}H NMR (400 MHz, CD_3OD): δ 1.20 (3H, *t*, *J* = 7.2), 2.78 (3H, *s*), 3.67 (3H, *s*), 3.77 (3H, *s*), 4.12 (2H, *q*, *J* = 7.2), 4.33 (2H, *s*), 6.56 (2H, *d*, *J* = 8.8), 6.68 (1H, *dd*, *J* = 8.4 and 2.4), 6.73 (1H, *d*, *J* = 2.4), 6.80 (1H, *d*, *J* = 8.4), 7.36 (2H, *d*, *J* = 8.8). ^{13}C NMR (100 MHz, CD_3OD): δ 13.0 (CH_3), 28.4 (CH_3), 52.6 (CH_2), 54.9 (CH_3), 55.0 (CH_3), 60.9 (CH_3), 110.2 (CH), 110.9 (2CH), 112.9 (CH), 121.2 (CH), 123.2 (C), 129.5 (2CH), 133.1 (C), 148.8 (C), 149.9 (C), 153.8 (C), 169.5 (C). HRMS ($C_{19}H_{24}N_2O_6S + Na^+$): calcd 431.1247 (M + Na^+), found 431.1240.

N-(2-bromo-4,5-dimethoxyphenyl)-4-(methylamino)benzenesulfonamide (**164**). To a solution of **158** (320 mg, 0.77 mmol) and $NaBH_4$ (44 mg, 1.16 mmol) in dry THF (15 mL) at 0°C, trichloroacetic acid (189 mg, 1.16 mmol) diluted in dry THF (10 mL) was added dropwise under nitrogen atmosphere. The reaction mixture was stirred at 0°C to room temperature for 48 h, concentrated and re-dissolved in EtOAc, washed with brine, dried over anhydrous Na_2SO_4, filtered, and solvent evaporated in vacuum to afford the compound **164** (262 mg, 0.65 mmol, 85%). Crude reaction product was purified by crystallization in methanol (103 mg, 0.26 mmol, 33%). M.p.: 150-152 °C (MeOH). IR (KBr): 3394, 3232, 1602, 1147, 817 cm^{-1}. ^{1}H NMR (400 MHz, CD_3OD): δ 2.77 (3H, s), 3.74 (3H, s), 3.75 (3H, s), 6.52 (2H, d, J = 8.8), 6.97 (1H, s), 6.98 (1H, s), 7.40 (2H, d, J = 8.8). ^{13}C NMR (100 MHz, acetone-D_6): δ 29.5 (CH_3), 55.3 (CH_3), 55.5 (CH_3), 107.8 (C), 109.4 (CH), 110.6 (2CH), 115.0 (CH), 125.1 (C), 128.5 (C), 129.3 (2CH), 147.8 (C), 148.9 (C), 153.5 (C). HRMS ($C_{15}H_{17}BrN_2O_4S + Na^+$): calcd 422.9985 and 424.9964 (M + Na^+), found 422.9977 and 424.9939.

N-(2-bromo-4,5-dimethoxyphenyl)-*N*-methyl-4-(methylamino)benzenesulfonamide (**165**). 56 mg (0.14 mmol) of **164** were dissolved in CH_3CN (30 mL) with 16 mg (0.28 mmol) of KOH. After 30 min stirring at room temperature, CH_3I (17.5 µL, 0.28 mmol) was added to the solution and the reaction mixture was stirred for 48 h. The solvent was removed under reduced pressure. The residue was dissolved in EtOAc and washed with brine, dried (Na_2SO_4) and concentrated in vacuo. The crude residue (54 mg) was purified by preparative TLC in CH_2Cl_2/MeOH 99:1 (**165**, 40 mg, 0.10 mmol, 69%). M.p.: 135-140 °C (MeOH). ^{1}H NMR (400 MHz, CD_3OD): δ 2.82 (3H, *s*), 3.07 (3H, *s*), 3.62 (3H, *s*), 3.82 (3H, *s*), 6.45 (1H, *s*), 6.65 (2H, *d*, *J* = 8.8), 7.15 (1H, *s*), 7.49 (2H, *d*, *J* = 8.8). ^{13}C NMR (100 MHz, $CDCl_3$): δ 30.1 (CH_3), 38.3 (CH_3), 56.0 (CH_3), 56.2 (CH_3), 111.1 (2CH), 112.5 (CH), 115.0 (C), 115.4 (CH), 125.1 (C), 130.1 (2CH), 132.9 (C), 148.3 (C), 149.2 (C), 152.6 (C). HRMS ($C_{16}H_{19}BrN_2O_4S + Na^+$): calcd 439.0121 (M + Na^+), found 439.0111.

N-(2-bromo-4,5-dimethoxyphenyl)-*N*-ethyl-4-(methylamino)benzenesulfonamide (**166**). 65 mg (0.16 mmol) of compound **164** were dissolved in dry DMF (3 mL) and 44 mg (0.32 mmol) of crushed K_2CO_3 were added. After 30 min stirring at room temperature, 24 µL (0.32 mmol) of bromoethane were added to the solution. The reaction mixture was stirred at room temperature for 48 h. The mixture was evaporated to dryness. The residue was diluted with water, and the solution was extracted with EtOAc. The extract was dried over Na_2SO_4, filtered, and evaporated to dryness. The residue (46 mg) was purified by preparative TLC (CH_2Cl_2/MeOH 99:1) to give 28 mg (0.06 mmol, 41%) of compound **166**. ^{1}H NMR (400 MHz, CD_3OD): δ 1.03 (3H, *t*, *J* = 7.2), 2.81 (3H, *s*), 3.61 (3H, *s*), 3.75 (2H, *m*), 3.82 (3H, *s*), 6.39 (1H, *s*), 6.63 (2H, *d*, *J* = 8.8),

7.17 (1H, *s*), 7.47 (2H, *d*, *J* = 8.8). ^{13}C NMR (100 MHz, $CDCl_3$): δ 13.7 (CH_3), 30.1 (CH_3), 45.9 (CH_2), 56.0 (CH_3), 56.1 (CH_3), 111.1 (2CH), 113.6 (CH), 115.4 (CH), 116.8 (C), 125.9 (C), 130.0 (2CH), 130.3 (C), 148.1 (C), 149.2 (C), 152.5 (C). HRMS ($C_{17}H_{21}BrN_2O_4S$ + Na^+): calcd 451.0298 (M + Na^+), found 451.0299.

N-(2-bromo-4,5-dimethoxyphenyl)-*N*-(cyanomethyl)-4-(methylamino)benzenesulfonamide (**167**). A mixture of **164** (72 mg, 0.18 mmol) and K_2CO_3 (49 mg, 0.36 mmol) in dry DMF (3 mL) was stirred at room temperature for 30 min. Then, 2-chloroacetonitrile (22.7 µL, 0.36 mmol) was added. After 48 h, the solvent was evaporated under reduced pressure. The residue was dissolved in EtOAc and washed with brine, dried (Na_2SO_4), filtered, and concentrated in vacuo. After concentration (66 mg), the title compound was isolated by preparative TLC in CH_2Cl_2/MeOH 99:1 (**167**, 30 mg, 0.07 mmol, 38%). M.p.: 173-177 °C (MeOH). ^{1}H NMR (400 MHz, $CDCl_3$): δ 2.88 (3H, *s*), 3.71 (3H, *s*), 3.87 (3H, *s*), 4.17 (1H, *d*, *J* = 18), 4.87 (1H, *d*, *J* = 18), 6.57 (2H, *d*, *J* = 8.8), 6.75 (1H, *s*), 7.04 (1H, *s*), 7.58 (2H, *d*, *J* = 8.8). ^{13}C NMR (100 MHz, $CDCl_3$): δ 30.0 (CH_3), 38.7 (CH_2), 56.0 (CH_3), 56.2 (CH_3), 111.2 (2CH), 113.9 (CH), 115.2 (C), 115.4 (C), 115.5 (CH), 124.4 (C), 128.9 (C), 130.3 (2CH), 148.5 (C), 150.2 (C), 153.2 (C). HRMS ($C_{17}H_{18}BrN_3O_4S$ + Na^+): calcd 462.0094 and 464.0073 (M + Na^+), found 462.0083 and 464.0039.

N-(4-(*N*-(3,4-dimethoxyphenyl)sulfamoyl)phenyl)-*N*-methylformamide (**168**). The compound **159** (80 mg, 0.25 mmol) was stirred in a mixture of CH_2Cl_2 (40 mL), pyridine (1 mL) and formic acid (2 mL) at room temperature for 48 h. Then, the reaction mixture was poured onto ice and treated with 2N HCl and 5% $NaHCO_3$, washed to neutrality with brine, dried over anhydrous Na_2SO_4, filtered and concentrated under vacuum. The residue (68 mg) was purified by preparative TLC (toluene/EtOAc 1:1) to isolate compound **168** (20 mg, 0.06 mmol, 23%). ^{1}H NMR (400 MHz, CD_3OD): δ 3.27 (3H, *s*), 3.70 (3H, *s*), 3.72 (3H, *s*), 6.57 (1H, *dd*, *J* = 8.4 and 2.4), 6.71 (1H, *d*, *J* = 2.4), 6.75 (1H, *d*, *J* = 8.4), 7.39 (2H, *d*, *J* = 8.8), 7.74 (2H, *d*, *J* = 8.8), 8.61 (1H, *s*). ^{13}C NMR (100 MHz, acetone-D_6): δ 29.9 (CH_3), 55.1 (CH_3), 55.3 (CH_3), 107.2 (CH), 112.0 (CH), 114.3 (CH), 120.2 (2CH), 128.6 (2CH), 130.6 (C), 136.1 (C), 146.1 (C), 147.2 (C), 149.6 (C), 161.4 (CH). HRMS ($C_{16}H_{18}N_2O_5S$ + Na^+): calcd 373.0829 (M + Na^+), found 373.0824.

2-Methoxy-4,6-dinitrophenol (**169**). To a stirred solution at 0°C of 2-methoxyphenol (5 g, 4.52 mL, 40.3 mmol) in acetic acid (60 mL), nitric acid (5.54 mL, 80.6 mmol) in acetic acid (40 mL) was slowly added under nitrogen atmosphere. After 6 h at 0°C, the reaction mixture was poured onto ice and kept at 4°C for 1 h. Then, the precipitate formed was filtered and washed with water under vacuum to dryness to obtain 7.77 g (36.6 mmol, 90%) of **169**. ^{1}H NMR (400 MHz, $CDCl_3$): δ 4.06 (3H, *s*), 7.95 (1H, *d*, *J* = 2.8), 8.67 (1H, *d*, *J* = 2.8), 11.18 (1H, *bs*). ^{13}C NMR (100 MHz, $CDCl_3$): δ 57.3 (CH_3), 111.0 (CH), 112.7 (CH), 139.3 (2C), 150.6 (C), 150.9 (C). HRMS ($C_7H_6N_2O_6$ + H^+): calcd 215.0299 (M + H^+), found 215.0299.

1,2-Dimethoxy-3,5-dinitrobenzene (**170**). To a solution of **169** (5.27 g, 24.6 mmol) and K_2CO_3 (11.9 g, 86 mmol) in acetone (100 mL), $(CH_3)_2SO_4$ (11.7 mL, 123 mmol) was dropwise added. The reaction mixture was stirred at room temperature for 48 h and then heated at reflux for 8 h. The mixture was filtered through Celite® and evaporated to dryness to afford compound **170** (5.52 g, 24.2 mmol, 98%). The product was then used without further purification. ^{1}H NMR (400 MHz, $CDCl_3$): δ 4.03 (3H, *s*), 4.09 (3H, *s*), 7.95 (1H, *d*, *J* = 2.8), 8.25 (1H, *d*, *J* = 2.8). ^{13}C NMR (100 MHz, $CDCl_3$): δ 57.0 (CH_3), 62.4 (CH_3), 110.2 (CH), 112.1 (CH), 142.4 (C), 143.8 (C), 148.0 (C), 154.3 (C). HRMS ($C_8H_8N_2O_6$ + H^+): calcd 229.0455 (M + H^+), found 229.0470.

4,5-Dimethoxybenzene-1,3-diamine (**171**). A mixture of **170** (5.48 g, 24 mmol), 20 mg of Pd (C) and 125 mL of EtOAc was maintained under low hydrogen pressure and stirred at room temperature. After 4 days, uptake of H_2 was completed and the solution was filtered through

Celite®. The filtrate was concentrated in vacuo to give product **171** (3.32 g, 19.7 mmol, 82%). The product was then used without further purification. ^{1}H NMR (400 MHz, $CDCl_3$): δ 3.76 (3H, *s*), 3.78 (3H, *s*), 5.72 (1H, *d*, *J* = 2.8), 5.74 (1H, *d*, *J* = 2.8). ^{13}C NMR (100 MHz, $CDCl_3$): δ 55.5 (CH_3), 60.1 (CH_3), 90.6 (CH), 95.1 (CH), 140.9 (C), 143.2 (C), 147.0 (C), 153.5 (C). GC-MS ($C_8H_{12}N_2O_2$): 168 (M^+).

N-(3-amino-4,5-dimethoxyphenyl)-4-methoxybenzenesulfonamide (**172**). To a solution of **171** (2.82 g, 16.7 mmol) in CH_2Cl_2 (100 mL) and pyridine (2.7 mL, 35.5 mmol), 4-methoxybenzenesulfonyl chloride (865 mg, 8.38 mmol) was slowly added. After complete uptake of 4-methoxybenzenesulfonyl chloride, another 865 mg (8.35 mmol) were slowly added. The reaction mixture was stirred at room temperature for 4 h. Then, it was washed with brine, dried over Na_2SO_4, filtered, and concentrated under vacuum. The residue (4.48 g) was dissolved again in CH_2Cl_2 and treated with 2N HCl. Both layers were then treated separately. Organic layer was washed with brine, dried, filtered and evaporated to afford 2.20 g (4.33 mmol, 52%) of the uncharacterized compound *N*,*N*'-(4,5-dimethoxy-1,3-phenylene)bis(4-methoxybenzenesulfonamide). Aqueous layer was then neutralized with 5% $NaHCO_3$ and extracted with CH_2Cl_2. The resulted organic layer was washed with brine, dried over Na_2SO_4, filtered, and concentrated under vacuum to afford 1.18 g (3.49 mmol, 21%) of the desired compound **172**, which was purified by flash column chromatography (hexane/EtOAc 1:1) (916 mg, 2.71 mmol, 16%). M.p.: 132-133 °C (CH_2Cl_2/hexane). ^{1}H NMR (400 MHz, CD_3OD): δ 3.64 (3H, *s*), 3.65 (3H, *s*), 3.74 (3H, *s*), 6.08 (1H, *d*, *J* = 2.4), 6.21 (1H, *d*, *J* = 2.4), 6.90 (2H, *d*, *J* = 8.8), 7.67 (2H, *d*, *J* = 8.8). ^{13}C NMR (100 MHz, CD_3OD): δ 54.7 (CH_3), 54.7 (CH_3), 58.9 (CH_3), 95.8 (CH), 101.8 (CH), 113.7 (2CH), 129.0 (2CH), 130.9 (C), 132.9 (C), 133.8 (C), 141.1 (C), 152.9 (C), 163.0 (C). HRMS ($C_{15}H_{18}N_2O_5S + H^+$): calcd 339.1009 ($M + H^+$), found 339.1013.

N-(3-amino-4,5-dimethoxyphenyl)-4-methoxy-*N*-methylbenzenesulfonamide (**173**). To 110 mg (0.32 mmol) of **172** and 45 mg (0.65 mmol) of KOH in CH_3CN (50 mL), 40.7 µL (0.65 mmol) of CH_3I were added and it was stirred for 24 h. The CH_3CN solution was concentrated under reduced pressure, the residue dissolved in EtOAc and washed with brine. The organics were dried over Na_2SO_4, filtered and evaporated. The crude material (91 mg) was purified by column chromatography using hexane/EtOAc 1:1 as eluant to give 60 mg (0.17 mmol, 52%) of **173.** ^{1}H NMR (400 MHz, $CDCl_3$): δ 3.06 (3H, *s*), 3.70 (3H, *s*), 3.78 (3H, *s*), 3.84 (3H, *s*), 6.05 (1H, *d*, *J* = 2.4), 6.07 (1H, *d*, *J* = 2.4), 6.91 (2H, *d*, *J* = 8.8), 7.54 (2H, *d*, *J* = 8.8). ^{13}C NMR (100 MHz, $CDCl_3$): δ 38.4 (CH_3), 55.6 (CH_3), 55.7 (CH_3), 59.9 (CH_3), 101.7 (CH), 107.0 (CH), 113.7 (2CH), 128.3 (C), 130.1 (2CH), 134.8 (C), 137.7 (C), 140.3 (C), 152.6 (C), 162.9 (C). HRMS ($C_{16}H_{20}N_2O_5S + H^+$): calcd 353.1166 ($M + H^+$), found 353.1171.

N-(2,3-dimethoxy-5-((4-methoxyphenyl)sulfonamido)phenyl)formamide (**174**). Compound **172** (197 mg, 0.58 mmol) was stirred in a mixture of CH_2Cl_2 (40 mL), pyridine (1 mL) and formic acid (3 mL) at room temperature for 48 h. Then, the reaction mixture was poured onto ice and treated with 2N HCl and 5% $NaHCO_3$, washed to neutrality with brine, dried over anhydrous Na_2SO_4, filtered and solvent evaporated to produce 142 mg (0.39 mmol, 67%) of crude reaction product **174**, which was purified by crystallization in methanol (104 mg, 0.28 mmol, 48%). M.p.: 213-217 °C (MeOH). ^{1}H NMR (400 MHz, CD_3OD): δ 3.76 (3H, *s*), 3.77 (3H, *s*), 3.82 (3H, *s*), 6.61 (1H, *d*, *J* = 2.8), 6.98 (2H, *d*, *J* = 9.2), 7.66 (1H, *d*, *J* = 2.8), 7.72 (2H, *d*, *J* = 9.2), 8.25 (1H, *s*). ^{13}C NMR (100 MHz, DMSO-D_6): δ 55.7 (CH_3), 55.7 (CH_3), 60.5 (CH_3), 100.3 (CH), 104.5 (CH), 114.4 (2CH), 129.2 (2CH), 131.2 (C), 131.7 (C), 133.9 (C), 134.1 (C), 152.1 (C), 160.3 (CH), 162.5 (C). HRMS ($C_{16}H_{18}N_2O_6S + H^+$): calcd 367.0958 ($M + H^+$), found 367.0963.

N-(3,4-dimethoxy-5-(methylamino)phenyl)-4-methoxybenzenesulfonamide (**175**). To a solution of **174** (110 mg, 0.30 mmol) and $NaBH_4$ (17 mg, 0.45 mmol) in dry THF (15 mL) at 0°C, trichloroacetic acid (74 mg, 0.45 mmol) diluted in dry THF (5 mL) was added dropwise under nitrogen atmosphere. The reaction mixture was stirred at 0°C to room temperature for 48 h, concentrated and re-dissolved in EtOAc, washed with brine, dried over anhydrous Na_2SO_4, filtered and solvent evaporated in vacuum to afford the compound **175** (99 mg, 0.28 mmol, 93%). Crude reaction product was purified by crystallization (22 mg, 0.06 mmol, 21%). M.p.: 156-161 °C (CH_2Cl_2/hexane). ^{1}H NMR (400 MHz, $CDCl_3$): δ 2.71 (3H, *s*), 3.71 (3H, *s*), 3.73 (3H, *s*), 3.83 (3H, *s*), 5.89 (1H, *d*, *J* = 2.4), 6.06 (1H, *d*, *J* = 2.4), 6.26 (1H, *bs*), 6.89 (2H, *d*, *J* = 8.8), 7.71 (2H, *d*, *J* = 8.8). ^{13}C NMR (100 MHz, $CDCl_3$): δ 31.4 (CH_3), 56.7 (CH_3), 56.9 (CH_3), 61.1 (CH_3), 96.5 (CH), 98.7 (CH), 115.2 (2CH), 130.7 (2CH), 131.8 (C), 133.7 (C), 134.5 (C), 144.7 (C), 153.4 (C), 164.1 (C). HRMS ($C_{16}H_{20}N_2O_5S$ + H^+): calcd 353.1166 (M + H^+), found 353.1161.

N-(3,4-dimethoxy-5-(methylamino)phenyl)-4-methoxy-*N*-methylbenzenesulfonamide (**176**). 58 mg (0.16 mmol) of **175** were dissolved in CH_3CN (25 mL) with 19 mg (0.33 mmol) of KOH. After 30 min stirring at room temperature, CH_3I (20.6 µL, 0.33 mmol) was added to the solution and the reaction mixture was stirred for 24 h. The solvent was removed under reduced pressure. The residue was dissolved in EtOAc and washed with brine, dried (Na_2SO_4) and concentrated in vacuo to afford 57 mg (0.15 mmol, 94%) of **176**. The crude product was purified by crystallization in CH_2Cl_2/hexane (11 mg, 0.03 mmol, 18%). M.p.: 138-146 °C (CH_2Cl_2/hexane). IR (KBr): 3411, 1602, 1497, 1175, 825 cm^{-1}. ^{1}H NMR (400 MHz, $CDCl_3$): δ 2.69 (3H, *d*, *J* = 4.4), 3.11 (3H, *s*), 3.72 (3H, *s*), 3.77 (3H, *s*), 3.86 (3H, *s*), 4.30 (1H, *bs*), 5.91 (1H, *d*, *J* = 2.4), 6.05 (1H, *d*, *J* = 2.4), 6.93 (2H, *d*, *J* = 8.8), 7.59 (2H, *d*, *J* = 8.8). ^{13}C NMR (100 MHz, $CDCl_3$): δ 30.2 (CH_3), 38.6 (CH_3), 55.6 (CH_3), 55.7 (CH_3), 59.8 (CH_3), 100.6 (CH), 102.5 (CH), 113.7 (2CH), 128.5 (C), 130.2 (2CH), 134.3 (C), 138.1 (C), 143.1 (C), 151.8 (C), 162.9 (C). HRMS ($C_{17}H_{22}N_2O_5S$ + H^+): calcd 367.1322 (M + H^+), found 367.1318.

N-(3-(dimethylamino)-4,5-dimethoxyphenyl)-4-methoxy-*N*-methylbenzenesulfonamide (**177**). To a solution of **172** (100 mg, 0.29 mmol) and K_2CO_3 (408 mg, 2.96 mmol) in acetone (20 mL), $(CH_3)_2SO_4$ (212 µL, 2.21 mmol) was dropwise added and heated at reflux for 1 h. Then, the reaction mixture was filtered, poured onto ice, and extracted with CH_2Cl_2. The organic layers were dried over anhydrous Na_2SO_4, filtered and evaporated to dryness (50 mg). Compound **177** (8 mg, 0.02 mmol, 7%) was isolated by preparative TLC (hexane/EtOAc 4:6). ^{1}H NMR (400 MHz, $CDCl_3$): δ 2.64 (6H, *s*), 3.05 (3H, *s*), 3.66 (3H, *s*), 3.72 (3H, *s*), 3.79 (3H, *s*), 6.07 (1H, *bs*), 6.23 (1H, *bs*), 6.86 (2H, *d*, *J* = 8.4), 7.48 (2H, *d*, *J* = 8.4). ^{13}C NMR (100 MHz, $CDCl_3$): δ 38.6 (CH_3), 42.7 ($2CH_3$), 55.6 (CH_3), 56.0 (CH_3), 59.3 (CH_3), 104.9 (CH), 109.5 (CH), 113.7 (2CH), 128.4 (C), 130.2 (2CH), 137.1 (C), 140.2 (C), 146.2 (C), 153.1 (C), 162.9 (C). HRMS ($C_{18}H_{24}N_2O_5S$ + H^+): calcd 381.1479 (M + H^+), found 381.1467.

2-Hydroxy-3-methoxy-5-nitrobenzonitrile (**178**). A mixture of 2-hydroxy-3-methoxy-5-nitrobenzaldehyde (404 mg, 2.05 mmol), hydroxylamine hydrochloride (1.42 g, 20.5 mmol) and pyridine (one drop) in methanol (15 mL) was heated at reflux. After 24 h, the methanolic solution was concentrated under reduced pressure and the residue was re-dissolved in EtOAc, washed with brine, dried over Na_2SO_4 and concentrated. The residue was then re-dissolved in pyridine (10 mL) and acetic anhydride (0.5 mL) and heated at reflux for 48 h. The reaction mixture was poured into ice, acidified with 2N HCl solution and extracted with EtOAc. The organic layers were washed with brine, dried over Na_2SO_4 and concentrated under vacuum to give compound **178** (277 mg, 1.43 mmol, 70%). The product was then used without further purification. ^{1}H NMR (400

MHz, CD_3OD): δ 4.00 (3H, *s*), 7.94 (1H, *d*, *J* = 2.8), 8.09 (1H, *d*, *J* = 2.8). GC-MS ($C_8H_6N_2O_4$): 194 (M^+).

2,3-Dimethoxy-5-nitrobenzonitrile (**179**). To a solution of **178** (277 mg, 1.43 mmol) and K_2CO_3 (988 mg, 7.15 mmol) in acetone (20 mL), $(CH_3)_2SO_4$ (239 µL, 2.50 mmol) was dropwise added and heated at reflux overnight. Then, the reaction mixture was concentrated under vacuum, re-dissolved in EtOAc and washed with brine. The organics were dried over anhydrous Na_2SO_4, filtered and evaporated to dryness to afford compound **179** (270 mg, 1.32 mmol, 91%). The product was then used without further purification. ^{1}H NMR (400 MHz, $CDCl_3$): δ 3.99 (3H, *s*), 4.19 (3H, *s*), 7.93 (1H, *d*, *J* = 2.8), 8.06 (1H, *d*, *J* = 2.8). GC-MS ($C_9H_8N_2O_4$): 204 (M^+).

5-Amino-2,3-dimethoxybenzonitrile (**180**). The nitro precursor **179** (270 mg, 1.32 mmol) in ethyl acetate (50 mL) and Pd (C) (10 mg) was stirred at room temperature under H_2 atmosphere for 48 h. The reaction mixture was filtered over Celite®, and the filtrate was evaporated to dryness to give the title compound (**180,** 225 mg, 1.26 mmol, 97%). The crude reaction product was then used without further purification. ^{1}H NMR (400 MHz, $CDCl_3$): δ 3.82 (3H, *s*), 3.87 (3H, *s*), 6.37 (1H, *d*, *J* = 2.8), 6.43 (1H, *d*, *J* = 2.8). GC-MS ($C_9H_{10}N_2O_2$): 178 (M^+).

N-(3-cyano-4,5-dimethoxyphenyl)-4-methoxybenzenesulfonamide (**181**). To a solution of the aniline **180** (220 mg, 1.23 mmol) in CH_2Cl_2 (50 mL) and pyridine (2 mL), 4-methoxybenzenesulfonyl chloride (306 mg, 1.48 mmol) was slowly added. The reaction mixture was stirred at room temperature for 4 h. Then, it was treated with 2N HCl and 5% $NaHCO_3$. The organics were washed with brine, dried over Na_2SO_4, filtered, and concentrated under vacuum to yield compound **181** (423 mg, 1.21 mmol, 98%), which was purified by crystallization in CH_2Cl_2 (220 mg, 0.63 mmol, 51%). M.p.: 170-180 °C (CH_2Cl_2). IR (KBr): 3222, 2228, 1590, 1492, 1150, 851 cm^{-1}. ^{1}H NMR (400 MHz, $CDCl_3$): δ 3.84 (3H, *s*), 3.86 (3H, *s*), 3.96 (3H, *s*), 6.65 (1H, *d*, *J* = 2.4), 6.73 (1H, *bs*), 6.93 (2H, *d*, *J* = 8.8), 7.01 (1H, *d*, *J* = 2.4), 7.68 (2H, *d*, *J* = 8.8). ^{13}C NMR (100 MHz, $CDCl_3$): δ 55.5 (CH_3), 56.1 (CH_3), 61.7 (CH_3), 106.6 (C), 111.1 (CH), 114.3 (2CH), 115.6 (CH), 115.8 (C), 129.4 (2CH), 130.8 (C), 133.7 (C), 148.7 (C), 152.9 (C), 163.2 (C). HRMS ($C_{16}H_{16}N_2O_5S$ + H^+): calcd 349.0853 (M + H^+), found 349.0849.

N-(3-cyano-4,5-dimethoxyphenyl)-4-methoxy-*N*-methylbenzenesulfonamide (**182**). To a stirred solution of **181** (67 mg, 0.19 mmol) in CH_3CN (30 mL), 21 mg (0.38 mmol) of KOH were added. After 1 h at room temperature 24 µL (0.38 mmol) of CH_3I were added and stirred for 24 h. The solution was concentrated in vacuo, re-dissolved with EtOAc, washed with brine, dried over Na_2SO_4 and evaporated to dryness to give 62 mg (0.17 mmol, 89%) of **182**. The crude reaction product was purified by crystallization in methanol (38 mg, 0.10 mmol, 54%). M.p.: 129-135 °C (MeOH). IR (KBr): 3435, 2236, 1594, 1163, 810 cm^{-1}. ^{1}H NMR (400 MHz, $CDCl_3$): δ 3.09 (3H, *s*), 3.87 (3H, *s*), 3.87 (3H, *s*), 4.02 (3H, *s*), 6.53 (1H, *d*, *J* = 2.4), 6.95 (2H, *d*, *J* = 9.2), 7.17 (1H, *d*, *J* = 2.4), 7.47 (2H, *d*, *J* = 9.2). ^{13}C NMR (100 MHz, $CDCl_3$): δ 37.9 (CH_3), 55.6 (CH_3), 56.2 (CH_3), 61.7 (CH_3), 106.2 (C), 114.2 (2CH), 115.6 (C), 117.6 (CH), 120.0 (CH), 127.1 (C), 129.9 (2CH), 137.9 (C), 150.7 (C), 152.5 (C), 163.4 (C). HRMS ($C_{17}H_{18}N_2O_5S$ + H^+): calcd 363.1009 (M + H^+), found 363.1008.

N-(3-cyano-4,5-dimethoxyphenyl)-*N*-ethyl-4-methoxybenzenesulfonamide (**183**). 70 mg (0.20 mmol) of **181** and 44 mg (0.40 mmol) of K_2CO_3 were dissolved in dry DMF (3 mL). After 30 min stirring at room temperature, 2-bromoethano (60 µL, 0.80 mmol) was added to the solution and stirred for 48 h. The reaction mixture was concentrated under reduced pressure, dissolved with EtOAc, washed with brine, dried (Na_2SO_4), filtered, and concentrated in vacuo to give 72 mg (0.19 mmol, 95%) of crude reaction product **183**, from which 45 mg (0.12 mmol, 59%) were

purified by crystallization in methanol. M.p.: 148-153 °C (MeOH). ^{1}H NMR (200 MHz, $CDCl_3$): δ 1.07 (3H, *t*, *J* = 7), 3.53 (2H, *q*, *J* = 7), 3.85 (3H, *s*), 3.88 (3H, *s*), 4.04 (3H, *s*), 6.57 (1H, *d*, *J* = 2.4), 6.96 (2H, *d*, *J* = 9), 7.04 (1H, *d*, *J* = 2.4), 7.53 (2H, *d*, *J* = 9). ^{13}C NMR (100 MHz, $CDCl_3$): δ 13.8 (CH_3), 45.4 (CH_2), 55.6 (CH_3), 56.2 (CH_3), 61.7 (CH_3), 106.4 (C), 114.2 (2CH), 115.5 (C), 119.5 (CH), 122.6 (CH), 129.0 (C), 129.7 (2CH), 135.2 (C), 151.2 (C), 152.7 (C), 163.2 (C). HRMS ($C_{18}H_{20}N_2O_5S + H^+$): calcd 377.1166 ($M + H^+$), found 377.1176.

N-(3-cyano-4,5-dimethoxyphenyl)-*N*-(cyanomethyl)-4-methoxybenzenesulfonamide (**184**). 2-chloroacetonitrile (31 µL, 0.48 mmol) was added after 30 min to a stirred solution of **181** (85 mg, 0.24 mmol) and K_2CO_3 (66 mg, 0.48 mmol) in DMF (3 mL). After 24 h, the reaction mixture was dried under vacuum, re-dissolved in EtOAc and washed with brine. After drying over Na_2SO_4 and removal of the solvent, the residue (76 mg) was purified by preparative TLC (CH_2Cl_2/EtOAc 9:1) to give **184** (13 mg, 0.03 mmol, 14%). ^{1}H NMR (200 MHz, $CDCl_3$): δ 3.83 (3H, *s*), 3.89 (3H, *s*), 4.06 (3H, *s*), 4.51 (2H, *s*), 6.82 (1H, *d*, *J* = 2.4), 7.00 (2H, *d*, *J* = 9), 7.07 (1H, *d*, *J* = 2.4), 7.61 (2H, *d*, *J* = 9). ^{13}C NMR (100 MHz, $CDCl_3$): δ 39.4 (CH_2), 55.7 (CH_3), 56.3 (CH_3), 61.8 (CH_3), 106.9 (C), 114.5 (C), 114.5 (2CH), 115.0 (C), 118.1 (CH), 123.1 (CH), 127.9 (C), 130.2 (2CH), 134.3 (C), 152.3 (C), 153.0 (C), 164.1 (C). HRMS ($C_{18}H_{17}N_3O_5S + Na^+$): calcd 410.0781 ($M + Na^+$), found 410.0775.

Ethyl *N*-(3-cyano-4,5-dimethoxyphenyl)-*N*-((4-methoxyphenyl)sulfonyl)glycinate (**185**). To a stirred solution of **181** (80 mg, 0.23 mmol) in dry DMF (3 mL), 63 mg (0.46 mmol) of K_2CO_3 were added. After 1 h at room temperature, 51 µL (0.46 mmol) of ethyl 2-bromoacetate were added and stirred for 24 h. The reaction mixture was concentrated, re-dissolved in EtOAc, washed with brine, dried over anhydrous Na_2SO_4, filtered and concentrated under vacuum to produce 96 mg (0.22 mmol, 96%) of crude reaction product **185**, from which 70 mg (0.16 mmol, 70%) were purified by crystallization. M.p.: 110-118 °C (MeOH). ^{1}H NMR (200 MHz, $CDCl_3$): δ 1.24 (3H, *t*, *J* = 7.2), 3.84 (3H, *s*), 3.88 (3H, *s*), 4.02 (3H, *s*), 4.16 (2H, *q*, *J* = 7.2), 4.33 (2H, *s*), 6.75 (1H, *d*, *J* = 2.6), 6.95 (2H, *d*, *J* = 9), 7.23 (1H, *d*, *J* = 2.6), 7.61 (2H, *d*, *J* = 9). ^{13}C NMR (100 MHz, $CDCl_3$): δ 14.0 (CH_3), 52.5 (CH_2), 55.6 (CH_3), 56.2 (CH_3), 61.6 (CH_2), 61.6 (CH_3), 106.5 (C), 114.1 (2CH), 115.4 (C), 119.3 (CH), 123.2 (CH), 129.7 (C), 129.9 (2CH), 135.9 (C), 151.5 (C), 152.7 (C), 163.4 (C), 168.4 (C). HRMS ($C_{20}H_{22}N_2O_7S + H^+$): calcd 435.1220 ($M + H^+$), found 435.1221.

1,4-Dimethoxy-2-nitrobenzene (**186**).

*Compound **19** article 2. Available at Materials and methods, chemical synthesis.*
*Compound **74** article 3. Available at Materials and methods, chemical synthesis (2.1).*

2,5-Dimethoxyaniline (**187**).

*Compound **20** article 2. Available at Materials and methods, chemical synthesis.*
*Compound **75** article 3. Available at Materials and methods, chemical synthesis (2.1).*

N-(2,5-dimethoxyphenyl)-4-methoxybenzenesulfonamide (**188**).

*Compound **21** article 2. Available at Materials and methods, chemical synthesis.*
*Compound **76** article 3. Available at Materials and methods, chemical synthesis (2.1).*

N-(2,5-dimethoxyphenyl)-4-methoxy-*N*-methylbenzenesulfonamide (**189**).

*Compound **22** article 2. Available at Materials and methods, chemical synthesis.*

N-(2,5-dimethoxy-4-nitrophenyl)-4-methoxybenzenesulfonamide (**190**).

*Compound **96** article 3. Available at Materials and methods, chemical synthesis (2.1).*

N-(4-amino-2,5-dimethoxyphenyl)-4-methoxybenzenesulfonamide (**191**).

*Compound **104** article 3. Available at Materials and methods, chemical synthesis (2.1).*

N-(2,5-dimethoxy-4-((4-methoxyphenyl)sulfonamido)phenyl)formamide (**192**). Sulfonamide **191** (180 mg, 0.53 mmol) was dissolved in CH_2Cl_2 (50 mL) and pyridine (1 mL). 48 µL (1.06 mmol) of formic acid were added and stirred at room temperature for 48 h. The reaction mixture was washed with 2N HCl, 5% $NaHCO_3$ and brine, dried over anhydrous Na_2SO_4 and concentrated in vacuo to afford 174 mg (0.47 mmol, 89%) of **192**. Crude reaction product was purified by preparative TLC in hexane/EtOAc 2:8 (146 mg, 0.40 mmol, 75%). IR (KBr): 3325, 3253, 1664, 1498, 841 cm^{-1}. ^1H NMR (400 MHz, $CDCl_3$): δ 3.57 (3H, *s*), 3.81 (3H, *s*), 3.87 (3H, *s*), 6.85 (2H, *d, J* = 8.8), 7.19 (1H, *s*), 7.63 (2H, *d, J* = 8.8) 7.97 (1H, *s*), 8.39 (1H, *s*). ^{13}C NMR (100 MHz, $CDCl_3$): δ 55.9 (CH_3), 56.6 (CH_3), 56.8 (CH_3), 104.7 (CH), 106.2 (CH), 114.3 (2CH), 121.4 (C), 124.6 (C), 129.6 (2CH), 130.9 (C), 142.2 (C), 144.4 (C), 159.3 (CH), 163.4 (C). HRMS ($C_{16}H_{18}N_2O_6S$ + Na^+): calcd 389.0778 (M + Na^+), found 389.0786.

N-(2,5-dimethoxy-4-(methylamino)phenyl)-4-methoxybenzenesulfonamide (**193**). To a solution of **192** (185 mg, 0.50 mmol) and $NaBH_4$ (29 mg, 0.76 mmol) in dry THF (10 mL) at 0°C, trichloroacetic acid (124 mg, 0.76 mmol) diluted in dry THF (2 mL) was added dropwise under nitrogen atmosphere. The reaction mixture was stirred at 0°C to room temperature for 24 h, concentrated and re-dissolved in EtOAc, washed with brine, dried over anhydrous Na_2SO_4, filtered, and solvent evaporated in vacuum to afford 175 mg of crude reaction. Compound **193** (142 mg, 0.40 mmol, 80%) was isolated by flash column chromatography (hexane/EtOAc 6:4). ^1H NMR (400 MHz, $CDCl_3$): δ 2.80 (3H, *s*), 3.40 (3H, *s*), 3.81 (3H, *s*), 3.82 (3H, *s*), 5.97 (1H, *s*), 6.49 (1H, *bs*), 6.82 (2H, *d, J* = 8.8), 7.00 (1H, *s*), 7.58 (2H, *d, J* = 8.8). ^{13}C NMR (100 MHz, $CDCl_3$): δ 30.3 (CH_3), 55.5 (CH_3), 56.0 (CH_3), 56.1 (CH_3), 94.0 (CH), 107.6 (CH), 112.9 (C), 113.5 (2CH), 129.4 (2CH), 130.8 (C), 138.3 (C), 140.6 (C), 146.5 (C), 162.7 (C). HRMS ($C_{16}H_{20}N_2O_5S$ + H^+): calcd 353.1166 (M + H^+), found 353.1164.

N-(2,5-dimethoxy-4-(methylamino)phenyl)-4-methoxy-*N*-methylbenzenesulfonamide (**194**). To a solution of **191** (149 mg, 0.44 mmol) in acetone (50 mL), K_2CO_3 (609 mg, 4.40 mmol) and $(CH_3)_2SO_4$ (316 µL, 3.30 mmol) were added, heated at reflux, and stirred overnight. Then, the reaction mixture was filtered, poured onto ice, and extracted with CH_2Cl_2. The organic layers were dried over anhydrous Na_2SO_4, filtered, and evaporated to dryness to afford 70 mg of crude reaction. By preparative TLC (toluene/EtOAc 4:6) compound **194** (25 mg, 0.07 mmol, 15%) was isolated. ^1H NMR (400 MHz, $CDCl_3$): δ 2.84 (3H, *s*), 3.18 (3H, *s*), 3.38 (3H, *s*), 3.76 (3H, *s*), 3.86 (3H, *s*), 6.01 (1H, *s*), 6.67 (1H, *s*), 6.91 (2H, *d, J* = 9.2), 7.64 (2H, *d, J* = 9.2). ^{13}C NMR (100 MHz, $CDCl_3$): δ 30.1 (CH_3), 38.2 (CH_3), 55.3 (CH_3), 55.5 (CH_3), 55.9 (CH_3), 93.8 (CH), 112.9 (CH), 113.4 (2CH), 115.9 (C), 129.8 (2CH), 131.6 (C), 139.9 (C), 140.2 (C), 151.5 (C), 162.4 (C). HRMS ($C_{17}H_{22}N_2O_5S$ + H^+): calcd 367.1322 (M + H^+), found 367.1321.

N-(2,5-dimethoxy-4-((4-methoxyphenyl)sulfonamido)phenyl)acetamide (**195**). A mixture of **191** (97 mg, 0.28 mmol), acetic anhydride (32 µL, 0.34 mmol) and pyridine (2 mL) in CH_2Cl_2 (50 mL) was stirred at room temperature for 24 h. Then, it was poured onto ice and extracted with CH_2Cl_2. Organic layers were washed with 2N HCl, 5% $NaHCO_3$ and brine, dried (Na_2SO_4), filtered, and evaporated to dryness to give 98 mg (0.26 mmol, 90 %) of **195**. Crude reaction product was purified by crystallization in CH_2Cl_2/hexane (54 mg, 0.14 mmol, 49%). M.p.: 178-184 °C (CH_2Cl_2/hexane). IR (KBr): 3220, 1668, 1598, 1499, 829 cm^{-1}. ^1H NMR (400 MHz, $CDCl_3$): δ 2.15 (3H, *s*), 3.52 (3H, *s*), 3.78 (3H, *s*), 3.83 (3H, *s*), 6.81 (2H, *d, J* = 9.2), 7.14 (1H, *s*), 7.60 (2H, *d, J* = 9.2), 7.72 (1H, *bs*), 7.97 (1H, *s*). ^{13}C NMR (100 MHz, $CDCl_3$): δ 24.9 (CH_3), 55.6 (CH_3), 56.2 (CH_3), 56.4 (CH_3), 103.6 (CH), 105.7 (CH), 113.8 (2CH), 120.4 (C), 125.3 (C), 129.3 (2CH), 130.5 (C), 141.5

(C), 144.2 (C), 162.9 (C), 168.2 (C). HRMS ($C_{17}H_{20}N_2O_6S + H^+$): calcd 381.1115 (M + H^+), found 381.1126.

N-(2,5-dimethoxy-4-((4-methoxy-*N*-methylphenyl)sulfonamido)phenyl)-*N*-methylacetamide (**196**). 80 mg (0.21 mmol) of **195** were dissolved in CH_3CN (40 mL) and 23 mg (0.42 mmol) of KOH were added. After 30 min stirring at room temperature, CH_3I (26 µL, 0.42 mmol) was added to the solution. The reaction mixture was stirred for 24 h, concentrated under reduced pressure, dissolved in EtOAc, washed with brine, dried (Na_2SO_4), filtered, and evaporated to dryness. 72 mg (0.17 mmol, 87%) of compound **196** were yielded and purified by crystallization in CH_2Cl_2/hexane (44 mg, 0.11 mmol, 53%). M.p.: 170-171 °C (CH_2Cl_2/hexane). IR (KBr): 1676, 1654, 1597, 1514, 834 cm^{-1}. ^1H NMR (400 MHz, $CDCl_3$): δ 1.82 (3H, *s*), 3.15 (3H, *s*), 3.20 (3H, *s*), 3.40 (3H, *s*), 3.78 (3H, *s*), 3.87 (3H, *s*), 6.60 (1H, *s*), 6.93 (2H, *d, J* = 9.2), 6.97 (1H, *s*), 7.65 (2H, *d, J* = 9.2). ^{13}C NMR (100 MHz, $CDCl_3$): δ 21.7 (CH_3), 35.9 (CH_3), 37.7 (CH_3), 55.5 (CH_3), 55.6 (CH_3), 56.0 (CH_3), 112.2 (CH), 113.6 (2CH), 116.0 (CH), 129.2 (C), 129.7 (2CH), 131.0 (C), 132.9 (C), 148.6 (C), 150.3 (C), 162.8 (C), 171.1 (C). HRMS ($C_{19}H_{24}N_2O_6S + H^+$): calcd 409.1428 (M + H^+), found 409.1413.

2-Chloro-*N*-(2,5-dimethoxy-4-((4-methoxyphenyl)sulfonamido)phenyl)acetamide (**197**).

*Compound **129** article 3. Available at Materials and methods, chemical synthesis (2.1).*

3-Chloro-*N*-(2,5-dimethoxy-4-((4-methoxyphenyl)sulfonamido)phenyl)propanamide (**198**).

*Compound **138** article 3. Available at Materials and methods, chemical synthesis (2.1).*

N-(4-(3-ethylureido)-2,5-dimethoxyphenyl)-4-methoxybenzenesulfonamide (**199**). To 98 mg (0.29 mmol) of **191** in CH_2Cl_2 (7 mL), 34 µL (0.43 mmol) of ethyl isocyanate were added. After 6 h stirring at room temperature, the precipitate formed was filtered to afford 87 mg (0.21 mmol, 73%) of **199**. The obtained solid was recrystallized from CH_2Cl_2 to give pure product **199** (70 mg, 0.17 mmol, 59%). M.p.: 208-211 °C (CH_2Cl_2). IR (KBr): 3354, 3231, 1651, 1498, 829 cm^{-1}. ^1H NMR (400 MHz, $CDCl_3$): δ 1.18 (3H, *t, J*= 7.2), 3.28 (2H, *m*), 3.51 (3H, *s*), 3.81 (3H, *s*), 3.83 (3H, *s*), 4.50 (1H, *bs*), 6.71 (1H, *bs*), 6.74 (1H, *bs*), 6.83 (2H, *d, J* = 9.2), 7.13 (1H, *s*), 7.60 (2H, *d, J* = 9.2), 7.79 (1H, *s*). ^{13}C NMR (100 MHz, acetone-D_6): δ 14.8 (CH_3), 34.2 (CH_3), 55.1 (CH_3), 55.5 (CH_3), 55.9 (CH_3), 102.5 (CH), 107.8 (CH), 113.6 (2CH), 118.1 (C), 128.4 (C), 129.3 (2CH), 131.9 (C), 141.0 (C), 145.7 (C), 154.9 (C), 162.9 (C). HRMS ($C_{18}H_{23}N_3O_6S + H^+$): calcd 410.1380 (M + H^+), found 410.1374.

N-(4-(3-ethyl-1-methylureido)-2,5-dimethoxyphenyl)-4-methoxy-*N*-methylbenzenesulfonamide (**200**). To a stirred solution of **199** (60 mg, 0.15 mmol) in CH_3CN (25 mL), 17 mg (0.30 mmol) of KOH were added. After 30 min at room temperature, CH_3I (19 µL, 0.30 mmol) was added. The solution was stirred for 24 h; then the mixture was evaporated to dryness. The residue was dissolved with EtOAc and washed with brine, dried over Na_2SO_4, filtered, and evaporated to dryness to give 64 mg (0.15 mmol, 98%) of **200**. The residue was purified by preparative TLC (CH_2Cl_2/MeOH 98:2) (57 mg, 0.13 mmol, 87%) and recrystallized from MeOH (35 mg, 0.08 mmol, 53%). M.p.: 120-123 °C (MeOH). IR (KBr): 3436, 1648, 1597, 807 cm^{-1}. ^1H NMR (400 MHz, CD_3OD): δ 1.04 (3H, *t, J* = 6.8), 3.09 (3H, *s*), 3.13 (2H, *q, J* = 6.8), 3.16 (3H, *s*), 3.44 (3H, *s*), 3.75 (3H, *s*), 3.88 (3H, *s*), 6.83 (1H, *s*), 6.93 (1H, *s*), 7.07 (2H, *d, J* = 9.2), 7.66 (2H, *d, J* = 9.2). ^{13}C NMR (100 MHz, CD_3OD): δ 14.6 (CH_3), 35.0 (CH_3), 35.4 (CH_3), 36.7 (CH_2), 54.8 ($2CH_3$), 55.2 (CH_3), 113.4 (CH), 113.5 (2CH), 115.8 (CH), 128.8 (C), 129.5 (2CH), 130.7 (C), 131.8 (C), 149.1 (C), 150.9 (C), 158.7 (C), 163.2 (C). HRMS ($C_{20}H_{27}N_3O_6S + H^+$): calcd 438.1693 (M + H^+), found 438.1689.

N-(4-bromo-2,5-dimethoxyphenyl)-4-methoxybenzenesulfonamide (**201**).

*Compound **23** article 2. Available at Materials and methods, chemical synthesis.*

N-(4-bromo-2,5-dimethoxyphenyl)-4-methoxy-*N*-methylbenzenesulfonamide (**202**).

*Compound **24** article 2. Available at Materials and methods, chemical synthesis.*

N-(4-bromo-2,5-dimethoxyphenyl)-*N*-(cyanomethyl)-4-methoxybenzenesulfonamide (**203**).

*Compound **25** article 2. Available at Materials and methods, chemical synthesis.*

Ethyl *N*-(4-bromo-2,5-dimethoxyphenyl)-*N*-((4-methoxyphenyl)sulfonyl)glycinate (**204**).

*Compound **26** article 2. Available at Materials and methods, chemical synthesis.*

N-(4-bromo-2,5-dimethoxyphenyl)-*N*-((4-methoxyphenyl)sulfonyl)glycine (**205**).

*Compound **29** article 2. Available at Materials and methods, chemical synthesis.*

Ethyl (4-bromo-2,5-dimethoxyphenyl)((4-methoxyphenyl)sulfonyl)carbamate (**206**).

*Compound **27** article 2. Available at Materials and methods, chemical synthesis.*

N-(4-bromo-2,5-dimethoxyphenyl)-4-methoxy-*N*-(oxiran-2-ylmethyl)benzenesulfonamide (**207**).

*Compound **28** article 2. Available at Materials and methods, chemical synthesis.*

N-(2,5-dimethoxyphenyl)-4-nitrobenzenesulfonamide (**208**).

*Compound **130** article 3. Available at Materials and methods, chemical synthesis (2.1).*

N-(4-bromo-2,5-dimethoxyphenyl)-4-nitrobenzenesulfonamide (**209**).

*Compound **296** article 3. Available at Materials and methods, chemical synthesis (2.1).*

4-Amino-*N*-(2,5-dimethoxyphenyl)benzenesulfonamide (**210**). A mixture of **208** (1.91 g, 5.65 mmol) and Pd (C) (10 mg) in EtOAc (250 mL) was equipped with a balloon of hydrogen gas and stirred at room temperature for 72 h. The solution was filtered through Celite® and the filtrate was concentrated in vacuum. The residue (1.51 g) was purified by flash chromatography on silica gel column eluting with toluene/EtOAc 8:2 to give 1.45 g (4.71 mmol, 83%) of **210**. ^{1}H NMR (400 MHz, $CDCl_3$): δ 3.63 (3H, *s*), 3.74 (3H, *s*), 4.05 (2H, *bs*), 6.51 (1H, *dd*, *J* = 8.8 and 3.2), 6.56 (2H, *d, J* = 8.8), 6.65 (1H, *d, J* = 8.8), 6.98 (1H, *bs*), 7.12 (1H, *d, J* = 3.2), 7.56 (2H, *d, J* = 8.8). ^{13}C NMR (100 MHz, CD_3OD): δ 56.4 (CH_3), 57.1 (CH_3), 110.6 (CH), 111.2 (CH), 113.4 (CH), 114.4 (2CH), 127.1 (C), 128.8 (C), 130.7 (2CH), 146.9 (C), 154.6 (C), 155.3 (C). HRMS ($C_{14}H_{16}N_2O_4S + H^+$): calcd 309.0904 ($M + H^+$), found 309.0895.

4-Amino-*N*-(4-bromo-2,5-dimethoxyphenyl)benzenesulfonamide (**211**).

*Compound **302** article 3. Available at Materials and methods, chemical synthesis (2.1).*

N-(2,5-dimethoxyphenyl)-4-(dimethylamino)benzenesulfonamide (**212**). Compound **210** (270 mg, 0.87 mmol) was dissolved in MeOH (50 mL) with paraformaldehyde (263 mg, 8.76 mmol) and acetic acid (200 µL). After 1 h stirring at room temperature sodium cyanoborohydride (110 mg, 1.75 mmol) was added to the solution. The reaction mixture was allowed to react for 4 days and then the solution was concentrated under reduced pressure. The residue was dissolved in EtOAc and washed with 5% $NaHCO_3$ and brine. The organics layers were dried over Na_2SO_4 and evaporated to afford **212** (229 mg, 0.68 mmol, 77%). The residue was purified by crystallization

in CH_2Cl_2/hexane (126 mg, 0.37 mmol, 43%). M.p.: 166-170 °C (CH_2Cl_2/hexane). ^{1}H NMR (400 MHz, $CDCl_3$): δ 2.94 (6H, *s*), 3.61 (3H, *s*), 3.70 (3H, *s*), 6.46 (1H, *dd, J* = 8.8 and 3.2), 6.51 (2H, *d, J* = 8.8), 6.63 (1H, *d, J* = 8.8), 7.06 (1H, *bs*), 7.11 (1H, *d, J* = 3.2), 7.59 (2H, *d, J* = 8.8). ^{13}C NMR (100 MHz, $CDCl_3$): δ 39.9 ($2CH_3$), 55.7 (CH_3), 56.3 (CH_3), 106.2 (CH), 108.8 (CH), 110.6 (2CH), 111.5 (CH), 124.1 (C), 127.4 (C), 129.0 (2CH), 143.2 (C), 152.9 (C), 153.8 (C). HRMS ($C_{16}H_{20}N_2O_4S + H^+$): calcd 337.1217 ($M + H^+$), found 337.1223.

N-(2,5-dimethoxyphenyl)-4-(dimethylamino)-*N*-methylbenzenesulfonamide (**213**). To a solution of **212** (98 mg, 0.29 mmol) in CH_3CN (25 mL), crushed KOH (32 mg, 0.58 mmol) was added and stirred for 30 min. Then, CH_3I (36 µL, 0.58 mmol) was added. After 24 h, CH_3CN was evaporated and the residue was re-dissolved in EtOAc. The solution was washed with brine, dried over Na_2SO_4, filtered, and evaporated to dryness to afford crude product **213** (85 mg, 0.24 mmol, 84%). Compound **213** was purified by silica gel column chromatography in hexane/EtOAc 1:1 (78 mg, 0.22 mmol, 77%). ^{1}H NMR (400 MHz, $CDCl_3$): δ 2.89 (6H, *s*), 3.00 (3H, *s*), 3.36 (3H, *s*), 3.59 (3H, *s*), 6.49 (2H, *d, J* = 8.8), 6.65 (1H, *dd, J* = 8.8 and 3.2), 6.68 (1H, *d, J* = 3.2), 7.41 (2H, *d, J* = 8.8). ^{13}C NMR (100 MHz, $CDCl_3$): δ 37.6 (CH_3), 39.5 ($2CH_3$), 55.5 ($2CH_3$), 110.3 (2CH), 112.4 (CH), 114.3 (CH), 116.4 (CH), 124.7 (C), 129.3 (2CH), 130.2 (C), 150.7 (C), 152.5 (C), 152.9 (C). HRMS ($C_{17}H_{22}N_2O_4S + H^+$): calcd 351.1373 ($M + H^+$), found 351.1360.

N-(4-bromo-2,5-dimethoxyphenyl)-4-(dimethylamino)benzenesulfonamide (**214**). A solution of paraformaldehyde (194 mg, 6.46 mmol), acetic acid (200 µL) and **211** (250 mg, 0.64 mmol) in MeOH (50 mL) was stirred at room temperature for 1 h. Sodium cyanoborohydride (81 mg, 1.29 mmol) was added to the solution and stirred at reflux for 24 h. Reaction mixture was concentrated under vacuum, poured onto ice, and extracted with EtOAc. Organic layers were washed with 5% $NaHCO_3$ and brine, dried (Na_2SO_4), filtered and evaporated to dryness to give **214** (251 mg, 0.60 mmol, 93%). Crude reaction product was purified by crystallization in CH_2Cl_2/hexane (166 mg, 0.40 mmol, 62%). M.p.: 117-118 °C (CH_2Cl_2/hexane). ^{1}H NMR (400 MHz, $CDCl_3$): δ 3.00 (6H, *s*), 3.64 (3H, *s*), 3.84 (3H, *s*), 6.55 (2H, *d, J* = 9.2), 6.90 (1H, *s*), 6.96 (1H, *bs*), 7.20 (1H, *s*), 7.58 (2H, *d, J* = 9.2). ^{13}C NMR (100 MHz, $CDCl_3$): δ 39.9 ($2CH_3$), 56.5 (CH_3), 56.8 (CH_3), 104.9 (CH), 105.2 (C), 110.6 (2CH), 115.8 (CH), 123.6 (C), 126.7 (C), 129.0 (2CH), 143.4 (C), 150.1 (C), 152.9 (C). HRMS ($C_{16}H_{19}BrN_2O_4S + H^+$): calcd 415.0322 and 417.0301 ($M + H^+$), found 415.0336 and 417.0284.

N-(4-bromo-2,5-dimethoxyphenyl)-4-(dimethylamino)-*N*-methylbenzenesulfonamide (**215**). To a stirred solution of **214** (90 mg, 0.22 mmol) and KOH (24 mg, 0.43 mmol) in CH_3CN (25 mL), CH_3I (27 µL, 0.43 mmol) was added after 30 min. After 24 h, the solvent was evaporated, the residue was re-dissolved in EtOAc and washed with brine, dried (Na_2SO_4), filtered and concentrated in vacuo to afford 85 mg (0.20 mmol, 91%) of the desired compound **215**. The residue was purified by crystallization in methanol (57 mg, 0.13 mmol, 61%). M.p.: 172-174 °C (MeOH). ^{1}H NMR (400 MHz, $CDCl_3$): δ 3.01 (6H, *s*), 3.12 (3H, *s*), 3.42 (3H, *s*), 3.78 (3H, *s*), 6.60 (2H, *d, J* = 8.8), 6.85 (1H, *s*), 6.97 (1H, *s*), 7.49 (2H, *d, J* = 8.8). ^{13}C NMR (100 MHz, $CDCl_3$): δ 37.7 (CH_3), 40.1 ($2CH_3$), 55.9 (CH_3), 56.8 (CH_3), 110.5 (2CH), 111.1 (C), 115.6 (CH), 116.8 (CH), 124.6 (C), 127.8 (C), 129.4 (2CH), 149.6 (C), 150.8 (C), 152.8 (C). HRMS ($C_{17}H_{21}BrN_2O_4S + Na^+$): calcd 451.0298 and 453.0277 ($M + Na^+$), found 451.0292 and 453.0272.

N-(4-bromo-2,5-dimethoxyphenyl)-4-(dimethylamino)-*N*-ethylbenzenesulfonamide (**216**). 85 mg (0.21 mmol) of **214** and 55 mg (0.40 mmol) of K_2CO_3 were mixed in dry DMF (3 mL). After 30 min stirring at room temperature, bromoethane (30 µL, 0.40 mmol) was added to the mixture and stirred 24 h. The reaction mixture was concentrated, re-dissolved in EtOAc, washed with brine, dried over anhydrous Na_2SO_4, filtered, and concentrated in vacuum to obtain 83 mg (0.19 mmol, 91%) of **216** and crystalized in methanol (58 mg, 0.13 mmol, 64%). M.p.: 143-158 °C (MeOH). ^{1}H NMR (400 MHz, CD_3OD): δ 1.01 (3H, *t, J* = 7.2), 3.04 (6H, *s*), 3.45 (3H, *s*), 3.58 (2H, *q, J* = 7.2), 3.75 (3H, *s*), 6.75 (2H, *d, J* = 8.8), 6.77 (1H, *s*), 7.13 (1H, *s*), 7.46 (2H, *d, J* = 8.8). ^{13}C NMR

(100 MHz, $CDCl_3$): δ 14.3 (CH_3), 40.1 ($2CH_3$), 44.4 (CH_2), 55.8 (CH_3), 56.8 (CH_3), 110.6 (2CH), 111.4 (C), 116.6 (CH), 117.1 (CH), 125.8 (C), 126.7 (C), 129.3 (2CH), 149.6 (C), 151.4 (C), 152.6 (C). HRMS ($C_{18}H_{23}BrN_2O_4S + H^+$): calcd 445.0614 ($M + H^+$), found 445.0610.

N-(4-bromo-2,5-dimethoxyphenyl)-*N*-(cyanomethyl)-4-(dimethylamino)benzenesulfonamide (**217**). A mixture of **215** (83 mg, 0.20 mmol) and K_2CO_3 (55 mg, 0.40 mmol) in dry DMF (3 mL) was stirred for 30 min. Then, 2-chloroacetonitrile (25 µL, 0.40 mmol) was added and stirred for 24 h. After concentration, the reaction residue was re-dissolved in EtOAc, washed with brine, dried (Na_2SO_4), filtered, and the solvent was evaporated to dryness. Crude product **217** was obtained (83 mg, 0.18 mmol, 91%) and it was purified by crystallization in methanol (30 mg, 0.07 mmol, 33%). M.p.: 160-162 °C (MeOH). ^{1}H NMR (400 MHz, $CDCl_3$): δ 3.04 (6H, *s*), 3.48 (3H, *s*), 3.76 (3H, *s*), 4.54 (2H, *s*), 6.61 (2H, *d, J* = 8.8), 6.92 (1H, *s*), 7.03 (1H, *s*), 7.50 (2H, *d, J* = 8.8). ^{13}C NMR (100 MHz, $CDCl_3$): δ 38.1 (CH_2), 40.0 ($2CH_3$), 55.9 (CH_3), 56.8 (CH_3), 110.5 (2CH), 112.7 (C), 115.5 (C), 115.9 (CH), 116.9 (CH), 123.5 (C), 125.4 (C), 129.5 (2CH), 149.9 (C), 150.3 (C), 153.2 (C). HRMS ($C_{18}H_{20}BrN_3O_4S + Na^+$): calcd 476.0250 and 478.0230 ($M + Na^+$), found 476.0243 and 478.0212.

Ethyl *N*-(4-bromo-2,5-dimethoxyphenyl)-*N*-((4-(dimethylamino)phenyl)sulfonyl)glycinate (**218**). Ethyl 2-bromoacetate (40 µL, 0.36 mmol) was added, after 30 min, to a stirred mixture of compound **214** (75 mg, 0.18 mmol) and K_2CO_3 (50 mg, 0.36 mmol) in dry DMF (3 mL). After 24 h, the solvent was evaporated under reduced pressure and the residue was dissolved in EtOAc, washed with brine, dried over anhydrous Na_2SO_4, filtered, and concentrated in vacuum to afford 89 mg (0.18 mmol, 98%) of crude reaction product **218**, from which, 52 mg (0.10 mmol, 57%) were purified by crystallization in methanol. M.p.: 135-138 °C (MeOH). ^{1}H NMR (400 MHz, CD_3OD): δ 1.23 (3H, *t, J* = 7.2), 3.04 (6H, *s*), 3.39 (3H, *s*), 4.14 (2H, *q, J* = 7.2), 4.33 (2H, *s*), 6.73 (2H, *d, J* = 9.2), 7.09 (1H, *s*), 7.13 (1H, *s*), 7.44 (2H, *d, J* = 9.2). ^{13}C NMR (100 MHz, $CDCl_3$): δ 14.0 (CH_3), 40.1 ($2CH_3$), 50.8 (CH_2), 55.8 (CH_3), 56.8 (CH_3), 61.1 (CH_2), 110.5 (2CH), 111.6 (C), 116.4 (CH), 117.6 (CH), 125.4 (C), 126.9 (C), 129.4 (2CH), 149.5 (C), 150.2 (C), 152.8 (C), 169.6 (C). HRMS ($C_{20}H_{25}BrN_2O_6S + H^+$): calcd 501.0689 ($M + H^+$), found 501.0678.

N-benzyl-*N*-(4-bromo-2,5-dimethoxyphenyl)-4-(dimethylamino)benzenesulfonamide (**219**). A solution of **214** (70 mg, 0.17 mmol) and K_2CO_3 (47 mg, 0.34 mmol) in dry DMF (3 mL) was stirred for 30 min. Benzyl chloride (39 µL, 0.34 mmol) was added to the solution and stirred for 24 h. Reaction mixture was concentrated under vacuum, re-dissolved in EtOAc and washed with brine, dried (Na_2SO_4), filtered, and evaporated to dryness to give **219** (62 mg, 0.12 mmol, 73%). The crude reaction product was purified by preparative TLC in hexane/EtOAc 6:4 (48 mg, 0.09 mmol, 56%). IR (KBr): 1594, 1496, 815 cm^{-1}. ^{1}H NMR (200 MHz, CD_3OD): δ 3.06 (6H, *s*), 3.41 (3H, *s*), 3.59 (3H, *s*), 4.71 (2H, *s*), 6.54 (1H, *s*), 6.78 (2H, *d, J* = 9.2), 7.03 (1H, *s*), 7.19 (5H, *bs*), 7.52 (2H, *d, J* = 9.2). ^{13}C NMR (100 MHz, $CDCl_3$): δ 40.1 ($2CH_3$), 53.3 (CH_2), 55.7 (CH_3), 56.7 (CH_3), 110.5 (2CH), 111.4 (C), 116.5 (CH), 117.5 (CH), 125.8 (C), 126.5 (C), 127.4 (CH), 128.2 (2CH), 128.8 (2CH), 129.4 (2CH), 136.8 (C), 149.4 (C), 151.1 (C), 152.7 (C). HRMS ($C_{23}H_{25}BrN_2O_4S + H^+$): calcd 505.0791 and 507.0771 ($M + H^+$), found 505.0783 and 507.0761.

N-(4-(*N*-(2,5-dimethoxyphenyl)sulfamoyl)phenyl)formamide (**220**). A solution of **210** (348 mg, 1.13 mmol) and formic acid (4.31 mL, 11.29 mmol) in pyridine (2 mL) and CH_2Cl_2 (48 mL) was stirred at room temperature for 48 h. The reaction mixture was poured onto ice and extracted with CH_2Cl_2. Organics layers were washed with 2N HCl, 5% $NaHCO_3$ and brine, dried over Na_2SO_4, filtered, and evaporated to dryness. 357 mg (1.06 mmol, 94%) of **220** was obtained and purified by crystallization in CH_2Cl_2 (305 mg, 0.91 mmol, 80%). M.p.: 158-164 °C (CH_2Cl_2). IR (KBr): 3325, 3251, 1692, 1592, 802 cm^{-1}. ^{1}H NMR (400 MHz, CD_3OD): δ 3.50 (3H, *s*), 3.71 (3H, *s*), 6.62 (1H, *dd, J* = 9.2 and 3.2), 6.74 (1H, *d, J* = 9.2), 7.03 (1H, *d, J* = 3.2), 7.65 (2H, *d, J* = 9.2), 7.67 (2H, *d, J* = 9.2), 8.29 (1H, *s*). ^{13}C NMR (100 MHz, DMSO-D_6): δ 55.7 (CH_3), 56.5 (CH_3), 110.5 (CH), 110.6 (CH), 113.1

(CH), 119.1 (2CH), 126.8 (C), 128.5 (2CH), 135.0 (C), 142.2 (C), 146.3 (C), 153.3 (C), 160.6 (CH). HRMS ($C_{15}H_{16}N_2O_5S$ + Na^+): calcd 359.0672 (M + Na^+), found 359.0681.

N-(4-(*N*-(4-bromo-2,5-dimethoxyphenyl)sulfamoyl)phenyl)formamide (**221**).

*Compound **315** article 3. Available at Materials and methods, chemical synthesis (2.1).*

N-(2,5-dimethoxyphenyl)-4-(methylamino)benzenesulfonamide (**222**). Formamide **220** (300 mg, 0.89 mmol) was dissolved in dry THF (10 mL). After it was cooled to 0°C, $NaBH_4$ (50 mg, 1.34 mmol) was added, followed by the dropwise addition of trichloroacetic acid (219 mg, 1.34 mmol) dissolved in dry THF (10 mL). The reaction mixture was stirred from 0°C to room temperature for 24 h, then, it was concentrated, poured into ice, and extracted with EtOAc. The organics layers were dried (Na_2SO_4), filtered and concentrated in vacuo to afford 281 mg (0.87 mmol, 97%) of the desired compound, **222**. The residue was crystallized in CH_2Cl_2/hexane (157 mg, 0.49 mmol, 54%). M.p.: 128-130 °C (CH_2Cl_2/hexane). ^{1}H NMR (400 MHz, $CDCl_3$): δ 2.83 (3H, *d, J* = 4.4), 3.64 (3H, *s*), 3.74 (3H, *s*), 4.20 (1H, *bs*), 6.47 (2H, *d, J* = 8.4), 6.50 (1H, *dd, J* = 9.2 and 3.2), 6.65 (1H, *d, J* = 9.2), 7.01 (1H, *bs*), 7.13 (1H, *d, J* = 3.2), 7.59 (2H, *d, J* = 8.4). ^{13}C NMR (100 MHz, $CDCl_3$): δ 30.1 (CH_3), 55.9 (CH_3), 56.5 (CH_3), 106.8 (CH), 109.2 (CH), 111.3 (2CH), 111.8 (CH), 125.1 (C), 127.6 (C), 129.5 (2CH), 143.6 (C), 153.1 (C), 154.0 (C). HRMS ($C_{15}H_{18}N_2O_4S$ + Na^+): calcd 345.0879 (M + Na^+), found 345.0896.

N-(2,5-dimethoxyphenyl)-*N*-methyl-4-(methylamino)benzenesulfonamide (**223**). 150 mg (0.46 mmol) of **222** were dissolved in CH_3CN (40 mL) with 52 mg (0.93 mmol) of KOH. After 30 min stirring at room temperature, CH_3I (58 µL, 0.93 mmol) was added to the solution and the reaction mixture was stirred for 24 h. The solvent was removed under reduced pressure. The residue was dissolved in EtOAc and washed with brine and dried over Na_2SO_4. After concentration, the residue (154 mg) was purified by silica gel column chromatography (hexane/EtOAc 7:3) to give 133 mg (0.39 mmol, 85%) of **223**. ^{1}H NMR (400 MHz, $CDCl_3$): δ 2.87 (3H, *bs*), 3.15 (3H, *s*), 3.49 (3H, *s*), 3.73 (3H, *s*), 4.20 (1H, *bs*), 6.54 (2H, *d, J* = 8.8), 6.74 (1H, *d, J* = 9.2), 6.80 (1H, *dd, J* = 9.2 and 3.2), 6.82 (1H, *d, J* = 3.2), 7.51 (2H, *d, J* = 8.8). ^{13}C NMR (100 MHz, $CDCl_3$): δ 30.0 (CH_3), 37.8 (CH_3), 55.7 ($2CH_3$), 110.8 (2CH), 112.6 (CH), 114.3 (CH), 116.7 (CH), 125.3 (C), 129.6 (2CH), 130.2 (C), 150.8 (C), 152.6 (C), 153.0 (C). HRMS ($C_{16}H_{20}N_2O_4S$ + H^+): calcd 337.1217 (M + H^+), found 337.1217.

N-(4-bromo-2,5-dimethoxyphenyl)-4-(methylamino)benzenesulfonamide (**224**).

*Compound **323** article 3. Available at Materials and methods, chemical synthesis (2.1).*

N-(4-bromo-2,5-dimethoxyphenyl)-*N*-methyl-4-(methylamino)benzenesulfonamide (**225**). To a stirred solution of **224** (72 mg, 0.18 mmol) in CH_3CN (25 mL), 20 mg (0.36 mmol) of crushed KOH were added. After 1 h at room temperature 22 µL (0.36 mmol) of CH_3I were added and stirred for 24 h. The mixture was evaporated to dryness. The residue was diluted with water, and the solution was extracted with EtOAc. The extract was dried over Na_2SO_4, filtered, and evaporated to dryness to yield 73 mg (0.18 mmol, 98%) of **225**. The residue was crystallized from methanol to give 34 mg (0.08 mmol, 45%) of the purified compound **225**. M.p.: 184-188 °C (MeOH). ^{1}H NMR (400 MHz, $CDCl_3$): δ 2.83 (3H, *s*), 3.13 (3H, *s*), 3.42 (3H, *s*), 3.78 (3H, *s*), 6.50 (2H, *d, J* = 8.8), 6.85 (1H, *s*), 6.98 (1H, *s*), 7.44 (2H, *d, J* = 8.8). ^{13}C NMR (100 MHz, $CDCl_3$): δ 30.1 (CH_3), 37.7 (CH_3), 55.8 (CH_3), 56.8 (CH_3), 110.8 (2CH), 111.1 (C), 115.6 (CH), 116.8 (CH), 124.5 (C), 125.6 (C), 129.6 (2CH), 149.6 (C), 150.8 (C), 152.4 (C). HRMS ($C_{16}H_{19}BrN_2O_4S$ + Na^+): calcd 437.0141 and 439.0121 (M + Na^+), found 437.0132 and 439.0113.

N-(4-bromo-2,5-dimethoxyphenyl)-*N*-(cyanomethyl)-4-(methylamino)benzenesulfonamide (**226**). 2-chloroacetonitrile (28 µL, 0.44 mmol) was added after 30 min to a stirred solution of **224** (89 mg, 0.22 mmol) and K_2CO_3 (61 mg, 0.44 mmol) in DMF (3 mL). After 24 h, the reaction mixture was dried under vacuum, re-dissolved in EtOAc and washed with brine. After drying over

Na_2SO_4 and removal of the solvent, crude reaction product **226** (90 mg, 0.20 mmol, 92%) was purified by crystallization in methanol (60 mg, 0.14 mmol, 61%). M.p.: 105-112 °C (MeOH). ^{1}H NMR (400 MHz, CD_3OD): δ 2.79 (3H, *s*), 3.45 (3H, *s*), 3.77 (3H, *s*), 4.58 (2H, *s*), 6.57 (2H, *d, J* = 8.8), 6.94 (1H, *s*), 7.16 (1H, *s*), 7.38 (2H, *d, J* = 8.8). ^{13}C NMR (100 MHz, $CDCl_3$): δ 30.0 (CH_3), 38.2 (CH_2), 55.8 (CH_3), 56.8 (CH_3), 110.9 (2CH), 112.9 (C), 115.5 (C), 116.0 (CH), 116.9 (CH), 124.6 (C), 125.4 (C), 129.8 (2CH), 149.9 (C), 150.3 (C), 153.0 (C). HRMS ($C_{17}H_{18}BrN_3O_4S$ + H^+): calcd 440.0274 and 442.0254 (M + H^+), found 440.0270 and 442.0243.

N-benzyl-*N*-(4-bromo-2,5-dimethoxyphenyl)-4-(methylamino)benzenesulfonamide (**227**).

*Compound **332** article 3. Available at Materials and methods, chemical synthesis (2.1).*

3-Bromo-*N*-(2,5-dimethoxyphenyl)-*N*-methyl-4-(methylamino)benzenesulfonamide (**228a**) and 3-bromo-*N*-(4-bromo-2,5-dimethoxyphenyl)-*N*-methyl-4-(methylamino)benzenesulfonamide (**228b**). A solution of **223** (102 mg, 0.30 mmol) and *N*-bromosuccinimide (54 mg, 0.30 mmol) in CH_2Cl_2 (30 mL) was stirred at room temperature for 24 h. The reaction mixture was washed with brine, dried over Na_2SO_4, and concentrated under reduced pressure. The residue (78 mg) was purified by preparative TLC (hexane/EtOAc 7:3) to give compounds **228a** (15 mg, 0.04 mmol, 12%) and **228b** (22 mg, 0.04 mmol, 15%). **228a:** ^{1}H NMR (400 MHz, $CDCl_3$): δ 2.95 (3H, *s*), 3.15 (3H, *s*), 3.49 (3H, *s*), 3.75 (3H, *s*), 6.56 (1H, *d*, *J* = 8.8), 6.74 (1H, *d, J* = 8.8), 6.82 (1H, *dd, J* = 8.8 and 3.2), 6.87 (1H, *d, J* = 3.2), 7.56 (1H, *dd, J* = 8.8 and 2), 7.76 (1H, *d, J* = 2). ^{13}C NMR (100 MHz, $CDCl_3$): δ 30.3 (CH_3), 37.7 (CH_3), 55.5 (CH_3), 55.7 (CH_3), 108.1 (C), 108.7 (CH), 112.3 (CH), 114.8 (CH), 116.9 (CH), 126.9 (C), 128.9 (CH), 129.7 (C), 131.9 (CH), 148.6 (C), 150.6 (C), 153.2 (C). HRMS ($C_{16}H_{19}BrN_2O_4S$ + H^+): calcd 415.0322 and 417.0301 (M + H^+), found 415.0300 and 417.0282. **228b:** IR (KBr): 3409, 1591, 1496, 846 cm^{-1}. ^{1}H NMR (400 MHz, $CDCl_3$): δ 2.95 (3H, *d, J* = 5.2), 3.14 (3H, *s*), 3.46 (3H, *s*), 3.83 (3H, *s*), 4.85 (1H, *bs*), 6.55 (1H, *d, J* = 8.8), 6.91 (1H, *s*), 7.01 (1H, *s*), 7.52 (1H, *dd, J* = 8.8 and 2), 7.74 (1H, *d, J* = 2). ^{13}C NMR (100 MHz, $CDCl_3$): δ 30.3 (CH_3), 37.6 (CH_3), 55.7 (CH_3), 56.8 (CH_3), 106.8 (C), 108.1 (C), 108.6 (CH), 115.8 (CH), 116.7 (CH), 126.5 (C), 128.8 (C), 128.9 (CH), 131.7 (CH), 148.7 (C), 149.7 (C), 150.6 (C). HRMS ($C_{16}H_{18}Br_2N_2O_4S$ + H^+): calcd 492.9427 and 494.9406 (M + H^+), found 492.9383 and 494.9384.

3-Bromo-*N*-(4-bromo-2,5-dimethoxyphenyl)-4-(methylamino)benzenesulfonamide (**229**). Compound **222** (90 mg, 0.28 mmol) and *N*-bromosuccinimide (100 mg, 0.56 mmol) dissolved in CH_2Cl_2 (30 mL) were stirred for 2 h. The solution was washed with brine, dried, and evaporated to dryness to afford 112 mg (0.23 mmol, 83%) of crude product **229** which was crystallized in methanol (78 mg, 0.16 mmol, 58%). M.p.: 136-147 °C (MeOH). ^{1}H NMR (400 MHz, $CDCl_3$): δ 2.88 (3H, *d, J* = 5.2), 3.63 (3H, *s*), 3.83 (3H, *s*), 4.85 (1H, *bs*), 6.45 (1H, *d, J* = 8.8), 6.90 (1H, *s*), 6.95 (1H, *bs*), 7.15 (1H, *s*), 7.51 (1H, *dd, J* = 8.8 and 2), 7.81 (1H, *d, J* = 2). ^{13}C NMR (100 MHz, $CDCl_3$): δ 30.2 (CH_3), 56.4 (CH_3), 56.9 (CH_3), 105.6 (CH), 106.0 (C), 108.1 (C), 108.9 (CH), 115.8 (CH), 125.7 (C), 126.0 (C), 128.5 (CH), 131.5 (CH), 143.6 (C), 149.2 (C), 150.2 (C). HRMS ($C_{15}H_{16}Br_2N_2O_4S$ + H^+): calcd 478.9270 and 480.9250 (M + H^+), found 478.9256 and 480.9244.

N-(2,5-dimethoxyphenyl)-4-methoxy-3-nitrobenzenesulfonamide (**230**).

*Compound **183** article 3. Available at Materials and methods, chemical synthesis (2.1).*

N-(4-bromo-2,5-dimethoxyphenyl)-4-methoxy-*N*-methyl-3-nitrobenzenesulfonamide (**231**).

*Compound **204** article 3. Available at Materials and methods, chemical synthesis (2.1).*

3-Amino-*N*-(2,5-dimethoxyphenyl)-4-methoxybenzenesulfonamide (**232**). The nitro sulfonamide **230** (1.22 g, 3.31 mmol) in ethyl acetate (125 mL) and Pd (C) (10 mg) was stirred at room temperature under H_2 atmosphere for 48 h. The reaction mixture was filtered through Celite® and the filtrate was evaporated to dryness to afford the amine sulfonamide **232** (975 mg, 2.88 mmol, 87%), which was purified by crystallization in methanol (802 mg, 2.37 mmol, 71%).

M.p.: 132-134 °C (MeOH). ^{1}H NMR (400 MHz, $CDCl_3$): δ 3.64 (3H, *s*), 3.73 (3H, *s*), 3.85 (3H, *s*), 3.92 (2H, *bs*), 6.51 (1H, *dd, J* = 8.8 and 3.2), 6.67 (1H, *d, J* = 8.8), 6.71 (1H, *d, J* = 8.8), 7.02 (1H, *bs*), 7.08 (1H, *d, J* = 2.4), 7.12 (1H, *d, J* = 3.2), 7.19 (1H, *dd, J* = 8.8 and 2.4). ^{13}C NMR (100 MHz, $CDCl_3$): δ 55.6 (CH_3), 55.7 (CH_3), 56.3 (CH_3), 106.5 (CH), 109.0 (CH), 109.2 (CH), 111.5 (CH), 112.4 (CH), 118.3 (CH), 127.1 (C), 130.9 (C), 136.7 (C), 143.3 (C), 150.4 (C), 153.8 (C). HRMS ($C_{15}H_{18}N_2O_5S + H^+$): calcd 339.1009 (M + H^+), found 339.1006.

3-Amino-*N*-(4-bromo-2,5-dimethoxyphenyl)-4-methoxybenzenesulfonamide (**233**). 644 mg (1.90 mmol) of **232** and 373 mg (2.09 mmol) of *N*-bromosuccinimide in CH_2Cl_2 (50 mL) were stirred for 3 h. Then, it was washed with brine, dried over Na_2SO_4, filtered, and concentrated in vacuum. The residue (766 mg) was chromatographed in silica gel column (toluene/EtOAc 8:2) to afford the desired compound **233** (542 mg, 1.30 mmol, 68%). ^{1}H NMR (400 MHz, $CDCl_3$): δ 3.64 (3H, *s*), 3.84 (3H, *s*), 3.86 (3H, *s*), 3.94 (2H, *bs*), 6.71 (1H, *d, J* = 8.8), 6.93 (1H, *s*), 7.05 (1H, *d, J* = 2.4), 7.14 (1H, *dd, J* = 8.8 and 2.4), 7.20 (1H, *s*). ^{13}C NMR (100 MHz, $CDCl_3$): δ 55.6 (CH_3), 56.5 (CH_3), 56.8 (CH_3), 105.3 (CH), 109.3 (CH), 109.5 (C), 112.2 (CH), 115.9 (CH), 118.4 (CH), 126.3 (C), 130.6 (C), 136.6 (C), 143.5 (C), 150.2 (C), 150.5 (C). HRMS ($C_{15}H_{17}BrN_2O_5S + Na^+$): calcd 438.9934 and 440.9913 (M + Na^+), found 438.9921 and 440.9885.

3-Amino-*N*-(4-bromo-2,5-dimethoxyphenyl)-4-methoxy-*N*-methylbenzenesulfonamide (**234**). To 155 mg (0.37 mmol) of **233** in CH_3CN (25 mL), 41 mg (0.74 mmol) of crushed KOH were added and stirred for 30 min. Then, 46 µL (0.74 mmol) of CH_3I were added and stirred for 24 h. The solvent was evaporated to dryness and the residue was re-dissolved in EtOAc, washed with brine, dried (Na_2SO_4) and filtered. After concentration, the residue (150 mg) was purified by silica gel column chromatography (toluene/EtOAc 8:2) to give pure product **234** (129 mg, 0.30 mmol, 80%). ^{1}H NMR (400 MHz, $CDCl_3$): δ 3.15 (3H, *s*), 3.43 (3H, *s*), 3.80 (3H, *s*), 3.89 (3H, *s*), 6.77 (1H, *d, J* = 8.8), 6.85 (1H, *s*), 6.96 (1H, *d, J* = 2.4), 6.99 (1H, *s*), 7.08 (1H, *dd, J* = 8.8 and 2.4). ^{13}C NMR (100 MHz, $CDCl_3$): δ 37.7 (CH_3), 55.7 (CH_3), 55.9 (CH_3), 56.7 (CH_3), 109.1 (CH), 111.2 (C), 112.9 (CH), 115.4 (CH), 116.8 (CH), 118.4 (CH), 129.0 (C), 130.7 (C), 136.5 (C), 149.5 (C), 150.1 (C), 150.9 (C). HRMS ($C_{16}H_{19}BrN_2O_5S + Na^+$): calcd 455.0070 (M + Na^+), found 455.0064.

3-Amino-*N*-(4-bromo-2,5-dimethoxyphenyl)-*N*-(cyanomethyl)-4-methoxybenzenesulfonamide (**235**). A mixture of **233** (92 mg, 0.22 mmol) and K_2CO_3 (60 mg, 0.44 mmol) in dry DMF (3 mL) was stirred at room temperature for 30 min. Then, 2-chloroacetonitrile (28 µL, 0.44 mmol) was added. After 24 h, the solvent was evaporated under reduced pressure. The residue was dissolved in EtOAc and washed with brine, dried (Na_2SO_4) and concentrated in vacuo to afford 84 mg (0.18 mmol, 83%) of **235**. The title compound was purified by preparative TLC (CH_2Cl_2 /MeOH 98:2) (75 mg, 0.16 mmol, 74%). ^{1}H NMR (200 MHz, $CDCl_3$): δ 3.47 (3H, *s*), 3.81 (3H, *s*), 3.90 (3H, *s*), 4.09 (2H, *bs*), 4.53 (2H, *s*), 6.77 (1H, *d, J* = 8.2), 6.91 (1H, *s*), 6.94 (1H, *d, J* = 2.4), 7.04 (1H, *s*), 7.07 (1H, *dd, J* = 8.2 and 2.4). ^{13}C NMR (100 MHz, $CDCl_3$): δ 38.3 (CH_2), 55.8 (CH_3), 55.9 (CH_3), 56.8 (CH_3), 109.3 (CH), 112.6 (CH), 113.0 (C), 115.3 (C), 115.9 (CH), 116.9 (CH), 118.7 (CH), 125.1 (C), 130.3 (C), 136.7 (C), 149.9 (C), 150.3 (C), 150.7 (C). HRMS ($C_{17}H_{18}BrN_3O_5S + H^+$): calcd 456.0223 and 458.0203 (M + H^+), found 456.0223 and 458.0208.

Ethyl (5-(*N*-(4-bromo-2,5-dimethoxyphenyl)-*N*-methylsulfamoyl)-2-methoxyphenyl)carbamate (**236**). To a stirred solution of **234** (95 mg, 0.22 mmol) in dry DMF (3 mL), 60 mg (0.44 mmol) of K_2CO_3 were added. After 1 h at room temperature 85 µL (0.88 mmol) of ethyl chloroformate were added and stirred for 48 h. The reaction mixture was evaporated to dryness. After concentration, the residue was re-dissolved in EtOAc, washed with brine, dried over Na_2SO_4, filtered, and concentrated in vacuum to produce 101 mg (0.20 mmol, 91%) of compound **236**. Crude reaction product was purified by crystallization in CH_2Cl_2/hexane (73 mg, 0.14 mmol, 66%). M.p.: 151-157 °C (CH_2Cl_2/hexane). ^{1}H NMR (400 MHz, $CDCl_3$): δ 1.32 (3H, *t, J* = 7.2), 3.22 (3H, *s*), 3.47 (3H, *s*), 3.85 (3H, *s*), 3.95 (3H, *s*), 4.24 (2H, *q, J* = 7.2), 6.85 (1H, *d, J* = 8.8), 6.92 (1H, *s*), 7.00 (1H, *s*), 7.22 (1H, *bs*), 7.35 (1H, *dd, J* = 8.8 and 2.4). ^{13}C NMR (100 MHz, $CDCl_3$): δ 14.5

(CH_3), 37.8 (CH_3), 55.8 (CH_3), 56.1 (CH_3), 56.8 (CH_3), 61.5 (CH_2), 108.9 (CH), 111.4 (C), 115.6 (CH), 116.9 (CH), 117.3 (CH), 123.0 (CH), 128.0 (C), 128.9 (C), 131.7 (C), 149.7 (C), 150.4 (C), 150.8 (C), 153.1 (C). HRMS ($C_{19}H_{23}BrN_2O_7S + Na^+$): calcd 525.0302 and 527.0281 ($M + Na^+$), found 525.0299 and 527.0266.

1,2,4-Trimethoxy-5-nitrobenzene (**237**).

*Compound **30** article 2. Available at Materials and methods, chemical synthesis.*

2,4,5-Trimethoxyaniline (**238**).

*Compound **31** article 2. Available at Materials and methods, chemical synthesis.*

4-Methoxy-*N*-(2,4,5-trimethoxyphenyl)benzenesulfonamide (**239**).

*Compound **32** article 2. Available at Materials and methods, chemical synthesis.*

4-Methoxy-*N*-methyl-*N*-(2,4,5-trimethoxyphenyl)benzenesulfonamide (**240**).

*Compound **33** article 2. Available at Materials and methods, chemical synthesis.*

N-ethyl-4-methoxy-*N*-(2,4,5-trimethoxyphenyl)benzenesulfonamide (**241**).

*Compound **34** article 2. Available at Materials and methods, chemical synthesis.*

N-(cyanomethyl)-4-methoxy-*N*-(2,4,5-trimethoxyphenyl)benzenesulfonamide (**242**).

*Compound **35** article 2. Available at Materials and methods, chemical synthesis.*

Ethyl *N*-((4-methoxyphenyl)sulfonyl)-*N*-(2,4,5-trimethoxyphenyl)glycinate (**243**).

*Compound **36** article 2. Available at Materials and methods, chemical synthesis.*

N-benzyl-4-methoxy-*N*-(2,4,5-trimethoxyphenyl)benzenesulfonamide (**244**).

*Compound **37** article 2. Available at Materials and methods, chemical synthesis.*

4-Nitro-*N*-(2,4,5-trimethoxyphenyl)benzenesulfonamide (**245**). To 1.44 g of aniline **238** (7.85 mmol) in CH_2Cl_2 (50 mL) and pyridine (2 mL), 2.09 g of 4-nitrobenzenesulfonyl chloride (9.43 mmol) was slowly added and stirred at room temperature overnight. The reaction was treated with 2N HCl and 5% $NaHCO_3$, washed with brine, dried over anhydrous Na_2SO_4 and the solvent evaporated to obtain 2.73 g (7.42 mmol, 94%) of **245**. Crude product was crystallized in methanol to afford the purified compound (2.17 g, 5.89 mmol, 75%). M.p.: 189-195 °C (MeOH). IR (KBr): 3295, 1606, 1529, 1167, 850 cm^{-1}. ^1H NMR (200 MHz, CD_3OD): δ 3.36 (3H, *s*), 3.78 (3H, *s*), 3.79 (3H, *s*), 6.48 (1H, *s*), 7.04 (1H, *s*), 7.88 (2H, *d*, *J* = 9), 8.30 (2H, *d*, *J* = 9). ^{13}C NMR (100 MHz, acetone-D_6): δ 55.5 (CH_3), 55.5 (CH_3), 56.0 (CH_3), 98.0 (CH), 112.0 (CH), 116.1 (C), 123.7 (2CH), 128.7 (2CH), 143.1 (C), 146.0 (C), 147.4 (C), 149.1 (C), 150.1 (C). HRMS ($C_{15}H_{16}N_2O_7S + Na^+$): calcd 391.0570 ($M + Na^+$), found 391.0572.

4-Amino-*N*-(2,4,5-trimethoxyphenyl)benzenesulfonamide (**246**). A mixture of **245** (1.75 g, 4.75 mmol), 10 mg of Pd (C) and 125 mL of EtOAc was maintained under low hydrogen pressure and stirred at room temperature. After 48 h, uptake of H_2 was completed and the solution was filtered through Celite®. The filtrate was concentrated in vacuo to give product **246** (1.52 g, 4.50 mmol, 94%). The residue was purified by crystallization in methanol (806 mg, 2.38 mmol, 50%). M.p.: 160-165 °C (MeOH). IR (KBr): 3479, 3379, 3328, 1594, 1513, 1152, 876 cm^{-1}. ^1H NMR (200 MHz, CD_3OD): δ 3.49 (3H, *s*), 3.75 (3H, *s*), 3.77 (3H, *s*), 6.51 (1H, *s*), 6.55 (2H, *d*, *J* = 9), 6.99 (1H, *s*), 7.32 (2H, *d*, *J* = 9). ^{13}C NMR (100 MHz, $CDCl_3$): δ 56.3 (CH_3), 56.5 ($2CH_3$), 97.5 (CH), 107.9 (CH),

113.6 (2CH), 118.4 (C), 127.0 (C), 129.3 (2CH), 143.1 (C), 144.7 (C), 146.8 (C), 150.6 (C). HRMS ($C_{15}H_{18}N_2O_5S + Na^+$): calcd 361.0829 ($M + Na^+$), found 361.0824.

4-(Dimethylamino)-*N*-(2,4,5-trimethoxyphenyl)benzenesulfonamide (**247**). Compound **246** (800 mg, 2.36 mmol) was dissolved in MeOH (50 mL) with paraformaldehyde (710 mg, 23.6 mmol) and acetic acid (one drop). After 1 h stirring at room temperature sodium cyanoborohydride (297 mg, 4.72 mmol) was added to the solution. The reaction mixture was heated at reflux overnight. Then, the methanolic solution was concentrated under reduced pressure, the residue dissolved in EtOAc and washed with 5% $NaHCO_3$ and brine. The organics were dried over sodium sulphate and evaporated to afford **247** (843 mg, 2.30 mmol, 97%). The residue was purified by crystallization in methanol (612 mg, 1.67 mmol, 70%). M.p.: 118-126 °C (MeOH). ^{1}H NMR (200 MHz, CD_3OD): δ 2.99 (6H, *s*), 3.47 (3H, *s*), 3.75 (3H, *s*), 3.77 (3H, *s*), 6.50 (1H, *s*), 6.65 (2H, *d*, *J* = 9.2), 7.01 (1H, *s*), 7.45 (2H, *d*, *J* = 9.2). ^{13}C NMR (100 MHz, $CDCl_3$): δ 40.0 ($2CH_3$), 56.3 (CH_3), 56.4 (CH_3), 56.6 (CH_3), 97.7 (CH), 107.3 (CH), 110.4 (2CH), 118.9 (C), 124.2 (C), 129.0 (2CH), 143.1 (C), 144.4 (C), 146.5 (C), 152.8 (C). HRMS ($C_{17}H_{22}N_2O_5S + Na^+$): calcd 389.1142 ($M + Na^+$), found 389.1140.

4-(Dimethylamino)-*N*-methyl-*N*-(2,4,5-trimethoxyphenyl)benzenesulfonamide (**248**). To a stirred solution of **247** (83 mg, 0.22 mmol) in CH_3CN (40 mL), 25 mg (0.45 mmol) of crushed KOH were added. After 1 h at room temperature 28.3 µL (0.45 mmol) of CH_3I were added and stirred for 24 h. The solution was concentrated in vacuo, re-dissolved with EtOAc, washed with brine, dried over Na_2SO_4 and evaporated to dryness to give 83 mg (0.22 mmol, 96%) of **248**. The crude reaction product was purified by crystallization in methanol (62 mg, 0.16 mmol, 72%). M.p.: 154-159 °C (MeOH). IR (KBr): 1599, 1515, 1154, 790 cm^{-1}. ^{1}H NMR (200 MHz, CD_3OD): δ 3.04 (6H, *s*), 3.11 (3H, *s*), 3.47 (3H, *s*), 3.69 (3H, *s*), 3.83 (3H, *s*), 6.56 (1H, *s*), 6.69 (1H, *s*), 6.75 (2H, *d*, *J* = 9), 7.45 (2H, *d*, *J* = 9). ^{13}C NMR (100 MHz, $CDCl_3$): δ 38.0 (CH_3), 40.1 ($2CH_3$), 56.0 (CH_3), 56.1 (CH_3), 56.4 (CH_3), 97.6 (CH), 110.5 (2CH), 114.6 (CH), 121.6 (C), 125.0 (C), 129.5 (2CH), 142.3 (C), 149.3 (C), 151.1 (C), 152.7 (C). HRMS ($C_{18}H_{24}N_2O_5S + H^+$): calcd 381.1479 ($M + H^+$), found 381.1473.

4-(Dimethylamino)-*N*-ethyl-*N*-(2,4,5-trimethoxyphenyl)benzenesulfonamide (**249**). 90 mg (0.24 mmol) of **247** and 67 mg (0.49 mmol) of K_2CO_3 were dissolved in dry DMF (3 mL). After 30 min stirring at room temperature, 2-bromoethane (36.7 µL, 0.49 mmol) was added to the solution and stirred for 24 h. The reaction mixture was concentrated under reduced pressure, dissolved with EtOAc, washed with brine, dried (Na_2SO_4), filtered, and concentrated in vacuo to give 96 mg (0.24 mmol, 99%) of crude reaction product **249**, from which 68 mg (0.17 mmol, 70%) were purified by crystallization in methanol. M.p.: 119-128 °C (MeOH). ^{1}H NMR (200 MHz, CD_3OD): δ 1.00 (3H, *t*, *J* = 7), 3.04 (6H, *s*), 3.49 (3H, *s*), 3.55 (2H, *q*, *J* = 7), 3.69 (3H, *s*), 3.84 (3H, *s*), 6.58 (1H, *s*), 6.64 (1H, *s*), 6.75 (2H, *d*, *J* = 9), 7.46 (2H, *d*, *J* = 9). ^{13}C NMR (100 MHz, $CDCl_3$): δ 14.2 (CH_3), 40.1 ($2CH_3$), 44.7 (CH_2), 55.9 (CH_3), 56.0 (CH_3), 56.4 (CH_3), 97.4 (CH), 110.5 (2CH), 116.0 (CH), 118.6 (C), 126.2 (C), 129.3 (2CH), 142.3 (C), 149.4 (C), 151.7 (C), 152.6 (C). HRMS ($C_{19}H_{26}N_2O_5S + H^+$): calcd 395.1635 ($M + H^+$), found 395.1629.

N-(cyanomethyl)-4-(dimethylamino)-*N*-(2,4,5-trimethoxyphenyl)benzenesulfonamide (**250**). 2-chloroacetonitrile (31 µL, 0.49 mmol) was added after 30 min to a stirred solution of **247** (90 mg, 0.24 mmol) and K_2CO_3 (67 mg, 0.49 mmol) in DMF (3 mL). After 24 h, the reaction mixture was dried under vacuum, re-dissolved in EtOAc and washed with brine. After drying over Na_2SO_4 and removal of the solvent, 99 mg (0.24 mmol, 99%) of compound **250** were obtained. Crude product was purified by crystallization in methanol (79 mg, 0.19 mmol, 79%). M.p.: 140-146 °C (MeOH). ^{1}H NMR (400 MHz, $CDCl_3$): δ 3.01 (6H, *s*), 3.48 (3H, *s*), 3.78 (3H, *s*), 3.87 (3H, *s*), 4.51 (2H, *s*), 6.39 (1H, *s*), 6.59 (2H, *d*, *J* = 8.8), 6.78 (1H, *s*), 7.48 (2H, *d*, *J* = 8.8). ^{13}C NMR (100 MHz, $CDCl_3$): δ 38.6 (CH_2), 40.0 ($2CH_3$), 55.8 (CH_3), 56.2 (CH_3), 56.4 (CH_3), 97.1 (CH), 110.5 (2CH), 115.2 (CH), 115.8 (C), 117.4 (C), 123.9 (C), 129.5 (2CH), 142.5 (C), 150.4 (C), 150.8 (C), 153.1 (C). HRMS ($C_{19}H_{23}N_3O_5S + H^+$): calcd 406.1431 ($M + H^+$), found 406.1433.

Ethyl *N*-((4-(dimethylamino)phenyl)sulfonyl)-*N*-(2,4,5-trimethoxyphenyl)glycinate (**251**). To a solution of **247** (90 mg, 0.24 mmol) in DMF (3 mL), was added K_2CO_3 (67 mg, 0.49 mmol) and the resulting mixture was stirred for 30 min. Then, ethyl 2-bromoacetate (54.7 µL, 0.49 mmol) was added. After 24 h, the solvent was evaporated to dryness and the residue was dissolved in brine and extracted with EtOAc. The organics were dried over Na_2SO_4 before concentration under reduced pressure to yield the compound **251** (109 mg, 0.24 mmol, 98%). Crude product was crystallized from methanol to give the purified product (44 mg, 0.10 mmol, 39%). M.p.: 94-99 °C (MeOH). ^{1}H NMR (400 MHz, $CDCl_3$): δ 1.20 (3H, *t*, *J* = 7.2), 2.98 (6H, *s*), 3.44 (3H, *s*), 3.72 (3H, *s*), 3.82 (3H, *s*), 4.10 (2H, *q*, *J* = 7.2), 4.34 (2H, *s*), 6.34 (1H, *s*), 6.56 (2H, *d*, *J* = 8.8), 6.95 (1H, *s*), 7.48 (2H, *d*, *J* = 8.8). ^{13}C NMR (100 MHz, $CDCl_3$): δ 14.1 (CH_3), 40.0 ($2CH_3$), 51.3 (CH_2), 55.8 (CH_3), 56.1 (CH_3), 56.3 (CH_3), 61.1 (CH_2), 96.9 (CH), 110.3 (2CH), 116.7 (CH), 118.9 (C), 125.7 (C), 129.4 (2CH), 142.1 (C), 149.6 (C), 150.5 (C), 152.7 (C), 169.8 (C). HRMS ($C_{21}H_{28}N_2O_7S + H^+$): calcd 453.1690 (M + H^+), found 453.1689.

N-benzyl-4-(dimethylamino)-*N*-(2,4,5-trimethoxyphenyl)benzenesulfonamide (**252**). A solution of **247** (90 mg, 0.24 mmol) and K_2CO_3 (67 mg, 0.49 mmol) in dry DMF (3 mL) was stirred at room temperature for 30 min, then 57 µL (0.49 mmol) of benzyl chloride were added and the mixture stirred for 24 h. When completed, solvent was removed under vacuum and the residue was washed with brine, extracted with EtOAc, dried (Na_2SO_4), filtered, and evaporated to dryness to afford 110 mg (0.24 mmol, 98%) of **252**. The crude reaction product was purified by crystallization in methanol (43 mg, 0.09 mmol, 38%). M.p.: 125-129 °C (MeOH). ^{1}H NMR (200 MHz, CD_3OD): δ 3.06 (6H, *s*), 3.43 (3H, *s*), 3.55 (3H, *s*), 3.78 (3H, *s*), 4.68 (2H, *bs*), 6.44 (1H, *s*), 6.48 (1H, *s*), 6.77 (2H, *d*, *J* = 9), 7.18 (5H, *bs*), 7.52 (2H, *d*, *J* = 9). ^{13}C NMR (100 MHz, $CDCl_3$): δ 39.7 ($2CH_3$), 53.3 (CH_2), 55.4 (CH_3), 55.5 (CH_3), 55.9 (CH_3), 96.6 (CH), 110.1 (2CH), 116.0 (CH), 118.1 (C), 125.7 (C), 126.8 (CH), 127.6 (2CH), 128.5 (2CH), 128.9 (2CH), 136.7 (C), 141.6 (C), 148.9 (C), 150.9 (C), 152.2 (C). HRMS ($C_{24}H_{28}N_2O_5S + H^+$): calcd 457.1792 (M + H^+), found 457.1790.

N-(4-(*N*-(2,4,5-trimethoxyphenyl)sulfamoyl)phenyl)formamide (**253**). A solution of **246** (650 mg, 1.92 mmol) and formic acid (10 mL) in pyridine (5 mL) and CH_2Cl_2 (70 mL) was stirred for 24 h. Then, the reaction mixture was washed with 2N HCl, 5% $NaHCO_3$ and brine, dried over Na_2SO_4, filtered, and evaporated to dryness to afford 650 mg (1.78 mmol, 92%) of **253**. The crude reaction product was purified by crystallization in methanol (414 mg, 1.13 mmol, 59%). M.p.: 204-214 °C (MeOH). IR (KBr): 3331, 3260, 1701, 1592, 1526, 1163, 845 cm^{-1}. ^{1}H NMR (200 MHz, CD_3OD): δ 3.42 (3H, *s*), 3.77 (3H, *s*), 3.77 (3H, *s*), 6.49 (1H, *s*), 7.02 (1H, *s*), 7.63 (4H, *bs*), 8.29 (1H, *s*). ^{13}C NMR (100 MHz, DMSO-D_6): δ 56.2 (CH_3), 56.5 (CH_3), 56.6 (CH_3), 99.0 (CH), 112.5 (CH), 117.0 (C), 118.9 (2CH), 128.5 (2CH), 135.3 (C), 141.9 (C), 142.5 (2C), 148.2 (C), 160.6 (CH). HRMS ($C_{16}H_{18}N_2O_6S + Na^+$): calcd 389.0778 (M + Na^+), found 389.0774.

4-(Methylamino)-*N*-(2,4,5-trimethoxyphenyl)benzenesulfonamide (**254**). To a solution of formamide **253** (570 mg, 1.55 mmol) and $NaBH_4$ (88 mg, 2.33 mmol) in dry THF (15 mL) at 0°C, trichloroacetic acid (381 mg, 2.33 mmol) in dry THF (10 mL) was added dropwise under nitrogen atmosphere. The reaction mixture was stirred at 0°C to room temperature for 24 h and then concentrated and re-dissolved in EtOAc, washed with brine, dried over anhydrous Na_2SO_4, filtered and solvent evaporated in vacuum. The residue (520 mg) was purified by silica gel chromatography using hexane/EtOAc (7:3) to yield 404 mg (1.08 mmol, 74%) of **254**. ^{1}H NMR (200 MHz, CD_3OD): δ 2.74 (3H, *s*), 3.48 (3H, *s*), 3.74 (3H, *s*), 3.75 (3H, *s*), 6.48 (2H, *d*, *J* = 9), 6.50 (1H, *s*), 7.00 (1H, *s*), 7.38 (2H, *d*, *J* = 9). ^{13}C NMR (100 MHz, $CDCl_3$): δ 29.9 (CH_3), 56.3 (CH_3), 56.5 (CH_3), 56.6 (CH_3), 97.6 (CH), 107.7 (CH), 110.8 (2CH), 118.7 (C), 125.3 (C), 129.2 (2CH), 143.1 (C), 144.5 (C), 146.6 (C), 152.5 (C). HRMS ($C_{16}H_{20}N_2O_5S + Na^+$): calcd 375.0985 (M + Na^+), found 375.0986.

N-methyl-4-(methylamino)-*N*-(2,4,5-trimethoxyphenyl)benzenesulfonamide (**255**). A mixture of **254** (96 mg, 0.27 mmol) and crushed KOH (30 mg, 0.54 mmol) in CH_3CN (40 mL) was stirred at room temperature for 30 min. Then, CH_3I (34 µL, 0.54 mmol) was added to the solution and stirred for 24 h. The solvent was evaporated under reduced pressure and the residue was re-dissolved in EtOAc, washed with brine, dried over Na_2SO_4 and concentrated to afford compound **255** (91 mg, 0.25 mmol, 91%). Then, it was crystallized in methanol to isolate the pure compound (69 mg, 0.19 mmol, 69%). M.p.: 141-156 °C (MeOH). ^{1}H NMR (400 MHz, $CDCl_3$): δ 2.86 (3H, *s*), 3.14 (3H, *s*), 3.50 (3H, *s*), 3.76 (3H, *s*), 3.86 (3H, *s*), 6.40 (1H, *s*), 6.53 (2H, *d*, *J* = 8.8), 6.73 (1H, *s*), 7.49 (2H, *d*, *J* = 8.8). ^{13}C NMR (100 MHz, $CDCl_3$): δ 30.2 (CH_3), 38.0 (CH_3), 55.9 (CH_3), 56.1 (CH_3), 56.4 (CH_3), 97.6 (CH), 110.8 (2CH), 114.5 (CH), 121.4 (C), 126.1 (C), 129.7 (2CH), 142.3 (C), 149.3 (C), 151.0 (C), 152.2 (C). HRMS ($C_{17}H_{22}N_2O_5S + H^+$): calcd 367.1322 ($M + H^+$), found 367.1322.

N-(cyanomethyl)-4-(methylamino)-*N*-(2,4,5-trimethoxyphenyl)benzenesulfonamide (**256**). A solution of **254** (57 mg, 0.16 mmol) and K_2CO_3 (44 mg, 0.32 mmol) in dry DMF (3 mL) was stirred at room temperature for 1 h. To this solution 2-chloroacetonitrile (20.5 µL, 0.32 mmol) was added and the reaction mixture was stirred for 24 h. The solvent was removed under reduced pressure. The residue was dissolved in EtOAc and washed with brine, dried (Na_2SO_4) and concentrated in vacuo to afford 57 mg (0.15 mmol, 90%) of **256**. The crude product was purified by crystallization in methanol (45 mg, 0.12 mmol, 71%). M.p.: 168-173 °C (MeOH). IR (KBr): 3397, 1598, 1517, 1150, 869 cm^{-1}. ^{1}H NMR (200 MHz, CD_3OD): δ 2.80 (3H, *s*), 3.49 (3H, *s*), 3.72 (3H, *s*), 3.84 (3H, *s*), 4.57 (2H, *s*), 6.57 (2H, *d*, *J* = 9), 6.59 (1H, *s*), 6.82 (1H, *s*), 7.38 (2H, *d*, *J* = 9). ^{13}C NMR (100 MHz, $CDCl_3$): δ 30.0 (CH_3), 38.6 (CH_2), 55.8 (CH_3), 56.1 (CH_3), 56.5 (CH_3), 97.0 (CH), 110.9 (2CH), 115.2 (CH), 115.7 (C), 117.4 (C), 125.2 (C), 129.8 (2CH), 142.6 (C), 150.4 (C), 150.8 (C), 152.8 (C). HRMS ($C_{18}H_{21}N_3O_5S + Na^+$): calcd 414.1094 ($M + Na^+$), found 414.1089.

Ethyl *N*-((4-(methylamino)phenyl)sulfonyl)-*N*-(2,4,5-trimethoxyphenyl)glycinate (**257**). To a solution of **254** (56 mg, 0.16 mmol) and K_2CO_3 (44 mg, 0.32 mmol) in dry DMF (3 mL), ethyl 2-bromoacetate (35.5 µL, 0.32 mmol) was added after 30 min stirring. The reaction mixture was then stirred for 48 h, concentrated under vacuum, re-dissolved in EtOAc, washed with brine, dried (Na_2SO_4) and evaporated to dryness. The residue (70 mg) was purified by preparative TLC (hexane/EtOAc 2:8) to give **257** (63 mg, 0.14 mmol, 90%). IR (KBr): 3402, 1747, 1599, 1505, 884 cm^{-1}. ^{1}H NMR (400 MHz, $CDCl_3$): δ 1.20 (3H, *t*, *J* = 7.2), 2.81 (3H, *s*), 3.44 (3H, *s*), 3.73 (3H, *s*), 3.82 (3H, *s*), 4.10 (2H, *q*, *J* = 7.2), 4.35 (2H, *s*), 6.34 (1H, *s*), 6.47 (2H, *d*, *J* = 8.8), 6.97 (1H, *s*), 7.43 (2H, *d*, *J* = 8.8). ^{13}C NMR (100 MHz, $CDCl_3$): δ 14.1 (CH_3), 30.1 (CH_3), 51.3 (CH_2), 55.7 (CH_3), 56.0 (CH_3), 56.3 (CH_3), 61.0 (CH_2), 96.8 (CH), 110.7 (2CH), 116.8 (CH), 118.8 (C), 126.6 (C), 129.6 (2CH), 142.1 (C), 149.6 (C), 150.5 (C), 152.4 (C), 169.8 (C). HRMS ($C_{20}H_{26}N_2O_7S + H^+$): calcd 439.1533 ($M + H^+$), found 439.1536.

4-Methoxy-3-nitro-*N*-(2,4,5-trimethoxyphenyl)benzenesulfonamide (**258**). To a solution of aniline **238** (430 mg, 2.35 mmol) in CH_2Cl_2 (50 mL) and pyridine (2 mL), benzenesulfonyl chloride **53** (650 mg, 2.58 mmol) was slowly added. The mixture was stirred at room temperature overnight. Then, the reaction was treated with 2N HCl and 5% $NaHCO_3$, washed with brine, dried over anhydrous Na_2SO_4 and concentrated in vacuum to yield 816 mg (2.05 mmol, 87%) of sulfonamide **258**, which was purified by crystallization in methanol (491 mg, 1.23 mmol, 52%). M.p.: 185-194 °C (MeOH). IR (KBr): 3257, 1606, 1510, 1143, 833 cm^{-1}. ^{1}H NMR (200 MHz, $CDCl_3$): δ 3.57 (3H, *s*), 3.83 (3H, *s*), 3.86 (3H, *s*), 3.98 (3H, *s*), 6.34 (1H, *s*), 6.70 (1H, *bs*), 7.03 (1H, *d*, *J* = 8.8), 7.13 (1H, *s*), 7.80 (1H, *dd*, *J* = 8.8 and 2.4), 8.18 (1H, *d*, *J* = 2.4). ^{13}C NMR (100 MHz, $CDCl_3$): δ 56.0 (CH_3), 56.3 (CH_3), 56.6 (CH_3), 57.0 (CH_3), 96.9 (CH), 108.9 (CH), 113.1 (CH), 116.4 (C), 125.1 (CH), 131.1 (C), 133.1 (CH), 133.1 (C), 143.2 (C), 145.1 (C), 147.9 (C), 155.5 (C). HRMS ($C_{16}H_{18}N_2O_8S + Na^+$): calcd 421.0676 ($M + Na^+$), found 421.0677.

3-Amino-4-methoxy-*N*-(2,4,5-trimethoxyphenyl)benzenesulfonamide (**259**). Nitro sulfonamide **258** (700 mg, 1.76 mmol) in ethyl acetate (125 mL) and Pd (C) (10 mg) was stirred at room temperature under H_2 atmosphere for 48 h. The reaction mixture was filtered over Celite®, and the filtrate was evaporated to dryness to yield 551 mg (1.50 mmol, 85%) of **259**, which was purified by crystallization in methanol (311 mg, 0.85 mmol, 48%). M.p.: 153-160 °C (MeOH). IR (KBr): 3459, 3365, 3232, 1617, 1510, 1156, 856 cm^{-1}. ^1H NMR (200 MHz, $CDCl_3$): δ 3.54 (3H, *s*), 3.82 (3H, *s*), 3.85 (6H, *s*), 3.89 (2H, *bs*), 6.37 (1H, *s*), 6.65 (1H, *bs*), 6.69 (1H, *d*, *J* = 8.6), 6.99 (1H, *d*, *J* = 2.4), 7.08 (1H, *dd*, *J* = 8.6 and 2.4), 7.15 (1H, *s*). ^{13}C NMR (100 MHz, $CDCl_3$): δ 55.6 (CH_3), 56.3 (CH_3), 56.5 (CH_3), 56.6 (CH_3), 97.6 (CH), 107.6 (CH), 109.1 (CH), 112.6 (CH), 118.4 (CH), 118.5 (C), 130.9 (C), 136.4 (C), 143.1 (C), 144.6 (C), 146.7 (C), 150.3 (C). HRMS ($C_{16}H_{20}N_2O_6S$ + Na^+): calcd 391.0934 (M + Na^+), found 391.0930.

3-Amino-4-methoxy-*N*-methyl-*N*-(2,4,5-trimethoxyphenyl)benzenesulfonamide (**260**). To 75 mg (0.20 mmol) of **259** and 22 mg (0.40 mmol) of crushed KOH in CH_3CN (40 mL), 25.4 µL of CH_3I (0.40 mmol) were added and it was stirred for 24 h. The CH_3CN solution was concentrated under reduced pressure, the residue dissolved in EtOAc and washed with brine. The organics were dried over Na_2SO_4, filtered, and evaporated to afford compound **260** (72 mg, 0.19 mmol, 92%). The crude material was purified by column chromatography using hexane/EtOAc 1:1 as eluant to give 62 mg (0.16 mmol, 79%). IR (KBr): 3474, 3372, 1615, 1151, 882 cm^{-1}. ^1H NMR (200 MHz, $CDCl_3$): δ 3.13 (3H, *s*), 3.49 (3H, *s*), 3.74 (3H, *s*), 3.84 (3H, *s*), 3.87 (3H, *s*), 6.40 (1H, *s*), 6.70 (1H, *s*), 6.76 (1H, *d*, *J* = 8.2), 6.98 (1H, *d*, *J* = 2.4), 7.07 (1H, *dd*, *J* = 8.2 and 2.4). ^{13}C NMR (100 MHz, $CDCl_3$): δ 38.1 (CH_3), 55.7 (CH_3), 55.9 (CH_3), 56.1 (CH_3), 56.3 (CH_3), 97.6 (CH), 109.1 (CH), 113.3 (CH), 114.6 (CH), 118.6 (CH), 121.2 (C), 131.2 (C), 136.3 (C), 142.3 (C), 149.4 (C), 150.0 (C), 151.1 (C). HRMS ($C_{17}H_{22}N_2O_6S$ + Na^+): calcd 405.1091 (M + Na^+), found 405.1083.

3-Amino-*N*-ethyl-4-methoxy-*N*-(2,4,5-trimethoxyphenyl)benzenesulfonamide (**261**). 100 mg (0.27 mmol) of compound **259** were dissolved in dry DMF (3 mL) and 75 mg (0.54 mmol) of K_2CO_3 were added. After 30 min stirring at room temperature, 80.8 µL (1.08 mmol) of bromoethane were added to the solution. The reaction mixture was stirred at room temperature for 48 h. The solution was concentrated in vacuo and re-dissolved with EtOAc. Then, it was washed with brine, dried over Na_2SO_4 and evaporated to dryness to give 100 mg (0.25 mmol, 92%) of **261**. The crude product was purified by preparative TLC (CH_2Cl_2/EtOAc 7:3) (61 mg, 0.15 mmol, 56%). IR (KBr): 3479, 3373, 1614, 1537, 900 cm^{-1}. ^1H NMR (200 MHz, $CDCl_3$): δ 1.02 (3H, *t*, *J* = 7.2), 3.50 (3H, *s*), 3.56 (1H, *m*), 3.76 (3H, *s*), 3.84 (1H, *m*), 3.87 (3H, *s*), 3.88 (3H, *s*), 6.42 (1H, *s*), 6.67 (1H, *s*), 6.76 (1H, *d*, *J* = 8.6), 7.01 (1H, *d*, *J* = 2.2), 7.10 (1H, *dd*, *J* = 8.6 and 2.2). ^{13}C NMR (100 MHz, $CDCl_3$): δ 14.2 (CH_3), 44.8 (CH_2), 55.7 (CH_3), 55.9 (CH_3), 56.0 (CH_3), 56.4 (CH_3), 97.3 (CH), 109.1 (CH), 113.2 (CH), 115.9 (CH), 118.2 (C), 118.5 (CH), 132.3 (C), 136.2 (C), 142.2 (C), 149.5 (C), 149.9 (C), 151.7 (C). HRMS ($C_{18}H_{24}N_2O_6S$ + H^+): calcd 397.1428 (M + H^+), found 397.1427.

3-Amino-*N*-(cyanomethyl)-4-methoxy-*N*-(2,4,5-trimethoxyphenyl)benzenesulfonamide (**262**). A mixture of **259** (81 mg, 0.22 mmol) and K_2CO_3 (60 mg, 0.44 mmol) in dry DMF (3 mL) was stirred at room temperature for 30 min. Then, 2-chloroacetonitrile (28 µL, 0.44 mmol) was added. After 24 h, the solvent was evaporated under reduced pressure. The residue was dissolved in EtOAc and washed with brine, dried (Na_2SO_4) and concentrated in vacuo to isolate 60 mg (0.15 mmol, 66%) of **262**. The title compound was purified by crystallization in methanol (37 mg, 0.09 mmol, 41%). M.p.: 173-178 °C (MeOH). ^1H NMR (200 MHz, $CDCl_3$): δ 3.51 (3H, *s*), 3.77 (3H, *s*), 3.88 (3H, *s*), 3.90 (3H, *s*), 4.54 (2H, *s*), 6.41 (1H, *s*), 6.78 (1H, *d, J* = 8.2), 6.80 (1H, *s*), 6.97 (1H, *d, J* = 2.4), 7.10 (1H, *dd, J* = 8.2 and 2.4). ^{13}C NMR (100 MHz, $CDCl_3$): δ 38.7 (CH_2), 55.8 (CH_3), 56.1 ($2CH_3$), 56.3 (CH_3), 97.2 (CH), 109.3 (CH), 112.9 (CH), 115.2 (CH), 115.5 (C), 117.2 (C), 118.8 (CH), 130.7 (C), 136.6 (C), 142.6 (C), 150.5 (2C), 150.9 (C). HRMS ($C_{18}H_{21}N_3O_6S$ + Na^+): calcd 430.1043 (M + Na^+), found 430.1041.

Ethyl *N*-((3-amino-4-methoxyphenyl)sulfonyl)-*N*-(2,4,5-trimethoxyphenyl)glycinate (**263a**) and ethyl (5-(*N*-(2-ethoxy-2-oxoethyl)-*N*-(2,4,5-trimethoxyphenyl)sulfamoyl)-2-methoxyphenyl)glycinate (**263b**). A mixture of **259** (83 mg, 0.22 mmol) and K_2CO_3 (61 mg, 0.45 mmol) in dry DMF (3 mL), was stirred for 1 h. Then, ethyl 2-bromoacetate (50 µL, 0.45 mmol) was added. After 24 h, the reaction mixture was concentrated under reduced pressure, diluted with EtOAc, washed with brine, dried (Na_2SO_4), filtered, and concentrated in vacuo. The residue (94 mg) was then purified by preparative TLC (CH_2Cl_2/EtOAc 7:3) to afford compounds **263a** (51 mg, 0.11 mmol, 50%) and **263b** (35 mg, 0.06 mmol, 29%). **263a:** ^{1}H NMR (400 MHz, $CDCl_3$): δ 1.22 (3H, *t*, *J* = 7), 3.44 (3H, *s*), 3.77 (3H, *s*), 3.83 (3H, *s*), 3.87 (3H, *s*), 4.09 (4H, *q*, *J* = 7), 4.35 (2H, *s*), 6.35 (1H, *s*), 6.73 (1H, *d*, *J* = 8.6), 6.98 (1H, *d*, *J* = 2.4), 7.02 (1H, *s*), 7.07 (1H, *dd*, *J* = 8.6 and 2.4). ^{13}C NMR (100 MHz, $CDCl_3$): δ 14.1 (CH_3), 51.4 (CH_2), 55.6 (CH_3), 56.0 ($2CH_3$), 56.3 (CH_3), 61.0 (CH_2), 96.8 (CH), 109.0 (CH), 113.2 (CH), 116.7 (CH), 118.6 (CH), 118.6 (C), 132.1 (C), 136.3 (C), 142.1 (C), 149.7 (C), 150.1 (C), 150.5 (C), 169.6 (C). HRMS ($C_{20}H_{26}N_2O_8S + Na^+$): calcd 477.1302 (M + Na^+), found 477.1301. **263b:** ^{1}H NMR (200 MHz, $CDCl_3$): δ 1.23 (3H, *t*, *J* = 7), 1.29 (3H, *t*, *J* = 7), 3.41 (3H, *s*), 3.77 (3H, *s*), 3.85 (5H, *s*), 3.90 (3H, *s*), 4.14 (2H, *q*, *J* = 7), 4.22 (2H, *q*, *J* = 7), 4.37 (2H, *s*), 6.34 (1H, *s*), 6.71 (1H, *d*, *J* = 2.4), 6.74 (1H, *d*, *J* = 8.6), 7.01 (1H, *s*), 7.08 (1H, *dd*, *J* = 8.6 and 2.4). ^{13}C NMR (100 MHz, $CDCl_3$): δ 14.1 ($2CH_3$), 45.0 (CH_2), 51.6 (CH_2), 55.8 (CH_3), 56.1 ($2CH_3$), 56.2 (CH_3), 61.6 (CH_2), 61.8 (CH_2), 96.8 (CH), 108.1 (CH), 108.2 (CH), 116.9 (CH), 118.0 (CH), 118.4 (C), 132.1 (C), 136.8 (C), 142.1 (C), 149.7 (C), 150.0 (C), 150.5 (C), 169.6 (C), 170.4 (C). HRMS ($C_{24}H_{32}N_2O_{10}S + Na^+$): calcd 563.1670 (M + Na^+), found 563.1669.

3-Amino-*N*-benzyl-4-methoxy-*N*-(2,4,5-trimethoxyphenyl)benzenesulfonamide (**264**). To a solution of **259** (95 mg, 0.26 mmol) and K_2CO_3 (71 mg, 0.52 mmol) in dry DMF (3 mL), benzyl chloride (60 µL 0.52 mmol) was added after 30 min stirring at room temperature. Then, the reaction mixture was stirred for 24 h. When completed, solvent was removed under vacuum and the residue was washed with brine, extracted with EtOAc, dried (Na_2SO_4), filtered and evaporated to dryness to afford 108 mg (0.24 mmol, 91%) of **264.** Crude reaction product was purified by preparative TLC (CH_2Cl_2/EtOAc 7:3) to give 67 mg (0.15 mmol, 57%) of pure product. IR (KBr): 3477, 3374, 1612, 1508, 1150, 872 cm^{-1}. ^{1}H NMR (200 MHz, $CDCl_3$): δ 3.42 (3H, *s*), 3.61 (3H, *s*), 3.81 (3H, *s*), 3.90 (3H, *s*), 4.69 (2H, *bs*), 6.32 (1H, *s*), 6.46 (1H, *s*), 6.78 (1H, *d*, *J* = 8.6), 7.03 (1H, *d*, *J* = 2.4), 7.14 (1H, *dd*, *J* = 8.6 and 2.4), 7.18 (5H, *bs*). ^{13}C NMR (100 MHz, $CDCl_3$): δ 53.8 (CH_2), 55.7 ($2CH_3$), 55.9 (CH_3), 56.3 (CH_3), 97.0 (CH), 109.1 (CH), 113.3 (CH), 116.4 (CH), 118.2 (C), 118.6 (CH), 127.3 (CH), 128.0 (2CH), 128.8 (2CH), 132.4 (C), 136.3 (C), 136.9 (C), 142.0 (C), 149.4 (C), 150.0 (C), 151.3 (C). HRMS ($C_{23}H_{26}N_2O_6S + H^+$): calcd 459.1584 (M + H^+), found 459.1584.

N-(4-chloro-2,5-dimethoxyphenyl)-4-methoxybenzenesulfonamide (**265**). To 107 mg (0.57 mmol) of 5-chloro-2,4-dimethoxyaniline in CH_2Cl_2 (25 mL) and pyridine (1 mL), 118 mg (0.57 mmol) of 4-methoxybenzenesulfonyl chloride was slowly added and stirred at room temperature for 12 h. The reaction was treated with 2N HCl and 5% $NaHCO_3$, washed with brine, dried over anhydrous Na_2SO_4 and the solvent evaporated to obtain 199 mg (0.56 mmol, 98%) of **265**. The residue was crystallized in methanol to afford the purified compound (139 mg, 0.39 mmol, 68%). M.p.: 131-133 °C (MeOH). IR (KBr): 3236, 1596, 1496, 1025, 709 cm^{-1}. ^{1}H NMR (400 MHz, $CDCl_3$): δ 3.59 (3H, *s*), 3.82 (3H, *s*), 3.83 (3H, *s*), 6.32 (1H, *s*), 6.62 (1H, *bs*), 6.86 (2H, *d*, *J* = 9.2), 7.55 (1H, *s*), 7.65 (2H, *d*, *J* = 9.2). ^{13}C NMR (100 MHz, $CDCl_3$): δ 55.6 (CH_3), 56.0 (CH_3), 56.4 (CH_3), 96.5 (CH), 113.7 (C), 113.8 (2CH), 118.9 (C), 124.6 (CH), 129.4 (2CH), 130.4 (C), 150.2 (C), 153.1 (C), 163.0 (C). HRMS ($C_{15}H_{16}ClNO_5S + H^+$): calcd 358.0510 (M + H^+), found 358.0512.

N-(4-chloro-2,5-dimethoxyphenyl)-4-methoxy-*N*-methylbenzenesulfonamide (**266**). 102 mg (0.28 mmol) of **265** were dissolved in CH_3CN (50 mL) with 33 mg (0.57 mmol) of KOH. After 30 min stirring at room temperature, CH_3I (35.6 µL, 0.57 mmol) was added to the solution and the

reaction mixture was stirred for 48 h. The solvent was removed under reduced pressure. The residue was dissolved in EtOAc and washed with brine, dried (Na_2SO_4) and concentrated in vacuo to afford 100 mg (0.27 mmol, 94%) of **266**. The crude product was purified by crystallization in CH_2Cl_2/hexane (47 mg, 0.13 mmol, 44%). M.p.: 194-201 °C (CH_2Cl_2/hexane). ^{1}H NMR (400 MHz, $CDCl_3$): δ 3.13 (3H, *s*), 3.52 (3H, *s*), 3.87 (3H, *s*), 3.89 (3H, *s*), 6.38 (1H, *s*), 6.94 (2H, *d*, *J* = 9.2), 7.20 (1H, *s*), 7.64 (2H, *d*, *J* = 9.2). ^{13}C NMR (100 MHz, $CDCl_3$): δ 37.8 (CH_3), 55.5 (CH_3), 55.7 (CH_3), 56.4 (CH_3), 96.6 (CH), 112.8 (C), 113.7 (2CH), 122.1 (CH), 129.6 (2CH), 130.8 (C), 132.3 (C), 155.6 (C), 156.2 (C), 162.7 (C). HRMS ($C_{16}H_{18}ClNO_5S + H^+$): calcd 372.0667 ($M + H^+$), found 372.0675.

2,6-Dibromo-4-nitrophenol (**267**). To a solution of 4-nitrophenol (2.5 g, 18 mmol) in CH_2Cl_2 (125 mL) *N*-bromosuccinimide (6.4 g, 36 mmol) was added. After 48 stirring at room temperature the precipitate formed was filtered to afford compound **267** (5.08g, 17.1 mmol, 95%) which was used without further purification. ^{1}H NMR (400 MHz, $CDCl_3$): δ 8.41 (2H, *s*). GC-MS ($C_6H_3Br_2NO_3$): 297 (M^+).

1,3-Dibromo-2-methoxy-5-nitrobenzene (**268**). To a solution of **267** (2.11 g, 7.11 mmol) and K_2CO_3 (1.96 g, 14.2 mmol) in acetone (50 mL), $(CH_3)_2SO_4$ (1.19 mL, 12.4 mmol) was dropwise added and heated at reflux overnight. Then, the reaction mixture was concentrated under vacuum, re-dissolved in EtOAc and washed with brine. The organics were dried over anhydrous Na_2SO_4, filtered, and evaporated to dryness to afford compound **268** (1.52 g, 4.89 mmol, 69%). The product was then used without further purification. ^{1}H NMR (400 MHz, $CDCl_3$): δ 3.97 (3H, *s*), 8.41 (2H, *s*). GC-MS ($C_7H_5Br_2NO_3$): 311 (M^+).

3,5-Dibromo-4-methoxyaniline (**269**). The nitro precursor **268** (1.52 g, 4.89 mmol) in ethyl acetate (125 mL) and Pd (C) (10 mg) was stirred at room temperature under H_2 atmosphere for 48 h. The reaction mixture was filtered through Celite®, and the filtrate was evaporated to dryness to give the title compound (**269,** 819 mg, 2.91 mmol, 60%). The crude reaction product was then used without further purification. ^{1}H NMR (400 MHz, $CDCl_3$): δ 3.79 (3H, *s*), 6.83 (2H, *s*). GC-MS ($C_7H_7Br_2NO$): 281 (M^+).

N-(3,5-dibromo-4-methoxyphenyl)-4-methoxybenzenesulfonamide (**270**). To a solution of **269** (800 mg, 2.85 mmol) in CH_2Cl_2 (50 mL) and pyridine (1 mL), 4-methoxybenzenesulfonyl chloride was slowly added (588 mg, 2.85 mmol) and stirred at room temperature. After 24 h, the reaction was treated with 2N HCl and 5% $NaHCO_3$, washed with brine to neutrality, dried over anhydrous Na_2SO_4 and concentrated under vacuum to yield 1.25 g (2.78 mmol, 97%) of the sulfonamide **270**. The product was purified by crystallization in CH_2Cl_2 (978 mg, 2.17 mmol, 76%). M.p.: 105-114 °C (CH_2Cl_2). ^{1}H NMR (400 MHz, $CDCl_3$): δ 3.82 (3H, *s*), 3.86 (3H, *s*), 6.94 (2H, *d*, *J* = 8.8), 7.71 (2H, *d*, *J* = 8.8). ^{13}C NMR (100 MHz, $CDCl_3$): δ 55.6 (CH_3), 60.7 (CH_3), 114.5 (2CH), 118.3 (2C), 125.0 (2CH), 129.4 (2CH), 129.6 (C), 134.3 (C), 151.5 (C), 163.5 (C). HRMS ($C_{14}H_{13}Br_2NO_4S + Na^+$): calcd 473.8804 ($M + Na^+$), found 473.8796.

N-(3,5-dibromo-4-methoxyphenyl)-4-methoxy-*N*-methylbenzenesulfonamide (**271**). 390 mg (0.86 mmol) of **270** were dissolved in CH_3CN (50 mL) with 99 mg (1.72 mmol) of KOH. After 30 min stirring at room temperature, CH_3I (108 µL, 1.72 mmol) was added to the solution and the reaction mixture was stirred for 48 h. The solvent was removed under reduced pressure. The residue was dissolved in EtOAc and washed with brine, dried (Na_2SO_4) and concentrated in vacuo to afford 316 mg (0.68 mmol, 79%) of **271**. The crude product was purified by crystallization in methanol (263 mg, 0.57 mmol, 65%). IR (KBr): 1593, 1467, 1150, 808 cm^{-1}. ^{1}H NMR (400 MHz, $CDCl_3$): δ 3.09 (3H, *s*), 3.88 (6H, *s*), 6.97 (2H, *d*, *J* = 8.8), 7.27 (2H, *s*), 7.51 (2H, *d*, *J* = 8.8). ^{13}C NMR (100 MHz, $CDCl_3$): δ 37.9 (CH_3), 55.6 (CH_3), 60.7 (CH_3), 114.1 (2CH), 117.6 (2C), 127.4 (C), 129.9

(2CH), 130.7 (2CH), 139.0 (C), 153.2 (C), 163.3 (C). HRMS ($C_{15}H_{15}Br_2NO_4S + Na^+$): calcd 485.8981 and 487.8960 ($M + Na^+$), found 485.8982 and 487.8962.

N-(3,5-dibromo-4-methoxyphenyl)-*N*-ethyl-4-methoxybenzenesulfonamide (**272**). A solution of **270** (82 mg, 0.18 mmol) and K_2CO_3 (50 mg, 0.36 mmol) in dry DMF (3 mL) was stirred for 30 min. Then, 2-bromoethano (81 µL, 1.08 mmol) was added to the solution and was stirred for 72 h. The solution was concentrated in vacuo and re-dissolved with EtOAc. Then, it was washed with brine, dried over Na_2SO_4 and evaporated to dryness to give 78 mg (0.16 mmol, 89%) of **272**. Crude product was purified by crystallization in methanol (56 mg, 0.12 mmol, 64%). M.p.: 110-115 °C (MeOH). ^{1}H NMR (200 MHz, $CDCl_3$): δ 1.06 (3H, *t*, *J* = 7), 3.48 (2H, *q*, *J* = 7), 3.88 (3H, *s*), 3.89 (3H, *s*), 6.97 (2H, *d*, *J* = 9.4), 7.20 (2H, *s*), 7.55 (2H, *d*, *J* = 9.4). ^{13}C NMR (100 MHz, $CDCl_3$): δ 13.9 (CH_3), 45.5 (CH_2), 55.6 (CH_3), 60.7 (CH_3), 114.1 (2CH), 117.7 (2C), 129.2 (C), 129.8 (2CH), 133.0 (2CH), 136.5 (C), 153.8 (C), 163.2 (C). HRMS ($C_{16}H_{17}Br_2NO_4S + H^+$): calcd 479.9297 ($M + H^+$), found 479.9332.

Ethyl *N*-(3,5-dibromo-4-methoxyphenyl)-*N*-((4-methoxyphenyl)sulfonyl)glycinate (**273**). To a stirred solution of **270** (88 mg, 0.19 mmol) in dry DMF (3 mL), 52 mg (0.38 mmol) of K_2CO_3 were added. After 1 h at room temperature, 43 µL (0.38 mmol) of ethyl 2-bromoacetate were added and stirred for 24 h. The reaction mixture was concentrated, re-dissolved in EtOAc, washed with brine, dried over anhydrous Na_2SO_4, filtered, and concentrated under vacuum to produced 85 mg (0.16 mmol, 81%) of crude reaction product from which 63 mg (0.12 mmol, 60%) of **273** were purified by crystallization in methanol. M.p.: 90-95 °C (MeOH). ^{1}H NMR (200 MHz, $CDCl_3$): δ 1.24 (3H, *t*, *J* = 7.2), 3.87 (3H, *s*), 3.88 (3H, *s*), 4.16 (2H, *q*, *J* = 7.2), 4.13 (2H, *s*), 6.96 (2H, *d*, *J* = 9), 7.38 (2H, *s*), 7.64 (2H, *d*, *J* = 9). ^{13}C NMR (100 MHz, $CDCl_3$): δ 14.0 (CH_3), 52.5 (CH_2), 55.6 (CH_3), 60.7 (CH_3), 61.7 (CH_2), 114.1 (2CH), 117.8 (2C), 129.8 (C), 130.0 (2CH), 133.0 (2CH), 137.2 (C), 154.1 (C), 163.4 (C), 168.4 (C). HRMS ($C_{18}H_{19}Br_2NO_6S + H^+$): calcd 535.9373 and 537.9352 ($M + H^+$), found 535.9372 and 537.9370.

4-Methoxy-3-nitrobenzonitrile (**274**).

*Compound **250** article 3. Available at Materials and methods, chemical synthesis (2.1).*

3-Amino-4-methoxybenzonitrile (**275**).

*Compound **258** article 3. Available at Materials and methods, chemical synthesis (2.1).*

N-(5-cyano-2-methoxyphenyl)-4-methoxybenzenesulfonamide (**276a**) and 4-cyano-2-((4-methoxyphenyl)sulfonamido)phenyl 4-methoxybenzenesulfonate (**276b**).

*Compounds **276A** and **276B** article 3. Available at Materials and methods, chemical synthesis (2.1).*

N-(5-cyano-2-methoxyphenyl)-4-methoxy-*N*-methylbenzenesulfonamide (**277**). To a solution of **276a** (55 mg, 0.17 mmol) in CH_3CN (40 mL) KOH (19 mg, 0.34 mmol) was added and stirred for 30 min. Then, CH_3I (21 µL, 0.34 mmol) was added. The reaction mixture was stirred at room temperature for 48 h and evaporated to dryness. The residue was dissolved in EtOAc, washed with brine, and dried over Na_2SO_4. After concentration, the residue (53 mg) was purified by preparative TLC (hexane/CH_2Cl_2/EtOAc 4:1:5) to give 34 mg (0.10 mmol, 59%) of **277**. IR (KBr): 2226, 1597, 1500, 1157, 814 cm^{-1}. ^{1}H NMR (200 MHz, $CDCl_3$): δ 3.15 (3H, *s*), 3.58 (3H, *s*), 3.87 (3H, *s*), 6.88 (1H, *d*, *J* = 8.6), 6.95 (2H, *d*, *J* = 9), 7.53-7.63 (4H, *m*). ^{13}C NMR (100 MHz, $CDCl_3$): δ 37.5 (CH_3), 55.6 (CH_3), 55.7 (CH_3), 104.2 (C), 112.5 (CH), 113.8 (2CH), 118.2 (C), 129.6 (2CH), 130.3 (C), 130.5 (C), 133.9 (CH), 135.4 (CH), 160.1 (C), 162.9 (C). HRMS ($C_{16}H_{16}N_2O_4S + H^+$): calcd 333.0904 ($M + H^+$), found 333.0900.

N-(4-bromophenyl)-4-methoxybenzenesulfonamide (**278**). To a solution of 4-bromoaniline (180 mg, 1.04 mmol) in CH_2Cl_2 (50 mL) and pyridine (1 mL), 4-methoxybenzenesulfonyl chloride (216 mg, 1.04 mmol) was slowly added. The reaction mixture was stirred at room temperature for 8 h. Then, it was treated with 2N HCl and 5% $NaHCO_3$. The organics were washed with brine, dried over Na_2SO_4, filtered, and concentrated under vacuum. The residue (326 mg) was purified by flash column chromatography (hexane/EtOAc 1:1) to afford compound **278** (320 mg, 0.93 mmol, 89%). ^{1}H NMR (400 MHz, $CDCl_3$): δ 3.73 (3H, *s*), 6.81 (2H, *d*, *J* = 8.8), 6.91 (2H, *d*, *J* = 8.8), 7.24 (2H, *d*, *J* = 8.8), 7.49 (1H, *bs*), 7.66 (2H, *d*, *J* = 8.8). ^{13}C NMR (100 MHz, $CDCl_3$): δ 55.6 (CH_3), 114.3 (2CH), 118.3 (C), 122.8 (2CH), 129.4 (2CH), 129.9 (C), 132.3 (2CH), 135.8 (C), 163.2 (C). HRMS ($C_{13}H_{12}BrNO_3S$ + Na^+): calcd 363.9613 and 365.9593 (M + Na^+), found 363.9604 and 365.9591.

N-(4-bromophenyl)-4-methoxy-*N*-methylbenzenesulfonamide (**279**). 97 mg (0.28 mmol) of **278** were dissolved in CH_3CN (50 mL) with 32 mg (0.56 mmol) of KOH. After 30 min stirring at room temperature, CH_3I (35 µL, 0.56 mmol) was added to the solution and the reaction mixture was stirred for 48 h. The solvent was removed under reduced pressure. The residue was dissolved in EtOAc and washed with brine, dried (Na_2SO_4) and concentrated in vacuo to afford 90 mg (0.25 mmol, 90%) of **279**. The crude product was purified by crystallization in CH_2Cl_2/hexane (20 mg, 0.06 mmol, 20%). M.p.: 118-125 °C (CH_2Cl_2/hexane). ^{1}H NMR (400 MHz, $CDCl_3$): δ 3.12 (3H, *s*), 3.86 (3H, *s*), 6.92 (2H, *d*, *J* = 8.8), 6.98 (2H, *d*, *J* = 8.8), 7.41 (2H, *d*, *J* = 8.8), 7.46 (2H, *d*, *J* = 8.8). ^{13}C NMR (100 MHz, $CDCl_3$): δ 37.8 (CH_3), 55.6(CH_3), 114.0 (2CH), 120.8 (C), 127.5 (C), 128.1 (2CH), 129.9 (2CH), 131.9 (2CH), 140.7 (C), 163.1 (C). HRMS ($C_{14}H_{14}BrNO_3S$ + Na^+): calcd 377.9770 and 379.9750 (M + Na^+), found 377.9774 and 379.9748.

5-Amino-2-methoxyphenol (**280**). 2-Methoxy-5-nitrophenol (248 mg, 1.47 mmol) in ethyl acetate (50 mL) and Pd (C) (10 mg) was stirred at room temperature under H_2 atmosphere for 72 h. The reaction mixture was filtered through Celite®, and the filtrate was evaporated to dryness to give the title compound (**280,** 201 mg, 1.44 mmol, 98%). The crude reaction product was then used without further purification. ^{1}H NMR (200 MHz, $CDCl_3$): δ 3.77 (3H, *s*), 5.40 (2H, *bs*), 6.14 (1H, *dd*, *J* = 8.4 and 2.6), 6.33 (1H, *d*, *J* = 2.6), 6.65 (1H, *d*, *J* = 8.4). GC-MS ($C_7H_9NO_2$): 139 (M^+).

N-(3-hydroxy-4-methoxyphenyl)-4-nitrobenzenesulfonamide (**281**). To a solution of **280** (174 mg, 1.25 mmol) in CH_2Cl_2 (50 mL) and pyridine (2 mL), 4-nitrobenzenesulfonyl chloride (277 mg, 1.25 mmol) was slowly added and stirred at room temperature. After 24 h, the reaction was treated with 2N HCl and 5% $NaHCO_3$, washed with brine to neutrality, dried over anhydrous Na_2SO_4 and concentrated under vacuum. The residue (249 mg) was purified by flash column chromatography (CH_2Cl_2/EtOAc) to yield compound **281** (192 mg, 0.59 mmol, 47%). ^{1}H NMR (400 MHz, CD_3OD): δ 3.75 (3H, *s*), 6.47 (1H, *dd*, *J* = 8.4 and 2.4), 6.59 (1H *d*, *J* = 2.4), 6.73 (1H, *d*, *J* = 8.4), 7.90 (2H, *d*, *J* = 9.2), 8.29 (2H, *d*, *J* = 9.2). ^{13}C NMR (100 MHz, CD_3OD): δ 55.1 (CH_3), 110.4 (CH), 111.4 (CH), 113.8 (CH), 123.7 (2CH), 128.2 (2CH), 129.7 (C), 145.1 (C), 145.9 (C), 146.6 (C), 150.0 (C). HRMS ($C_{13}H_{12}N_2O_6S$ + Na^+): calcd 347.0308 (M + Na^+), found 347.0322.

4-Methoxy-*N*-(2-methoxy-5-(trifluoromethyl)phenyl)benzenesulfonamide (**282**). To a solution of 2-methoxy-5-(trifluoromethyl)aniline (303 mg, 1.58 mmol) in CH_2Cl_2 (50 mL) and pyridine (2 mL), 4-methoxybenzenesulfonyl chloride (328 mg, 1.58 mmol) was slowly added. The reaction mixture was stirred at room temperature overnight. Then, it was treated with 2N HCl and 5% $NaHCO_3$. The organics were washed with brine, dried over Na_2SO_4, filtered, and concentrated under vacuum to yield compound **282** (443 mg, 1.23 mmol, 77%), which was purified by crystallization in CH_2Cl_2/hexane (233 mg, 0.64 mmol, 41%). M.p.: 117-119 °C (CH_2Cl_2/hexane). IR (KBr): 3235, 1594, 1518, 1261, 1118, 817 cm^{-1}. ^{1}H NMR (400 MHz, $CDCl_3$): δ 3.76 (3H, *s*), 3.82

(3H, *s*), 6.80 (1H, *d*, *J* = 8.4), 6.88 (2H, *d*, *J* = 8.8), 7.07 (1H, *bs*), 7.28 (1H, *dd*, *J* = 8.4 and 2), 7.72 (2H, *d*, *J* = 8.8), 7.78 (1H, *d*, *J* = 2). ^{13}C NMR (100 MHz, CD_3OD): δ 54.7 (CH_3), 55.0 (CH_3), 110.8 (CH), 113.5 (2CH), 120.1 (CH), 122.1 (C), 122.8 (CH), 122.9 (C), 126.5 (C), 129.0 (2CH), 131.1 (C), 154.0 (C), 163.2 (C). HRMS ($C_{15}H_{14}F_3NO_4S + H^+$): calcd 362.0668 ($M + H^+$), found 362.0669.

4-Methoxy-*N*-(2-methoxy-5-(trifluoromethyl)phenyl)-*N*-methylbenzenesulfonamide (**283**). 83 mg (0.23 mmol) of **282** and 26 mg (0.46 mmol) of KOH were mixed in in CH_3CN (50 mL). After 30 min stirring at room temperature, CH_3I (58 µL, 0.92 mmol) was added to the mixture and stirred 24 h. The reaction mixture was concentrated, re-dissolved in EtOAc, washed with brine, dried over anhydrous Na_2SO_4, filtered, and concentrated in vacuum. The residue (87 mg) was purified by preparative TLC in hexane/EtOAc 1:1 to afford compound **283** (70 mg, 0.18 mmol, 81%). IR (film): 1597, 1498, 1139, 810 cm^{-1}. ^{1}H NMR (400 MHz, $CDCl_3$): δ 3.17 (3H, *s*), 3.57 (3H, *s*), 3.86 (3H, *s*), 6.89 (1H, *d*, *J* = 8.4), 6.94 (2H, *d*, *J* = 8.8), 7.48 (1H, *d*, *J* = 2), 7.52 (1H, *dd*, *J* = 8.4 and 2), 7.62 (2H, *d*, *J* = 8.8). ^{13}C NMR (100 MHz, $CDCl_3$): δ 37.6 (CH_3), 55.5 (CH_3), 55.6 (CH_3), 111.8 (CH), 113.7 (2CH), 122.7 (C), 123.1 (C), 126.7 (C), 126.8 (CH), 128.8 (CH), 129.7 (2CH), 130.8 (C), 158.9 (C), 162.8 (C). HRMS ($C_{16}H_{16}F_3NO_4S + H^+$): calcd 376.0825 ($M + H^+$), found 376.0819.

N-benzyl-4-methoxy-*N*-(2-methoxy-5-(trifluoromethyl)phenyl)benzenesulfonamide (**284**). A solution of **282** (58 mg, 0.16 mmol) and K_2CO_3 (44 mg, 0.32 mmol) in dry DMF (3 mL) was stirred for 30 min. Benzyl chloride (38 µL, 0.32 mmol) was added to the solution and stirred for 48 h. Reaction mixture was concentrated under vacuum, re-dissolved in EtOAc and washed with brine, dried (Na_2SO_4), filtered, and evaporated to dryness to give **284** (65 mg, 0.14 mmol, 89%). Crude reaction product was purified by crystallization in CH_2Cl_2/hexane (25 mg, 0.05 mmol, 34%). M.p.: 123-124 °C (CH_2Cl_2/hexane). IR (KBr): 1596, 1498, 1351, 1156, 814 cm^{-1}. ^{1}H NMR (400 MHz, $CDCl_3$): δ 3.53 (3H, *s*), 3.88 (3H, *s*), 4.72 (2H, *s*), 6.80 (1H, *d*, *J* = 8.4), 6.94 (2H, *d*, *J* = 8.8), 7.20 (5H, *m*), 7.23 (1H, *d*, *J* = 2.4), 7.45 (1H, *dd*, *J* = 8.4 and 2.4), 7.65 (2H, *d*, *J* = 8.8). ^{13}C NMR (100 MHz, $CDCl_3$): δ 53.3 (CH_2), 55.2 (CH_3), 55.3 (CH_3), 111.3 (CH), 113.5 (2CH), 122.3 (C), 122.6 (C), 126.6 (CH), 126.8 (C), 127.4 (CH), 127.9 (2CH), 128.3 (2CH), 129.4 (2CH), 130.2 (CH), 131.6 (C), 135.7 (C), 158.9 (C), 162.6 (C). HRMS ($C_{22}H_{20}F_3NO_4S + H^+$): calcd 452.1138 ($M + H^+$), found 452.1141.

N-(4-bromo-3-(trifluoromethyl)phenyl)-4-methoxybenzenesulfonamide (**285**). To 300 mg (1.25 mmol) of 4-bromo-3-(trifluoromethyl)aniline in CH_2Cl_2 (50 mL) and pyridine (2 mL), 258 mg (1.25 mmol) of the 4-methoxybenzenesulfonyl chloride was slowly added and stirred at room temperature for 4 h. The reaction was treated with 2N HCl and 5% $NaHCO_3$, washed with brine, dried over anhydrous Na_2SO_4 and the solvent evaporated to obtain 482 mg (1.17 mmol, 94%) of **285**. Crude product was crystallized in CH_2Cl_2/hexane to afford the purified compound (361 mg, 0.88 mmol, 70%). M.p.: 110-111 °C (CH_2Cl_2/hexane). IR (KBr): 3265, 1597, 1498, 1177, 828 cm^{-1}. ^{1}H NMR (400 MHz, $CDCl_3$): δ 3.85 (3H, *s*), 6.66 (1H, *bs*), 6.93 (2H, *d*, *J* = 8.8), 7.15 (1H, *dd*, *J* = 8.8 and 2.8), 7.33 (1H, *d*, *J* = 2.8), 7.57 (1H, *d*, *J* = 8.8), 7.72 (2H, *d*, *J* = 8.8). ^{13}C NMR (100 MHz, $CDCl_3$): δ 55.6 (CH_3), 114.5 (2CH), 115.1 (C), 119.9 (CH), 120.8 (C), 123.6 (C), 124.6 (CH), 129.4 (2CH), 129.6 (C), 135.8 (CH), 136.4 (C), 163.6 (C). HRMS ($C_{14}H_{11}BrF_3NO_3S + Na^+$): calcd 431.9487 and 433.9467 ($M + Na^+$), found 431.9484 and 433.9467.

N-(4-bromo-3-(trifluoromethyl)phenyl)-4-methoxy-*N*-methylbenzenesulfonamide (**286**). To a stirred solution of **285** (92 mg, 0.22 mmol) in CH_3CN (25 mL), 25 mg (0.44 mmol) of KOH were added. After 30 min at room temperature, CH_3I (28 µL, 0.44 mmol) was added. The solution was stirred for 24 h; then the mixture was evaporated to dryness. The residue was dissolved with EtOAc and washed with brine, dried over Na_2SO_4, filtered, and evaporated to dryness. The residue (89 mg) was purified by preparative TLC (hexane/EtOAc 7:3) to isolate compound **286**

(82 mg, 0.19 mmol, 86%). ^{1}H NMR (400 MHz, $CDCl_3$): δ 3.14 (3H, *s*), 3.86 (3H, *s*), 6.94 (2H, *d*, *J* = 8.8), 7.19 (1H, *dd*, *J* = 8.8 and 2.8), 7.37 (1H, *d*, *J* = 2.8), 7.46 (2H, *d*, *J* = 8.8), 7.64 (1H, *d*, *J* = 8.8). ^{13}C NMR (100 MHz, $CDCl_3$): δ 37.6 (CH_3), 55.6 (CH_3), 114.1 (2CH), 118.0 (C), 120.9 (C), 123.7 (C), 125.6 (CH), 127.2 (C), 129.8 (2CH), 130.6 (CH), 135.4 (CH), 141.2 (C), 163.4 (C). HRMS ($C_{15}H_{13}BrF_3NO_3S + H^+$): calcd 423.9824 and 425.9804 ($M + H^+$), found 423.9841 and 425.9810.

4-Methoxy-*N*-(3-(trifluoromethyl)phenyl)benzenesulfonamide (**287**). To 233 µL (1.86 mmol) of 3-(trifluoromethyl)aniline in CH_2Cl_2 (50 mL) and pyridine (2 mL), 385 mg (1.86 mmol) of 4-methoxybenzenesulfonyl chloride were slowly added and stirred at room temperature for 12 h. The reaction was treated with 2N HCl and 5% $NaHCO_3$, washed with brine, dried over anhydrous Na_2SO_4 and the solvent evaporated to dryness. Crude residue (522 mg) was purified by flash column chromatography (hexane/EtOAc 6:4) to afford 516 mg (1.56 mmol, 84%) of pure product **287**. IR (film): 3255, 1594, 1496, 1145, 834 cm^{-1}. ^{1}H NMR (400 MHz, $CDCl_3$): δ 3.83 (3H, *s*), 6.86 (1H, *bs*), 6.91 (2H, *d*, *J* = 8.8), 7.27-7.37 (4H, *m*), 7.73 (2H, *d*, *J* = 8.8). ^{13}C NMR (100 MHz, $CDCl_3$): δ 55.5 (CH_3), 114.4 (2CH), 117.4 (CH), 121.4 (CH), 123.8 (CH), 124.9 (C), 129.4 (2CH), 129.9 (CH), 131.4 (C), 131.8 (C), 137.5 (C), 163.4 (C). HRMS ($C_{14}H_{12}F_3NO_3S + Na^+$): calcd 354.0382 ($M + Na^+$), found 354.0389.

4-Methoxy-*N*-methyl-*N*-(3-(trifluoromethyl)phenyl)benzenesulfonamide (**288**). A mixture of **287** (77 mg, 0.23 mmol) and KOH (26 mg, 0.46 mmol) in CH_3CN (50 mL) was stirred for 30 min. Then, CH_3I (29 µL, 0.46 mmol) was added and stirred at room temperature for 48 h. The solvent was removed under reduced pressure. The residue was dissolved in EtOAc and washed with brine, dried (Na_2SO_4) and concentrated in vacuum to afford 78 mg (0.22 mmol, 97%) of **288**. The crude product was purified by crystallization in CH_2Cl_2/hexane (58 mg, 0.17 mmol, 72%). M.p.: 103-104 °C (CH_2Cl_2/hexane). IR (KBr): 1592, 1496, 1257, 898 cm^{-1}. ^{1}H NMR (400 MHz, $CDCl_3$): δ 3.16 (3H, *s*), 3.86 (3H, *s*), 6.92 (2H, *d*, *J* = 8.8), 7.27 (1H, *bs*), 7.39 (1H, *bd*, *J* = 7.6), 7.42 (1H, *bs*), 7.45 (2H, *d*, *J* = 8.8), 7.52 (1H, *bd*, *J* = 7.6). ^{13}C NMR (100 MHz, $CDCl_3$): δ 37.8 (CH_3), 55.6 (CH_3), 114.0 (2CH), 123.0 (CH), 123.8 (CH), 127.5 (C), 129.4 (CH), 129.9 (2CH), 130.2 (CH), 131.1 (C), 131.4 (C), 142.4 (C), 163.3 (C). HRMS ($C_{15}H_{14}F_3NO_3S + H^+$): calcd 346.0719 ($M + H^+$), found 346.0719.

N-benzyl-4-methoxy-*N*-(3-(trifluoromethyl)phenyl)benzenesulfonamide (**289**). 74 mg (0.53 mmol) of K_2CO_3 were added to a stirred solution of **287** (88 mg, 0.26 mmol) in 3 mL of dry DMF. After 1 h at room temperature 62 µL (0.53 mmol) of benzyl chloride were added and stirred for 24 h. The reaction mixture was concentrated, re-dissolved in EtOAc, washed with brine, dried over anhydrous Na_2SO_4, filtered, and concentrated in vacuum to obtain 110 mg (0.26 mmol, 98%) of **289**. It was purified by crystallization in CH_2Cl_2/hexane (74 mg, 0.17 mmol, 66%). M.p.: 108-109 °C (CH_2Cl_2/hexane). IR (KBr): 1596, 1495, 1263, 1123, 898 cm^{-1}. ^{1}H NMR (400 MHz, $CDCl_3$): δ 3.88 (3H, *s*), 4.71 (2H, *s*), 6.96 (2H, *d*, *J* = 8.8), 7.14 (1H, *bs*), 7.18-7.23 (6H, *m*), 7.33 (1H, *bt*, *J* = 7.6), 7.44 (1H, *bd*, *J* = 7.6), 7.56 (2H, *d*, *J* = 8.8). ^{13}C NMR (100 MHz, $CDCl_3$): δ 54.4 (CH_3), 55.6 (CH_2), 114.2 (2CH), 124.4 (CH), 124.6 (C), 125.2 (CH), 127.8 (CH), 128.5 (4CH), 129.5 (CH), 129.8 (2CH), 130.8 (C), 131.2 (C), 132.8 (CH), 135.2 (C), 139.8 (C), 163.2 (C). HRMS ($C_{21}H_{18}F_3NO_3S + H^+$): calcd 422.1032 ($M + H^+$), found 422.1039.

4-Methoxy-*N*-(4-(trifluoromethyl)phenyl)benzenesulfonamide (**290**). To a solution of 4-(trifluoromethyl)aniline (294 mg, 1.82 mmol) in CH_2Cl_2 (50 mL) and pyridine (2 mL), 4-methoxybenzenesulfonyl chloride (377 mg, 1.82 mmol) was slowly added and stirred at room temperature for 12 h. Then the reaction mixture was treated with 2N HCl and 5% $NaHCO_3$. Organic layers were washed to neutrality with brine, dried over anhydrous Na_2SO_4 and concentrated under vacuum. The residue (490 mg) was purified by flash column chromatography (hexane/EtOAc 6:4) to yield compound **290** (473 mg, 1.43 mmol, 78%) which

was then crystallized in CH_2Cl_2/hexane (376 mg, 1.13 mmol, 62%). M.p.: 117-118 °C (CH_2Cl_2/hexane). IR (KBr): 3299, 1595, 1498, 1116, 833 cm^{-1}. ^1H NMR (400 MHz, $CDCl_3$): δ 3.81 (3H, *s*), 6.91 (2H, *d*, *J* = 9.2), 7.20 (2H, *d*, *J* = 8.4), 7.46 (2H, *d*, *J*, = 8.4), 7.79 (1H, *bs*), 7.82 (2H, *d*, *J* = 9.2). ^{13}C NMR (100 MHz, $CDCl_3$): δ 55.6 (CH_3), 114.5 (2CH), 119.5 (2CH), 122.3 (C), 125.2 (C), 126.6 (2CH), 129.4 (2CH), 129.9 (C), 140.0 (C), 163.5 (C). HRMS ($C_{14}H_{12}F_3NO_3S$ + Na^+): calcd 354.0382 (M + Na^+), found 354.0377.

4-Methoxy-*N*-methyl-*N*-(4-(trifluoromethyl)phenyl)benzenesulfonamide (**291**). To a solution of **290** (77 mg, 0.23 mmol) in CH_3CN (50 mL), crushed KOH (26 mg, 0.46 mmol) was added and stirred for 30 min. Then, CH_3I (29 µL, 0.46 mmol) was added. After 24 h, CH_3CN was evaporated and the residue was re-dissolved in EtOAc. The solution was washed with brine, dried over Na_2SO_4, filtered, and evaporated to dryness. Crude residue (76 mg) was purified by preparative TLC in hexane/EtOAc 7:3 to afford compound **291** (71 mg, 0.20 mmol, 89%). IR (film): 1596, 1498, 1169, 869 cm^{-1}. ^1H NMR (400 MHz, $CDCl_3$): δ 3.17 (3H, *s*), 3.85 (3H, *s*), 6.92 (2H, *d*, *J* = 8.8), 7.25 (2H, *d*, *J* = 8.4), 7.46 (2H, *d*, *J* = 8.8), 7.56 (2H, *d*, *J* = 8.4). ^{13}C NMR (100 MHz, $CDCl_3$): δ 37.6 (CH_3), 55.6 (CH_3), 114.0 (2CH), 125.9 (2CH), 126.2 (2CH), 127.7 (C), 128.8 (C), 129.0 (C), 129.8 (2CH), 144.9 (C), 163.2 (C). HRMS ($C_{15}H_{14}F_3NO_3S$ + Na^+): calcd 368.0539 (M + Na^+), found 368.0534.

N-benzyl-4-methoxy-*N*-(4-(trifluoromethyl)phenyl)benzenesulfonamide (**292**). To a stirred solution of **290** (77 mg, 0.23 mmol) in dry DMF (3 mL) 64 mg (0.46 mmol) of K_2CO_3 were added. After 1 h at room temperature, 54 µL (0.46 mmol) of benzyl chloride were added and stirred for 24 h. The reaction mixture was concentrated, re-dissolved in EtOAc, washed with brine, dried over anhydrous Na_2SO_4, filtered and concentrated under vacuum to produced 93 mg (0.22 mmol, 95%) of crude reaction product from which 69 mg (0.16 mmol, 70%) of **292** were purified by crystallization in CH_2Cl_2/hexane. M.p.: 135-136 °C (CH_2Cl_2/hexane). IR (KBr): 1596, 1498, 1133, 836 cm^{-1}. ^1H NMR (400 MHz, $CDCl_3$): δ 3.89 (3H, *s*), 4.74 (2H, *s*), 6.96 (2H, *d*, *J* = 8.8), 7.14 (2H, *d*, *J* = 8.4), 7.21 (5H, *m*), 7.46 (2H, *d*, *J* = 8.4), 7.57 (2H, *d*, *J* = 8.8). ^{13}C NMR (100 MHz, $CDCl_3$): δ 54.2 (CH_3), 55.6 (CH_2), 114.2 (2CH), 125.8 (C), 125.9 (2CH), 127.8 (CH), 128.3 (2CH), 128.5 (2CH), 128.7 (2CH), 129.4 (C), 129.7 (2CH), 129.8 (C), 135.3 (C), 142.4 (C), 163.2 (C). HRMS ($C_{21}H_{18}F_3NO_3S$ + Na^+): calcd 444.0852 (M + Na^+), found 444.0850.

3,4,5-Trimethoxy-2-((4-methoxyphenyl)sulfonamido)benzoic acid (**293a**) and 3,4,5-trimethoxy-2-(3,4,5-trimethoxy-2-((4-methoxyphenyl)sulfonamido)benzamido) benzoic acid (**293b**).

*Compounds **63A** and **63B** article 3. Available at Materials and methods, chemical synthesis (2.1).*

Methyl 2-amino-3,4,5-trimethoxybenzoate (**294**). To a solution of 2-amino-3,4,5-trimethoxybenzoic acid (174 mg, 0.76 mmol) in CH_2Cl_2 (12 mL), 1 mL of (trimethylsilyl)diazomethane 2 M in hexane and 3 mL of methanol were added. After 1 h stirring at room temperature the reaction mixture was poured onto ice and extracted with CH_2Cl_2. The organics were dried over Na_2SO_4, filtered, and evaporated to dryness to afford compound **294** (170 mg, 0.70 mmol, 92%) which was used without further purification. ^1H NMR (400 MHz, $CDCl_3$): δ 3.64 (3H, *s*), 3.70 (6H, *s*), 3.80 (3H, *s*), 5.56 (2H, *bs*), 6.99 (1H, *s*). GC-MS ($C_{11}H_{15}NO_5$): 241 (M^+).

Methyl 3,4,5-trimethoxy-2-((4-methoxyphenyl)sulfonamido)benzoate (**295**). To a solution of **294** (170 mg, 0.70 mmol) in CH_2Cl_2 (50 mL) and pyridine (1 mL), 4-methoxybenzenesulfonyl chloride (146 mg, 0.70 mmol) was slowly added. The mixture was stirred at room temperature for 24 h. Then the reaction was treated with 2N HCl, washed with brine, dried over anhydrous Na_2SO_4 and the solvent evaporated to obtain 154 mg (0.37 mmol, 53%) of **295**. It was purified by crystallization in ethanol (36 mg, 0.09 mmol, 12%). M.p.: 84-85 °C (EtOH). IR (KBr): 3146,

1686, 1598, 1495, 1126, 838 cm^{-1}. ^{1}H NMR (400 MHz, $CDCl_3$): δ 3.45 (3H, *s*), 3.79 (3H, *s*), 3.85 (3H, *s*), 3.87 (3H, *s*), 3.89 (3H, *s*), 6.91 (2H, *d*, *J* = 9.2), 7.14 (1H, *s*), 7.75 (2H, *d*, *J* = 9.2), 8.88 (1H, *bs*). ^{13}C NMR (100 MHz, $CDCl_3$): δ 52.4 (CH_3), 55.6 (CH_3), 56.1 (CH_3), 60.3 (CH_3), 61.0 (CH_3), 108.3 (CH), 113.5 (2CH), 117.8 (C), 127.3 (C), 129.4 (2CH), 132.4 (C), 146.8 (C), 148.5 (C), 150.5 (C), 162.6 (C), 167.4 (C). HRMS ($C_{18}H_{21}NO_8S + H^+$): calcd 412.1061 ($M + H^+$), found 412.1064.

4-Methoxy-*N*-(6-methoxypyridin-3-yl)benzenesulfonamide (**296**).

*Compound **240** article 3. Available at Materials and methods, chemical synthesis (2.1).*

4-Methoxy-*N*-(6-methoxypyridin-3-yl)-*N*-methylbenzenesulfonamide (**297**). 83 mg (0.28 mmol) of **296** were dissolved in CH_3CN (40 mL) and 31 mg (0.56 mmol) of KOH were added. After 30 min stirring at room temperature, CH_3I (35 µL, 0.56 mmol) was added to the solution. The reaction mixture was stirred for 24 h, concentrated under reduced pressure, dissolved in EtOAc, washed with brine, dried (Na_2SO_4), filtered, and evaporated to dryness. The residue (86 mg) was purified by preparative TLC (hexane/EtOAc 6:4) to isolate compound **297** (64 mg, 0.21 mmol, 74%). ^{1}H NMR (400 MHz, $CDCl_3$): δ 3.12 (3H, *s*), 3.84 (3H, *s*), 3.88 (3H, *s*), 6.65 (1H, *d*, *J* = 9.2), 6.92 (2H, *d*, *J* = 8.8), 7.32 (1H, *dd*, *J* = 9.2 and 2.4), 7.49 (2H, *d*, *J* = 8.8), 7.80 (1H, *d*, *J* = 2.4). ^{13}C NMR (100 MHz, $CDCl_3$): δ 38.3 (CH_3), 53.7 (CH_3), 55.6 (CH_3), 110.7 (C), 114.1 (2CH), 127.8 (C), 129.9 (2CH), 132.0 (C), 137.6 (CH), 145.0 (CH), 162.8 (C), 163.1 (C). HRMS ($C_{14}H_{16}N_2O_4S + H^+$): calcd 309.0904 ($M + H^+$), found 309.0899.

N-(cyanomethyl)-4-methoxy-*N*-(6-methoxypyridin-3-yl)benzenesulfonamide (**298**). A mixture of **296** (100 mg, 0.34 mmol) and K_2CO_3 (93 mg, 0.68 mmol) in dry DMF (3 mL) was stirred at room temperature for 30 min. Then, 2-chloroacetonitrile (43 µL, 0.68 mmol) was added. After 72 h, the solvent was evaporated under reduced pressure. The residue was dissolved in EtOAc and washed with brine, dried (Na_2SO_4) and concentrated in vacuo. Crude residue (57 mg) was purified by preparative TLC (toluene/EtOAc 7:3) to yield compound **298** (9 mg, 0.03 mmol, 8%). ^{1}H NMR (400 MHz, $CDCl_3$): δ 3.81 (3H, *s*), 3.85 (3H, *s*), 4.47 (2H, *s*), 6.66 (1H, *d*, *J* = 8.8), 6.91 (2H, *d*, *J* = 8.8), 7.35 (1H, *dd*, *J* = 8.8 and 2.8), 7.56 (2H, *d*, *J* = 8.8), 7.89 (1H, *d*, *J* = 2.8). ^{13}C NMR (100 MHz, $CDCl_3$): δ 39.7 (CH_2), 53.9 (CH_3), 55.7 (CH_3), 111.7 (CH), 114.5 (2CH), 114.7 (C), 128.6 (C), 130.1 (2CH), 131.2 (C), 138.9 (CH), 147.3 (CH), 163.8 (C), 164.0 (C). HRMS ($C_{15}H_{15}N_3O_4S + H^+$): calcd 334.0856 ($M + H^+$), found 334.0856.

N-benzyl-4-methoxy-*N*-(6-methoxypyridin-3-yl)benzenesulfonamide (**299**).

*Compound **279** article 3. Available at Materials and methods, chemical synthesis (2.1).*

N-(6-methoxypyridin-3-yl)-4-nitrobenzenesulfonamide (**300**).

*Compound **283** article 3. Available at Materials and methods, chemical synthesis (2.1).*

4-Amino-*N*-(6-methoxypyridin-3-yl)benzenesulfonamide (**301**).

*Compound **287** article 3. Available at Materials and methods, chemical synthesis (2.1).*

4-(Dimethylamino)-*N*-(6-methoxypyridin-3-yl)benzenesulfonamide (**302**). A solution of paraformaldehyde (475 mg, 15.8 mmol), acetic acid (500 µL) and **301** (442 mg, 1.58 mmol) in MeOH (50 mL) was stirred at room temperature for 1 h. Sodium cyanoborohydride (199 mg, 3.16 mmol) was added to the solution and stirred at reflux for 24 h. Reaction mixture was concentrated under vacuum, poured onto ice, and extracted with EtOAc. Organic layers were washed with 5% $NaHCO_3$ and brine, dried (Na_2SO_4), filtered, and evaporated to dryness to give **302** (446 mg, 1.44 mmol, 92%). Crude reaction product was purified by crystallization in methanol (253 mg, 0.82 mmol, 52%). M.p.: 139-145 °C (MeOH). IR (KBr): 3015, 1598, 1487, 1092, 825 cm^{-1}. ^{1}H NMR (400 MHz, CD_3OD): δ 3.00 (6H, *s*), 3.82 (3H, *s*), 6.67 (1H, *d*, *J* = 8.8), 6.68 (2H,

d, *J* = 9.2), 7.41 (1H, *dd*, *J* = 8.8 and 2.8), 7.46 (2H, *d*, *J* = 9.2), 7.70 (1H, *d*, *J* = 2.8). ^{13}C NMR (100 MHz, $CDCl_3$): δ 39.9 ($2CH_3$), 53.6 (CH_3), 110.8 (2CH), 110.9 (CH), 123.5 (C), 127.3 (C), 129.1 (2CH), 135.7 (CH), 142.2 (CH), 152.9 (C), 162.1 (C). HRMS ($C_{14}H_{17}N_3O_3S$ + Na^+): calcd 330.0883 (M + Na^+), found 330.0879.

4-(Dimethylamino)-*N*-(6-methoxypyridin-3-yl)-*N*-methylbenzenesulfonamide (**303**). To a solution of **302** (80 mg, 0.26 mmol) in CH_3CN (25 mL), crushed KOH (29 mg, 0.52 mmol) was added and stirred for 30 min. Then, CH_3I (33 µL, 0.52 mmol) was added. After 24 h, CH_3CN was evaporated and the residue was re-dissolved in EtOAc. The solution was washed with brine, dried over Na_2SO_4, filtered, and evaporated to dryness to afford product **303** (76 mg, 0.24 mmol, 90%) which was purified by crystallization in methanol (15 mg, 0.05 mmol, 18%). M.p.: 95-100 °C (MeOH). ^{1}H NMR (400 MHz, CD_3OD): δ 3.03 (6H, *s*), 3.09 (3H, *s*), 3.87 (3H, *s*), 6.71 (1H, *d*, *J* = 8.8), 6.73 (2H, *d*, *J* = 9.2), 7.32 (2H, *d*, *J* = 9.2), 7.35 (1H, *dd*, *J* = 8.8 and 2.4), 7.83 (1H, *d*, *J* = 2.4). ^{13}C NMR (100 MHz, $CDCl_3$): δ 38.1 (CH_3), 39.9 ($2CH_3$), 53.6 (CH_3), 110.5 (CH), 110.6 (2CH), 121.2 (C), 129.6 (2CH), 132.5 (C), 137.7 (CH), 144.9 (CH), 152.9 (C), 162.6 (C). HRMS ($C_{15}H_{19}N_3O_3S$ + H^+): calcd 322.1220 (M + H^+), found 322.1220.

4-(Dimethylamino)-*N*-ethyl-*N*-(6-methoxypyridin-3-yl)benzenesulfonamide (**304**). 85 mg (0.28 mmol) of **302** and 76 mg (0.55 mmol) of K_2CO_3 were mixed in dry DMF (3 mL). After 30 min stirring at room temperature, bromoethane (41 µL, 0.55 mmol) was added to the mixture and stirred 24 h. The reaction mixture was concentrated, re-dissolved in EtOAc, washed with brine, dried over anhydrous Na_2SO_4, filtered, and concentrated in vacuum to obtain 91 mg (0.27 mmol, 98%) of **304** and crystalized in methanol (66 mg, 0.20 mmol, 71%). M.p.: 142-147 °C (MeOH). ^{1}H NMR (400 MHz, CD_3OD): δ 1.03 (3H, *t*, *J* = 7.6), 3.05 (6H, *s*), 3.56 (2H, *q*, *J* = 7.6), 3.89 (3H, *s*), 6.74 (1H, *d*, *J* = 8.8), 6.76 (2H, *d*, *J* = 9.2), 7.29 (1H, *dd*, *J* = 8.8 and 2.8), 7.39 (2H, *d*, *J* = 9.2), 7.80 (1H, *d*, *J* = 2.8). ^{13}C NMR (100 MHz, $CDCl_3$): δ 13.9 (CH_3), 40.0 ($2CH_3$), 45.4 (CH_2), 53.7 (CH_3), 110.7 (2CH), 110.8 (CH), 123.4 (C), 129.3 (2CH), 129.6 (C), 139.4 (CH), 147.2 (CH), 152.8 (C), 163.0 (C). HRMS ($C_{16}H_{21}N_3O_3S$ + H^+): calcd 336.1376 (M + H^+), found 336.1377.

N-(cyanomethyl)-4-(dimethylamino)-*N*-(6-methoxypyridin-3-yl)benzenesulfonamide (**305**). A mixture of **302** (65 mg, 0.21 mmol) and K_2CO_3 (58 mg, 0.42 mmol) in dry DMF (3 mL) was stirred for 30 min. Then, 2-chloroacetonitrile (27 µL, 0.42 mmol) was added and stirred for 24 h. After concentration, the reaction residue was re-dissolved in EtOAc, washed with brine, dried (Na_2SO_4), filtered, and the solvent was evaporated to dryness. Crude product **305** was obtained (66 mg, 0.19 mmol, 90%) and it was purified by crystallization in methanol (21 mg, 0.06 mmol, 29%). M.p.: 85-91 °C (MeOH). IR (KBr): 3435, 2906, 1594, 1495, 821 cm^{-1}. ^{1}H NMR (400 MHz, CD_3OD): δ 3.05 (6H, *s*), 3.89 (3H, *s*), 4.66 (2H, *s*), 6.76 (3H, *t*, *J* = 9.2), 7.44 (3H, *d*, *J* = 9.2), 7.91 (1H, *d*, *J* = 2.4). ^{13}C NMR (100 MHz, $CDCl_3$): δ 39.6 (CH_2), 40.0 ($2CH_3$), 53.9 (CH_3), 110.8 (2CH), 111.5 (CH), 115.1 (C), 121.5 (C), 129.1 (C), 129.7 (2CH), 139.0 (CH), 147.3 (CH), 153.4 (C), 163.8 (C). HRMS ($C_{16}H_{18}N_4O_3S$ + H^+): calcd 347.1172 (M + H^+), found 347.1171.

Ethyl *N*-((4-(dimethylamino)phenyl)sulfonyl)-*N*-(6-methoxypyridin-3-yl)glycinate (**306**). Ethyl 2-bromoacetate (61 µL, 0.55 mmol) was added, after 30 min, to a stirred mixture of compound **302** (84 mg, 0.27 mmol) and K_2CO_3 (76 mg, 0.55 mmol) in dry DMF (3 mL). After 24 h, the solvent was evaporated under reduced pressure and the residue was dissolved in EtOAc, washed with brine, dried over anhydrous Na_2SO_4, filtered, and concentrated in vacuum. The residue (102 mg) was purified by preparative TLC (hexane/EtOAc 1:1) to afford compound **306** (59 mg, 0.15 mmol, 55%). ^{1}H NMR (400 MHz, CD_3OD): δ 1.21 (3H, *t*, *J* = 7.2), 3.02 (6H, *s*), 3.86 (3H, *s*), 4.13 (2H, *q*, *J* = 7.2), 4.37 (2H, *s*), 6.70 (1H, *d*, *J* = 8.8), 6.72 (2H, *d*, *J* = 9.2), 7.44 (2H, *d*, *J* = 9.2), 7.46 (1H, *dd*, *J* = 8.8 and 2.4), 7.91 (1H, *d*, *J* = 2.4). ^{13}C NMR (100 MHz, $CDCl_3$): δ 14.0 (CH_3), 40.0 ($2CH_3$), 52.7 (CH_2),

53.7 (CH_3), 61.4 (CH_2), 110.6 (2CH), 110.9 (CH), 123.5 (C), 129.5 (2CH), 130.5 (C), 140.1 (CH), 147.4 (CH), 152.9 (C), 163.2 (C), 168.8 (C). HRMS ($C_{18}H_{23}N_3O_5S + H^+$): calcd 394.1431 ($M + H^+$), found 394.1434.

N-(4-(*N*-(6-methoxypyridin-3-yl)sulfamoyl)phenyl)formamide (**307**).

*Compound **309** article 3. Available at Materials and methods, chemical synthesis (2.1).*

N-(6-methoxypyridin-3-yl)-4-(methylamino)benzenesulfonamide (**308**).

*Compound **316** article 3. Available at Materials and methods, chemical synthesis (2.1).*

N-(6-methoxypyridin-3-yl)-*N*-methyl-4-(methylamino)benzenesulfonamide (**309**). Compound **308** (90 mg, 0.31 mmol) was dissolved in CH_3CN (40 mL) and 34 mg (0.62 mmol) of KOH were added. After 30 min stirring, 58 µL (0.93 mmol) of CH_3I were added. The reaction mixture was stirred at room temperature for 24 h and evaporated to dryness. The residue was dissolved in EtOAc, washed with brine, dried over Na_2SO_4 and concentrated under vacuum. The residue (90 mg) was purified by preparative TLC (CH_2Cl_2/EtOAc 8:2) to give products **309** (22 mg, 0.07 mmol, 23%) and **303** (30 mg, 0.09 mmol, 30%). IR (KBr): 3408, 2944, 1600, 1489, 1148, 814 cm^{-1}. ^1H NMR (400 MHz, CD_3OD): δ 2.80 (3H, *s*), 3.09 (3H, *s*); 3.87 (3H, *s*), 6.58 (2H, *d*, *J* = 9.2), 6.71 (1H, *d*, *J* = 8.8), 7.25 (2H, *d*, *J* = 9.2), 7.35 (1H, *dd*, *J* = 8.8 and 2.8), 7.84 (1H, *d*, *J* = 2.8). ^{13}C NMR (100 MHz, $CDCl_3$): δ 30.0 (CH_3), 38.2 (CH_3), 53.7 (CH_3), 110.6 (CH), 111.1 (2CH), 122.4 (C), 129.9 (2CH), 132.4 (C), 137.7 (CH), 144.9 (CH), 152.7 (C), 162.7 (C). HRMS ($C_{14}H_{17}N_3O_3S + H^+$): calcd 308.1063 ($M + H^+$), found 308.1066.

N-(cyanomethyl)-*N*-(6-methoxypyridin-3-yl)-4-(methylamino)benzenesulfonamide (**310**). To a solution of **308** (115 mg, 0.39 mmol) and K_2CO_3 (107 mg, 0.78 mmol) in dry DMF (3 mL), 2-chloroacetonitrile (49 µL, 0.78 mmol) was added after 1 h stirring at room temperature. After 24 h, the solution was concentrated in vacuo and re-dissolved with EtOAc. Then, it was washed with brine, dried over Na_2SO_4 and evaporated to dryness. The residue (76 mg) was purified by preparative TLC (hexane/EtOAc 1:1) to afford compound **310** (15 mg, 0.05 mmol, 10%). ^1H NMR (400 MHz, CD_3OD): δ 2.81 (3H, *s*), 3.90 (3H, *s*), 4.65 (2H, *s*), 6.60 (2H, *d*, *J* = 8.8), 6.77 (1H, *d*, *J* = 9.2), 7.37 (2H, *d*, *J* = 8.8), 7.44 (1H, *dd*, *J* = 9.2 and 2.8), 7.92 (1H, *d*, *J* = 2.8). ^{13}C NMR (100 MHz, $CDCl_3$): δ 29.9 (CH_3), 39.6 (CH_2), 53.9 (CH_3), 111.3 (2CH), 111.5 (CH), 115.0 (C), 122.9 (C), 129.0 (C), 130.0 (2CH), 139.0 (CH), 147.3 (CH), 153.3 (C), 163.9 (C). HRMS ($C_{15}H_{16}N_4O_3S + H^+$): calcd 333.1016 ($M + H^+$), found 333.1018.

N-(4-(*N*-(6-methoxypyridin-3-yl)sulfamoyl)phenyl)-*N*-methylformamide (**311**).

*Compound **320** article 3. Available at Materials and methods, chemical synthesis (2.1).*

2,3,4-Trimethoxybenzenesulfonyl chloride (**312**). To a solution of 1,2,3-trimethoxybenzene (1.06 g, 6.33 mmol) chlorosulfonic acid (445 µL, 6.65 mmol) was carefully added dropwise in ice-cooled 1,2-dichloroethane (25 mL) under N_2. After 90 min, thionyl chloride was slowly added (919 µL, 12.6 mmol) and warmed to room temperature. After 90 min, the reaction was evaporated under vacuum to afford compound **312** (1.59 g, 5.98 mmol, <95%) with minor impurities. The unpurified product was then used without further purification. ^1H NMR (400 MHz, $CDCl_3$): δ 3.90 (3H, *s*), 3.96 (3H, *s*), 4.13 (3H, *s*), 6.74 (1H, *d*, *J* = 9.2), 7.67 (1H, *d*, *J* = 9.2). ^{13}C NMR (100 MHz, $CDCl_3$): δ 57.9 (CH_3), 62.4 (CH_3), 63.3 (CH_3), 107.5 (CH), 126.4 (CH), 130.9 (C), 144.3 (C), 153.6 (C), 161.7 (C). GC-MS ($C_9H_{11}ClO_5S$): 266 (M^+).

2,3,4-Trimethoxy-*N*-(4-methoxyphenyl)benzenesulfonamide (**313**). To a solution of 4-methoxyaniline (311 mg, 2.52 mmol) in CH_2Cl_2 (80 mL) and trimethylamine (100 µL), sulfonyl chloride **312** (1.12 g, 4.20 mmol) was slowly added. The reaction mixture was stirred at room

temperature for 8 h and then washed with brine, dried over Na_2SO_4, filtered, and evaporated to dryness. The residue (810 mg) was purified by flash column chromatography (toluene/EtOAc 8:2) to give compound **313** (451 mg, 1.28 mmol, 51%). ^{1}H NMR (400 MHz, $CDCl_3$): δ 3.67 (3H, *s*), 3.82 (3H, *s*), 3.86 (3H, *s*), 4.09 (3H, *s*), 6.56 (1H, *d*, *J* = 8.8), 6.67 (2H, *d*, *J* = 9.2), 6.86 (1H, *bs*), 6.99 (2H, *d*, *J* = 9.2), 7.34 (1H, *d*, *J* = 8.8). ^{13}C NMR (100 MHz, $CDCl_3$): δ 54.7 (CH_3), 55.5 (CH_3), 60.4 (CH_3), 61.6 (CH_3), 105.9 (CH), 113.6 (2CH), 123.5 (C), 124.3 (2CH), 124.9 (CH), 128.9 (C), 141.9 (C), 150.1 (C), 157.1 (C), 157.4 (C). HRMS ($C_{16}H_{19}NO_6S$ + H^+): calcd 354.1006 (M + H^+), found 354.1012.

2,3,4-Trimethoxy-*N*-(4-methoxyphenyl)-*N*-methylbenzenesulfonamide (**314**). A mixture of **313** (91 mg, 0.26 mmol) and KOH (29 mg, 0.52 mmol) in CH_3CN (40 mL) was stirred at room temperature for 30 min. Then, CH_3I (32 µL, 0.52 mmol) was added to the solution and stirred for 24 h. The solvent was evaporated under reduced pressure and the residue was re-dissolved in EtOAc, washed with brine, dried over Na_2SO_4 and concentrated. The residue (101 mg) was purified by preparative TLC (hexane/EtOAc 6:4) to afford compound **314** (87 mg, 0.24 mmol, 92%). ^{1}H NMR (400 MHz, $CDCl_3$): δ 3.35 (3H, *s*), 3.75 (3H, *s*), 3.88 (3H, *s*), 3.90 (3H, *s*), 3.98 (3H, *s*), 6.57 (1H, *d*, *J* = 8.8), 6.75 (2H, *d*, *J* = 9.2), 7.10 (2H, *d*, *J* = 9.2), 7.34 (1H, *d*, *J* = 8.8). ^{13}C NMR (100 MHz, $CDCl_3$): δ 39.3 (CH_3), 55.3 (CH_3), 56.1 (CH_3), 60.9 (CH_3), 61.5 (CH_3), 106.1 (CH), 114.0 (2CH), 124.9 (C), 126.6 (CH), 128.3 (2CH), 134.2 (C), 142.7 (C), 151.7 (C), 157.6 (C), 158.4 (C). HRMS ($C_{17}H_{21}NO_6S$ + H^+): calcd 368.1162 (M + H^+), found 368.1155.

N-(cyanomethyl)-2,3,4-trimethoxy-*N*-(4-methoxyphenyl)benzenesulfonamide (**315**). 90 mg (0.25 mmol) of **313** were dissolved in DMF (3 mL) and K_2CO_3 (69 mg, 0.50 mmol) was added. After 30 min stirring at room temperature 2-chloroacetonitrile (32 µL, 0.50 mmol) was added to the solution and stirred for 48 h. The solvent was removed under reduced pressure. The residue was dissolved in EtOAc and washed with brine, dried (Na_2SO_4) and concentrated in vacuo. The crude product (89 mg) was purified by preparative TLC (hexane/EtOAc 6:4) to yield compound **315** (81 mg, 0.20 mmol, 81%). ^{1}H NMR (400 MHz, $CDCl_3$): δ 3.73 (3H, *s*), 3.87 (3H, *s*), 3.92 (3H, *s*), 4.07 (3H, *s*), 4.70 (2H, *s*), 6.58 (1H, *d*, *J* = 9.2), 6.78 (2H, *d*, *J* = 9.2), 7.07 (2H, *d*, *J* = 9.2), 7.28 (1H, *d*, *J* = 9.2). ^{13}C NMR (100 MHz, $CDCl_3$): δ 40.9 (CH_2), 55.4 (CH_3), 56.2 (CH_3), 61.1 (CH_3), 61.7 (CH_3), 106.4 (CH), 114.8 (2CH), 115.7 (C), 124.3 (C), 126.5 (CH), 130.1 (2CH), 130.2 (C), 142.7 (C), 151.4 (C), 158.3 (C), 159.8 (C). HRMS ($C_{18}H_{20}N_2O_6S$ + H^+): calcd 393.1115 (M + H^+), found 393.1116.

2,4-Dimethoxy-*N*-(4-methoxyphenyl)benzenesulfonamide (**316**). To 293 mg (2.38 mmol) of 4-methoxyaniline in CH_2Cl_2 (50 mL) and pyridine (2 mL), 563 mg (2.38 mmol) of 2,4-dimethoxybenzenesulfonyl chloride were slowly added and stirred at room temperature for 4 h. The reaction was treated with 2N HCl and 5% $NaHCO_3$, washed with brine, dried over anhydrous Na_2SO_4 and the solvent evaporated to obtain 705 mg (2.18 mmol, 92%) of **316**. The product was purified by crystallization in CH_2Cl_2/hexane (174 mg, 0.54 mmol, 23%). M.p.: 159 °C (CH_2Cl_2/hexane). IR (KBr): 3301, 1595, 1509, 1163, 839 cm^{-1}. ^{1}H NMR (400 MHz, $CDCl_3$): δ 3.71 (3H, *s*), 3.81 (3H, *s*), 4.02 (3H, *s*), 6.42 (1H, *dd*, *J* = 8.8 and 2.4), 6.50 (1H, *d*, *J* = 2.4), 6.71 (2H, *d*, *J* = 8.4), 6.97 (2H, *d*, *J* = 8.4), 7.64 (1H, *d*, *J* = 8.8). ^{13}C NMR (100 MHz, acetone-D_6): δ 54.7 (CH_3), 55.2 (CH_3), 55.7 (CH_3), 98.8 (CH), 104.5 (CH), 113.9 (2CH), 119.1 (C), 123.4 (2CH), 130.8 (C), 132.1 (CH), 157.1 (C), 158.1 (C), 164.9 (C). HRMS ($C_{15}H_{17}NO_5S$ + Na^+): calcd 346.0720 (M + Na^+), found 346.0724.

2,4-Dimethoxy-*N*-(4-methoxyphenyl)-*N*-methylbenzenesulfonamide (**317**). To 88 mg (0.27 mmol) of **316** in CH_3CN (40 mL), 30 mg (0.54 mmol) of crushed KOH were added and stirred for 30 min. Then, 34 µL (0.54 mmol) of CH_3I were added and stirred for 24 h. The solvent was evaporated to dryness and the residue was re-dissolved in EtOAc, washed with brine, dried

(Na_2SO_4) and filtered. After concentration, the residue (106 mg) was purified by preparative TLC (hexane/EtOAc 4:6) to give pure product **317** (86 mg, 0.25 mmol, 93%). IR (KBr): 1574, 1505, 1245, 833 cm^{-1}. ^1H NMR (400 MHz, $CDCl_3$): δ 3.30 (3H, *s*), 3.75 (3H, *s*), 3.79 (3H, *s*), 3.82 (3H, *s*), 6.40 (1H, *dd*, *J* = 8.4 and 2.4), 6.45 (1H, *d*, *J* = 2.4), 6.76 (2H, *d*, *J* = 8.8), 7.08 (2H, *d*, *J* = 8.8), 7.63 (1H, *d*, *J* = 8.4). ^{13}C NMR (100 MHz, $CDCl_3$): δ 39.2 (CH_3), 55.3 (CH_3), 55.6 (CH_3), 55.8 (CH_3), 99.1 (CH), 104.0 (CH), 113.9 (2CH), 119.1 (C), 128.0 (2CH), 133.6 (CH), 134.6 (C), 158.2 (C), 158.4 (C), 164.6 (C). HRMS ($C_{16}H_{19}NO_5S + H^+$): calcd 338.1057 ($M + H^+$), found 338.1059.

N-(cyanomethyl)-2,4-dimethoxy-*N*-(4-methoxyphenyl)benzenesulfonamide (**318**). 2-chloroacetonitrile (20 µL, 0.31 mmol) was added after 30 min to a stirred solution of **316** (51 mg, 0.16 mmol) and K_2CO_3 (43 mg, 0.31 mmol) in dry DMF (3 mL). After 24 h, the reaction mixture was dried under vacuum, re-dissolved in EtOAc and washed with brine. After drying over Na_2SO_4 and removal of the solvent, crude reaction product **318** (45 mg, 0.12 mmol, 79%) was purified by crystallization in methanol (7 mg, 0.02 mmol, 12%). IR (KBr): 3435, 2991, 1604, 1510, 1216, 869 cm^{-1}. ^1H NMR (400 MHz, $CDCl_3$): δ 3.77 (3H, *s*), 3.86 (3H, *s*), 4.02 (3H, *s*), 4.75 (2H, *s*), 6.42 (1H, *dd*, *J* = 8.8 and 2.4), 6.56 (1H, *d*, *J* = 2.4), 6.81 (2H, *d*, *J* = 8.8), 7.07 (2H, *d*, *J* = 8.8), 7.57 (1H, *d*, *J* = 8.8). ^{13}C NMR (100 MHz, CD_3OD): δ 40.3 (CH_2), 54.5 (CH_3), 54.9 (CH_3), 55.4 (CH_3), 98.8 (CH), 104.5 (CH), 114.2 (2CH), 116.2 (C), 118.2 (C), 129.9 (2CH), 130.6 (C), 132.8 (CH), 158.5 (C), 159.9 (C), 165.7 (C). HRMS ($C_{17}H_{18}N_2O_5S + Na^+$): calcd 385.0829 ($M + Na^+$), found 385.0823.

N-benzyl-2,4-dimethoxy-*N*-(4-methoxyphenyl)benzenesulfonamide (**319**). A solution of **316** (80 mg, 0.25 mmol) and K_2CO_3 (69 mg, 0.50 mmol) in dry DMF (3 mL) was stirred for 30 min. Benzyl chloride (58 µL, 0.50 mmol) was added to the solution and stirred for 24 h. Reaction mixture was concentrated under vacuum, re-dissolved in EtOAc and washed with brine, dried (Na_2SO_4), filtered, and evaporated to dryness to give **319** (98 mg, 0.24 mmol, 96%). The crude reaction product was purified by crystallization in methanol (61 mg, 0.15 mmol, 60%). M.p.: 113 °C (MeOH). IR (KBr): 1606, 1578, 1508, 1253, 833 cm^{-1}. ^1H NMR (400 MHz, $CDCl_3$): δ 3.69 (3H, *s*), 3.84 (3H, *s*), 3.96 (3H, *s*), 4.89 (2H, *s*), 6.40 (1H, *dd*, *J* = 8.8 and 2.4), 6.53 (1H, *d*, *J* = 2.4), 6.65 (2H, *d*, *J* = 8.8), 6.90 (2H, *d*, *J* = 8.8), 7.23 (5H, *m*), 7.63 (1H, *d*, *J* = 8.8). ^{13}C NMR (100 MHz, $CDCl_3$): δ 55.2 (CH_3), 55.6 (CH_3), 55.9 (CH_3), 56.4 (CH_2), 99.3 (CH), 104.0 (CH), 113.9 (2CH), 120.0 (C), 127.3 (CH), 128.3 (2CH), 128.5 (2CH), 130.3 (2CH), 131.7 (C), 133.6 (CH), 137.5 (C), 158.2 (C), 158.6 (C), 164.6 (C). HRMS ($C_{22}H_{23}NO_5S + H^+$): calcd 414.1370 ($M + H^+$), found 414.1363.

3,4-Dimethoxy-*N*-(4-methoxyphenyl)benzenesulfonamide (**320**). To a solution of 4-methoxyaniline (293 mg, 2.38 mmol) in CH_2Cl_2 (50 mL) and pyridine (2 mL), 3,4-dimethoxybenzenesulfonyl chloride (563 mg, 2.38 mmol) was slowly added. The mixture was stirred at room temperature for 8 h. Then the reaction was treated with 2N HCl and 5% $NaHCO_3$, washed with brine, dried over anhydrous Na_2SO_4 and the solvent evaporated to obtain 525 mg (1.62 mmol, 68%) of **320**. It was purified by crystallization in CH_2Cl_2/hexane (305 mg, 0.94 mmol, 40%). M.p.: 126 °C (CH_2Cl_2/hexane). IR (KBr): 3252, 1587, 1251, 841 cm^{-1}. ^1H NMR (400 MHz, $CDCl_3$): δ 3.76 (3H, *s*), 3.78 (3H, *s*), 3.91 (3H, *s*), 6.16 (1H, *bs*), 6.77 (2H, *d*, *J* = 8.8), 6.84 (1H, *d*, *J* = 8.4), 6.96 (2H, *d*, *J* = 8.8), 7.06 (1H, *d*, *J* = 2.4), 7.30 (1H, *dd*, *J* = 8.4 and 2.4). ^{13}C NMR (100 MHz, $CDCl_3$): δ 55.4 (CH_3), 56.0 (CH_3), 56.1 (CH_3), 109.7 (CH), 110.3 (CH), 114.3 (2CH), 121.3 (CH), 125.3 (2CH), 129.1 (C), 130.4 (C), 148.8 (C), 152.6 (C), 157.8 (C). HRMS ($C_{15}H_{17}NO_5S + Na^+$): calcd 346.0720 ($M + Na^+$), found 346.0722.

3,4-Dimethoxy-*N*-(4-methoxyphenyl)-*N*-methylbenzenesulfonamide (**321**). A mixture of **320** (81 mg, 0.25 mmol) and KOH (28 mg, 0.50 mmol) in CH_3CN (25 mL) was stirred at room temperature for 30 min. Then, CH_3I (31 µL, 0.50 mmol) was added to the solution and stirred for 24 h. The solvent was evaporated under reduced pressure and the residue was re-dissolved in EtOAc,

washed with brine, dried over Na_2SO_4 and concentrated to afford 74 mg (0.22 mmol, 87%) of compound **321** which was purified by preparative TLC (hexane/EtOAc 4:6) (60 mg, 0.18 mmol, 71%). IR (film): 1586, 1508, 1138, 862 cm^{-1}. ^1H NMR (400 MHz, $CDCl_3$): δ 3.12 (3H, *s*), 3.74 (3H, *s*), 3.79 (3H, *s*), 3.94 (3H, *s*), 6.81 (2H, *d*, *J* = 8.8), 6.88 (1H, *d*, *J* = 2.4), 6.90 (1H, *d*, *J* = 8.8), 7.01 (2H, *d*, *J* = 8.8), 7.24 (1H, *dd*, *J* = 8.8 and 2.4). ^{13}C NMR (100 MHz, CD_3OD): δ 37.4 (CH_3), 54.5 (CH_3), 55.0 (CH_3), 55.2 (CH_3), 110.5 (2CH), 113.5 (2CH), 121.6 (CH), 127.6 (C), 127.8 (2CH), 134.3 (C), 148.8 (C), 153.0 (C), 158.9 (C). HRMS ($C_{16}H_{19}NO_5S$ + H^+): calcd 338.1057 (M + H^+), found 338.1068.

N-(cyanomethyl)-3,4-dimethoxy-*N*-(4-methoxyphenyl)benzenesulfonamide (**322**). A solution of **320** (110 mg, 0.34 mmol) and K_2CO_3 (94 mg, 0.68 mmol) in dry DMF (3 mL) was stirred at room temperature for 1 h. To this solution 2-chloroacetonitrile (43 µL, 0.68 mmol) was added and the reaction mixture was stirred for 48 h. The solvent was removed under reduced pressure. The residue was dissolved in EtOAc and washed with brine, dried (Na_2SO_4) and concentrated in vacuo to afford 114 mg (0.31 mmol, 93%) of **322**. The crude product was purified by crystallization in methanol (81 mg, 0.22 mmol, 66%). M.p.: 123 °C (MeOH). ^1H NMR (400 MHz, CD_3OD): δ 3.78 (3H, *s*), 3.79 (3H, *s*), 3.90 (3H, *s*), 4.68 (2H, *s*), 6.90 (2H, *d*, *J* = 9.2), 7.07 (1H, *d*, *J* = 8.4), 7.09 (2H, *d*, *J* = 9.2), 7.10 (1H, *d*, *J* = 2.4), 7.25 (1H, *dd*, *J* = 8.4 and 2.4). ^{13}C NMR (100 MHz, CD_3OD): δ 39.1 (CH_2), 54.6 (CH_3), 55.1 (CH_3), 55.2 (CH_3), 110.3 (CH), 110.5 (CH), 114.1 (2CH), 115.6 (C), 121.9 (CH), 128.7 (C), 129.6 (2CH), 131.1 (C), 149.1 (C), 153.5 (C), 160.1 (C). HRMS ($C_{17}H_{18}N_2O_5S$ + H^+): calcd 363.1009 (M + H^+), found 363.1009.

N-benzyl-3,4-dimethoxy-*N*-(4-methoxyphenyl)benzenesulfonamide (**323**). A solution of **320** (70 mg, 0.22 mmol) and K_2CO_3 (60 mg, 0.44 mmol) in dry DMF (3 mL) was stirred at room temperature for 30 min, then 51 µL (0.44 mmol) of benzyl chloride were added and the mixture stirred for 48 h. When completed, solvent was removed under vacuum and the residue was washed with brine, extracted with EtOAc, dried (Na_2SO_4), filtered, and evaporated to dryness to afford 77 mg (0.18 mmol, 85%) of **323.** The crude reaction product was purified by crystallization in CH_2Cl_2/hexane (47 mg, 0.11 mmol, 52%). M.p.: 138 °C (CH_2Cl_2/hexane). IR (KBr): 1587, 1454, 1155, 808 cm^{-1}. ^1H NMR (400 MHz, $CDCl_3$): δ 3.73 (3H, *s*), 3.78 (3H, *s*), 3.96 (3H, *s*), 4.66 (2H, *s*), 6.71 (2H, *d*, *J* = 8.8), 6.88 (2H, *d*, *J* = 8.8), 6.93 (1H, *d*, *J* = 8.4), 7.01 (1H, *d*, *J* = 2), 7.22 (5H, *bs*), 7.34 (1H, *dd*, *J* = 8.4 and 2). ^{13}C NMR (100 MHz, $CDCl_3$): δ 54.9 (CH_3), 55.3 ($2CH_3$), 56.1 (CH_2), 110.3 (CH), 110.4 (CH), 113.9 (2CH), 121.5 (CH), 127.5 (CH), 128.3 (2CH), 128.6 (2CH), 129.4 (C), 130.3 (2CH), 131.6 (C), 136.1 (C), 148.7 (C), 152.4 (C), 158.9 (C). HRMS ($C_{22}H_{23}NO_5S$ + H^+): calcd 414.1370 (M + H^+), found 414.1366.

Anexo 2.c. Biological evaluation of the synthesized sulfonamide library.

Table: Antiproliferative activity against human tumor cell lines U937 (lung histiocytic lymphoma), HeLa (cervical carcinoma), MCF7 (breast carcinoma), and HT-29 (colon carcinoma) expressed as drug concentration required to inhibit the growth by 50%, relative to untreated controls after 72 h of drug exposure (IC_{50}). Cytotoxicity against HT-29 cell line in the presence of the Pgp/MDR1 inhibitor Verapamil (10 µM). Percentage of the *in vitro* Tubulin Polymerization Inhibition (TPI) at 10 µM ligand concentration. Aqueous solubility in pH 7.0 phosphate buffer expressed in µg/mL. [a] Cytotoxic. [b] Non-cytotoxic. [c] Not determined.

	Antiproliferative activity						
	U937	HeLa	MCF7	HT-29 IC_{50} (nM)		TPI (%)	Solub.
Nº Comp.	10 µM	IC_{50} (nM)	IC_{50} (nM)	Standard	Verap. 10µM	10 µM	(µg/mL)
1a	C [a]	240	375	897	975	0	83
1b	NC [b]	>1000	>1000	>1000	n.d. [c]	0	108
2a	C	71	127	143	117	35	27
2b	NC	>1000	>1000	>1000	n.d.	0	n.d.
3	C	99	87	913	328	25	30
4	C	94	340	503	460	30	n.d.
5	C	287	270	747	683	0	38
6	C	143	275	230	458	0	33
7	C	217	335	237	398	21	n.d.
8	NC	>1000	>1000	>1000	n.d.	0	n.d.
9	C	750	830	>1000	n.d.	21	n.d.
10	C	>1000	>1000	>1000	n.d.	11	n.d.
11	NC	>1000	>1000	>1000	n.d.	10	88
12	NC	>1000	>1000	>1000	n.d.	0	158
13	NC	>1000	>1000	>1000	n.d.	0	n.d.
14	NC	>1000	>1000	>1000	n.d.	0	n.d.
15	NC	>1000	>1000	>1000	n.d.	0	230
16	NC	>1000	>1000	>1000	n.d.	0	n.d.
17	NC	>1000	>1000	>1000	n.d.	4	n.d.
18	NC	>1000	>1000	>1000	n.d.	0	n.d.
19	NC	>1000	>1000	>1000	n.d.	0	n.d.
20	NC	>1000	>1000	>1000	n.d.	0	87
21	NC	>1000	>1000	>1000	n.d.	0	357
22	NC	>1000	>1000	>1000	n.d.	0	1690
23	NC	>1000	>1000	>1000	n.d.	0	41
24	NC	>1000	>1000	>1000	n.d.	0	n.d.
25	NC	>1000	>1000	>1000	n.d.	0	n.d.
26	NC	>1000	>1000	>1000	n.d.	0	28
27	C	>1000	>1000	>1000	n.d.	0	25
28	C	230	173	887	1170	0	15
29a	C	63	30	103	43	40	7
29b	NC	>1000	>1000	>1000	n.d.	0	4
30	C	66	81	460	84	45	6
31	C	183	135	140	240	38	18
32	C	55	120	123	237	17	8
33	C	99	91	863	850	14	n.d.
34	C	>1000	>1000	>1000	n.d.	6	n.d.
35a	C	330	100	165	287	72	n.d.
35b	C	>1000	>1000	690	n.d.	0	n.d.
36	NC	>1000	n.d.	>1000	n.d.	n.d.	17
37	NC	>1000	>1000	>1000	n.d.	0	27
38	C	607	>1000	807	n.d.	7	43
39	C	44	61	59	50	47	16

40	C	18	13	44	50	34	29
41	C	77	42	89	53	24	29
42	C	143	73	500	515	22	50
43	C	53	12	81	45	78	19
44a	C	2570	>1000	>1000	n.d.	0	165
44b	NC	>1000	>1000	>1000	n.d.	0	n.d.
45	C	527	>1000	>1000	n.d.	0	38
46	C	21	8	28	27	36	26
47	C	>1000	>1000	>1000	n.d.	8	3.3
48	C	110	100	500	587	14	5.7
49	C	413	505	500	578	11	n.d.
50	C	595	480	500	500	0	9.1
51	C	407	160	360	390	52	n.d.
52	C	>1000	>1000	>1000	n.d.	11	n.d.
54	NC	>1000	>1000	>1000	n.d.	n.d.	n.d.
55	C	260	96	277	260	15	89
56	C	23	26	81	79	41	108
57	C	38	14	63	58	37	58
58	C	60	8	61	62	5	46
59	C	25	48	300	276	75	14
60	C	210	48	113	317	13	n.d.
61	C	>1000	>1000	>1000	n.d.	0	n.d.
62	C	440	1190	>1000	n.d.	2	n.d.
63	C	1170	>1000	>1000	n.d.	0	n.d.
64a	NC	>1000	n.d.	n.d.	n.d.	n.d.	1551
65	C	>1000	n.d.	n.d.	n.d.	n.d.	677
66a	NC	>1000	n.d.	n.d.	n.d.	0	1206
66b	NC	>1000	n.d.	n.d.	n.d.	31	146
67	NC	>1000	n.d.	n.d.	n.d.	0	1066
68	NC	>1000	n.d.	n.d.	n.d.	0	376
69	NC	>1000	>1000	>1000	n.d.	0	n.d.
70	C	877	765	>1000	n.d.	10	35
71	C	>1000	>1000	>1000	n.d.	0	n.d.
72	C	>1000	>1000	>1000	n.d.	0	n.d.
73	NC	>1000	>1000	>1000	n.d.	0	n.d.
74	C	>1000	>1000	>1000	n.d.	0	n.d.
75	NC	>1000	>1000	>1000	n.d.	0	n.d.
76	NC	>1000	>1000	>1000	n.d.	0	n.d.
77	NC	>1000	>1000	>1000	n.d.	0	41
78	NC	>1000	n.d.	>1000	n.d.	n.d.	n.d.
79	C	877	n.d.	2000	n.d.	10	66
80	C	>1000	n.d.	>1000	n.d.	19	n.d.
81	C	>1000	n.d.	>1000	n.d.	n.d.	n.d.
82	NC	>1000	n.d.	>1000	n.d.	n.d.	n.d.
83	C	>1000	>1000	>1000	n.d.	25	n.d.
84	NC	>1000	>1000	>1000	n.d.	0	39
85	NC	>1000	>1000	>1000	n.d.	0	4
86	C	1000	>1000	1000	n.d.	15	548
87	C	920	>1000	>1000	n.d.	10	n.d.
88	C	>1000	>1000	>1000	n.d.	15	n.d.
89	NC	>1000	n.d.	>1000	n.d.	n.d.	n.d.
90	NC	>1000	n.d.	>1000	n.d.	n.d.	n.d.
91	NC	>1000	n.d.	>1000	n.d.	n.d.	n.d.
92	C	233	465	300	290	3	27
93	C	410	430	360	660	7	n.d.
94	C	370	n.d.	1000	n.d.	0	n.d.
95a	C	1230	n.d.	>1000	n.d.	0	n.d.

96	C	367	n.d.	1000	n.d.	23	n.d.
95b	C	>1000	n.d.	>1000	n.d.	0	n.d.
97a	C	497	99	495	293	10	n.d.
97b	NC	>1000	>1000	>1000	n.d.	0	n.d.
98a	C	417	n.d.	610	n.d.	0	n.d.
98b	C	>1000	>1000	>1000	n.d.	0	n.d.
99a	C	310	335	450	533	0	n.d.
99b	C	>1000	>1000	>1000	n.d.	0	n.d.
99c	C	>1000	>1000	>1000	n.d.	0	n.d.
101	NC	>1000	n.d.	>1000	n.d.	0	1
102	NC	995	n.d.	>1000	n.d.	0	120
103	NC	>1000	>1000	>1000	n.d.	n.d.	n.d.
104	NC	>1000	>1000	>1000	n.d.	0	n.d.
105	C	>1000	>1000	>1000	n.d.	0	16
106	NC	>1000	n.d.	>1000	n.d.	n.d.	n.d.
107	NC	1160	n.d.	>1000	n.d.	0	17
108	NC	>1000	n.d.	>1000	n.d.	n.d.	n.d.
109	NC	>1000	>1000	>1000	n.d.	0	5
110	NC	>1000	>1000	>1000	n.d.	0	1
111	C	1030	>1000	2000	n.d.	17	22
112	NC	>1000	n.d.	>1000	n.d.	n.d.	n.d.
115a	NC	>1000	>1000	>1000	n.d.	7	n.d.
115b	NC	>1000	n.d.	>1000	n.d.	n.d.	n.d.
116	NC	>1000	n.d.	>1000	n.d.	n.d.	n.d.
117	NC	>1000	n.d.	>1000	n.d.	n.d.	n.d.
118	NC	>1000	>1000	>1000	n.d.	n.d.	n.d.
119	NC	>1000	n.d.	>1000	n.d.	n.d.	n.d.
120	NC	>1000	>1000	>1000	n.d.	4	82
121a	NC	>1000	>1000	>1000	n.d.	0	70
121b	NC	>1000	n.d.	>1000	n.d.	0	59
122	NC	>1000	>1000	>1000	n.d.	0	15
123	NC	>1000	>1000	>1000	n.d.	3	460
124	NC	>1000	>1000	>1000	n.d.	0	n.d.
125a	NC	>1000	>1000	>1000	n.d.	0	454
126	NC	>1000	>1000	>1000	n.d.	0	n.d.
125b	NC	>1000	>1000	>1000	n.d.	0	480
127	NC	>1000	>1000	>1000	n.d.	0	n.d.
128	NC	>1000	>1000	>1000	n.d.	0	n.d.
129	C	630	n.d.	1000	n.d.	0	30
130	NC	>1000	n.d.	>1000	n.d.	0	7.1
131	NC	>1000	>1000	>1000	n.d.	0	1172
132	NC	>1000	>1000	>1000	n.d.	0	255
133	NC	>1000	>1000	>1000	n.d.	0	220
134	NC	>1000	>1000	>1000	n.d.	0	4489
135	C	510	n.d.	543	n.d.	0	22
136	C	557	n.d.	907	n.d.	0	61
137	C	313	660	365	500	24	26
138	C	407	575	360	750	16	13
139	C	>1000	>1000	>1000	n.d.	0	n.d.
140	C	>1000	>1000	>1000	n.d.	38	n.d.
141	NC	>1000	n.d.	>1000	n.d.	0	11
142	NC	>1000	>1000	>1000	n.d.	0	n.d.
143	NC	>1000	n.d.	>1000	n.d.	0	n.d.
144	NC	>1000	>1000	>1000	n.d.	3	55
145	NC	>1000	>1000	>1000	n.d.	0	n.d.
146	NC	>1000	>1000	>1000	n.d.	0	8
147a	C	1000	n.d.	>1000	n.d.	20	53

147b	NC	>1000	n.d.	>1000	n.d.	0	n.d.
148	NC	>1000	n.d.	>1000	n.d.	0	4.6
149	NC	1000	>1000	>1000	n.d.	n.d.	118
150	NC	>1000	n.d.	>1000	n.d.	0	45
151	NC	>1000	>1000	>1000	n.d.	0	n.d.
152a	NC	>1000	n.d.	>1000	n.d.	0	n.d.
152b	NC	>1000	n.d.	>1000	n.d.	n.d.	n.d.
153	NC	>1000	>1000	>1000	n.d.	0	n.d.
154	C	745	180	510	500	0	12
155	C	283	715	310	500	10	60
156	C	1160	>1000	1200	n.d.	8	2.2
157	NC	>1000	>1000	>1000	n.d.	0	n.d.
158	NC	1000	>1000	>1000	n.d.	0	n.d.
159	NC	>1000	>1000	>1000	n.d.	0	52
160	C	>1000	n.d.	>1000	n.d.	n.d.	56
161	C	>1000	n.d.	>1000	n.d.	n.d.	n.d.
162	NC	>1000	n.d.	>1000	n.d.	n.d.	36
163	NC	>1000	n.d.	>1000	n.d.	n.d.	n.d.
164	C	313	420	320	365	11	20
165	C	747	306	750	740	11	9.3
166	C	3000	n.d.	1200	n.d.	11	62
167	C	497	n.d.	750	n.d.	14	6.2
168	NC	>1000	n.d.	>1000	n.d.	n.d.	n.d.
172	NC	>1000	>1000	>1000	n.d.	7	243
173	C	3470	>1000	>1000	n.d.	11	47
174	NC	>1000	>1000	>1000	n.d.	0	16
175	C	411	530	>1000	n.d.	0	60
176	C	71	71	410	130	25	164
177	C	337	390	662	450	0	71
181	NC	>1000	n.d.	>1000	n.d.	n.d.	n.d.
182	C	1100	n.d.	>1000	n.d.	0	n.d.
183	C	3500	n.d.	2500	n.d.	13	n.d.
184	C	>1000	n.d.	>1000	n.d.	7	n.d.
185	C	>1000	n.d.	>1000	n.d.	16	n.d.
188	C	227	350	187	187	0	13
189	C	177	153	250	305	4	25
190	C	>1000	>1000	>1000	n.d.	0	n.d.
191	NC	>1000	>1000	>1000	n.d.	0	51
192	NC	>1000	>1000	>1000	n.d.	0	44
193	NC	630	n.d.	>1000	n.d.	18	189
194	C	1070	>1000	>1000	n.d.	0	20
195	NC	>1000	>1000	>1000	n.d.	0	n.d.
196	NC	>1000	>1000	>1000	n.d.	0	n.d.
197	NC	>1000	>1000	>1000	n.d.	0	n.d.
198	NC	>1000	>1000	>1000	n.d.	0	n.d.
199	NC	>1000	>1000	>1000	n.d.	0	n.d.
200	NC	>1000	>1000	>1000	n.d.	0	n.d.
201	C	45	25	72	30	65	9
202	C	33	19	123	160	59	1
203	C	36	86	97	85	51	1
204	C	577	700	2100	867	28	n.d.
205	NC	>1000	>1000	>1000	n.d.	8	n.d.
206	C	377	220	525	170	44	n.d.
207	C	495	n.d.	860	n.d.	32	n.d.
208	NC	>1000	>1000	>1000	n.d.	0	n.d.
209	NC	>1000	>1000	>1000	n.d.	0	n.d.
210	NC	>1000	>1000	>1000	n.d.	0	56

211	NC	>1000	>1000	>1000	n.d.	0	14
212	NC	>1000	>1000	>1000	n.d.	0	5.8
213	C	867	>1000	>1000	n.d.	0	8.3
214	C	233	540	877	940	8	6.3
215	C	111	62	217	250	15	1.4
216	C	347	98	360	360	10	2
217	C	300	195	673	110	16	8.9
218	C	>1000	n.d.	>1000	n.d.	5	n.d.
219	C	>1000	>1000	>1000	n.d.	15	n.d.
220	NC	>1000	>1000	>1000	n.d.	0	n.d.
221	NC	>1000	>1000	>1000	n.d.	0	n.d.
222	NC	>1000	>1000	>1000	n.d.	0	28
223	C	803	>1000	>1000	n.d.	0	45
224	C	347	210	370	425	10	4.8
225	C	193	71	360	243	16	11
226	C	327	105	220	383	25	8.7
227	C	2370	4000	1500	n.d.	30	n.d.
228a	C	1040	>1000	>1000	n.d.	5	18
228b	C	115	545	1030	1010	10	28
229	C	>1000	>1000	>1000	n.d.	5	10
230	NC	>1000	>1000	>1000	n.d.	5	n.d.
231	C	175	975	903	1430	0	n.d.
232	C	350	615	>1000	n.d.	0	38
233	C	38	48	117	102	8	9.4
234	C	71	16	917	65	10	3.7
235	C	47	10	51	57	23	17
236	C	1010	n.d.	>1000	n.d.	0	n.d.
239	C	410	580	360	553	3	213
240	C	413	99	500	577	0	157
241	C	313	715	500	1070	19	122
242	C	500	67	365	415	5	15
243	C	>1000	>1000	>1000	n.d.	0	n.d.
244	C	833	n.d.	1250	n.d.	7	n.d.
245	NC	>1000	n.d.	>1000	n.d.	n.d.	n.d.
246	NC	>1000	>1000	>1000	n.d.	0	n.d.
247	C	>1000	>1000	>1000	n.d.	0	61
248	C	220	300	360	390	10	12
249	C	500	360	265	510	0	18
250	C	823	n.d.	1500	n.d.	0	13
251	C	>1000	n.d.	>1000	n.d.	0	n.d.
252	C	>1000	>1000	>1000	n.d.	0	n.d.
253	NC	>1000	>1000	>1000	n.d.	0	n.d.
254	C	>1000	>1000	>1000	n.d.	0	n.d.
255	C	730	n.d.	1000	n.d.	0	n.d.
256	C	555	n.d.	1000	n.d.	3	6
257	C	>1000	n.d.	>1000	n.d.	0	n.d.
258	NC	>1000	n.d.	>1000	n.d.	n.d.	n.d.
259	C	337	170	365	377	12	126
260	C	407	67	220	320	0	138
261	C	503	370	500	507	0	204
262	C	407	51	500	370	0	11
263a	C	>1000	n.d.	>1000	n.d.	0	n.d.
264	C	410	303	500	565	15	n.d.
263b	C	>1000	n.d.	>1000	n.d.	5	n.d.
265	C	800	n.d.	>1000	n.d.	2	n.d.
266	C	950	n.d.	>1000	n.d.	5	n.d.
270	C	>1000	n.d.	>1000	n.d.	0	n.d.

271	C	280	735	1630	277	18	n.d.
272	C	357	565	500	373	57	n.d.
273	NC	>1000	n.d.	>1000	n.d.	n.d.	n.d.
276a	C	>1000	n.d.	>1000	n.d.	0	n.d.
276b	NC	>1000	>1000	>1000	n.d.	0	n.d.
277	NC	>1000	n.d.	>1000	n.d.	0	n.d.
278	NC	>1000	n.d.	>1000	n.d.	0	n.d.
279	NC	3670	n.d.	>1000	n.d.	0	n.d.
281	NC	>1000	n.d.	n.d.	n.d.	0	n.d.
282	NC	>1000	n.d.	n.d.	n.d.	n.d.	n.d.
283	NC	>1000	n.d.	n.d.	n.d.	n.d.	n.d.
284	NC	>1000	n.d.	n.d.	n.d.	n.d.	n.d.
285	NC	>1000	n.d.	n.d.	n.d.	n.d.	n.d.
286	NC	>1000	n.d.	n.d.	n.d.	n.d.	n.d.
287	NC	>1000	n.d.	n.d.	n.d.	n.d.	n.d.
288	NC	>1000	n.d.	n.d.	n.d.	n.d.	n.d.
289	NC	>1000	n.d.	n.d.	n.d.	n.d.	n.d.
290	NC	>1000	n.d.	n.d.	n.d.	n.d.	n.d.
291	NC	>1000	n.d.	n.d.	n.d.	n.d.	n.d.
292	NC	>1000	n.d.	n.d.	n.d.	n.d.	n.d.
293a	NC	>1000	n.d.	>1000	n.d.	n.d.	1759
293b	NC	>1000	>1000	>1000	n.d.	n.d.	1889
295	NC	>1000	n.d.	>1000	n.d.	n.d.	110
296	NC	>1000	n.d.	>1000	n.d.	n.d.	n.d.
297	NC	>1000	n.d.	>1000	n.d.	n.d.	n.d.
298	NC	>1000	n.d.	>1000	n.d.	n.d.	n.d.
299	NC	>1000	>1000	>1000	n.d.	n.d.	n.d.
300	NC	>1000	n.d.	>1000	n.d.	n.d.	n.d.
301	NC	>1000	n.d.	>1000	n.d.	n.d.	n.d.
302	NC	>1000	n.d.	>1000	n.d.	n.d.	n.d.
303	NC	>1000	n.d.	>1000	n.d.	n.d.	n.d.
304	NC	>1000	n.d.	>1000	n.d.	n.d.	n.d.
305	NC	>1000	n.d.	>1000	n.d.	n.d.	n.d.
306	NC	>1000	n.d.	>1000	n.d.	n.d.	n.d.
307	NC	>1000	n.d.	>1000	n.d.	n.d.	n.d.
308	NC	>1000	>1000	>1000	n.d.	n.d.	n.d.
309	C	>1000	n.d.	>1000	n.d.	8	n.d.
310	NC	>1000	n.d.	>1000	n.d.	n.d.	n.d.
311	NC	>1000	>1000	>1000	n.d.	n.d.	n.d.
313	NC	>1000	n.d.	>1000	n.d.	n.d.	n.d.
314	NC	>1000	n.d.	>1000	n.d.	n.d.	n.d.
315	NC	>1000	n.d.	>1000	n.d.	n.d.	n.d.
316	NC	>1000	n.d.	n.d.	n.d.	n.d.	n.d.
317	NC	>1000	n.d.	n.d.	n.d.	n.d.	n.d.
318	NC	>1000	n.d.	n.d.	n.d.	n.d.	n.d.
319	NC	>1000	n.d.	n.d.	n.d.	n.d.	n.d.
320	NC	>1000	n.d.	n.d.	n.d.	n.d.	n.d.
321	NC	>1000	n.d.	n.d.	n.d.	n.d.	n.d.
322	NC	>1000	n.d.	n.d.	n.d.	n.d.	n.d.
323	NC	>1000	n.d.	n.d.	n.d.	n.d.	n.d.

Anexo digital 2.d. ^{1}H and ^{13}C NMR spectra of the synthesized sulfonamide library.

Los espectros de RMN de ^{1}H y de ^{13}C de los compuestos descritos en el anexo 2.b están disponibles en el CD adjunto al presente trabajo de Tesis Doctoral como material suplementario digital.